



UNIVERSITAT DE
BARCELONA

Development of New Multicomponent Processes based on Unexplored Chemistry of Isocyanides: Access to Heterocyclic Scaffolds and Applications

Ouldouz Ghashghaei

ADVERTIMENT. La consulta d'aquesta tesi queda condicionada a l'acceptació de les següents condicions d'ús: La difusió d'aquesta tesi per mitjà del servei TDX (www.tdx.cat) i a través del Dipòsit Digital de la UB (diposit.ub.edu) ha estat autoritzada pels titulars dels drets de propietat intel·lectual únicament per a usos privats emmarcats en activitats d'investigació i docència. No s'autoritza la seva reproducció amb finalitats de lucre ni la seva difusió i posada a disposició des d'un lloc aliè al servei TDX ni al Dipòsit Digital de la UB. No s'autoritza la presentació del seu contingut en una finestra o marc aliè a TDX o al Dipòsit Digital de la UB (framing). Aquesta reserva de drets afecta tant al resum de presentació de la tesi com als seus continguts. En la utilització o cita de parts de la tesi és obligat indicar el nom de la persona autora.

ADVERTENCIA. La consulta de esta tesis queda condicionada a la aceptación de las siguientes condiciones de uso: La difusión de esta tesis por medio del servicio TDR (www.tdx.cat) y a través del Repositorio Digital de la UB (diposit.ub.edu) ha sido autorizada por los titulares de los derechos de propiedad intelectual únicamente para usos privados enmarcados en actividades de investigación y docencia. No se autoriza su reproducción con finalidades de lucro ni su difusión y puesta a disposición desde un sitio ajeno al servicio TDR o al Repositorio Digital de la UB. No se autoriza la presentación de su contenido en una ventana o marco ajeno a TDR o al Repositorio Digital de la UB (framing). Esta reserva de derechos afecta tanto al resumen de presentación de la tesis como a sus contenidos. En la utilización o cita de partes de la tesis es obligado indicar el nombre de la persona autora.

WARNING. On having consulted this thesis you're accepting the following use conditions: Spreading this thesis by the TDX (www.tdx.cat) service and by the UB Digital Repository (diposit.ub.edu) has been authorized by the titular of the intellectual property rights only for private uses placed in investigation and teaching activities. Reproduction with lucrative aims is not authorized nor its spreading and availability from a site foreign to the TDX service or to the UB Digital Repository. Introducing its content in a window or frame foreign to the TDX service or to the UB Digital Repository is not authorized (framing). Those rights affect to the presentation summary of the thesis as well as to its contents. In the using or citation of parts of the thesis it's obliged to indicate the name of the author.

Programa de Doctorado de Química Orgánica Experimental y Industrial

Tesis Doctoral

Development of New Multicomponent Processes based on Unexplored Chemistry of Isocyanides: Access to Heterocyclic Scaffolds and Applications.

Memoria presentada por
Ouldouz Ghashghaei

Dirigida y revisada por:

Prof. Rodolfo Lavilla Grifols
(Universitat de Barcelona)

Universitat de Barcelona
Barcelona, 2017

The present thesis has been developed in the Faculty of Pharmacy, Department of Pharmacology, Toxicology and Therapeutical Chemistry, Unit of Organic Chemistry at the Laboratories in the Parc Científic de Barcelona (January 2013-June 2017). This work was supported by DGICYT, Spain (projects BQUCTQ2012-30930; CTQ2015- 67870-P), and Generalitat de Catalunya (project 2009 SGR 1024)

UNIVERSITAT DE BARCELONA

Facultat de Farmàcia i Ciències de l'Alimentació
Departament de Farmacologia, Toxicologia i Química Terapèutica

**Development of New Multicomponent Processes
based on Unexplored Chemistry of Isocyanides:
Access to Heterocyclic Scaffolds and Applications.**

**Ouldouz Ghashghaei
2017**



UNIVERSITAT DE
BARCELONA

To my father

**To strive,
to seek,
to find,
and not to yield.**

Ulysses (Alfred Tennyson, 1842)

Acknowledgements

This dissertation would not have been possible without the guidance and the help of several individuals who in one way or another contributed and extended their valuable assistance in the preparation and completion of this study.

First and foremost, my utmost gratitude to Dr. Rodolfo Lavilla, for giving me the opportunity to join his group and his unfailing support and encouragement. He has been my inspiration as I hurdle all the obstacles in the past four years.

I consider it an honor to have been in collaboration with all the groups who have contributed to this study: Dr Ramon Eritja, Dr Ana Avino, Dr Javier Luque, Dr Carolina Estarellas, Dr Marc Vendrell, Dr John Kelly, Dr Diego Moñoz-Torrero and Dr Javier Sánchez Céspedes.

I share the credit of my work with my amazing colleagues: Dr Nicola Kielland, Dr Marc Reves, Dr Krathi Kishore, Dr Samantha Caputo, Consiglia A. Manna and Miquel Sintes. Without their support, dedication and contributions, this study would not have been possible.

I would also like to thank my wonderful lab mates and friends at the PCB: Dr Lorena Mendive for her unconditional support all the way to the end. The staff from UQC: Jose, Unai, Sergi, Marta M, Marta, Patri, Dani, Natalia and Sonia, the people in ChemBioLab: Juan, Ivan, Helena, Alex, Gerardo, Jesus, Carlos, Omar, Nuria and Gloria as well as the staff from NMR and Mass Spectroscopy Service for their assistance and support.

I would like to thank Dr Josep Bonjoch and the administrative staff at the Faculty of Pharmacy for their kind consideration regarding the academic procedures I was very little familiar with.

And eventually this journey would not have been possible without my family and friends who generously offered their support in the hard times.

همراهان روزهای سخت،

بابای بی نظیرم،

نسرین و جمال جانم،

ایپیلی، ژاله جان، شعله و ولفگانگ عزیزم،

بشارت، حجت و فرزانه‌گانی‌های نازنینم،

بدون شما این سفر به انتها نمی رسید. از داشتن شما بی نهایت خوشبختم و سپاسگزار همیشگی لطف و محبت بی منتتان.

Ouldouz Ghashghaei

Barcelona, June 2017

Table of Contents

Introduction and Objectives	1
Main Strategies in Organic Synthesis	3
Multicomponent Reactions (MCRs)	7
Synthesis and functionalization of Heterocycles Using MCRs.....	17
Multiple Multicomponent Reactions:	24
Objectives.....	25
Chapter I	29
Publication I: Studies on the interaction of isocyanides with imines: Reaction scope and mechanistic variations.....	31
Publication I: Selected Supporting Information	32
Chapter II	69
Publication II: Modular Access to Tetrasubstituted Imidazolium Salts through Acid-Catalyzed Addition of Isocyanides to Propargylamines.....	71
Publication II: Selected Supporting Information	72
Addendum to Chapter II: Antiparasitical Properties of Novel Tetrasubstituted Imidazolium Salts Arising from the Interaction of Isocyanides and Propargylamines (Unpublished Results)	105
Chapter III	113
Publication III: Insertion of Isocyanides into N–Si Bonds: Multicomponent Reactions with Azines Leading to Potent Antiparasitic Compounds	115
Publication III: Selected Supporting Information	116
Chapter IV	197
Publication IV: Multiple Multicomponent Reaction Platform for the Selective Access to N-PolyHeterocyclic Chemotypes with Relevant Applications in Biology, Medicine and Materials Science	199
Publication IV: Selected Supporting Information	227
Conclusions	287
Summaries	291
Chapter I.....	293
Chapter II.....	295
Chapter III.....	297
Chapter IV.....	299
Personal Contributions	301

*Complete Supporting Information is Available in the Digital Version

Introduction and Objectives

Main Strategies in Organic Synthesis

The photochemist G. S. Hammond believed that “The most fundamental and lasting objective of synthesis is not the production of new compounds, but production of properties”¹. This idea is having an impact in the way Organic Synthesis should be envisaged. The immense investigation in this field attempts to meet the society’s growing demands for functional chemotypes in various sectors i.e. health, industry, energy, etc. Traditionally, most functional molecules were originated from nature which offers a vast variety of functional chemotypes. The exceptional functions of these compounds make them attractive targets for synthesis.²

In this way, Organic Synthesis was initially approached through what is called Target Oriented Synthesis (TOS). TOS investigates processes to access organic compounds in an efficient manner. In a TOS process, simple and readily available building blocks are transformed into a single target structure. However, due to the complex structure of the target, usually long multi-step procedures are inevitable.³ (Figure 1)

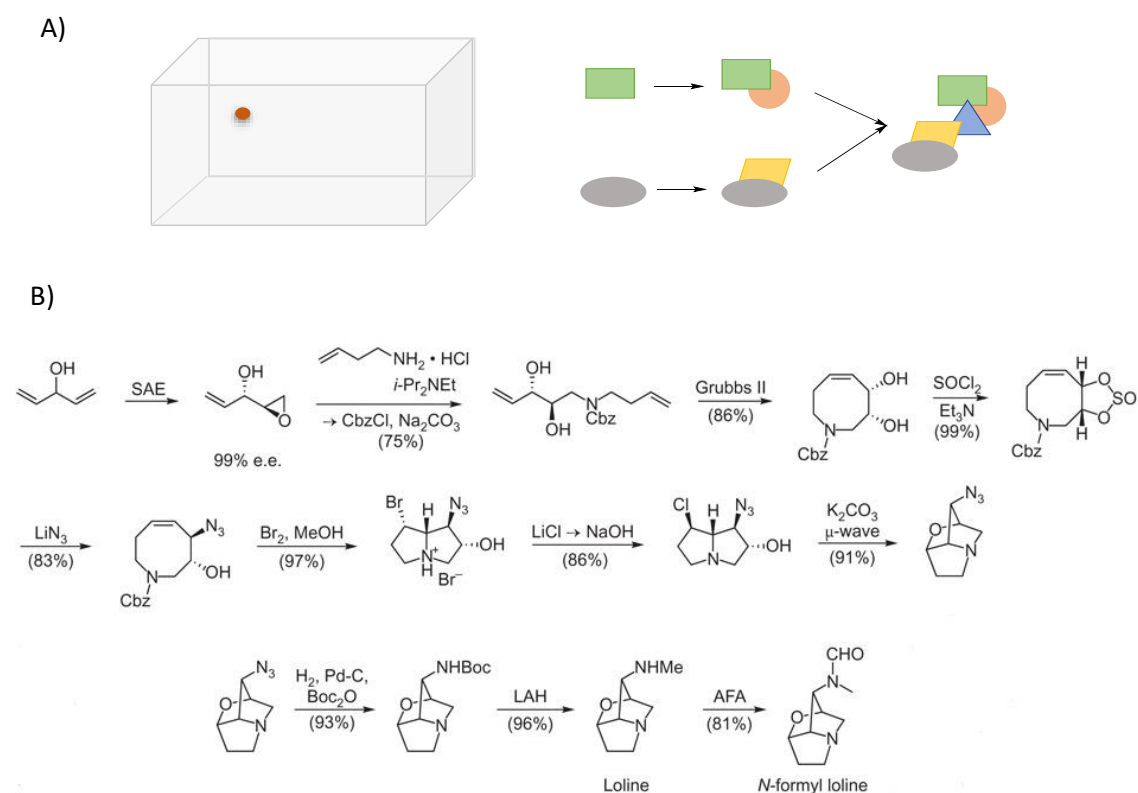


Figure 1. A) Schematic Presentation of TOS, B) Total synthesis of loline alkaloids (Taken from Ref.4)⁴

Discovery of new reactions and advances in catalysis enabled chemists to synthesize non-natural chemotypes, some of which displaying equally valuable (or even improved) properties.⁵ Being structurally simpler, they easily undergo screening and modification processes. This leads to higher efficiency, shorter synthetic routes, and more diverse properties compared to their naturally occurring counterparts. The aforementioned approach, normally referred to as Function Oriented Synthesis (FOS), focuses on the simpler yet better functioning analogs of known chemotypes.⁶ (Figure 2)

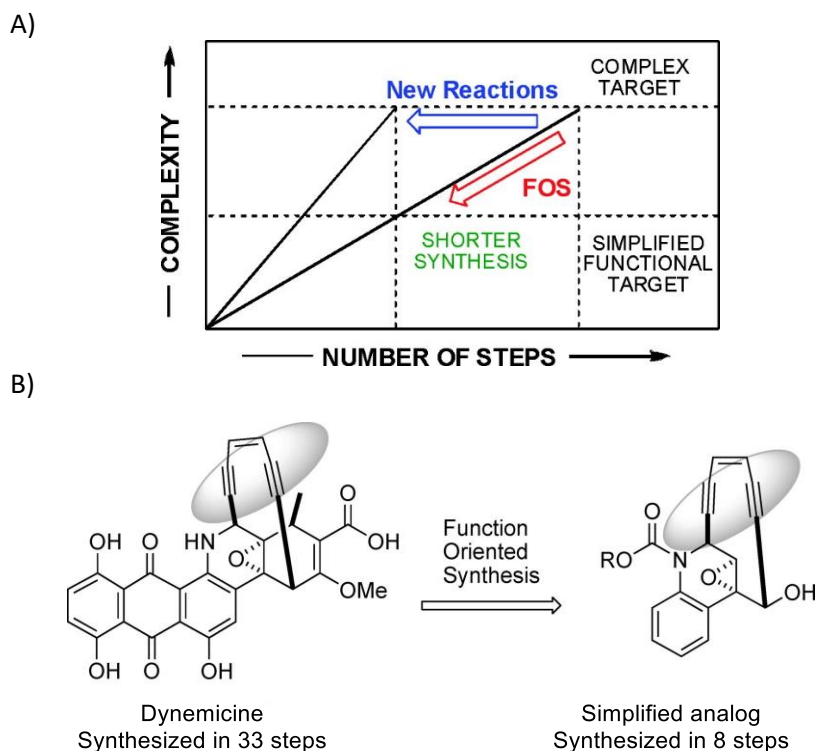


Figure 2. A) FOS and its role in synthesis strategy (Adapted from Wender et al.⁶) B) Complex antitumoral compound Dynemicin was synthesized in 33 steps,⁷ while its simplified analog could be obtained in 8 steps.⁸

Another common strategy in Organic Synthesis is Combinatorial Chemistry. It refers to the rapid access to a large array of compounds (called library) with a common scaffold. Screening the obtained libraries leads to the discovery of compounds with much improved properties. Higher levels of structural diversity are achieved through variations in substrates or reactivity modes. However, the exploration of the chemical space remains quite limited, very close to the parent scaffold.⁹ (Figure 3)

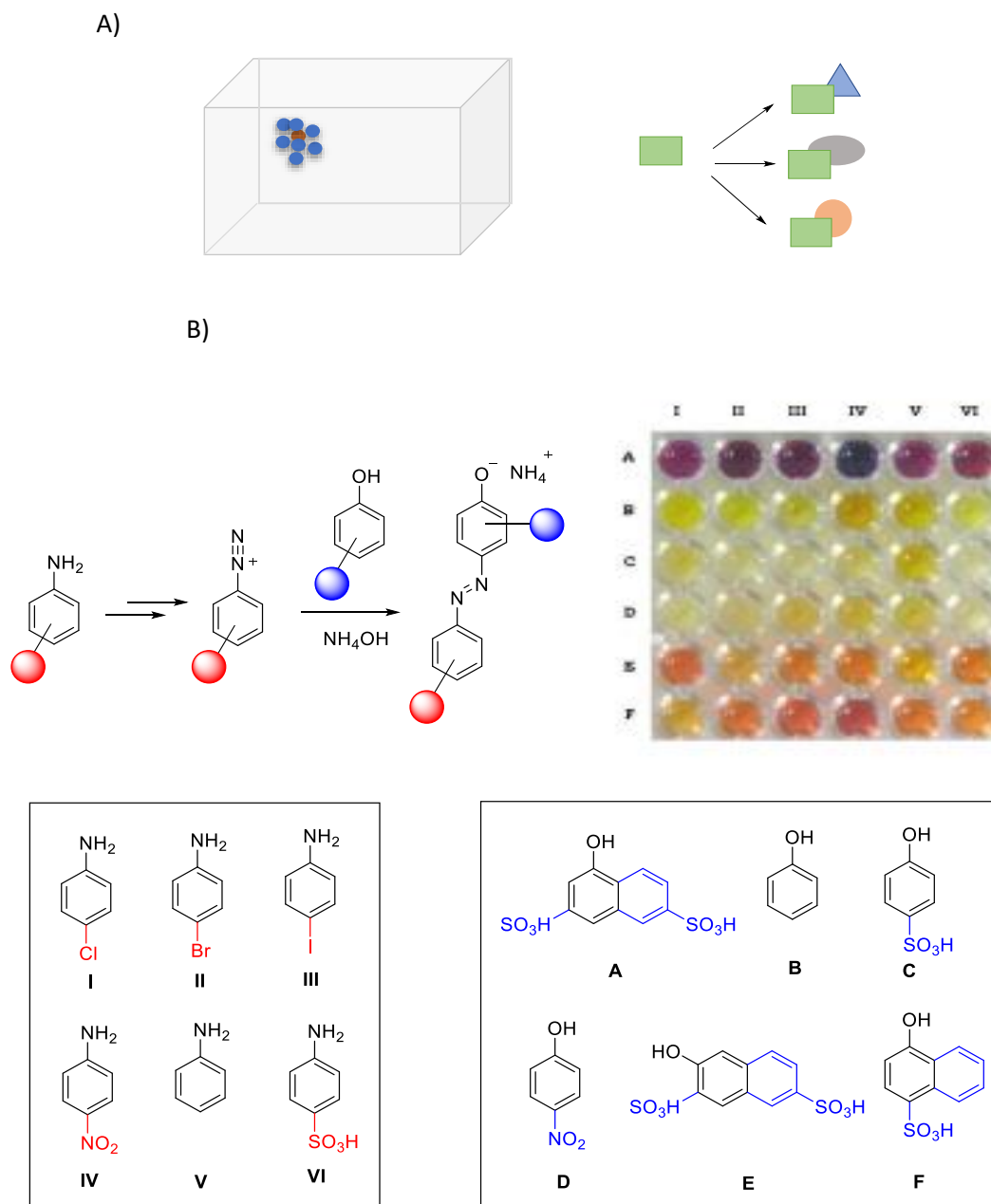


Figure 3. A) Schematic presentation of Combinatorial Chemistry. B) Solid-phase combinatorial synthesis of azo dyes.¹⁰

Meanwhile, many scientists believe that function may not be limited to known scaffolds. In other words, “unprecedented chemotypes” could potentially be alternative sources of properties. This growing approach is termed Diversity Oriented Synthesis (DOS). (Figure 4) DOS is defined as investigating the unexplored chemical space around privileged scaffolds by means of a family of transformations which upon reactive intermediates (i.e. furans, dienes, etc.) amenable to distinct reactivity modes lead to structurally different scaffolds. The ultimate goal of DOS is to achieve novel chemotypes with exceptional properties.¹¹

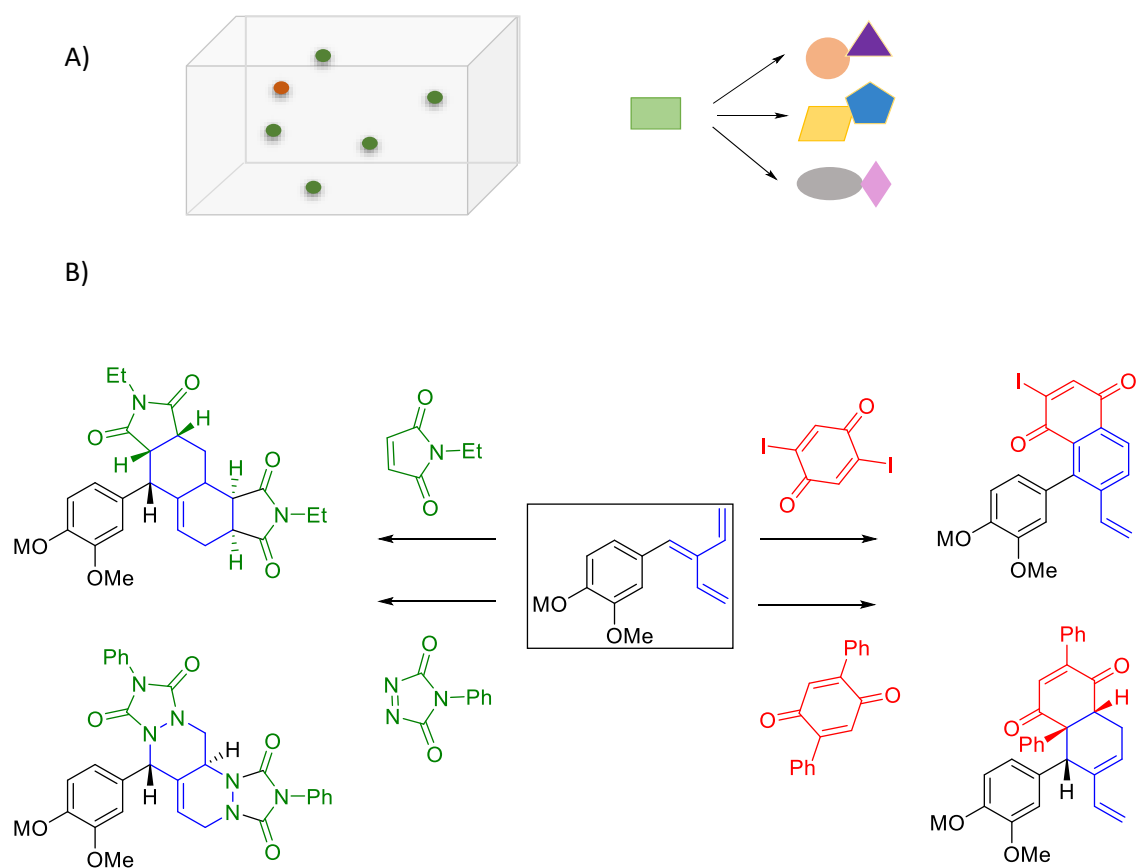


Figure 4. A) Schematic Presentation of DOS. B) The Diversity oriented synthesis of polycyclic compounds through cycloadditions and aza Diels Alder reactions, where skeletal diversity is achieved through the incorporation of different reagents. ¹²

Multicomponent Reactions (MCRs)

Multicomponent reactions (MCRs) are processes in which three or more components are incorporated into a final adduct in a one pot manner. They differ from tandem reactions in the sense that in MCRs all the components are added in the beginning of the reaction and the process proceeds through a unified reaction mechanism involving all reactants and intermediates thus generated (Figure 5).

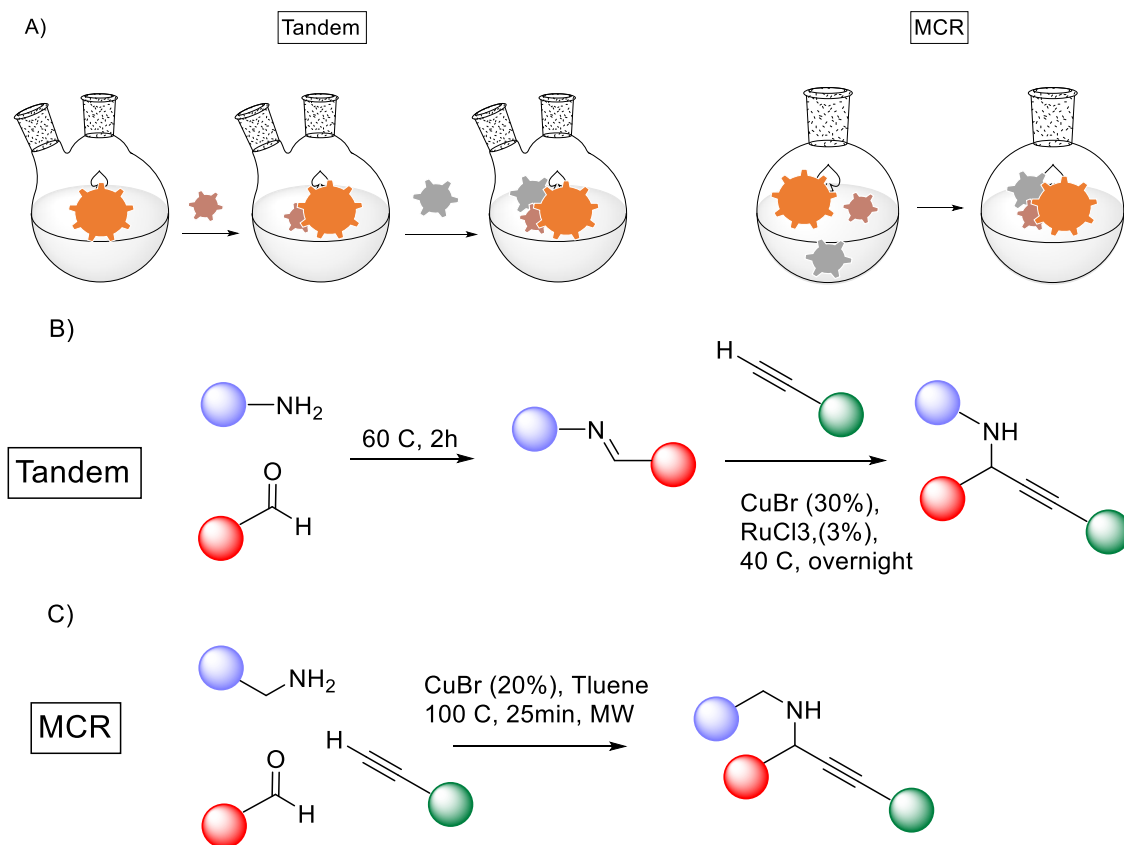


Figure 5. A) Schematic presentation of a tandem process vs an MCR. B) A³ coupling: Tandem¹³ vs Multicomponent approach for the synthesis of propargylamines.¹⁴

The key features of MCRs compared to classic reactions could be summarized as followed:¹⁵ (Figure 6)

- MCRs are experimentally simple procedures, adding all the starting material into a reaction mixture followed by a single isolation step.
- They are atom economic processes as all or a major number of the components' atoms appear in the final product structure.
- They have high bond-forming efficiency (BFE).
- MCRs are convergent, as all components end up into the final product.

- MCRs are selective processes, as the complex reaction cocktail yields a single product, although several other reactivity patterns are statistically possible. This is achieved by the intelligent design of such reactions, exploiting the distinct kinetic, and thermodynamic connectivity preferences of the building blocks.
- They are versatile processes, as variable (diversifiable) components are assembled into the final adduct, giving access to more diversity points (reactive functional groups amenable to further transformation) in the shortest synthetic routes. Moreover, they provide increased levels of structural complexity in a single step. Therefore, MCRs are defined as processes with high exploratory potential.

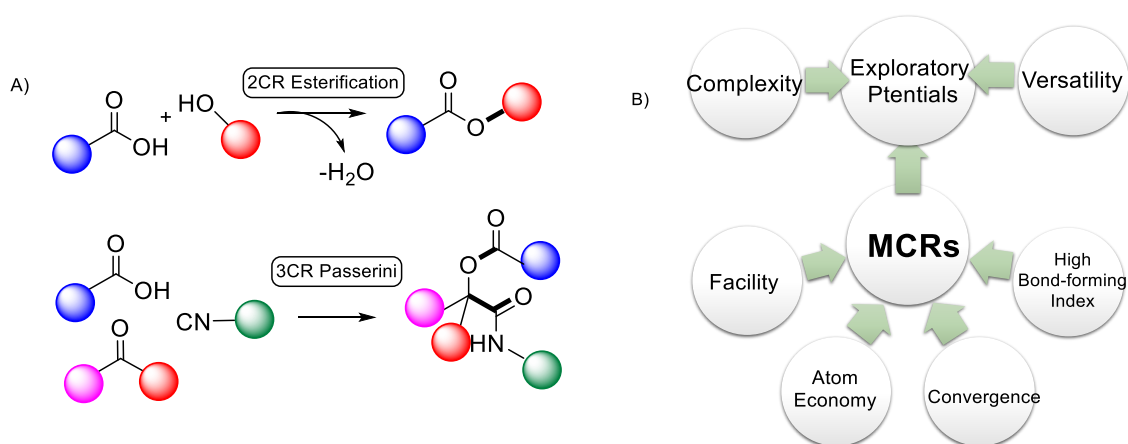


Figure 6. A) Schematic comparison of a 2-C Esterification vs a 3-C Passerini reaction. B) Advantageous features of MCRs.

Having featured several synthetic advantages, MCRs have turned into powerful tools in organic synthesis, having found a wide variety of applications in different fields:

- MCRs have been influential in TOS processes, offering solutions for synthetic challenges. They have facilitated synthetic access to several sophisticated scaffolds. Moreover, MCRs have been exploited to achieve shorter synthetic routes. Thus, they frequently appear as key steps in the total synthesis of natural products and other complex scaffolds¹⁶ (Figure 7).
- MCRs have been a popular strategy for the assembly of combinatorial libraries for screening purposes. MCRs can provide rapid and facile access to a large number of adducts with common skeleton. In these processes, a multidimensional matrix of adducts is achieved in a single step, exploiting a combination of diverse components¹⁷ (Figure 9).
- MCRs are among the most common strategies in DOS, as they yield high orders of structural diversity, making it possible to efficiently cover larger areas of unexplored chemical space.

Moreover, potent exploratory potentials of MCRs lead to the formation of unprecedented chemotypes¹⁸ (Figure 8).

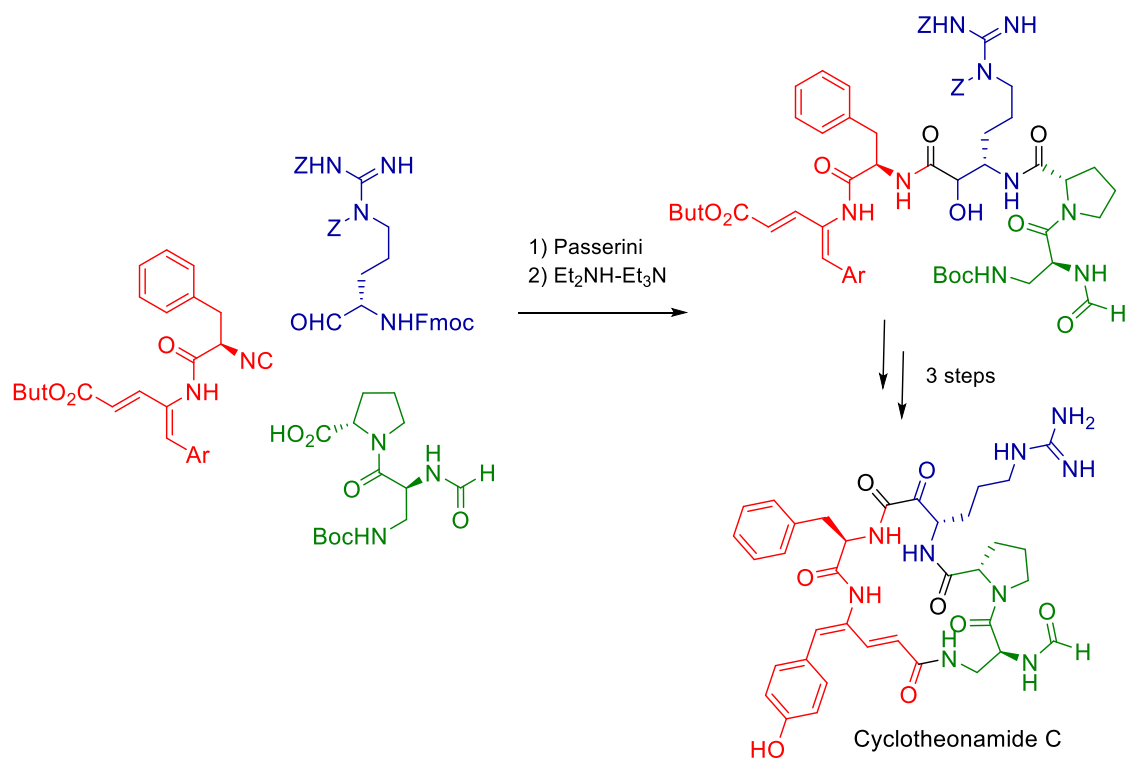


Figure 7. Applications of MCRs in TOS: Convergent synthesis of potent protease inhibitor cyclotheonamide C featuring 3CR Passerini by Aitken et al. (Ref 16)

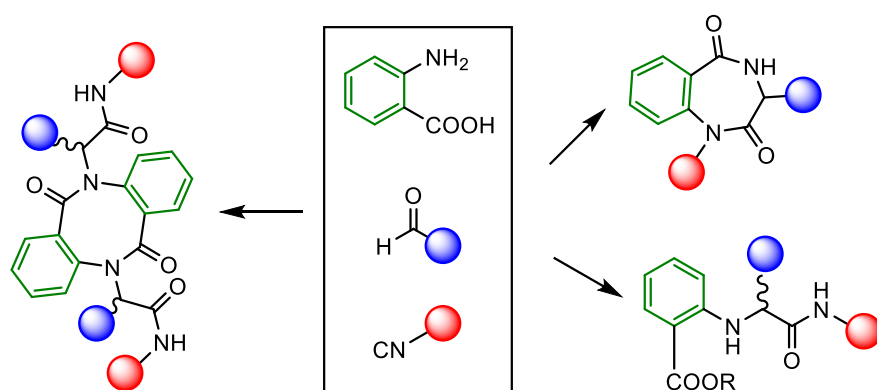


Figure 8. Application of MCRs in DOS: Structural diversity of an Ugi-Type MCR adducts.

Introduction and objectives

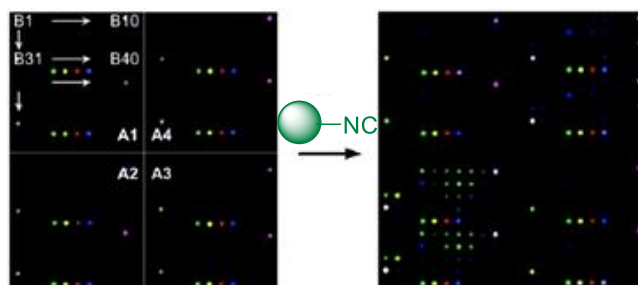
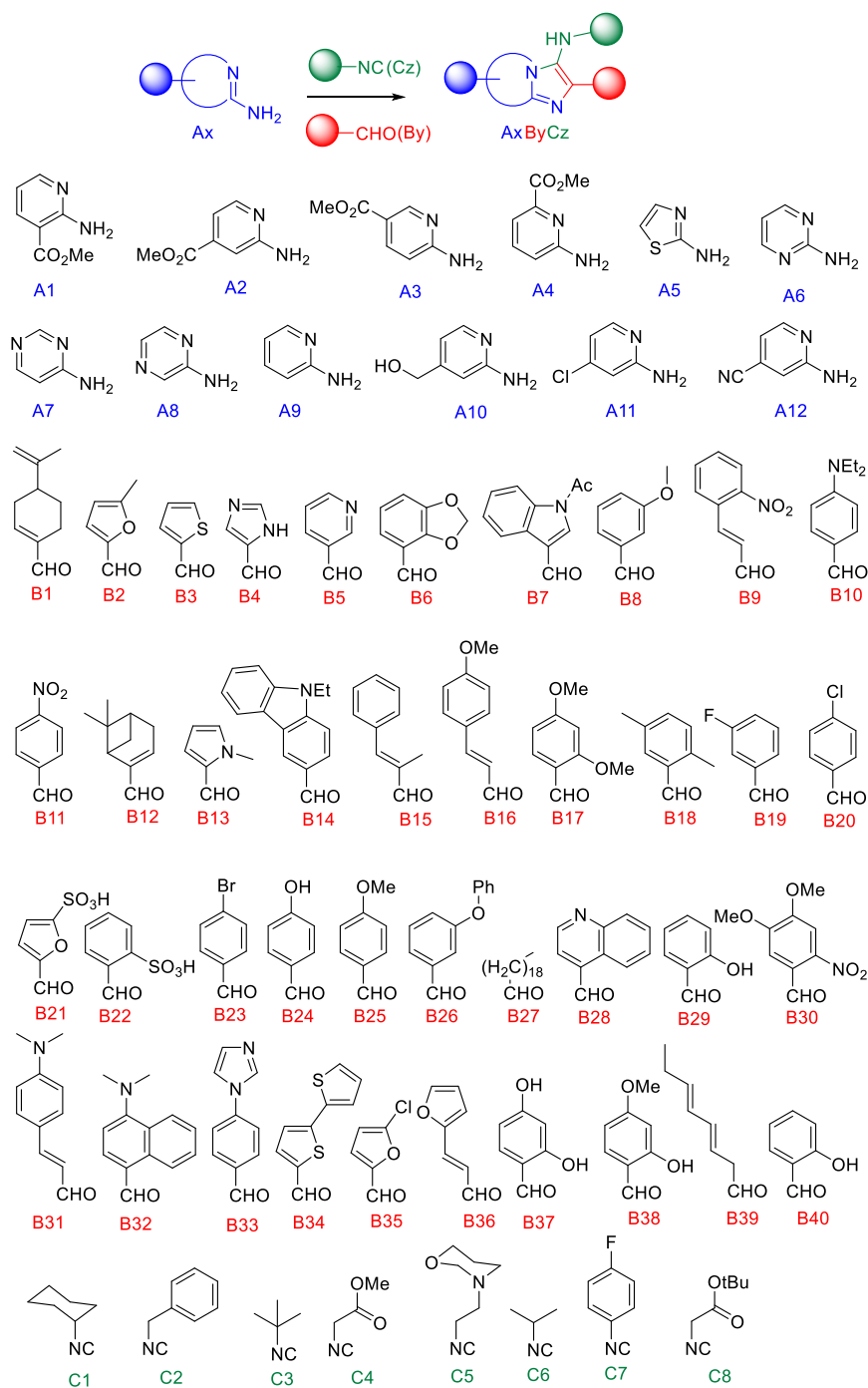


Figure 9. Application of MCRs in Combinatorial Chemistry: Combinatorial synthesis of a library of autofluorescing druglike molecules with an Ugi-type MCR. (Taken from Ref. 17)

The first Multicomponent reaction was reported by Strecker in 1850s. He initially obtained the amino acid alanine from the MCR of acetaldehyde, ammonia, and hydrogen cyanide followed by the acid-mediated hydrolysis of the α -aminonitrile intermediate (Figure 10).¹⁹

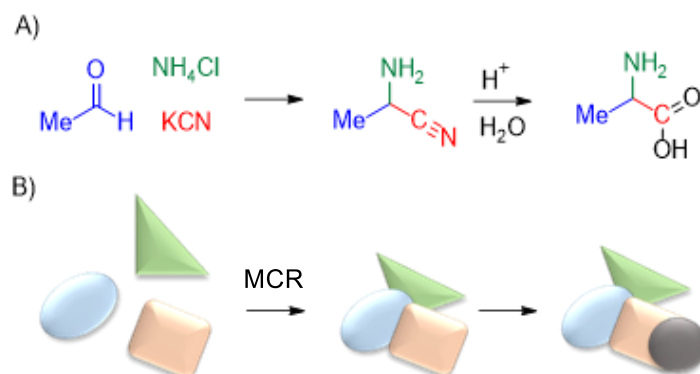


Figure 10. A) The Strecker MCR for the synthesis of aminoacids. B) Schematic representation of a typical Multicomponent Process

In the past 170 years, a growing number of new MCR processes are being reported. However, despite their incredible diversity in terms of building blocks, mechanisms and yielding scaffolds, they normally follow a general concept in design. In Figure 11 the core logic of most MCR processes has been illustrated, taking a 3-CR process involving A, B and C.²⁰ First, components A and B go through a usually reversible reaction to form the intermediate M. This primary reaction is normally favoured over undesired combinations. The reversibility factor is of critical importance as it dynamically controls the concentration of M, reducing the formation of undesired reactions. Intermediate M is consequently trapped and a sequence of irreversible transformations involving component C yields the final product.

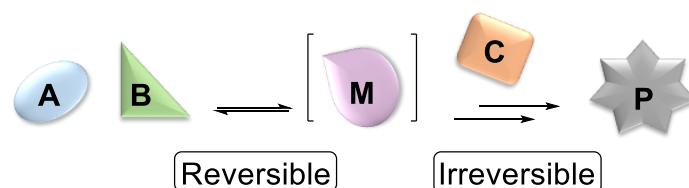


Figure 11. The general mechanistical route of an MCR: It consist of a primary reversible phase, followed by a set of irreversible transformations

A variety of reversible reactions have been exploited in MCR designs, imine formation being the most common of them. Ugi and Passerini MCRs, which are believed to be the most influential multicomponent transformations, feature carbonyls, imines or surrogates. Other common reactions include Knoevenagel reaction, Biginelli, metal-catalyzed-transformations, Dihydropyridine Hantzsch reactions, Povarov reaction, Michael-type condensations, etc. On the other hand, irreversible outputs

mainly feature electrophilic/nucleophilic additions, cyclization, aromatization, and rearrangements²¹ (Figure 12).

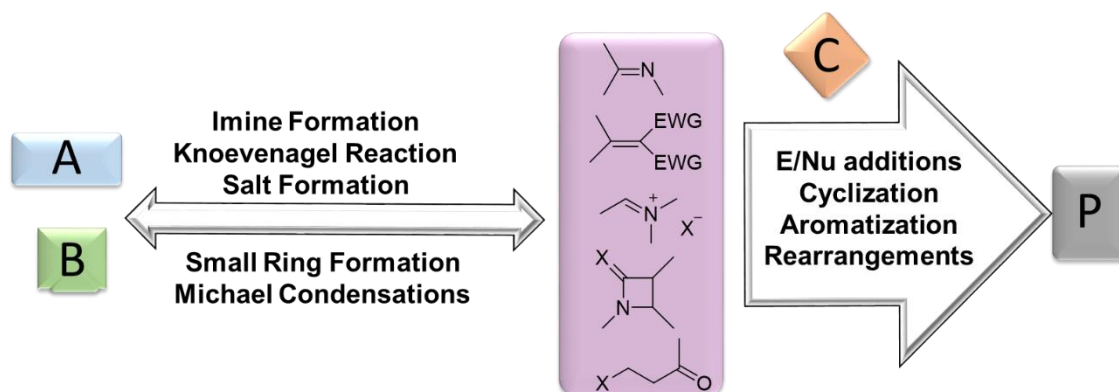


Figure 12. Some of the common reactions used in the design of MCRs

More complex versions of MCRs are achieved through combinations of different MCRs and/or classic reactions along with programmed elaboration of the irreversible transformations to achieve highly sophisticated structures (Figure 13).

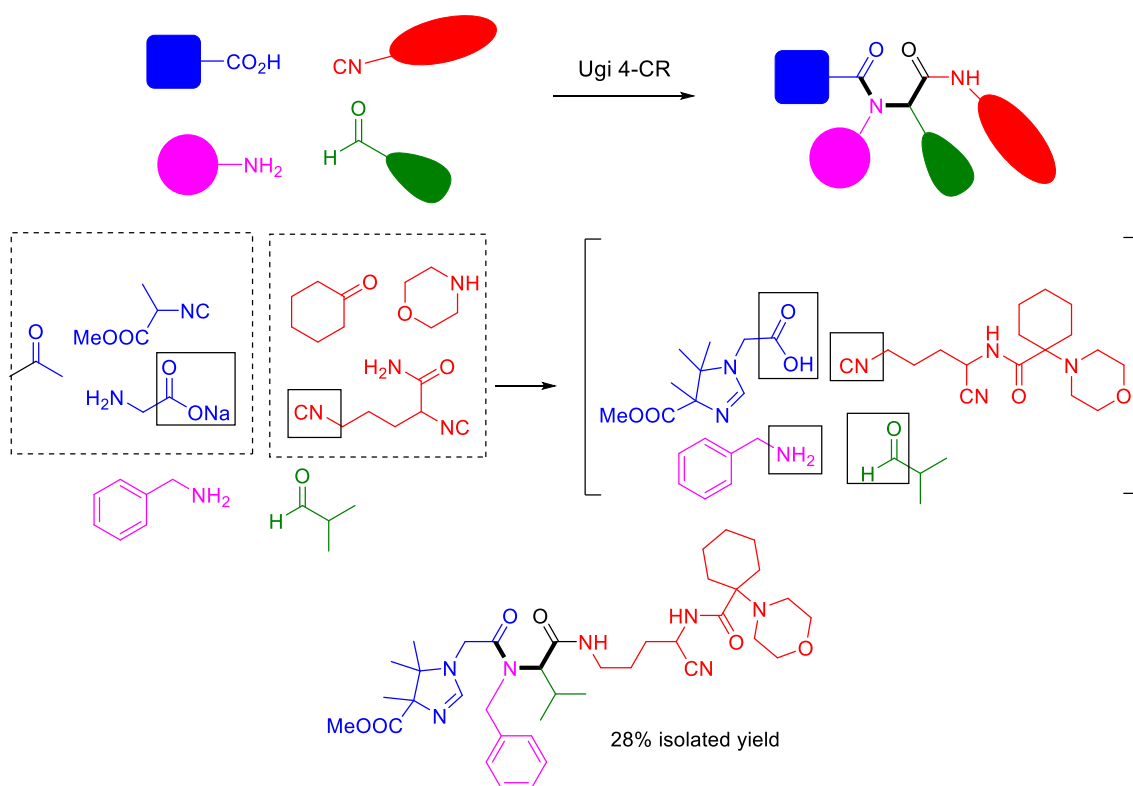


Figure 13. An eight-component reaction: the products of MCR1 and MCR2 serve as the new components of an Ugi-Type 4CR²²

Isocyanide-Based Multicomponent Reactions (IMCRs)

Isocyanides play a central role in a variety of multicomponent reactions. Their significant presence in MCR arises from their versatile reactivity pattern. Isocyanides can be described through two resonance forms (Figure 14A). Their specific electronic structure featuring an electron pair as well as a vacant orbital, enables them to react as nucleophiles and/or electrophiles. This property makes them a uniquely efficient component in MCRs. In an IMCR assembly, isocyanides are mainly exploited in the irreversible output, trapping the present intermediate M by Nucleophilic attacks and/or Electrophilic additions. Moreover, due to their bivalent (carbenic) nature, they facilitate cyclization strategies. This feature is widely exploited to assemble heterocyclic scaffolds (Figure 14B)²³.

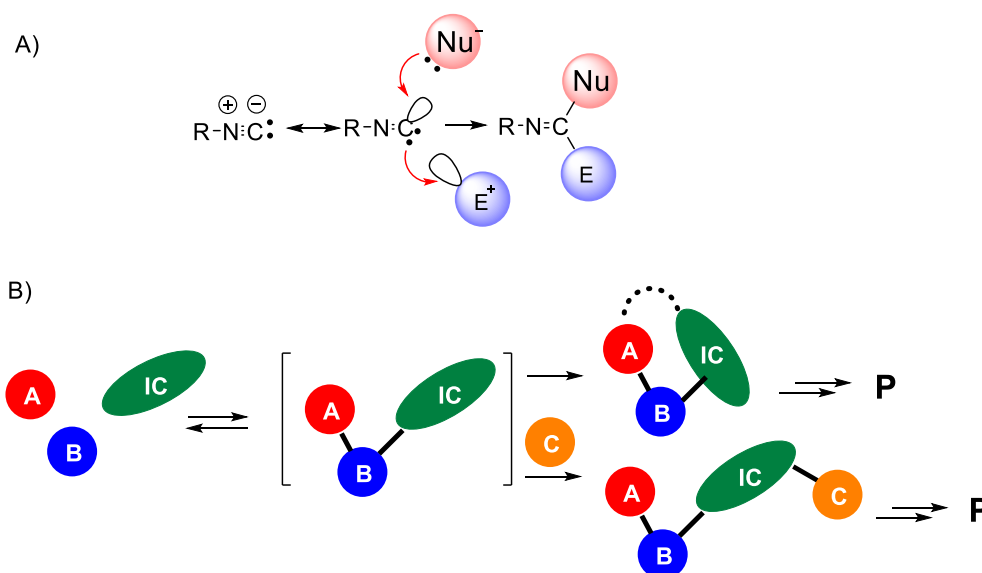


Figure 14. A) Chemical reactivity of isocyanides towards electrophiles and nucleophiles. B) Schematic representation of IMCRs.

Ugi IMCRs are one of the main highlights of multicomponent processes. The original Ugi Reaction is a 4-CR, which is itself an elaboration on the aforementioned Passerini 3-CR. In this reaction, an amine, an aldehyde or ketone, an isocyanide and a carboxylic acid are condensed in a polar media to yield an α -N-acylaminoamide. The reaction exploits a reversible imine formation step, followed by the nucleophilic attack of the isocyanide, subsequent trapping of the nitrilium ion by the nucleophilic carboxylate, where divalent carbon of the isocyanide becomes tetravalent. The formed intermediate undergoes the Mumm rearrangement to yield the thermodynamically stable final adduct (Figure 15)²⁴.

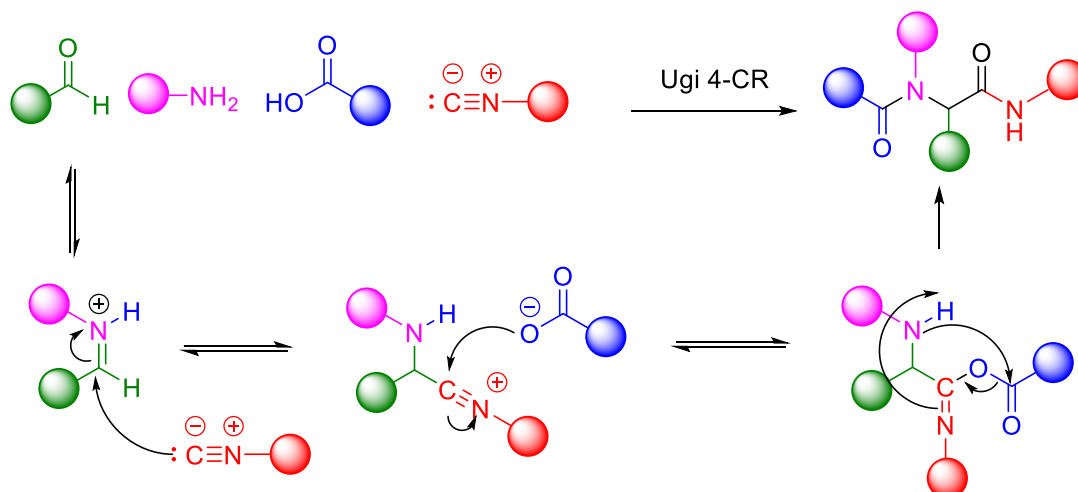


Figure 15. Plausible reaction mechanism of Ugi-4CR

Employing multiple diversity points of the Ugi adduct, a vast variety of secondary transformations have been incorporated, leading to further enrichment of the reaction output. For instance, cyclization strategies have been utilized to synthesize highly functionalized heterocyclic scaffolds. Ugi-4CR has been successfully paired with other MCRs to achieve union MCRs (Figure 17). Ugi-type reactions therefore have been widely exploited for the synthesis of natural products as well as screening libraries.²⁵

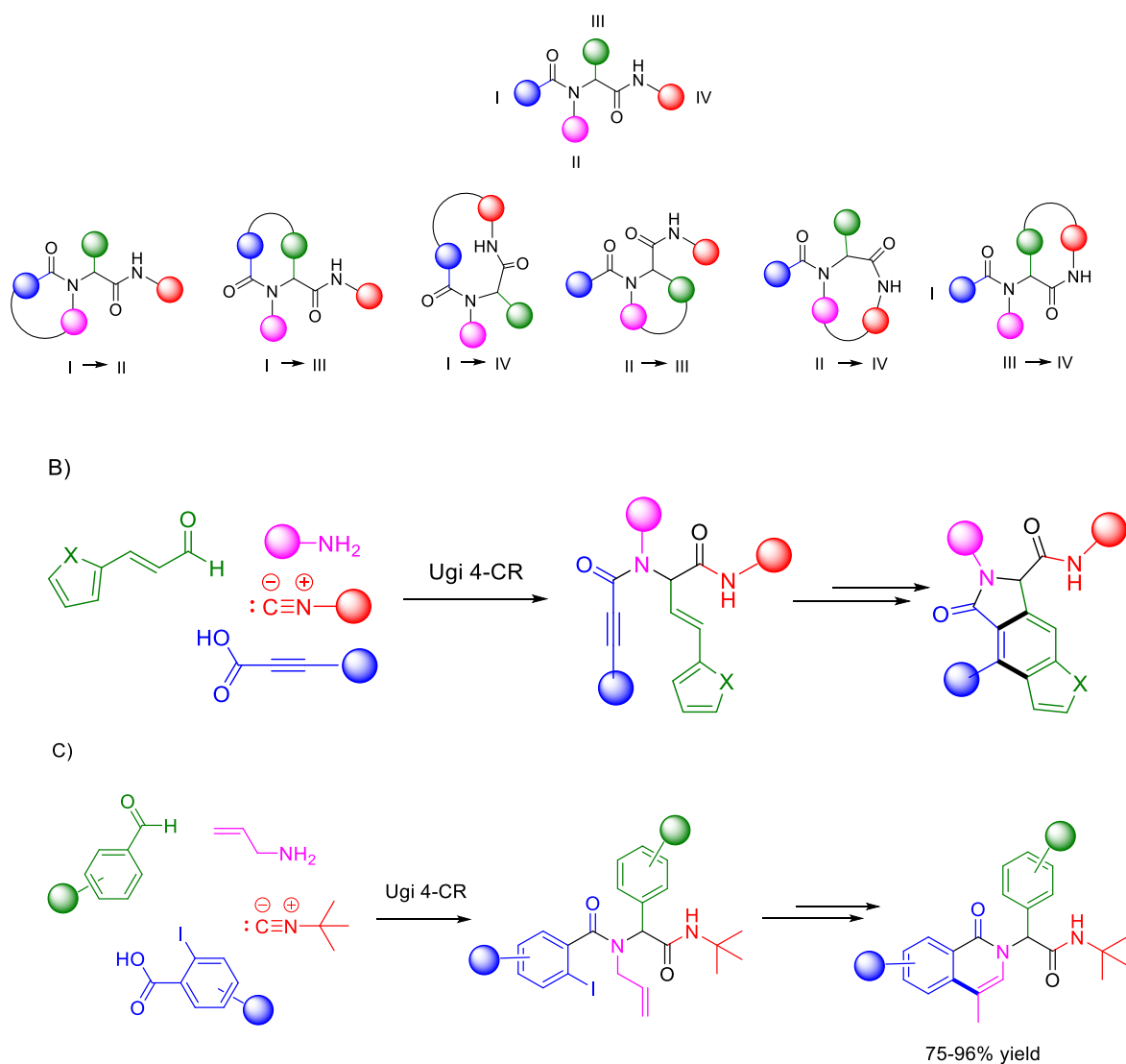


Figure 16. A) Possible heterocyclic Ugi-type scaffolds arising from cyclization strategies B) Modification of Ugi adduct via Diels Alder reaction²⁶. C) Modification of Ugi adduct via Heck coupling²⁷.

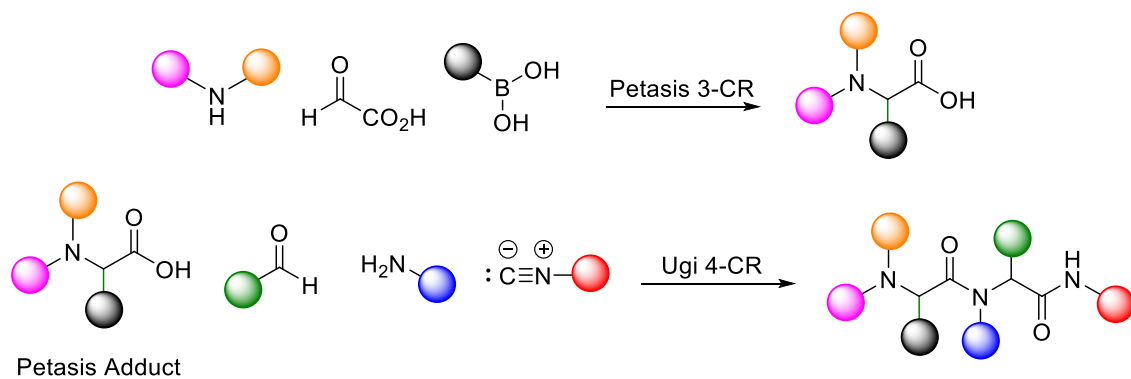


Figure 17. A) Tandem Petasis- Ugi MCRs to achieve formal 7-CR processes.

Isocyanide Insertion Reactions

Nucleophilicity and electrophilicity of isocyanides in IMCRs have been thoroughly studied in the recent years, giving rise to a large collection of MCRs yielding valued N-containing scaffold. However, reactivity of isocyanides is not restricted to E/N additions. Isocyanide insertion imidoylative reactions (also referred to as imidoylative reactions) are another useful, yet lesser studied aspect of Isocyanide chemistry. Research in the field can lead to a new class of IMCRs featuring isocyanide insertions.

Isocyanide insertions are normally promoted by either acid (Lewis or Brønsted) mediated processes or transition metal-catalyzed transformations (mainly Pd catalyzed insertions). They can take place on a variety of connectivities including C-Heteroatom, C-C, Heteroatom-H, or Heteroatom-Heteroatom bonds. The same structural diversity is observed in the resulting scaffolds, reinforcing the huge potential of isocyanide insertion in Organic synthesis (Figure 18).²⁸

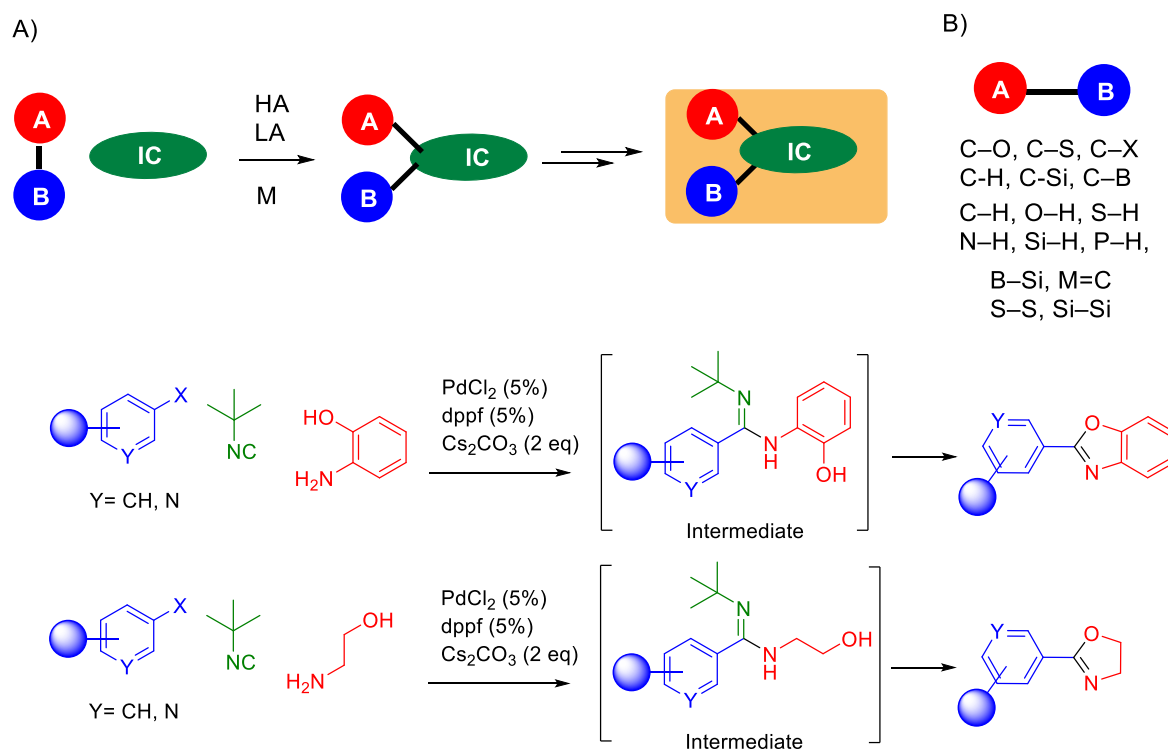


Figure 18. A) Schematic representation of Isocyanide Insertion (IC = isocyanide). B) Common bonds on which isocyanides are inserted. C) Utilizing Pd-catalyzed isocyanide insertion into C-X bonds in the multicomponent synthesis of oxazolines and benzoxazoles.²⁹

Synthesis and functionalization of Heterocycles Using MCRs

Having reviewed the main strategies for the design of MCRs, it is worth remembering that one of the main objectives of research for new/improved MCRs is to access functional compounds. Heterocycles are highly valued chemotypes in Organic Chemistry due to their various applications in industry, medicine, etc. In this way, synthesis of functional heterocycles is a popular trend in MCRs.³⁰ Heterocyclic moieties could be introduced into MCR adducts by exploiting Heterocyclic components and/or generating them in the MCR process itself or through post-MCR modifications. A combination of these strategies leads to facile synthesis of complex polyheterocyclic outputs (Figure 19).

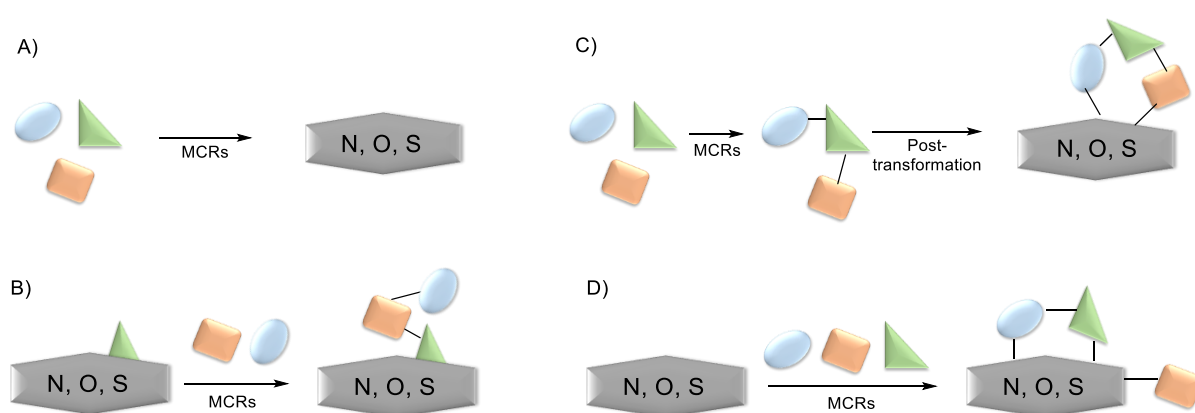


Figure 19. A) Formation of Heterocycles by MCRs, B Heterocycles as substituents in MCRs, C) Formation of Heterocycles by MCRs-Posttransformation, D) Functionalization of Heterocycles by MCRs.

In the context of the PhD thesis, we take a more detailed look at Reissert-type reactions and Groebke-Blackburn-Bienaymé MCRs. They are illustrative examples on the facile and versatile access to a diverse variety of functionalized azines using MCRs.

Groebke-Blackburn-Bienaymé MCR

Groebke-Blackburn-Bienaymé MCR (normally abbreviated as GBB) is an Ugi-type-3-CR and was discovered almost simultaneously by the three scientists.³¹ It assembles an aldehyde, an α -aminoazine and an isocyanide into aminoimidazoles, a highly valued drug-like core. GBB processes can deliver rapid diversification due to their MCR nature. Therefore, this MCR has been widely applied in modern medicinal chemistry³² (Figure 20).

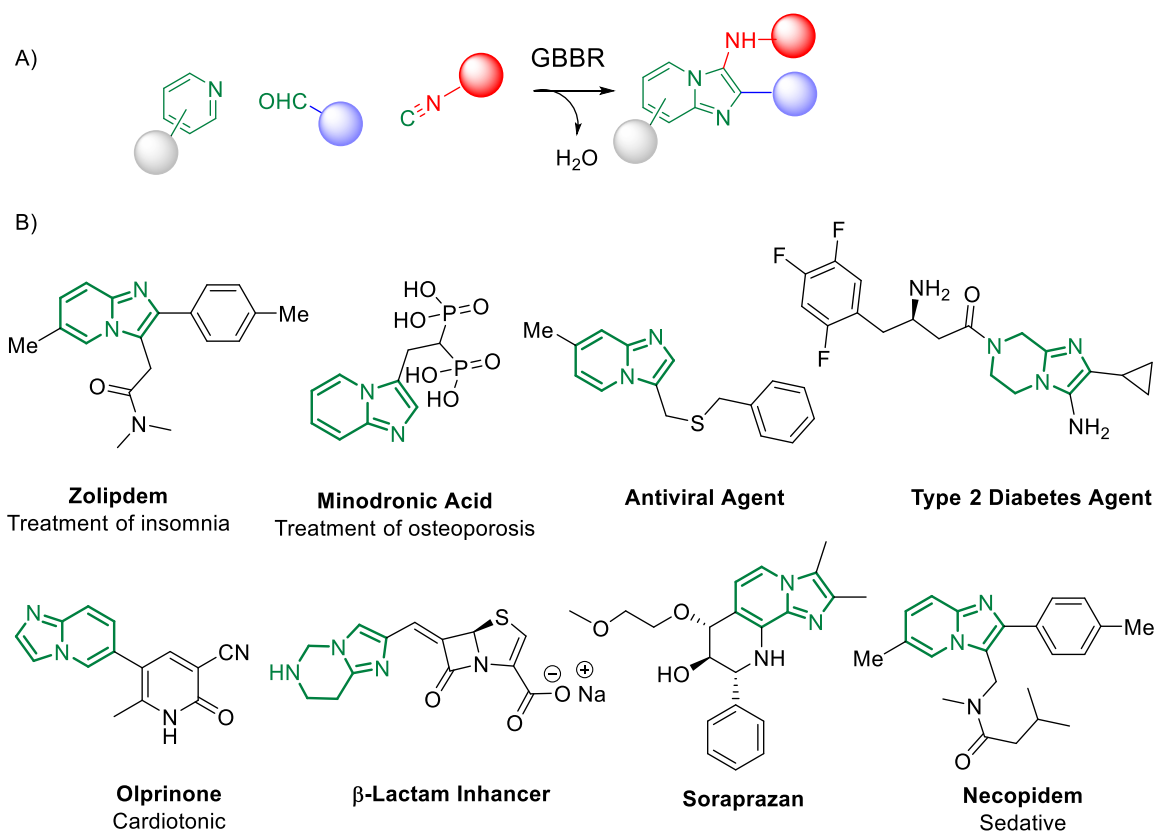


Figure 20. A) Schematic representation of a GBBR MCR. B) Examples of therapeutic agents containing the pyridoimidazole moiety.

The reaction mechanism involves the formation of iminoazine intermediate, which is attacked by the isocyanide component. The resulting iminium ion is then trapped by the azine nitrogen. Finally, the nitrilium intermediate is rearranged into the final structure through a 1,3-H shift. (Figure 21)

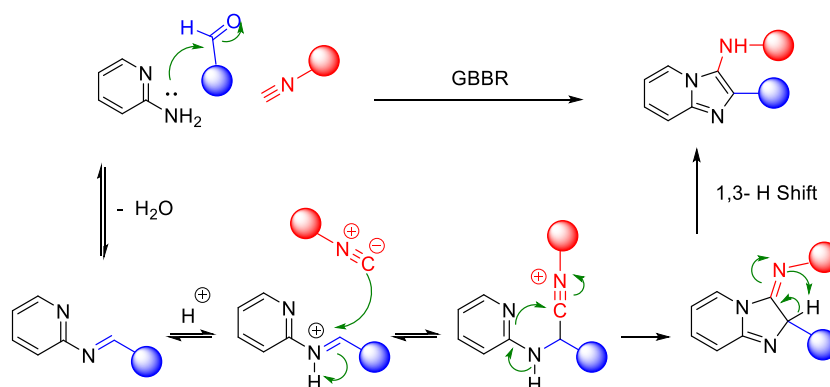


Figure 21. Proposed reaction mechanism for the classic GBBR.

Structural diversity in GBB adducts normally arise from the variations in the aminoazines (Figure 22), carbonyl surrogates and isocyanides as well as the ensuing post-modifications. As a rule of thumb, the vast majority of isocyanides and aldehydes yield useful GBB adducts, and many primary α -aminoazines or unsubstituted amidines react as well.³³ The post-transformations normally exploit the programmed (usually orthogonal) decoration of functional groups present on the starting components. Post-transformations normally feature cyclization, nucleophilic substitutions, coupling strategies and other tandem processes (Figure 23). The impressive diversity of GBB processes to yield a variety of heterocyclic scaffolds, has made them one of the most useful reactions for the synthesis of bioactive compounds, natural products, and combinatorial libraries in the context of medicinal chemistry projects. It must be added that functionalized reactants (for instance, aldehydes featuring carboxylic acid residues) can yield subsequent MCRs after a post-transformation involving a standard Ugi 4-CR, then leading to complex scaffolds with up to six diversity points (figure 24).

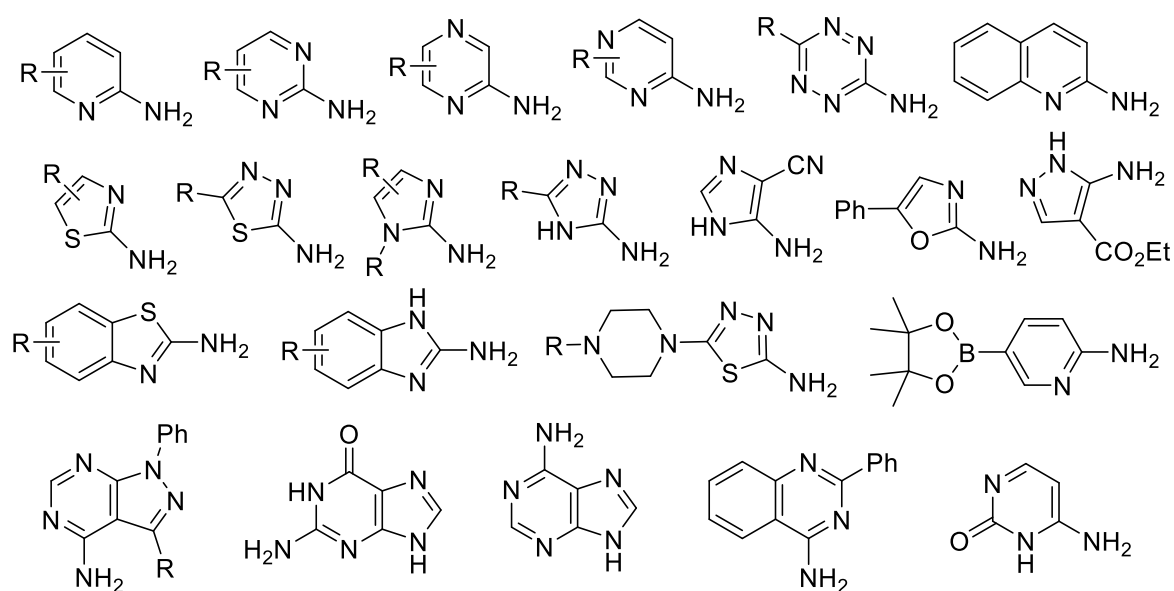


Figure 22. The scope of aminoazines in GBB processes.

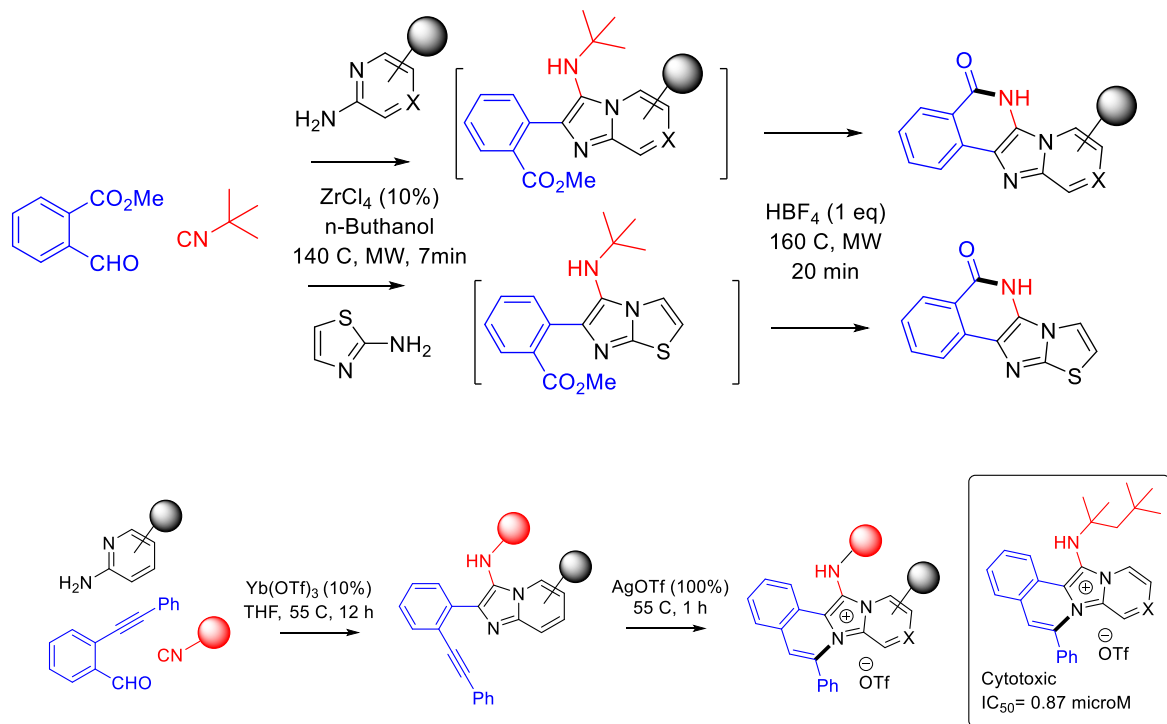


Figure 23. Examples of post transformations on GBB adducts arising from functionalized aminoazines.^{34 35}

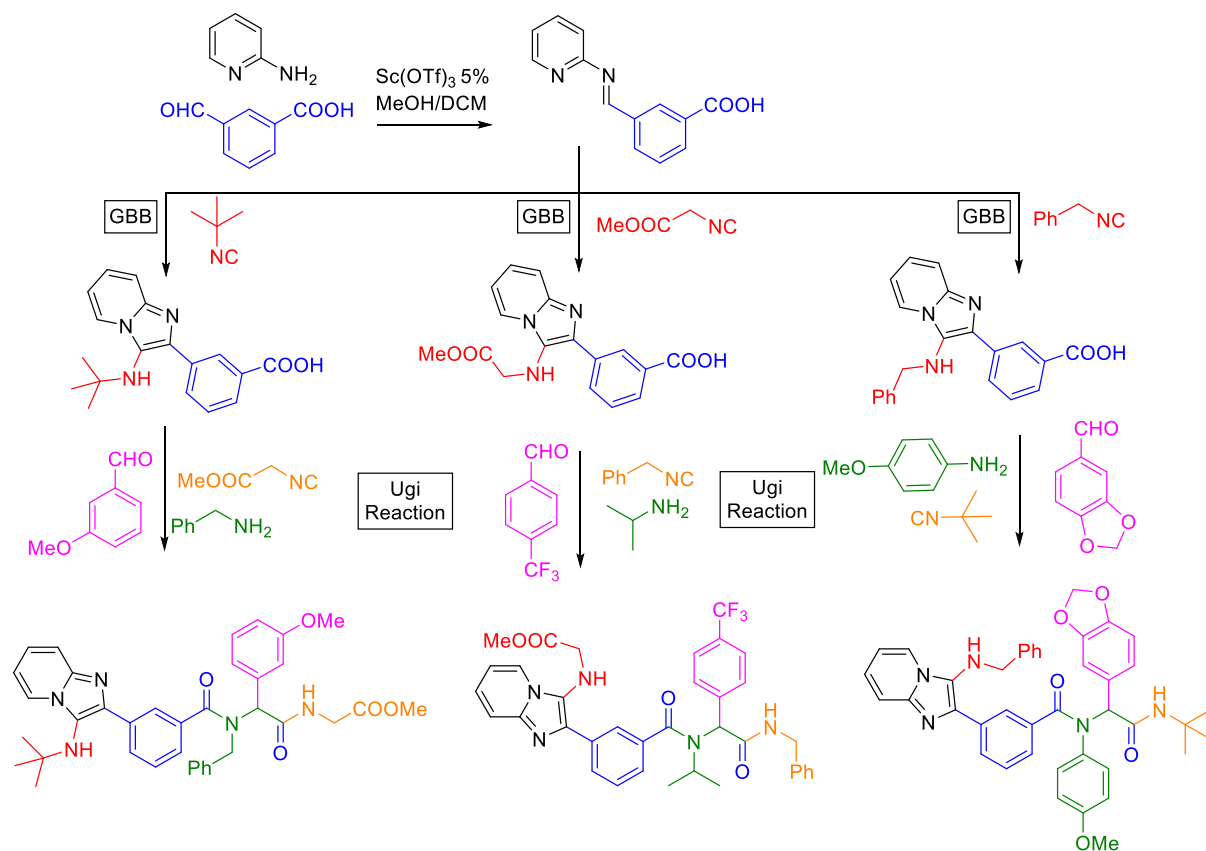


Figure 24. Orthogonal union of GBB and Ugi reactions for the synthesis of polyfunctionalized heterocycles with six diversity points (Ref 35).

Reissert-Type MCRs

Azines are useful components in MCRs as they have a rich reactivity suitable for producing complex heterocyclic scaffolds in simple protocols. This is of great importance in organic synthesis, as N-heterocycles are a frequently appearing moiety in natural products, drugs and bioactive compounds. In terms of reaction design, they are often regarded as imine surrogates. MCRs in which azines mimic imines, normally follow a general pattern (Figure 25): the first step which is the addition of electrophile, and this electrophilic activation of the heterocyclic N atom, is fast and reversible. Component E formally acts as an activating agent. The attack of nucleophile is considered slow and demanding, as the aromaticity is disturbed. Thus, the evolution of intermediate I to intermediate II is the rate determining step. The resulting intermediate II is very reactive and can easily evolve into the final product, usually recovering aromaticity in some cases.

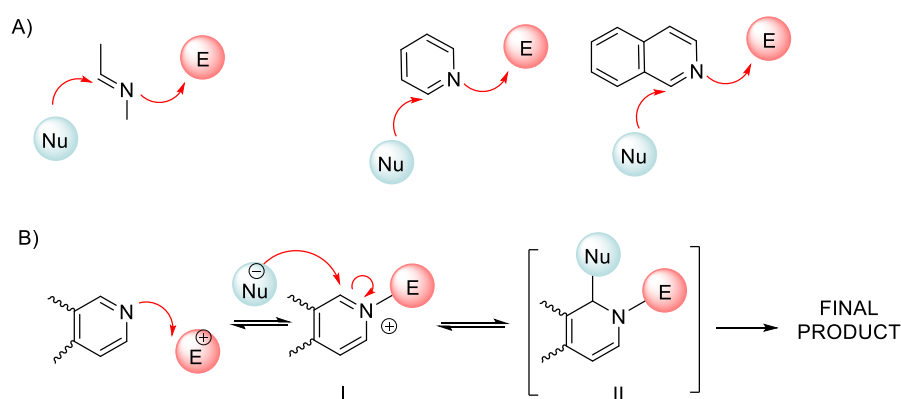


Figure 25. A) Imines and azines in Reissert-type MCR processes B) The general reaction route of MCRs involving azines as imine surrogates.

The earliest example of such reactions was reported by Reissert in 1900s³⁶. The original Reissert reaction involves the participation of isoquinoline, potassium cyanide and an acid chloride to yield the N-acylated α -cyano-(dihydro)azine. Over years, Reissert-type reactions have diversified in several directions, yielding a vast variety of heterocyclic chemotypes. However, they all share the general sequence of azine activation, nucleophilic addition and transformation into a stable adduct. Structural diversity in Reissert-type reactions arise from the variations in the components involved (azines, activating agents and nucleophiles) as well as from the transformations the Reissert adduct undergoes to evolve into the final products. (Figure 26)³⁷ For instance in Figure 27A, a four component Reissert process is illustrated, in which the nucleophile (dicarbonyl species) is formed *in situ* and a

complex polyheterocyclic adduct is obtained through an intramolecular cyclization of the initial zwitterionic intermediate.³⁸

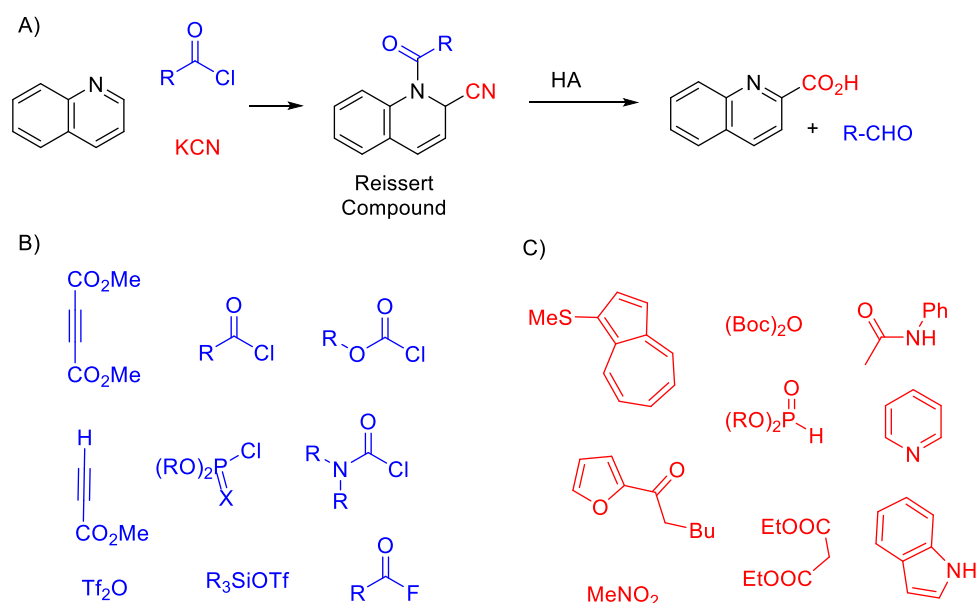


Figure 26. A) The original Reissert reaction. B) The scope of activating agents and C) The scope of nucleophiles in Reissert-type reactions.

It is worth mentioning that pyridines require more potent activation mode, due to the loss of aromaticity in the course of reaction. An illustrative example has been reported by Charette,³⁹ in which pyridines and lactams preform an ionic intermediate in the presence of triflic anhydride. Afterwards, a nucleophile (in this case a metal enolate) is added to the reaction mixture and a Reissert process, followed by an intramolecular cyclization, affords the tricyclic dihydropyridine adduct. The final product is an advanced intermediate in the total synthesis of the natural alkaloid tetraopenerine T4 (Figure 27B).

In this respect, it is relevant to note that isocyanides have been included in Reissert-type MCRs.⁴⁰ The first example was the carbamoylation of isoquinoline with isocyanides, upon activation with acid chlorides (figure 28A).⁴¹ This example follows almost the same mechanism as the original process with cyanide as nucleophile. On the other hand, the use of stronger electrophilic activating agents, such as fluorinated anhydrides (trifluoroacetic anhydride) leads to a drastic modification of the reaction mechanism, leading to a completely different connectivity: a dipolar heterocyclic acid fluoride (Figure 28B).⁴²

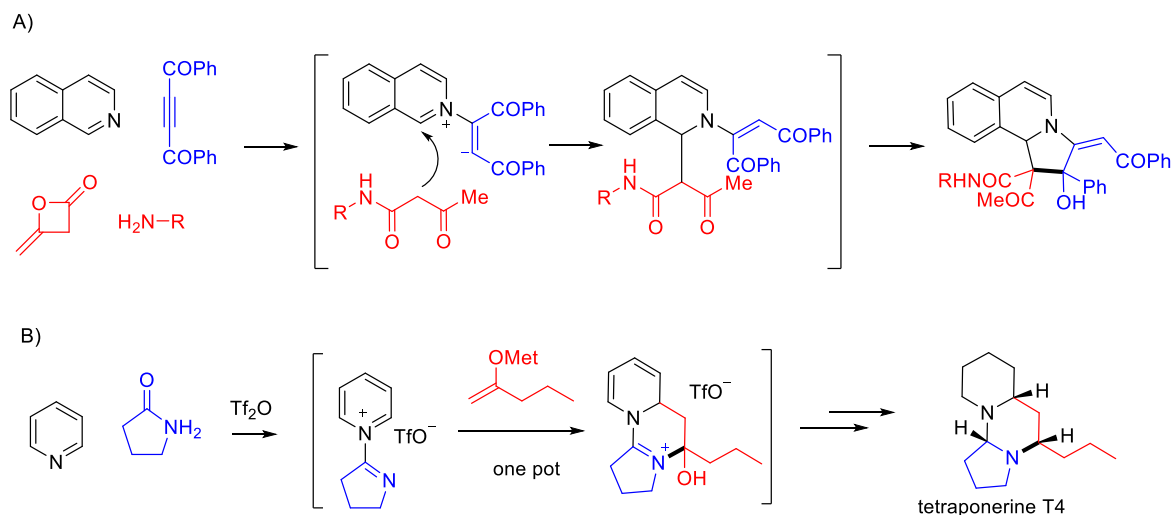


Figure 27. A) 4-CR Reissert reaction featuring the *in situ* formation of the carbonyl nucleophile and an intramolecular addition to form a tricyclic adduct. B) Application of Reissert reaction in the synthesis of the natural product tetraponerine T4.

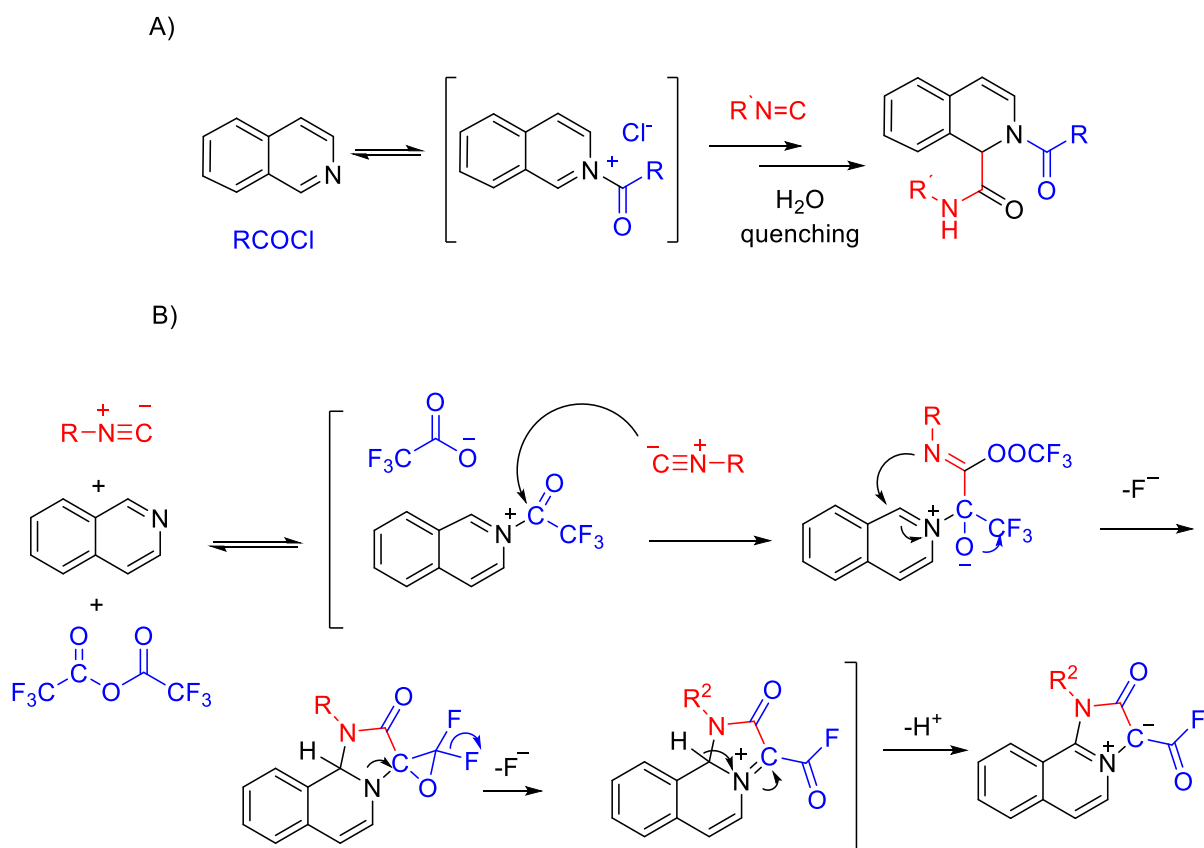


Figure 28. Isocyanide Reissert MCRs. A) Carbamoylation of Isoquinoline with isocyanides and acid chlorides. B) Inverted reaction with trifluoroacetic anhydride leading to a dipolar acid fluoride

Multiple Multicomponent Reactions:

In the quest for expanding the synthetic features of MCRs, it is relevant to note the fundamental improvements made in Multiple MultiComponent Reactions (MMCRs), which is the programmed use of divalent reactants in known processes, giving rise to the final adduct through a series sequential MCRs, taking place essentially in a one-pot manner (Figure 29).

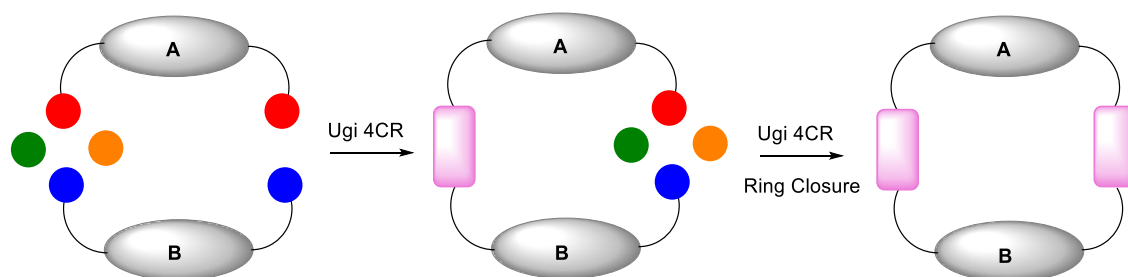


Figure 29. General approach for Multiple MCRs

Wessjohann has made fundamental contributions in this field, and has developed efficient approaches to the one-step preparation of highly functionalized complex compounds, often with very large dimension using this methodology.⁴³ Especially relevant are some examples of macrocyclic cages using multifunctional (bi/tri) components (Figure 30)⁴⁴. So far, the exploration of this approach is rather limited, and mainly standard substrates in Ugi 4-CRs have been significantly examined. Many other MCRs await for a similar development along these lines.

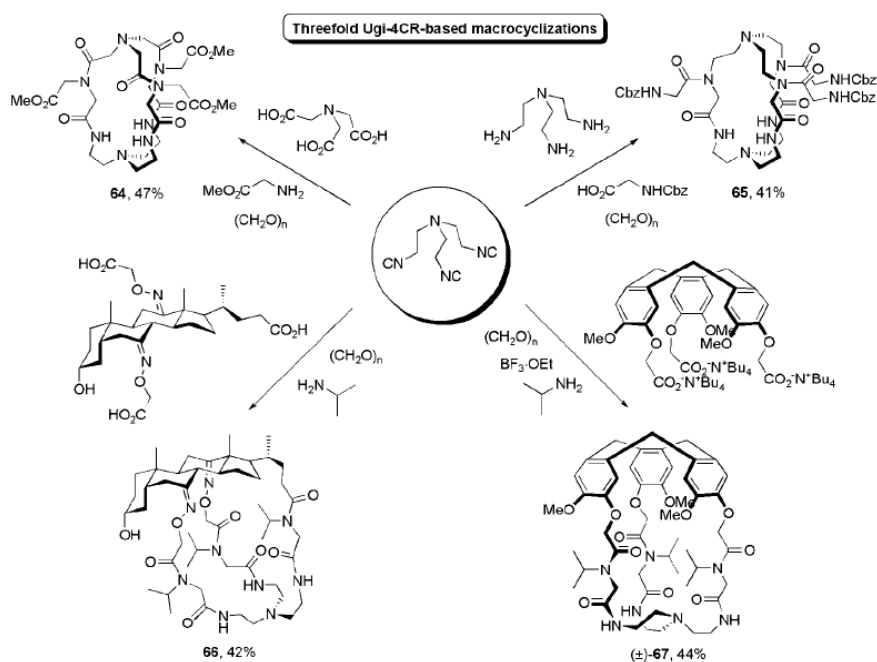


Figure 30. Preparation of macrocyclic cages through MMCRs. (taken from ref 44)

Objectives

In the present thesis, we focus on the development of new processes for the modular formation of novel and/or privileged heterocyclic scaffolds using isocyanide-based multicomponent reactions. We are particularly interested in processes that offer experimental facility and structural diversity, as well as functional final products. In this regard, lesser studied reactivity modes of isocyanides as key component in MCRs are explored. We study the interaction of isocyanides with imines, propargylamines and N-silylated species. We also investigate possible applications of the obtained adducts. In the final chapter, we study a multiple multicomponent process and explore the previously mentioned potentials of MCRs in a more elaborate manner. The detailed objectives of each chapter are as follows:

1) Studies on the interactions of Imines and Isocyanides

The main goal of this chapter was to study the interaction between the components of the Ugi reaction in the absence of the carboxylic acid component. Especially when replaced by a second equivalent of isocyanide. The study investigates the various mechanistical pathways of the process. We are particularly interested in the formation of diimioazetidines in an ABB-type process. The reaction conditions are to be optimized to yield the azetidine adduct as the main product. Also, the scope and the mechanistical interpretations are to be described.

2) Studies on the Interaction of Isocyanides and Propargylamines

The central idea of this chapter was to study the interaction of isocyanides and alkynes. The propargylamines were chosen as the substrate, as they could trap the expected intermediate of isocyanide addition to alkynes in an intramolecular manner. However, the preliminary experiments revealed that the reaction takes a different pathway, yielding substituted imidazoliums salts. Hence, we focus on the study of the new process investigating optimized reaction conditions, the scope and mechanistical considerations. We also use other alkynyl substrates to further study the possibility of isocyanide/triple-bond interaction. Furthermore, as imidazolium salts are considered a valued scaffold in several fields, we started the exploration of the potential applications for the obtained compounds.

3) Studies on the Interaction of Isocyanides and N-silylated species

Looking for the new reaction modes of isocyanides, we initially intended direct interaction of isocyanides and TMSCl. However, the first reactions led to a cocktail of unstable species we could not properly characterize. To have a more stabilized silylated moieties, we focused on to the interaction

of N-silylated azines and isocyanides. We realized that the interaction yields imidazolium salts in a Reissert type condensation. Hence, we aim to study the scope, regioselectivity pattern and the detailed mechanism of the process. Moreover, we intend to trap the silylated intermediate to using common electrophiles to define the role of silyl moiety in the process. Also, we try to define relevant functions for the obtained compounds, mainly in medicinal chemistry and catalysis.

4) Studies on Multiple Groebke-Blackburn-Bienaymé Multicomponent Reactions

In the last chapter, we study the behavior of a some polyaminoazines as substrates for multiple Groebke-Blackburn-Bienaymé MCR. We study the optimized conditions, the scope, post modifications as well as the reaction mechanism to explain the observed selectivity. We also try to design a regioselective methodology for non-symmetric substrates. Moreover, as the obtained adducts are N-fused polycyclic scaffolds, we expect to find relevant applications in medicinal and biological chemistry as well as bioimaging and material science.

References

- ¹ Editorial. (Chief Editor: Peter Kirkpatrick), *Nature Reviews Drug Discovery* 3, 375 (2004)
- ²Wender, P. A., & Miller, B. L. (2009). Synthesis at the molecular frontier. *Nature*, 460(7252), 197-201.
- ³ Schreiber, S. L. (2000). Target-oriented and diversity-oriented organic synthesis in drug discovery. *Science*, 287(5460), 1964-1969.
- ⁴ Cakmak, M., Mayer, P., & Trauner, D. (2011). An efficient synthesis of loline alkaloids. *Nature Chemistry*, 3(7), 543-545.
- ⁵ Bergbreiter, D. E., & Kobayashi, S. (2009). Introduction to facilitated synthesis. 257-258.
- ⁶ Wender, P. A., Verma, V. A., Paxton, T. J., & Pillow, T. H. (2007). Function-oriented synthesis, step economy, and drug design. *Accounts of chemical research*, 41(1), 40-49.
- ⁷ Shair, M. D., Yoon, T. Y., Mosny, K. K., Chou, T. C., & Danishefsky, S. J. (1996). The total synthesis of dynemicin A leading to development of a fully contained bioreductively activated enediyne prodrug. *Journal of the American Chemical Society*, 118(40), 9509-9525.
- ⁸ Wender, P. A., & Zercher, C. K. (1991). Studies on DNA-cleaving agents: synthesis of a functional dynemicin analogue. *Journal of the American Chemical Society*, 113(6), 2311-2313.
- ⁹ Feher, M., & Schmidt, J. M. (2003). Property distributions: differences between drugs, natural products, and molecules from combinatorial chemistry. *Journal of Chemical Information and Computer Sciences*, 43(1), 218-227.
- ¹⁰ Merrington, J., James, M., & Bradley, M. (2002). Supported diazonium salts—convenient reagents for the combinatorial synthesis of azo dye. *Chemical Communications*, (2), 140-141.

- ¹¹ Burke, M. D., & Schreiber, S. L. (2004). A planning strategy for diversity-oriented synthesis. *Angewandte Chemie International Edition*, 43(1), 46-58.
- ¹² Kwon, O., Park, S. B., & Schreiber, S. L. (2002). Skeletal diversity via a branched pathway: efficient synthesis of 29 400 discrete, polycyclic compounds and their arraying into stock solutions. *Journal of the American Chemical Society*, 124(45), 13402-13404.
- ¹³ Li, C. J., & Wei, C. (2002). Highly efficient Grignard-type imine additions via C-H activation in water and under solvent-free conditions. *Chemical Communications*, (3), 268-269.
- ¹⁴ Bariwal, J. B., Ermolat'ev, D. S., & Van der Eycken, E. V. (2010). Efficient Microwave-Assisted Synthesis of Secondary Alkylpropargylamines by Using A3-Coupling with Primary Aliphatic Amines. *Chemistry-a European Journal*, 16(11), 3281-3284.
- ¹⁵ Dömling, A., & Ugi, I. (2000). Multicomponent reactions with isocyanides. *Angewandte Chemie International Edition*, 39(18), 3168-3210.
- ¹⁶ Roche, S. P., Faure, S., & Aitken, D. J. (2008). Total Synthesis of Cyclotheonamide C using a Tandem Backbone-Extension-Coupling Methodology. *Angewandte Chemie International Edition*, 47(36), 6840-6842.
- ¹⁷ Burchak, O. N., Mughlerli, L., Ostuni, M., Lacapere, J. J., & Balakirev, M. Y. (2011). Combinatorial discovery of fluorescent pharmacophores by multicomponent reactions in droplet arrays. *Journal of the American Chemical Society*, 133(26), 10058-10061
- ¹⁸ Ugi, I. (2001). Recent progress in the chemistry of multicomponent reactions. *Pure and Applied Chemistry*, 73(1), 187-191.
- ¹⁹ Strecker, A. (1850). Ueber die künstliche Bildung der Milchsäure und einen neuen, dem Glycocoll homologen Körper. *European Journal of Organic Chemistry*, 75(1), 27-45.
- ²⁰ Domling, A., Wang, W., & Wang, K. (2012). Chemistry and biology of multicomponent reactions. *Chemical reviews*, 112(6), 3083-3135.
- ²¹ Mironov, M. A. (2006). Design of Multi-Component Reactions: From Libraries of Compounds to Libraries of Reactions. *Molecular Informatics*, 25(5-6), 423-431.
- ²² Elders, Niels, et al. "The Efficient One-Pot Reaction of up to Eight Components by the Union of Multicomponent Reactions." *Angewandte Chemie International Edition* 48.32 (2009): 5856-5859.
- ²³ Sung, K., & Chen, C. C. (2001). Kinetics and mechanism of acid-catalyzed hydrolysis of cyclohexyl isocyanide and pK_a determination of N-cyclohexylnitrilium ion. *Tetrahedron Letters*, 42(29), 4845-4848.
- ²⁴ Marcaccini, S., & Torroba, T. (2007). The use of the Ugi four-component condensation. *Nature Protocols*, 2(3), 632-639.
- ²⁵ Bonnaterre, F., Bois-Choussy, M., & Zhu, J. (2006). Rapid access to oxindoles by the combined use of an Ugi four-component reaction and a microwave-assisted intramolecular buchwald-hartwig amidation reaction. *Organic letters*, 8(19), 4351-4354.
- ²⁶ Ugi, I. (1982). From isocyanides via four-component condensations to antibiotic syntheses. *Angewandte Chemie International Edition in English*, 21(11), 810-819.
- ²⁷ Endo, A., Yanagisawa, A., Abe, M., Tohma, S., Kan, T., & Fukuyama, T. (2002). Total synthesis of ecteinascidin 743. *Journal of the American Chemical Society*, 124(23), 6552-6554.

- ²⁸ Qiu, G., Ding, Q., & Wu, J. (2013). Recent advances in isocyanide insertion chemistry. *Chemical Society Reviews*, 42(12), 5257-5269.
- ²⁹ Boissarie, P. J., Hamilton, Z. E., Lang, S., Murphy, J. A., & Suckling, C. J. (2011). A powerful palladium-catalyzed multicomponent process for the preparation of oxazolines and benzoxazoles. *Organic letters*, 13(23), 6256-6259.
- ³⁰ Vicente-García, E., Kielland, N., & Lavilla, R. (2014). Functionalization of Heterocycles by MCRs. In *Multicomponent Reactions in Organic Synthesis* (pp. 159-182). Wiley-VCH Verlag GmbH & Co. KGaA.
- ³¹ Bienayme, H., & Bouzid, K. (1998). A new heterocyclic multicomponent reaction for the combinatorial synthesis of fused 3-aminoimidazoles. *Angewandte Chemie International Edition*, 37(16), 2234-2237.
- ³² De Coen, L. M., Heugebaert, T. S., García, D., & Stevens, C. V. (2015). Synthetic entries to and biological activity of pyrrolopyrimidines. *Chemical reviews*, 116(1), 80-139.
- ³³ Devi, N., Rawal, R. K., & Singh, V. (2015). Diversity-oriented synthesis of fused-imidazole derivatives via Groebke–Blackburn–Bienayme reaction: a review. *Tetrahedron*, 71(2), 183-232.
- ³⁴ Guchhait, S. K., & Madaan, C. (2010). Towards molecular diversity: dealkylation of tert-butyl amine in Ugi-type multicomponent reaction product establishes tert-butyl isocyanide as a useful convertible isonitrile. *Organic & biomolecular chemistry*, 8(16), 3631-3634.
- ³⁵ Zhou, H., Wang, W., Khorev, O., Zhang, Y., Miao, Z., Meng, T., & Shen, J. (2012). Three-Component, One-Pot Sequential Synthesis of Tetracyclic Pyrido [2', 1': 2, 3] imidazo [5, 1-a] isoquinolinium Compounds as Potent Anticancer Agents. *European Journal of Organic Chemistry*, 2012(28), 5585-5594.
- ³⁶ Reissert, A. (1905). Ueber die Einführung der Benzoyl-gruppe in tertiäre cyclische Basen. *Berichte der deutschen chemischen Gesellschaft*, 38(3), 3415-3435.
- ³⁷ Blaskó, Gábor, Péter Kerekes, and Sándor Makleit. "Reissert Synthesis of Isoquinoline and Indole Alkaloids." *The Alkaloids: Chemistry and Pharmacology* 31 (1987): 1-28.
- ³⁸ Alizadeh, A., & Zohreh, N. (2008). A One-Pot Synthesis of 1, 2-Dihydroisoquinoline Derivatives from Isoquinoline via a Four-Component Reaction. *Helvetica Chimica Acta*, 91(5), 844-849.
- ³⁹ Charette, A. B., Mathieu, S., & Martel, J. (2005). Electrophilic Activation of Lactams with Tf₂O and Pyridine: Expedient Synthesis of (±)-Tetraoponerine T4. *Organic letters*, 7(24), 5401-5404.
- ⁴⁰ Kielland, N., & Lavilla, R. (2010). Recent developments in Reissert-type multicomponent reactions. In *Synthesis of Heterocycles via Multicomponent Reactions II* (pp. 127-168). Springer Berlin Heidelberg.
- ⁴¹ Díaz, J. L., Miguel, M., & Lavilla, R. (2004). N-Acylazinium salts: A new source of iminium ions for Ugi-type processes. *The Journal of organic chemistry*, 69(10), 3550-3553.
- ⁴² Arévalo, M. J., Kielland, N., Masdeu, C., Miguel, M., Isambert, N., & Lavilla, R. (2009). Multicomponent access to functionalized mesoionic structures based on TFAA activation of isocyanides: Novel domino reactions. *European Journal of Organic Chemistry*, 2009(5), 617-625.
- ⁴³ Wessjohann, Ludger A., Ricardo AW Neves Filho, and Daniel G. Rivera. "Multiple multicomponent reactions with isocyanides." *Isocyanide Chemistry: Applications in Synthesis and Material Science* (2012): 233-262.
- ⁴⁴ Wessjohann, L. A., Rivera, D. G., & Vercillo, O. E. (2009). Multiple multicomponent macrocyclizations (MiBs): a strategic development toward macrocycle diversity. *Chemical reviews*, 109(2), 796-814.

Chapter I

Publication I: Studies on the interaction of isocyanides with imines: Reaction scope and mechanistic variations

Studies on the interaction of isocyanides with imines: reaction scope and mechanistic variations

Ouldouz Ghashghaei¹, Consiglia Annamaria Manna¹,
Esther Vicente-García¹, Marc Revés¹ and Rodolfo Lavilla^{*1,2}

Letter

Open Access

Address:

¹Barcelona Science Park, University of Barcelona, Baldiri Reixac 10–12, 08028 Barcelona, Spain and ²Laboratory of Organic Chemistry, Faculty of Pharmacy, University of Barcelona, Av. Joan XXIII sn, 08028 Barcelona, Spain

Email:

Rodolfo Lavilla* - rlavilla@pcb.ub.es

* Corresponding author

Keywords:

azetidines; heterocycles; imines; isocyanides; multicomponent reactions

Beilstein J. Org. Chem. **2014**, *10*, 12–17.

doi:10.3762/bjoc.10.3

Received: 30 September 2013

Accepted: 29 November 2013

Published: 06 January 2014

This article is part of the Thematic Series "Multicomponent reactions II".

Guest Editor: T. J. J. Müller

© 2014 Ghashghaei et al; licensee Beilstein-Institut.

License and terms: see end of document.

Abstract

The interaction of imines with isocyanides has been studied. The main product results from a sequential process involving the attack of two units of isocyanide, under Lewis acid catalysis, upon the carbon–nitrogen double bond of the imine to form the 4-membered ring system. The scope of the reaction regarding the imine and isocyanide ranges has been determined, and also some mechanistic variations and structural features have been described.

Introduction

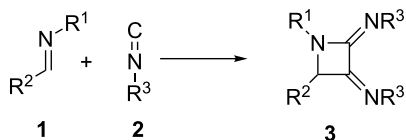
The interaction of imines with isocyanides is mainly focused on to the well-known Ugi multicomponent reaction (MCR) [1]. This fundamental process features the participation of a carboxylic acid group which attacks the intermediate nitrilium ion thus leading, after the Mumm rearrangement, to α -amidoamides. However, the direct reaction of imines and isocyanides has been considerably less studied and, in the absence of a carboxylate, the mechanistic outcome is considerably modified [2]. A relevant precedent was described by Deyrup in the late sixties, demonstrating the double incorporation of an isocyanide moiety to an imine [3,4]. Interestingly, the 3CR between a carbonyl, an amine and an isocyanide, taking place through the intermediacy of the in situ generated

imine, leads to α -aminoamidines, resulting from the trapping of the nitrilium cation by the remaining amine [5–8]. Taking into account the intrinsic interest in the azetidine scaffold in medicinal chemistry [9], we decided to study in detail the formation of bis(imino)azetidines **3** from the interaction of imines **1** and isocyanides **2** (Scheme 1), including the scope of the reaction and mechanistic features of this interesting ABB' process [10].

Results and Discussion

Reaction scope

In this section we analyze the reaction conditions, the structural features of the products and the scope of the reactants.



Scheme 1: Azetidine formation from the interaction of imines with isocyanides.

Reaction conditions

We began our studies with the experimental screening of the solvents, catalysts and temperatures suitable for this transformation. In this respect, taking imine **1a** ($R^1 = p\text{-MeOC}_6\text{H}_4$; $R^2 = p\text{-ClC}_6\text{H}_4$) and isocyanide **2a** ($R^3 = t\text{-Bu}$), we tested the standard reaction in THF, MeCN, and CH_2Cl_2 as solvents using a variety of Lewis and Brønsted acid activating agents (20–100 mol %) including: InCl_3 , $\text{Sc}(\text{OTf})_3$, AuCl_3 , AgOTf , GaCl_3 , NbCl_5 , camphorsulfonic acid, I_2 , $\text{Br}_2\cdot\text{SMe}_2$ and $\text{BF}_3\cdot\text{OEt}_2$, at temperatures ranging from rt to 80°C . The transformations were tested under standard heating or microwave irradiation, with reaction times lasting from 30 min to 48 h. The imine **1a** was generated in situ, using MS 4 Å, or previously prepared by condensation of the corresponding aldehyde and aniline. It was found that the best conditions were obtained using $\text{BF}_3\cdot\text{Et}_2\text{O}$ as the activating agent in stoichiometric amounts in THF, at rt for 24 hours or under MW irradiation for 30 min at 65°C , allowing the formation of the expected azetidine **3a** in 43% and 48%, respectively. Compounds **4** and **5** could not be detected (Scheme 2). When the process was run as a true MCR (mixing the amine, the aldehyde and two equivalents of isocyanide **2a**), the adduct **3a** was produced in trace amounts and the main product was the α -amino-amidine **4**, in good agreement with previous reports [5–8]. In a different experiment, the addition of a 9-fold excess of isocyanide **2a** to the imine **1a** under the usual conditions led to detection of tris(imino)pyrrolidine **5** (9%) as the minor product, and azetidine **3a** as the major component (24%, Scheme 2).

Structural elucidation

Although we could confirm the constitution of the azetidine **3a** by spectroscopic methods (NMR, MS), the stereochemistry of the $\text{C}=\text{N}$ bonds present in the structure remained unsolved. Furthermore, no conclusive nOe's were observed to assign these stereogenic centers, and there were no reports in the literature regarding this point. A monocrystal of the bis(imino)azetidine **3a** was subjected to X-ray diffraction analysis and the solid state structure is depicted in Figure 1 [11].

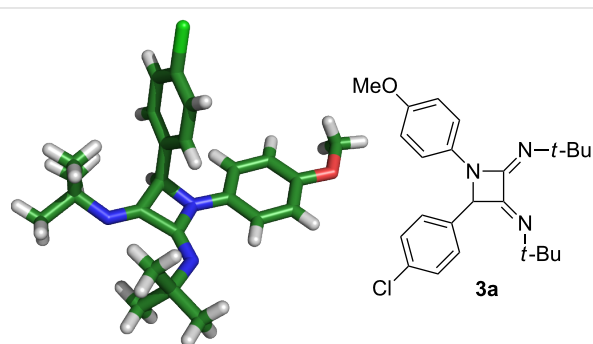
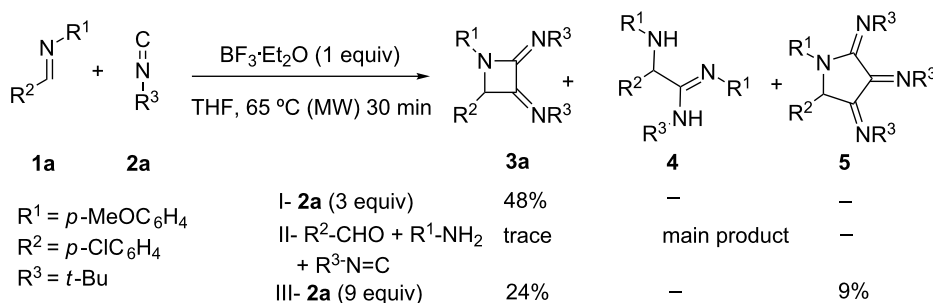
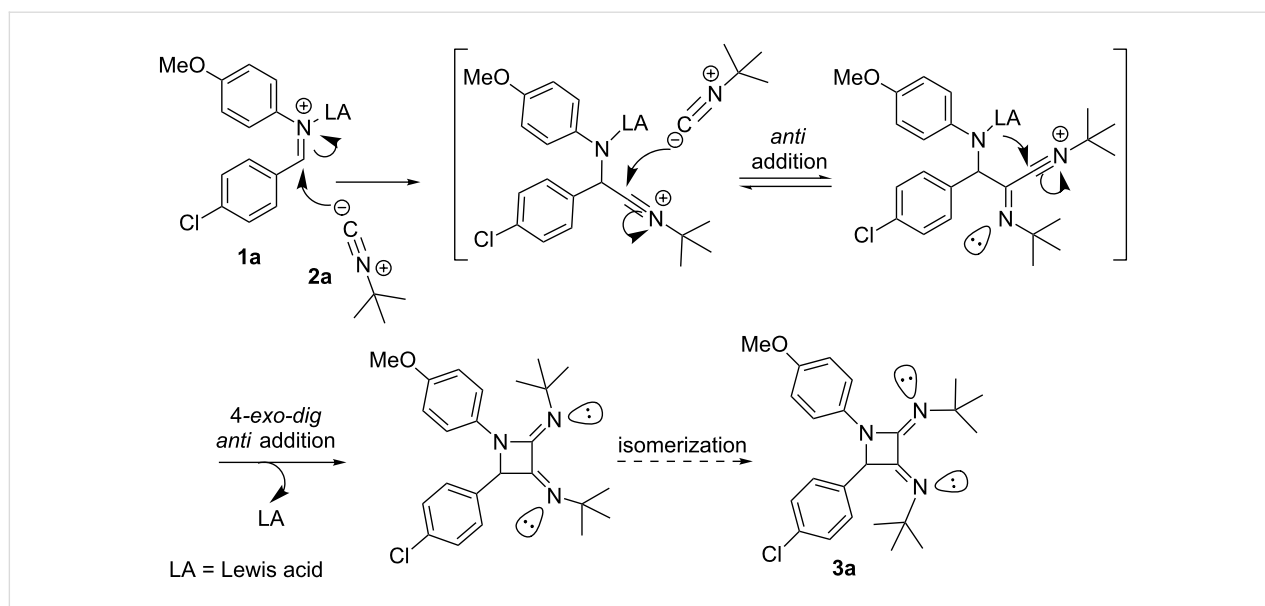


Figure 1: X-ray diffraction analysis of azetidine **3a**.

This result confirms the structural features associated to this scaffold, and also raises some questions on the origin of the stereochemistry associated to the $\text{C}=\text{N}$ moieties. First of all, the process can be explained by an attack of one isocyanide equivalent to the Lewis acid (LA)-activated imine, leading to a first nitrilium intermediate (Scheme 3), then a subsequent attack would give rise to a second nitrilium ion [12–15], which is trapped by the nucleophilic nitrogen of the imine. This last step is formally a disfavoured nucleophilic 4-*exo-dig* process [16], although recent results and calculations show that it should be feasible and some examples have been disclosed [17]. Interestingly, the expected *anti*-addition mode towards the carbon–nitrogen triple bonds should generate *Z* configurations [18,19], which are not observed in the solid-state, thus suggesting isomerization processes affecting the $\text{C}=\text{N}$ moieties,



Scheme 2: Reaction conditions.



Scheme 3: Stepwise mechanism for the formation of azetidine **3a**.

likely mediated by acid-catalyzed prototropy or other tautomerization steps. Computational calculations (MMFF, AM1 and BL3YP/6-31G* performed in a Spartan suite) suggest that the differences in the heat of formation among some geometrical isomers are small. Furthermore, NMR spectra nearly always display a single set of signals, thus discarding further isomerization events once the compounds are detected or isolated.

Reactant scope

Next, the scope of the reaction was investigated, and a variety of imines was subjected to the interaction with a range of isocyanides under the optimized conditions to determine the generality of the process and to detect possible restrictions. Results are depicted in Table 1.

The scan of isocyanides shows that their nucleophilicity plays a determining role in the reactivity, since *tert*-butyl, cyclohexyl and benzyl isocyanides (Table 1, entries 1–3, 5–12) show a relatively high conversion, whereas the aromatic isocyanide was less reactive (entry 4) and the weaker nucleophiles TOSMIC and methyl isocyanoacetate were not productive (Table 1, entries 13 and 14) [20]. Additionally, with respect to imines, the reaction works well for substrates generated from aromatic aldehydes and anilines displaying *o*-, *m*- and *p*-substituents (Table 1, entries 1–7). Moreover, in one case the 3-aminoindole **6** was detected (27%), in agreement with a recent report (Table 1, entry 5) [21].

N-Alkylimines seem to react appropriately (Table 1, entry 8). Furthermore, we have observed some *tert*-butyl eliminations, probably due to competing reactions under the acidic condi-

tions (Table 1, entries 5, 6 and 8). In general, imines containing electron-rich *N*-aryl moieties showed higher reactivities, and we were not able to isolate azetidine adducts **3** from the reaction of arylimines containing strong electron-withdrawing groups at the aniline moiety (*p*-CF₃, *p*-F and *p*-COOEt), likely because of their low conversions. However, the presence of such groups linked to the carbon of the imine did not seem to disturb their reactivity (Table 1, entries 1–8). Interestingly, the reaction of glyoxylate imine (Table 1, entry 9) with *tert*-butyl isocyanide led to the formation of minor amounts of the azetidine adduct **3i** (9%) whereas the α -aminoamide **7** (34%) was the major component. The formation of amidoamides has been reported in the *p*-toluenesulfonic acid-catalyzed interaction of anilines, amines and isocyanides [8]. On the other hand, the reaction of the same imine with cyclohexyl isocyanide gave azetidine **3j** (34%) in a selective manner (Table 1, entry 10), without traces of the corresponding α -aminoamide. Different types of activated substrates displaying C=N bonds (*N*-sulfinylimines, oximes and hydrazones) were studied, but none of them reacted productively with isocyanides under the described conditions. Finally, the reaction with isatinimines led to the formation of the spiroazetidines **3k** (14%) and **3l** (28%, Table 1, entries 11 and 12). Remarkably, in the former case an intramolecular cyclization of the nitrilium ion upon the electron rich *p*-methoxyphenyl group took place and led to the formation of the bis(imino)tetrahydroquinoline **8** (17%, Table 1, entry 11).

Mechanistic analysis

Taking into account the structural variety observed in this family of reactions, a rational explanation is needed to understand the formation of such products. Here we describe a

Table 1: Scope of the imine and isocyanide starting materials.

entry	R ¹	R ²	R ³	yield
1	4-MeOC ₆ H ₄	4-ClC ₆ H ₄	<i>t</i> -Bu	3a (48%)
2	4-MeOC ₆ H ₄	4-ClC ₆ H ₄	<i>c</i> -C ₆ H ₁₁	3b (41%) ^a
3	4-MeOC ₆ H ₄	4-ClC ₆ H ₄	Bn	3c (63%) ^a
4	4-MeC ₆ H ₄	4-ClC ₆ H ₄	4-MeOC ₆ H ₄	3d (19%) ^b
5	3-MeOC ₆ H ₄	4-ClC ₆ H ₄	<i>t</i> -Bu	3e (19%) + 6 (27%)
6	4-MeOC ₆ H ₄	2-ClC ₆ H ₄	<i>t</i> -Bu	3f (12%) + 3f' (15%)
7	2-MeC ₆ H ₄	4-ClC ₆ H ₄	<i>t</i> -Bu	3g (31%)
8	<i>n</i> -C ₃ H ₇	4-ClC ₆ H ₄	<i>t</i> -Bu	3h' (32%)
9	4-MeOC ₆ H ₄	EtOCO	<i>t</i> -Bu	3i (9%) ^a + 7 (34%)
10	4-MeOC ₆ H ₄	EtOCO	<i>c</i> -C ₆ H ₁₁	3j (34%) ^a
11	4-MeOC ₆ H ₄		<i>t</i> -Bu	3k (14%) ^b + 8 (17%)
12	4-MeC ₆ H ₄		<i>t</i> -Bu	3l (28%)
13	4-MeOC ₆ H ₄	4-ClC ₆ H ₄	Ts-CH ₂	–
14	4-MeOC ₆ H ₄	4-ClC ₆ H ₄	MeO ₂ C-CH ₂	–

^aThe reaction was performed at rt. 20% of catalyst was used. ^bThe adduct could not be isolated in pure form.

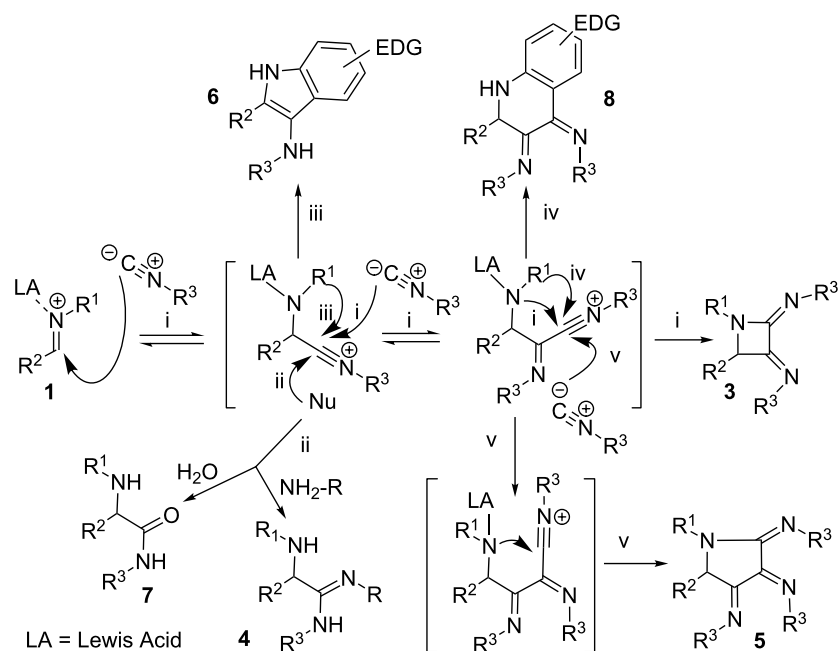
simplified hypothesis based on the well-known nucleophilic addition of isocyanides to Lewis acid-activated imines (Scheme 3). The first nitrilium intermediate can evolve through a second addition and ring-closure to yield the azetidinium adduct **3** (Scheme 4, route i), or can also be trapped by water or amine/imine nucleophiles leading to α -aminoamides **7** and α -aminoamidines **4**, respectively (Scheme 4, route ii). The formation of aminoamide **7** was restricted to the use of glyoxylate imines, and happens only with *tert*-butyl isocyanide, but not with cyclohexyl isocyanide. On the other hand, the aminoamidines **4**, the standard adducts from the amine–aldehyde–isocyanide 3CR were observed in some occasions [5–7] under our conditions presumably by attack of the unreacted imine upon the nitrilium cation. These facts suggest that either a good nucleophile (amines, imines) may act intermolecularly to undergo fast addition to this intermediate or, when an alkyl carboxylate group is present it may stabilize the nitrilium intermediate precluding

further addition events and leading to the aminoamides **7** after the final aqueous treatment.

Furthermore, we have detected indole **6** arising from the cyclization of electron-rich aromatic rings linked to the imine nitrogen upon the electrophilic nitrilium intermediate, in agreement with a Sorensen report (Scheme 4, route iii) [21]. Finally, the imino-nitrilium cation can be trapped by an aromatic ring when using isatin imines, leading to bis(imino)tetrahydroquinoline **8**, (Scheme 4, route iv). In a reaction using a large isocyanide excess, a triple insertion of the isocyanide moiety has been observed, the adduct being the tris(imino)pyrrolidine **5** (Scheme 4, route v).

Conclusion

As a summary, we have described structural and mechanistic features for the bis(imino)azetidines arising from the



Scheme 4: Manifold reaction mechanism.

imine–isocyanide interaction, finding that the process involves a sequential double isocyanide incorporation into the C=N bond. The final step is a nucleophilic 4-*exo-dig* cyclization, and the anti addition modes likely lead to less stable stereoisomers which spontaneously isomerize to the observed compounds. Furthermore, we have determined the scope of the reaction, according to the imine and isocyanide starting materials, and a small collection of multicomponent adducts has been prepared. These structures bear a novel azetidine scaffold of potential interest in medicinal chemistry [22,23]. Although the yields are modest, the compounds can be conveniently prepared in a straightforward manner. A part of the azetidine structure distinct scaffolds have been obtained from the interaction of different reactant combinations: α -aminoamides, α -aminoamidines, indoles, bis(imino)tetrahydroquinolines and tris(imino)pyrrolidines. Finally, a unified reaction mechanism that can account for the production of this rich structural outcome has been proposed.

Supporting Information

Supporting Information File 1

Experimental procedures, characterization data, copies of the NMR spectra for all new compounds and X-ray views of azetidine **3a**.

[<http://www.beilstein-journals.org/bjoc/content/supplementary/1860-5397-10-3-S1.pdf>]

Acknowledgements

This work was supported by DGICYT (Spain, project BQU-CTQ2012-30930), and Generalitat de Catalunya (project 2009 SGR 1024). C.M. thanks the Leonardo da Vinci Project Unipharma-Graduates 8 for a fellowship.

References

- Dömling, A. *Chem. Rev.* **2006**, *106*, 17–89. doi:10.1021/cr0505728 And references cited therein.
- El Kaïm, L.; Grimaud, L. In *Isocyanide Chemistry*; Nenajdenko, V. G., Ed.; Wiley-VCH: Weinheim, 2005; pp 159–194. See for an overview of acid surrogates in isocyanide MCRs.
- Deyrup, J. A.; Vestling, M. M.; Hagan, W. V.; Yun, H. Y. *Tetrahedron* **1969**, *25*, 1467–1478. doi:10.1016/S0040-4020(01)82718-6
- Morel, G.; Marchand, E.; Malvaut, Y. *Heteroat. Chem.* **2000**, *11*, 370–376. doi:10.1002/1098-1071(2000)11:5<370::AID-HC8>3.0.CO;2-J
- McFarland, J. W. *J. Org. Chem.* **1963**, *28*, 2179–2181. doi:10.1021/jo01044a006
- Keung, W.; Bakir, F.; Patron, A. P.; Rogers, D.; Priest, C. D.; Darmohusodo, V. *Tetrahedron Lett.* **2004**, *45*, 733–737. doi:10.1016/j.tetlet.2003.11.051
- Khan, A. T.; Basha, S.; Lal, M.; Mir, M. H. *RSC Adv.* **2012**, *2*, 5506–5509. doi:10.1039/c2ra20539d
- Saha, B.; Frett, B.; Wang, Y.; Li, H.-Y. *Tetrahedron Lett.* **2013**, *54*, 2340–2343. doi:10.1016/j.tetlet.2013.02.055
- Brandi, A.; Cicchi, S.; Cordero, F. M. *Chem. Rev.* **2008**, *108*, 3988–4035. doi:10.1021/cr800325e
- Tejedor, D.; García-Tellado, F. *Chem. Soc. Rev.* **2007**, *36*, 484–491. doi:10.1039/b608164a

11. CCDC 963354 contains the supplementary crystallographic data of product **3a**. These data can be obtained free of charge from The Cambridge Crystallographic Data Centre via http://www.ccdc.cam.ac.uk/data_request/cif.
12. Bez, G.; Zhao, C.-G. *Org. Lett.* **2003**, *5*, 4991–4993. doi:10.1021/ol0359618
13. Oshita, M.; Yamashita, K.; Tobisu, M.; Chatani, N. *J. Am. Chem. Soc.* **2005**, *127*, 761–766. doi:10.1021/ja0450206
14. Korotkov, V. S.; Larionov, O. V.; de Meijere, A. *Synthesis* **2006**, 3542–3546. doi:10.1055/s-2006-942514
15. Masdeu, C.; Gómez, E.; Williams, N. A. O.; Lavilla, R. *Angew. Chem., Int. Ed.* **2007**, *46*, 3043–3046. doi:10.1002/anie.200605070
16. Baldwin, J. E. *J. Chem. Soc., Chem. Commun.* **1976**, 734–736. doi:10.1039/C39760000734
17. Alabugin, I. V.; Gilmore, K.; Manoharan, M. *J. Am. Chem. Soc.* **2011**, *133*, 12608–12623. doi:10.1021/ja203191f
And references cited therein.
18. Nguyen, M. T.; Hegarty, A. F.; Sana, M.; Leroy, G. *J. Am. Chem. Soc.* **1985**, *107*, 4141–4145. doi:10.1021/ja00300a008
19. Johnson, J. E.; Cornell, S. C. *J. Org. Chem.* **1980**, *45*, 4144–4148. doi:10.1021/jo01309a015
20. Tumanov, V. V.; Tishkov, A. A.; Mayr, H. *Angew. Chem., Int. Ed.* **2007**, *46*, 3563–3566. doi:10.1002/anie.200605205
21. Schneekloth, J. S., Jr.; Kim, J.; Sorensen, E. J. *Tetrahedron* **2009**, *65*, 3096–3101. doi:10.1016/j.tet.2008.08.055
22. Burkhard, J. A.; Wagner, B.; Fischer, H.; Schuler, F.; Müller, K.; Carreira, E. M. *Angew. Chem., Int. Ed.* **2010**, *49*, 3524–3527. doi:10.1002/anie.200907108
23. Lowe, J. T.; Lee, M. D., IV; Akella, L. B.; Davoine, E.; Donckele, E. J.; Durak, L.; Duvall, J. R.; Gerard, B.; Holson, E. B.; Joliton, A.; Kesavan, S.; Lemercier, B. C.; Liu, H.; Marié, J.-C.; Mulrooney, C. A.; Muncipinto, G.; Welzel-O'Shea, M.; Panko, L. M.; Rowley, A.; Suh, B.-C.; Thomas, M.; Wagner, F. F.; Wei, J.; Foley, M. A.; Marcaurelle, L. A. *J. Org. Chem.* **2012**, *77*, 7187–7211. doi:10.1021/jo300974j

License and Terms

This is an Open Access article under the terms of the Creative Commons Attribution License (<http://creativecommons.org/licenses/by/2.0>), which permits unrestricted use, distribution, and reproduction in any medium, provided the original work is properly cited.

The license is subject to the *Beilstein Journal of Organic Chemistry* terms and conditions: (<http://www.beilstein-journals.org/bjoc>)

The definitive version of this article is the electronic one which can be found at:
[doi:10.3762/bjoc.10.3](https://doi.org/10.3762/bjoc.10.3)

Publication I: Selected Supporting Information

Experimental procedures

General information

Unless stated otherwise, all reactions were carried out under argon atmosphere in dried glassware. Commercially available reactants were used without further purification. Thin-layer chromatography was performed on pre-coated Merk silica gel 60 F254 plates and visualized under an UV lamp. ^1H , and ^{13}C NMR spectra were recorded on a Varian Mercury 400 (at 400 MHz, and 100 MHz respectively). Unless otherwise quoted, NMR spectra were recorded in CDCl_3 solution with TMS as an internal reference. Data for ^1H NMR spectra are reported as follows: chemical shift (δ ppm), multiplicity, integration and coupling constants (Hz). Data for ^{13}C NMR spectra are reported in terms of chemical shift (δ ppm). IR spectra were recorded using a Thermo Nicolet Nexus spectrometer and are reported in frequency of absorption (cm^{-1}). High resolution mass spectrometry was performed by the University of Barcelona Mass Spectrometry Service.

The microwave-assisted reactions were performed by setting the temperature at reported number and the maximum power and pressure at 250 W and 200 psi respectively. The power is automatically altered by the device to maintain the set temperature for the reported duration of time. A ramp period of 10 min is set to reach the desired temperature and the device automatically starts the emission period as soon as the set temperature is obtained. During the reactions the stirring option is on and a stream of nitrogen cools the reactor. The Max Power option is also on to maintain the reaction temperature while cooling. This option should not be used for polar solvents.

The *N*-aryl-aromatic imines **1** were prepared by mixing the amine and carbonyl components in ACN, in the presence of 4 Å MS at room temperature, according to a standard method. *N*-alkyl imines and activated substrates were prepared following the described procedures (see below).

Preparation of imines and related compounds (1)

General procedure

Equimolar amounts of the corresponding aldehyde and amine (1:1, 2 mmol) together with 2 g of activated MS 4 Å were placed in a 50 mL flask, 10 mL of dry ACN were added and the solution was stirred under nitrogen for 24 h or until all the starting material was consumed. The reaction progress was monitored by TLC or HPLC. After the reaction was complete, 10 mL of saturated aqueous NaHCO_3 solution were added. Molecular sieves were filtered and washed with 20 mL of EtOAc. The aqueous layer was extracted with 3 × 10 mL of EtOAc. The combined organic layers were dried over Na_2SO_4 , filtered and concentrated in vacuo. The resulting crude imine was used without further purification.

General procedure for isatin imines

Equimolar amounts of isatin and the corresponding amine (1:1, 5 mmol) were placed in a 100 mL flask, 20 mL of absolute EtOH and 0.2 mL glacial acetic acid were added and the mixture was refluxed for 12 h or until all the starting material was consumed. The reaction progress was monitored by TLC or HPLC. After the reaction was complete, the solution was set aside to gradually cool down overnight. The formed crystals were filtered, washed with cold EtOH and dried in vacuo ^[1].

The following compounds were prepared according to literature procedures:

N-(4-Chlorobenzylidene)propan-1-amine ^[2]

(*E*)-Ethyl 2-((4-methoxyphenyl)imino)acetate ^[3]

(*S*)-(+)-*N*-(4-Chlorobenzylidene)-4-methylbenzenesulfinamide ^[4]

1-(4-Chlorobenzylidene)-2-(4-methoxyphenyl)hydrazine ^[5]

4-Chlorobenzaldehyde oxime ^[6]

General procedures for the azetidine formation

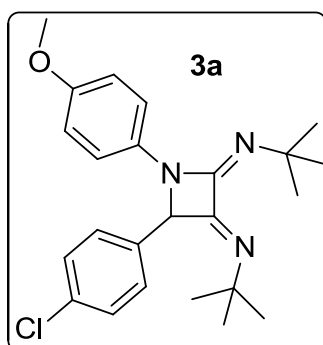
General procedure A

0.5 mmol (1 equiv) of imine **1** were dissolved in 2 mL of dry THF. To this solution was dropwise syringed 0.5 mmol (1 equiv) of $\text{BF}_3 \cdot \text{Et}_2\text{O}$ while stirring. In case of using a solid isocyanide, it was first dissolved in 1 mL of THF. After 2 min, 1.5 mmol (3 equiv.) of the corresponding isocyanide was gradually added. The solution was stirred for 24 h or until the reaction was complete or showed no evolution. The reaction was quenched with 10 mL of saturated NaHCO_3 solution and extracted with 3×10 mL of AcOEt. The combined organic phases were dried over Na_2SO_4 , concentrated in vacuo and purified by flash chromatography (Hexanes/EtOAc).

General procedure B

In a microwave reactor tube, 0.5 mmol (1 equiv) of imine **1** were dissolved in 2 mL of dry THF. To this solution was dropwise syringed 0.5 mmol (1 equiv) of $\text{BF}_3 \cdot \text{Et}_2\text{O}$ while stirring. After 2 minutes, 1.5 mmol (3 equiv) of the corresponding isocyanide was gradually added. In case of using a solid isocyanide, it was first dissolved in 1 mL of THF. The solution was irradiated in the microwave for 30 min at 65 °C. Then it was allowed to cool to room temperature. The reaction was quenched with 10 mL of saturated NaHCO_3 solution and extracted with 3×10 mL of EtOAc. The combined organic phases were dried over Na_2SO_4 , concentrated in vacuo and purified by flash chromatography (hexanes/EtOAc).

Characterization data



N,N'-(4-(4-Chlorophenyl)-1-(4-methoxyphenyl)azetidine-2,3-diylidene)bis(2-methylpropan-2-amine) (**3a**).

According to procedure B, azetidine **3a** was obtained as a pale yellow solid (48%).

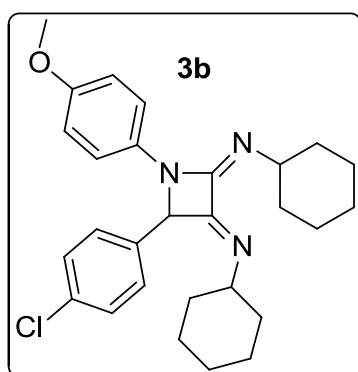
$\text{C}_{24}\text{H}_{30}\text{ClN}_3\text{O}$ ($M = 411.97 \text{ g}\cdot\text{mol}^{-1}$).

IR (neat, cm^{-1}): 3417, 2969, 2930, 2860, 1719, 1668, 1508, 1380, 1303, 1245, 1207, 1130, 1028, 932, 829.

¹H NMR (400 MHz, CDCl₃) δ 7.42 (d, *J* = 9.1 Hz, 2H), 7.33 (s, 4H), 6.76 (d, *J* = 9.1 Hz, 2H), 5.38 (s, 1H), 3.71 (s, 3H), 1.49 (s, 9H), 1.09 (s, 9H).

¹³C NMR (101 MHz, CDCl₃) δ 154.6, 153.9, 152.3, 136.8, 134.4, 134.0, 129.36, 129.35, 117.2, 114.2, 70.3, 58.1, 55.5, 53.9, 53.5, 30.8, 30.2.

HRMS (ESI): calculated for **C₂₄H₃₁ClN₃O** [*M* + *H*]⁺: 412.215, found 412.215.



***N,N'*-(4-(4-Chlorophenyl)-1-(4-methoxyphenyl)azetidine-2,3-diylidene)dicyclohexanamine (3b).**

According to procedure B, using 20% BF₃·Et₂O, **3b** was obtained as an amorphous solid (41%).

C₂₈H₃₄ClN₃O (*M* = 464.04 g·mol⁻¹).

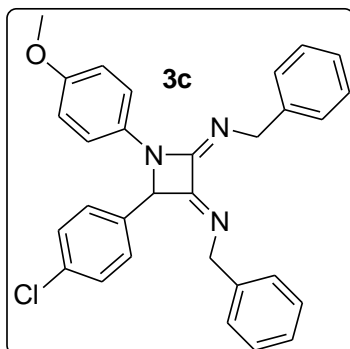
IR (neat, cm⁻¹): 2930, 2853, 1713, 1674, 1508, 1444,

1367, 1297, 1245, 1137, 1008, 823, 733.

¹H NMR (400 MHz, CDCl₃) δ 7.29 (d, *J* = 9.1 Hz, 2H), 7.25 (d, *J* = 9.6 Hz, 2H), 7.20 (d, *J* = 9.6 Hz, 2H), 6.69 (d, *J* = 9.1 Hz, 2H), 5.39 (s, 1H), 4.21 (m, 2H), 3.64 (s, 3H), 3.18 (m, 4H), 1.81 – 0.75 (m, 16H).

¹³C NMR (101 MHz, CDCl₃) δ 157.1, 154.5, 152.2, 135.6, 134.1, 133.8, 129.3, 128.2, 116.9, 114.3, 69.3, 61.2, 57.1, 55.49, 55.44, 35.34, 35.26, 33.6, 32.8, 25.9, 25.5, 24.8, 23.87, 23.72.

HRMS (ESI): calculated for **C₂₈H₃₅ClN₃O** [*M* + *H*]⁺ 464.2463, found 464.2452.



2,3-Bis(benzylimino)-4-(4-chlorophenyl)-1-(4-methoxyphenyl)azetidine (3c).

According to procedure A, using 20% BF₃·Et₂O, azetidine **3c** was obtained as an amorphous solid (63%).

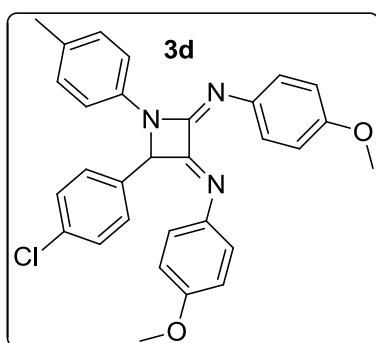
C₃₀H₂₆ClN₃O (M = 480.00 g·mol⁻¹).

IR (neat, cm⁻¹): 3058, 3026, 2930, 1726, 1687, 1508, 1450, 1245, 1130, 1028, 829.

¹H NMR (400 MHz, CDCl₃) 7.41 (ddd, *J* = 6.2, 1.3, 0.7 Hz, 2H), 7.35 – 7.31 (m, 2H), 7.28 (cs, 6H), 7.21 – 7.12 (m, 4H), 6.96 (dd, *J* = 7.9, 1.6 Hz, 2H), 6.70 (d, *J* = 9.1 Hz, 2H), 5.51 (s, 1H), 5.09 (s, 2H), 4.45 (d, *J* = 14.4 Hz, 1H), 4.41 (d, *J* = 14.4 Hz, 1H), 3.64 (s, 3H).

¹³C NMR (101 MHz, CDCl₃) δ 160.0, 154.0, 152.3, 140.7, 136.7, 133.8, 133.2, 132.1, 128.6, 127.6, 127.4, 127.2, 126.6, 126.47, 126.1, 125.3, 116.2, 113.3, 68.9, 55.3, 54.4, 52.4.

HRMS (ESI) : calculated for **C₃₀H₂₇ClN₃O** [M + H]⁺ 480.1837., found 480.1835.



***N,N'*-(4-(4-Chlorophenyl)-1-(*p*-tolyl)azetidine-2,3-diylidene)bis(4-methoxyaniline) (3d)**

According to procedure B, azetidine **3d** was obtained as a yellow amorphous solid (19%).

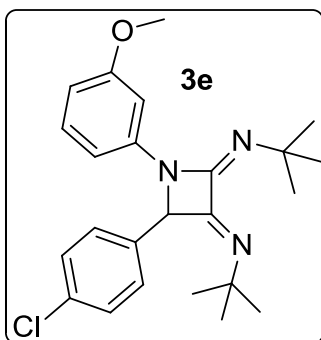
C₃₀H₂₆ClN₃O₂ (M = 495.99 g·mol⁻¹).

IR (neat, cm⁻¹): 1656, 1504, 1499, 1378, 1294, 1241, 1030, 830.

¹H NMR (400 MHz, CDCl₃) 7.54 (d, *J* = 8.9 Hz, 2H), 7.44 (d, *J* = 8.5 Hz, 2H), 7.15 (d, *J* = 8.5 Hz, 2H), 7.07 (d, *J* = 8.0 Hz, 4H), 6.89 (d, *J* = 8.9 Hz, 2H), 6.74 (bs, 4H), 5.84 (s, 1H), 3.81 (s, 3H), 3.78 (s, 3H), 2.28 (s, 3H).

¹³C NMR (101 MHz, CDCl₃) δ 159.1, 158.1, 156.6, 150.2, 139.71, 139.58, 136.8, 134.4, 133.1, 132.8, 129.7, 129.1, 128.4, 124.9, 122.6, 116.7, 114.05, 113.87, 69.3, 55.65, 55.58, 21.1.

HRMS (ESI): calculated for **C₃₀H₂₇ClN₃O₂** [M + H]⁺ 496.1786., found 496.1787.



***N,N'*-(4-(4-Chlorophenyl)-1-(3-methoxyphenyl)azetidine-2,3-diylidene)bis(2-methylpropan-2-amine) (3e)**

According to procedure B, azetidine **3e** was obtained as a cream amorphous solid (19%).

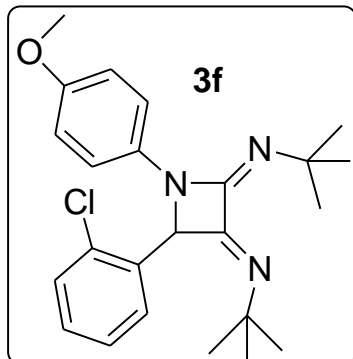
C₂₄H₃₀ClN₃O (M = 411.97 g·mol⁻¹).

IR (neat, cm⁻¹): 2962, 2861, 1722, 1671, 1477, 1203, 837.

¹H NMR (400 MHz, CDCl₃) δ 7.51 (t, *J* = 2.1 Hz, 1H), 7.34 (bs, 4H), 7.04 (t, *J* = 8.2 Hz, 1H), 6.72 (dd, *J* = 8.2, 1.2 Hz, 1H), 6.45 (ddd, *J* = 8.2, 2.1, 1.2 Hz, 1H), 5.39 (s, 1H), 3.74 (s, 3H), 1.48 (s, 9H), 1.09 (s, 9H).

¹³C NMR (101 MHz, CDCl₃) δ 159.9, 153.6, 152.3, 141.1, 136.5, 134.4, 129.32, 129.26, 129.20, 107.90, 107.81, 101.9, 70.4, 58.1, 55.0, 53.9, 30.6, 30.0.

HRMS (ESI): calculated for **C₂₄H₃₁ClN₃O** [M + H]⁺: 412.215, found 412.215.



***N,N'*-(4-(2-Chlorophenyl)-1-(4-methoxyphenyl)azetidine-2,3-diylidene)bis(2-methylpropan-2-amine) (3f)**

According to procedure B, azetidine **3f** was obtained as a cream solid (12%).

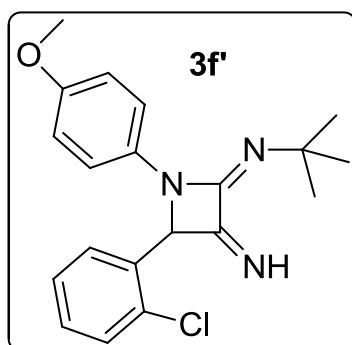
C₂₄H₃₀ClN₃O (M = 411.97 g·mol⁻¹).

IR (neat, cm⁻¹): 3084, 2952, 2819, 1721, 1660, 1507, 1233, 1121, 754.

¹H NMR (400 MHz, CDCl₃) δ 7.47 (d, *J* = 9.0 Hz, 2H), 7.40 (dd, *J* = 6.9, 2.9 Hz, 1H), 7.35 (dd, *J* = 6.9, 3.6 Hz, 1H), 7.21 (m, 2H), 6.77 (d, *J* = 9.0 Hz, 2H), 5.99 (s, 1H), 3.71 (s, 3H), 1.48 (s, 9H), 1.09 (s, 9H).

^{13}C NMR (101 MHz, CDCl_3) δ 154.7, 154.4, 153.4, 152.5, 135.8, 133.66, 133.56, 131.8, 129.89, 129.79, 129.69, 128.9, 127.8, 122.5, 117.1, 114.2, 65.7, 57.6, 55.4, 53.7, 30.7, 29.6.

HRMS (ESI): calculated for $\text{C}_{24}\text{H}_{31}\text{ClN}_3\text{O}$ $[\text{M} + \text{H}]^+$: 412.215, found 412.215.



N-(4-(2-Chlorophenyl)-3-imino-1-(4-methoxyphenyl)-
azetidin-2-ylidene)-2-methylpropan-2-amine (**3f'**)

According to procedure B, azetidine **3f'** was obtained as yellow oil (15%).

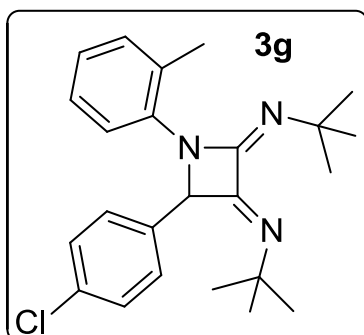
$\text{C}_{20}\text{H}_{22}\text{ClN}_3\text{O}$ ($M = 355.86 \text{ g}\cdot\text{mol}^{-1}$).

IR (neat, cm^{-1}): 3379, 2962, 2820, 1640, 1508, 1233, 1040, 806.

^1H NMR (400 MHz, CDCl_3) δ 7.47 – 7.43 (m, 1H), 7.37 – 7.33 (m, 1H), 7.31 – 7.14 (m, 2H), 6.73 (d, $J = 9.0 \text{ Hz}$, 2H), 6.59 (d, $J = 9.0 \text{ Hz}$, 2H), 5.68 (d, $J = 5.4 \text{ Hz}$, 1H), 5.25 (d, $J = 5.4 \text{ Hz}$, 1H), 3.71 (s, 3H), 1.43 (s, 9H).

^{13}C NMR (101 MHz, CDCl_3) δ 152.7, 139.7, 137.8, 135.2, 134.6, 130.2, 129.8, 128.8, 127.7, 115.1, 114.8, 111.2, 61.3, 58.7, 55.7, 29.3.

HRMS (ESI): calculated for $\text{C}_{20}\text{H}_{23}\text{ClN}_3\text{O}$ $[\text{M} + \text{H}]^+$: 356.1524, found 356.1513.



N,N'-(4-(4-Chlorophenyl)-1-(*o*-tolyl)azetidine-2,3-
diylidene)bis(2-methylpropan-2-amine) (**3g**)

According to procedure B, azetidine **3g** was obtained as a brown paste (31%).

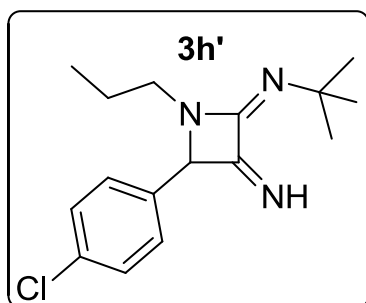
$\text{C}_{24}\text{H}_{30}\text{ClN}_3$ ($M = 395.97 \text{ g}\cdot\text{mol}^{-1}$).

IR (neat, cm^{-1}): 2952, 2861, 2850, 1671, 1488, 1203, 837.

¹H NMR (400 MHz, CDCl₃) δ 7.45 (d, *J* = 8.1 Hz, 1H), 7.25 (d, *J* = 8.7 Hz, 2H), 7.20 (d, *J* = 8.7 Hz, 2H), 7.04 (m, 2H), 6.94 (m, 1H), 5.56 (s, 1H), 2.29 (s, 3H), 1.47 (s, 9H), 1.11 (s, 9H).

¹³C NMR (101 MHz, CDCl₃) δ 154.9, 153.0, 137.0, 136.4, 134.2, 132.0, 131.2, 129.4, 129.0, 125.9, 125.0, 122.8, 118.6, 114.9, 71.6, 58.2, 53.6, 30.7, 30.0, 20.1.

HRMS (ESI): calculated for C₂₄H₃₁ClN₃ [M + H]⁺: 396.2201, found 396.2194.



***N*-(4-(4-Chlorophenyl)-3-imino-1-propylazetidino-2-ylidene)-2-methylpropan-2-amine (3h')**

According to procedure B, azetidine **3h'** was obtained as a lemon amorphous solid (32%).

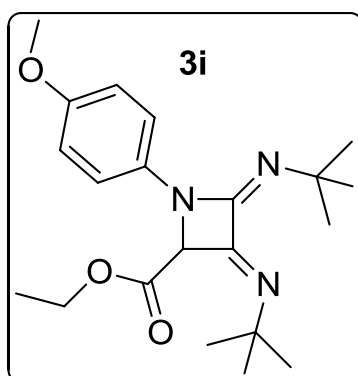
C₁₆H₂₂ClN₃ (M = 291.82 g·mol⁻¹).

IR (neat, cm⁻¹): 3359, 3318, 2952, 2861, 2149, 1579, 1091, 837.

¹H NMR (400 MHz, CDCl₃) δ 7.42 (d, *J* = 8.4 Hz, 2H), 7.32 (d, *J* = 8.4 Hz, 2H), 5.79 (s, 1H), 2.75 (cs, 2H), 1.57 (s, 1H), 1.41 (cs, 2H), 1.17 (s, 9H), 0.76 (t, *J* = 7.4 Hz, 3H).

¹³C NMR (101 MHz, CDCl₃) δ 161.1, 136.0, 131.1, 130.5, 129.1, 123.4, 54.7, 46.1, 29.6, 29.1, 24.5, 11.3.

HRMS (ESI): calculated for C₁₆H₂₃ClN₃ [M + H]⁺: 292.1575, found 292.1575.



Ethyl 3,4-bis(tert-butylimino)-1-(4-methoxyphenyl)azetidine-2-carboxylate (3i)

According to procedure A, using 20% BF₃, Et₂O, azetidine **3i** was obtained as a white amorphous solid (9%).

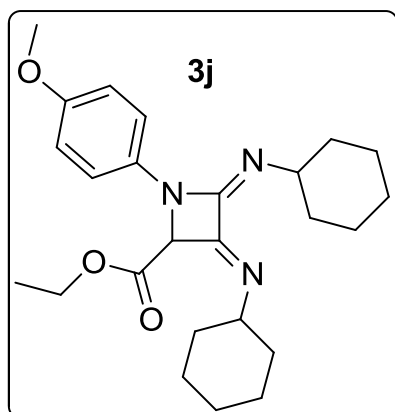
C₂₁H₃₁N₃O₃ (M = 373.49 g·mol⁻¹).

IR (neat, cm^{-1}): 2960, 1737, 1717, 1674, 1187.

$^1\text{H NMR}$ (400 MHz, CDCl_3) δ 7.46 (d, $J = 9.1$ Hz, 2H), 6.85 (d, $J = 9.1$ Hz, 2H), 4.95 (s, 1H), 4.19 (cs, 2H), 3.77 (s, 3H), 1.42 (s, 9H), 1.30 (s, 9H), 1.20 (t, $J = 7.1$ Hz, 3H).

$^{13}\text{C NMR}$ (126 MHz, CDCl_3) δ 169.6, 154.8, 151.4, 147.7, 134.2, 116.7, 114.5, 68.5, 62.0, 58.5, 55.7, 54.0, 30.7, 29.9, 14.1.

HRMS (ESI): calculated for $\text{C}_{21}\text{H}_{32}\text{N}_3\text{O}_3$ $[\text{M} + \text{H}]^+$: 374.2438, found 374.2441.



Ethyl 3,4-bis(cyclohexylimino)-1-(4-methoxyphenyl)azetidine-2-carboxylate (3j)

According to procedure A, using 20% $\text{BF}_3 \cdot \text{Et}_2\text{O}$, azetidine **3j** was obtained as an amorphous white solid (34%).

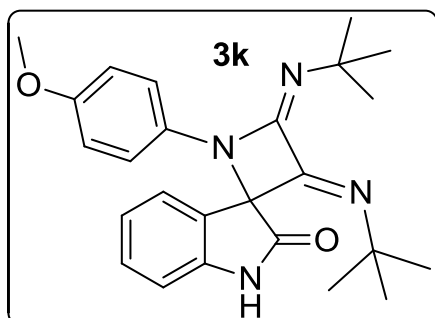
$\text{C}_{25}\text{H}_{35}\text{N}_3\text{O}_3$ ($M = 425.56 \text{ g}\cdot\text{mol}^{-1}$).

IR (neat, cm^{-1}): 2930, 2854, 1720, 1687, 1514.

$^1\text{H NMR}$ (400 MHz, CDCl_3) δ 7.27 (d, $J = 8.0$ Hz, 2H), 6.79 (d, $J = 8.0$ Hz, 2H), 4.98 (s, 1H), 4.16 (m, Hz, 2H), 4.07 (m, 2H), 3.70 (s, 3H), 3.38 (m, 4H), 1.72 - 1.25(m, 16H), 1.18 (t, $J = 7.0$ Hz, 3H).

$^{13}\text{C NMR}$ (101 MHz, CDCl_3) δ 206.5, 154.5, 134.0, 116.5, 114.4, 67.0, 62.00, 61.98, 61.9, 57.3, 55.5, 35.1, 33.6, 33.4, 30.9, 25.8, 25.5, 24.6, 23.8, 23.7, 14.1 (three quaternary carbon signals not detected)

HRMS (ESI): calculated for $\text{C}_{25}\text{H}_{30}\text{N}_4\text{O}$ $[\text{M} + \text{H}]^+$: 426.2751, found 426.2745.



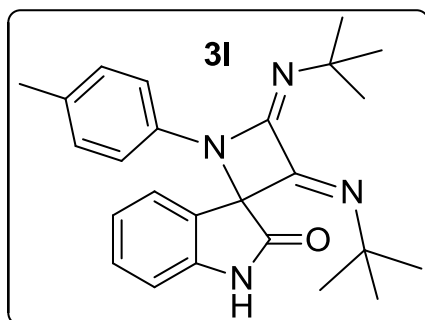
3,4-bis(tert-Butylimino)-1-(4-methoxyphenyl)spiro[azetidine-2,3'-indolin]-2'-one (3k)

According to procedure B, azetidine **3k** was obtained as a brown paste (14%).

$C_{25}H_{30}N_4O_2$ ($M = 418.53 \text{ g}\cdot\text{mol}^{-1}$).

$^1\text{H NMR}$ (400 MHz, $CDCl_3$) δ 9.05 (bs, 1H), 7.45 (m, 1H), 7.35 (m, 1H), 7.31 – 7.14 (m, 2H), 6.73 (d, $J = 9.0 \text{ Hz}$, 2H), 6.59 (d, $J = 9.0 \text{ Hz}$, 2H), 3.71 (s, 3H), 1.43 (s, 9H), 0.98 (s, 9H).

LRMS (HPLC-MS): calculated for $C_{25}H_{31}N_4O_2$ $[M + H]^+$: 419.24, found 419.



3,4-bis(tert-Butylimino)-1-(p-tolyl)spiro[azetidine-2,3'-indolin]-2'-one (3l)

According to procedure A, azetidine **3l** was obtained as an amorphous cream solid (28%).

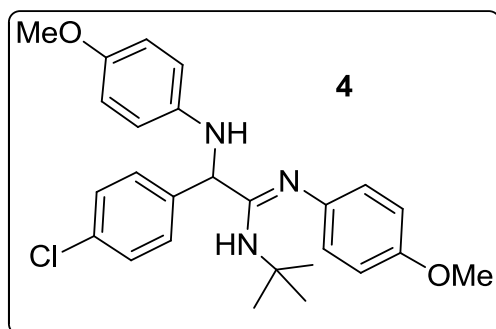
$C_{25}H_{30}N_4O$ ($M = 402.53 \text{ g}\cdot\text{mol}^{-1}$).

IR (neat, cm^{-1}): 2962, 2861, 1742, 1691, 1508, 1355, 1183, 928.

$^1\text{H NMR}$ (400 MHz, $CDCl_3$) δ 9.42 (s, 1H), 7.27 (m, $J = 7.8, 1.2 \text{ Hz}$, 1H), 7.22 (cs, 3H), 7.01 (m, $J = 7.8, 0.8 \text{ Hz}$, 1H), 6.93 – 6.90 (m, 2H), 6.89 (s, 1H), 2.17 (s, 3H), 1.50 (s, 9H), 1.02 (s, 9H).

$^{13}\text{C NMR}$ (101 MHz, $CDCl_3$) δ 175.4, 150.7, 147.3, 140.4, 136.9, 131.6, 130.5, 129.4, 125.44, 124.5, 123.5, 116.0, 111.3, 77.4, 58.5, 54.1, 30.6, 29.5, 20.8.

HRMS (ESI): calculated for $C_{25}H_{31}N_4O$ $[M + H]^+$: 403.2492, found 403.249.



N-(tert-Butyl)-2-(4-chlorophenyl)-N'-(4-methoxyphenyl)-2-((4-methoxyphenyl)amino)acetimidamide (4)

Amidine **4a** was obtained by direct stirring aniline **1a**, aldehyde **2a** and tert-butyl

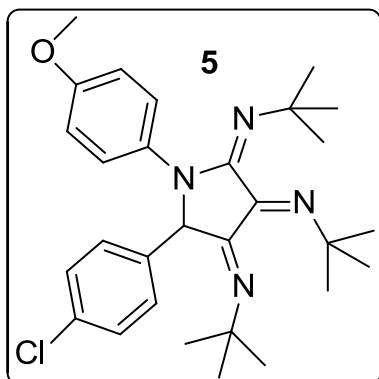
isocyanide, with $\text{Sc}(\text{OTf})_3$ (20% mol) at rt. for 14 h in ACN. After standard aqueous work up and EtOAc extraction, the crude was purified through column chromatography (SiO_2 , Hexanes-EtOAc 50:50) to yield amidine **4** (28%).

$\text{C}_{26}\text{H}_{30}\text{ClN}_3\text{O}_2$ ($M = 451.99 \text{ g}\cdot\text{mol}^{-1}$).

$^1\text{H NMR}$ (400 MHz, CDCl_3) δ 7.25 (d, $J = 8.5 \text{ Hz}$, 2H), 7.08 (d, $J = 8.5 \text{ Hz}$, 2H), 6.83 (d, $J = 9.0 \text{ Hz}$, 2H), 6.65 (cs, 4H), 6.40 (d, $J = 8.8 \text{ Hz}$, 2H), 6.00 (m, 1H), 4.86 (s, 1H), 3.78 (s, 3H), 3.73 (s, 3H), 3.46 (bs, 1H), 1.46 (s, 9H).

$^{13}\text{C NMR}$ (101 MHz, CDCl_3) δ 154.5, 153.4, 143.8, 141.0, 138.5, 134.0, 129.4, 128.9, 122.9, 116.4, 114.93, 114.80, 114.8, 113.96, 59.7, 55.7, 55.5, 50.8, 28.4.

LRMS (HPLC-MS): calculated for $\text{C}_{26}\text{H}_{31}\text{ClN}_3\text{O}_2$ $[\text{M} + \text{H}]^+$: 452.20, found 452.



N,N',N''-(5-(4-Chlorophenyl)-1-(4-methoxyphenyl)pyrrolidine-2,3,4-triylidene)tris(2-methylpropan-2-amine) (5)

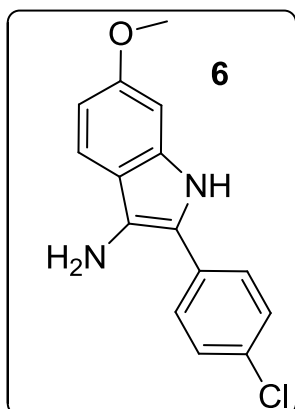
According to procedure B, pyrrolidine **5** was obtained as a brown paste (9%).

$\text{C}_{29}\text{H}_{39}\text{ClN}_4\text{O}$ ($M = 495.10 \text{ g}\cdot\text{mol}^{-1}$).

IR (neat, cm^{-1}): 2962, 1691, 1640, 1508, 1355, 1233, 816.

$^1\text{H NMR}$ (400 MHz, CDCl_3) δ 7.32 (d, $J = 9.2 \text{ Hz}$, 2H), 7.26 (d, $J = 8.5 \text{ Hz}$, 2H), 7.16 (d, $J = 8.5 \text{ Hz}$, 2H), 6.73 (d, $J = 9.2 \text{ Hz}$, 2H), 5.59 (s, 1H), 3.74 (s, 3H), 1.45 (s, 9H), 1.43 (s, 9H), 1.29 (s, 9H).

HRMS (ESI): calculated for $\text{C}_{29}\text{H}_{40}\text{ClN}_4\text{O}$ $[\text{M} + \text{H}]^+$: 495.2885, found 495.2875.



2-(4-Chlorophenyl)-6-methoxy-1H-indol-3-amine (6)

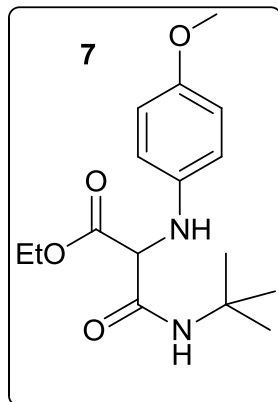
According to procedure B, indole **6** was obtained as an slightly unstable amorphous cream solid (27%).

C₁₅H₁₃ClN₂O (M = 272.72 g·mol⁻¹).

IR (neat, cm⁻¹): 3237, 2952, 2881, 2393, 2220, 1488, 1152, 1020, 827.

¹H NMR (400 MHz, DMSO) δ 12.45 (m, 1H), 7.96 (d, *J* = 8.6 Hz, 2H), 7.71 (d, *J* = 8.6 Hz, 2H), 7.54 (d, *J* = 8.7 Hz, 1H), 7.01 (d, *J* = 2.2 Hz, 1H), 6.93 (dd, *J* = 8.7, 2.2 Hz, 1H), 3.84 (s, 3H), 1.25 (s, 2H).

¹³C NMR (101 MHz, DMSO) δ 157.8, 142.8, 137.0, 134.6, 129.8, 128.7, 122.5, 119.7, 112.9, 95.8, 55.9.



Ethyl 3-(tert-butylamino)-2-(4-methoxyphenylamino)-3-oxopropanoate (7)

According to procedure A, aminoamide **7** was obtained as light brown paste (41%).

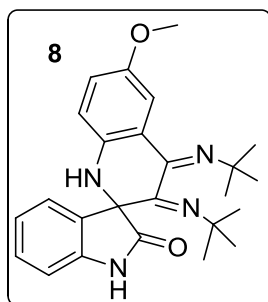
C₁₆H₂₄N₂O₄ (M = 308.37 g·mol⁻¹).

IR (neat, cm⁻¹): 3381, 2968, 1741, 1699, 1619, 1512, 1464, 1367, 1244, 1179, 1033.

¹H NMR (400 MHz, CDCl₃) δ 6.79 (d, *J* = 8.9 Hz, 2H), 6.64 (s, 1H), 6.60 (d, *J* = 8.9 Hz, 2H), 4.71 (s, 1H), 4.36 – 4.20 (m, 2H), 3.75 (s, 3H), 1.32 (s, 9H), 1.30 (t, *J* = 7.1 Hz, 3H).

¹³C NMR (101 MHz, CDCl₃) δ 169.4, 165.5, 153.4, 139.6, 115.3, 114.8, 64.2, 62.4, 55.5, 51.3, 28.4, 14.0.

HRMS (ESI): calculated for $C_{16}H_{25}N_2O_4$ $[M + H]^+$: 309.1809, found 309.1809.



3',4'-bis(tert-Butylimino)-6'-methoxy-3',4'-dihydro-1'H-spiro[indoline-3,2'-quinolin]-2-one (8)

According to procedure B, tetrahydroquinoline **8** was obtained as a brown solid (17%)

$C_{25}H_{30}N_4O_2$ ($M = 418.53 \text{ g}\cdot\text{mol}^{-1}$).

IR (neat, cm^{-1}): 3420, 3227, 2962, 1681, 1508, 1223, 1040, 755.

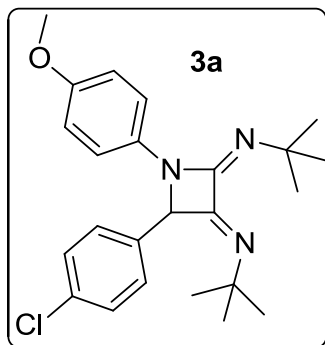
^1H NMR (400 MHz, CDCl_3) δ 7.84 (dd, $J = 7.8, 1.5 \text{ Hz}$, 1H), 7.70 (m, 1H), 7.42 (dd, $J = 7.6, 1.3 \text{ Hz}$, 1H), 7.32 (m, $J = 7.6, 1.3 \text{ Hz}$, 1H), 7.20 (bs, 2H), 7.12 (dd, $J = 8.0, 1.0 \text{ Hz}$, 1H), 6.45 (bs, 1H), 5.27 (bs, 1H), 3.77 (s, 3H), 1.60 (s, 9H), 1.20 (s, 9H).

^{13}C NMR (101 MHz, CDCl_3) δ 167.2, 154.8, 153.4, 140.7, 130.3, 129.6, 128.4, 127.1, 125.7, 123.7, 121.5, 120.7, 119.6, 115.7, 105.7, 59.8, 55.6, 51.7, 29.7, 29.1.

HRMS (ESI): calculated for $C_{25}H_{31}N_4O_2$ $[M + H]^+$: 419.2442, found 419.2438.

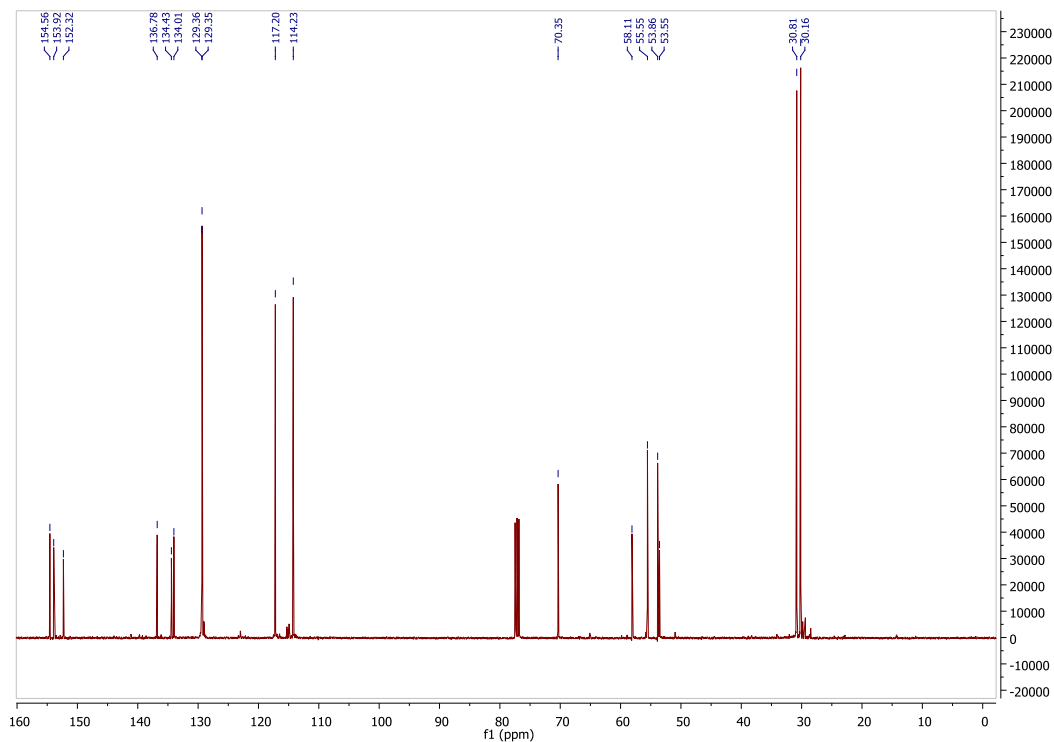
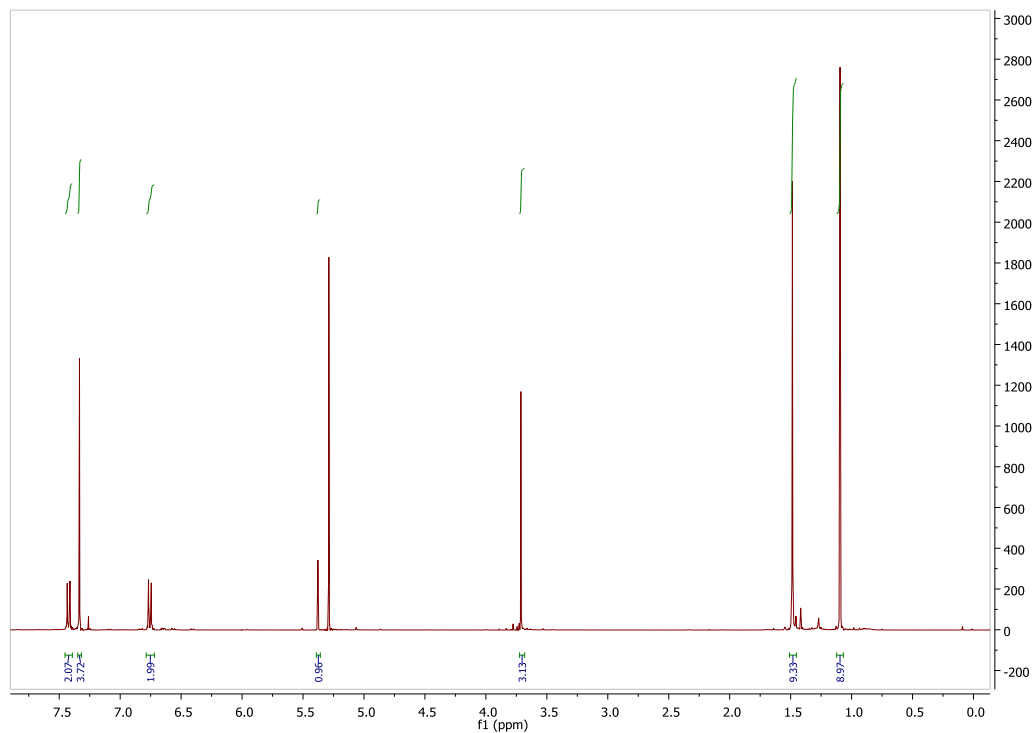
References

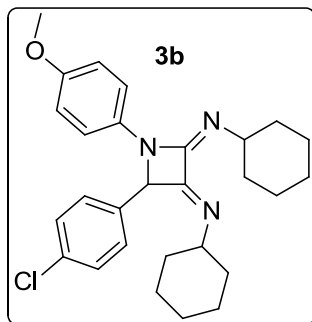
1. Kahveci, B. *Molecules* **2005**, *10*, 376-382.
2. Renault, S. V.; Bertrand, S.; Carreaux, F. O.; Bazureau, J. P. *Journal of Combinatorial Chemistry* **2007**, *9*, 935-942.
3. Gerard, B.; O'Shea, M. W.; Donckele, E.; Kesavan, S.; Akella, L. B.; Xu, H.; Jacobsen, E. N.; Marcaurelle, L. A. *ACS combinatorial science* **2012**, *14*, 621-630.
4. Davis, F. A.; Zhang, Y.; Andemichael, Y.; Fang, T.; Fanelli, D. L.; Zhang, H., *J. Org. Chem.* **1999**, *64*, 1403-1406.
5. Hania, M. M., *Journal of Chemistry* **2009**, *6*, S508-S514.
6. Galvis, C. E. P.; Kouznetsov, V. V. *Org. Biomol. Chem.* **2013**, *11*, 407-411.



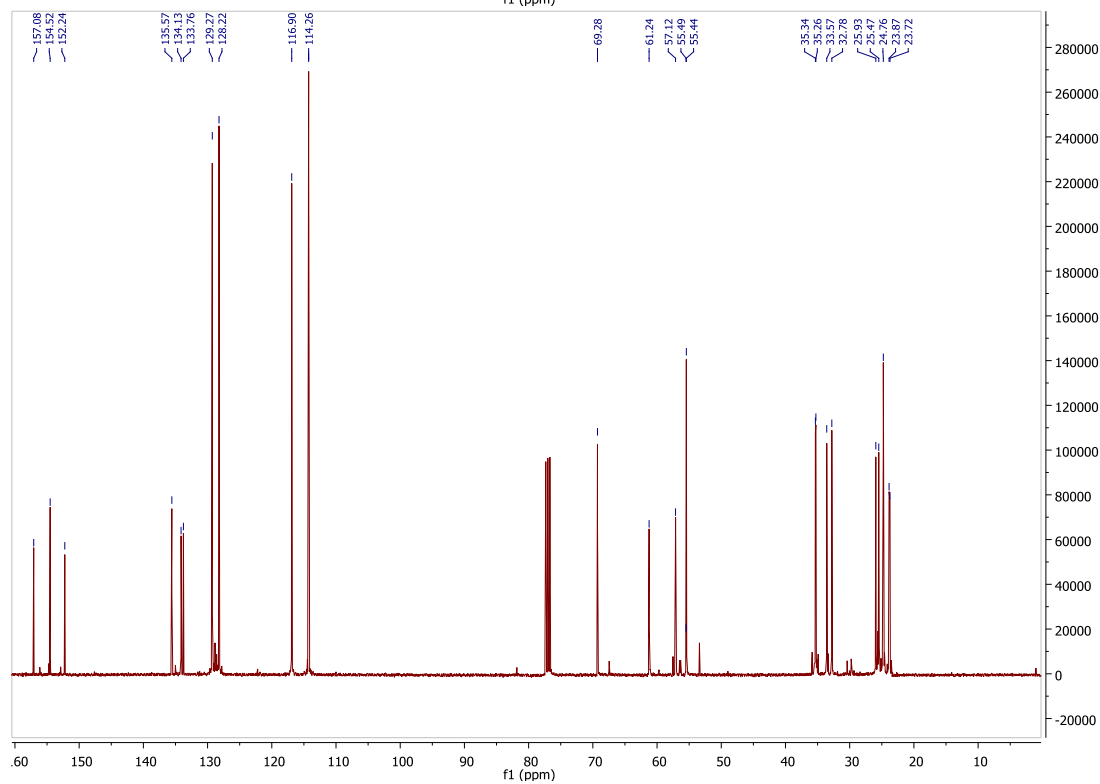
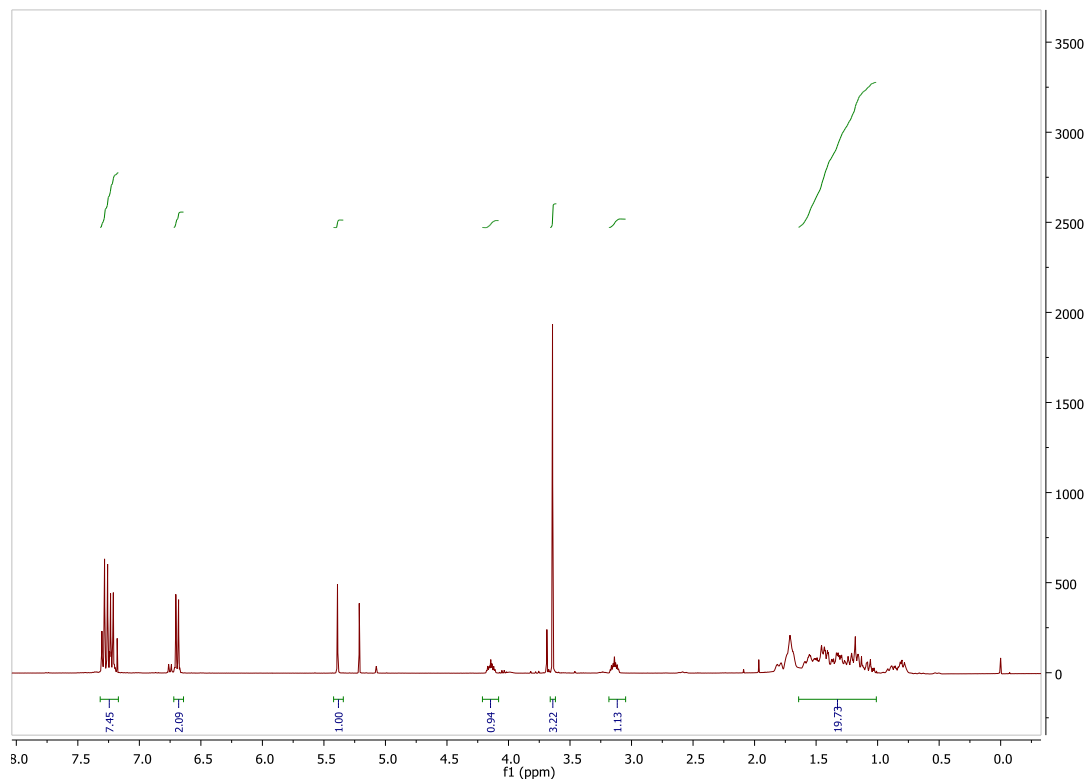
Copies of the NMR spectra

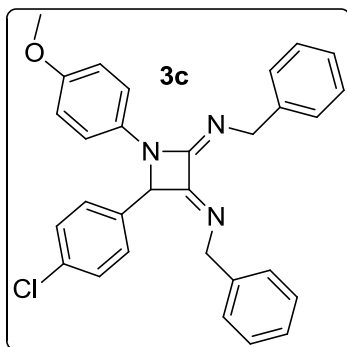
N,N'-(4-(4-Chlorophenyl)-1-(4-methoxyphenyl)azetidene-2,3-diylidene)bis(2-methylpropan-2-amine) (**3a**)



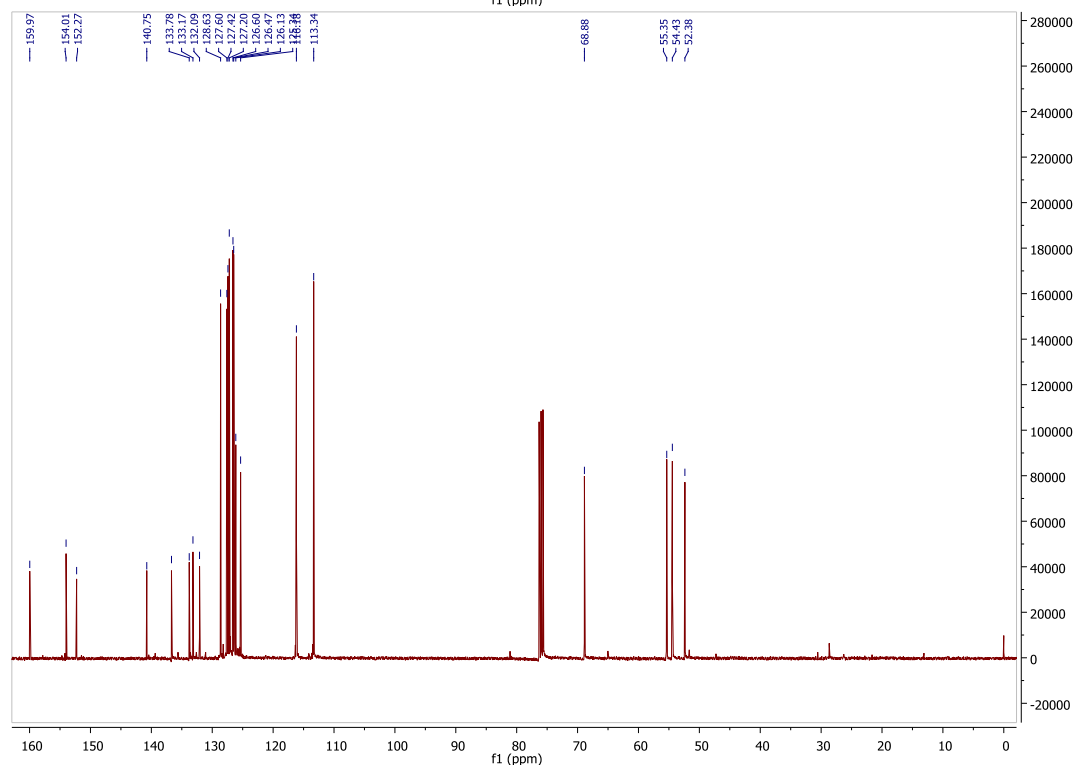
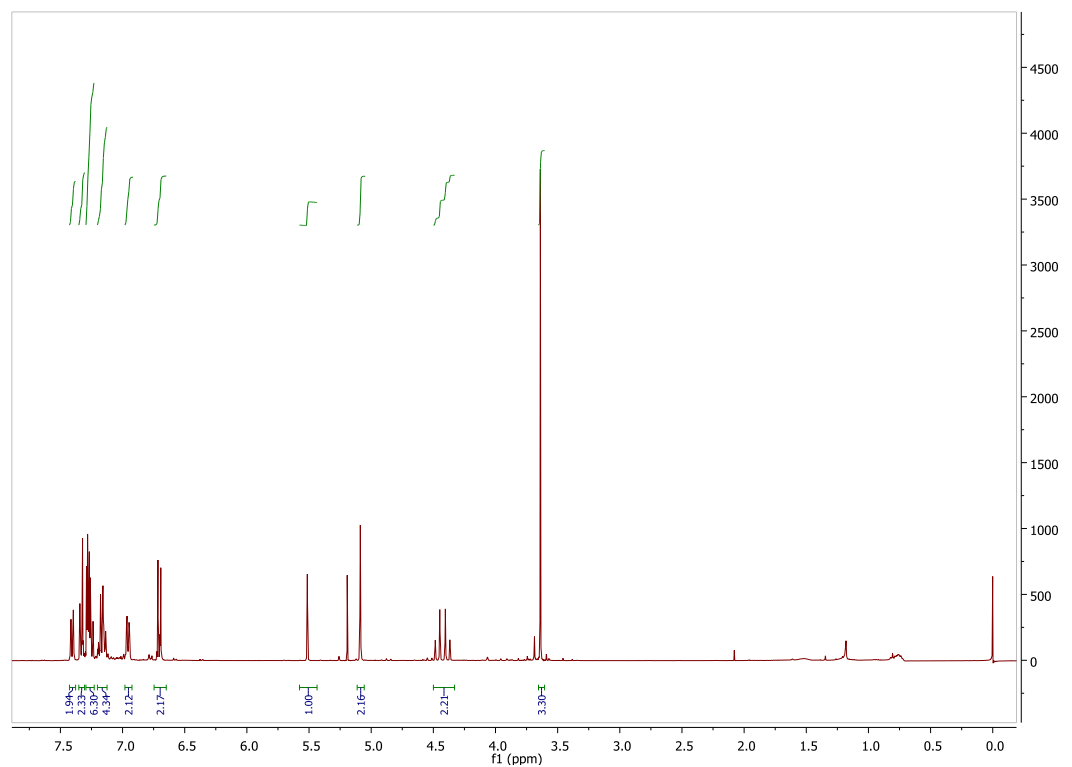


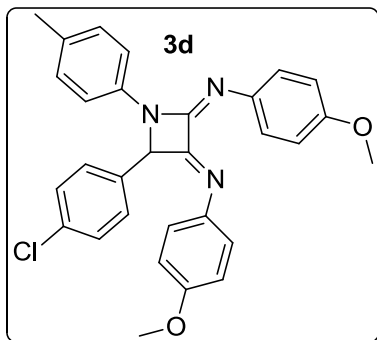
***N,N'*-(4-(4-Chlorophenyl)-1-(4-methoxyphenyl)azetidine-2,3-diylidene)dicyclohexanamine (3b)**



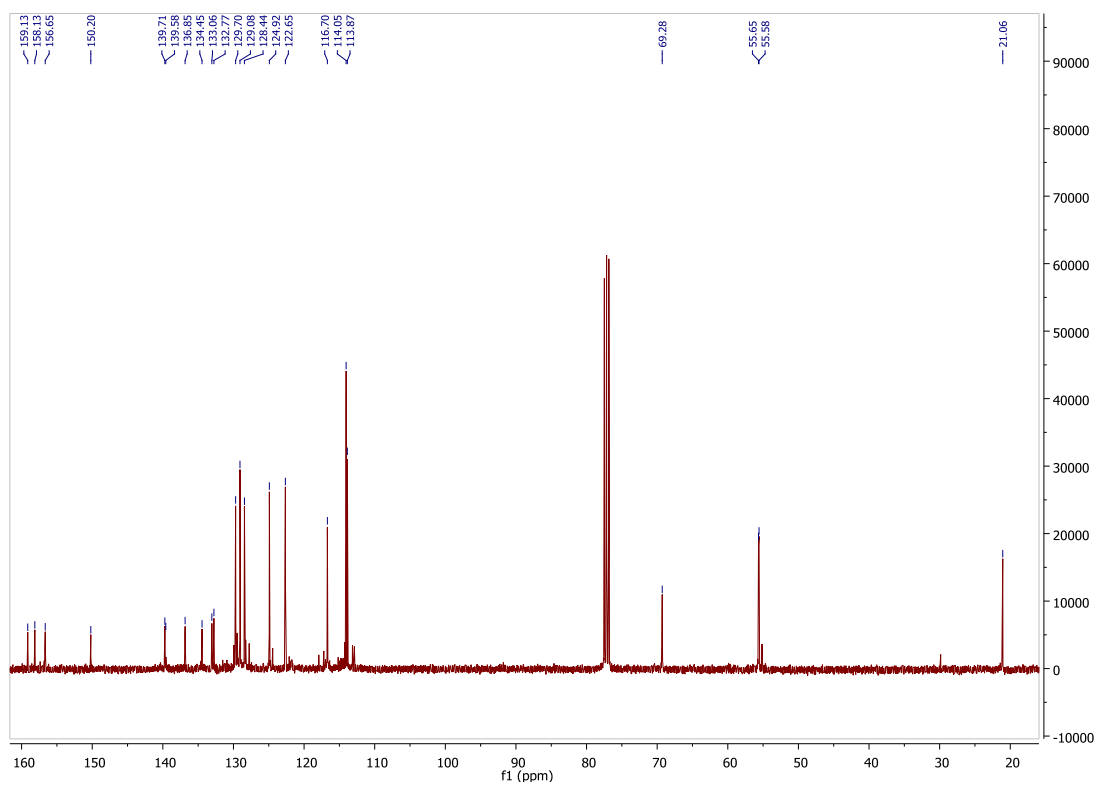
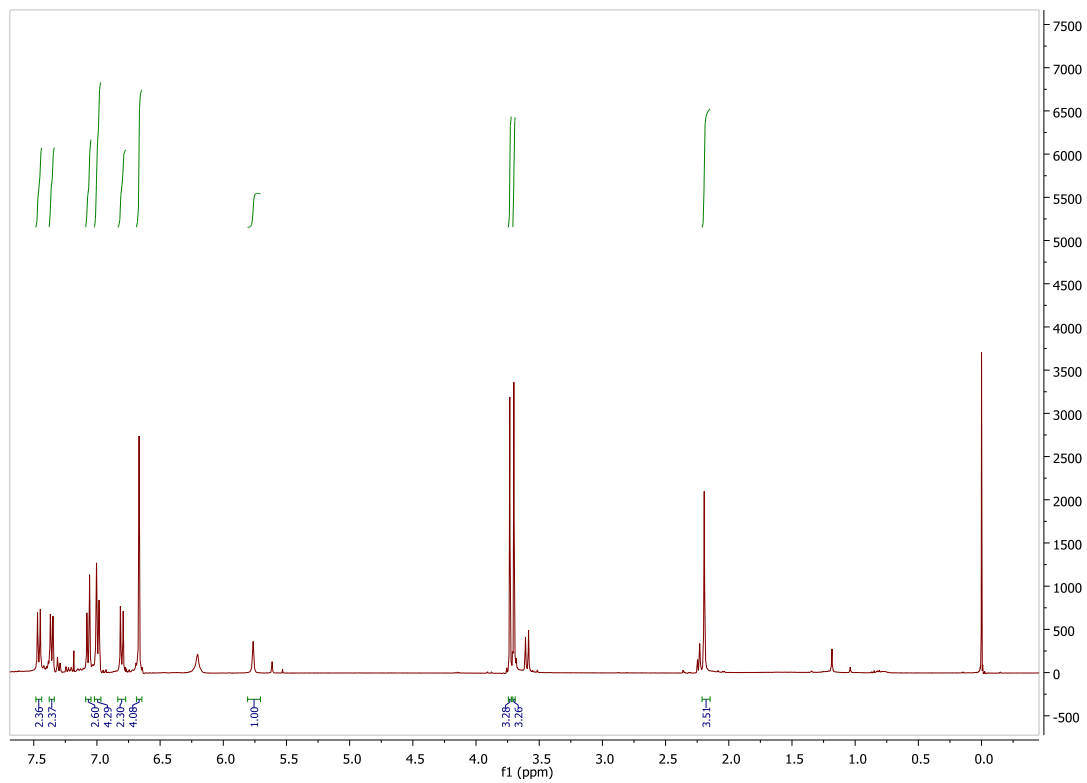


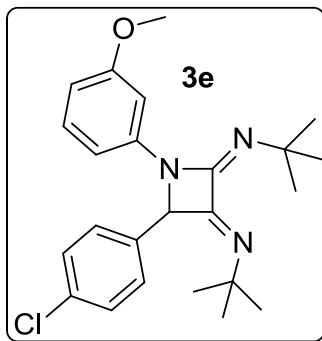
***N,N'*-(4-(4-Chlorophenyl)-1-(4-methoxyphenyl)azetidine-2,3-diyldene)bis(1-phenylmethanamine) (3c)**



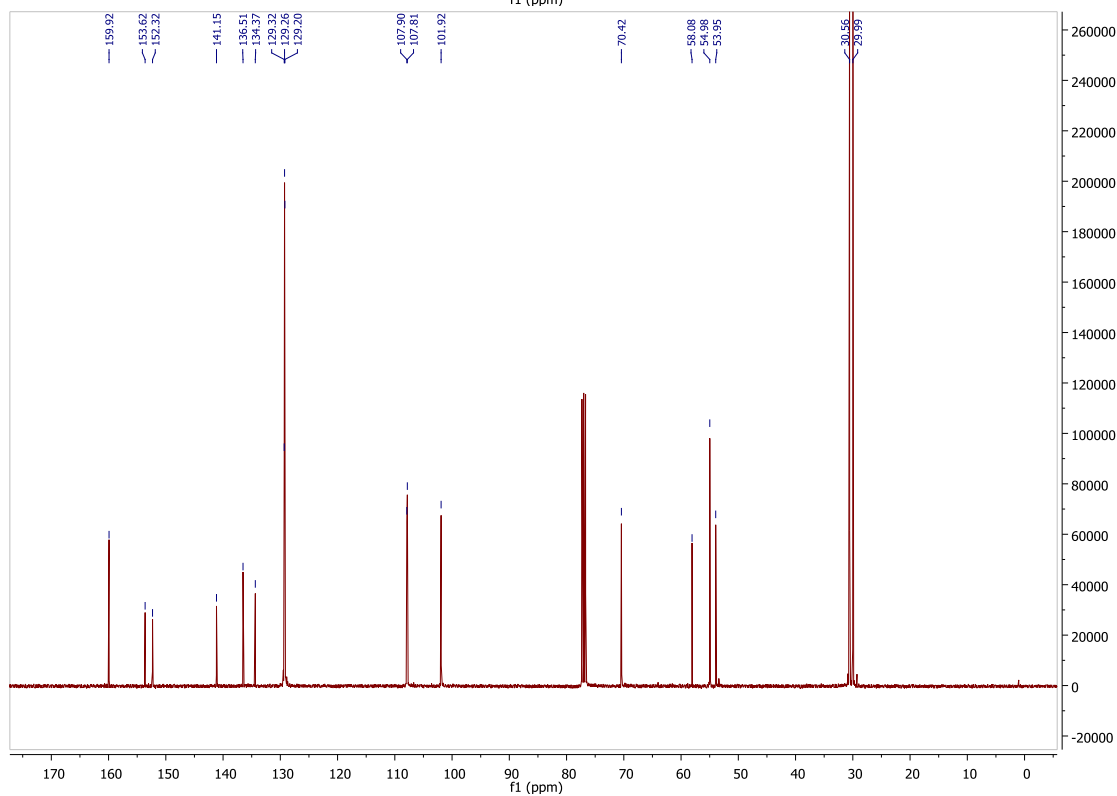
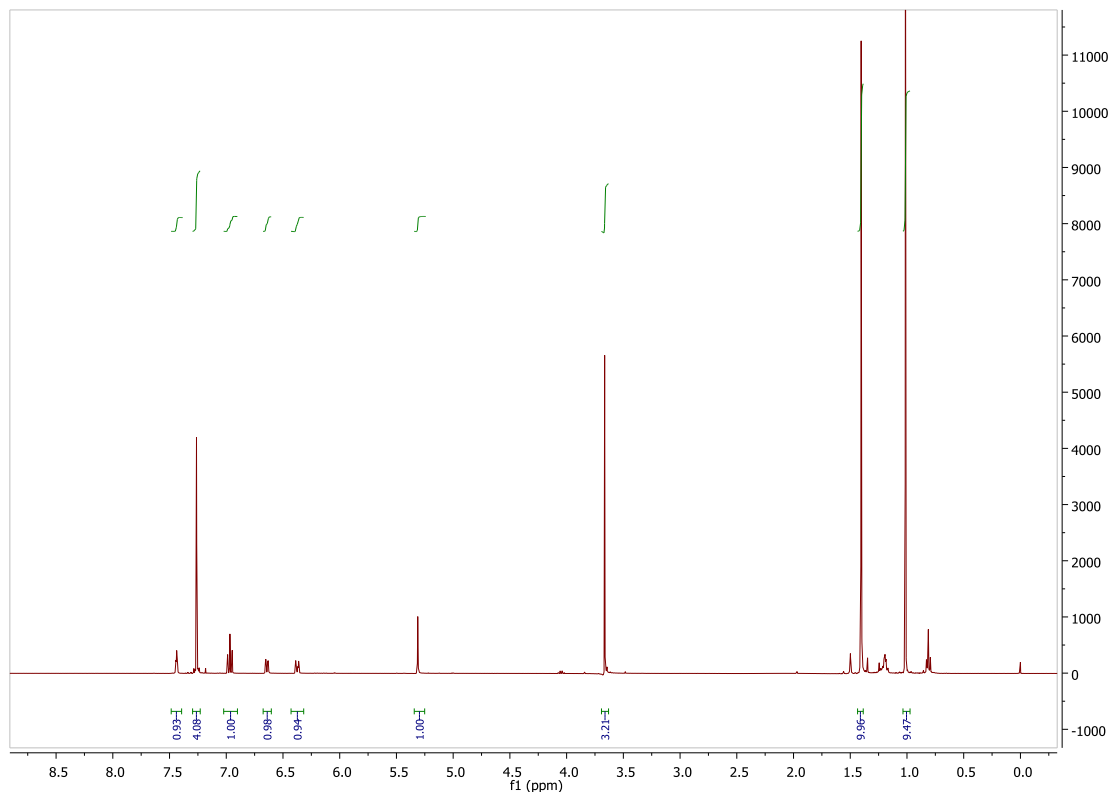


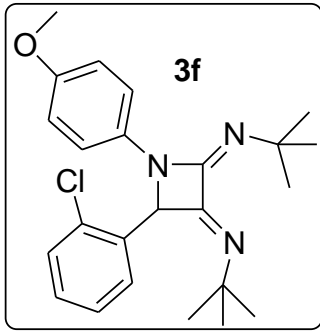
(N,N',N,N')-*N,N'*-(4-(4-Chlorophenyl)-1-(*p*-tolyl)azetidine-2,3-diylidene)bis(4-methoxyaniline) (**3d**)



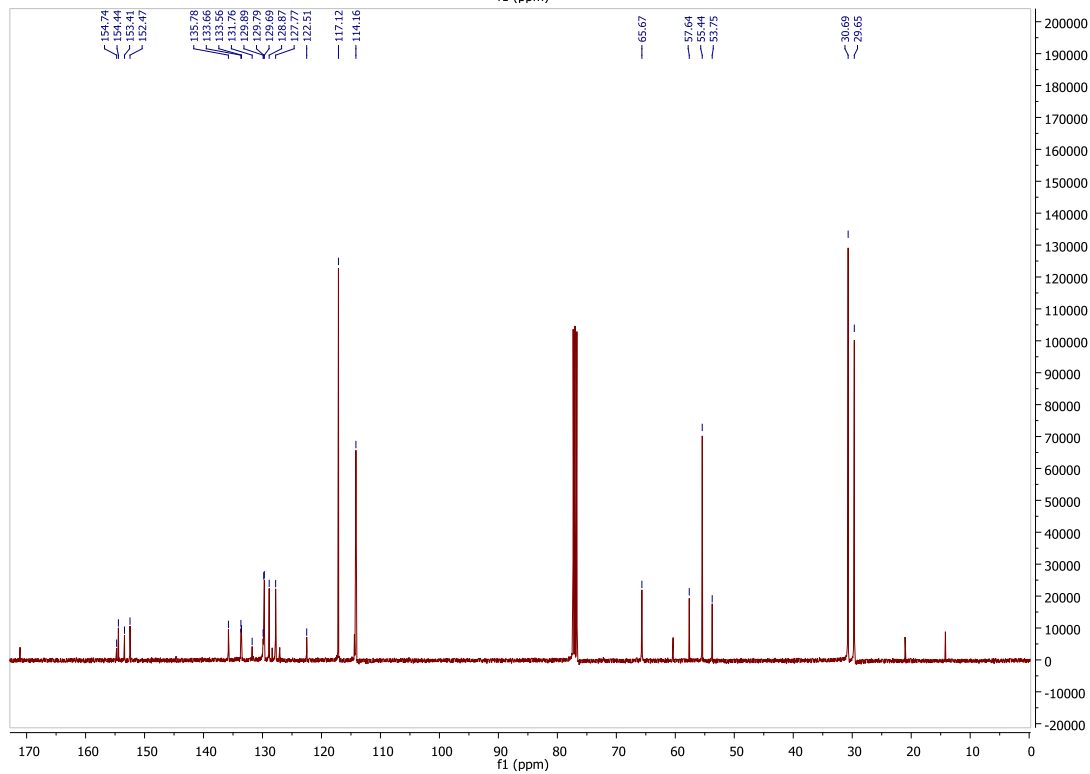
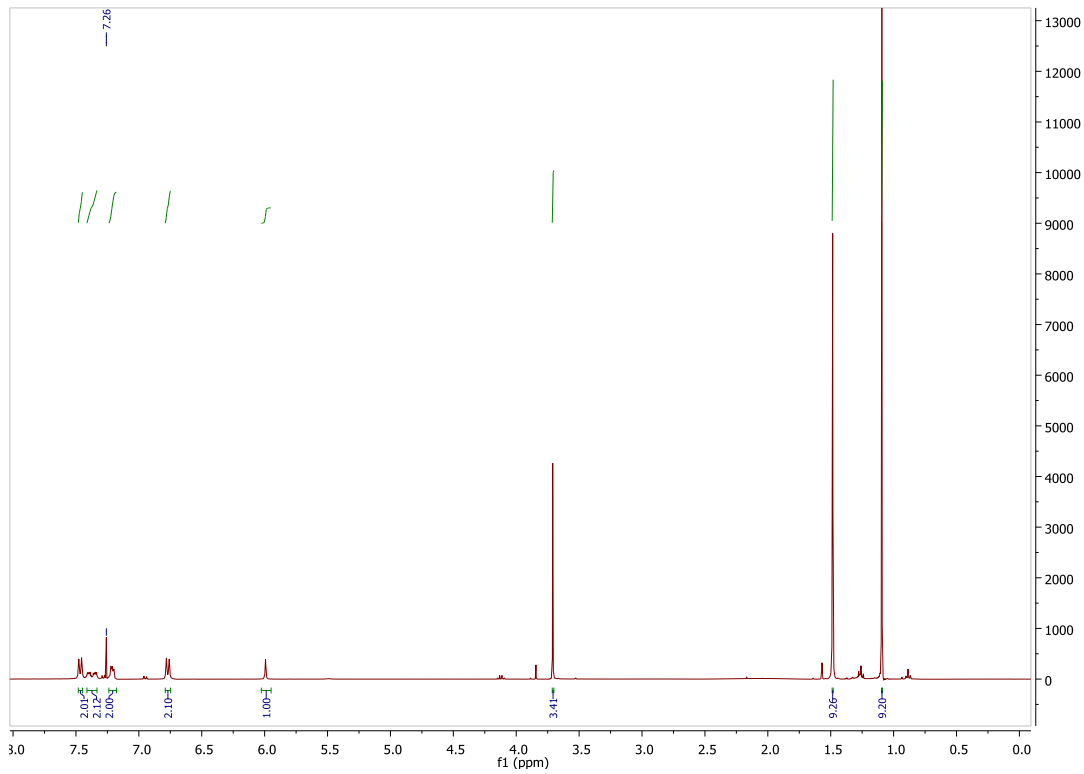


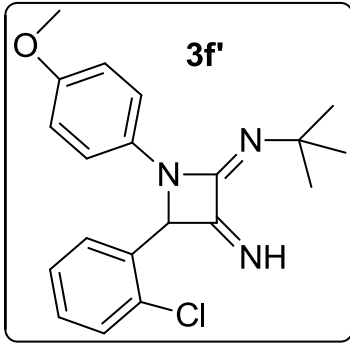
***N,N'*-(4-(4-Chlorophenyl)-1-(3-methoxyphenyl)azetidene-2,3-diyldene)bis(2-methylpropan-2-amine) (3e)**



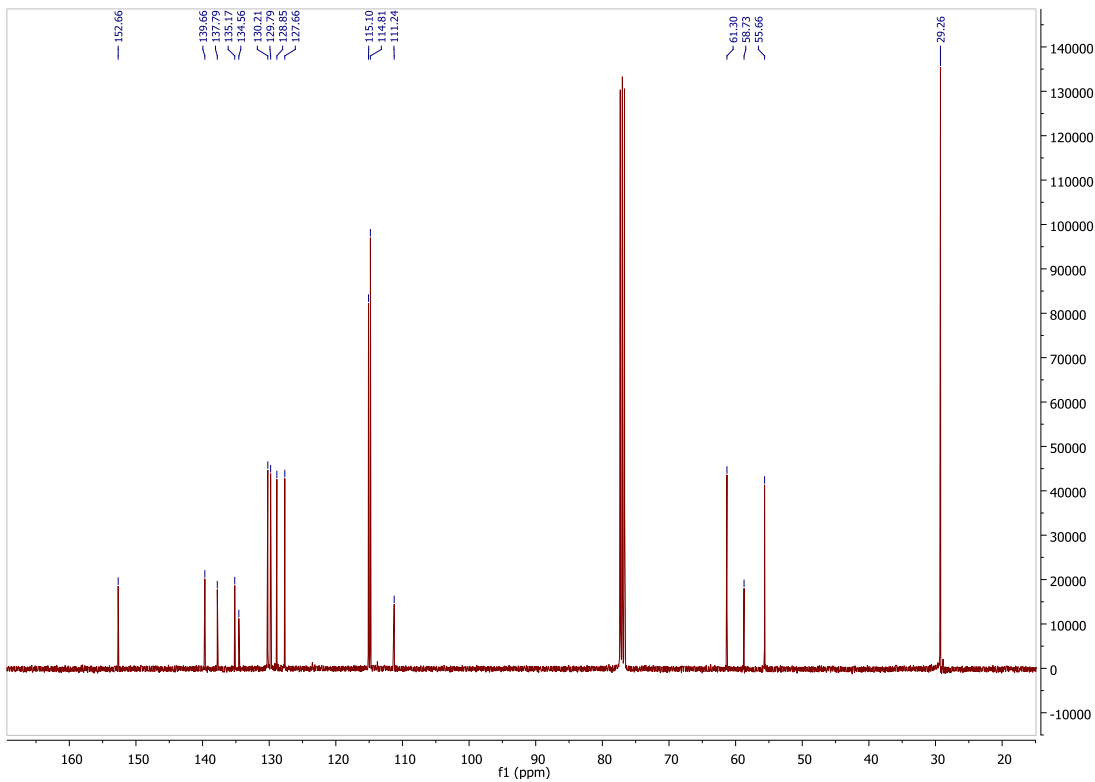
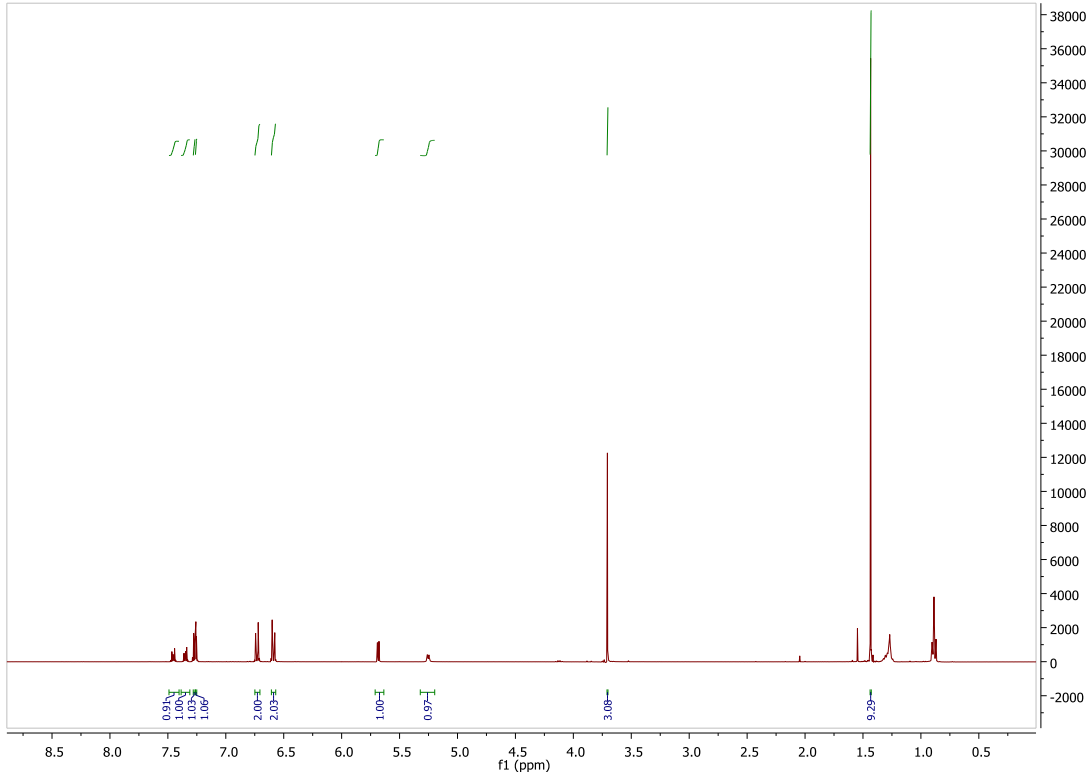


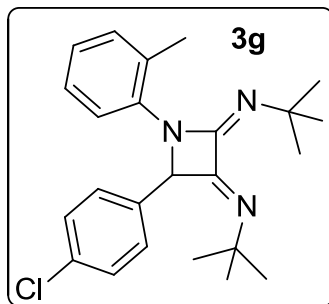
***N,N'*-(4-(2-Chlorophenyl)-1-(4-methoxyphenyl)azetidene-2,3-diylidene)bis(2-methylpropan-2-amine) (3f)**



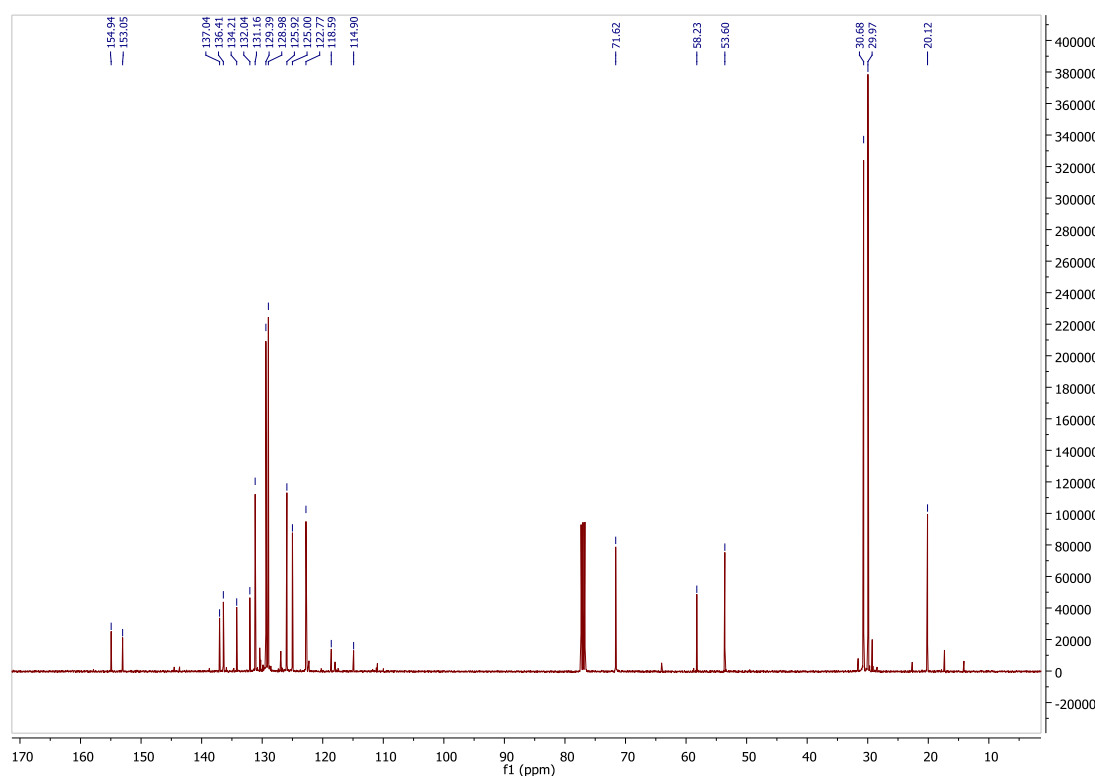
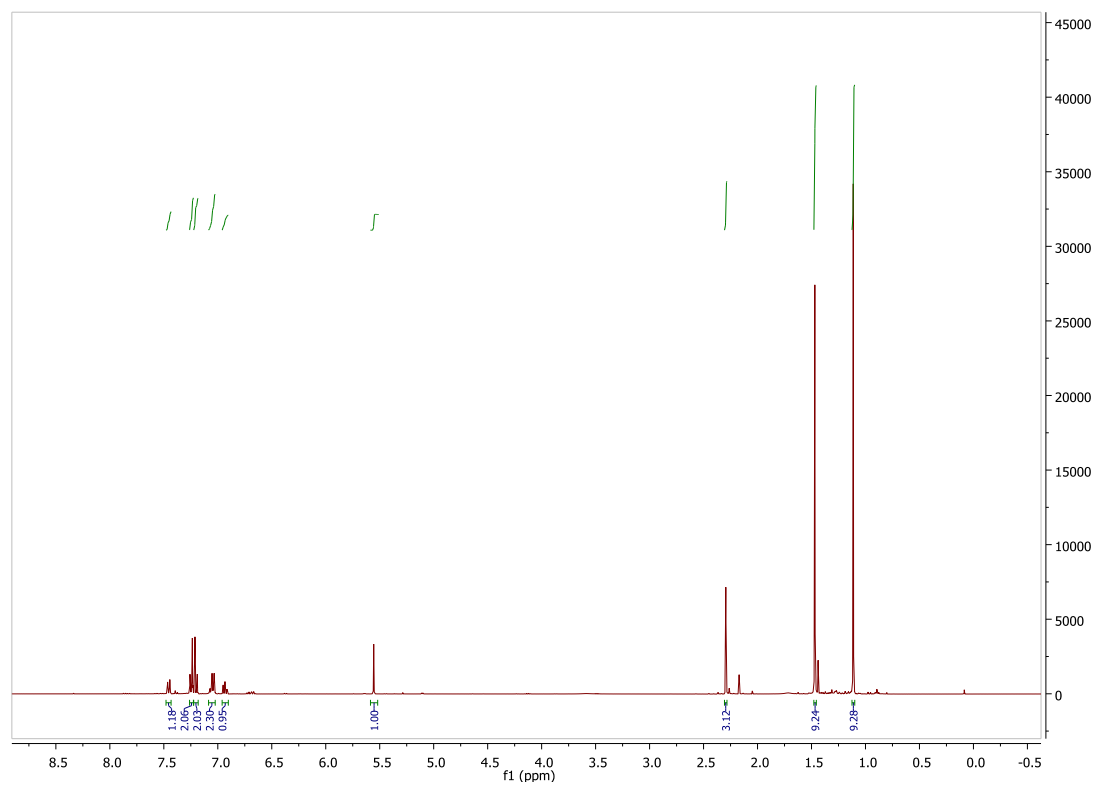


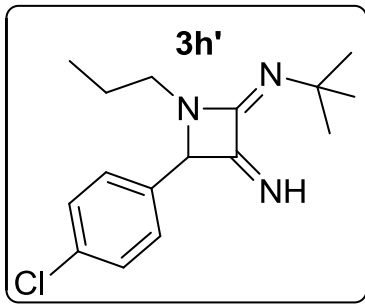
***N*-(4-(2-Chlorophenyl)-3-imino-1-(4-methoxyphenyl)azetidin-2-ylidene)-2-methylpropan-2-amine (3f')**



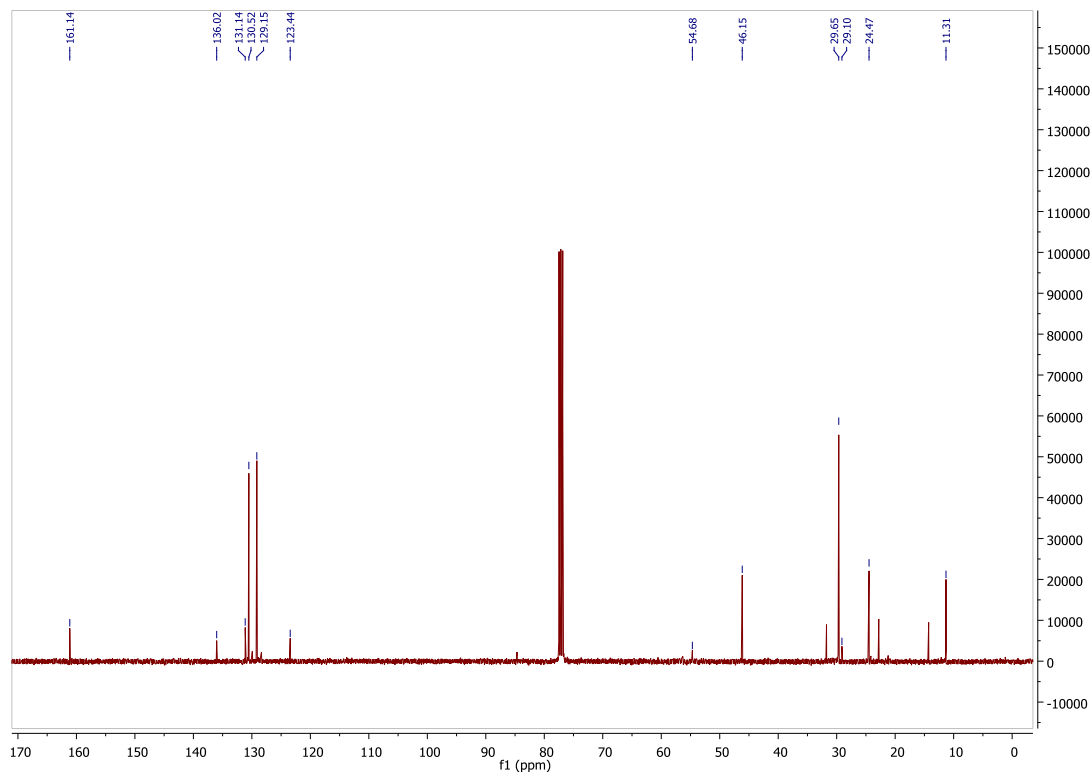
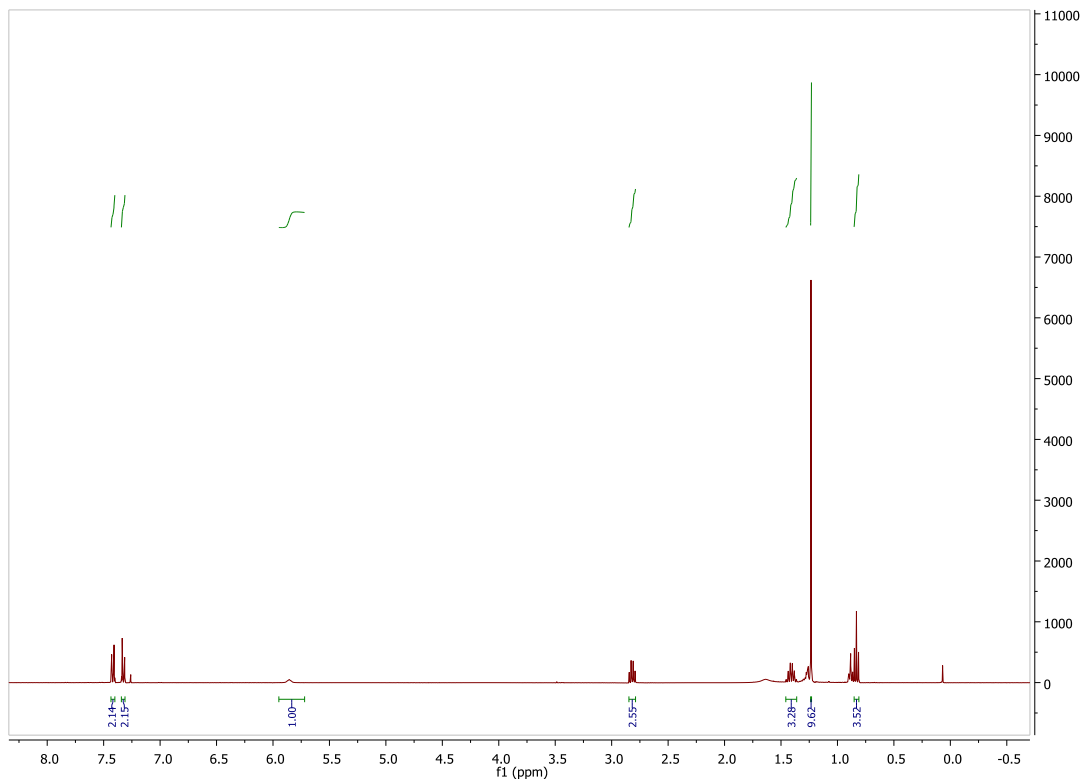


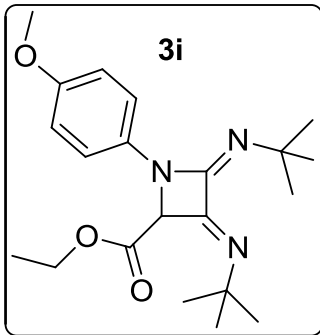
***N,N'*-(4-(4-Chlorophenyl)-1-*o*-tolylazetidine-2,3-diylidene)bis(2-methylpropan-2-amine) (3g)**



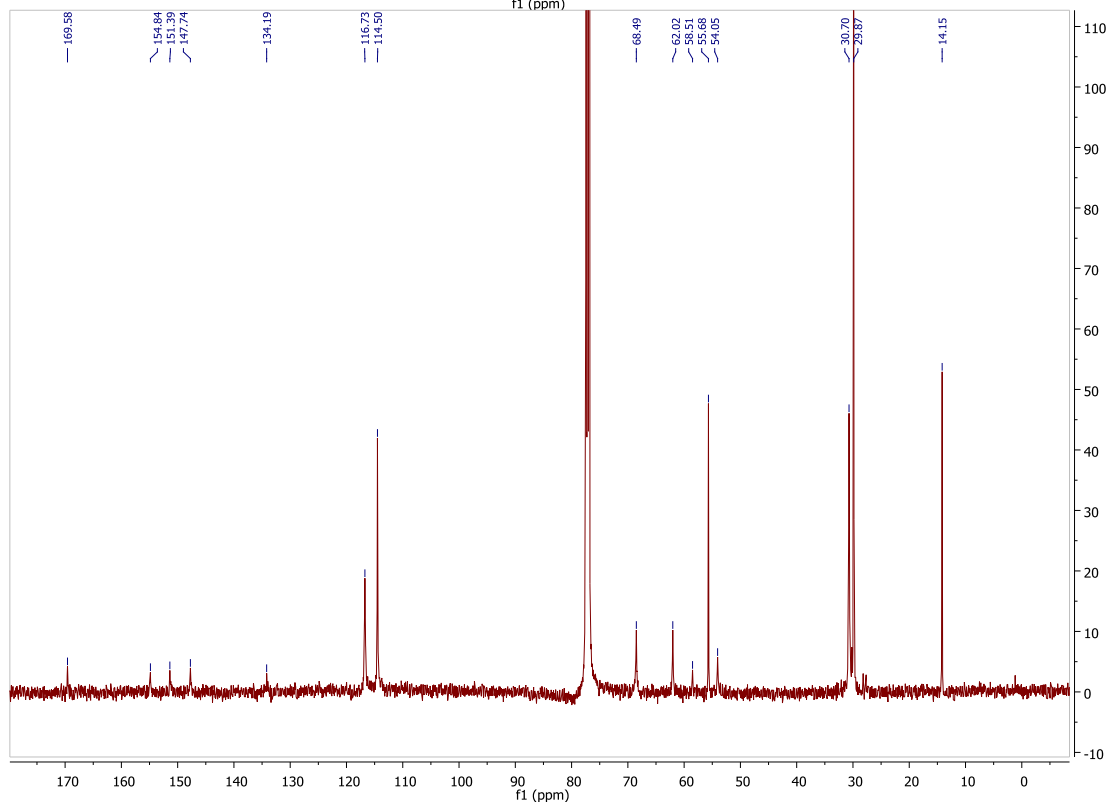
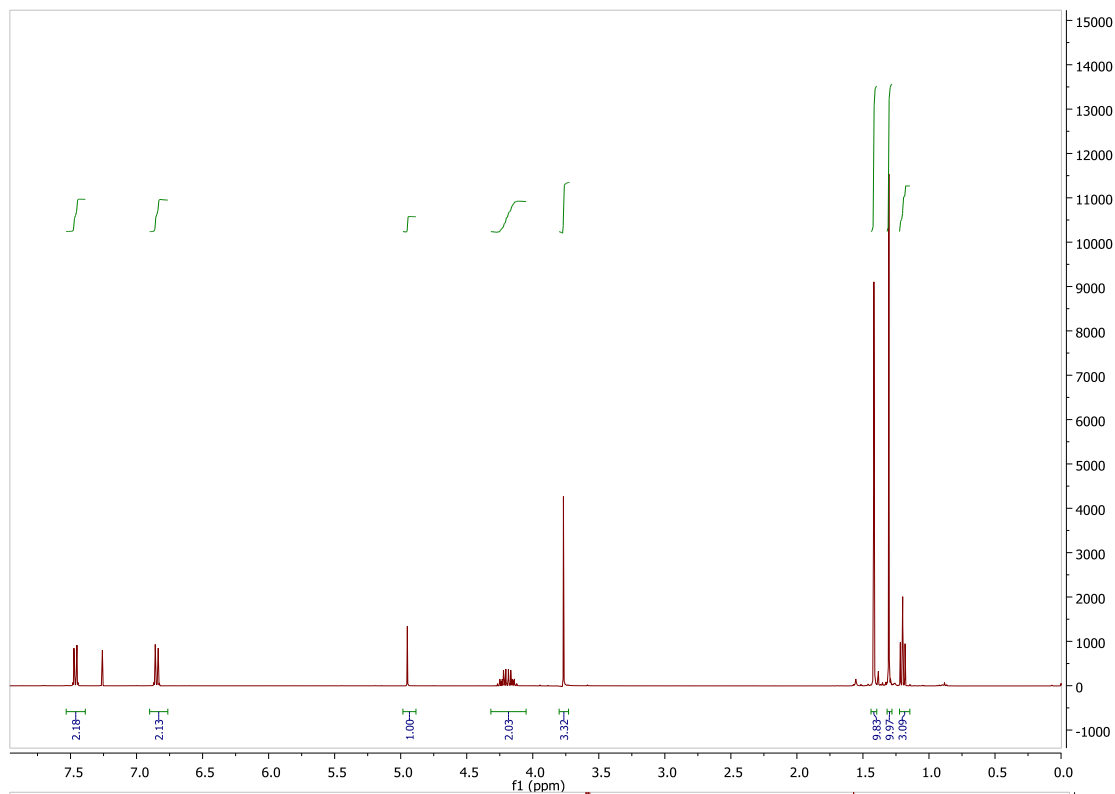


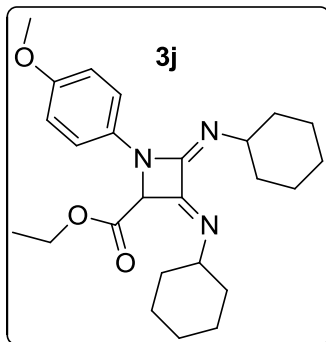
N-(4-(4-Chlorophenyl)-3-imino-1-propylazetidin-2-ylidene)-2-methylpropan-2-amine (3h')



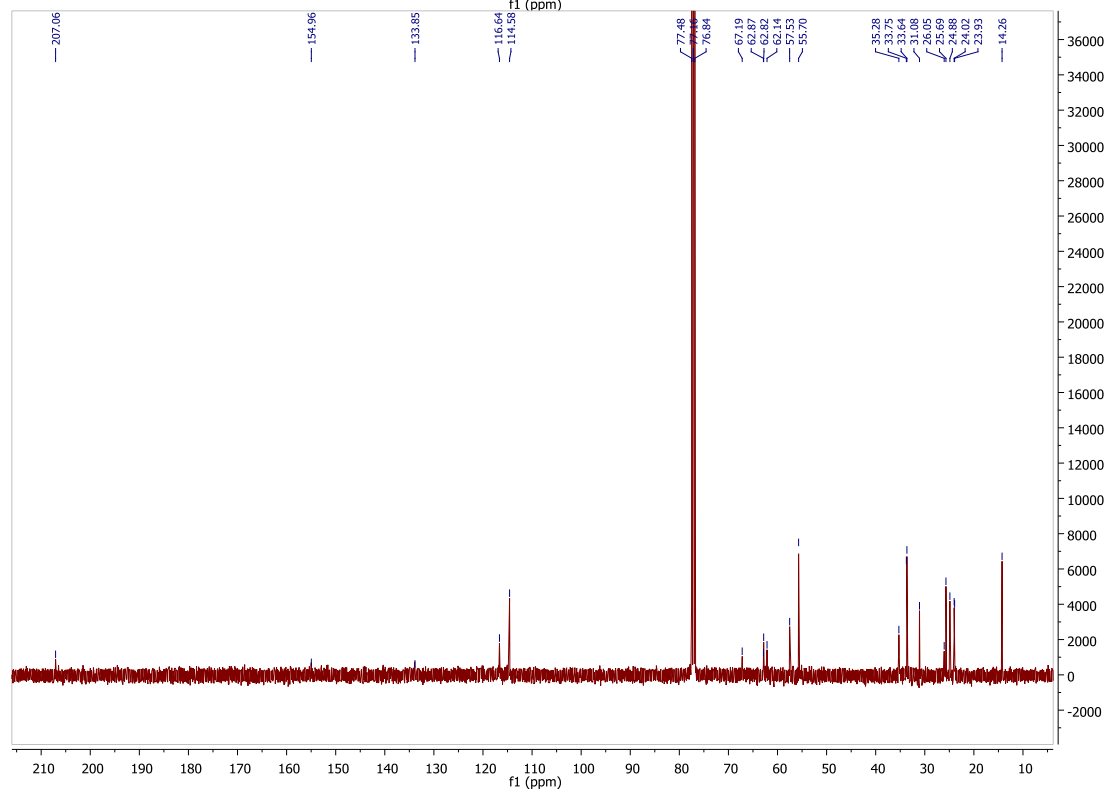
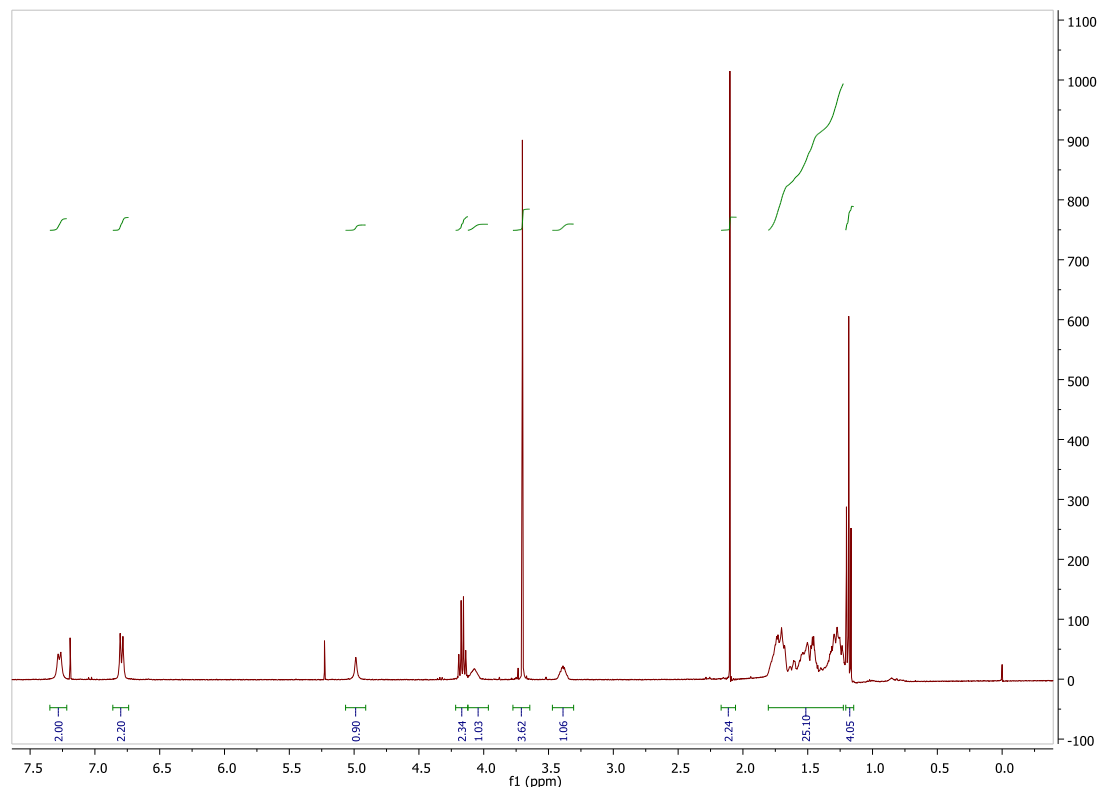


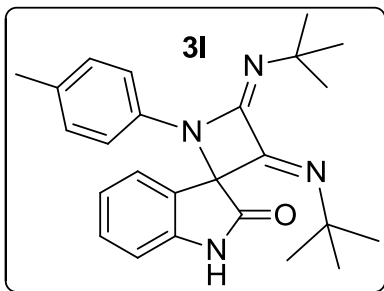
Ethyl 3,4-bis(tert-butylimino)-1-(4-methoxyphenyl)azetidine-2-carboxylate (3i)



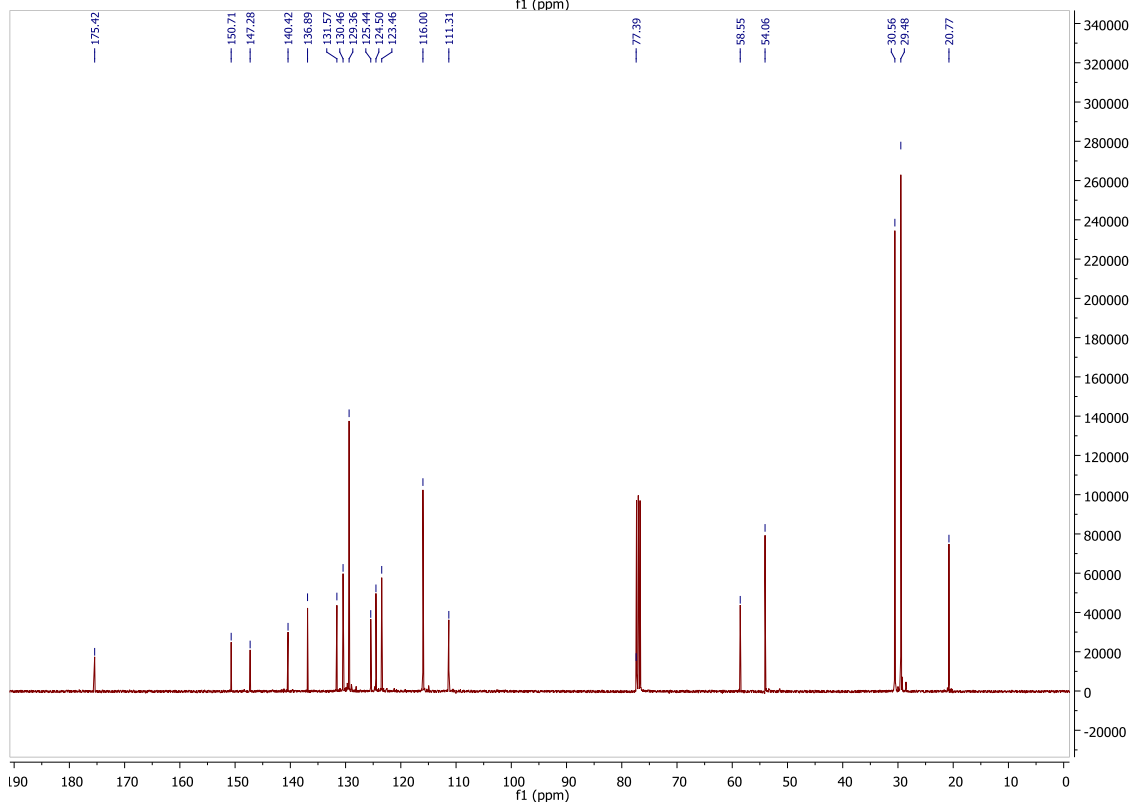
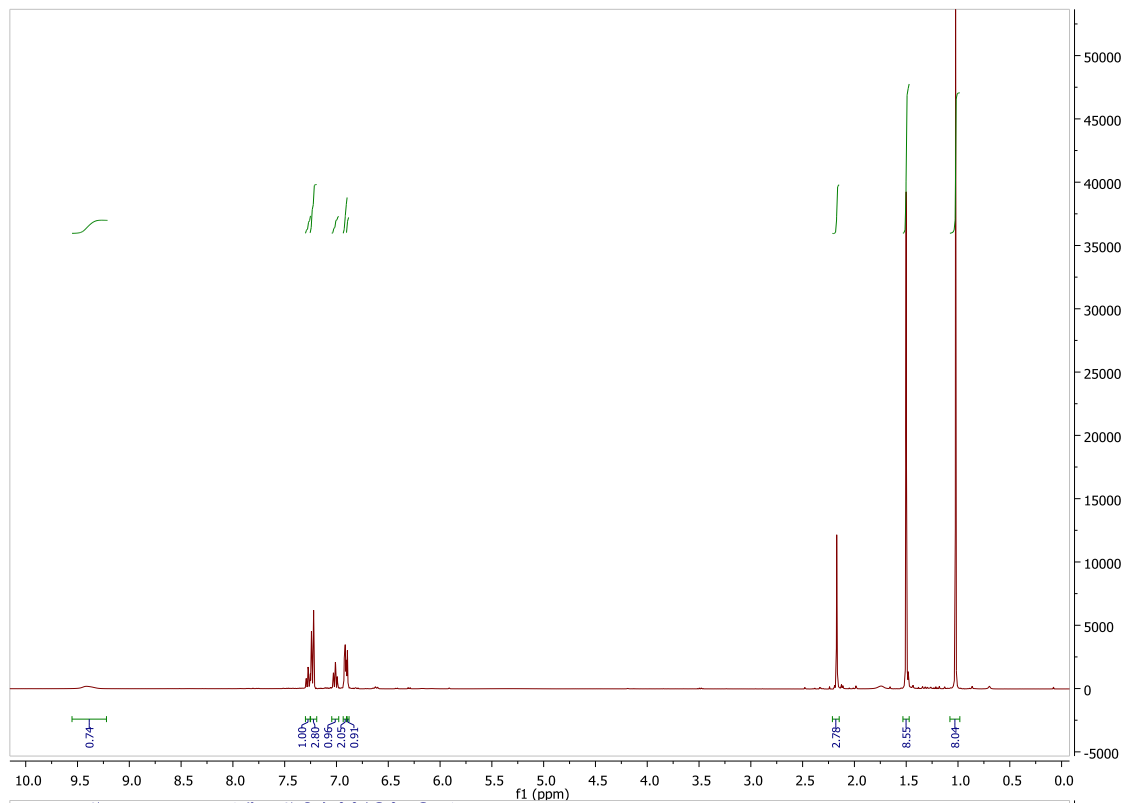


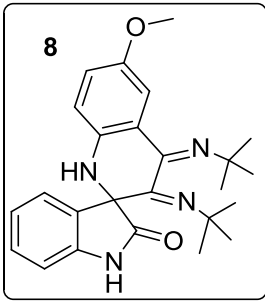
Ethyl 3,4-bis(cyclohexylimino)-1-(4-methoxyphenyl)azetidine-2-carboxylate (3j)



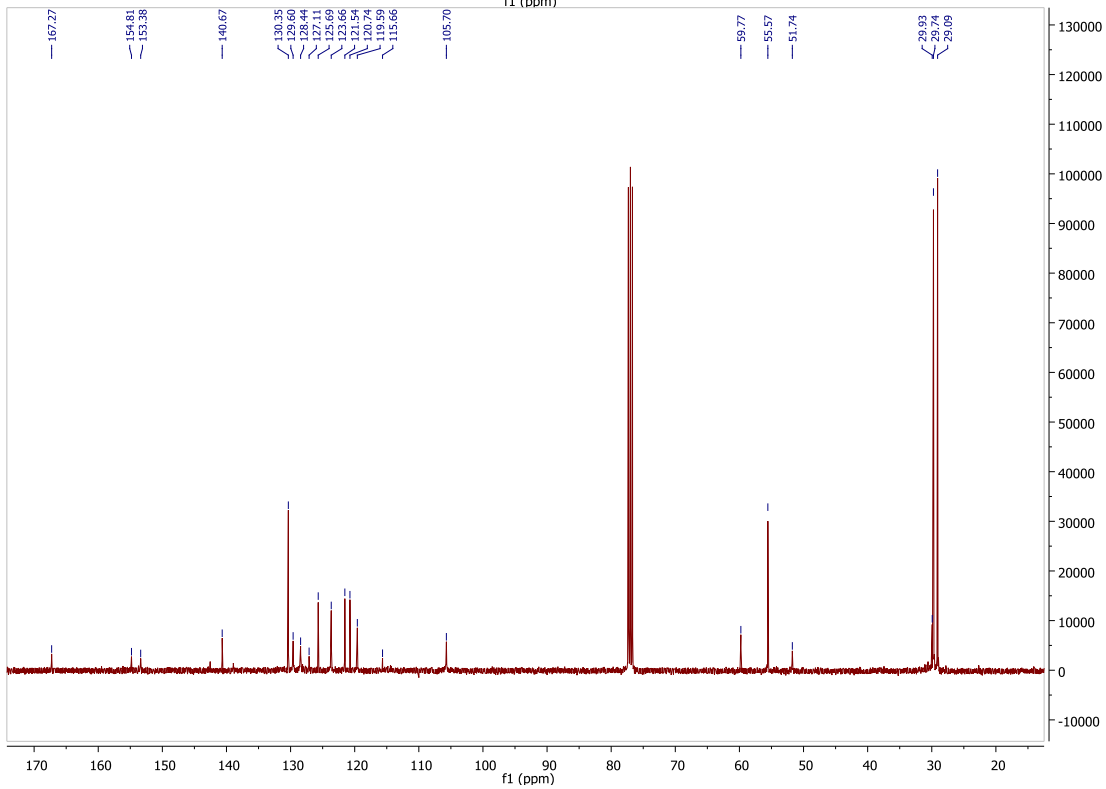
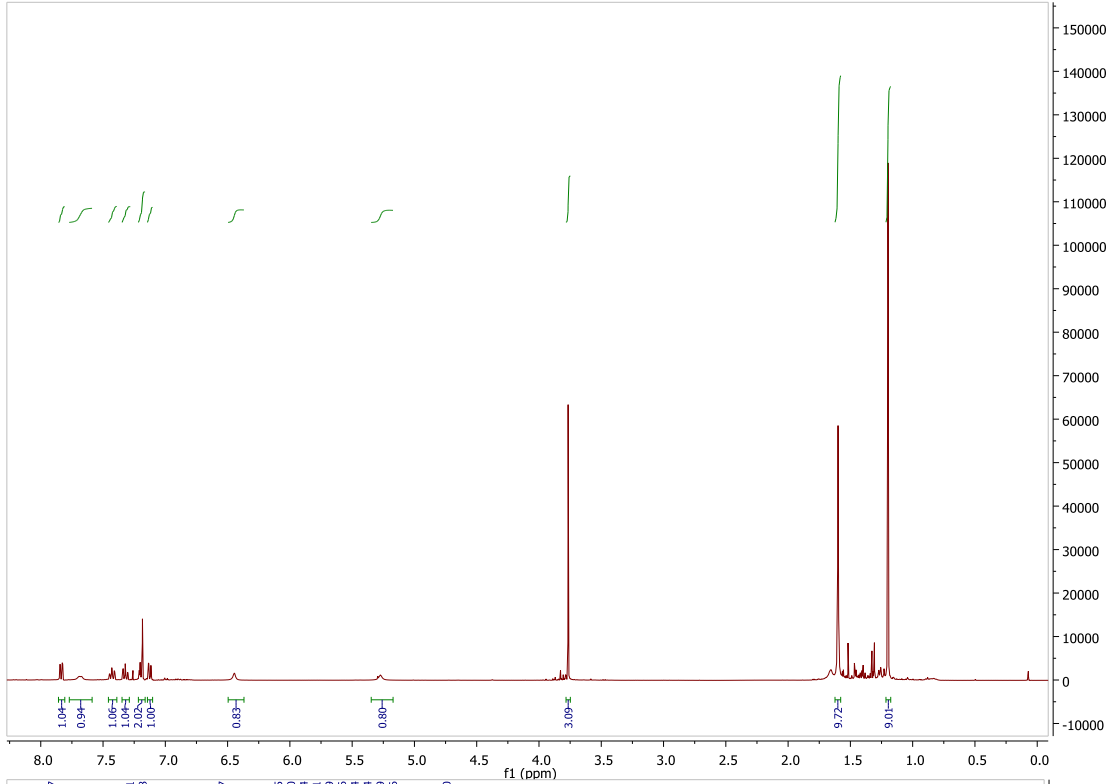


3,4-bis(tert-Butylimino)-1-p-tolylspiro[azetidine-2,3'-indolin]-2'-one (3I)



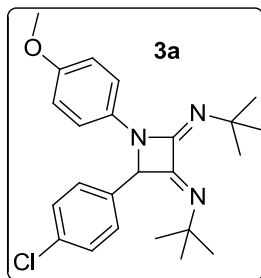


3',4'-bis(tert-Butylimino)-6'-methoxy-3',4'-dihydro-1'H-spiro[indoline-3,2'-quinolin]-2-one (8)

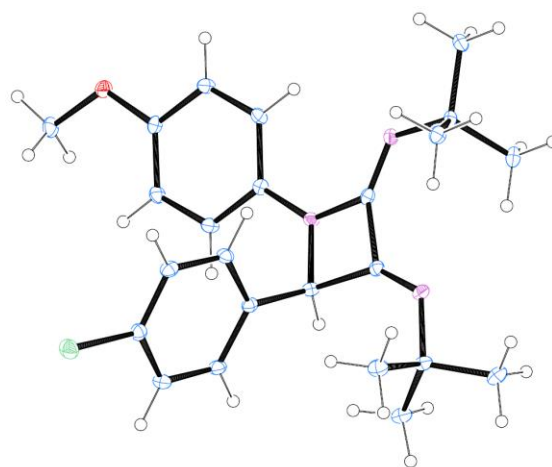
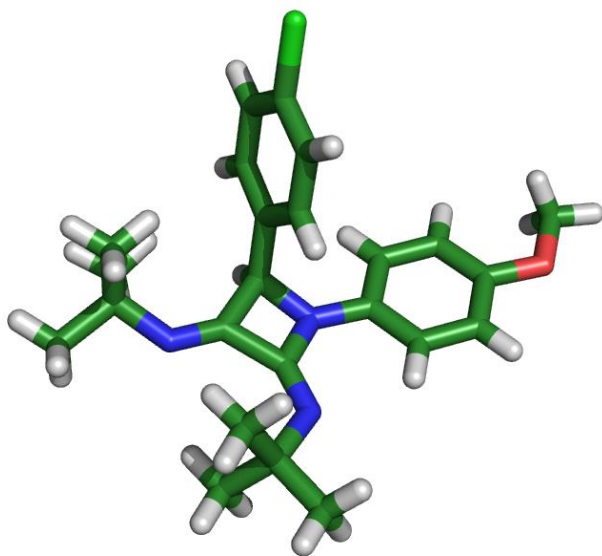


X-ray Structure of bis-aminoazetidine 3a

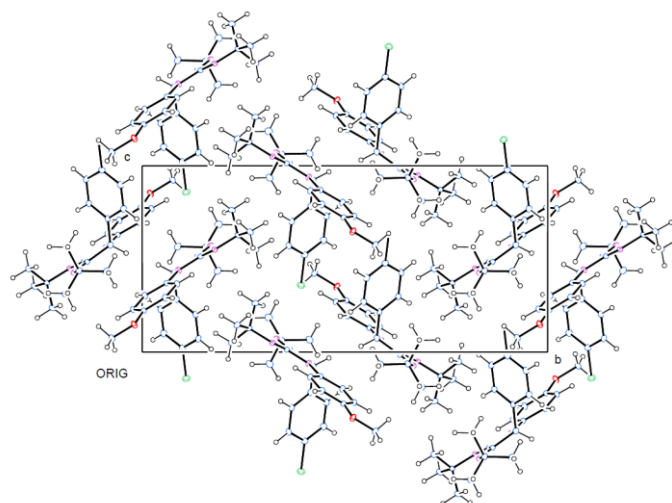
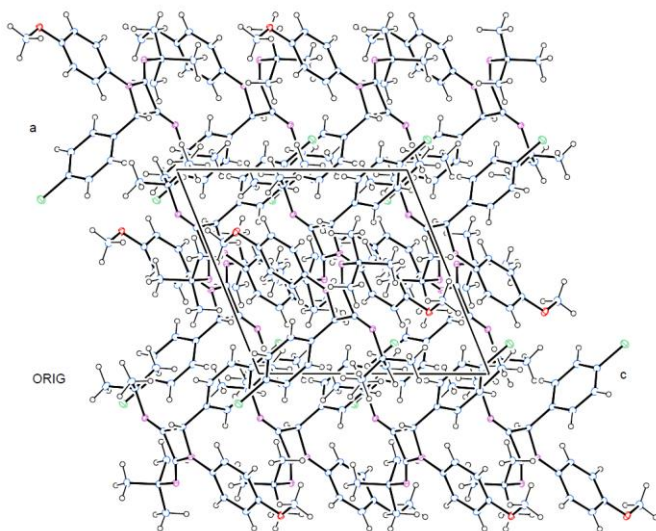
(CCDC 963354)



N,N'-(4-(4-Chlorophenyl)-1-(4-methoxyphenyl) azetidine -2,3-diyldiene)bis(2-methylpropan-2-amine



Cell views of bis-iminoazetidine 3a



Chapter II

**Publication II: Modular Access to
Tetrasubstituted Imidazolium Salts
through Acid-Catalyzed Addition of
Isocyanides to Propargylamines**

Modular Access to Tetrasubstituted Imidazolium Salts through Acid-Catalyzed Addition of Isocyanides to Propargylamines

Ouldouz Ghashghaei,^[a] Marc Revés,^[a] Nicola Kielland,^[b] and Rodolfo Lavilla*^[a,b]

Keywords: Synthetic methods / Homogeneous catalysis / Multicomponent reactions / Nitrogen heterocycles / N ligands

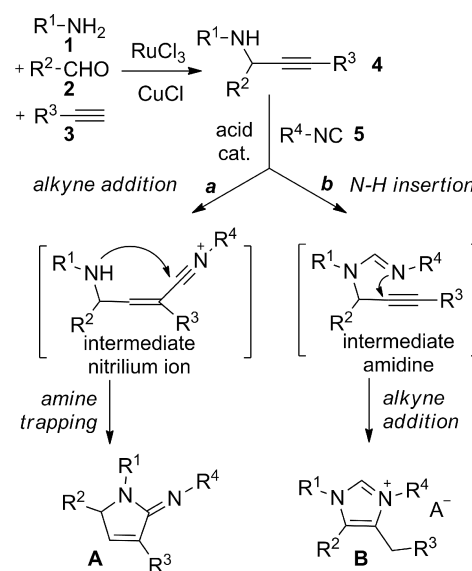
Propargylamines, prepared through A³-coupling of primary amines, aldehydes and terminal alkynes, react with isocyanides in an HCl-catalyzed process to yield tetrasubstituted imidazolium salts. The key step of the mechanism involves the generation of an amidine intermediate, from the isocyanide insertion into the N–H bond of the propargylamine, which in situ evolves by cyclization upon the alkyne moiety. The scope of the process is analyzed and only shows restric-

tions for aliphatic amines, whereas it is quite general regarding the aldehyde, alkyne and isocyanide inputs. The protocol allows the preparation of a wide array of adducts, tandem one-pot processes being also feasible. Mechanistic studies using selected substrates have been used to determine the profile of the reaction and some substitution and functional group limitations. Some post-synthetic transformations of the imidazolium salts have been performed as well.

Introduction

Multicomponent reactions (MCRs) and domino processes, being transformations in which several bonds are generated in a single step, represent an optimized way for the synthesis of complex compounds in a fast manner, especially suitable for the generation of chemical libraries.^[1] In this context, following our interest in isocyanide MCR chemistry,^[2] we decided to tackle the interaction of these substrates with alkynes.^[3] So far, this interaction mostly involves metal-catalyzed processes and conjugated additions to electron-deficient alkynes.^[4] Although remarkable processes have been described by the Van der Eycken group, where the alkyne is a manifold substituent in some inputs of the Ugi MCR;^[5] the direct transformation remains largely unexplored. We envisaged a new reaction profile where the isocyanide would undergo addition to an acid activated triple bond,^[6] and the nitrilium ion so generated would be captured by a nucleophilic amine (Scheme 1, pathway *a*) to yield iminopyrrolines **A** or tautomeric species. Alternatively, the process may proceed by isocyanide insertion^[7] into the N–H bond of the secondary amine, to trigger an intramolecular amidine addition upon the alkyne^[8] through a 5-*exo-dig* route^[9] (Scheme 1, pathway *b*) and [1,3]-H shift, leading to the imidazolium salts **B**. The recent report of Zhu and co-workers, describing an analogous process using

double catalysis of Ag⁺/Yb³⁺ cations,^[10] prompted us to disclose our findings.



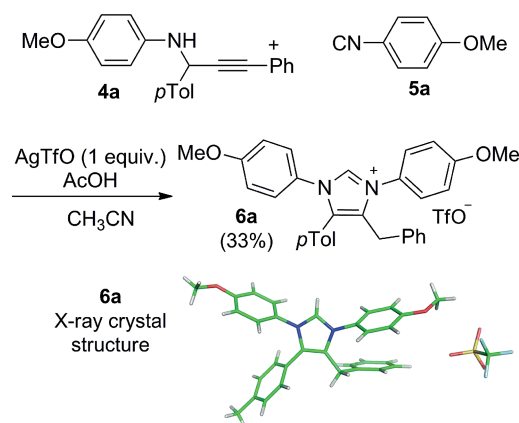
Scheme 1. Hypothetical mechanistic profiles on the interaction of isocyanides and propargylamines.

In this way, we prepared A³ adducts,^[11] arising from the metal-catalyzed interaction of, a primary amine **1**, an aldehyde **2** and a terminal alkyne **3**, to afford propargylamines **4** (Scheme 1). Then, these compounds were treated with isocyanides **5** under variety of acid catalysts (see below). These processes allowed the formation of imidazolium salts **6** (Scheme 2), thus revealing the prevalence of the latter mechanistic choice.

[a] Laboratory of Organic Chemistry, Faculty of Pharmacy, University of Barcelona, Av. Joan XXIII sn, 08028 Barcelona, Spain
E-mail: rlavilla@pcb.ub.es

[b] Barcelona Science Park, Baldiri Reixac, 10–12, 08028 Barcelona, Spain

Supporting information for this article is available on the WWW under <http://dx.doi.org/10.1002/ejoc.201500502>.



Scheme 2. Synthesis of imidazolium salts through silver-catalyzed propargylamine-isocyanide interaction.

Results and Discussion

First the preparation of propargylamines **4** was troublesome, as there are few reports involving the participation of primary amines.^[11c] We were concerned about the incompatibility of the Cu^I cation used in the A³ couplings with isocyanides **5**, via the formation of inert complexes, therefore requiring purification of the A³ adducts. After much experimentation, it was shown that the concomitant use of Ru^{III}/Cu^I catalysis in THF (Li-Wei method)^[11d] was productive and, importantly, allowed the subsequent isocyanide interaction to be performed in tandem (see below). The aniline-derived substrates were prepared in this way, whereas those arising from benzylamine were synthesized using van Eycken conditions.^[11c]

Next, the reaction of propargylamine **4a** and isocyanide **5a** was investigated (Scheme 2). Several Lewis acids such as CuBr, InCl₃, AuCl₃, AgOTf, Sc(OTf)₃, I₂ and ICl allowed the detection of the corresponding salt **6a** in low yields. However, the combination of AgOTf/AcOH was more productive and afforded the imidazolium salt **6a** in 33% yield. The X-ray diffraction of a monocrystal of this compound secured the proposed structure.^[12]

The best results were observed when propargylamine **4a** was treated with a stoichiometric amount of HCl (dioxane solution), in a 1:1 mixture of ACN/THF at room temp., affording the final adduct in 82% yield (Table 1). For unknown reasons, the imidazolium salts were better isolated after aqueous Na₂CO₃ extraction^[13] (clean HPLC profiles), and analytical samples can be obtained by standard flash chromatography (SiO₂), although some decomposition was observed during purification. Consequently, we assume that the anion of the imidazolium species is CO₃²⁻, although its unequivocal identification was not possible (MS-Ve technique).

The use of imidazolium salts and their derivatives is widespread in several areas such as medicinal chemistry or biology.^[14] Imidazolium salts belong to a very common class of ionic liquids,^[15] and constitute the primary source of N-heterocyclic carbenes,^[16] frequently used ligands in organometallic chemistry. In this respect, PEPSI catalysts

Table 1. Range of the components.

Entry	Adduct	R ¹ , R ² , R ³ , R ⁴	Yield ^[a]
1	6a	4-MeOC ₆ H ₄ , <i>p</i> Tol, Ph, 4-MeOC ₆ H ₄	82%
2	6b	<i>p</i> Tol, Ph, Ph, <i>t</i> Bu	82%
3	6c	4-MeOC ₆ H ₄ , <i>p</i> Tol, Ph, <i>t</i> Bu	92%
4	6d	Bn, <i>i</i> Pr, Ph, <i>c</i> Hex	23% ^[b]
5	6e	4-MeOC ₆ H ₄ CH ₂ , Ph, Ph, <i>c</i> Hex	10% ^[b]
6	6f	4-MeOC ₆ H ₄ , 4-ClC ₆ H ₄ , <i>p</i> Tol, <i>t</i> Bu	56% ^[c]
7	6g	4-MeOC ₆ H ₄ , 4-ClC ₆ H ₄ , <i>n</i> -C ₅ H ₁₁ , <i>t</i> Bu	85%
8	6h	<i>p</i> Tol, Ph, Ph, <i>c</i> Hex	82%
9	6i	<i>p</i> Tol, Ph, Ph, EtCO ₂ CH ₂	96% ^[c]
10	6j	<i>p</i> Tol, Ph, Ph, 2,6-(H ₃ C) ₂ C ₆ H ₃	27% ^[d]
11	6k	<i>p</i> Tol, 4-ClC ₆ H ₄ , Ph, 2-naphthyl	75% ^[e]

[a] Obtained from general procedure A (see Supporting Information). [b] AcOH (1 equiv.) and AgTfO (20%) were used instead of HCl (see SI). [c] The hydrolyzed betaine **6i'** was also generated during purification. [d] Reaction performed at 60 °C. [e] Reaction performed with MeSO₃H (1 equiv.) instead of HCl, due to the low solubility of the propargylamine hydrochloride.

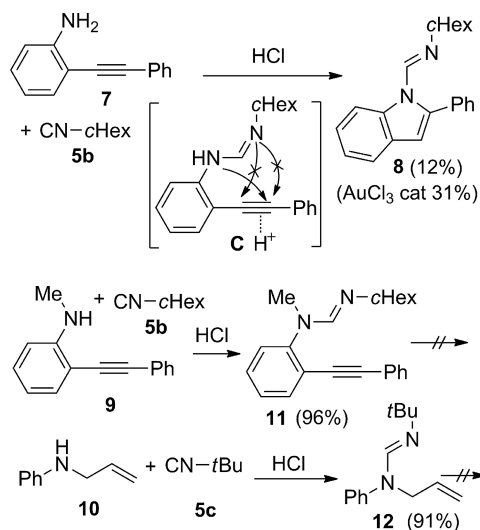
rank among the most active catalysts for Pd-coupling reactions.^[17] Unfortunately the preparations of polysubstituted imidazolium salts usually involve complex multistep syntheses.^[18] Therefore, many of the previously mentioned applications have been tested only on simple, easily accessible salts, usually obtained by alkylation of the parent imidazoles.^[19] Thus, a general and direct access to these compounds would allow a programmed preparation of diversely substituted derivatives and hence a finer and more rational modulation of their properties.

Next the scope of the reaction was tested. Propargylamines **4** having N-aromatic residues smoothly reacted with isocyanides to afford the corresponding products (Table 1, entries 1–3, 6–11). On the other hand, the N-benzyl derivatives afforded imidazolium salts **6d** and **6e** in lower yields (Table 1, entries 4 and 5), whereas N-alkyl derivatives did not react under these conditions. The use of milder acids (AcOH, citric acid) was inefficient, *p*TosOH gave low yields and the HCl-promoted addition remained as the only productive transformation (23% and 10% respectively). This fact constitutes the main practical limitation of the procedure. Referring to the aldehyde moiety, the process allows a wider scope; including aromatic (both electron-rich and electron-poor, Table 1, entries 1–3, 5–11) and alkyl derivatives (Table 1, entry 4). With respect to the terminal alkyne substitution, a variety of aromatic (Table 1, entry 1–6, 8–11) and aliphatic residues (Table 1, entry 7) are tolerated.

Finally, a wide range of isocyanides yielded the corresponding products, allowing the introduction of bulky aliphatic groups such as *t*Bu and *c*Hex (Table 1, entries 2–8). Aromatic isocyanides were also productive, either displaying electron-donating groups (MeO) or bulky residues such as xylyl and naphthyl groups (Table 1, entries 1, 10, 11). Methyl isocyanoacetate afforded the corresponding imidazolium salt **6i** (entry 9) and partially hydrolyzed during chromatographic purification, presumably to the betaine **6i'** (see SI). Although PhosMIC and TosMIC underwent satisfactory conversions, the corresponding adducts

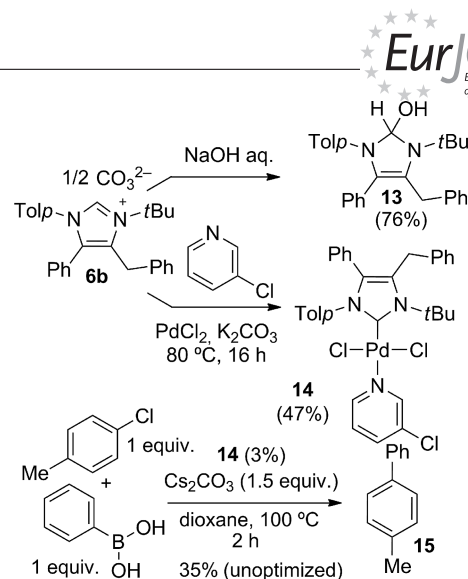
(detected by HPLC/MS) quickly decomposed during chromatographic purification.

In order to further explore the range of the reaction upon distinct substrates, we performed a series of experiments. First of all, the intermolecular version of this interaction was tested. In this way, disubstituted alkynes (diphenylacetylene or 1-phenyl-1-hexyne) were treated with primary anilines and isocyanides, under a variety of catalysts, but no imidazolium salts could be detected. This result reinforces the need of an intramolecular mode of action. The *o*-alkynylaniline **7** was treated with isocyanide **5b** to afford indole **8** in 12% yield (31% with AuCl₃ catalysis, Scheme 3). The process may start with an N–H isocyanide insertion to generate amidine **C**, which would subsequently cyclize (*5-endo-dig*) to afford the final product (Scheme 3), in a transformation related to the Larock indole synthesis.^[20] Noteworthy, when 2-phenylindole reacted with isocyanide **5b** under the same conditions, product **8** was not formed, suggesting that the formation of the amidine moiety takes place first.



Scheme 3. Mechanistic probes.

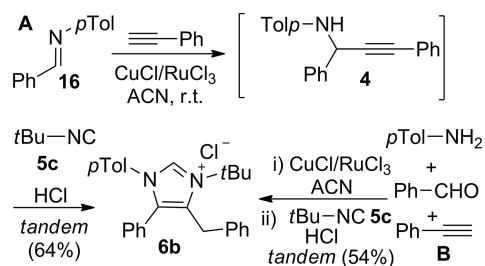
Interestingly, the substituted anilines **9** and **10** afforded, on interaction with isocyanides **5b** and **5c**, amidines **11** (96%) and **12** (91%) respectively (Scheme 3). The processes stop at the amidine formation stage and the cyclizations upon the π systems do not proceed, although imidazolium rings have been formed this way in related systems.^[21] When attempting a different extraction procedure, using aq. NaOH (1 M) as a basic quencher, the hydroxy derivative **13** (Scheme 4) cleanly precipitated, and was isolated in 76% yield and purified simply by filtration. Its structure was clearly established by spectroscopic methods. Interestingly, ¹H NMR showed two rotamers, probably due to the *tert*-butyl steric hindrance, albeit displaying a single peak in the HPLC profile. As a proof of concept, the PEPSI-type catalyst **14** was prepared from imidazolium salt **6b**, following Organ's procedure.^[22] The thus prepared palladium catalyst was used in a standard Suzuki reaction using 4-chlorotoluene as representative substrate, which was successfully cou-



Scheme 4. Post-transformation reactions and application.

pled with phenylboronic acid to furnish biphenyl **15** (35% yield, unoptimized, Scheme 4).

We next considered the feasibility of tandem procedures, to speed up the overall process. In this way, the pregenerated imine **16** was subjected to alkyne addition under Cu^I/Ru^{III} catalysis followed by in situ treatment with isocyanide **5c** and HCl to successfully afford the imidazolium salt **6b** (64%; Scheme 5, A). Furthermore, the direct synthesis of the same adduct by interaction of the four reactant inputs, without isolation of any intermediates was achieved by linking the standard A³ reaction with the isocyanide interaction (Scheme 5, B). Interestingly, this tandem/one-pot procedure, albeit less productive (54%) and clean than the original stepwise reaction, does not show synthetic restrictions due to incompatibilities of isocyanides with metal cations present in the medium. Likewise, imidazolium salts **6h** (49%) and **6i** (68%) were also prepared following this protocol.



Scheme 5. Tandem multicomponent approaches.

Conclusions

In conclusion, the formation of tetrasubstituted imidazolium salts by an HCl-promoted isocyanide/propargylamine interaction has been described. The scope of the process has been analyzed and some synthetic uses of the corresponding adducts determined. The reaction is not productive for aliphatic amines, whereas the Zhu reaction^[10] works well for these substrates. However, the milder condi-

tions used in our transformation allow the preparation of *N*-*tert*-butylimidazolium salts without elimination problems. Overall, our process shows that the stoichiometric use of HCl leads to the desired products, however in lower yields and parallels the mechanistic profile described for this interaction. Although for some sensitive substrates, the protic acid may be deleterious, the soft activation needed and the consumption of this reagent may prevent unwanted decomposition. Finally, tandem/one-pot protocols linking the synthesis of the propargylamines, by an A³ reaction, with the isocyanide addition step have been developed.

Experimental Section

Preparation of Propargylic Amines (4): *N*-(aryl)propargylamines were prepared using a modification of Li and Wei's procedure^[11d] in non-aqueous media: In a Schlenk tube, 2.0 mmol (1.00 equiv.) of aldehyde and 2.2 mmol (1.1 equiv.) of amine were dissolved in 5 mL of THF under inert atmosphere. The tube was sealed and the mixture was heated at 60 °C until complete consumption of the aldehyde (2 h). Next CuCl (30 mol-%), RuCl₃ (3 mol-%) and the alkyne (2.4 mmol, 1.2 equiv.) were added. The mixture was stirred at room temp. (30 min), and then heated at 50 °C until consumption of the imine (24 h). The solution was cooled, poured into water, and extracted with DCM. The combined organic phases were washed with water, dried with MgSO₄ and concentrated in vacuo. Purification by flash chromatography on silica gel (hexanes/AcOEt) afforded the corresponding propargylamines.

N-benzylpropargylamines were prepared following the procedure reported by Van der Eycken et al.^[11c]

General Procedure A: Propargylamine **4** (0.5 mmol, 1 equiv.) was dissolved in THF (1.5 mL) and ACN (1.5 mL) under inert atmosphere. Next isocyanide **5** (0.5 mmol, 1 equiv.) was added. A 4 M HCl solution in dioxane (125 μL, 1 equiv.) was added and the mixture stirred at room temp. until consumption of the propargylamine (4 h). Next the reaction was quenched with saturated Na₂CO₃ aq. solution (20 mL) and extracted with AcOEt (3 × 10 mL). The combined organic phases were dried with MgSO₄ and concentrated in vacuo to afford the corresponding imidazolium salts. Analytically pure samples of the products were obtained by flash chromatography on silica gel (hexanes/EtOH).

General Procedure B (tandem): In a Schlenk tube, the aldehyde (1.0 equiv.) and the amine (1.05 equiv.) were dissolved in THF (3 mL) under inert atmosphere. The tube was sealed and the mixture was heated at 60 °C until complete aldehyde consumption (2 h.). Next CuCl (30 mol-%), RuCl₃ (3 mol-%) and the alkyne (1.2 equiv.) were added. The mixture was first stirred at room temp. for 30 min, and then heated at 50 °C (24 h). The solution was cooled to room temp. and diluted with ACN (3 mL). The isocyanide (1.1 equiv.) was then added, followed by a 4 M HCl solution in dioxane (0.125 μL, 1 equiv.). The solution was stirred at room temp. until reaction completion (24 h) and then quenched with Na₂CO₃ (saturated aq. solution, 40 mL) and extracted with AcOEt (3 × 20 mL). The combined organic phases were dried with MgSO₄ and concentrated in vacuo, to afford the corresponding imidazolium salts. Analytically pure samples were obtained by flash chromatography on silica gel (hexanes/EtOH). In this way, from the corresponding inputs, imidazolium salts **6b** (54%), **6h** (49%), **6i** (68%) were obtained.

Typical Procedure C (tandem from the imine): In a Schlenk tube, imine **16** (204 mg, 1.05 mmol.), phenylacetylene **3** (122 mg,

1.2 mmol), CuCl (31 mg, 30 mol-%), RuCl₃ (6.5 mg, 3 mol-%) were dissolved in THF (3 mL) under inert atmosphere. The mixture was then stirred at 50 °C for 24 h. The solution was cooled to room temp. and diluted with ACN (3 mL). Then, *tert*-butyl isocyanide (91 mg, 1.1 mmol.) was then added, followed by a 4 M HCl solution in dioxane (0.125 mL, 1 equiv.). The resulting solution was stirred at room temp. until reaction completion (24 h) and then quenched with Na₂CO₃ (saturated aq. solution, 40 mL) and extracted with AcOEt (3 × 20 mL). The combined organic phases were dried with MgSO₄ and concentrated in vacuo, to afford imidazolium salt **6b** (412 mg, 64%). Analytically pure sample was obtained by flash chromatography on silica (hexanes/EtOH).

Preparation of Hydroxyldihydroimidazole (13): *N*-(1,3-diphenylprop-2-ynyl)-4-methylaniline (149 mg, 0.5 mmol) was dissolved in 1.5 mL of THF and ACN (1.5 mL) under inert atmosphere. *tert*-butyl isocyanide (50 mg, 0.6 mmol) was added, followed by a 4 M HCl solution in dioxane (0.125 μL, 1 equiv.). The solution was stirred at room temp. until reaction completion (24 h) and then quenched with a NaOH aq. solution (1 M, 3 mL) was added and the solution was stirred vigorously at room temperature overnight. Hydroxyldihydroimidazole **13** (151 mg, 76%), precipitated in the reaction mixture and was recovered by filtration, washed with hexanes (1 mL) and dried in vacuo.

Preparation of 2-(Phenylethynyl)aniline (7): Compound **7** was prepared through a Sonogashira coupling reaction as reported by Liang^[23] et al. in good yield (87%).

Preparation of *N*-(2-Phenyl-1*H*-indol-1-yl)methylene]cyclohexanamine (8): 2-(Phenylethynyl)aniline (**7**) (97 mg, 0.5 mmol), and AuCl₃ (15 mg, 0.05 mmol), were dissolved in ACN (1 mL) under inert atmosphere in a microwave tube. Cyclohexyl isocyanide (82 mg, 0.75 mmol) was added. The sealed tube was irradiated for 2 h at 75 °C (power: 80 W). The reaction was quenched with saturated aq. NaHCO₃ (10 mL) and extracted with AcOEt (3 × 10 mL). The combined organic phases were dried with MgSO₄, filtered, concentrated in vacuo and purified by flash chromatography on silica gel (hexanes/AcOEt) to afford compound indole **8** (47 mg, 31% yield). Unreacted starting material was also recovered (58%). The same reaction catalyzed by HCl (dioxane solution, 1 equiv.) gave the same compound in a modest 12% yield.

***N*-Methyl-2-(phenylethynyl)aniline (9):**^[24] 2-(Phenylethynyl)aniline (**7**) (193 mg, 1.0 mmol) was dissolved in THF (5 mL) under inert atmosphere and cooled to -78 °C. *n*BuLi solution (10 M in hexanes, 0.11 mL, 1.1 equiv.) was added dropwise and the mixture was stirred for 1 h. Methyl iodide (213 mg, 1.5 mmol) was added and the mixture was stirred at room temp. for 2 h. Upon reaction completion, the reaction was carefully quenched by dropwise addition of NH₄Cl aq. solution (1 mL) at 0 °C. A precipitate was filtered off, and the solution was added to of saturated aq. solution NaHCO₃ (10 mL) and extracted with AcOEt (3 × 10 mL). The combined organic phases were dried with MgSO₄, filtered, and concentrated in vacuo to yield aniline **9** (190 mg, 91% yield). The crude was used without further purification as the spectroscopic data matched with those described in the literature.

Preparation of *N*-Cyclohexyl-*N*-methyl-*N*-(2-(phenylethynyl)phenyl)formimidamide (11) and *N*-Allyl-*N*-*tert*-butyl-*N*-phenylformimidamide (12): Amidines **11** and **12** were prepared from *N*-methyl-2-(phenylethynyl)aniline (**9**) and *N*-allylaniline (**10**) respectively in 96% and 91% yield using general procedure A.

6b-PdCl₂-(3-chloropyridine) Complex (14): This catalysts was prepared from imidazolium salt **6b**, 3-chloropyridine and PdCl₂ following Organ's procedure^[25] (yield 47%).

4-Methyl-1,1'-biphenyl (15): A mixture of 4-chlorotoluene (24 mg, 0.205 mmol), phenylboronic acid (25 mg, 0.205 mmol), complex [6b-PdCl₂-(3-chloropyridine)] (14) (4 mg, 0.006 mmol), Cs₂CO₃ (99 mg, 0.307 mmol) in dioxane was heated at 100 °C for 2 h under nitrogen atmosphere. The mixture was filtered through a celite pad and concentrated under reduced pressure. The residue was purified by flash column chromatography on silica gel (hexanes/ethyl acetate) to obtain the desired product whose spectroscopic properties matched with the described in the literature^[26] (12 mg, 35%).

Acknowledgments

This work was supported by the Spanish Dirección General de Investigación Ciencia y Técnica (DGICYT) (project BQU-CTQ2012-30930) and Generalitat de Catalunya (grant number 2014 SGR 137). Profs. Carmen Nájera (Univ. Alicante), Rosario Fernández (Univ. Sevilla) and José M. Lassaletta (CSIC Sevilla) are thanked for useful suggestions.

- [1] For overviews on multicomponent reactions and domino processes, see: a) *Multicomponent Reactions in Organic Synthesis* (Eds.: J. Zhu, Q. Wang, M.-X. Wang), Wiley-VCH, Weinheim, Germany, 2015; b) *Domino Reactions* (Ed.: L. F. Tietze), Wiley-VCH, Weinheim, Germany, 2014; c) A. Domling, W. Wang, K. Wang, *Chem. Rev.* **2012**, *112*, 3083–3135, and references cited therein; d) *Multicomponent Reactions* (Eds.: J. Zhu, H. Bienayme), Wiley-VCH, Weinheim, Germany, 2005.
- [2] a) N. Kielland, E. Vicente-García, M. Revés, N. Isambert, M. J. Arévalo, R. Lavilla, *Adv. Synth. Catal.* **2013**, *355*, 3273–3284; b) A. Vazquez-Romero, N. Kielland, M. J. Arévalo, S. Preciado, R. J. Mellanby, Y. Feng, R. Lavilla, M. Vendrell, *J. Am. Chem. Soc.* **2013**, *35*, 16018–16021; c) M. J. Arévalo, N. Kielland, C. Masdeu, M. Miguel, N. Isambert, R. Lavilla, *Eur. J. Org. Chem.* **2009**, 617–625.
- [3] T. J. J. Müller, K. Deilhof, in: *Multicomponent Reactions in Organic Synthesis* (Eds.: J. Zhu, Q. Wang, M.-X. Wang), Wiley-VCH, Weinheim, Germany, 2015, p. 333–378.
- [4] For representative examples, see: a) G. Qiu, X. Qiu, J. Wu, *Adv. Synth. Catal.* **2013**, *355*, 3205–3209; b) Z. Hu, J. Wang, D. Liang, Q. Zhu, *Adv. Synth. Catal.* **2013**, *355*, 3290–3295; c) J. Liu, Z. Fang, Q. Zhang, Q. Liu, X. Bi, *Angew. Chem. Int. Ed.* **2013**, *52*, 6953–6957; *Angew. Chem.* **2013**, *125*, 7091–7095; d) M. Gao, C. He, H. Chen, R. Bai, B. Cheng, A. Lei, *Angew. Chem. Int. Ed.* **2013**, *52*, 6958–6961; *Angew. Chem.* **2013**, *125*, 7096–7099; e) S. Lang, *Chem. Soc. Rev.* **2013**, *42*, 4867–4880, and references cited therein; f) B. Liu, H. Gao, Y. Yu, W. Wu, H. Jiang, *J. Org. Chem.* **2013**, *78*, 10319–10328; g) H. Sun, H. Zhou, O. Khorev, R. Jiang, T. Yu, X. Wang, Y. Du, Y. Ma, T. Meg, J. Shen, *J. Org. Chem.* **2012**, *77*, 10745–10751; h) T. Mitamura, A. Ogawa, *J. Org. Chem.* **2011**, *76*, 1163–1166; i) F. Sha, Y. Lin, X. Huang, *Synthesis* **2009**, 424–430; j) C. Cao, Y. Shi, A. L. Odom, *J. Am. Chem. Soc.* **2003**, *125*, 2880–2881; k) see also: L. T. Nguyen, T. N. Le, F. De Proft, A. K. Chandra, W. Langenaeker, M. T. Nguyen, P. Geerlings, *J. Am. Chem. Soc.* **1999**, *121*, 5992–6001.
- [5] a) N. Sharma, Z. Li, U. K. Sharma, E. V. Van der Eycken, *Org. Lett.* **2014**, *16*, 3884–3887; b) Z. Li, A. Kumar, D. D. Vachhani, S. K. Sharma, V. S. Parmar, E. V. Van der Eycken, *Eur. J. Org. Chem.* **2014**, 2084–2091; c) A. Kumar, Z. Li, S. K. Sharma, V. S. Parmar, E. V. Van der Eycken, *Org. Lett.* **2013**, *15*, 1874–1877; d) for an overview, see: U. K. Sharma, N. Sharma, D. D. Vachhani, E. V. Van der Eycken, *Chem. Soc. Rev.* **2015**, *44*, 1836–1860.
- [6] a) Y. Yamamoto, *J. Org. Chem.* **2007**, *72*, 7817–7831; b) Y. Yamamoto, I. D. Gridnev, T. Patil, T. Jin, *Chem. Commun.* **2009**, 5075–5087.
- [7] For reviews on isocyanide insertion chemistry, see: a) G. Qiu, Q. Ding, J. Wu, *Chem. Soc. Rev.* **2013**, *42*, 5257–5269; b) A. V. Lygin, A. de Meijere, *Angew. Chem. Int. Ed.* **2010**, *49*, 9094–9124; *Angew. Chem.* **2010**, *122*, 9280–9311; c) for a recent example of isocyanide insertion into an N–H bond in a MCR process, see: F. Medda, C. Hulme, *Tetrahedron Lett.* **2014**, *55*, 3328–3331.
- [8] a) For a related process involving an isocyanide-metal complex interacting with a propargylamine, leading to N-heterocyclic carbene complexes, see: J. Ruiz, B. F. Perandones, G. García, M. E. G. Mosquera, *Organometallics* **2007**, *26*, 5687–5695; b) Also see: M. Joshi, M. Patel, R. Tiwari, A. K. Verma, *J. Org. Chem.* **2012**, *77*, 5633–5645.
- [9] For related transformations featuring 5-*exo* additions, see: a) R. L. Giles, J. D. Sullivan, A. M. Steiner, R. E. Loooper, *Angew. Chem. Int. Ed.* **2009**, *48*, 3116–3120; *Angew. Chem.* **2009**, *121*, 3162–3166; b) D. S. Ermolatev, J. B. Bariwal, P. L. Steenackers, S. C. J. De Keersmaecker, E. V. Van der Eycken, *Angew. Chem. Int. Ed.* **2010**, *49*, 9465–9468; *Angew. Chem.* **2010**, *122*, 9655–9658; c) B. P. Zavesky, N. R. Babji, J. P. Wolfe, *Org. Lett.* **2014**, *16*, 4952–4955; d) Also see: N. Kielland, C. J. Whiteoak, A. W. Kleij, *Adv. Synth. Catal.* **2013**, *355*, 2115–2138, and references cited therein.
- [10] S. Tong, Q. Wang, M.-X. Wang, J. Zhu, *Angew. Chem. Int. Ed.* **2015**, *54*, 1293–1297; *Angew. Chem.* **2015**, *127*, 1309–1313.
- [11] a) V. A. Peshkov, O. P. Pereshivko, E. V. Van der Eycken, *Chem. Soc. Rev.* **2012**, *41*, 3790–3807; b) W.-J. Yoo, L. Zhao, C.-J. Li, *Aldrichim. Acta* **2011**, *44*, 43–51; c) J. B. Bariwal, D. S. Ermolatev, E. V. Van der Eycken, *Chem. Eur. J.* **2010**, *16*, 3281–3284; d) C.-J. Li, C. Wei, *Chem. Commun.* **2002**, 268–269.
- [12] CCDC-1043645, -1043646 contain the supplementary crystallographic data for this paper. These data can be obtained free of charge from The Cambridge Crystallographic Data Centre via www.ccdc.cam.ac.uk/data_request/cif.
- [13] For the anion exchange of imidazolium chlorides with hydrogen carbonate and ensuing chemistry, see: M. Fèvre, J. Pinaud, A. Leteneur, Y. Gnanou, J. Vignolle, D. Taton, K. Miqueau, J.-M. Sotiropoulos, *J. Am. Chem. Soc.* **2012**, *134*, 6776–6784.
- [14] For recent reviews, see: a) S. N. Riduan, Y. Zhang, *Chem. Soc. Rev.* **2013**, *42*, 9055–9070; b) E. Alcalde, I. Dinares, N. Mesquida, in: *Anion Recognition in Supramolecular Chemistry* (Eds.: P. A. Gale, W. DeHaen), *Topics in Heterocyclic Chemistry*, Springer, Heidelberg, Germany, 2010, p. 267–300; c) K. M. Hindi, M. J. Panzner, C. A. Tessier, C. L. Cannon, W. J. Youngs, *Chem. Rev.* **2009**, *109*, 3859–3884.
- [15] For reviews, see: a) S.-G. Lee, *Chem. Commun.* **2006**, 1049–1063; b) K. Binnemans, *Chem. Rev.* **2005**, *105*, 4148–4204; c) J. Dupont, R. F. de Souza, P. A. Z. Suarez, *Chem. Rev.* **2002**, *102*, 3667–3692.
- [16] a) M. N. Hopkinson, C. Richter, M. Schedler, F. Glorius, *Nature* **2014**, *510*, 485–496; b) D. Enders, O. Niemeier, A. Henseler, *Chem. Rev.* **2007**, *107*, 5606–5655.
- [17] For a review see: E. Assen, B. Kantchev, C. J. O'Brien, M. G. Organ, *Angew. Chem. Int. Ed.* **2007**, *46*, 2768–2813; *Angew. Chem.* **2007**, *119*, 2824–2870.
- [18] See for example: a) A. Fürstner, M. Alcarazo, V. César, C. W. Lehmann, *Chem. Commun.* **2006**, 2176–2178; b) S. Li, F. Yang, T. Lv, J. Lan, G. Gao, J. You, *Chem. Commun.* **2014**, *50*, 3941–3943.
- [19] For an appraisal of the chemistry of imidazoles and derivatives, including synthetic methods, see: a) N. X. Huang, L. Liu, in: *Comprehensive Heterocyclic Chemistry III*, vol. 4 (Eds.: A. R. Katritzky, C. A. Ramsden, E. F. V. Scriven, R. J. K. Taylor), Pergamon, Oxford, UK, 2008, p. 143–364. For recent specific syntheses, see, inter alia: b) L. Hong, Y. Shao, L. Zhang, X. Zhou, *Chem. Eur. J.* **2014**, *20*, 8551–8555; c) G. Sapuppo, Q. Wang, D. Swinnen, J. Zhu, *Org. Chem. Front.* **2014**, *1*, 240–246; d) W. Hao, Y. Jiang, M. Cai, *J. Org. Chem.* **2014**, *79*, 3634–3640; e) F. de Moliner, C. Hulme, *Org. Lett.* **2012**, *14*, 1354–1357; f) H. Shen, Z. Xie, J. Am. Chem. Soc. **2010**, *132*, 11473–11480; g) F. Bellina, R. Rossi, *Adv. Synth. Catal.* **2010**, *352*, 1223–1276; h) B. A. Arndtsen, *Chem. Eur. J.* **2009**, *15*, 302–

- 313; i) S. Kamijo, Y. Yamamoto, *Chem. Asian J.* **2007**, *2*, 568–578.
- [20] a) S. Cacchi, G. Fabrizi, A. Goggiamani, *Org. React.* **2012**, *76*, 281–534; b) G. R. Humphrey, J. T. Kuethe, *Chem. Rev.* **2006**, *106*, 2875–2911.
- [21] R. Jazzar, J.-B. Bourg, R. D. Dewhurst, B. Donnadieu, G. Bertrand, *J. Org. Chem.* **2007**, *72*, 3492–3499.
- [22] C. J. O'Brien, E. A. B. Kantchev, C. Valente, N. Hadei, G. A. Chass, A. Lough, A. C. Hopkins, M. G. Organ, *Chem. Eur. J.* **2006**, *12*, 4743–4748.
- [23] X.-F. Xia, L.-L. Zhang, X.-R. Song, X.-Y. Liu, Y.-M. Liang, *Org. Lett.* **2012**, *14*, 2480–2483.
- [24] O. S. Morozov, A. V. Lunchev, A. A. Bush, A. A. Tukov, A. F. Asachenko, V. N. Khrustalev, S. S. Zaleskiy, V. P. Ananikov, M. S. Nechaev, *Chem. Eur. J.* **2014**, *20*, 6162–6170.
- [25] C. J. O'Brien, E. A. B. Kantchev, C. Valente, N. Hadei, G. A. Chass, A. Lough, A. C. Hopkins, M. G. Organ, *Chem. Eur. J.* **2006**, *12*, 4743–474.
- [26] S. Zhou, E. Doni, G. M. Anderson, R. G. Kane, S. W. MacDougall, V. M. Ironmonger, T. Tuttle, J. A. Murphy, *J. Am. Chem. Soc.* **2014**, *136*, 17818–17826.

Received: April 21, 2015
Published Online: June 9, 2015

Publication II: Selected Supporting Information

Experimental procedures

General Information

Unless stated otherwise, all reactions were carried out under argon atmosphere in dried glassware. Commercially available reactants were used without further purification. Thin-layer chromatography was performed on pre-coated Merck silica gel 60 F254 plates and visualized under a UV lamp. ^1H , and ^{13}C NMR spectra were recorded on a Varian Mercury 400 (at 400 MHz, and 100 MHz respectively). Unless otherwise quoted, NMR spectra were recorded in CDCl_3 solution with TMS as an internal reference. Data for ^1H -NMR spectra are reported as follows: chemical shift (δ ppm), multiplicity, integration and coupling constants (Hz). Data for ^{13}C -NMR spectra are reported in terms of chemical shift (δ ppm). IR spectra were recorded using a Thermo Nicolet Nexus spectrometer and are reported in frequency of absorption (cm^{-1}).

Preparation of propargylic amines (4)

N-(aryl)propargylamines were prepared using a modification of Li and Wei's procedure^[1] using non-aqueous media:

In a Schlenk tube, 2.0 mmol (1.00 equiv.) of aldehyde and 2.2 mmol (1.1 equiv.) of amine were dissolved in 5 mL of THF under inert atmosphere. The tube was sealed and the mixture was heated at 60 °C until complete consumption of the aldehyde (2 h). Next CuCl (30% mol), RuCl_3 (3% mol) and the alkyne (2.4 mmol, 1.2 equiv.) were added. The mixture was stirred at rt (30 min), and then heated at 50 °C until consumption of the imine (24 h). The solution was cooled, poured into water, and extracted with DCM. The combined organic phases were washed with water, dried over MgSO_4 and concentrated in vacuo. Purification by flash chromatography on silica gel (Hexanes/ AcOEt) afforded the corresponding propargylamines.

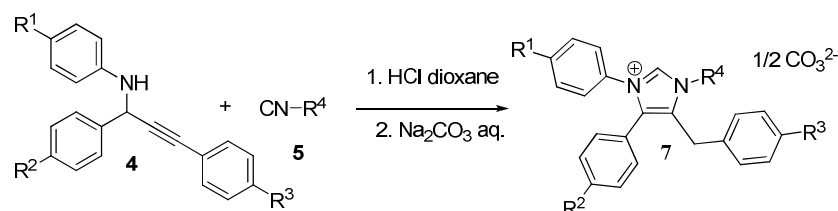
N-benzylpropargylamines were prepared following the procedure reported by Van der Eycken et al.^[2]

Described propargylamines

The following compounds were described in the literature, prepared as stated above, and their properties matched with the reported data: *N*-(1,3-diphenylprop-2-ynyl)-4-methylaniline^[3], *N*-benzyl-4-methyl-1-phenylpent-1-yn-3-amine^[2], *N*-(4-methoxybenzyl)-1,3-diphenylprop-2-yn-1-amine^[4], *N*-(1-(4-chlorophenyl)-3-phenylprop-2-ynyl)-4-methylaniline^[5]

Preparation of imidazolium salts (6)

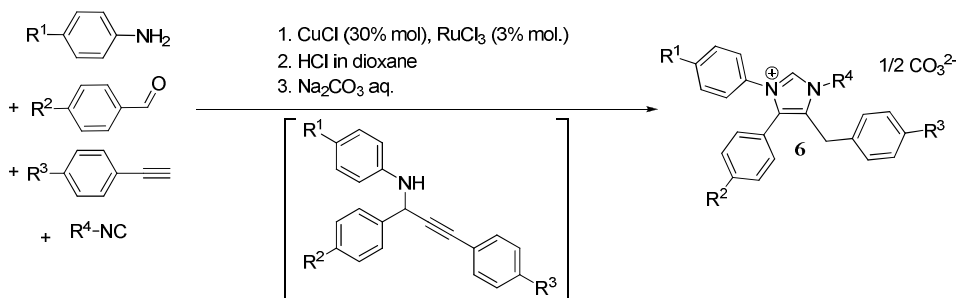
General procedure A:



Propargylamine 4 (0.5 mmol, 1 equiv.) was dissolved in THF (1.5 mL) and ACN (1.5 mL) under inert atmosphere. Next isocyanide 5 (0.5 mmol, 1 equiv.) was added. A 4 M HCl solution in dioxane (0.125 mL, 1 equiv.) was added and the mixture stirred until consumption of the propargylamine (4h). Next the reaction was quenched with saturated Na_2CO_3 aq. solution (20 mL) and extracted with AcOEt (3×10 mL). The combined organic phases were dried over MgSO_4 and concentrated in vacuo to afford the

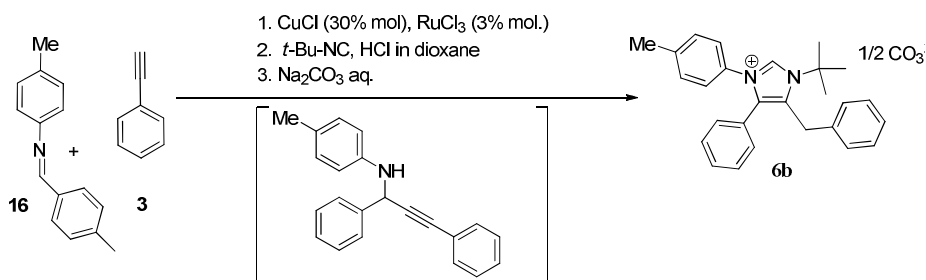
corresponding imidazolium salts. Analytically pure samples of the products were obtained by flash chromatography on silica gel (Hexanes/EtOH).

General procedure B (tandem):



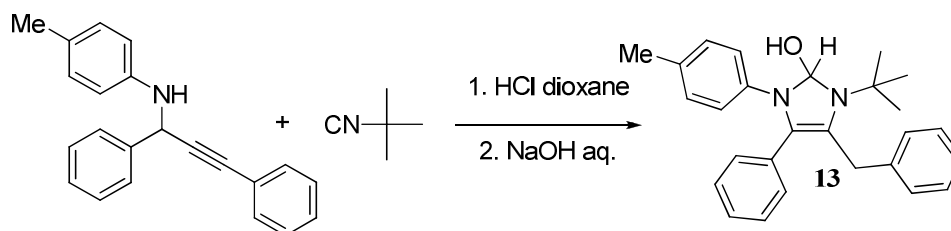
In a Schlenk tube, the aldehyde (1.00 mmol, 1.0 equiv.) and the amine (1.05 mmol, 1.05 equiv.) were dissolved in THF (3 mL) under inert atmosphere. The tube was sealed and the mixture was heated at 60 °C until complete aldehyde consumption (2 h.). Next CuCl (30% mol), RuCl₃ (3% mol.) and the alkyne (1.2 mmol, 1.2 equiv.) were added. The mixture was first stirred at rt for 30 min, and then heated at 50 °C for 24 h. The solution was cooled to rt and diluted with ACN (3 mL). The isocyanide (1.1 mmol, 1.1 equiv.) was then added, followed by a 4M HCl solution in dioxane (0.125 mL, 1 equiv.). The solution was stirred at rt until reaction completion (24 h) and then quenched with Na₂CO₃ (saturated aq. solution, 40 mL) and extracted with AcOEt (3×20 mL). The combined organic phases were dried over MgSO₄ and concentrated in vacuo, to afford the corresponding imidazolium salts. Analytically pure samples were obtained by flash chromatography on silica gel (Hexanes/EtOH). In this way, from the corresponding inputs, imidazolium salts **6b** (54%), **6h** (49%), **6i** (68%) were obtained.

General procedure C (tandem from the imine):



In a Schlenk tube, imine **16** (1.05 mmol.), phenylacetylene **3**, CuCl (30% mol), RuCl₃ (3% mol.) were dissolved in THF (3 mL) under inert atmosphere. The mixture was then stirred at 50 °C for 24 h. The solution was cooled at rt and diluted with ACN (3 mL). Then, *tert*-butylisocyanide (1.1 mmol, 1.1 equiv.) was then added, followed by a 4M HCl solution in dioxane (0.125 mL, 1 equiv.). The resulting solution was stirred at rt until reaction completion (24 h) and then quenched with Na₂CO₃ (saturated aq. solution, 40 mL) and extracted with AcOEt (3×20 mL). The combined organic phases were dried over MgSO₄ and concentrated in vacuo, to afford imidazolium salt **6b** (64%). Analytically pure sample was obtained by flash chromatography on silica gel (Hexanes/EtOH).

Preparation of dihydroimidazole (13)

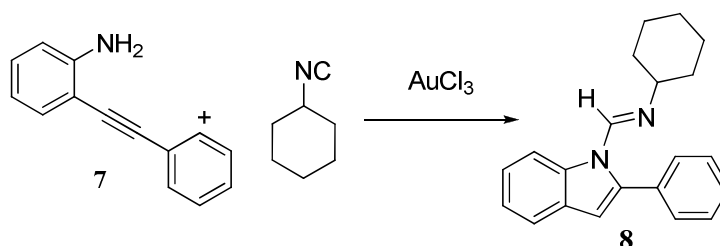


N-(1,3-diphenylprop-2-ynyl)-4-methylaniline (0.5 mmol, 1 equiv.) was dissolved in 1.5 mL of THF and ACN (1.5 mL) under inert atmosphere. *tert*-butylisocyanide 0.5 mmol (1 equiv.) was added, followed by a 4M HCl solution in dioxane (0.125 mL, 1 equiv.). The solution was stirred at rt until reaction completion (24 h) and then quenched with a NaOH aq. solution (1M, 3 mL) was added and the solution was stirred vigorously at room temperature overnight. Hydroxydihydroimidazole **13**, precipitated in the reaction mixture, was recovered by filtration, washed with hexanes (1 mL) and dried in vacuo.

Preparation of 2-(phenylethynyl)aniline (7)

Compound **7** was prepared through a Sonogashira coupling reaction as reported by Yong-Min Liang^[6] et al. in good yield (87%).

Preparation of *N*-((2-phenyl-1*H*-indol-1-yl)methylene)cyclohexanamine (8)

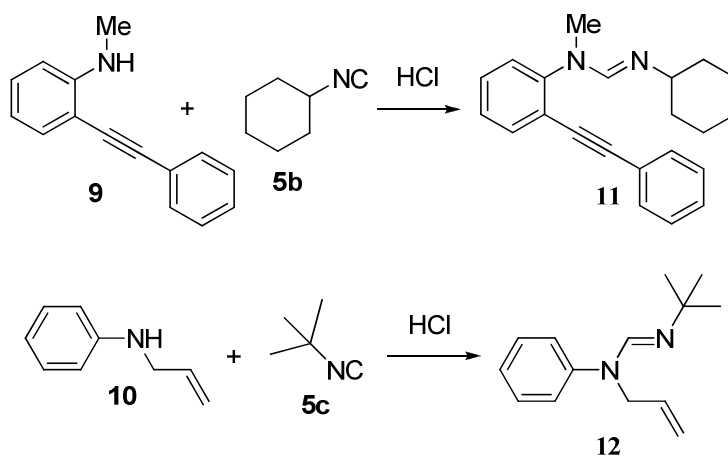


2-(Phenylethynyl)aniline **7** (0.5 mmol, 1 equiv.) and of AuCl₃ (0.05 mmol, 0.1 equiv.) were dissolved in ACN (1 mL) under inert atmosphere in a microwave tube. Cyclohexyl isocyanide (0.75 mmol, 1.5 equiv.) was added. The sealed tube was irradiated for 2 h at 75 °C (Power: 80W). The reaction was quenched with saturated aq. NaHCO₃ (10 mL) and extracted with AcOEt (3×10 mL). The combined organic phases were dried over MgSO₄, concentrated in vacuo and purified by flash chromatography on silica gel (Hexanes/AcOEt) to afford compound indole **8** in 31% yield. Unreacted starting material was also recovered (58%). The same reaction catalyzed by HCl (dioxane solution, 1 equiv) gave a modest 12%.

N-methyl-2-(phenylethynyl)aniline (9)^[7]

2-(Phenylethynyl)aniline **7** (1.0 mmol, 1 equiv.) was dissolved in THF (5 mL) under inert atmosphere and cooled to -78 °C. *n*-BuLi solution (10 M in hexanes, 0.11 mL, 1.1 equiv) was added dropwise and the mixture was stirred for 1 h. Methyl iodide (1.5 mmol, 1 equiv.) was added and the mixture was stirred at rt for 2 h. Upon reaction completion, the reaction was carefully quenched by dropwise addition of NH₄Cl aq. solution (1 mL) at 0 °C. A precipitate was filtered off, and the solution was added to saturated aq. solution NaHCO₃ (10 mL) and extracted with AcOEt (3×10 mL). The combined organic phases were dried over MgSO₄ and concentrated in vacuo. The crude was used without further purification. (Yield: 91%). The spectral data matched with those described in the literature.

Preparation of *N*'-cyclohexyl-*N*-methyl-*N*-(2-(phenylethynyl)phenyl)formimidamide (11) and *N*-allyl-*N*'-tert-butyl-*N*-phenylformimidamide (12)



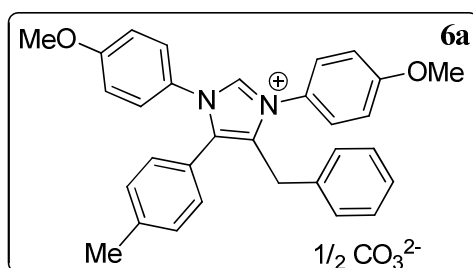
Compounds **11** and **12** were prepared respectively in 96% and 91% yield using **general procedure A**.

6b-PdCl₂-(3-chloropyridine) catalyst (14) was prepared following Organ's procedure.^[8] (Yield: 47%)

4-methyl-1,1'-biphenyl (15): A mixture of 4-chlorotoluene (24 mg, 0.205 mmol, 1 eq), phenylboronic acid (25mg, 0.205 mmol, 1 eq), complex **6b-PdCl₂-(3-chloropyridine) (14)** (4 mg, 0.006 mmol, 0.03eq), Cs₂CO₃ (99mg, 0.307 mmol, 1,5 eq.) in dioxane was heated at 100 °C for 2 h under nitrogen atmosphere. The mixture was filtered through a celite pad and concentrated under reduced pressure. The residue was purified by flash column chromatography (hexanes/ethyl acetate) to obtain the desired product whose spectroscopic properties matched with the described in the literature^[9] (12 mg, 35%).

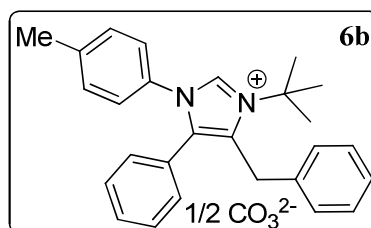
References:

- [1] C. Li, C. Wei, *Chem. Commun.*, **2002**, 268-269.
- [2] J. B. Bariwal, D. S. Ermolat'ev, E. V. Van der Eycken, *Chem. Eur. J.* **2010**, *16*, 3281-3284.
- [3] Z. Jiang, P. Lu, Y. Wang, *Org. Lett.* **2012**, *14*, 6266-6269
- [4] Y. Lu, T. C. Johnstone, B. A. Arndtsen, *J. Am. Chem. Soc.* **2009**, *131*, 11284-11285
- [5] Kui Zhang, You Huang, Ruyu Chen *Tetrahedron Letters* **2010**, *51*, 5463-5465
- [6] X-F. Xia, L-L. Zhang, X-R. Song, X-Y. Liu, Y-M. Liang, *Org. Lett.*, **2012**, *14*, 2480-2483.
- [7] Morozov, O. S.; Lunchev, A. V.; Bush, A. A.; Tukov, A. A.; Asachenko, A. F.; Khrustalev, V. N.; Zalesskiy, S. S.; Ananikov, V. P.; Nechaev, M. S. *Chem. Eur. J.* **2014**, *20*, 6162-6170.
- [8] C. J. O'Brien, E. A. B. Kantchev, C. Valente, N. Hadei, G. A. Chass, A. Lough, A. C. Hopkins, M. G. Organ, *Chem. Eur. J.* **2006**, *12*, 4743-474
- [9] Zhou, S.; Doni, E.; Anderson, G. M.; Kane, R. G.; MacDougall, S. W.; Ironmonger, V. M.; Tuttle, T.; Murphy, J.A. *J. Am. Chem. Soc.* **2014**, *136*, 17818-17826.



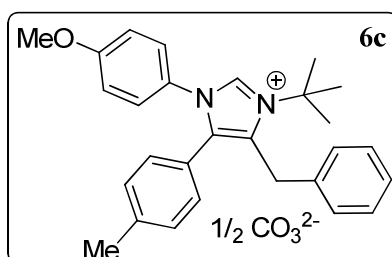
4-Benzyl-1,3-bis(4-methoxyphenyl)-5-(*p*-tolyl)-1*H*-imidazol-3-ium carbonate (6a): Following general procedure A afforded imidazolium salt **6a** as brown solid. (Yield: 82%)

^1H NMR (400 MHz, CDCl_3) δ 8.89 (s, 1H), 7.45 (d, $J = 9.0$ Hz, 2H), 7.40 (d, $J = 8.9$ Hz, 2H), 7.22 (d, $J = 8.2$ Hz, 2H), 7.19 – 7.14 (m, 5H), 6.91 (dd, $J = 8.9, 6.7$ Hz, 4H), 6.81 – 6.76 (m, 2H), 4.00 (s, 2H), 3.84 (s, 3H), 3.81 (s, 3H), 2.34 (s, 3H). ^{13}C NMR (100 MHz, CDCl_3) δ 161.4, 160.9, 140.7, 135.9, 135.9, 133.2, 132.2, 130.6, 130.0, 128.9, 128.2, 128.2, 127.6, 127.3, 126.2, 125.5, 121.9, 115.1, 115.1, 55.8, 55.8, 29.5, 21.6. IR (neat, cm^{-1}) 836.0, 1100.4, 1222.9, 1507.21, 1886.1, HRMS (ESI): calculated for $\text{C}_{31}\text{H}_{29}\text{N}_2\text{O}_2^+$ $[\text{M}]^+$: 461.2224, found 461.2227.



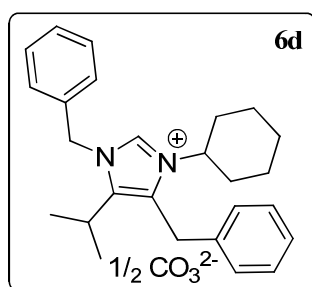
4-Benzyl-3-(*tert*-butyl)-5-phenyl-1-(*p*-tolyl)-1*H*-imidazol-3-ium carbonate (6b): Following general procedure A afforded imidazolium salt **6b** as clear brown oil. (Yield: 82%)

^1H NMR (400 MHz, CDCl_3) δ 9.67 (s, 1H), 7.28 – 7.24 (m, 3H), 7.23 (s, 2H), 7.19 (d, $J = 1.1$ Hz, 1H), 7.16 (dd, $J = 8.4, 1.2$ Hz, 2H), 7.08 (dd, $J = 8.6, 0.5$ Hz, 2H), 7.05 (dd, $J = 8.3, 1.3$ Hz, 2H), 7.01 – 6.95 (m, 2H), 4.24 (s, 2H), 2.24 (s, 3H), 1.68 (s, 9H). ^{13}C NMR (100 MHz, CDCl_3) δ 140.5, 136.8, 135.0, 131.3, 130.5, 130.4, 130.2, 129.8, 129.3, 129.1, 127.7, 127.4, 125.8, 125.4, 63.4, 31.2, 30.3, 21.3 (one quaternary carbon not detected). IR (neat, cm^{-1}): 823.2, 1024.3, 1340.6, 1539.7, 1742.8, HRMS (ESI): calculated for $\text{C}_{27}\text{H}_{29}\text{N}_2^+$ $[\text{M}]^+$: 381.2325, found 381.2323.



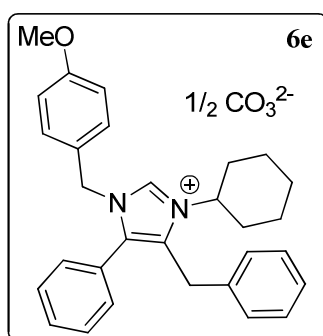
4-Benzyl-3-(*tert*-butyl)-1-(4-methoxyphenyl)-5-(*p*-tolyl)-1*H*-imidazol-3-ium carbonate (6c): Following general procedure A, afforded imidazolium salt **6c** as clear brown oil. (Yield: 92%)

^1H NMR (400 MHz, CDCl_3) 9.01 (s, 1H), 7.38 (d, $J = 9.0$ Hz, 2H), 7.34 – 7.27 (m, 2H), 7.23 (t, $J = 7.3$ Hz, 1H), 7.08 – 6.97 (m, 6H), 6.86 (d, $J = 8.9$ Hz, 2H), 4.29 (s, 2H), 3.78 (s, 3H), 2.26 (s, 3H), 1.72 (s, 9H). ^{13}C NMR (100 MHz, CDCl_3) δ 160.7, 140.5, 136.8, 135.7, 135.2, 130.4, 129.8, 129.8, 129.2, 127.7, 127.6, 127.4, 126.4, 122.2, 114.9, 63.4, 55.7, 31.2, 30.3, 21.5. IR (neat, cm^{-1}): 739.4, 831.2, 1025.3, 1265.2, 1501.6, 1670.7 HRMS (ESI): calculated for $\text{C}_{28}\text{H}_{31}\text{N}_2\text{O}^+$ $[\text{M}]^+$: 411.2431, found 411.2435.



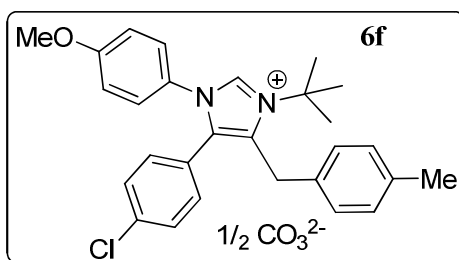
1,4-Dibenzyl-3-cyclohexyl-5-isopropyl-1*H*-imidazol-3-ium carbonate (6d): Following a modified procedure A, using AcOH instead of HCl and 20% of AgOTf, afforded 47 mg (23 %) of imidazolium salt **6d** as light brown oil, which was unstable and decomposed shortly after purification.

^1H NMR (400 MHz, CDCl_3) δ 10.50 (s, 1H), 7.42 – 7.26 (m, 8H), 7.03 (d, $J = 6.9$ Hz, 2H), 5.77 (s, 2H), 4.13 (s, 2H), 3.81 – 3.68 (m, 1H), 3.16 – 3.07 (m, 1H), 2.01 – 1.92 (m, 2H), 1.87 – 1.74 (m, 4H), 1.62 – 1.55 (m, 1H), 1.37 – 1.27 (m, 2H), 1.15 (s, 3H), 1.14 (s, 3H), 1.11 – 1.05 (m, 1H). HPLC.-MS (ESI): calculated for $\text{C}_{26}\text{H}_{33}\text{N}_2^+$ $[\text{M}]^+$: 373.26, found 373.26.



4-Benzyl-3-cyclohexyl-1-(4-methoxybenzyl)-5-phenyl-1*H*-imidazol-3-ium carbonate (6e): Following a modified procedure A, using AcOH instead of HCl and 20% of AgOTf, afforded imidazolium salt **6e** as light brown oil (10%), 69% of the starting material was recovered.

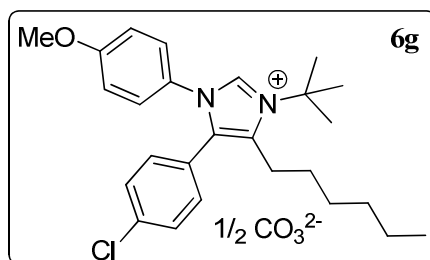
^1H NMR (400 MHz, CDCl_3) δ 10.60 (s, 1H), 7.52 – 7.45 (m, 1H), 7.46 – 7.38 (m, 2H), 7.25 – 7.14 (m, 5H), 6.93 – 6.85 (m, 4H), 6.64 (d, $J = 8.7$ Hz, 2H), 5.36 (s, 2H), 3.83 (s, 2H), 3.77 – 3.68 (m, 1H), 3.67 (s, 3H), 1.96 – 0.91 (m, 10H). HRMS (ESI): calculated for $\text{C}_{30}\text{H}_{33}\text{N}_2\text{O}^+$ $[\text{M}]^+$: 437.2587, found 437.2589.



3-(*tert*-Butyl)-5-(4-chlorophenyl)-1-(4-methoxyphenyl)-4-(4-methylbenzyl)-1*H*-imidazol-3-ium

carbonate (6f): Following a modified procedure A, (using MeSO₃H instead of HCl) afforded of imidazolium salt **6f** as clear brown oil. (Yield: 56%)

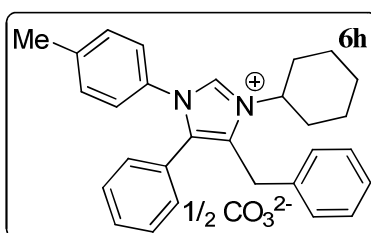
¹H NMR (400 MHz, CDCl₃) δ 8.93 (s, 1H), 7.38 (d, *J* = 9.0 Hz, 2H), 7.20 (d, *J* = 8.6 Hz, 2H), 7.09 (m, 4H), 6.92 (d, *J* = 8.0 Hz, 2H), 6.87 (d, *J* = 9.0 Hz, 2H), 4.25 (s, 2H), 3.78 (s, 3H), 2.30 (s, 3H), 1.73 (s, 9H). ¹³C NMR (100 MHz, CDCl₃) δ 160.8, 137.2, 136.6, 135.3, 134.4, 133.4, 132.0, 130.6, 129.9, 129.4, 127.8, 127.6, 126.2, 123.8, 115.0, 63.5, 55.7, 30.9, 30.2, 21.1. IR (neat, cm⁻¹): 823.2, 1024.3, 1340.6, 1539.7, 1742.8, HRMS (ESI): calculated for C₂₈H₃₀ClN₂O⁺ [M]⁺: 445.2041, found 445.2045.



3-(*tert*-Butyl)-5-(4-chlorophenyl)-4-hexyl-1-(4-methoxyphenyl)-1*H*-imidazol-3-ium carbonate (6g):

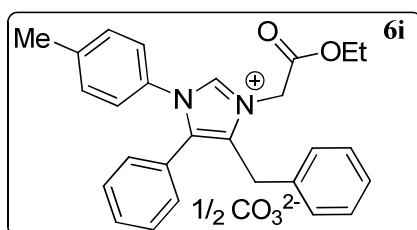
Following general procedure A, afforded imidazolium salt **6g** as clear brown oil. (Yield: 85%)

¹H NMR (400 MHz, CDCl₃) δ 9.37 (s, 1H), 7.29 (d, *J* = 8.6 Hz, 2H), 7.25 (d, *J* = 9.0 Hz, 2H), 7.11 (d, *J* = 8.6 Hz, 2H), 6.76 (d, *J* = 9.0 Hz, 2H), 3.70 (s, 3H), 2.87 – 2.69 (m, 2H), 1.81 (s, 9H), 1.43 – 1.28 (m, 2H), 1.21 – 0.98 (m, 6H), 0.75 (s, 3H). ¹³C NMR (100 MHz, CDCl₃) δ 159.5, 135.5, 134.2, 132.0, 131.2, 130.9, 128.5, 126.4, 125.0, 123.4, 113.8, 61.5, 54.5, 29.8, 29.1, 28.6, 28.1, 24.3, 21.3, 12.9. IR (neat, cm⁻¹): 823.2, 1024.3, 1340.6, 1539.7, 1742.8, HRMS (ESI): calculated for C₂₆H₃₄ClN₂O⁺ [M]⁺: 425.2354, found 425.2355.



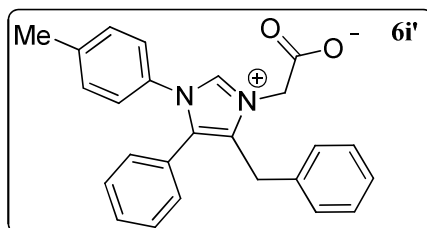
4-Benzyl-3-cyclohexyl-5-phenyl-1-(p-tolyl)-1H-imidazol-3-ium carbonate (6h): Following general procedure A afforded imidazolium salt **6h** as clear brown oil. (Yield: 82%)

^1H NMR (400 MHz, CDCl_3) δ 10.64 (s, 1H), 7.44 – 7.39 (m, 1H), 7.39 – 7.33 (m, 4H), 7.33 – 7.27 (m, 3H), 7.21 – 7.14 (m, 4H), 7.13 – 7.08 (m, 2H), 4.11 (s, 2H), 3.99 – 3.87 (m, 1H), 2.31 (s, 3H), 2.28 – 2.15 (m, 2H), 1.89 – 1.77 (m, 4H), 1.58 (d, $J = 13.4$ Hz, 1H), 1.46 – 1.31 (m, 1H), 1.19 – 1.05 (m, 2H). ^{13}C NMR (100 MHz, CDCl_3) δ 140.4, 137.8, 135.7, 131.8, 131.2, 130.5, 130.4, 130.3, 129.7, 129.5, 129.4, 127.9, 127.8, 125.5, 125.4, 59.5, 33.3, 29.4, 25.9, 24.3, 21.3. IR (neat, cm^{-1}): 823.2, 1024.3, 1340.6, 1539.7, 1742.8, HRMS (ESI): calculated for $\text{C}_{29}\text{H}_{31}\text{N}_2^+ [\text{M}]^+$: 407.2482, found 407.2481.



4-Benzyl-3-(2-ethoxy-2-oxoethyl)-5-phenyl-1-(p-tolyl)-1H-imidazol-3-ium carbonate (6i): Following general procedure A afforded of imidazolium salt **6i** as dark brown oil. (Yield: 96%)

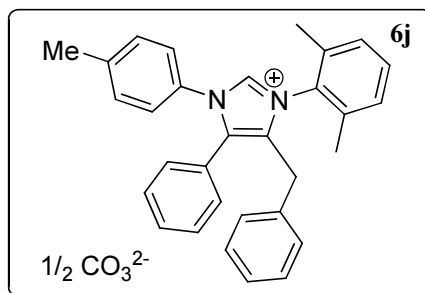
^1H NMR (400 MHz, CDCl_3) δ 10.22 (s, 1H), 7.46 – 7.40 (m, 1H), 7.40 – 7.36 (m, 2H), 7.35 – 7.33 (m, 1H), 7.33 – 7.26 (m, 4H), 7.23 – 7.17 (m, 4H), 7.12 – 7.08 (m, 2H), 5.37 (s, 2H), 4.13 – 4.05 (m, 4H), 2.35 (s, 3H), 1.22 (t, $J = 7.2$ Hz, 3H). ^{13}C NMR (100 MHz, CDCl_3) δ 166.2, 141.1, 138.7, 134.3, 132.3, 130.9, 131.0, 130.6, 130.5, 129.5, 129.4, 128.2, 128.0, 125.5, 124.8, 63.0, 49.1, 29.5, 21.3, 14.9, one quaternary carbon not detected. IR (neat, cm^{-1}): 823.2, 1024.3, 1340.6, 1539.7, 1742.8, HRMS (ESI): calculated for $\text{C}_{27}\text{H}_{27}\text{N}_2\text{O}_2^+ [\text{M}]^+$: 411.2067, found 411.2069.



2-(4-benzyl-5-phenyl-1-(p-tolyl)-1H-imidazol-3-ium-3-yl)acetate (6i'): during flash chromatography to obtain analytically pure sample of **6i**, imidazolium salt **6i'** was also isolated as dark brown oil. (Yield: 11%)

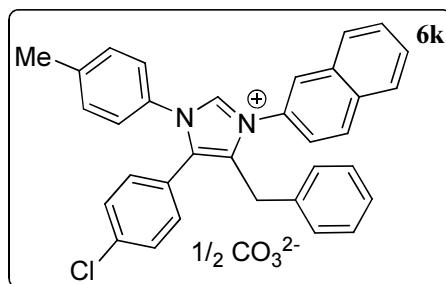
^1H NMR (400 MHz, CDCl_3) δ 9.73 (s, 1H), 7.33 – 7.27 (m, 1H), 7.27 – 7.20 (m, 4H), 7.19 – 7.12 (m, 3H), 7.12 – 7.06 (m, 4H), 7.02 (d, $J = 7.4$ Hz, 2H), 4.69 (s, 2H), 4.05 (s, 2H), 2.25 (d, $J = 1.9$ Hz, 3H), one missing mobile proton. ^{13}C NMR (100 MHz, CDCl_3) δ 168.3, 140.4, 138.2, 135.5, 131.7, 131.4, 131.1, 130.5, 130.1, 129.3, 129.1, 128.0, 127.5, 125.6, 125.5, 50.9, 29.1, 21.3, one quaternary carbon not

detected. IR (neat, cm^{-1}): 823.2, 1024.3, 1340.6, 1539.7, 1742.8, HRMS (ESI): calculated for $\text{C}_{25}\text{H}_{23}\text{N}_2\text{O}_2^+ [\text{M}]^+$: 383.1681, found 383.1679.



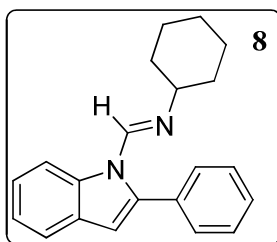
4-Benzyl-3-(2,6-dimethylphenyl)-5-phenyl-1-(*p*-tolyl)-1*H*-imidazol-3-ium carbonate (6j**):** Following a modified general procedure A, heating for 12 hours at 60 °C, afforded imidazolium salt **6j** as light brown oil. (Yield: 27%)

^1H NMR (400 MHz, CDCl_3) δ 11.04 (s, 1H), 7.51 – 7.41 (m, 5H), 7.37 – 7.33 (m, 2H), 7.34 – 7.30 (m, 1H), 7.17 (d, $J = 8.2$ Hz, 2H), 7.14 – 7.08 (m, 3H), 7.06 – 6.99 (m, 2H), 6.53 – 6.36 (m, 2H), 3.76 (s, 2H), 2.31 (s, 3H), 1.95 (s, 6H). ^{13}C NMR (100 MHz, CDCl_3) δ 140.6, 138.6, 135.8, 134.5, 131.8, 131.8, 131.4, 131.23, 130.8, 130.7, 130.6, 130.5, 129.6, 129.3, 128.7, 128.6, 127.6, 125.8, 125.2, 29.7, 21.3, 18.0. IR (neat, cm^{-1}): 823.2, 1024.3, 1340.6, 1539.7, 1742.8, HRMS (ESI): calculated for $\text{C}_{31}\text{H}_{29}\text{N}_2^+ [\text{M}]^+$: 429.2325, found 429.2324.



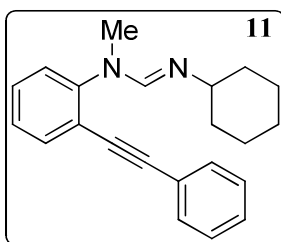
4-Benzyl-5-(4-chlorophenyl)-3-(naphthalen-2-yl)-1-(*p*-tolyl)-1*H*-imidazol-3-ium carbonate (6k**):** Following general procedure A, afforded imidazolium salt **6k** as light brown oil. (Yield: 75%)

^1H NMR (400 MHz, CDCl_3) δ 9.65 (s, 1H), 8.21 (s, 1H), 7.94 – 7.83 (m, 3H), 7.70 – 7.52 (m, 5H), 7.34-7.26 (m, 4H), 7.23 (d, $J = 7.5$ Hz, 2H), 7.16 – 7.10 (m, 3H), 6.80 (m, 2H), 4.04 (s, 2H), 2.36 (s, 3H). ^{13}C NMR (100 MHz, CDCl_3) δ 141.0, 137.5, 136.9, 135.7, 133.8, 132.9, 132.3, 132.1, 131.7, 130.9, 130.7, 130.3, 130.2, 129.6, 129.0, 128.9, 128.3, 128.2, 128.0, 127.8, 127.4, 127.0, 126.2, 123.7, 123.3, 29.7, 21.4. IR (neat, cm^{-1}): 823.2, 1024.3, 1340.6, 1539.7, 1742.8, HRMS (ESI): calculated for $\text{C}_{33}\text{H}_{26}\text{ClN}_2^+ [\text{M}]^+$: 485.1779, found 485.1782.



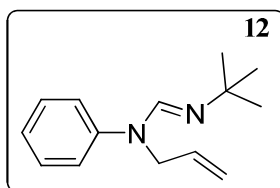
***N*-((1*H*-Indol-1-yl)methylene)cyclohexanamine (8):** Following aforementioned procedure afforded compound **8** was recovered (46.7 mg, 31%) as brown oil.

^1H NMR (400 MHz, CDCl_3) δ 8.78 (d, $J = 8.3$ Hz, 1H), 8.45 (s, 1H), 7.61 (d, $J = 7.7$, 1H), 7.52 – 7.49 (m, 4H), 7.48 – 7.43 (m, 1H), 7.35 (m, 1H), 7.26 (m, 1H), 6.62 (s, 1H), 3.20 – 3.03 (m, 1H), 1.89 – 1.29 (m, 10H). ^{13}C NMR (100 MHz, CDCl_3) δ 144.7, 140.3, 136.3, 131.9, 129.9, 129.3, 128.7, 128.4, 123.7, 122.5, 120.1, 116.1, 106.4, 65.5, 35.2, 25.8, 24.5. IR (neat, cm^{-1}): 823.2, 1024.3, 1340.6, 1539.7, 1742.8, HRMS (ESI): calculated for $\text{C}_{21}\text{H}_{23}\text{N}_2^+$ $[\text{M}+\text{H}]^+$: 303.1861, found 303.1860.



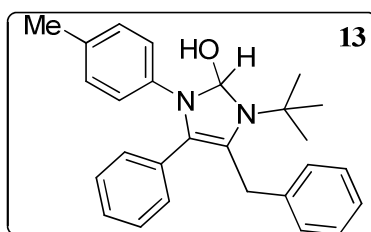
***N*'-Cyclohexyl-*N*-methyl-*N*-(2-(phenylethynyl)phenyl)formimidamide (11):** Following aforementioned procedure 65.2 mg (96%) of compound **11** as brown oil.

^1H NMR (400 MHz, CDCl_3) δ 7.94 (s, 1H), 7.55 (dd, $J = 7.7, 1.6$ Hz, 1H), 7.52 – 7.48 (m, 2H), 7.35 – 7.29 (m, 4H), 7.17 – 7.09 (m, 2H), 3.39 (s, 3H), 3.07 – 2.95 (m, 1H), 1.80 – 1.09 (m, 10H). IR (neat, cm^{-1}): 823.2, 1024.3, 1340.6, 1539.7, 1742.8, HRMS (ESI): calculated for $\text{C}_{22}\text{H}_{25}\text{N}_2^+$ $[\text{M}+\text{H}]^+$: 317.2018, found 317.2015.

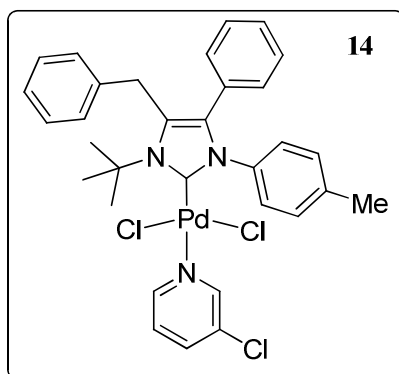


***N*-allyl-*N*'-(*tert*-butyl)-*N*-phenylformimidamide (12):** Following general procedure A, compound **13** was recovered (97.1 mg, 91%) as brown oil.

^1H NMR (400 MHz, CDCl_3) δ 7.95 (s, 1H), 7.34 – 7.27 (m, 2H), 7.08 – 6.99 (m, 3H), 5.98 – 5.85 (m, 1H), 5.18 – 5.09 (m, 2H), 4.53 – 4.47 (m, 2H), 1.22 (s, 9H). ^{13}C NMR (100 MHz, CDCl_3) δ 146.4, 134.0, 129.1, 122.5, 119.0, 115.7, 112.9, 54.0, 48.3, 31.0. IR (neat, cm^{-1}): 823.2, 1024.3, 1340.6, 1539.7, 1742.8, HRMS (ESI): calculated for $\text{C}_{14}\text{H}_{21}\text{N}_2^+$ $[\text{M}+\text{H}]^+$: 217.1705, found 217.1699.

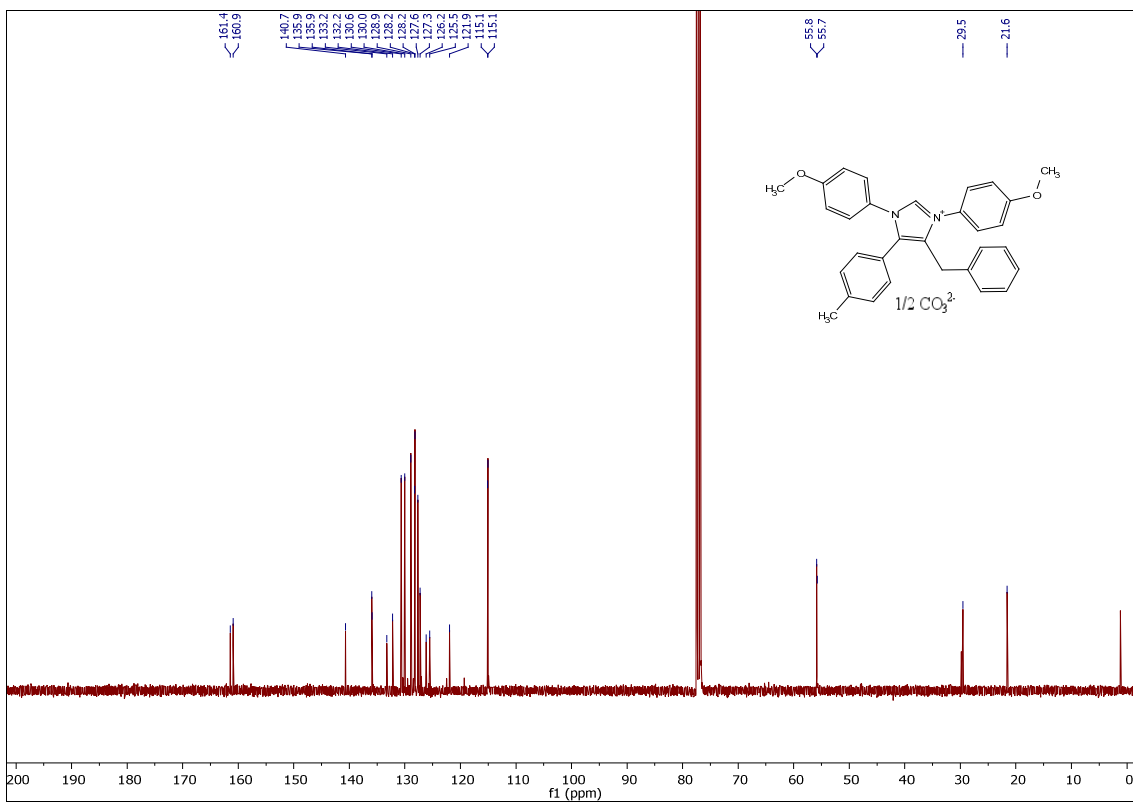
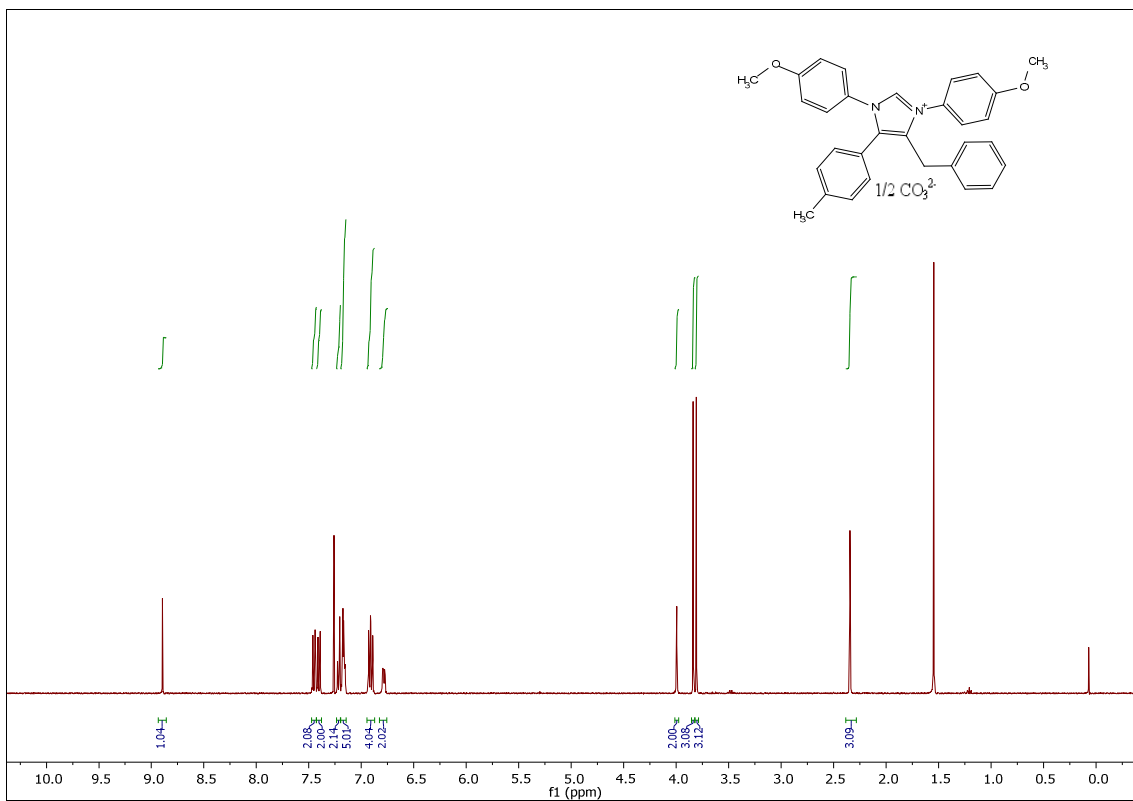


4-Benzyl-3-(*tert*-butyl)-5-phenyl-1-(*p*-tolyl)-2,3-dihydro-1*H*-imidazol-2-ol (13): Following aforementioned procedure, afforded 150 mg (76%) of hydroxyldiimidazole 7 as pale yellow solid. ^1H NMR (400 MHz, CDCl_3) Major rotamer reported δ 8.45 (s, 1H), 7.60 – 7.08 (m, 8H), 7.03 – 6.74 (m, 4H), 6.45 – 6.30 (m, 2H), 5.88 (s, 1H), 4.03 (d, $J = 14.6$ Hz, 1H), 3.11 (d, $J = 14.6$ Hz, 1H), 2.16 (s, 3H), 1.57 (s, 9H). ^{13}C NMR (100 MHz, CDCl_3) δ 164.4, 141.9, 139.8, 138.2, 134.9, 130.4, 129.5, 129.5, 128.8, 128.7, 128.0, 126.9, 119.1, 116.9, 57.4, 39.5, 31.3, 28.7, 20.6. HRMS (ESI): calculated for $\text{C}_{27}\text{H}_{31}\text{N}_2\text{O}^+$ $[\text{M}+\text{H}]^+$: 399.2436, found 399.2434.

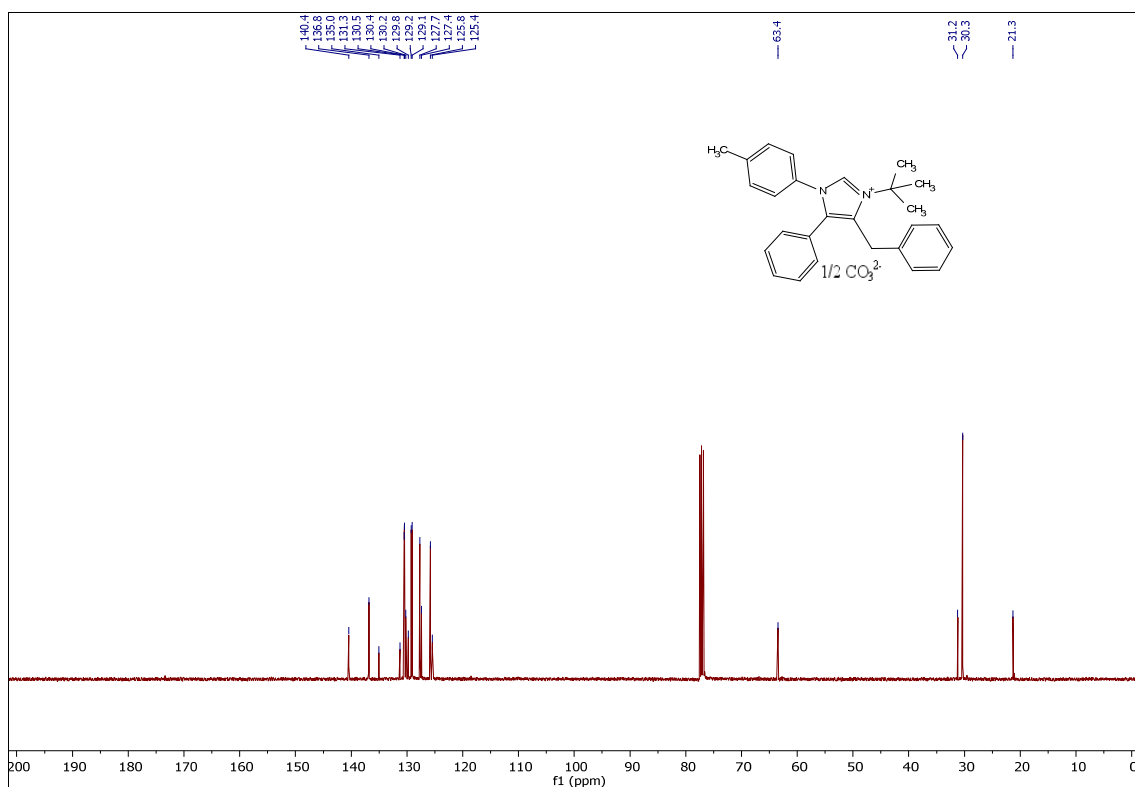
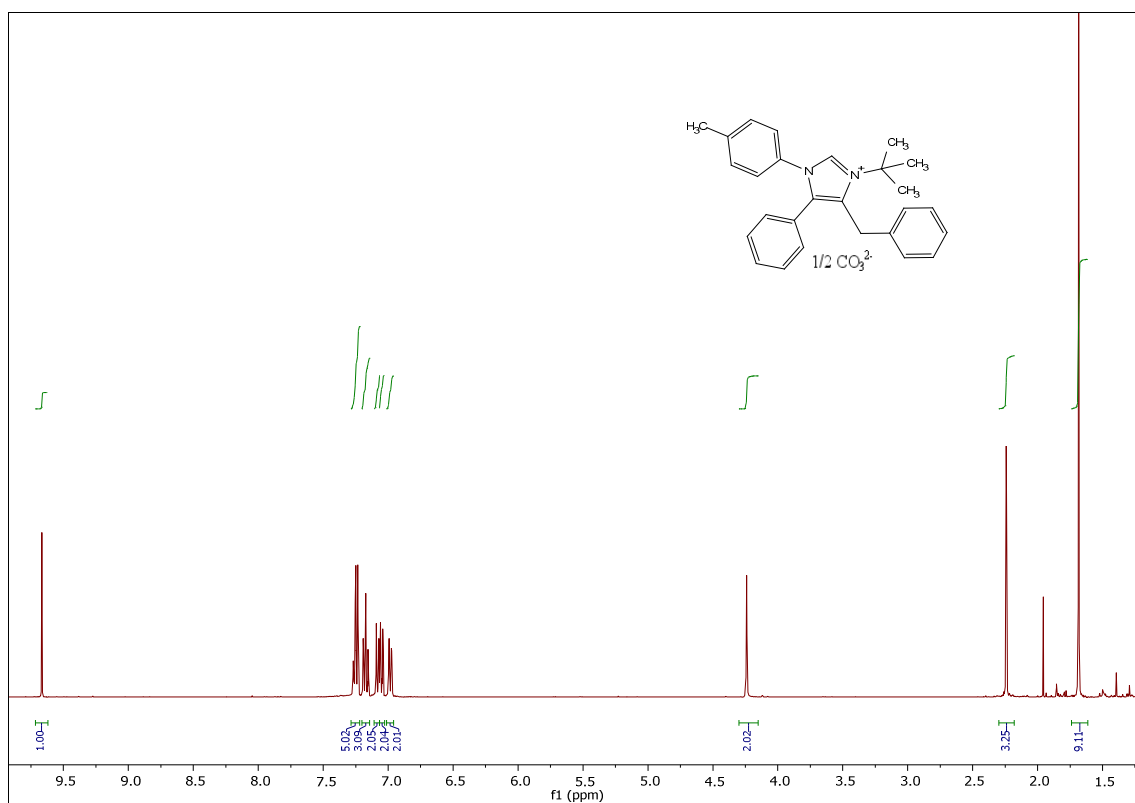


6b-PdCl₂-(3-chloropyridine) (14) ^1H NMR (400 MHz, CDCl_3) δ 8.67 (d, $J = 2.3$ Hz, 1H), 8.58 (dd, $J = 5.5, 1.3$ Hz, 1H), 7.66 (m, $J = 8.2, 2.3, 1.3$ Hz, 1H), 7.63 – 7.60 (m, 2H), 7.29 (m, 2H), 7.18 – 7.13 (m, 7H), 7.03 (m, $J = 8.1, 1.5$ Hz, 4H), 4.22 (s, 2H), 2.34 (s, 3H), 2.20 (s, 9H). ^{13}C NMR (100 MHz, CDCl_3) δ 150.5, 149.5, 145.9, 138.9, 138.5, 137.7, 136.9, 136.9, 132.6, 130.5, 130.2, 129.8, 129.2, 128.9, 128.7, 128.4, 128.2, 127.8, 126.7, 124.9, 61.4, 33.2, 32.8, 21.4 ppm. HRMS (ESI): calculated for $\text{C}_{32}\text{H}_{31}\text{Cl}_3\text{N}_3\text{Pd}$ $[\text{M}-\text{H}^+]$ 668.0613, found 668.0589

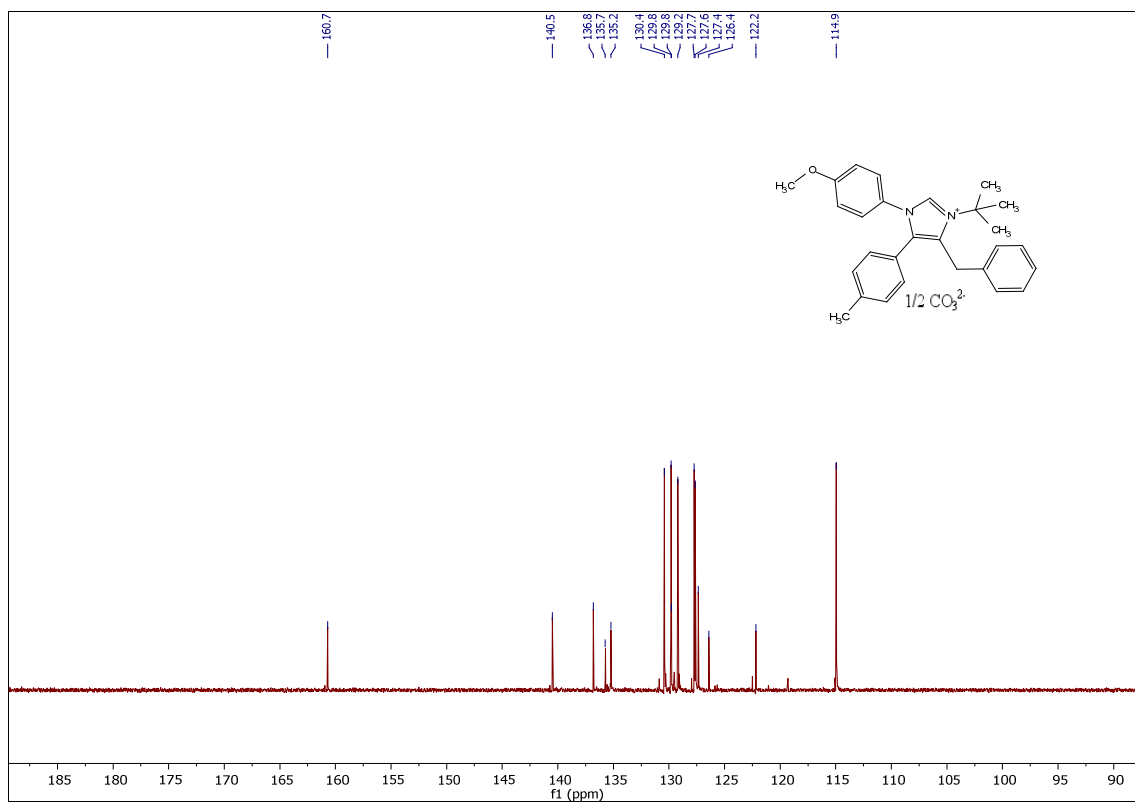
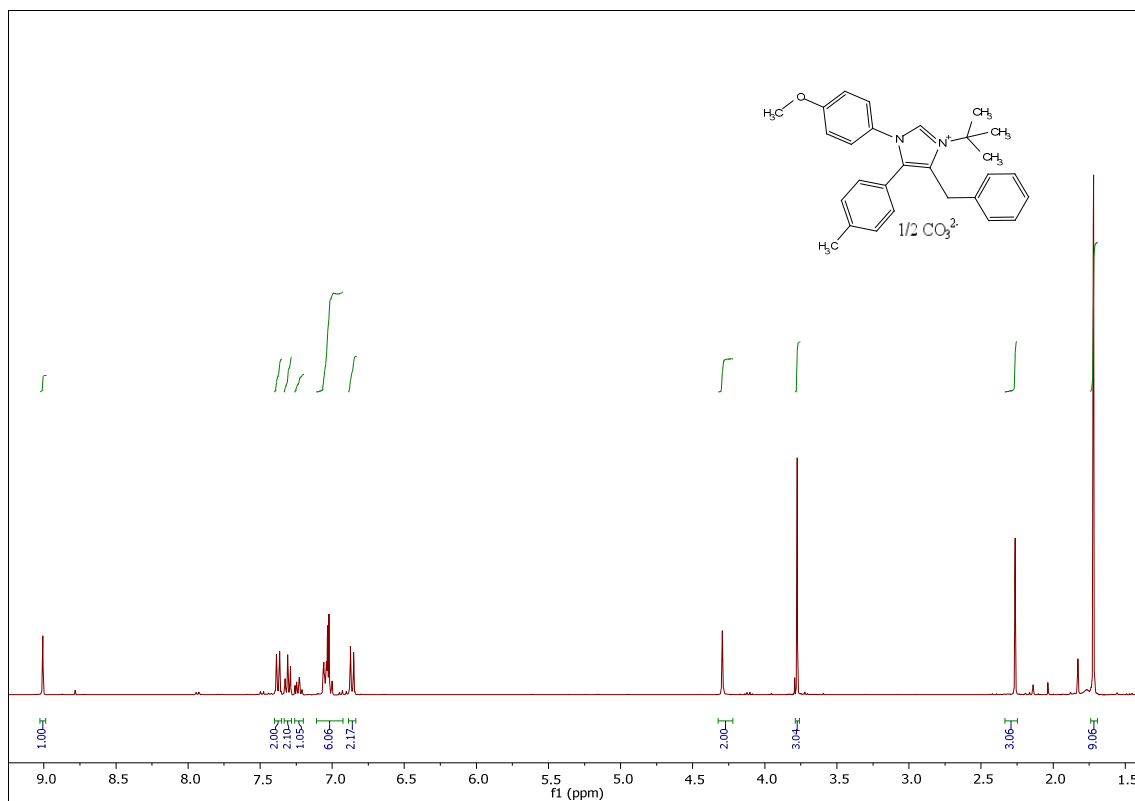
4-Benzyl-1,3-bis(4-methoxyphenyl)-5-(*p*-tolyl)-1*H*-imidazol-3-ium carbonate (6a)



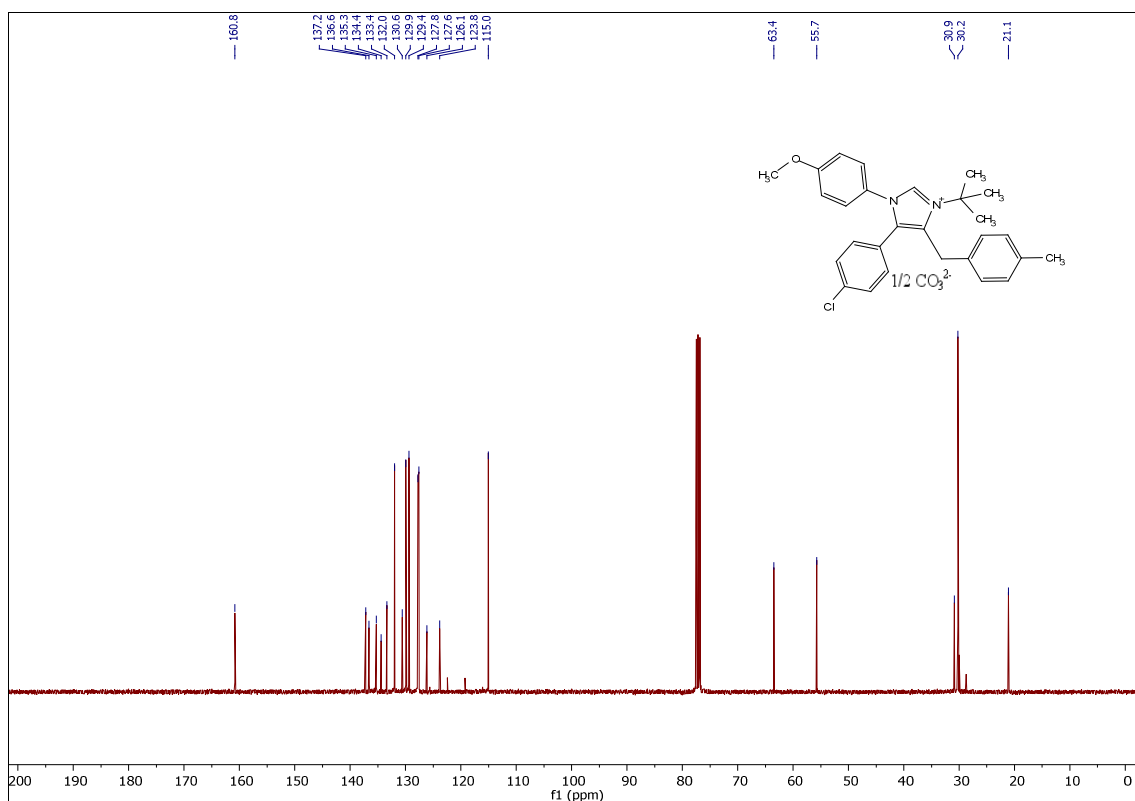
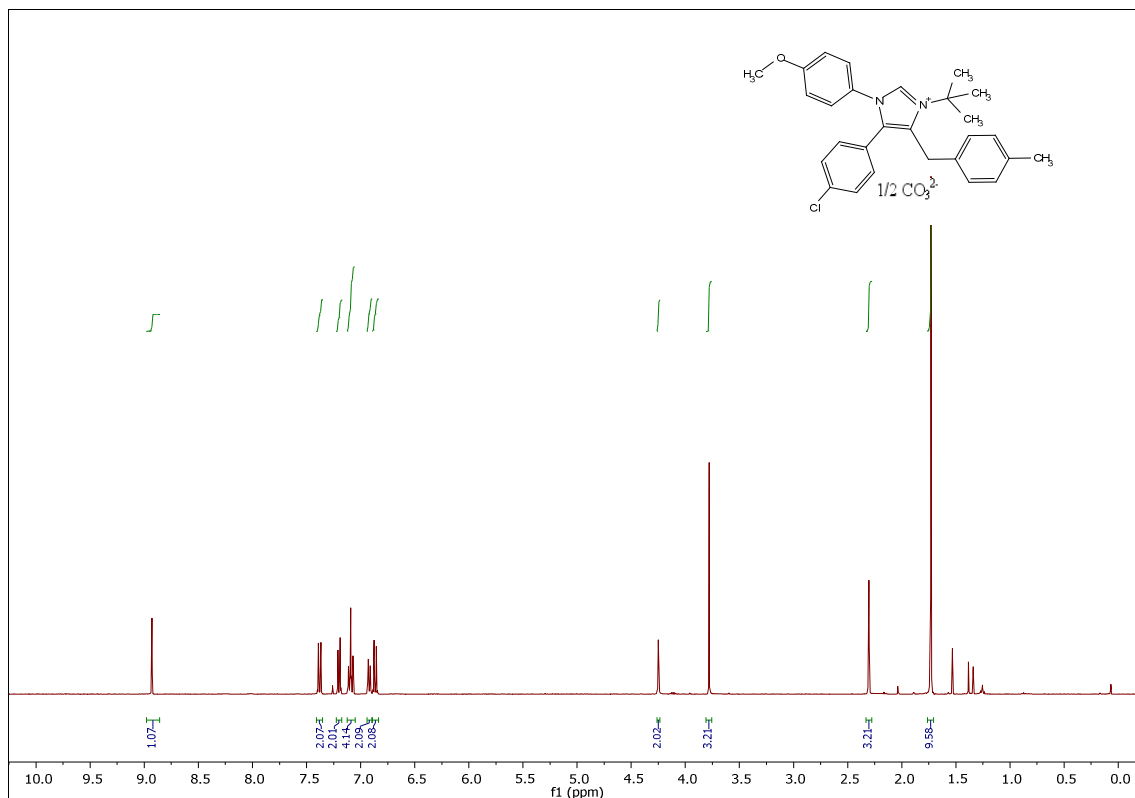
4-Benzyl-3-(*tert*-butyl)-5-phenyl-1-(*p*-tolyl)-1*H*-imidazol-3-ium carbonate (6b)



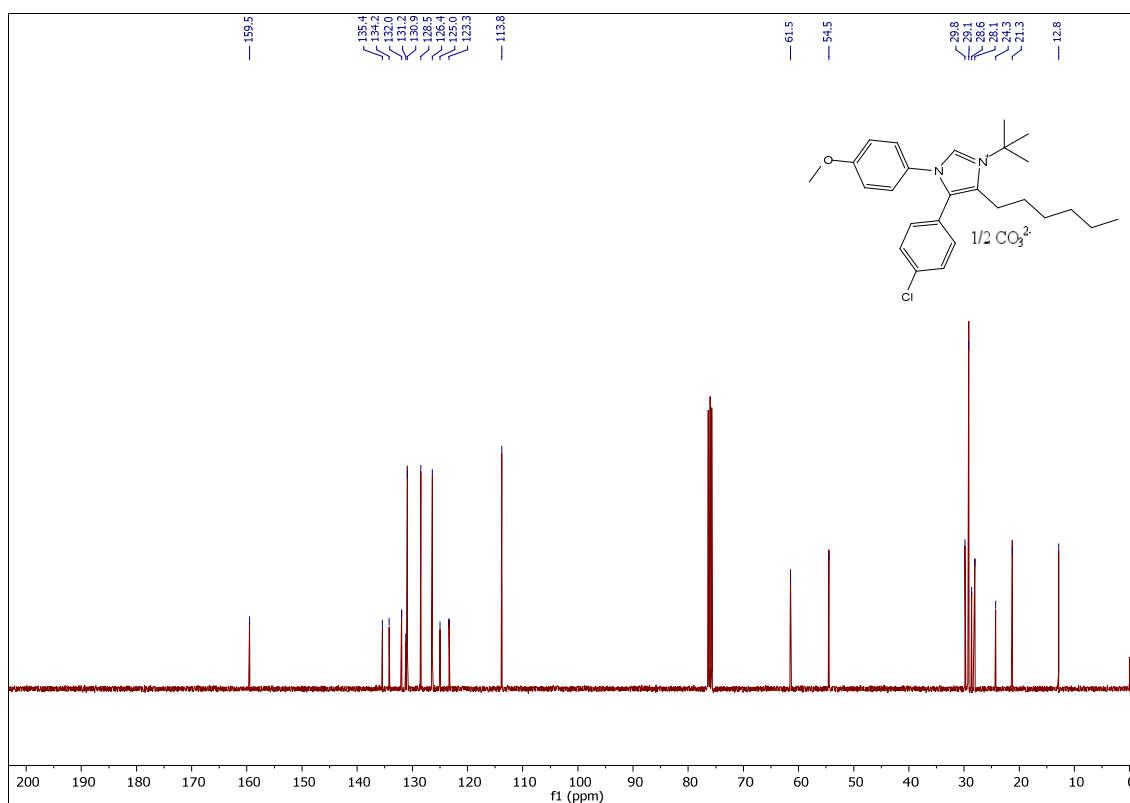
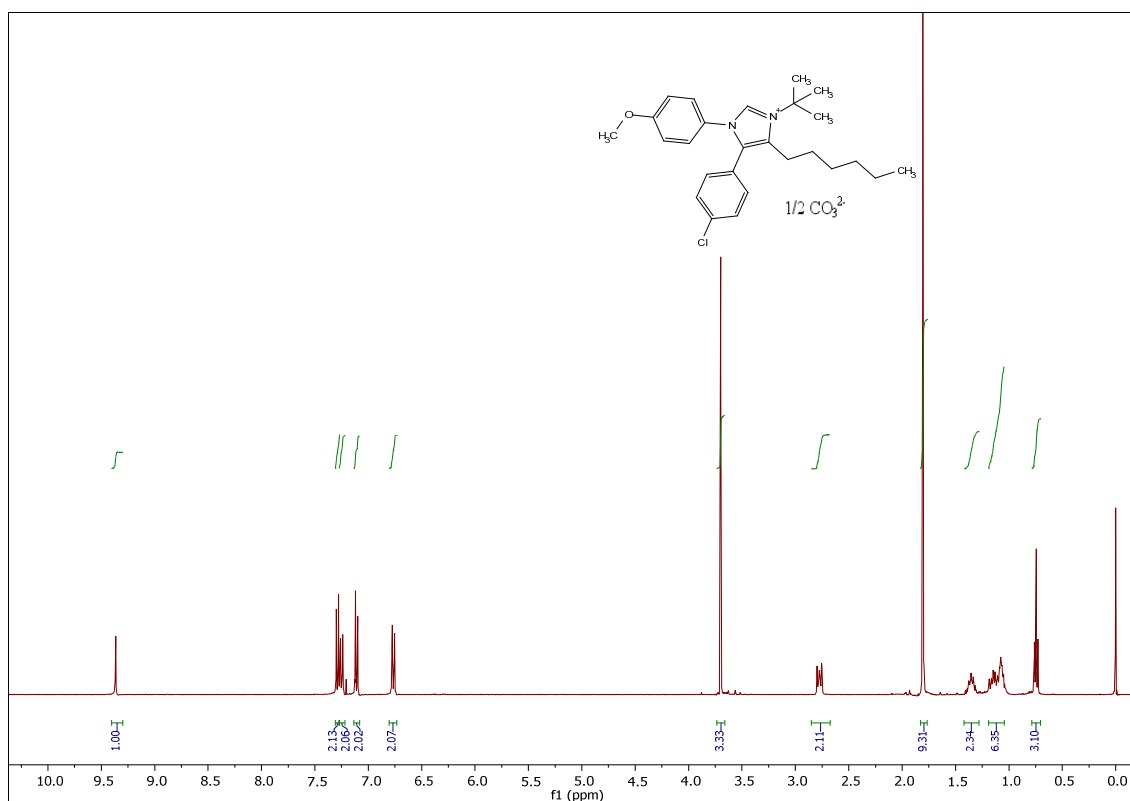
4-Benzyl-3-(*tert*-butyl)-1-(4-methoxyphenyl)-5-(*p*-tolyl)-1*H*-imidazol-3-ium carbonate (6c)



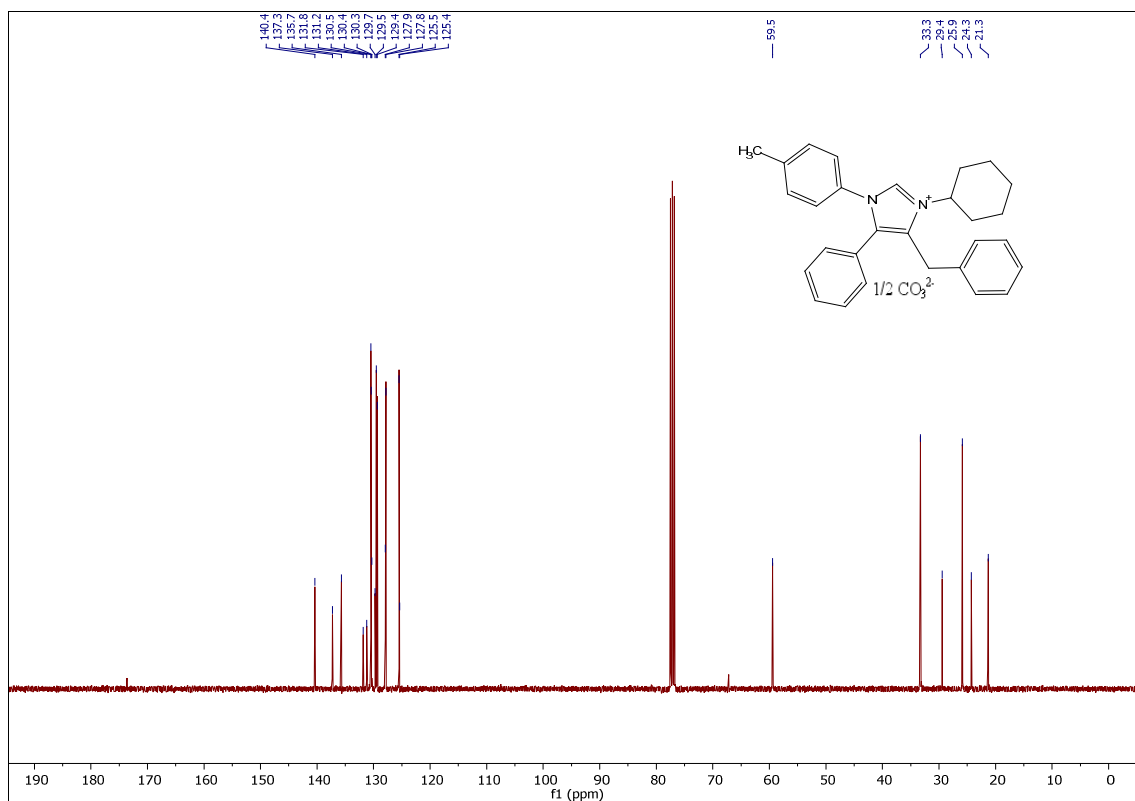
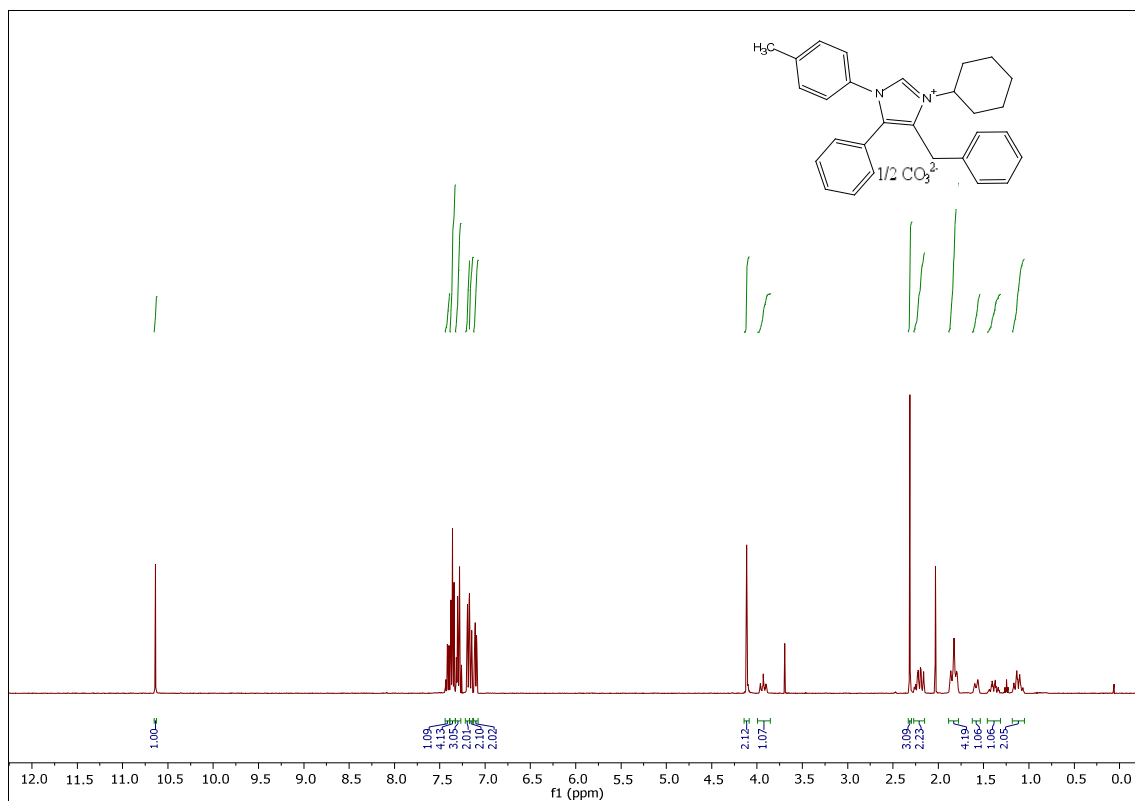
3-(*tert*-Butyl)-5-(4-chlorophenyl)-1-(4-methoxyphenyl)-4-(4-methylbenzyl)-1*H*-imidazol-3-ium carbonate (6f)



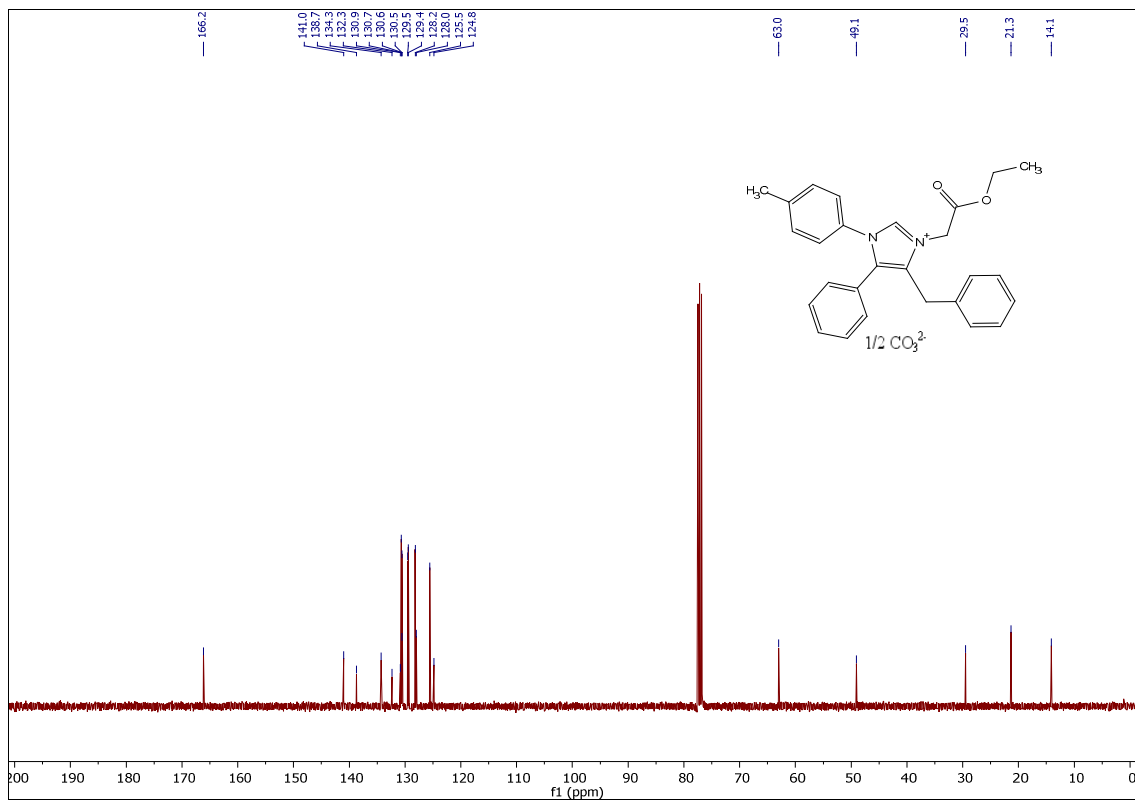
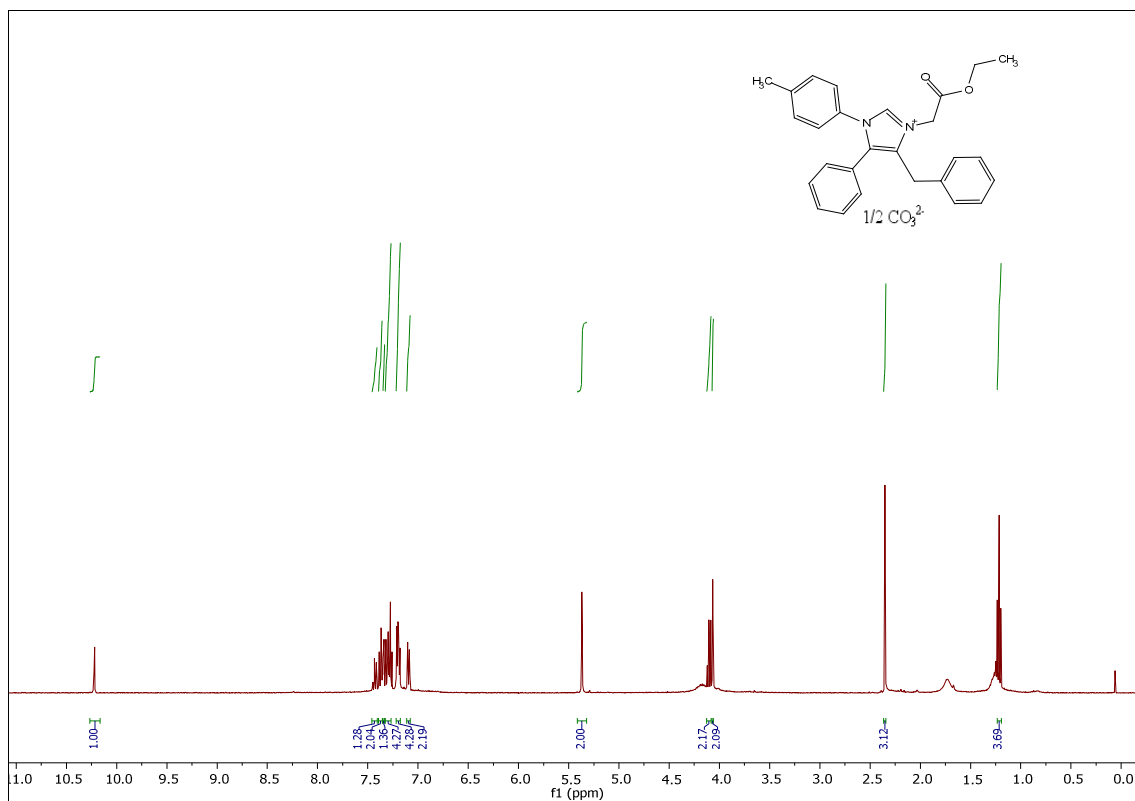
3-(*tert*-Butyl)-5-(4-chlorophenyl)-4-hexyl-1-(4-methoxyphenyl)-1*H*-imidazol-3-ium carbonate (6g)



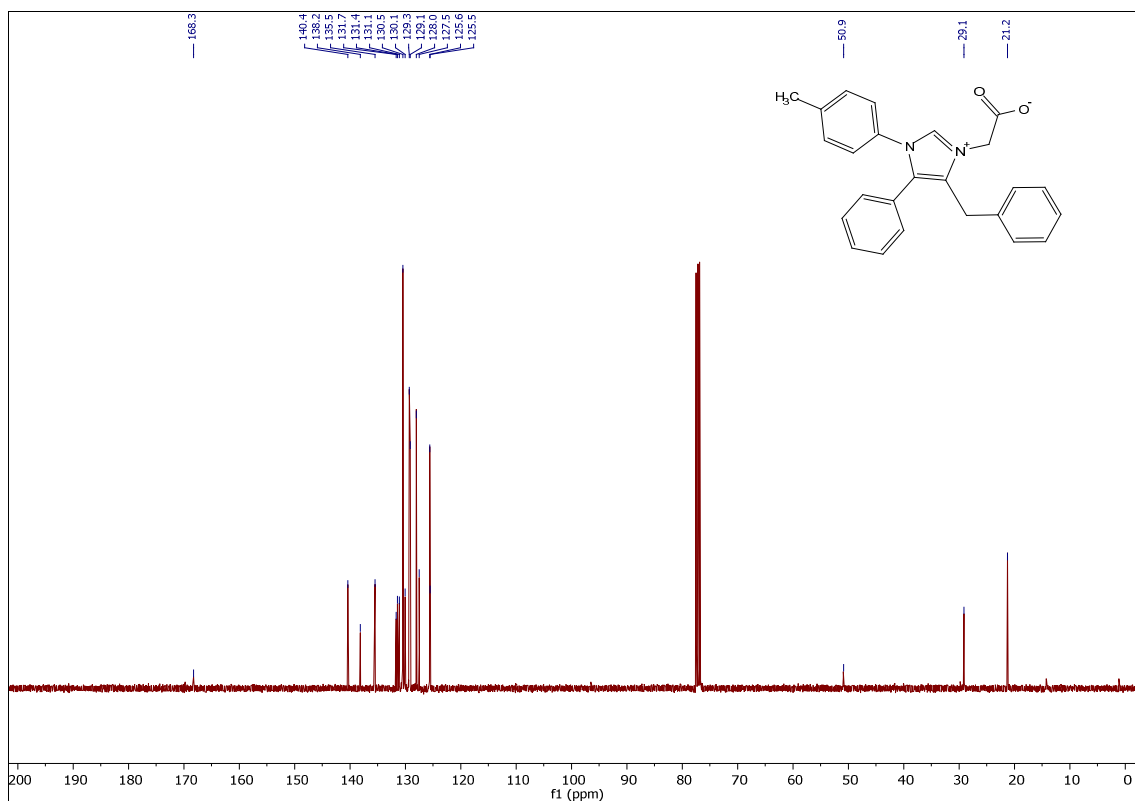
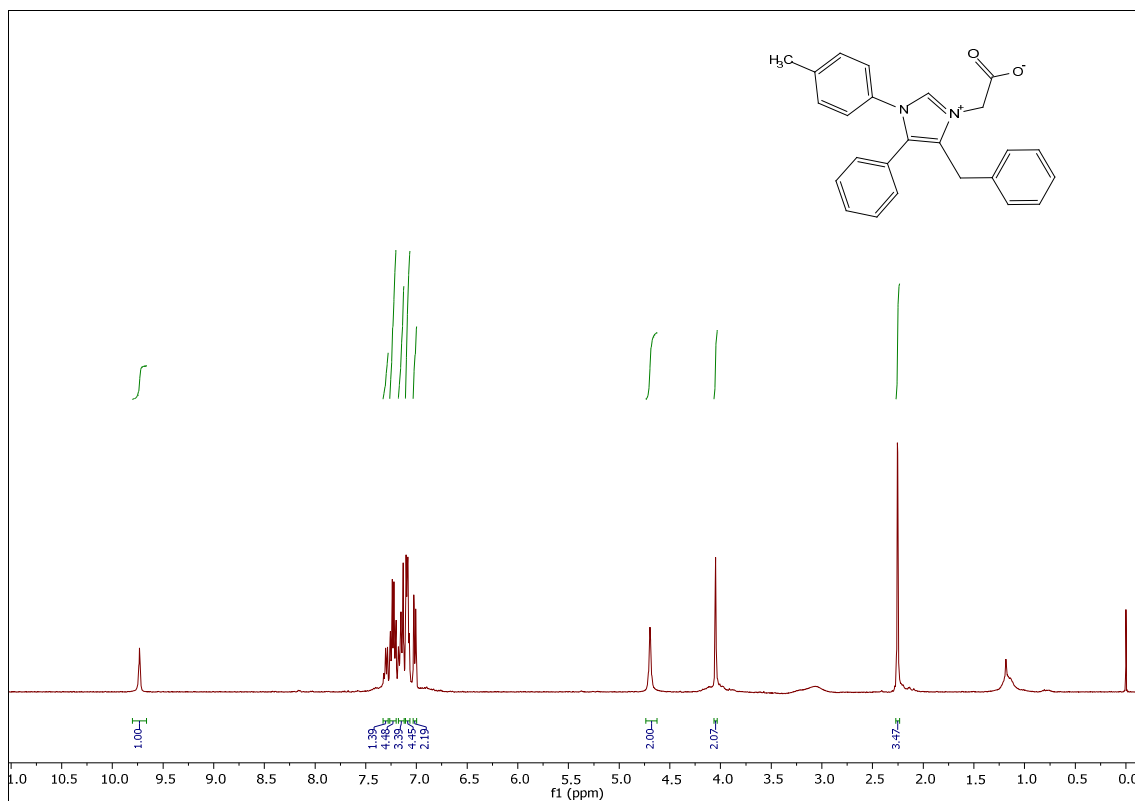
4-Benzyl-3-cyclohexyl-5-phenyl-1-(*p*-tolyl)-1*H*-imidazol-3-ium carbonate (6h)



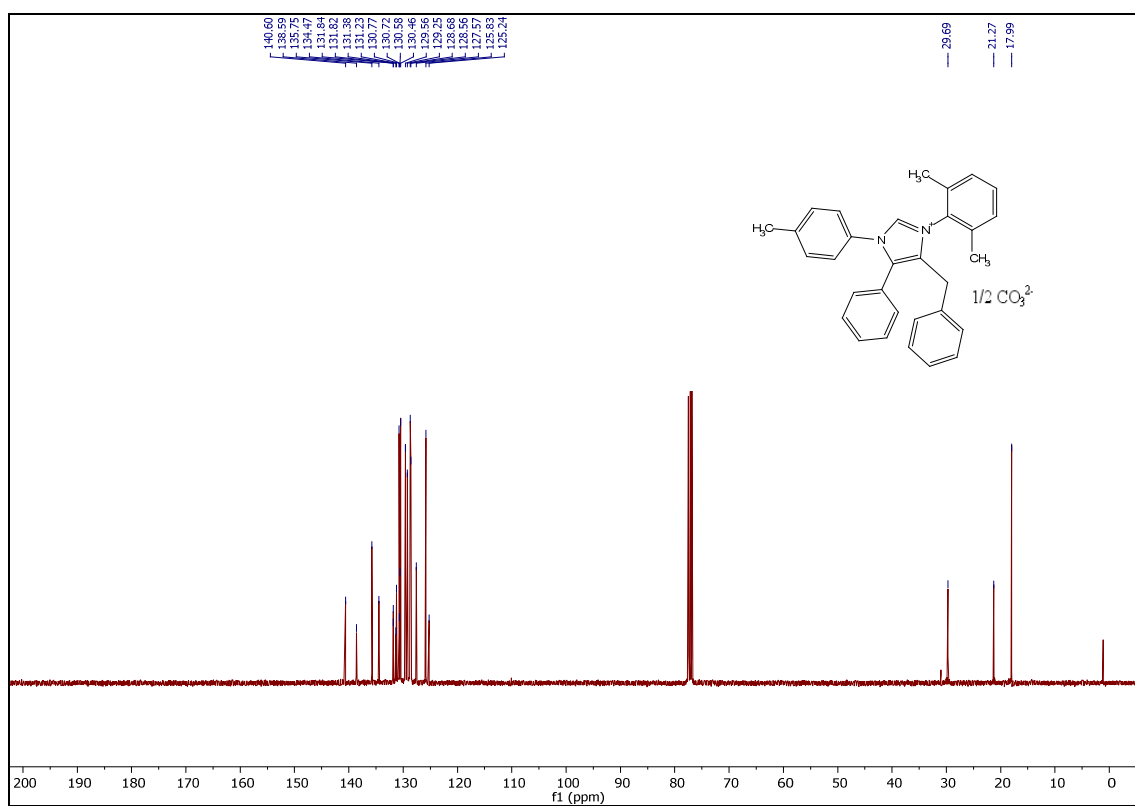
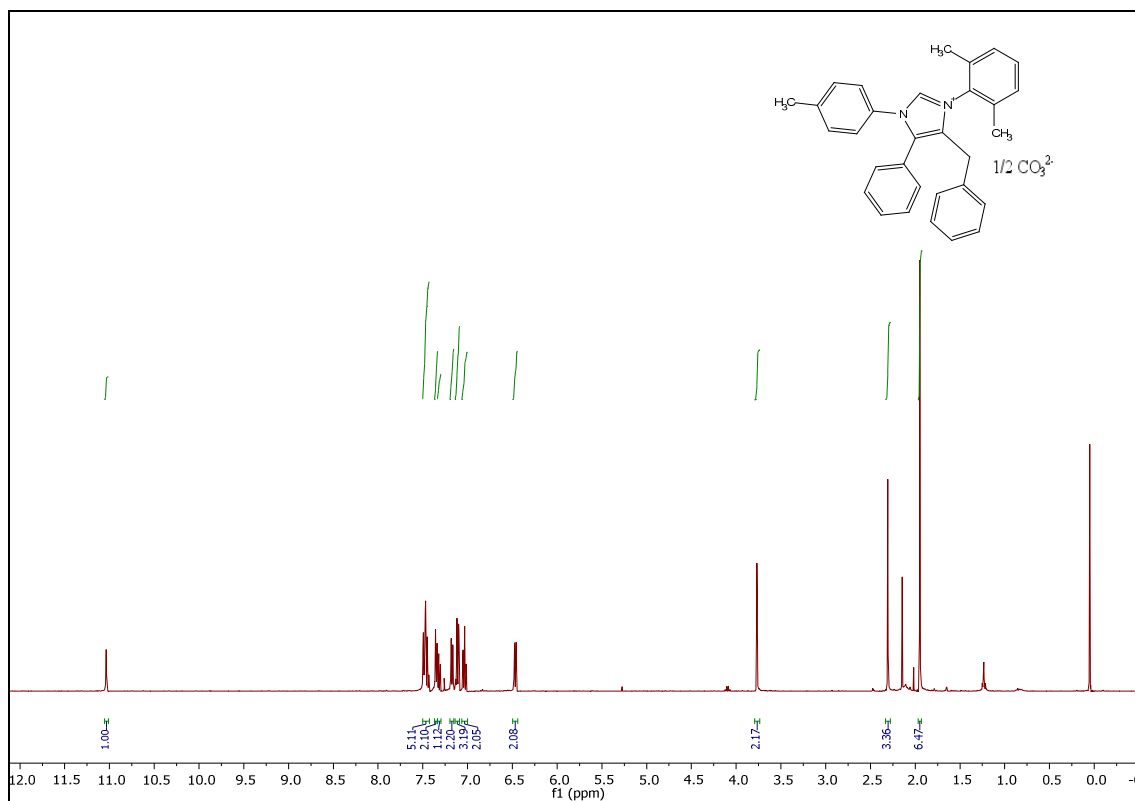
4-Benzyl-3-(2-ethoxy-2-oxoethyl)-5-phenyl-1-(*p*-tolyl)-1*H*-imidazol-3-ium carbonate (6i)



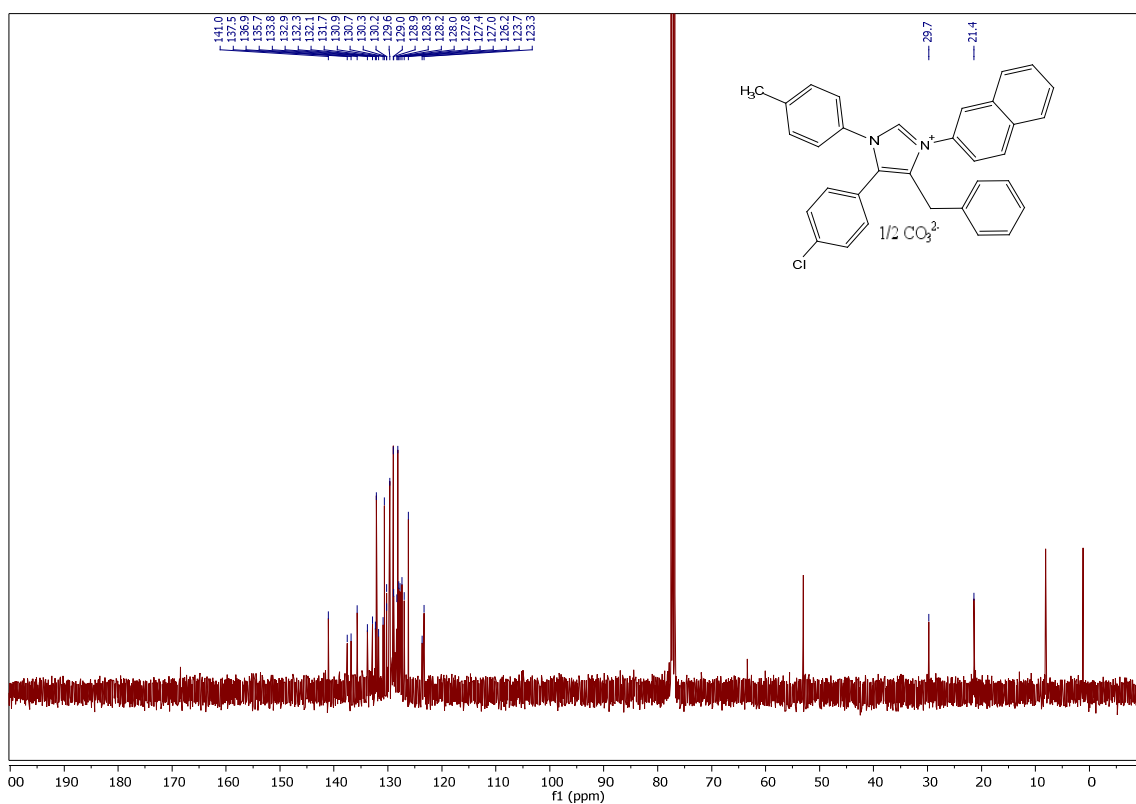
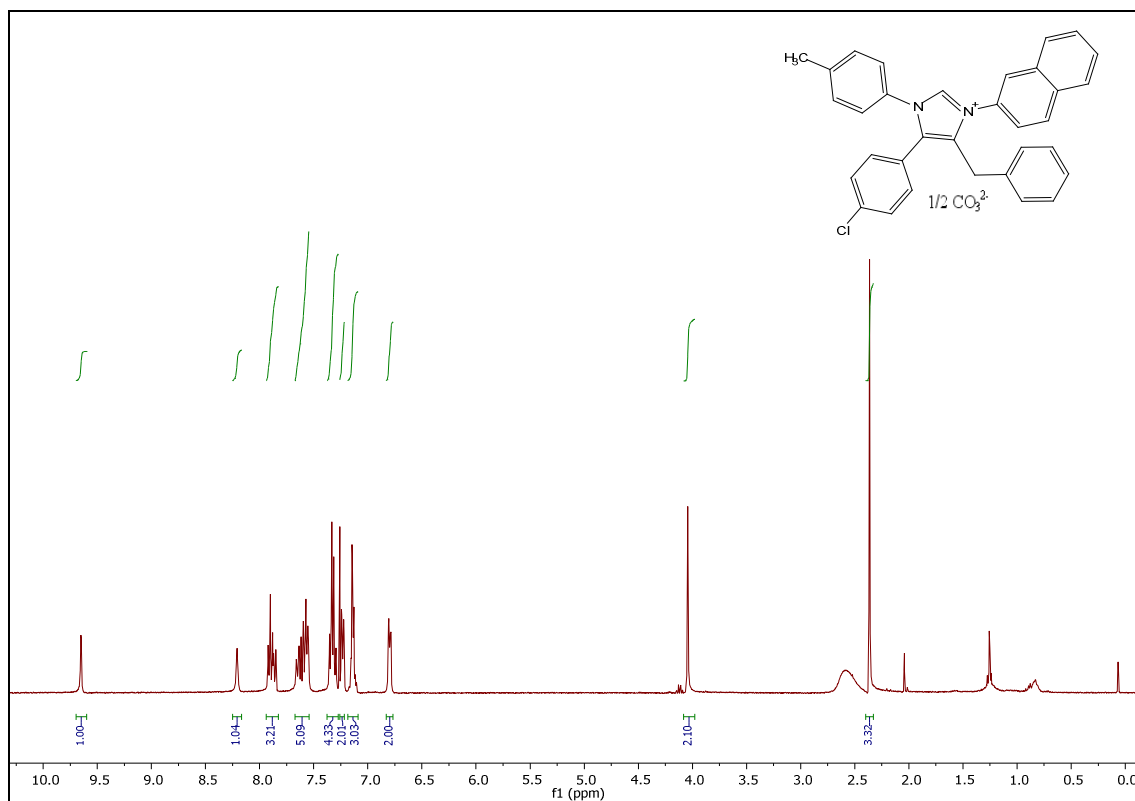
2-(4-benzyl-5-phenyl-1-(*p*-tolyl)-1H-imidazol-3-ium-3-yl)acetate (6i')



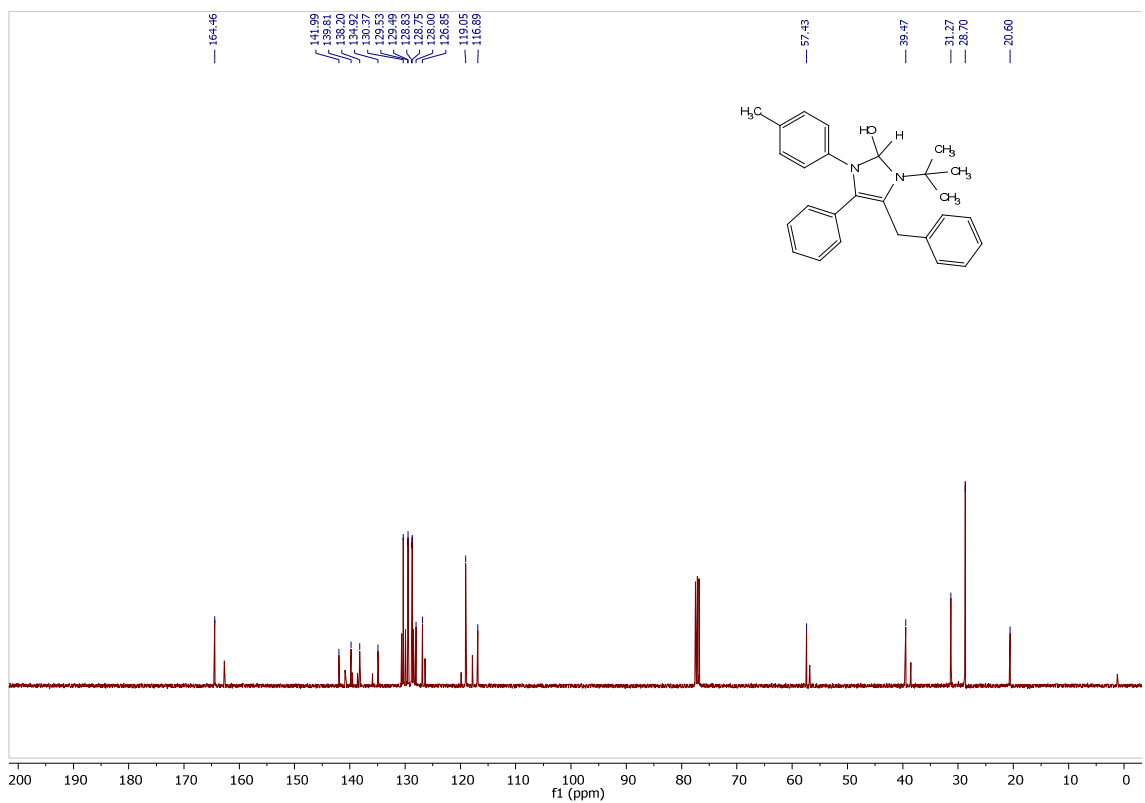
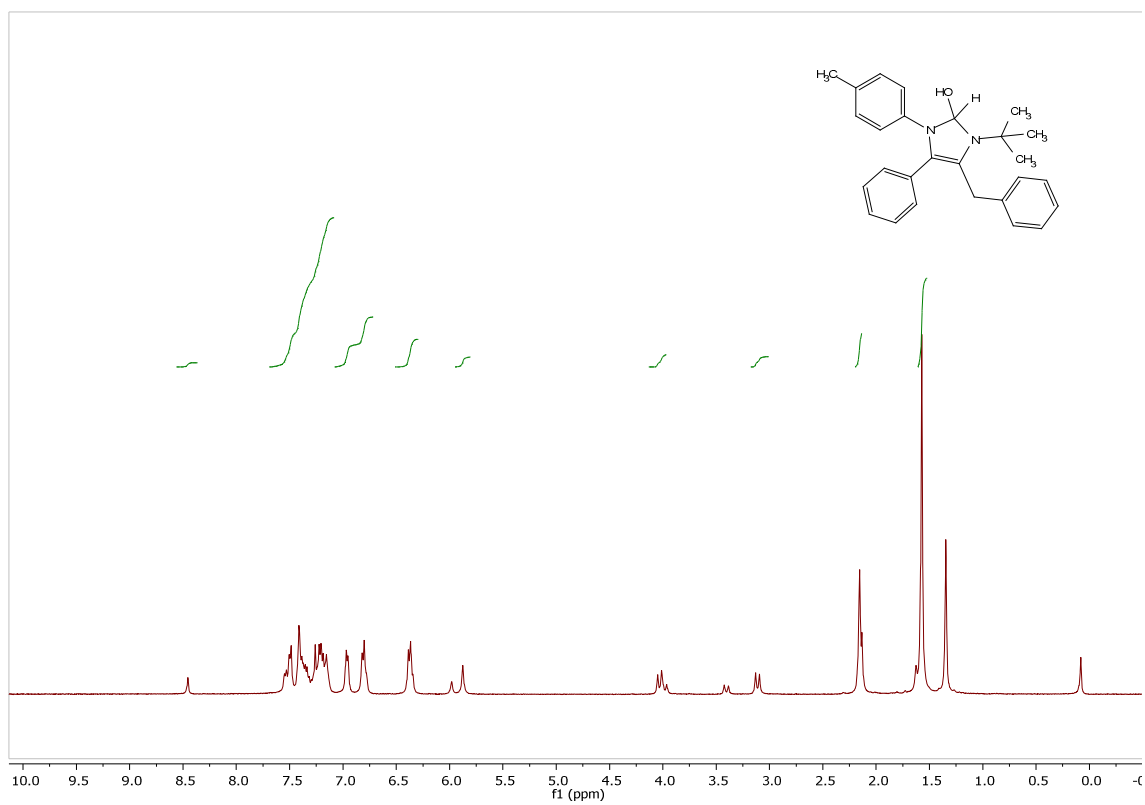
4-Benzyl-3-(2,6-dimethylphenyl)-5-phenyl-1-(*p*-tolyl)-1*H*-imidazol-3-ium carbonate (6j)



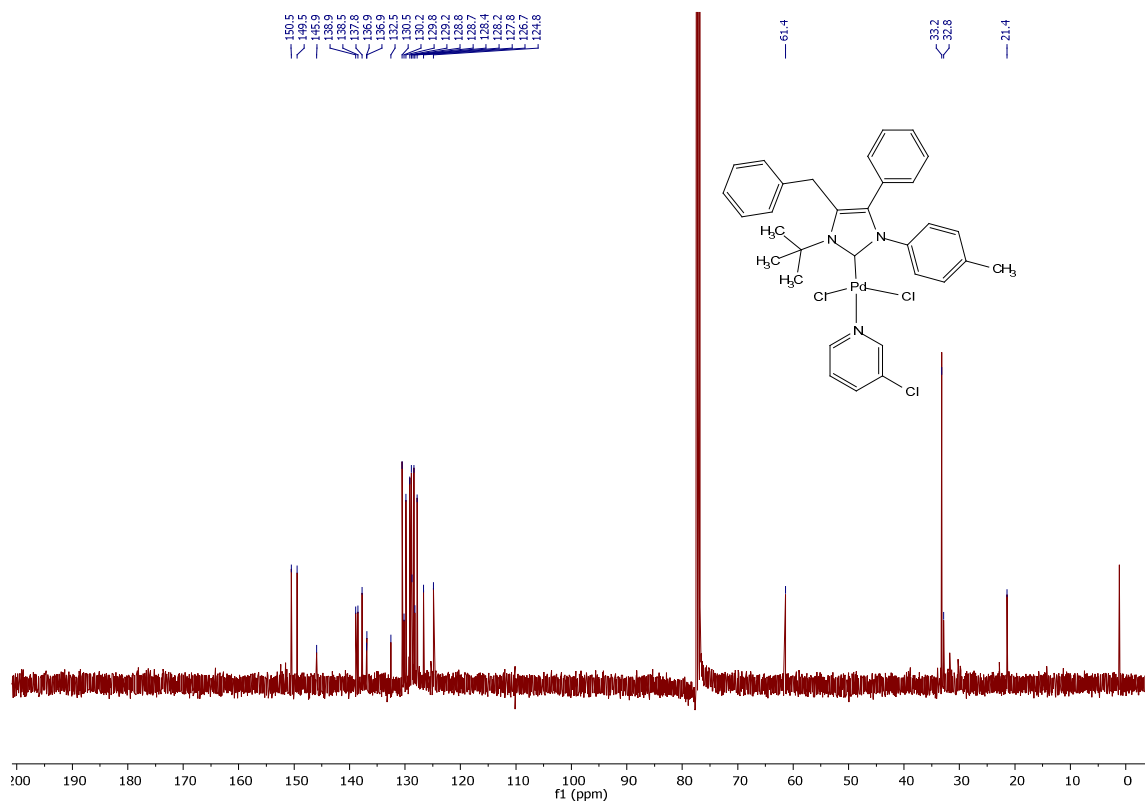
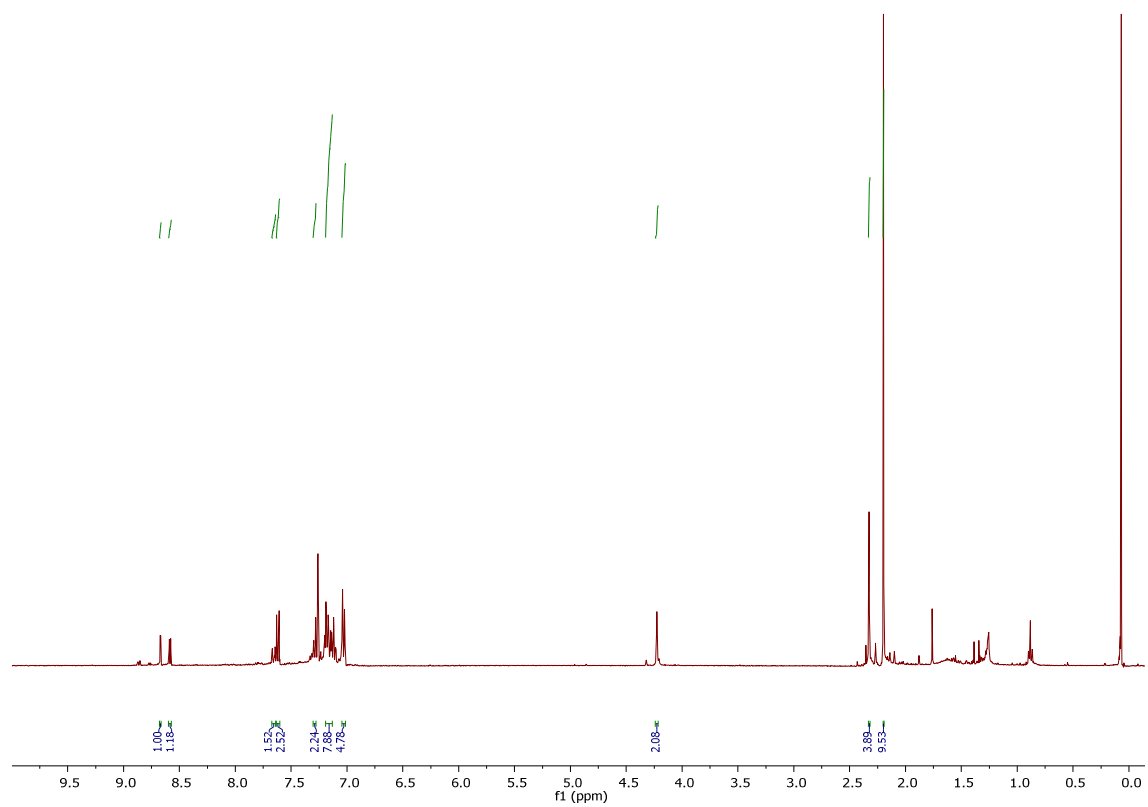
4-Benzyl-5-(4-chlorophenyl)-3-(naphthalen-2-yl)-1-(*p*-tolyl)-1*H*-imidazol-3-ium carbonate (6k)



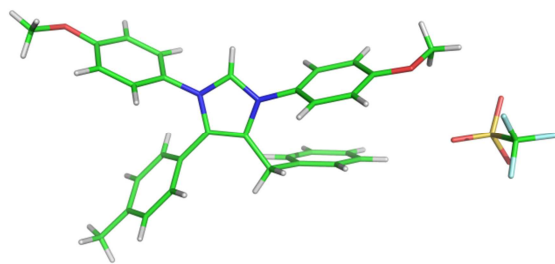
4-Benzyl-3-(*tert*-butyl)-5-phenyl-1-(*p*-tolyl)-2,3-dihydro-1*H*-imidazol-2-ol (13)



6b-PdCl₂-(3-chloropyridine) (14)



X-ray Structure of imidazolium salt **6a** (Triflate).



**Addendum to Chapter II: Antiparasitical
Properties of Novel Tetrasubstituted
Imidazolium Salts Arising from the
Interaction of Isocyanides and
Propargylamines (Unpublished Results)**

The antiparasitical properties of a small selection of novel tetrasubstituted imidazolium salts have been studied. These compounds arise from our group's recent publication¹ on the interaction of isocyanides and propargylamines. Imidazolium salts have been reported to be biologically active against Trypanosomes.² In the present study, the following five compounds have been investigated (Figure 1).

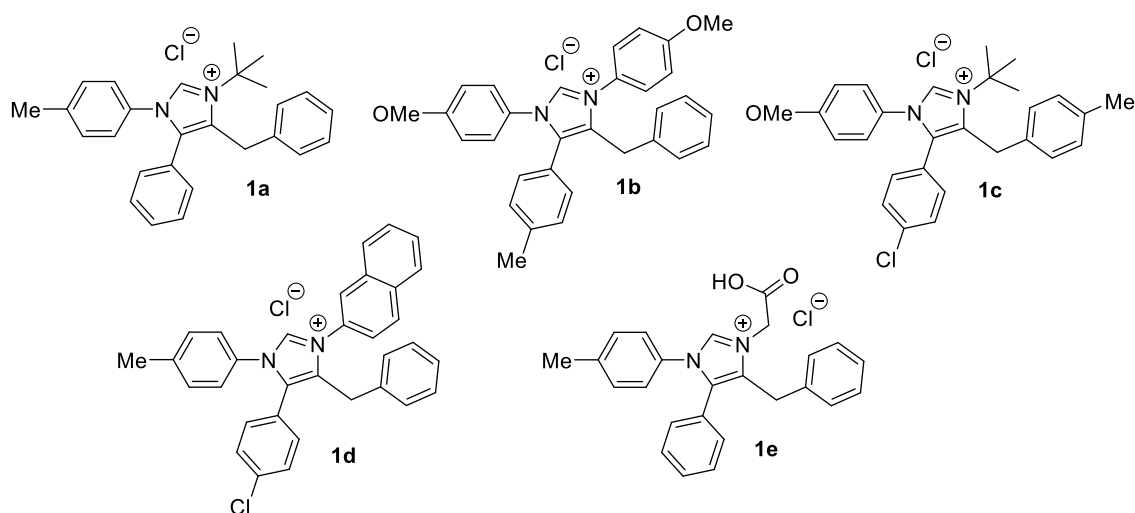


Figure 1. A3-Isocyanide imidazolium adducts studied for their biological activities.

Results and Discussion

T. brucei culturing and evaluation of trypanocidal activity

The antiparasitical properties were studied by Prof. Kelly (The London School of Hygiene & Tropical Medicine), following the methods reported in our common article.¹

Bloodstream form *T. brucei* (strain 221) were cultured at 37 °C in modified Iscove's medium³. Trypanocidal activity was assessed by growing parasites in the presence of various concentrations of the novel compounds and determining the levels which inhibited growth by 50% (IC₅₀) and 90% (IC₉₀). *T. brucei* in the logarithmic phase of growth were diluted back to 2.5×10⁴ mL⁻¹ and aliquoted into 96-well plates. The compounds were then added at a range of concentrations and the plates incubated at 37 °C. Each drug concentration was tested in triplicate. Resazurin was added after 48 h and the plates

¹ K. G. Kishore, O. Ghashghaei, C. Estarellas, M. M. Mestre, C. Monturiol, N. Kielland, J. M. Kelly, A. F. Francisco, S. Jayawardhana, D. Muñoz-Torrero, B. Pérez, F. J. Luque, R. Gámez-Montaño, R. Lavilla, *Angew. Chem.* **2016**, *128*, 9140.

² P. Faral-Tello, M. Liang, G. Mahler, P. Wipf, C. Robello. *Int. J. Antimicrob. Ag.* **2014**, *43*, 262-268.

³ S.R. Wilkinson, S.R. Prathalingam, M.C. Taylor, A. Ahmed, D. Horn, J.M. Kelly, *Free Radical Biol. Med.* **2006**, *40*, 98–209.

incubated for a further 16 h and the plates then read in a Spectramax plate reader. Results were analyzed using GraphPad Prism.

***T. cruzi* culturing and evaluation of trypanocidal activity**

T. cruzi epimastigotes (CL Brener stain) were cultured at 28 °C as described previously ⁴. Activity was determined by growing parasites in 96-well plates. Briefly, cultures were diluted to 2.5x10⁵ mL⁻¹, aliquoted into wells in triplicate at a range of drug concentrations, and allowed to grow for 4 days. Resazurin was added and the plates incubated for a further 3 days, then read in a Spectramax plate reader as outlined above.

Cytotoxic activity against rat skeletal myoblast L6 cells

Cytotoxicity against mammalian cells was assessed using microtitre plates following a described procedure ⁵. Briefly, rat skeletal muscle L6 cells were seeded at 1x10⁴ mL⁻¹ in 200 µL of growth medium containing different compound concentrations. The plates were incubated for 6 days at 37 °C and 20 µL resazurin was then added to each well. After a further 8 h incubation, the fluorescence was determined using a Spectramax plate reader.

Table 1: Compounds **1** vs bloodstream form *Trypanosoma brucei*.

Compd	EC₅₀ <i>T. brucei</i> (µM)	EC₉₀ <i>T. brucei</i> (µM)	EC₅₀ L cells (µM)	S.I.
1a	0.18 ± 0.01	0.28 ± 0.07	33.9 ± 3.3	188
1b	0.039 ± 0.001	0.048 ± 0.001	4.60 ± 0.38	118
1c	0.18 ± 0.01	0.20 ± 0.01	9.69 ± 0.58	54
1d	0.073 ± 0.001	0.093 ± 0.002	4.09 ± 0.28	44
1e	5.26 ± 0.10	6.79 ± 0.09	>130	>24

S.I.: Selectivity Index

⁴ G. Kendall, A.F. Wilderspin, F. Ashall, F., M.A. Miles, J. M. Kelly, *EMBO J.* **1990**, *9*, 2751-2758.

⁵ C. Bot, B.S. Hall, N. Bashir, M.C. Taylor, N.A. Helsby, S.R. Wilkinson, *Antimicrob. Agents Chemother.* **2010**, *54*, 4246–4252.

Table 2: Compounds **1** vs *Trypanosoma cruzi* epimastigotes.

Compd	EC ₅₀ <i>T. cruzi</i> (μ M)	EC ₉₀ <i>T. cruzi</i> (μ M)	EC ₅₀ L cells (μ M)	S.I.
1a	1.85 \pm 0.29	3.41 \pm 0.14	33.9 \pm 3.3	18
1b	0.44 \pm 0.01	1.29 \pm 0.05	4.60 \pm 0.38	10
1c	1.72 \pm 0.39	2.98 \pm 0.19	9.69 \pm 0.58	5.6
1d	0.54 \pm 0.08	1.00 \pm 0.04	4.09 \pm 0.28	7.6
1e	>20	>20	>130	-

S.I.: Selectivity Index

Determination of brain permeability: PAMPA-BBB assay

The in vitro permeability (P_e) of the novel compounds and fourteen commercial drugs through lipid extract of porcine brain membrane was determined by using a parallel artificial membrane permeation assay⁶. Commercial drugs and the target compounds were tested using a mixture of PBS:EtOH (70:30). Assay validation was made by comparing the experimental permeability with the reported values of the commercial drugs by bibliography and lineal correlation between experimental and reported permeability of the fourteen commercial drugs using the parallel artificial membrane permeation assay was evaluated ($y=1,6374x-1,3839$; $R^2=0,9203$). From this equation and the limits established by Di et al. for BBB permeation, three ranges of permeability were established: compounds of high BBB permeation (CNS+): P_e (10^{-6} cm s^{-1}) > 5.16; compounds of low BBB permeation (CNS-): P_e (10^{-6} cm s^{-1}) < 1.89; and compounds of uncertain BBB permeation (CNS \pm): $5.16 > P_e$ (10^{-6} cm s^{-1}) > 1.89.

Table **3** shows permeability results from the different commercial and assayed compounds (three different experiments in triplicate) and predictive penetration in the CNS. The tested compounds show different permeability to cross the barrier and to reach the central nervous system.

⁶ Di, L.; Kerns, E. H.; Fan, K.; McConnell, O. J.; CarTer, G. T. High throughput artificial membrane permeability assay for blood-brain barrier. *Eur. J. Med.Chem.* **2003**, *38*, 223-232.

Table 3. Permeability ($Pe \cdot 10^{-6} \text{ cm}\cdot\text{s}^{-1}$) in the PAMPA-BBB assay of 14 commercial drugs and tested compounds and predictive penetration in the CNS.

Compound	Bibliography value^(a)	Experimental value (n=3) \pm S.D.	CNS Prediction
Verapamil	16,0	25,9 \pm 0,4	
Testosterone	17,0	23,9 \pm 0,3	
Costicosterone	5,1	6,7 \pm 0,1	
Clonidine	5,3	6,5 \pm 0,05	
Ofloxacin	0,8	0,97 \pm 0,06	
Lomefloxacin	0,0	0,8 \pm 0,06	
Progesterone	9,3	16,8 \pm 0,0,3	
Promazine	8,8	13,8 \pm 0,3	
Imipramine	13,0	12,3 \pm 0,1	
Hidrocortisone	1,9	1,4 \pm 0,05	
Piroxicam	2,5	1,7 \pm 0,03	
Desipramine	12,0	17,8 \pm 0,1	
Cimetidine	0,0	0,7 \pm 0,03	
Norfloxacin	0,1	0,9 \pm 0,02	
1a		4,2 \pm 0,3	CNS+/-
1b		4,92 \pm 0,9	CNS+/-
1c		2,6 \pm 0,1	CNS+/-
1d		2,4 \pm 0,05	CNS+/-
1e		1,6 \pm 0,03	CNS-

a) Taken from Di et al. [3].

Calculated molecular properties and CNS MPO desirability scores of the novel isoquinolinium salts and related compounds

Table 4 Molecular properties (Log P, topological polar surface area (TPSA), molecular weight (MW), number of hydrogen bond acceptors (nON), number of hydrogen bond donors (nOHNH), number of rotatable bonds (nrotb), molecular volume (of the cation) , and number of violations of Lipinski's rules (n violations)) calculated using Molinspiration (<http://molinspiration.com>).

compd	miLogP	TPSA	nON	nOHNH	nrotb	nviolations	vol	MW
1a	3.30	8.82	2	0	<u>5</u>	0	382.26	381.54
1b	3.93	27.29	4	0	<u>7</u>	0	438.57	461.58
1e	1.36	46.12	4	1	<u>6</u>	0	359.88	383.47
1c	4.04	18.05	3	0	6	0	421.34	446.01
1d	5.67	8.82	2	0	5	1	445.01	486.04

Table 5. CNS MPO scores calculated using the algorithm reported in ref. ⁷TPSA values, MW, and the number of hydrogen bond donors (nOHNH), used in the algorithm, are shown also in Table 4.

compd	ClogP	clogD	TPSA	MW	HBD	pKa	CNS MPO
1c	4.04	2.24	18.05	446.01	0	-4.8	3.7
1e	1.36	0.31	46.12	383.47	1	2.45	5.7
1b	3.93	3.32	27.29	461.58	0	-4.53	3.5

In conclusion, compounds **1a** and **1b** show an in vitro potent activity (nanomolar) against *T. brucei* and also relevant against *T. cruzi*, with high selectivity indexes and suitable physicochemical parameters.

⁷ T.T. Wager, X. Hou, P.R. Verhoest, A. Villalobos, *ACS Chem. Neurosci.* **2010**, *1* 435-449.

Chapter III

Publication III: Insertion of Isocyanides
into N–Si Bonds: Multicomponent
Reactions with Azines Leading to Potent
Antiparasitic Compounds



Insertion of Isocyanides into N–Si Bonds: Multicomponent Reactions with Azines Leading to Potent Antiparasitic Compounds

Kranti G. Kishore⁺, Ouldouz Ghashghaei⁺, Carolina Estarellas⁺, M. Mar Mestre, Cristina Monturiol, Nicola Kielland, John M. Kelly, Amanda Fortes Francisco, Shiromani Jayawardhana, Diego Muñoz-Torrero, Belén Pérez, F. Javier Luque, Rocío Gámez-Montaña,* and Rodolfo Lavilla*

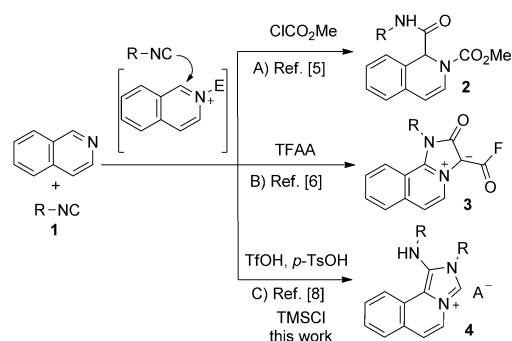
Abstract: Trimethylsilyl chloride is an efficient activating agent for azines in isocyanide-based reactions, which then proceed through a key insertion of the isocyanide into a N–Si bond. The reaction is initiated by N activation of the azine, followed by nucleophilic attack of an isocyanide in a Reissert-type process. Finally, a second equivalent of the same or a different isocyanide inserts into the N–Si bond leading to the final adduct. The use of distinct nucleophiles leads to a variety of α -substituted dihydroazines after a selective cascade process. Based on computational studies, a mechanistic hypothesis for the course of these reactions was proposed. The resulting products exhibit significant activity against *Trypanosoma brucei* and *T. cruzi*, featuring favorable drug-like properties and safety profiles.

Isocyanides hold a central role in several fields of chemistry.^[1] Their formally divalent character makes them ideal partners for multicomponent reactions (MCRs).^[2] However, their mild nucleophilicity, together with their affinity to metals, complicates their activation for many MCRs, which hence often require harsh reaction conditions. Transition-metal-catalyzed processes that involve isocyanides are synthetically useful,^[3] but complex, which is in part due to the metal coordination. In this context, the development of new facilitated MCR transformations is actively pursued, particularly those involving heterocycles, owing to their relevance in biological and medicinal chemistry.

As a testing ground for developing new activation modes, we selected isocyanide variants of the Reissert MCR.^[4] The interaction of isoquinoline with chloroformates or similar

reagents and isocyanides gives the MCR adduct **2**, following the typical mechanism of N activation and isocyanide attack at the α -position (Scheme 1A).^[5] However, interaction with trifluoroacetic anhydride (TFAA), a stronger electrophilic agent, gives rise to mesoionic acid fluorides **3** (Scheme 1B).^[6] Interestingly, strong Brønsted acid activation (TfOH, *p*-TsOH) of the isoquinoline enables an ABB' reaction^[7] with isocyanides (Scheme 1C), leading to isoquinoline-fused imidazolium salts.^[8] The latter reactions were productive, but mechanistic and selectivity issues have remained unsolved. Furthermore, the harsh reactions conditions required for these MCRs prevent the use of sensitive substrates.

In this context, we investigated the use of trimethylsilyl chloride (TMSCl) as a new activating agent in these trans-



Scheme 1. Reissert-type isocyanide multicomponent reactions. *p*-TsOH = *para*-toluenesulfonic acid, Tf = trifluoromethanesulfonyl, TFAA = trifluoroacetic anhydride, TMS = trimethylsilyl.

[*] K. G. Kishore,^[†] Prof. R. Gámez-Montaña
Departamento de Química
Universidad de Guanajuato
Noria Alta S/N, CP 36050 Guanajuato, Gto. (Mexico)
E-mail: rociogm@ugto.mx

O. Ghashghaei,^[†] M. M. Mestre, C. Monturiol, Dr. N. Kielland,
Prof. R. Lavilla
Laboratory of Organic Chemistry, Faculty of Pharmacy
University of Barcelona and Barcelona Science Park
Baldri Reixac 10-12, 08028 Barcelona (Spain)
E-mail: rlavilla@pcb.ub.es

Dr. C. Estarellas,^[†] Prof. F. J. Luque
Departament de Nutrició, Ciència dels Aliments i Gastronomia
Facultat de Farmàcia, and IBUB, Universitat de Barcelona
Prat de la Riba 171, 08921, Santa Coloma de Gramenet (Spain)

Prof. J. M. Kelly, Dr. A. F. Francisco, S. Jayawardhana
Department of Pathogen Molecular Biology
London School of Hygiene and Tropical Medicine
Keppel Street, London WC1E 7HT (UK)

Prof. D. Muñoz-Torrero
Laboratori de Química Farmacèutica, Facultat de Farmàcia, and
Institut de Biomedicina (IBUB), Universitat de Barcelona
Av. Joan XXIII, 27-31, 08028 Barcelona (Spain)

Prof. B. Pérez
Departament de Farmacologia, de Terapèutica i de Toxicologia
Institut de Neurociències, Universitat Autònoma de Barcelona
08193 Bellaterra, Barcelona (Spain)

[†] These authors contributed equally to this work.

Supporting information and the ORCID identification numbers for the authors of this article can be found under <http://dx.doi.org/10.1002/anie.201604109>.

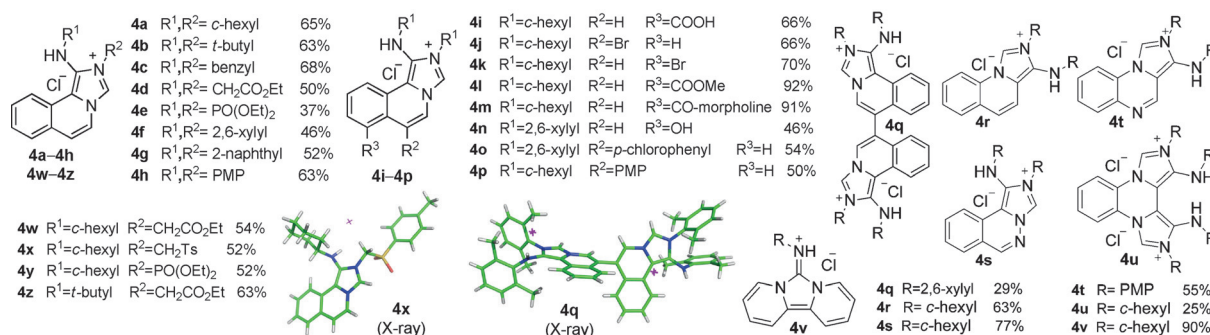


Figure 1. Reaction scope: azines and isocyanides. *c*-hex = cyclohexyl, PMP = *para*-methoxyphenyl.

formations, looking for milder conditions, wider synthetic scope, and selective processes. Incidentally, TMSCl and related derivatives have been used in MCRs almost exclusively to activate carbonyl compounds,^[9a,b] although Krasavin and co-workers reported an elegant example with imines.^[9c] The interaction of isoquinoline and cyclohexyl isocyanide with one equivalent of TMSCl in acetonitrile readily generated imidazolium salt **4a** (65%; Scheme 1C, Figure 1), which precipitated as the chloride salt, presumably after spontaneous hydrolysis of the initial TMS adduct. Owing to the relevance of this new activation mode, we further studied this process.

To determine the scope of the reaction, we screened a wide array of isocyanides and azines. Isoquinoline reacted with aliphatic isocyanides (cyclohexyl, *tert*-butyl, and benzyl isocyanides) to generate the expected adducts (**4a–4c**) in good yields (Figure 1). Functionalized isocyanides (ethyl isocynoacetate and diethyl isocyanomethylphosphonate (PhosMIC)) are compatible with the reaction conditions, and the corresponding imidazolium salts (**4d**, **4e**) were obtained in slightly lower yields. Aromatic isocyanides, such as 2,6-dimethylphenyl-, 2-naphthyl-, and 4-methoxyphenylisocyanide, also yielded the expected compounds (**4f–4h**). We then examined the azine component. Bromo-, carboxy-, and hydroxy-substituted isoquinolines reacted to yield the salts **4i–4k** and **4n**. These adducts can be derivatized in conventional post-transformation reactions. The acid **4i** was thus converted into ester **4l** and amide **4m** using standard procedures. However, the halogenated salts **4j** and **4k** do not react with boronic acids in standard Suzuki couplings, probably because their imidazolium moieties form stable NHC–Pd complexes.^[10] Experimental support came from the characterization of the Pd complex of **4s** and the observation of its low catalytic activity in Suzuki couplings (see the Supporting Information).

Furthermore, aryl-substituted isoquinolines reacted to generate the corresponding derivatives **4o** and **4p**. Remarkably, 4,4'-biisoquinoline underwent a double reaction to generate salt **4q** in a single step. Other azines were also tested, and whereas pyridine was unreactive even under forcing conditions, quinoline generated the corresponding adduct **4r** in good yields. Interestingly, phthalazine reacted with two equivalents of cyclohexyl isocyanide to selectively yield the salt **4s**, with no trace of the double reaction product being detected. Conversely, quinoxaline reacted with an

excess of the same isocyanide to render the double imidazolium salt **4u**. 4-Methoxyphenylisocyanide, however, yielded monoadduct **4t**. Interestingly, the reaction with 2,2'-bipyridine afforded the guanidinium salt **4v** in high yield, which is likely generated in a formal [4+1] cycloaddition (Figure 1).^[11,12]

Finally, we explored the possibility of introducing two distinct isocyanide residues. When a mixture of two isocyanides of similar nucleophilicity^[13] (cyclohexyl and *para*-methoxyphenyl) was reacted with isoquinoline and TMSCl, a roughly equimolecular mixture of the four possible products was obtained (see the Supporting Information). However, the use of one equivalent of an aliphatic isocyanide with another one of reduced nucleophilicity (isocynoacetate, toluenesulfonylmethyl isocyanide (TosMIC), or PhosMIC) dramatically changed the outcome, and we observed the formation of a single adduct in good yields. In this way, the isoquinoline-imidazolium salts **4w–4z** were obtained without detectable amounts of the homoadducts. The residues arising from the more nucleophilic species were attached to the azine α -position, whereas the less nucleophilic ones ended up linked to the heterocyclic nitrogen atom. Unequivocal structural assignment was achieved by X-ray diffraction of a monocrystal of salt **4x** (Figure 1). These results represent a breakthrough in the programmed synthesis of ABB' adducts, which had thus far been restricted to the use of two equivalents of the same input or required the separation of complex mixtures. Furthermore, the connectivity pattern outlined above was tested in other reactant combinations. When different nucleophiles (indole, dimedone) and one equivalent of an isocyanide were reacted with isoquinoline in TMSCl-promoted reactions,^[14] the adducts **5a–5e** (Figure 2) were conveniently obtained in high yields.

Control experiments with a proton scavenger support the participation of TMSCl as the activating agent (see the

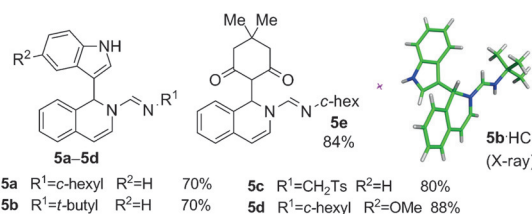
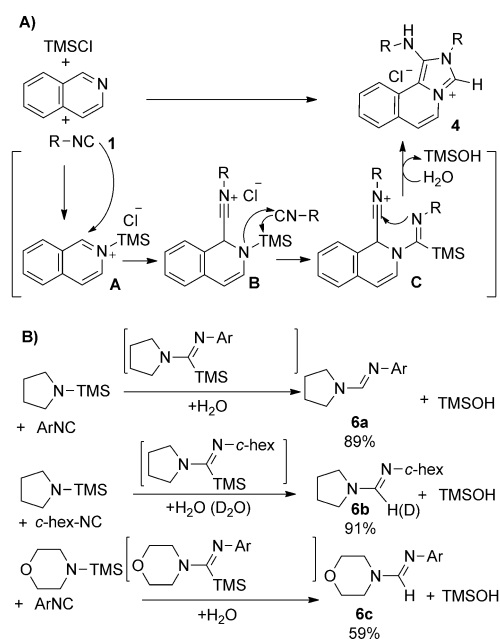


Figure 2. Interception of the MCR cascade with different nucleophilic species.



Scheme 2. Mechanistic proposal and control experiments. Ar = 4-MeOC₆H₄.

Supporting Information). We propose a novel mechanism that accounts for the experimental outcome (Scheme 2A). The reaction starts with the activation of the azine by TMSCl to generate in situ *N*-silyl azinium ion **A**,^[15] which is subsequently attacked by an isocyanide (or another nucleophilic species) to yield nitrilium cation **B**, likely stabilized by a chloride counterion. A second (less nucleophilic) isocyanide may insert into the N–Si bond of this intermediate to yield silylated amidine **C**, giving rise to the fused imidazolium salt **4** by intramolecular *N* addition to the nitrilium moiety and spontaneous hydrolysis of the resulting adduct. Although the azine activation by electrophiles and the isocyanide attack upon formation of the resulting intermediate are known,^[4] the *N*–Si isocyanide insertion^[16,17] is unprecedented.^[18] All attempts to isolate the silyl-substituted imidazolium salts under anhydrous conditions were unsuccessful, likely owing to the instability of the putative structure. Similarly, experiments performed to trap this silylated intermediate with a variety of electrophiles were unproductive, always leading to salts **4**. However,

the likelihood of the insertion step was supported by the generation of amidines **6a–6c** through reaction of isocyanides with *N*-silyl amines, albeit at higher temperatures (toluene, 110°C; Scheme 2B).^[19] In agreement with the proposed mechanism, deactivated or sterically hindered *N*-silyl derivatives failed to undergo the insertion reaction (see the Supporting Information). The course of the reaction was followed by NMR spectroscopy; the silylated intermediates were detected and evolved in situ into the C–H amidines by spontaneous hydrolysis with adventitious water. Although GC/MS analysis of the crude reaction mixtures confirmed the presence of silylated species and D₂O quenching gave amidine **6b** with partial isotopic labeling (see the Supporting Information), it was impossible to characterize the intermediates or trap them with distinct electrophiles.

Pivotal to this chemistry is the novel isocyanide insertion step, as contrary to the standard nucleophilic behavior commonly exhibited by isocyanides, the isocyanide seems to act as an electrophile in spite of the absence of metal cations or strong bases. To gain insight into the insertion process leading to amidines **6**, quantum-mechanical calculations were performed (see the Supporting Information). For the sake of simplicity, computations were performed with methyl isocyanide and trimethylsilyl dimethylamine (DMA-TMS) as the reagents. The reactive channel starts with the attack of the DMA-TMS amine nitrogen atom at the isocyanide in a process that involves the progressive loss of the *sp* hybridization of this latter reagent and the increased pyramidalization of the amine nitrogen atom (Figure 3). These structural changes are the major contribution to the reaction barrier. Furthermore, they afford the geometrical arrangement needed for the formation of the transition state (TS), where the isocyanide C atom is located 1.54 Å away from the amine

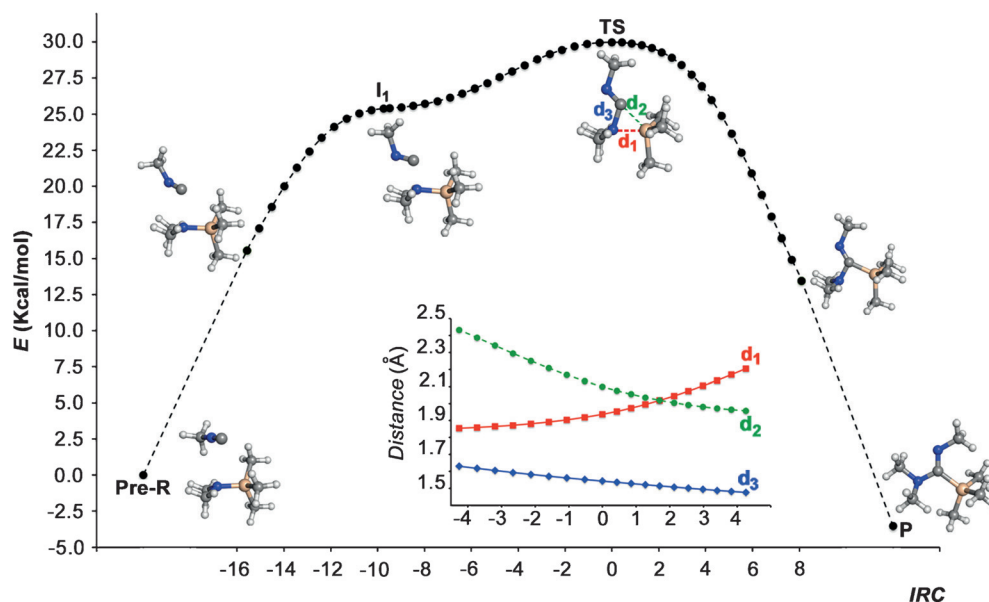
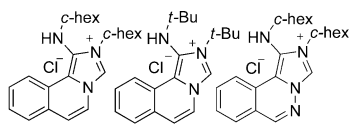


Figure 3. Reactive pathway along the intrinsic reaction coordinate (IRC) for the insertion of Me–N=C into DMA-TMS. Conversion of the pre-reactant (Pre-R) into the transition state (TS) occurs through a metastable intermediate (I1) orienting the isocyanide C atom towards the Si atom, enabling the insertion between the amine N and Si atoms in the final product (P). Inset: Changes in the distances between the isocyanide C atom and DMA-TMS (Si and N) around the TS (IRC = 0).

N atom, while it faces the Si atom (distance of 2.10 Å; Figure 3). Attack of the isocyanide C atom on the Si atom then leads to insertion into the N_{amine}-Si bond, which is enlarged to 2.84 Å in the final product, whereas the C-N_{amine} and C-Si bond lengths are 1.41 and 1.94 Å, respectively. The product is energetically favored by approximately 3.7 kcal mol⁻¹ with regard to the pre-reactant complex (see the Supporting Information, Table S1). These calculations support the mechanistic proposal, which involves the nucleophilic addition of the amine lone pair on the isocyanide and a transition state with a unique azasilainocyclopropane connectivity.

Recently, Wipf, Robello, and co-workers reported the activity of imidazolium salts against *Trypanosoma cruzi*.^[20] Inspired by their results, and considering the need for effective medicines for neglected tropical diseases,^[21] we tested the bioactivity of the synthesized compounds against the causative agents of two trypanosomiasis, namely *T. brucei* for African trypanosomiasis and *T. cruzi* for Chagas disease, which infect several million people. The search for simple, efficient hits is appealing,^[22] particularly if they can simultaneously treat more than one parasitic infection. We evaluated the in vitro trypanocidal activity of adducts **4** against bloodstream forms of *T. brucei* and the epimastigote form of *T. cruzi*. The results revealed an interesting spectrum of activities across the whole series, with many compounds having low micromolar (or even submicromolar) EC₅₀ and EC₉₀ values (Figure 4; see also the Supporting Information)



	4a	4b	4s
EC ₅₀ (<i>T. brucei</i> , μM)	0.55	0.50	0.71
EC ₅₀ (<i>T. cruzi</i> , μM)	1.02	1.53	1.14
SI (<i>T. brucei/cruzi</i>)	18/10	132/43	56/35
PAMPA BBB (Pe)	2.7	5.2	10.8
CNS MPO	4.8	4.8	5.5

Figure 4. Bioactivity data of selected compounds. SI = Selectivity index. High BBB permeation (Pe > 5.16) and CNS MPO scores suggest favorable pharmacokinetic properties (see the Supporting Information).

against both parasites. We observed clear correlations between structural features and bioactivity. Interestingly, the selectivity indexes, a measure of the differential activity against parasite and mammalian cells, were rather high, with values of up to 130 for *T. brucei* and up to 40 for *T. cruzi*. In a preliminary test, compounds **4b** and **4s** were found to display acceptable tolerability, although when evaluated in a bioluminescent murine model for acute *T. cruzi* infection,^[23] there was little significant activity in spite of the reasonable physicochemical profile (see the Supporting Information).^[24] Metabolic turnover and/or a poor biodistribution could be factors that limit efficacy, and these issues will require further assessment.

In summary, we have described the insertion of isocyanides into N-Si bonds, providing a mechanistic hypothesis

and a computational justification for this novel process. We have applied this activation mode to Reissert-type isocyanide MCRs, which can now be conducted with improved selectivity and benefit from an expanded scope. Some products displayed potent and selective in vitro activity against the causative agents of the African sleeping sickness and Chagas disease, paving the way for more detailed structure-activity relationship studies towards the development of convenient lead compounds.

Acknowledgements

We acknowledge support from DGICYT-Spain (CTQ-2015-67870P, SAF2014-57094R), the Generalitat de Catalunya (2014 SGR52, 137, 1189), and CONACYT-México (CB-2011-166747-Q). K.G.K. thanks CONACYT for Ph.D. graduate scholarships (481808/285150). F.J.L. is grateful to Icrea Academia for financial support. The Consorci de Serveis Universitaris de Catalunya (CSUC) is acknowledged for providing computational facilities. J.M.K. acknowledges support from the Drugs for Neglected Diseases Initiative (DNDi).

Keywords: azines · isocyanides · multicomponent reactions · silicon · trypanosomiasis

How to cite: *Angew. Chem. Int. Ed.* **2016**, *55*, 8994–8998
Angew. Chem. **2016**, *128*, 9140–9144

- [1] For an overview, see: *Isocyanide Chemistry* (Ed.: V. G. Nenajdenko), Wiley-VCH, Weinheim, **2012**.
- [2] a) *Multicomponent Reactions* (Eds.: J. Zhu, H. Bienaymé), Wiley-VCH, Weinheim, **2005**; b) *Multicomponent Reactions, Vol. 1, 2* (Ed.: T. J. J. Müller), Science of Synthesis, Thieme, Stuttgart, **2014**; c) *Multicomponent Reactions in Organic Synthesis* (Eds.: J. Zhu, Q. Wang, M.-X. Wang), Wiley-VCH, Weinheim, **2015**.
- [3] a) T. Vlaar, B. U. W. Maes, E. Ruijter, R. V. A. Orru, *Angew. Chem. Int. Ed.* **2013**, *52*, 7084–7097; *Angew. Chem.* **2013**, *125*, 7222–7236; b) S. Lang, *Chem. Soc. Rev.* **2013**, *42*, 4867–4880.
- [4] N. Kielland, R. Lavilla in *Synthesis of Heterocycles via Multicomponent Reactions II, Topics in Heterocyclic Chemistry 25* (Eds.: R. V. A. Orru, E. Ruijter, B. U. W. Maes), Springer, Heidelberg, **2010**.
- [5] J. L. Díaz, M. Miguel, R. Lavilla, *J. Org. Chem.* **2004**, *69*, 3550–3553.
- [6] M. J. Arévalo, N. Kielland, C. Masdeu, M. Miguel, N. Isambert, R. Lavilla, *Eur. J. Org. Chem.* **2009**, 617–625.
- [7] D. Tejedor, F. García-Tellado, *Chem. Soc. Rev.* **2007**, *36*, 484–491.
- [8] a) J.-C. Berthet, M. Nierlich, M. Ephritikhine, *Eur. J. Org. Chem.* **2002**, 375–378; b) A. Shaabaani, E. Soleimani, R. H. Khavasi, *J. Comb. Chem.* **2008**, *10*, 442–446.
- [9] a) J.-P. Wan, Y. Liu, *Curr. Org. Chem.* **2011**, *15*, 2758–2773; b) R. C. Cioc, D. J. H. van der Niet, E. Janssen, E. Ruijter, R. V. A. Orru, *Chem. Eur. J.* **2015**, *21*, 7808–7813; c) M. Krasavin, S. Tsurulnikov, M. Nikulnikov, V. Kysil, A. Ivachtchenko, *Tetrahedron Lett.* **2008**, *49*, 5241–5243.
- [10] E. A. B. Kantchev, C. J. O'Brien, M. G. Organ, *Angew. Chem. Int. Ed.* **2007**, *46*, 2768–2813; *Angew. Chem.* **2007**, *119*, 2824–2870.

- [11] Remarkably, this compound was also synthesized by Berthet and co-workers (Ref. [8a]) in a TfOH-promoted reaction at 100 °C with an excess of the isocyanide.
- [12] A. Kruithof, E. Ruitjer, R. V. A. Orru, *Chem. Asian J.* **2015**, *10*, 508–520.
- [13] V. V. Tumanov, A. A. Tishkov, H. Mayr, *Angew. Chem. Int. Ed.* **2007**, *46*, 3563–3566; *Angew. Chem.* **2007**, *119*, 3633–3636.
- [14] For a related reaction under strong acid activation, see: A. Shaabani, E. Soleimani, H. R. Khavasi, *Tetrahedron Lett.* **2007**, *48*, 4743–4747.
- [15] a) J. Bräckow, K. T. Wanner, *Tetrahedron* **2006**, *62*, 2395–2404; b) D. L. Comins, E. D. Smith, *Tetrahedron Lett.* **2006**, *47*, 1449–1451.
- [16] For reviews, see: a) A. V. Lygin, A. de Meijere, *Angew. Chem. Int. Ed.* **2010**, *49*, 9094–9124; *Angew. Chem.* **2010**, *122*, 9280–9311; b) G. Qiu, Q. Ding, J. Wu, *Chem. Soc. Rev.* **2013**, *42*, 5257–5269.
- [17] For recent examples of isocyanide insertion, see: a) Y. Tian, L. Tian, C. Li, X. Jia, J. Li, *Org. Lett.* **2016**, *18*, 840–843; b) S. Tong, Q. Wang, M.-X. Wang, J. Zhu, *Angew. Chem. Int. Ed.* **2015**, *54*, 1293–1297; *Angew. Chem.* **2015**, *127*, 1309–1313; c) Y. Fukumoto, H. Shimizu, A. Tashiro, N. Chatani, *J. Org. Chem.* **2014**, *79*, 8221–8227.
- [18] For insertions into Si–C and Si–H bonds, see: a) P. T. Nguyen, W. S. Palmer, K. A. Woerpel, *J. Org. Chem.* **1999**, *64*, 1843–1848; b) M. C. Lipke, T. D. Tilley, *J. Am. Chem. Soc.* **2013**, *135*, 10298–10301.
- [19] Amidines can also arise from isocyanide insertion into N–H bonds; see: F. Medda, C. Hulme, *Tetrahedron Lett.* **2014**, *55*, 3328–3331.
- [20] P. Faral-Tello, M. Liang, G. Mahler, P. Wipf, C. Robello, *Int. J. Antimicrob. Agents* **2014**, *43*, 262–268.
- [21] Centers for Disease Control and Prevention, Neglected Tropical Diseases, <http://www.cdc.gov/globalhealth/ntd/>.
- [22] K. Chibale, *Pure Appl. Chem.* **2005**, *77*, 1957–1964.
- [23] M. D. Lewis, A. Fortes Francisco, M. C. Taylor, H. Burrell-Saward, A. P. McLatchie, M. A. Miles, J. M. Kelly, *Cell. Microbiol.* **2014**, *16*, 1285–1300.
- [24] V. N. Viswanadhan, C. Balan, C. Hulme, J. C. Cheetham, Y. Sun, *Curr. Opin. Drug Discovery Dev.* **2002**, *5*, 400–406.

Received: May 3, 2016

Published online: June 17, 2016

Publication III: Selected Supporting Information

General information

Unless stated otherwise, all reactions were carried out under argon atmosphere in dried glassware. Commercially available reactants were used without further purification. Thin-layer chromatography was performed on pre-coated Merck silica gel 60 F254 plates and visualized under a UV lamp. ^1H , and ^{13}C NMR spectra were recorded on a Varian Mercury 400 (at 400 MHz, and 100 MHz respectively). Unless otherwise stated, NMR spectra were recorded in CDCl_3 solution with TMS as an internal reference. Data for ^1H NMR spectra are reported as follows: chemical shift (δ ppm), multiplicity, integration and coupling constants (Hz). Data for ^{13}C NMR spectra are reported in terms of chemical shift (δ ppm). IR spectra were recorded using a Thermo Nicolet Nexus spectrometer and are reported in frequency of absorption (cm^{-1}). High resolution mass spectrometry was performed by the University of Barcelona Mass Spectrometry Service.

Experimental procedures and Characterization data

General Procedures for the synthesis of characterized compounds

General Procedure A: A solution of isoquinoline (1 mmol, 1 eq) and TMS-Cl (1 mmol, 1 eq) in ACN (2 mL) was stirred for 10 min. at rt. The isocyanide (2 mmol, 2 eq) was then added and the mixture was stirred for 24 h at rt. After the completion of reaction the mixture was filtered and the residue was washed with ACN and diethyl ether to afford the pure imidazolium salt.

General Procedure B: Isoquinoline (1 mmol, 1 eq.) and TMS-Cl (1 mmol, 1 eq.) were stirred in ACN (2 mL) during 10 min. at rt. Isocyanide (2 mmol, 2 eq) was then added and stirred for 24 h at 60 °C. The mixture was filtered and washed with ACN and diethyl ether and then the solid was dried to afford the pure imidazolium salt.

General Procedure C: An isoquinoline solution (1 mmol, 1 eq.) in ACN (2 mL) was treated with TMS-Cl (1 mmol, 1 eq.). The mixture was stirred for 10 min at RT. Isocyanide (1 mmol, 1 eq) and indole (1 mmol, 1 eq.) were then added simultaneously and stirred for 2 to 24 h at rt. After reaction completion, the precipitate was filtered and washed with ACN and diethyl ether to afford the corresponding product.

General Procedure D: 1-(trimethylsilyl)pyrrolidine (1 mmol, 1 eq) and an isocyanide (1 mmol, 1 eq) were added simultaneously to stirring toluene (4 mL) under argon atmosphere at rt. The mixture was stirred at reflux for 2 days. After reaction completion, the mixture was quenched with water (5 mL). The organic layer was separated, dried over MgSO₄ and evaporated under reduced pressure to afford the final product.

2-cyclohexyl-1-(cyclohexylamino)-7-(methoxycarbonyl)imidazo[5,1-*a*]isoquinolin-2-ium chloride (4l)

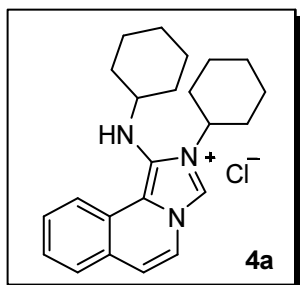
A solution of **4i** (0.11 mmol, 1 eq, 50 mg) and SOCl₂ (0.3 mmol, 3 eq, 27 μL) in MeOH (5 mL) was stirred during 72 h at rt. The reaction was quenched with 0.1M NaOH aqueous solution (5 mL and extracted with DCM 3x10mL). The solvent was removed and the residue washed with diethyl ether to afford 2-cyclohexyl-1-(cyclohexylamino)-7-(methoxycarbonyl)imidazo[5,1-*a*]isoquinolin-2-ium chloride **4l**.

2-cyclohexyl-1-(cyclohexylamino)-7-(morpholine-4-carbonyl)imidazo[5,1-*a*]isoquinolin-2-ium chloride (4m)

A solution of **4i** (0.11 mmol, 1 eq, 50 mg) and SOCl₂ (0.3 mmol, 3 eq, 24 μL) in DCM (5 mL) was stirred during 5 h at reflux. The mixture was evaporated under reduced pressure and the residue re-dissolved in DCM (5 mL). Morpholine (0.3 mmol, 3 eq, 29 μL) and HBT (0.3 mmol, 3 eq) were added and the mixture was stirred for 1 h. The mixture was quenched with NaOH (0.1 M, 5 mL) and extracted with DCM (3x10 mL). The organic phase was evaporated under reduced pressure and the residue was washed with diethyl ether and recrystallized by DCM/diethyl ether to afford pure 2-cyclohexyl-1-(cyclohexylamino)-7-(morpholine-4-carbonyl)imidazo[5,1-*a*]isoquinolin-2-ium chloride **4m**.

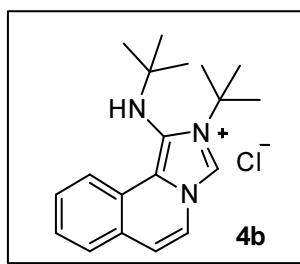
Characterization data for the final products

2-Cyclohexyl-1-(cyclohexylamino)imidazo[5,1-*a*]isoquinolin-2-ium chloride (**4a**)



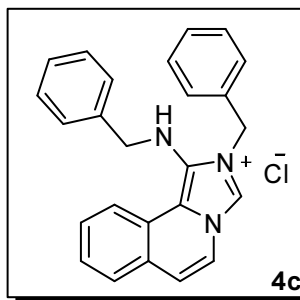
According to procedure A, compound **4a** was obtained as a white powder (65%). $^1\text{H NMR}$ (400 MHz, CDCl_3) δ 9.54 (s, 1H), 8.87 – 8.82 (m, 1H), 8.01 (d, $J = 7.4$ Hz, 1H), 7.82 – 7.77 (m, 1H), 7.70 – 7.64 (m, 2H), 7.33 (d, $J = 7.3$ Hz, 1H), 4.69 (s, 1H), 1.94 (s, 10H), 1.54 – 1.10 (m, 10H). $^{13}\text{C NMR}$ (100 MHz, CDCl_3) δ 129.30, 128.97, 128.80, 128.11, 127.62, 125.60, 123.27, 122.77, 122.15, 119.82, 118.12, 58.16, 56.02, 34.39, 33.95, 25.69, 25.38, 25.00, 24.44. **IR (KBr)** $\tilde{\nu}$ (cm^{-1}): 3171, 3070, 3008, 2911, 2849, 2723, 1588. **HRMS (ESI)**: calculated for $\text{C}_{23}\text{H}_{30}\text{N}_3$ [$\text{M}]^+$: 348.2434, found 348.2431.

2-(*tert*-butyl)-1-(*tert*-butylamino)imidazo[5,1-*a*]isoquinolin-2-ium chloride (**4b**)



According to procedure B, compound **4b** was obtained as a white powder (63%). $^1\text{H NMR}$ (400 MHz, CDCl_3) δ 11.45 (s, 1H), 8.81 (d, $J = 7.3$ Hz, 1H), 8.77 (d, $J = 9.4$ Hz, 1H), 7.59 (d, $J = 9.3$ Hz, 1H), 7.55 – 7.51 (m, 2H), 6.98 (d, $J = 7.3$ Hz, 1H), 3.58 (s, 1H), 2.16 (s, 1H), 1.92 (s, 10H), 1.26 (s, 10H). $^{13}\text{C NMR}$ δ 131.11, 130.72, 129.49, 129.43, 129.06, 127.44, 126.48, 125.59, 123.97, 121.99, 119.85, 64.92, 57.79, 31.37, 31.33. **IR (KBr)** $\tilde{\nu}$ (cm^{-1}): 3455, 3372, 3244, 3199, 3064, 2975, 2904. **HRMS (ESI)**: calculated for $\text{C}_{19}\text{H}_{26}\text{N}_3$ [$\text{M}]^+$: 296.2121, found 296.2124.

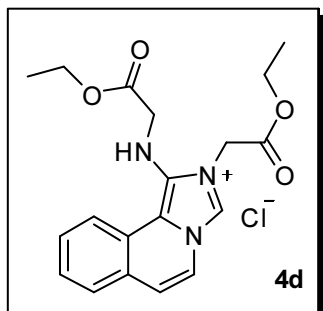
2-benzyl-3-(benzylamino)imidazo[5,1-*a*]isoquinolin-2-ium chloride (**4c**)



According to procedure A, compound **4c** was obtained as a white powder (68%). $^1\text{H NMR}$ (400 MHz, CD_3OD) δ 9.16 (s, 1H), 8.47 – 8.40 (m, 1H), 8.02 (d, $J = 7.4$ Hz, 1H), 7.81 – 7.75 (m, 1H), 7.64 (m, $J = 7.3, 1.5$ Hz, 2H), 7.46 – 7.38 (m, 3H), 7.34 – 7.24 (m, 8H), 5.32 (s, 2H), 4.19 (s, 2H). $^{13}\text{C NMR}$ (100 MHz, CD_3OD) δ 138.55, 133.39, 131.38, 129.53, 129.09, 128.88, 128.81, 128.52, 128.27, 128.21, 127.96, 127.59, 127.38, 124.54, 123.10, 122.48, 120.64, 120.61, 118.99, 51.93, 49.20. **IR (KBr)** $\tilde{\nu}$ (cm^{-1}): 3388,

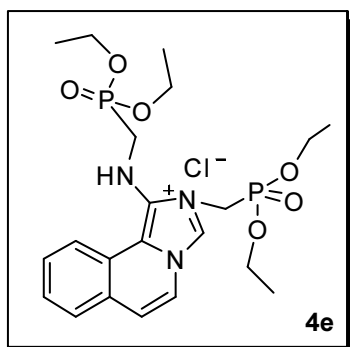
3158, 3078, 3058, 3023, 2909, 2979, 2850. **HRMS (ESI)**: calculated for $C_{25}H_{22}N_3 [M]^+$: 364.1808, found 364.1810.

2-(2-ethoxy-2-oxoethyl)-1-((2-ethoxy-2-oxoethyl)amino)imidazo[5,1-*a*]isoquinolin-2-ium chloride (4d)



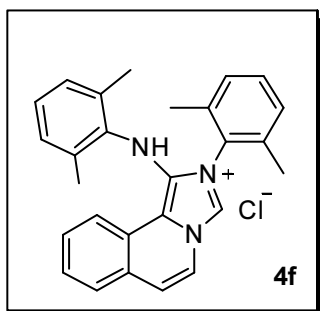
According to procedure B, compound **4d** was obtained as a white powder (50%) **¹H NMR** (400 MHz, $CDCl_3$) δ 10.72 (s, 1H), 8.41 (d, $J = 7.4$ Hz, 1H), 8.24 (d, $J = 7.9$ Hz, 1H), 7.62 – 7.57 (m, 1H), 7.51 (m, $J = 4.2, 1.7$ Hz, 2H), 6.92 (d, $J = 7.4$ Hz, 1H), 5.81 – 5.75 (m, 3H), 4.26 (q, $J = 7.1$ Hz, 2H), 4.10 (q, $J = 7.2$ Hz, 2H), 3.92 (d, $J = 6.0$ Hz, 2H), 1.31 (t, $J = 7.1$ Hz, 3H), 1.20 (t, $J = 7.1$ Hz, 3H). **¹³C NMR** (100 MHz, $CDCl_3$) δ 171.3, 167.2, 131.2, 129.7, 129.0, 127.9, 126.9, 126.4, 123.3, 122.0, 121.2, 118.8, 118.7, 62.7, 61.2, 48.3, 47.8, 14.0, 14.0. **IR (KBr)** $\tilde{\nu}$ (cm^{-1}): 3451, 3133, 3080, 2984, 3032, 2931, 1737, 1222. **HRMS (ESI)**: calculated for $C_{19}H_{22}N_3O_4 [M]^+$: 356.1605, found 356.1606.

2-((diethoxyphosphoryl)methyl)-1-(((diethoxyphosphoryl)methyl)amino)imidazo[5,1-*a*]isoquinolin-2-ium chloride (4e)



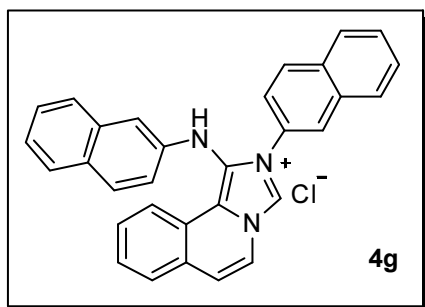
According to procedure A, compound **4e** was obtained as a white powder (37%) **¹H NMR** (400 MHz, DMSO) δ 9.69 (s, 1H), 8.50 (d, $J = 8.0$ Hz, 1H), 8.43 (d, $J = 6.2$ Hz, 1H), 7.91 (d, $J = 7.3$ Hz, 1H), 7.75 (m, $J = 22.8, 7.3$ Hz, 2H), 7.51 (d, $J = 7.3$ Hz, 1H), 5.81 (s, 1H), 5.26 (d, $J = 13.0$ Hz, 2H), 4.25 – 4.12 (m, 4H), 4.05 (p, $J = 7.1$ Hz, 4H), 3.63 (m, $J = 10.9, 6.2$ Hz, 2H), 1.26 (t, $J = 7.0$ Hz, 6H), 1.21 (t, $J = 7.0$ Hz, 6H). **¹³C NMR** (100 MHz, $CDCl_3$) δ 131.2, 130.0, 129.4, 128.2, 127.2, 126.6, 123.5, 122.1, 121.5, 119.3, 118.8, 64.6, 64.6, 62.8, 62.7, 44.1, 42.6, 16.4, 16.4, 16.4, 16.3. **IR (KBr)** $\tilde{\nu}$ (cm^{-1}): 3390, 3103, 3208, 3040, 2931, 2978, 2894, 1484, 1249. **HRMS (ESI)**: calculated for $C_{21}H_{32}N_3O_6P_2 [M]^+$: 484.1761, found 484.1769.

2-(2,6-dimethylphenyl)-1-((2,6-dimethylphenyl)amino)imidazo[5,1-*a*]isoquinolin-2-ium chloride (4f)



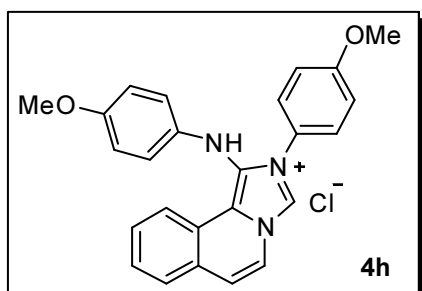
According to procedure B, compound **4f** was obtained as a white powder (46%) $^1\text{H NMR}$ (400 MHz, CD_3OD) δ 8.91 – 8.84 (m, 1H), 8.21 (d, $J = 7.4$ Hz, 1H), 7.96 – 7.91 (m, 1H), 7.84 – 7.73 (m, 2H), 7.54 (d, $J = 7.4$ Hz, 1H), 7.31 (t, $J = 7.7$ Hz, 1H), 7.09 (d, $J = 7.7$ Hz, 2H), 6.82 – 6.73 (m, 4H), 1.92 (d, $J = 6.6$ Hz, 12H). $^{13}\text{C NMR}$ (100 MHz, CD_3OD) δ 139.31, 135.79, 131.30, 131.20, 130.58, 129.79, 129.47, 129.45, 128.64, 128.57, 128.16, 127.66, 125.65, 123.95, 123.77, 122.95, 120.85, 120.28, 119.84, 17.28, 16.32. **IR (KBr)** $\tilde{\nu}$ (cm^{-1}): 3059, 3380, 2965, 3028, 2746, 2917, 2854 **HRMS (ESI)**: calculated for $\text{C}_{27}\text{H}_{26}\text{N}_3$ $[\text{M}]^+$: 392.2121, found 392.2129.

2-(naphthalen-2-yl)-1-(naphthalen-2-ylamino)imidazo[5,1-a]isoquinolin-2-ium chloride (**4g**)



According to procedure A, compound **4g** was obtained as a yellow powder (52%) $^1\text{H NMR}$ (400 MHz, DMSO) δ 10.47 (s, 1H), 9.28 (s, 1H), 8.51 (d, $J = 7.7$ Hz, 1H), 8.40 (s, 1H), 8.16 (d, $J = 7.8$ Hz, 1H), 8.11 (d, $J = 8.8$ Hz, 1H), 8.02 – 7.94 (m, 4H), 7.78 (m, $J = 8.8, 2.0$ Hz, 1H), 7.70 (d, $J = 8.7$ Hz, 2H), 7.68 – 7.62 (m, 5H), 7.59 (m, $J = 12.0, 4.5$ Hz, 1H), 7.48 (d, $J = 8.1$ Hz, 1H), 7.30 (t, $J = 7.0$ Hz, 1H), 7.19 (m, $J = 7.8, 6.2$ Hz, 2H), 7.04 (d, $J = 1.9$ Hz, 1H). $^{13}\text{C NMR}$ (100 MHz, DMSO) δ 142.84, 134.66, 133.53, 133.41, 132.69, 130.60, 130.27, 130.03, 129.84, 128.90, 128.80, 128.68, 128.47, 128.35, 128.25, 128.11, 128.09, 128.00, 126.86, 126.53, 126.38, 125.73, 124.58, 123.72, 123.37, 122.28, 122.22, 122.12, 119.50, 117.23, 107.59. **IR (KBr)** $\tilde{\nu}$ (cm^{-1}): 3381, 3110, 3045, 3004, 2926, 2843. **HRMS (ESI)**: calculated for $\text{C}_{31}\text{H}_{22}\text{N}_3$ $[\text{M}]^+$: 436.1808, found 436.1807.

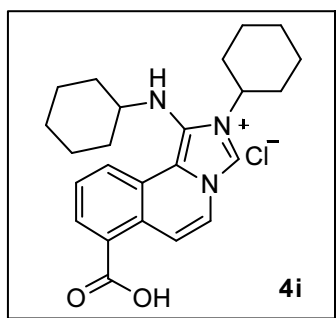
2-(4-methoxyphenyl)-1-((4-methoxyphenyl)amino)imidazo[5,1-a]isoquinolin-2-ium chloride (**4h**)



According to procedure A, compound **4h** was obtained as a grey powder (63%). $^1\text{H NMR}$ (400 MHz, DMSO) δ 10.30 (s, 1H), 8.69 (s, 1H), 8.45 (s, 1H), 8.10 (d, $J = 7.8$ Hz, 1H), 7.93 (d, $J = 7.6$ Hz, 1H), 7.69 – 7.61 (m, 3H), 7.57 (d, $J = 7.4$ Hz, 1H), 7.15 (d, $J = 8.5$ Hz, 2H), 6.71 (s, 4H), 3.81 (s, 3H),

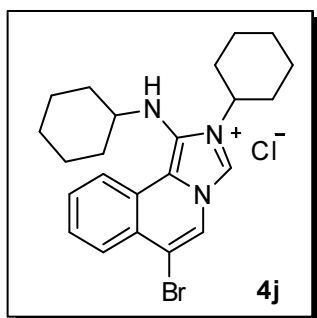
3.62 (s, 3H). ^{13}C NMR (100 MHz, DMSO) δ 160.90, 153.28, 138.45, 138.41, 130.06, 129.97, 128.61, 128.22, 127.89, 127.73, 125.72, 125.44, 123.70, 122.10, 122.08, 121.55, 119.12, 115.18, 115.15, 56.07, 55.53. IR (KBr) $\tilde{\nu}$ (cm^{-1}): 3143, 3074, 2988, 3041, 2952, 2891, 2830 HRMS (ESI): calculated for $\text{C}_{25}\text{H}_{22}\text{N}_3\text{O}_2$ $[\text{M}]^+$: 396.1707, found 396.1717.

7-carboxy-2-cyclohexyl-1-(cyclohexylamino)imidazo[5,1-*a*]isoquinolin-2-ium(4i)



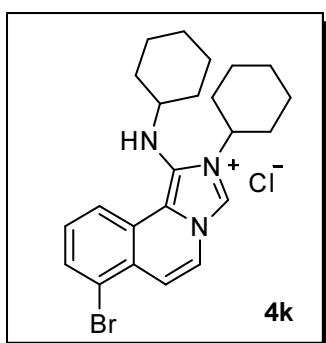
According to procedure B, compound **4i** was obtained as a white powder (66%). ^1H NMR (400 MHz, CD_3OD) δ 9.57 (s, 1H), 8.80 (d, $J = 8.1$ Hz, 1H), 8.45 (d, $J = 7.9$ Hz, 1H), 8.27 (m, $J = 7.7, 1.1$ Hz, 1H), 8.11 (d, $J = 7.9$ Hz, 1H), 7.80 (t, $J = 7.9$ Hz, 1H), 4.64 (m, $J = 12.0, 8.4, 3.6$ Hz, 1H), 3.03 (m, $J = 10.9, 7.1, 3.8$ Hz, 1H), 2.34 – 1.15 (m, 21H). ^{13}C NMR (100 MHz, CD_3OD) δ 166.44, 129.79, 128.95, 126.97, 126.96, 125.53, 125.13, 122.56, 121.72, 120.28, 117.53, 113.99, 56.30, 54.08, 32.40, 32.03, 23.75, 23.71, 23.30, 23.00. IR (KBr) $\tilde{\nu}$ (cm^{-1}): 3237, 3094, 2929, 2860, 1699, 1590, 1229 HRMS (ESI): calculated for $\text{C}_{24}\text{H}_{30}\text{O}_2\text{N}_3$ $[\text{M}]^+$: 392.2333, found 392.2336.

6-bromo-2-cyclohexyl-1-(cyclohexylamino)imidazo[5,1-*a*]isoquinolin-2-ium chloride (4j)



According to procedure A, compound **4j** was obtained as a white powder (66%). ^1H NMR (400 MHz, CD_3OD) δ 9.39 (s, 1H), 8.49 (d, $J = 7.5$ Hz, 1H), 8.39 (s, 1H), 8.05 (d, $J = 7.9$ Hz, 1H), 7.73 (t, $J = 7.1$ Hz, 1H), 7.66 (t, $J = 7.4$ Hz, 1H), 4.53 (s, 1H), 2.20 – 1.06 (m, 22H). ^{13}C NMR (100 MHz, CD_3OD) δ 131.49, 131.33, 130.29, 128.34, 127.15, 124.43, 124.21, 123.95, 123.07, 119.71, 115.76, 58.83, 56.66, 34.88, 34.55, 26.24, 26.20, 25.82, 25.48. IR (KBr) $\tilde{\nu}$ (cm^{-1}): 3167, 3076, 3003, 2912, 2753, 2719, 2849. HRMS (ESI): calculated for $\text{C}_{23}\text{H}_{29}\text{BrN}_3$ $[\text{M}]^+$: 426.1539, found 426.1528.

7-bromo-2-cyclohexyl-1-(cyclohexylamino)imidazo[5,1-*a*]isoquinolin-2-ium chloride (4k)

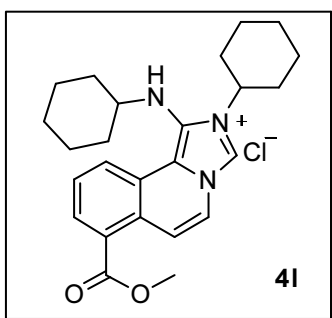


According to procedure A, compound **4k** was obtained as a white powder (70%). $^1\text{H NMR}$ (400 MHz, CDCl_3) δ 11.30 (s, 1H), 8.78 (d, $J = 6.5$ Hz, 1H), 8.44 (d, $J = 8.1$ Hz, 1H), 7.76 (d, $J = 7.7$ Hz, 1H), 7.46 (t, $J = 7.9$ Hz, 1H), 7.37 (d, $J = 7.0$ Hz, 1H), 4.99 (s, 1H), 4.71 (s, 1H), 2.95 (s, 1H), 2.25 – 1.67 (m, 10H), 1.65 – 0.99 (m, 10H). $^{13}\text{C NMR}$ (100 MHz, CDCl_3) δ 132.73, 130.66, 130.09, 126.43, 125.15,

124.77, 123.02, 122.82, 122.80, 118.24, 116.45, 58.36, 56.05, 34.71, 33.77, 25.60, 25.34, 25.15, 24.56. **IR (KBr)** $\tilde{\nu}$ (cm^{-1}): 3294, 3170, 2915, 3038, 3068, 2728, 2855.

HRMS (ESI): calculated for $\text{C}_{23}\text{H}_{29}\text{BrN}_3$ [$\text{M}]^+$: 426.1539, found 426.1539.

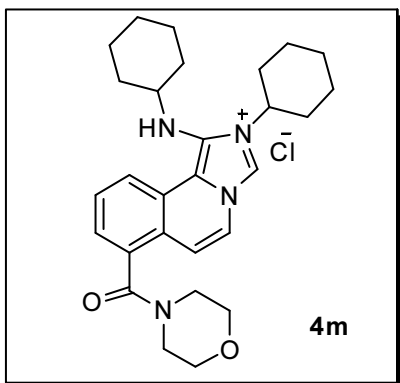
2-cyclohexyl-1-(cyclohexylamino)-7-(methoxycarbonyl)imidazo[5,1-a]isoquinolin-2-ium(4l)



Compound **4l** was obtained as a powder (92%) after esterification of acid **4i**. $^1\text{H NMR}$ (400 MHz, CDCl_3) δ 11.04 (s, 1H), 8.66 (d, $J = 8.0$ Hz, 1H), 8.62 (d, $J = 7.9$ Hz, 1H), 8.12 (d, $J = 7.8$ Hz, 1H), 8.10 – 8.07 (m, 1H), 7.59 (t, $J = 7.9$ Hz, 1H), 4.79 (d, $J = 5.6$ Hz, 1H), 4.62 (t, $J = 11.8$ Hz, 1H), 3.92 (s, 3H), 2.89 (d, $J = 5.8$ Hz, 1H), 2.15 – 1.76

(m, 10H), 1.66 – 1.05 (m, 10H). $^{13}\text{C NMR}$ (100 MHz, CDCl_3) δ 166.88, 131.71, 130.06, 128.68, 127.84, 127.75, 127.25, 125.40, 124.31, 123.32, 119.25, 115.26, 58.48, 56.40, 52.93, 34.74, 34.12, 25.92, 25.61, 25.32, 24.73. **IR (KBr)** $\tilde{\nu}$ (cm^{-1}): 3384, 3172, 3119, 3076, 2926, 2854, 1728, 1442, 1258. **HRMS(ESI)**: calculated for $\text{C}_{25}\text{H}_{32}\text{O}_2\text{N}_3$ [$\text{M}]^+$: 406.2489, found 406.2494.

2-cyclohexyl-1-(cyclohexylamino)-7-(morpholine-4-carbonyl)imidazo[5,1-a]isoquinolin-2-ium chloride (4m)

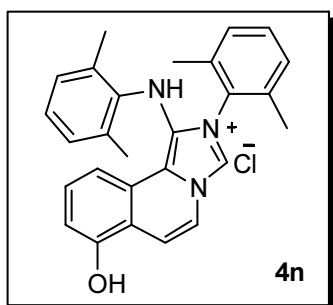


Compound **4m** was obtained as a white powder (72%) after amidation of acid **4i**. $^1\text{H NMR}$ (400 MHz, CDCl_3) δ 9.06 (s, 1H), 8.24 (d, $J = 8.1$ Hz, 1H), 7.92 (d, $J = 7.6$ Hz, 1H), 7.56 (t, $J = 7.8$ Hz, 1H), 7.33 (d, $J = 7.4$ Hz, 1H), 6.97 (d, $J = 7.6$ Hz, 1H), 4.51 (t, $J = 12.3$ Hz, 1H), 4.07 (d, $J = 4.7$ Hz, 1H), 3.94 (d, $J = 12.8$ Hz, 1H), 3.82 (s, 3H), 3.48 (dd, $J = 20.8, 13.8$ Hz, 2H), 3.14 (d, $J = 16.5$ Hz, 2H), 2.95 (d, $J = 4.1$

Hz, 1H), 2.24 – 1.73 (m, 10H), 1.67 – 1.14 (m, 10H). $^{13}\text{C NMR}$ (100 MHz, CDCl_3) δ

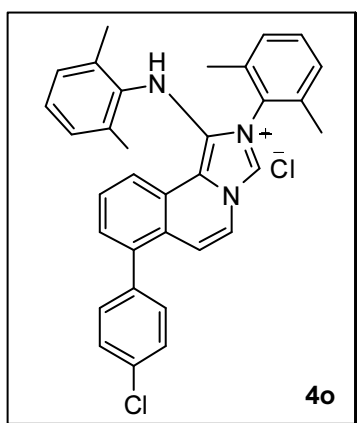
167.47, 133.86, 129.71, 129.36, 126.57, 124.16, 123.77, 123.14, 123.09, 122.14, 120.14, 115.00, 66.71, 57.76, 56.24, 47.64, 42.35, 33.65, 25.70, 25.32, 24.85, 24.50. **IR (KBr)** $\tilde{\nu}$ (cm⁻¹): 3377, 3259, 3153, 3076, 2934, 2849, 1619, 1449, 1281, 1119. **HRMS (ESI)**: calculated for C₂₈H₃₇N₄O₂ [M]⁺: 461.2911, found 461.2918.

2-(2,6-dimethylphenyl)-1-((2,6-dimethylphenyl)amino)-7-hydroxyimidazo[5,1-*a*]isoquinolin-2-ium chloride (4n)



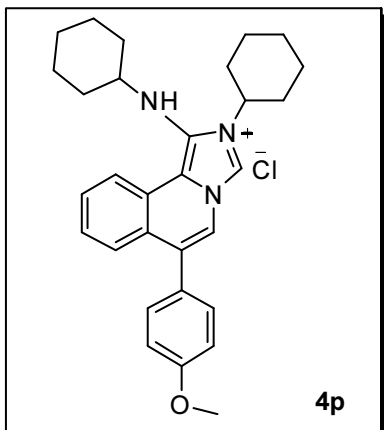
According to procedure B, compound **4n** was obtained as a white powder (46%). **¹H NMR** (400 MHz, DMSO) δ 11.00 (s, 1H), 9.88 (s, 1H), 8.23 (m, $J = 32.2, 7.2$ Hz, 2H), 7.88 (s, 1H), 7.62 (m, 2H), 7.29 (s, 2H), 7.08 (d, $J = 7.0$ Hz, 2H), 6.74 (s, 3H), 1.84 (m, 12H). **¹³C NMR** (100 MHz, DMSO) δ 154.39, 140.06, 136.09, 131.63, 131.43, 130.89, 130.74, 129.66, 128.96, 128.87, 126.55, 124.15, 123.77, 120.81, 119.81, 116.34, 115.28, 115.06, 113.89, 18.47, 17.47. **IR (KBr)** $\tilde{\nu}$ (cm⁻¹): 3201, 3230, 3052, 3013, 2970, 2931, 2796, 2618, 1521, 1463. **HRMS (ESI)**: calculated for C₂₇H₂₆O₂N₃ [M]⁺: 408.2070, found 408.2074.

7-(4-chlorophenyl)-2-(2,6-dimethylphenyl)-1-((2,6-dimethylphenyl)amino)imidazo[5,1-*a*]isoquinolin-2-ium chloride (4o)



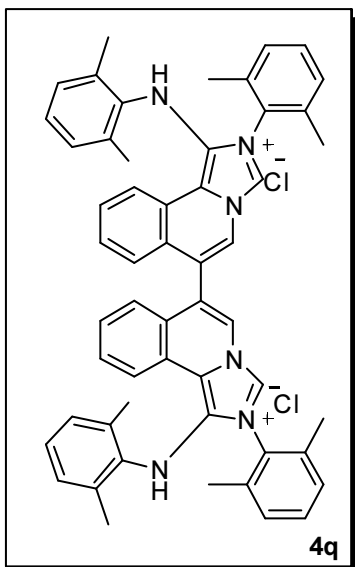
According to procedure B, compound **4o** was obtained as a white powder (54%). **¹H NMR** (400 MHz, CD₃OD) δ 8.97 (d, $J = 8.1$ Hz, 1H), 8.14 (d, $J = 7.7$ Hz, 1H), 7.85 (t, $J = 7.9$ Hz, 1H), 7.69 (m, $J = 7.6, 1.1$ Hz, 1H), 7.62 – 7.56 (m, 2H), 7.53 – 7.47 (m, 2H), 7.38 (d, $J = 7.7$ Hz, 1H), 7.30 (t, $J = 7.7$ Hz, 1H), 7.08 (d, $J = 7.7$ Hz, 2H), 6.80 (d, $J = 3.1$ Hz, 3H), 1.93 (s, 12H). **¹³C NMR** (100 MHz, CD₃OD) δ 139.98, 139.29, 137.58, 135.76, 134.06, 131.25, 131.21, 131.14, 130.61, 130.56, 130.16, 129.11, 128.67, 128.61, 128.60, 125.09, 123.79, 123.63, 123.61, 121.14, 120.22, 116.97, 17.32, 16.33, one quaternary carbon not detected. **IR (KBr)** $\tilde{\nu}$ (cm⁻¹): 3461, 3374, 3068, 3019, 2735, 2961, 2863. **HRMS (ESI)**: calculated for C₃₃H₂₉N₃ [M]⁺: 502.2045, found 502.2047.

2-cyclohexyl-1-(cyclohexylamino)-6-(4-methoxyphenyl)imidazo[5,1-*a*]isoquinolin-2-ium chloride (4p)



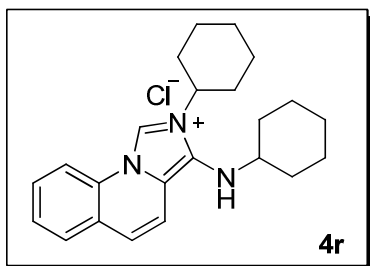
According to procedure A, compound **4p** was obtained as a white powder (50%). **¹H NMR** (400 MHz, CD₃OD) δ 9.49 (s, 1H), 8.64 (d, *J* = 8.1 Hz, 1H), 7.96 (s, 1H), 7.75 (t, *J* = 7.6 Hz, 1H), 7.66 (d, *J* = 7.9 Hz, 1H), 7.60 (t, *J* = 7.6 Hz, 1H), 7.44 (d, *J* = 8.6 Hz, 2H), 7.12 (d, *J* = 8.6 Hz, 2H), 4.66 (t, *J* = 12.0 Hz, 1H), 3.89 (s, 3H), 2.33 – 1.19 (m, 22H). **¹³C NMR** (100 MHz, CD₃OD) δ 160.37, 131.53, 130.68, 129.89, 129.16, 128.62, 127.99, 126.57, 126.50, 123.56, 123.17, 123.06, 119.24, 119.11, 113.99, 57.83, 55.48, 54.52, 33.96, 33.58, 25.30, 24.86, 24.56, one carbon not detected. **IR (KBr)** $\tilde{\nu}$ (cm⁻¹): 3378, 3182, 3147, 3072, 3044, 2986, 2931, 2848, 1610, 1588. **HRMS (ESI)**: calculated for C₃₀H₃₆N₃O [M]⁺: 454.2853, found 454.2854.

2,2'-bis(2,6-dimethylphenyl)-1,1'-bis((2,6-dimethylphenyl)amino)-[6,6'-biimidazo[5,1-*a*]isoquinoline]-2,2'-dium chloride (4q)



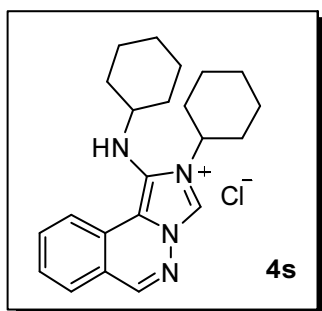
According to procedure A, compound **4q** was obtained as a white powder (29%). **¹H NMR** (400 MHz, CD₃OD) δ 9.75 (s, 2H), 9.06 (d, *J* = 8.0 Hz, 2H), 8.64 (s, 2H), 7.91 – 7.81 (m, 2H), 7.68 (d, *J* = 4.7 Hz, 4H), 7.34 (t, *J* = 7.7 Hz, 2H), 7.15 (d, *J* = 7.6 Hz, 2H), 7.11 (d, *J* = 7.6 Hz, 2H), 6.84 (s, 6H), 2.06 (d, *J* = 2.7 Hz, 12H), 2.00 (d, *J* = 3.6 Hz, 12H). **¹³C NMR** (100 MHz, CD₃OD) δ 139.28, 139.18, 135.87, 135.79, 131.68, 131.63, 131.49, 131.44, 131.22, 130.68, 130.36, 130.23, 129.96, 129.49, 129.47, 128.74, 128.66, 128.64, 127.76, 127.75, 126.85, 126.61, 126.56, 125.68, 124.39, 124.38, 123.97, 123.25, 123.23, 122.45, 119.95, 119.84, 17.44, 16.53, 16.47, seven carbons overlapped. **IR (KBr)** $\tilde{\nu}$ (cm⁻¹): 3418, 3129, 3061, 2959, 2919, 2857, 1644, 1576, 1463. **HRMS (ESI)**: calculated for C₅₄H₅₀N₆ [M]²⁺: 391.2043, found 391.2052.

2-cyclohexyl-3-(cyclohexylamino)imidazo[1,5-*a*]quinolin-2-ium chloride (4r)



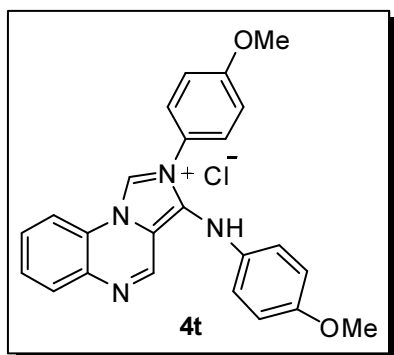
According to procedure B, compound **4r** was obtained as a grey powder (63%). $^1\text{H NMR}$ (400 MHz, CD_3OD) δ 9.92 (s, 1H), 8.28 (d, $J = 8.4$ Hz, 1H), 7.77 (m, $J = 7.8$, 1.3 Hz, 1H), 7.68 – 7.63 (m, 1H), 7.58 (m, $J = 11.0$, 4.2 Hz, 1H), 7.39 (d, $J = 9.7$ Hz, 1H), 7.28 (d, $J = 9.8$ Hz, 1H), 4.50 (m, $J = 12.1$, 3.8 Hz, 1H), 2.17 – 1.69 (m, 12H), 1.62 – 1.13 (m, 10H). $^{13}\text{C NMR}$ (100 MHz, CD_3OD) δ 130.78, 129.65, 129.35, 129.13, 128.34, 125.10, 123.00, 120.99, 118.47, 115.76, 114.79, 57.19, 56.05, 33.56, 33.43, 25.28, 24.67, 24.59, 23.77. **IR (KBr)** $\tilde{\nu}$ (cm^{-1}): 3381, 3110, 3045, 3004, 2926, 2843 **HRMS (ESI)**: calculated for $\text{C}_{23}\text{H}_{30}\text{N}_3$ $[\text{M}]^+$: 348.2434, found 348.2431.

2-cyclohexyl-1-(cyclohexylamino)imidazo[5,1-a]phthalazin-2-ium chloride (**4s**)



According to procedure B, compound **4s** was obtained as a yellow powder (77%). $^1\text{H NMR}$ (400 MHz, CD_3OD) δ 9.87 (s, 1H), 8.92 (s, 1H), 8.43 (d, $J = 8.0$ Hz, 1H), 8.09 – 8.06 (m, 1H), 8.05 – 8.00 (m, 1H), 4.65 (m, $J = 12.1$, 3.8 Hz, 1H), 3.05 (m, $J = 11.0$, 3.9 Hz, 1H), 2.25 – 1.77 (m, 12H), 1.69 – 1.23 (m, 10H). $^{13}\text{C NMR}$ (100 MHz, CD_3OD) δ 152.56, 134.56, 129.65, 129.50, 125.99, 124.47, 122.56, 120.73, 114.86, 58.24, 55.66, 33.75, 33.68, 25.31, 25.23, 24.85, 24.48. (one quaternary carbon not detected). **IR (KBr)** $\tilde{\nu}$ (cm^{-1}): 3160, 3045, 3000, 2923, 2853, 2726, 2665 **HRMS (ESI)**: calculated for $\text{C}_{22}\text{H}_{29}\text{N}_4$ $[\text{M}]^+$: 349.2387, found 349.2387.

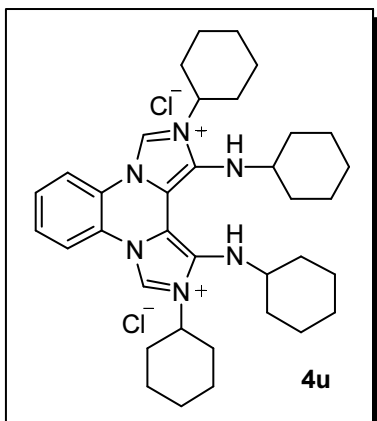
2-(4-methoxyphenyl)-3-((4-methoxyphenyl)amino)imidazo[1,5-a]quinoxalin-2-ium chloride (**4t**)



According to procedure A, compound **4t** was obtained as a dark red powder (58%). $^1\text{H NMR}$ (400 MHz, DMSO) δ 10.77 (s, 1H), 8.54 – 8.48 (m, 2H), 7.97 (d, $J = 7.3$ Hz, 1H), 7.83 – 7.75 (m, 3H), 7.68 (d, $J = 8.8$ Hz, 2H), 7.18 (d, $J = 8.9$ Hz, 2H), 7.06 (d, $J = 8.8$ Hz, 2H), 6.84 (d, $J = 8.8$ Hz, 2H), 3.83 (s, 3H), 3.70 (s, 3H). $^{13}\text{C NMR}$ (100 MHz, DMSO) δ 160.93, 155.85, 144.24, 136.28, 134.95, 134.45, 130.32, 130.05, 130.01, 127.81, 126.53, 125.44,

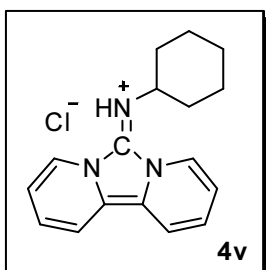
123.08, 121.46, 116.71, 115.22, 114.93, 110.90, 55.99, 55.55. **IR (KBr)** $\tilde{\nu}$ (cm^{-1}): 3406, 3103, 3043, 2939, 2999, 2939, 2830, 1628, 1499 **HRMS (ESI)**: calculated for $\text{C}_{24}\text{H}_{21}\text{ClN}_4\text{O}_2$ $[\text{M}]^+$: 397.1659, found 397.1666.

2,11-dicyclohexyl-1,12-bis(cyclohexylamino)diimidazo[1,5-*a*:5',1'-*c*]quinoxaline-2,11-diium chloride (4u)



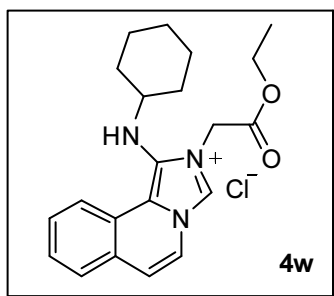
According to procedure A, compound **4u** was obtained as a dark grey powder (25%). **¹H NMR** (500 MHz, TFA) δ 9.68 (s, 2H), 8.30 (s, 2H), 7.85 (d, $J = 2.8$ Hz, 2H), 4.56 (t, $J = 11.8$ Hz, 2H), 3.27 (t, $J = 15.8$ Hz, 2H), 2.61 – 1.03 (m, 42H). **¹³C NMR** (126 MHz, TFA) δ 134.73, 133.51, 128.81, 124.25, 119.70, 113.02, 62.12, 61.66, 36.32, 35.48, 27.26, 26.75, 26.65, 26.09. **IR (KBr)** $\tilde{\nu}$ (cm^{-1}): 3403, 3197, 3087, 3042, 2927, 2841, 2651. **HRMS (ESI)**: calculated for $\text{C}_{36}\text{H}_{52}\text{N}_6$ $[\text{M}]^{2+}$: 284.2121, found 284.2122.

***N*-(6H-imidazo[1,5-*a*:3,4-*a'*]dipyridin-6-ylidene)cyclohexanaminium chloride (4v)**



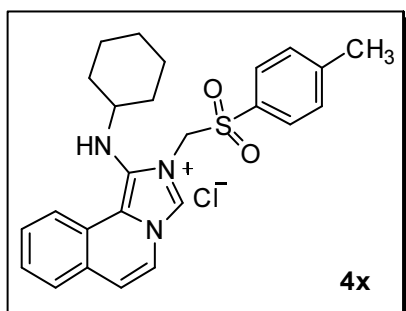
According to procedure A, compound **4v** was obtained as a dark red powder (90%). **¹H NMR** (400 MHz, CDCl_3) δ 8.76 (d, $J = 6.9$ Hz, 2H), 8.53 (s, 1H), 8.14 (d, $J = 9.0$ Hz, 2H), 7.17 (t, $J = 6.6$ Hz, 2H), 7.15 – 7.02 (m, 2H), 3.17 (s, 1H), 1.99 – 1.02 (m, 10H). **¹³C NMR** (100 MHz, CD_3OD) δ 126.56, 121.48, 119.95, 119.68, 119.19, 118.27, 56.48, 34.08, 25.00, 24.65. **IR (KBr)** $\tilde{\nu}$ (cm^{-1}): 3108, 3018, 2926, 2854. **HRMS (ESI)**: calculated for $\text{C}_{17}\text{H}_{20}\text{N}_3$ $[\text{M}]^+$: 266.1652, found 266.1654.

1-(cyclohexylamino)-2-(2-ethoxy-2-oxoethyl)imidazo[5,1-*a*]isoquinolin-2-ium chloride (4w)



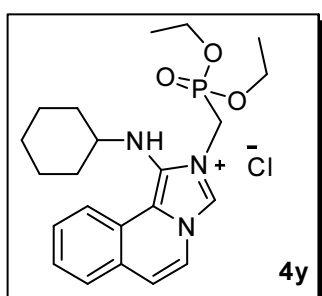
According to procedure A, compound **4w** was obtained as a white powder (54%). $^1\text{H NMR}$ (400 MHz, CDCl_3) δ 10.66 (s, 1H), 8.37 (d, $J = 7.9$ Hz, 1H), 8.29 (d, $J = 7.4$ Hz, 1H), 7.63 – 7.56 (m, 1H), 7.53 – 7.44 (m, 2H), 6.90 (d, $J = 7.4$ Hz, 1H), 5.60 (s, 2H), 4.27 (q, $J = 7.1$ Hz, 2H), 2.92 (tt, $J = 10.9, 3.7$ Hz, 1H), 1.91 – 1.34 (m, 7H), 1.31 (t, $J = 7.1$ Hz, 3H), 1.25 – 1.08 (m, 4H). $^{13}\text{C NMR}$ (100 MHz, CDCl_3) δ 166.74, 130.63, 129.44, 128.96, 127.89, 127.00, 126.88, 123.57, 122.58, 121.01, 119.66, 118.91, 62.89, 57.73, 47.27, 33.79, 25.33, 24.98, 14.08. **IR (KBr)** $\tilde{\nu}$ (cm^{-1}): 3188, 3131, 3086, 3029, 2980, 2927, 2851, 1738, 1467, 1232. **HRMS (ESI)**: calculated for $\text{C}_{21}\text{H}_{26}\text{N}_3\text{O}_2$ $[\text{M}]^+$: 352.2020, found 352.2025.

1-(cyclohexylamino)-2-(tosylmethyl)imidazo[5,1-*a*]isoquinolin-2-ium chloride (4x)



According to procedure A, compound **4x** was obtained as a white powder (52%). $^1\text{H NMR}$ (400 MHz, CD_3OD) δ 8.46 (d, $J = 7.5$ Hz, 1H), 8.15 (d, $J = 7.4$ Hz, 1H), 7.85 (d, $J = 7.6$ Hz, 1H), 7.82 – 7.77 (m, 2H), 7.76 – 7.67 (m, 3H), 7.49 (d, $J = 8.0$ Hz, 2H), 7.43 (d, $J = 7.4$ Hz, 1H), 3.03 – 2.92 (m, 1H), 2.47 (s, 3H), 1.88 – 1.11 (m, 13H). $^{13}\text{C NMR}$ (100 MHz, CD_3OD) δ 147.28, 132.47, 130.75, 130.35, 129.64, 129.49, 128.80, 128.22, 127.43, 123.34, 122.18, 120.48, 120.22, 120.06, 65.47, 57.97, 33.33, 25.10, 24.71, 20.34, 14.02. **IR (KBr)** $\tilde{\nu}$ (cm^{-1}): 3360, 3139, 3084, 3102, 3042, 2937, 2849, 1596, 1467, 1311. **HRMS (ESI)**: calculated for $\text{C}_{25}\text{H}_{28}\text{N}_3\text{O}_2\text{S}$ $[\text{M}]^+$: 434.1897, found 434.1903.

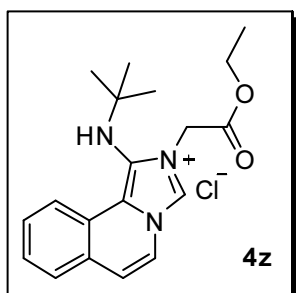
1-(cyclohexylamino)-2-(diethoxyphosphoryl)imidazo[5,1-*a*]isoquinolin-2-ium chloride (4y)



According to procedure A, compound **4y** was obtained as a white powder (52%). $^1\text{H NMR}$ (400 MHz, CDCl_3) δ 10.97 (d, $J = 14.8$ Hz, 1H), 8.37 (t, $J = 7.2$ Hz, 2H), 7.59 (d, $J = 3.9$ Hz, 2H), 7.56 – 7.48 (m, 1H), 7.13 – 7.02 (m, 1H), 5.32

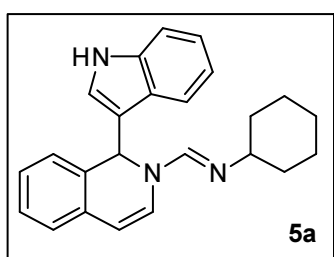
– 5.20 (m, 2H), 4.26 (m, $J = 14.5, 7.1$ Hz, 4H), 2.99 (s, 1H), 1.94 – 1.34 (m, 7H), 1.29 (m, $J = 7.0, 4.6, 2.0$ Hz, 6H), 1.19 (d, $J = 10.6$ Hz, 4H). ^{13}C NMR (100 MHz, CDCl_3) δ 131.66, 130.20, 129.68, 128.58, 127.74, 126.93, 124.22, 123.26, 121.75, 119.88, 119.80, 65.21, 65.14, 58.20, 43.35, 41.81, 34.90, 25.90, 25.53, 16.96, 16.91. IR (KBr) $\tilde{\nu}$ (cm^{-1}): 3364, 3101, 3036, 2971, 2916, 2851, 1590, 1317, 1248 HRMS (ESI): calculated for $\text{C}_{21}\text{H}_{29}\text{ClN}_3\text{O}_3\text{P}$ $[\text{M}]^+$: 416.2098, found 416.2109.

1-(*tert*-butylamino)-2-(2-ethoxy-2-oxoethyl)imidazo[5,1-*a*]isoquinolin-2-ium chloride (4z)



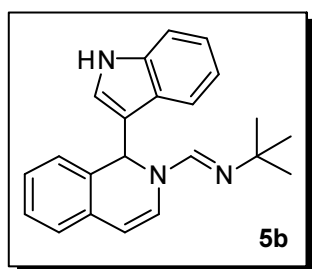
According to procedure A, compound **4z** was obtained as a white powder (63%). ^1H NMR (400 MHz, CDCl_3) δ 10.86 (s, 1H), 8.73 (d, $J = 7.9$ Hz, 1H), 8.34 (d, $J = 7.4$ Hz, 1H), 7.60 – 7.47 (m, 3H), 6.96 (d, $J = 7.4$ Hz, 1H), 5.60 (s, 2H), 4.28 (m, $J = 7.1$ Hz, 2H), 1.31 (t, $J = 7.1$ Hz, 3H), 1.26 (s, 10H). ^{13}C NMR (100 MHz, CD_3OD) δ 166.71, 129.42, 129.00, 128.85, 127.99, 127.72, 123.93, 122.60, 122.08, 120.62, 120.59, 119.26, 62.55, 56.34, 56.30, 29.12, 13.01. IR (KBr) $\tilde{\nu}$ (cm^{-1}): 3388, 3136, 3082, 3038, 2971, 2923, 2829, 2892, 1751, 1476 HRMS (ESI): calculated for $\text{C}_{19}\text{H}_{24}\text{ClN}_3\text{O}_2$ $[\text{M}]^+$: 326.1863, found 328.1869.

(*E*)-1-(1-(1*H*-indol-3-yl)isoquinolin-2-(1*H*)-yl)-*N*-cyclohexylmethanimine (5a)



According to procedure C, compound **5a** was obtained as a white powder (80%) ^1H NMR (400 MHz, pyridine- d_5) δ 11.45 (s, 1H), 7.72 (s, 3H), 7.21 (d, $J = 7.5$ Hz, 1H), 6.60 (d, $J = 7.3$ Hz, 1H), 6.26 (s, 1H), 6.24 (d, $J = 1.2$ Hz, 1H), 6.22 (d, $J = 1.8$ Hz, 1H), 6.13 – 6.07 (m, 1H), 5.35 (d, $J = 7.4$ Hz, 1H), 2.49 (s, 1H), 1.19 – 0.06 (m, 12H). ^{13}C NMR (100 MHz, pyridine) δ 151.07, 136.56, 131.43, 129.21, 128.11, 127.05, 126.81, 126.22, 125.57, 125.47, 124.45, 120.83, 120.47, 118.67, 113.79, 111.06, 59.16, 32.35, 31.81, 23.77, 23.76, 23.62. IR (KBr) $\tilde{\nu}$ (cm^{-1}): 3180, 3099, 3033, 2992, 2861, 2902, 2931, 2596, 2346 HRMS (ESI): calculated for $\text{C}_{24}\text{H}_{25}\text{N}_3$ $[\text{M} + \text{H}]^+$: 356.2802, found 356.2126.

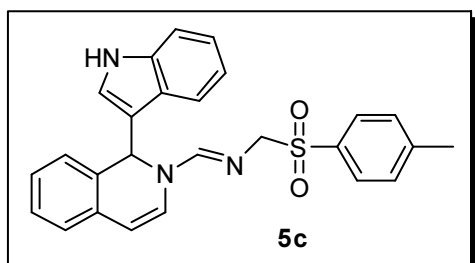
(E)-1-(1-(1H-indol-3yl)isoquinolin-2-(1H)-yl)-N-(tert-butyl)methanimine (5b)



According to procedure C, compound **5b** was obtained as a white powder (70%). ¹H NMR (400 MHz, CD₃OD) δ 8.36 (s, 1H), 7.52 (d, *J* = 7.4 Hz, 1H), 7.39 (s, 3H), 7.31 (s, 2H), 7.18 (d, *J* = 7.5 Hz, 2H), 7.07 (s, 1H), 6.97 – 6.83 (m, 2H), 6.71 (s, 1H), 1.39 (s, 9H). IR (KBr) $\tilde{\nu}$ (cm⁻¹): 3176, 3098, 3047, 2964, 2917, 2847, 2737, 2595 HRMS (ESI):

calculated for C₂₂H₂₃N₃ [M]⁺: 330.1926, found 330.1973.

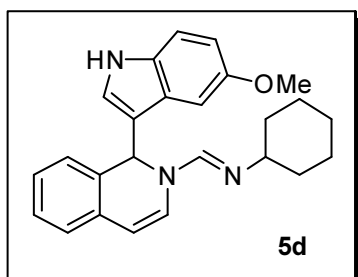
(E)-1-(1-(1H-indol-3yl)isoquinolin-2-(1H)-yl)-N-(tosylmethyl)methanimine (5c)



According to procedure C, compound **5c** was obtained as a white powder (80%). ¹H NMR (400 MHz, pyridine-*d*₅) δ 12.52 (s, 1H), 9.05 (s, 2H), 8.37 (d, *J* = 7.4 Hz, 2H), 8.26 – 8.02 (m, 3H), 7.88 (d, *J* = 12.2 Hz, 3H), 7.56 (d, *J* = 7.7 Hz, 3H), 7.51 – 7.38 (m, 3H), 6.32 (s, 1H), 5.36

(q, *J* = 12.6 Hz, 2H), 2.44 (s, 3H). ¹³C NMR (100 MHz, pyridine) δ ¹³C NMR (101 MHz, pyridine) δ 157.58, 144.85, 138.12, 133.14, 131.51, 130.08, 129.76, 128.12, 127.70, 127.55, 126.63, 125.68, 125.65, 125.37, 125.32, 122.17, 121.06, 120.14, 119.99, 118.28, 112.48, 77.75, 49.15, 21.55. IR (KBr) $\tilde{\nu}$ (cm⁻¹): 3506, 3429, 3058, 3180, 2987, 2904, 2782, 1683, 1617 HRMS (ESI): calculated for C₂₆H₂₃N₃O₂S [M + H]⁺: 442.1545, found 442.1572.

(E)-N-cyclohexyl-1-(1-(5-methoxy-1H-indol-3yl)isoquinolin-2-(1H)-yl)methanimine (5d)

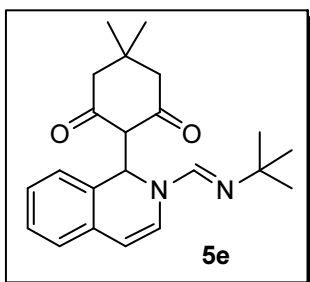


According to procedure C, compound **5d** was obtained as a white powder (88%). ¹H NMR (400 MHz, pyridine-*d*₅) δ 12.73 (d, *J* = 20.5 Hz, 1H), 9.10 (s, 2H), 8.22 (d, *J* = 5.5 Hz, 1H), 7.95 (s, 1H), 7.90 (t, *J* = 9.4 Hz, 1H), 7.82 (s, 1H), 7.58 (s, 4H), 7.42 (d, *J* = 8.6 Hz, 1H), 6.76 (s, 1H), 4.23 (s, 3H), 3.94 (s, 1H), 2.50 – 2.35 (m, 2H), 2.35

– 2.21 (m, 2H), 1.93 (s, 2H), 1.74 (s, 1H), 1.53 – 1.28 (m, 3H). ¹³C NMR (100 MHz, pyridine) δ 153.50, 151.58, 131.59, 131.51, 127.94, 127.28, 126.87, 126.15, 125.84,

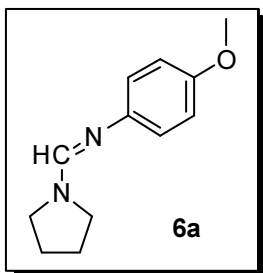
124.93, 124.50, 116.05, 113.52, 111.72, 111.13, 101.46, 58.69, 54.53, 32.31, 31.71, 23.76, 23.57, one quaternary carbon not detected. **IR (KBr)** $\tilde{\nu}$ (cm^{-1}): 3643, 3288, 3198, 3051, 2995, 2927, 2854, 2826. **HRMS (ESI)**: calculated for $\text{C}_{25}\text{H}_{27}\text{N}_3\text{O}$ $[\text{M} + \text{H}]^+$: 386.2188, found 386.2242.

(E)-2-(2-((tert-butylimino)methyl)-1,2-dihydroisoquinolin-1-yl)-5,5-dimethylcyclohexane-1,3-dione (5e)



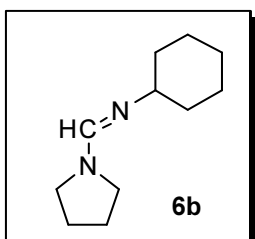
According to procedure C, using dimedone instead of the indole, compound **5e** was obtained as a white powder (84%). $^1\text{H NMR}$ (400 MHz, CDCl_3) δ 9.31 (d, $J = 14.0$ Hz, 1H), 8.95 (d, $J = 13.9$ Hz, 1H), 7.30 (d, $J = 7.6$ Hz, 1H), 7.22 – 7.12 (m, 2H), 7.04 – 6.99 (m, 1H), 6.85 (d, $J = 7.2$ Hz, 1H), 6.27 (s, 1H), 6.01 (d, $J = 7.4$ Hz, 1H), 2.53 (d, $J = 50.3$ Hz, 4H), 1.47 (s, 9H), 1.04 (s, 6H). $^{13}\text{C NMR}$ (100 MHz, CDCl_3) δ 151.72, 130.54, 128.59, 127.83, 127.82, 126.10, 125.49, 125.47, 114.36, 113.17, 56.59, 50.42, 32.26, 31.99, 29.83, 29.23. **IR (KBr)** $\tilde{\nu}$ (cm^{-1}): 3193, 3136, 3056, 3025, 2971, 2945, 2869, 2727, 2679, 2612, 1672, 1578, 1383, 1317. **HRMS (ESI)**: calculated for $\text{C}_{22}\text{H}_{28}\text{N}_2\text{O}_2$ $[\text{M} + \text{H}]^+$: 353.2151, found 353.2239.

N-(4-methoxyphenyl)-1-(pyrrolidin-1-yl)methanimine (6a)



According to procedure D, compound **6a** was obtained as an oily liquid (89%). $^1\text{H NMR}$ (400 MHz, CDCl_3) δ 7.66 (s, 1H), 6.83 (d, $J = 9.0$ Hz, 2H), 6.74 (d, $J = 9.0$ Hz, 2H), 3.70 (s, 3H), 3.44 – 3.39 (m, 4H), 1.86 (t, $J = 6.7$ Hz, 4H). $^{13}\text{C NMR}$ (100 MHz, CDCl_3) δ 155.35, 150.15, 145.89, 121.72, 114.25, 55.54, 55.47, 25.01. **IR (KBr)** $\tilde{\nu}$ (cm^{-1}): 2949, 2867, 2831, 1632, 1506. **HRMS (ESI)**: calculated for $\text{C}_{12}\text{H}_{17}\text{N}_2\text{O}$ $[\text{M} + \text{H}]^+$: 205.1296, found 205.1335.

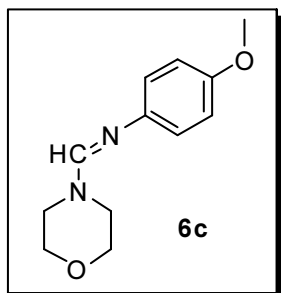
N-cyclohexyl-1-(pyrrolidin-1-yl)methanimine (6b)



According to procedure D, compound **6b** was obtained as an oily liquid (91%). $^1\text{H NMR}$ (400 MHz, CDCl_3) δ 7.58 (s, 1H), 3.38 – 3.24 (m, 4H), 2.81 (m, $J = 10.9, 4.1$ Hz, 1H), 1.88 – 1.82 (m,

4H), 1.79 – 1.05 (m, 10H). ^{13}C NMR (100 MHz, CDCl_3) δ 150.41, 65.22, 46.76, 36.25, 25.69, 25.59, 25.02. IR (KBr) $\tilde{\nu}$ (cm^{-1}): 2965, 2626, 2845, 1634 HRMS (ESI): calculated for $\text{C}_{11}\text{H}_{20}\text{N}_2$ $[\text{M}+\text{H}]^+$: 181.1660, found 181.1701.

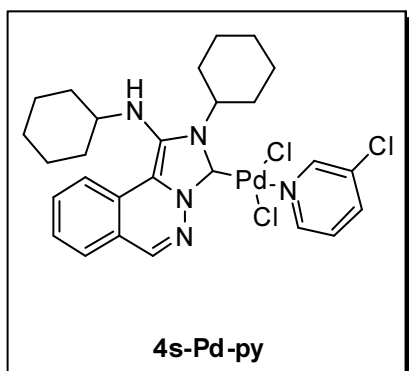
4-methoxy-*N*-(morpholinomethylene)aniline (6c)



According to procedure D, compound **6c** was obtained as an oily liquid (59%). ^1H NMR (400 MHz, CDCl_3) δ 7.49 (s, 1H), 6.93 – 6.87 (m, 2H), 6.85 – 6.79 (m, 2H), 3.78 (s, 3H), 3.76 – 3.72 (m, 4H), 3.49 (s, 4H). ^{13}C NMR (100 MHz, CDCl_3) δ 155.79, 152.00, 144.82, 121.63, 114.35, 109.99, 66.67, 55.49. HRMS (ESI): calculated for $\text{C}_{12}\text{H}_{17}\text{N}_2\text{O}_2$ $[\text{M}+\text{H}]^+$: 221.1290,

found 221.1285.

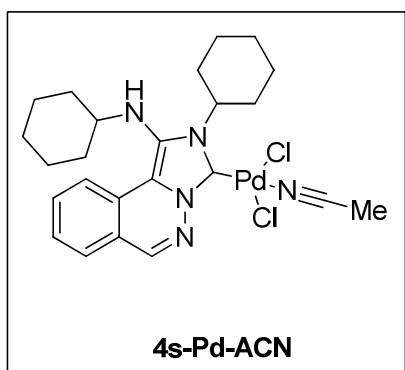
2-cyclohexyl-1-(cyclohexylamino)imidazo[5,1-*a*]phthalazin-2-ium chloride-PdCl₂ complex with 3-chloropyridine (4s-Pd-py)



According to the procedure reported by M. G. Organ et al.^[1], compound **4s-Pd-py** was obtained as a light yellow powder (82%) ^1H NMR(400 MHz, CDCl_3) δ 9.10 (d, J = 2.3 Hz, 1H), 9.01 (dd, J = 5.5, 1.3 Hz, 1H), 8.40 (s, 1H), 8.02 (d, J = 8.0 Hz, 1H), 7.70 (m, J = 8.2, 2.3, 1.3 Hz, 1H), 7.65 – 7.56 (m, 2H), 7.46 – 7.38 (m, 1H), 7.26 (dd, J = 8.2, 5.1 Hz, 1H), 4.64 (t, J

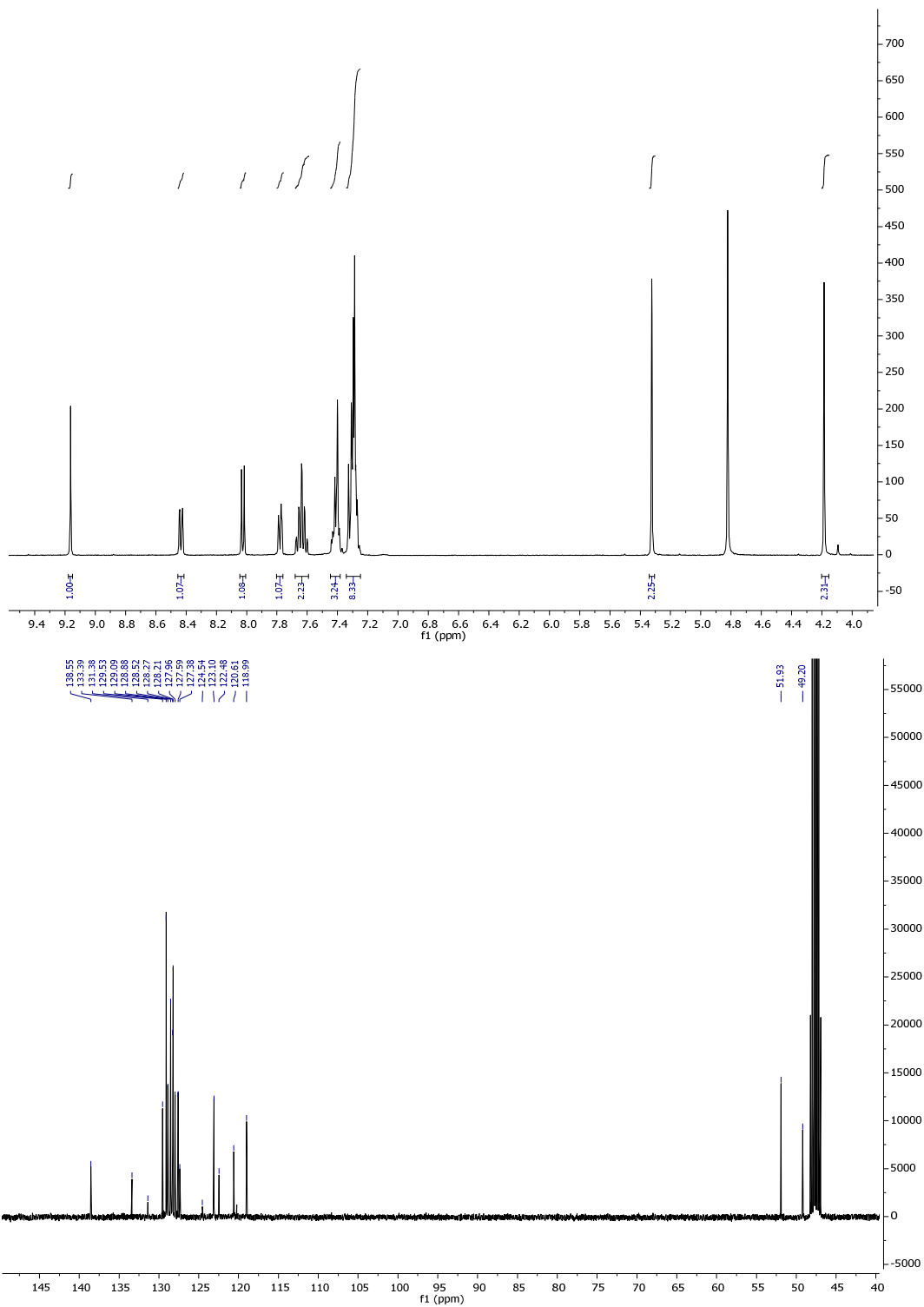
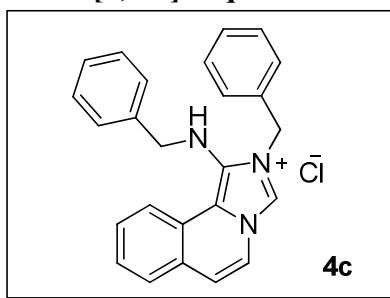
= 12.3 Hz, 1H), 3.30 (d, J = 9.8 Hz, 1H), 2.18 – 1.09 (m, 22H). ^{13}C NMR (100 MHz, CDCl_3) δ 150.61, 149.60, 148.47, 138.84, 137.85, 132.99, 132.41, 129.33, 128.47, 128.07, 126.00, 124.71, 121.62, 121.13, 117.45, 58.49, 57.64, 34.47, 34.17, 26.70, 25.53, 25.47, 25.08.

2-cyclohexyl-1-(cyclohexylamino)imidazo[5,1-*a*]phthalazin-2-ium chloride-PdCl₂ complex with CH₃CN (4s-Pd-ACN)

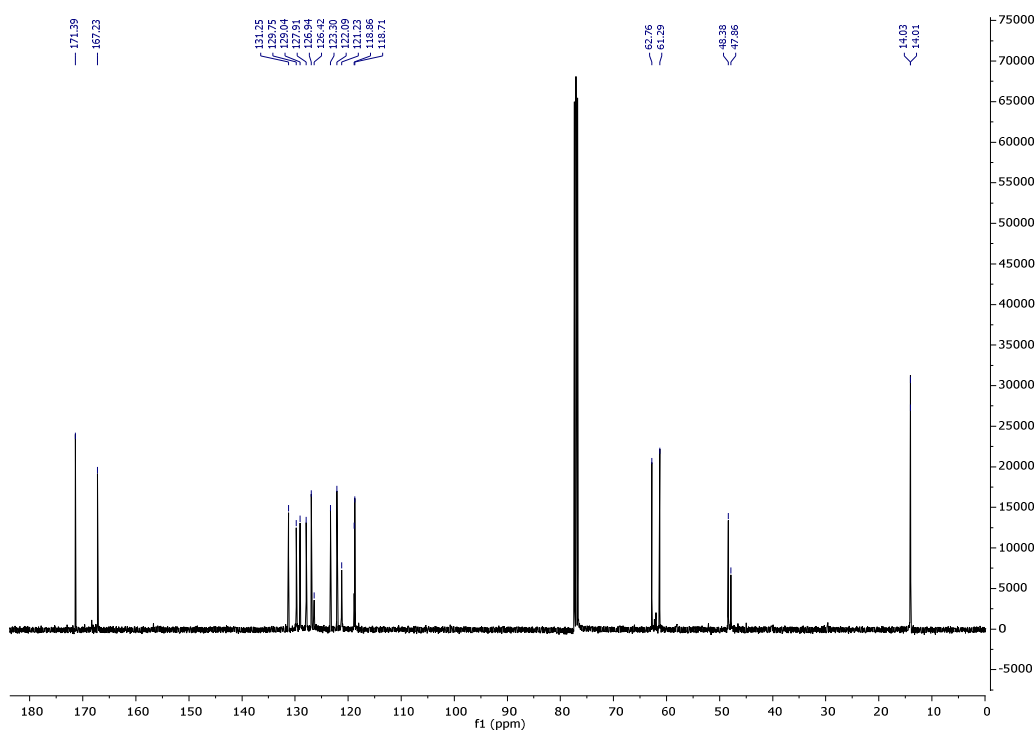
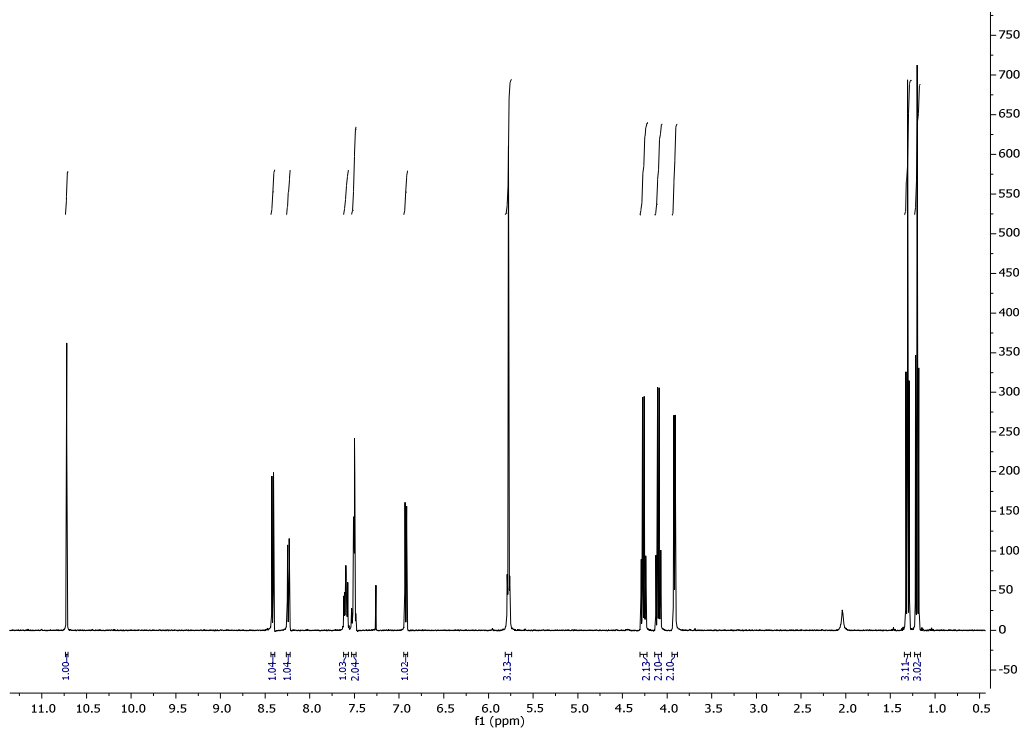
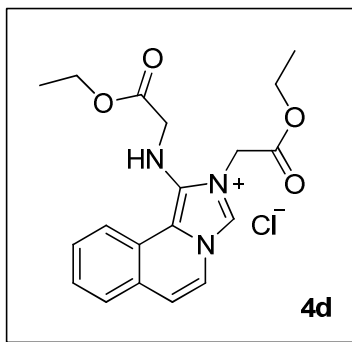


According to the procedure reported by Xu et al.^[2], starting from 1 mmol of **4s**, a compound was obtained as a grey solid (530 mg) which was recrystallized from CH_3CN . Due to solubility issues,

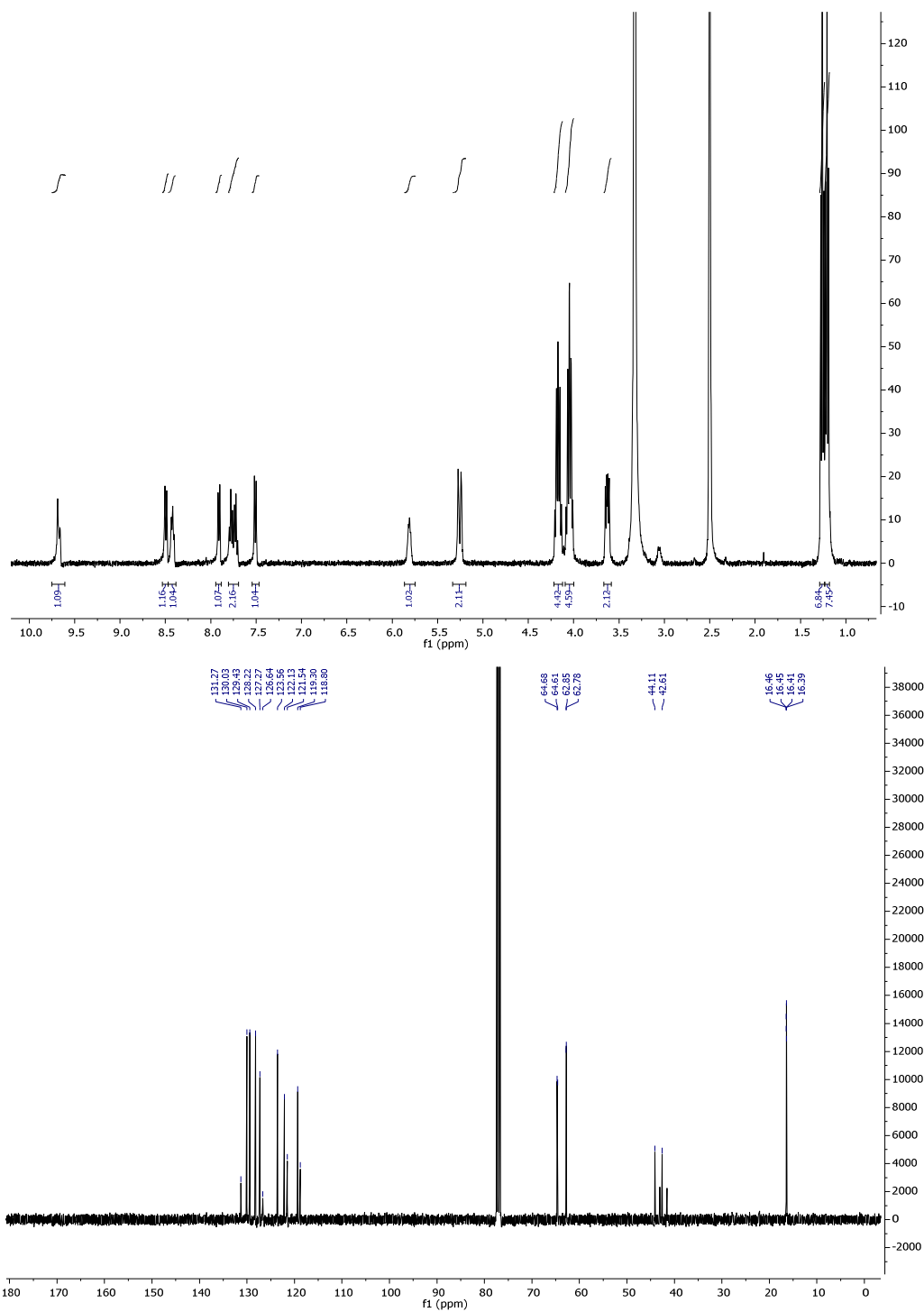
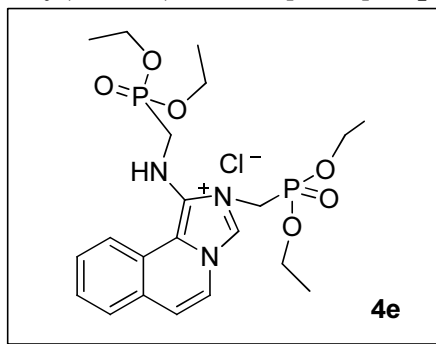
2-benzyl-3-(benzylamino)imidazo[5,1-a]isoquinolin-2-ium chloride (4c)



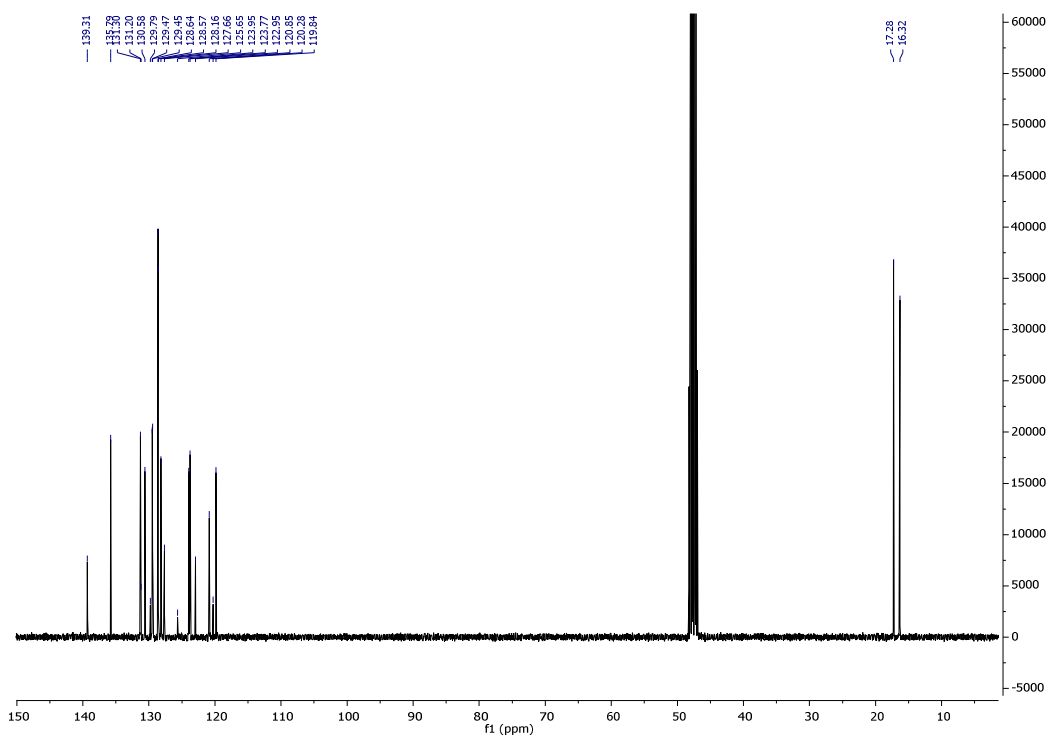
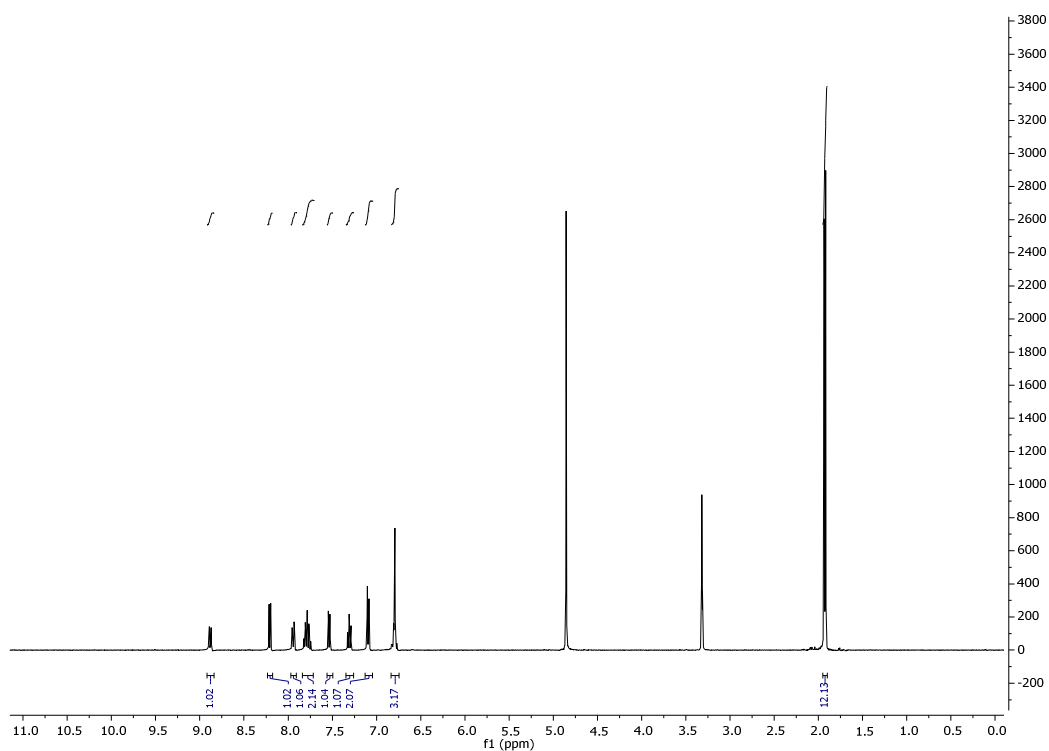
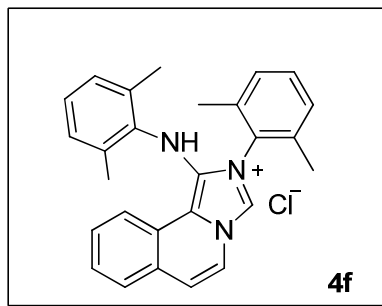
2-(2-ethoxy-2-oxoethyl)-1-((2-ethoxy-2-oxoethyl)amino)imidazo[5,1-a]isoquinolin-2-ium chloride (4d)



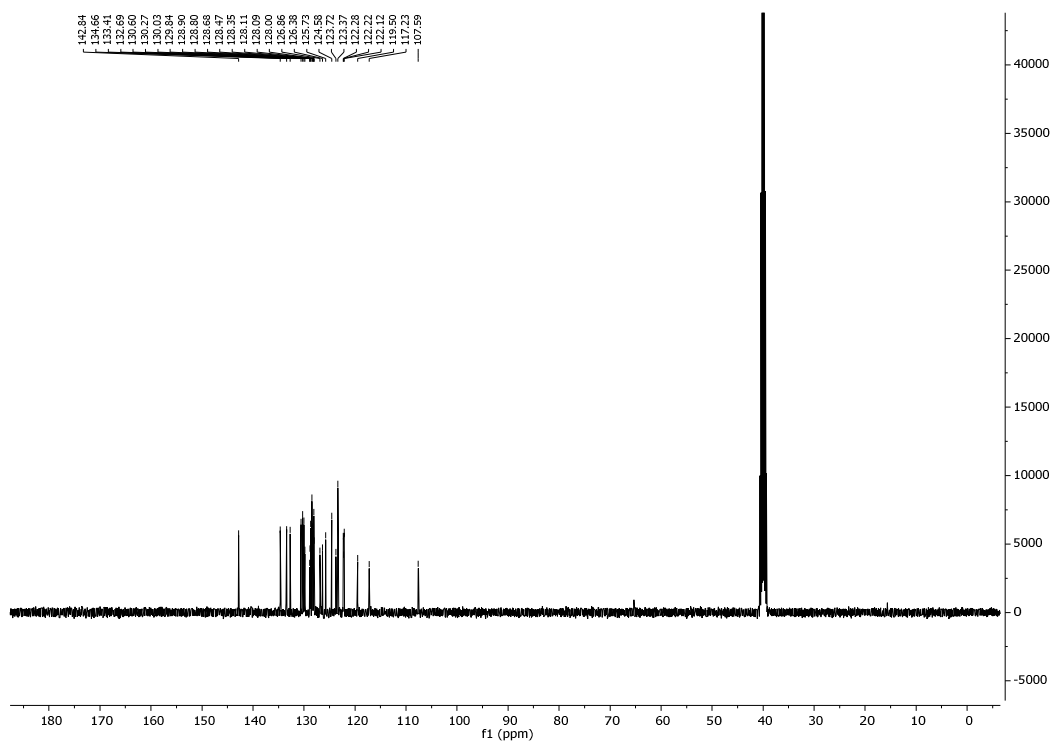
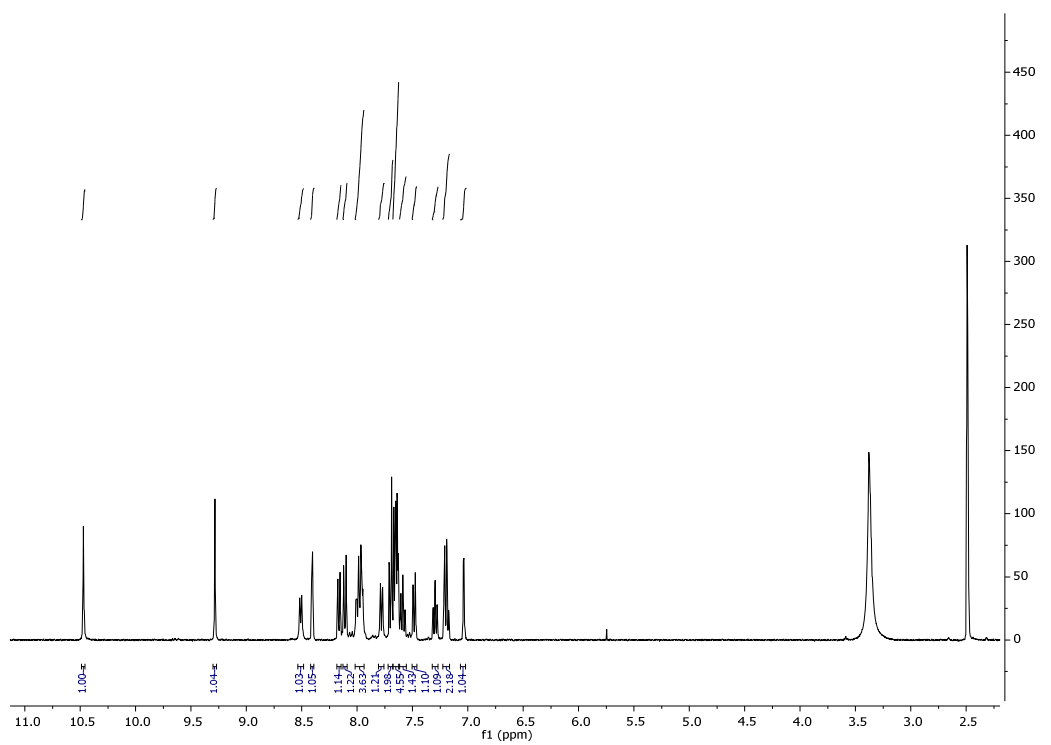
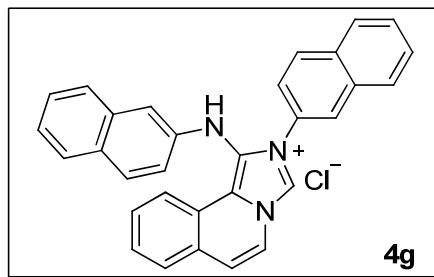
**2-((diethoxyphosphoryl)methyl)-1-
(((diethoxyphosphoryl)methyl)amino)imidazo[5,1-*a*]isoquinolin-2-ium chloride (4e)**



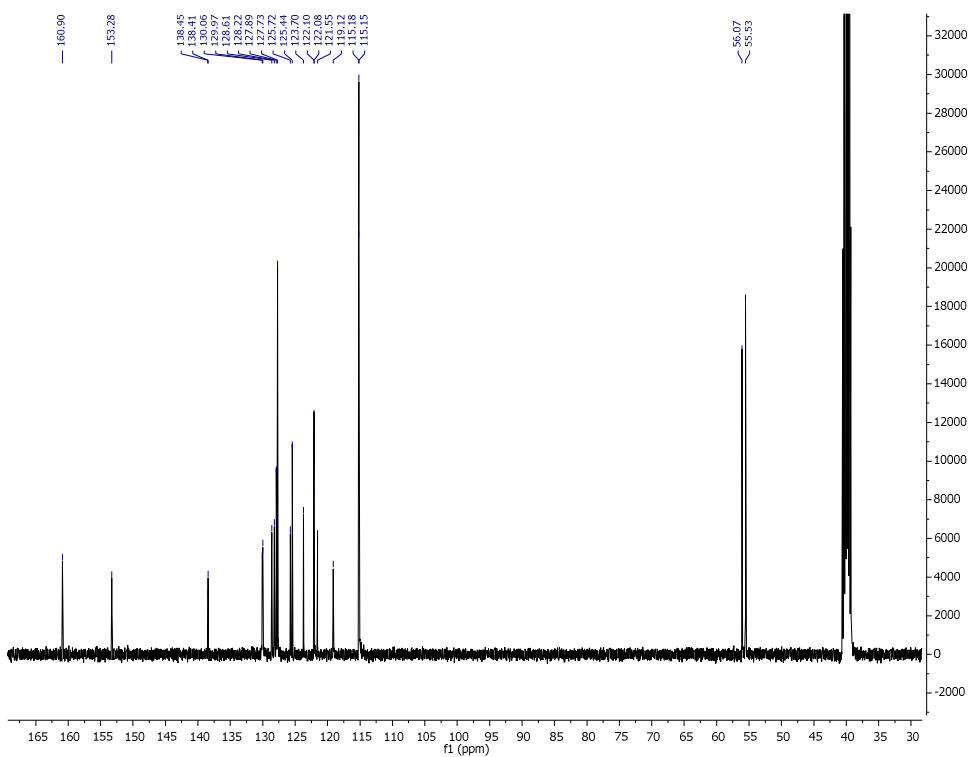
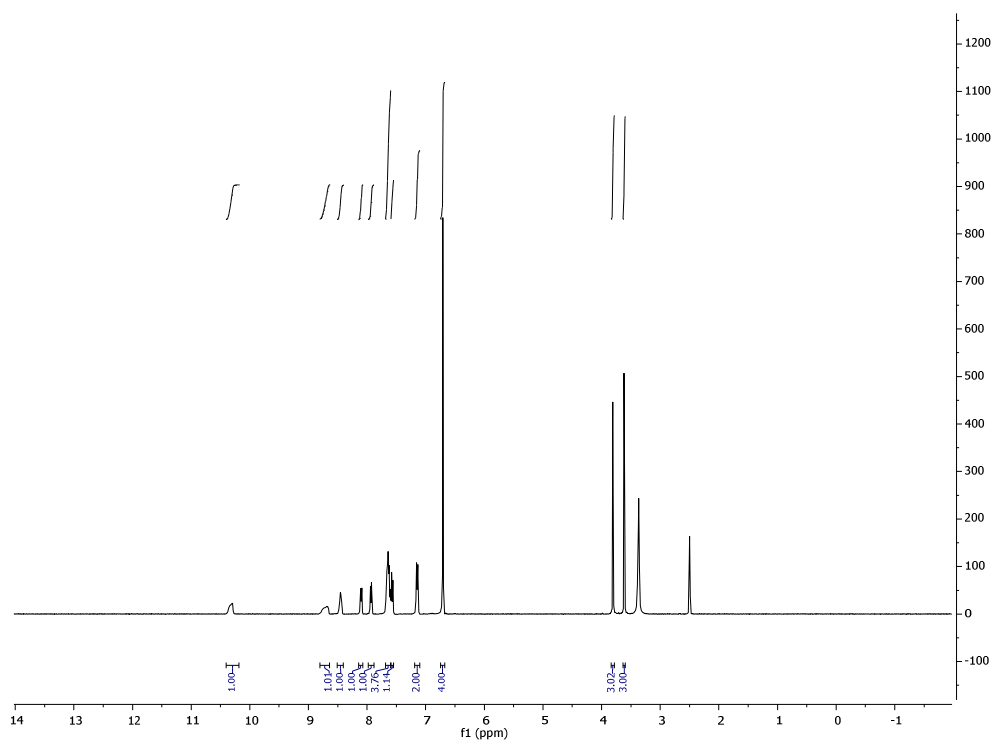
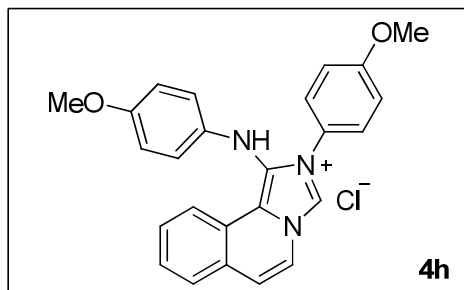
2-(2,6-dimethylphenyl)-1-((2,6-dimethylphenyl)amino)imidazo[5,1-*a*]isoquinolin-2-ium chloride (4f)



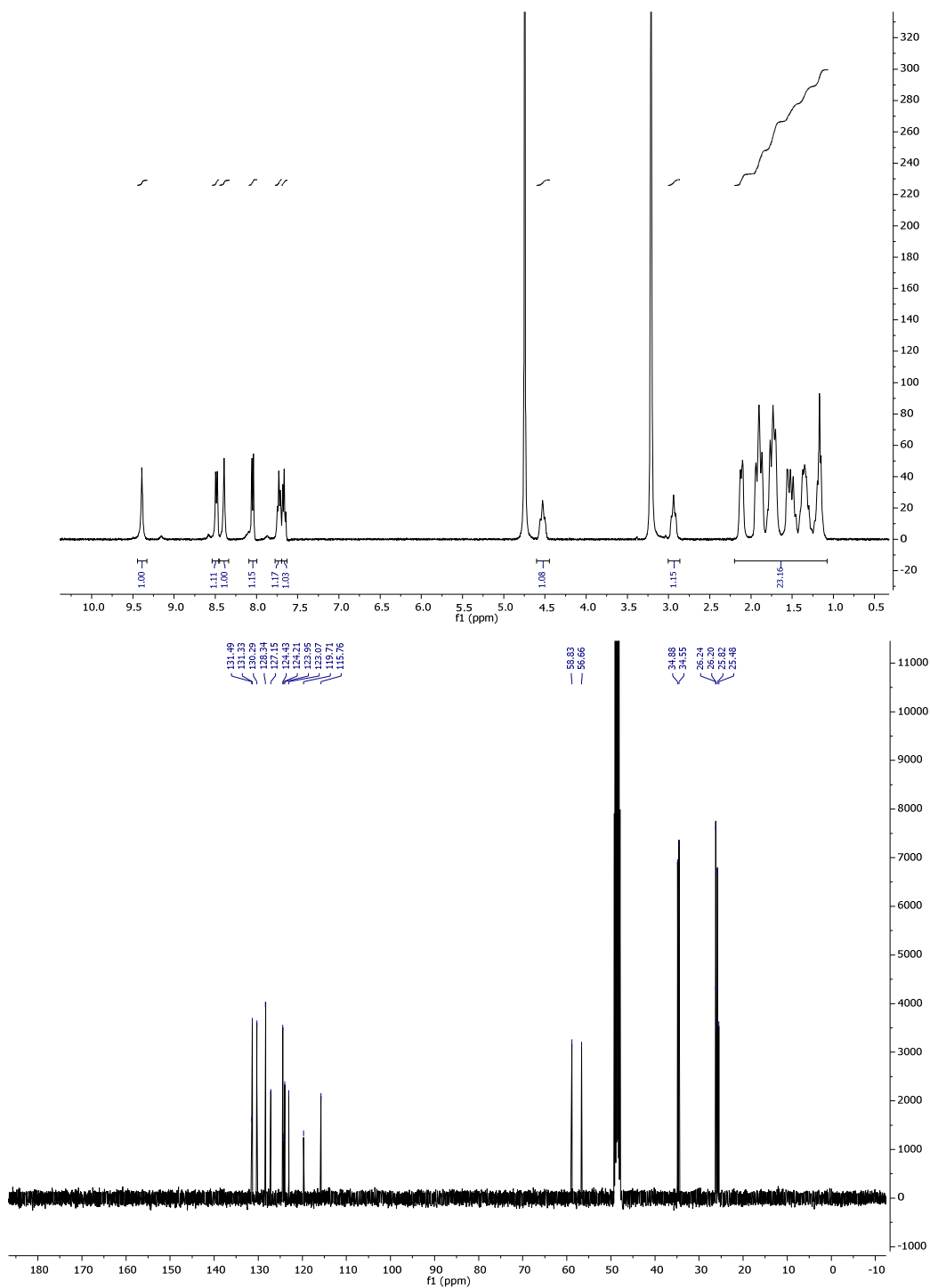
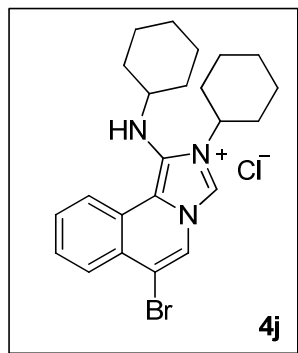
2-(naphthalen-2-yl)-1-(naphthalen-2-ylamino)imidazo[5,1-a]isoquinolin-2-ium chloride (4g)



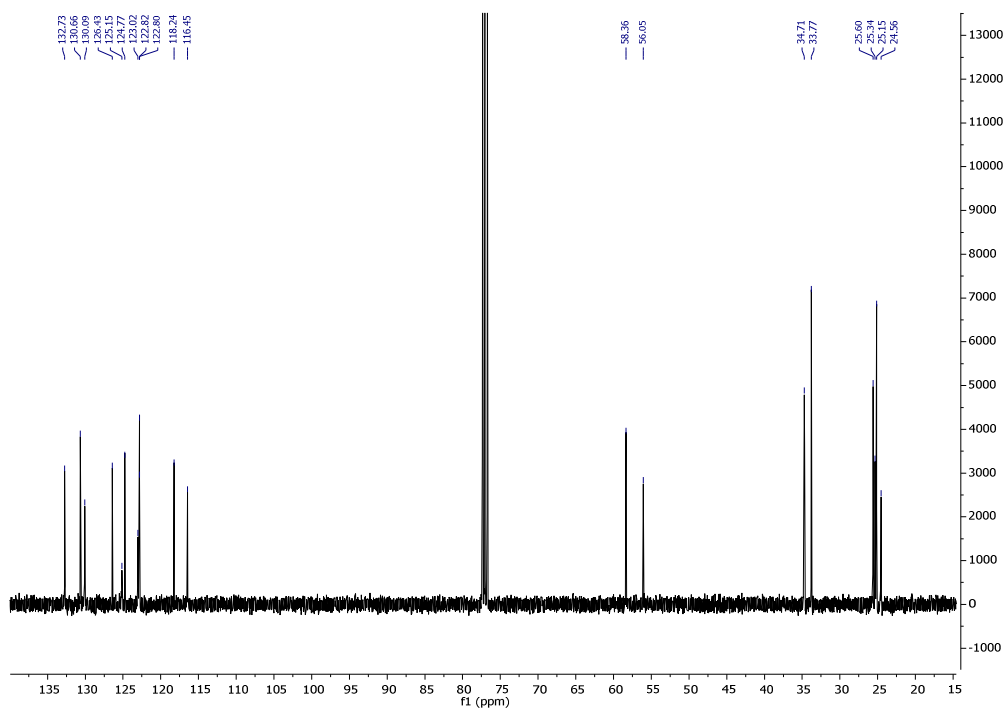
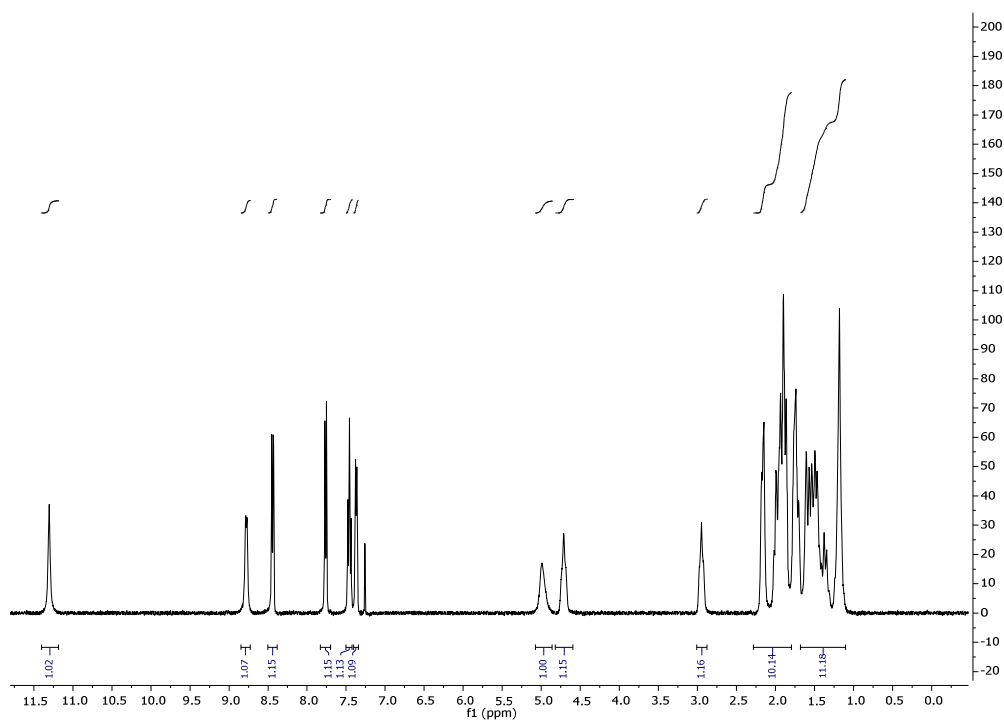
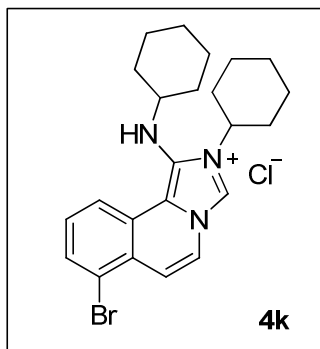
2-(4-methoxyphenyl)-1-((4-methoxyphenyl)amino)imidazo[5,1-a]isoquinolin-2-ium chloride (4h)



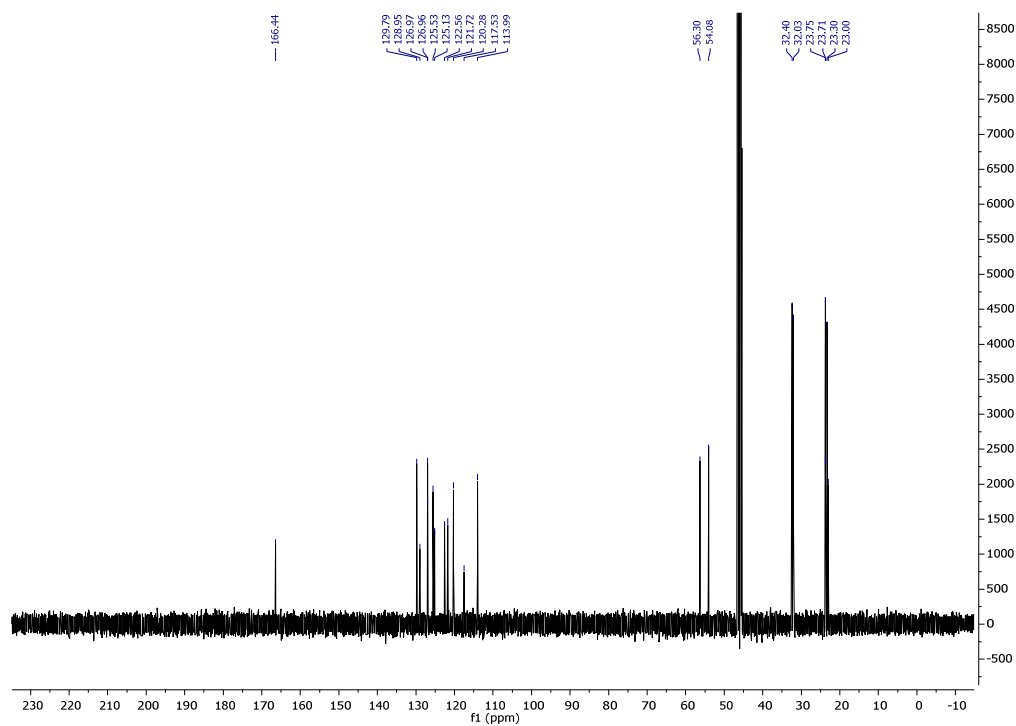
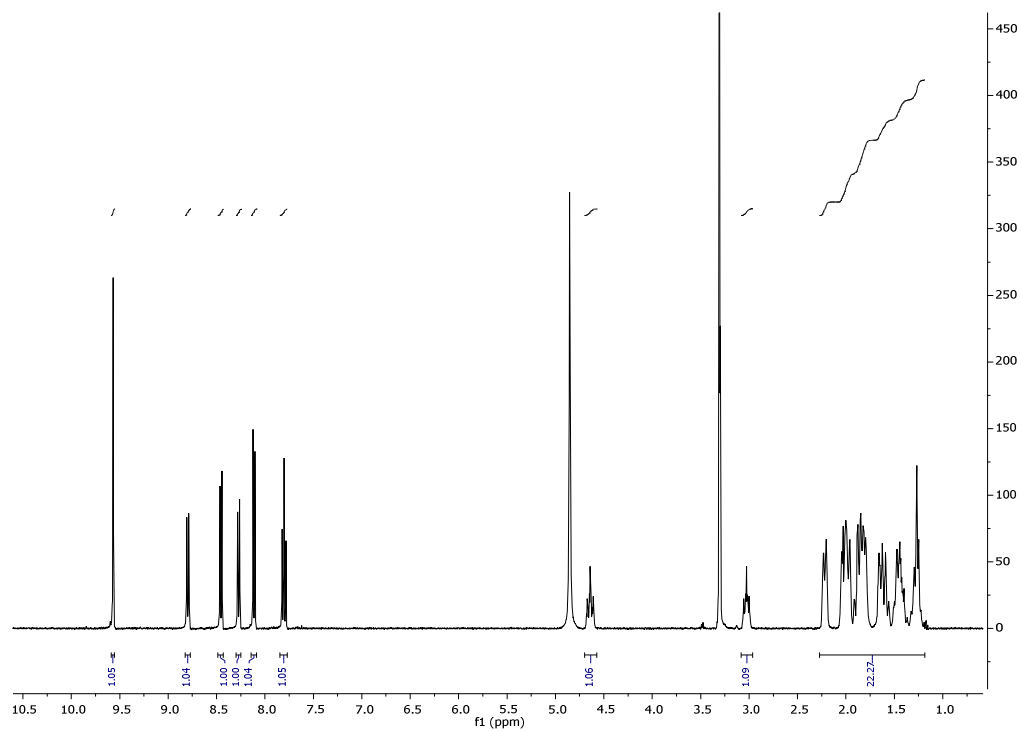
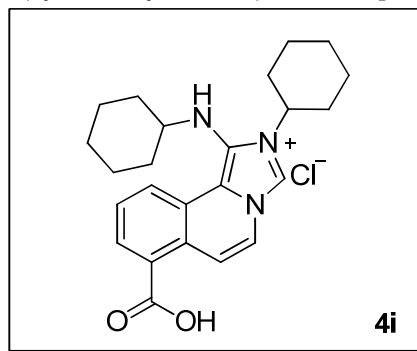
6-bromo-2-cyclohexyl-1-(cyclohexylamino)imidazo[5,1-a]isoquinolin-2-ium chloride (4j)



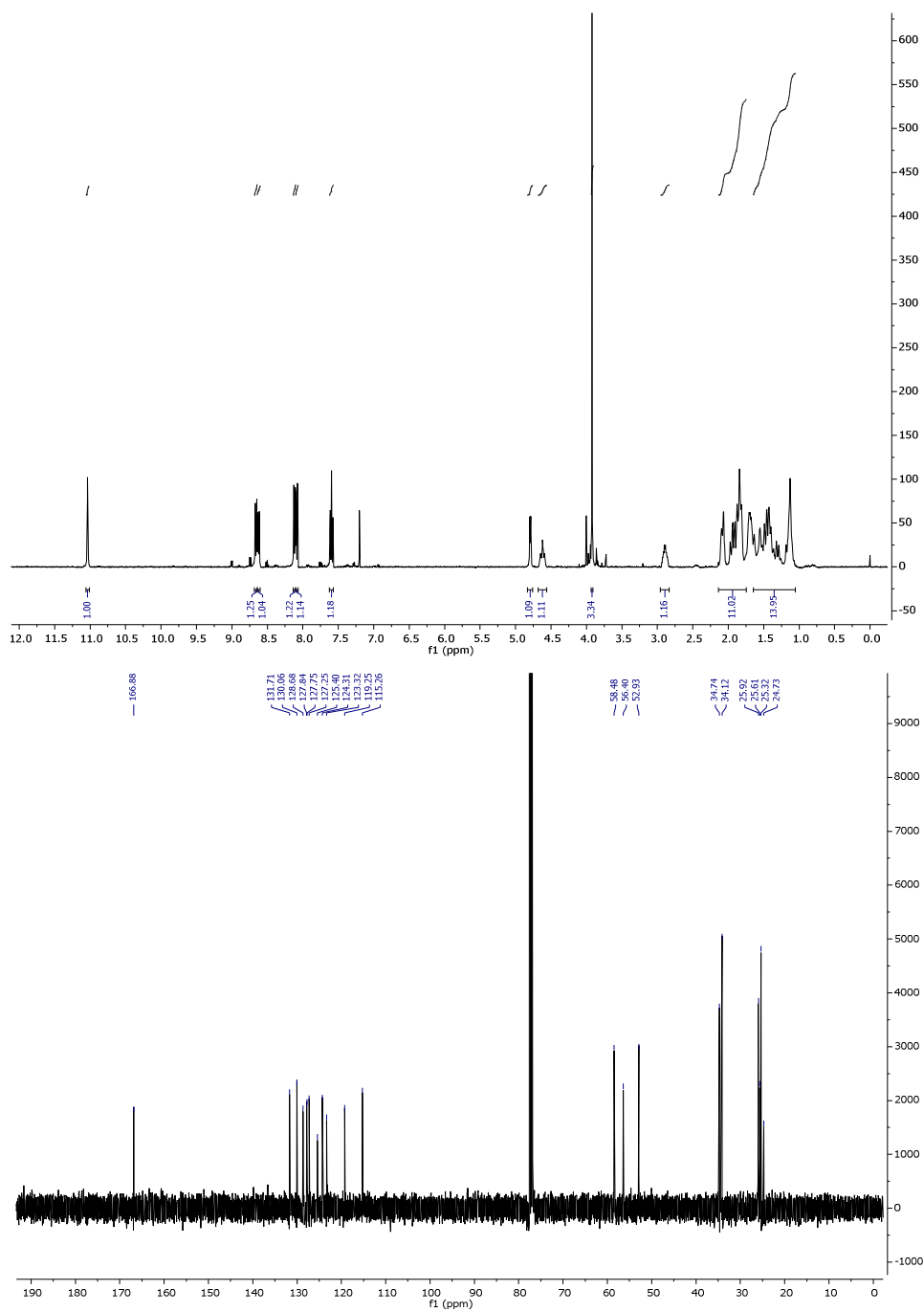
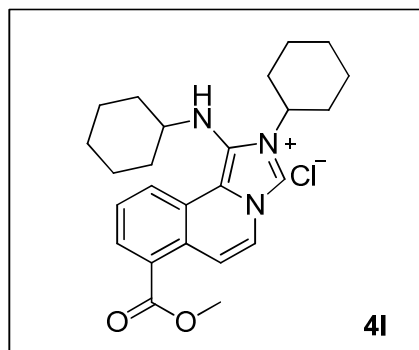
7-bromo-2-cyclohexyl-1-(cyclohexylamino)imidazo[5,1-a]isoquinolin-2-ium chloride (4k)



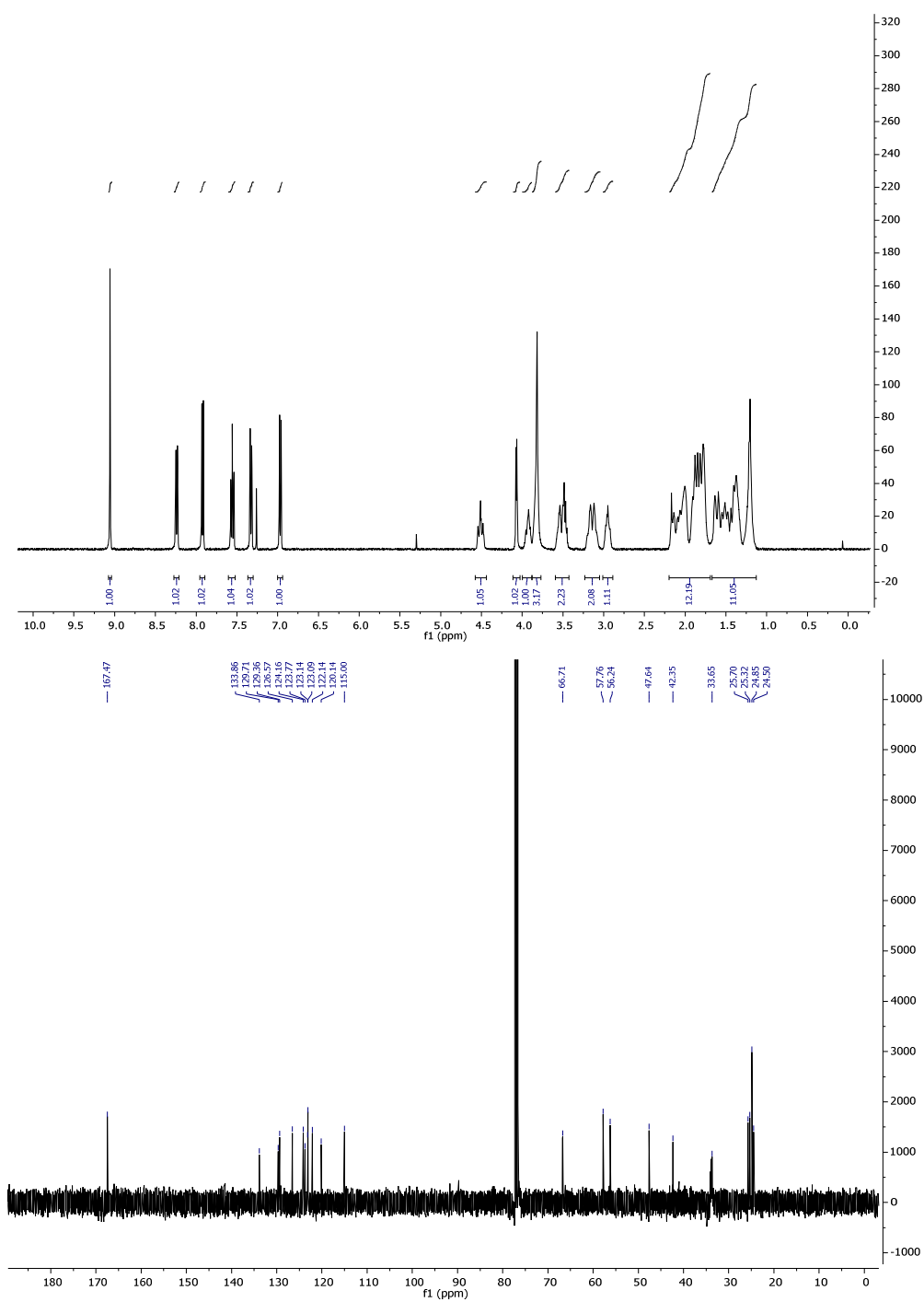
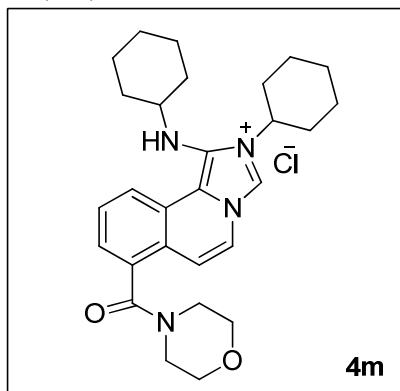
7-carboxy-2-cyclohexyl-1-(cyclohexylamino)imidazo[5,1-a]isoquinolin-2-ium(4i)



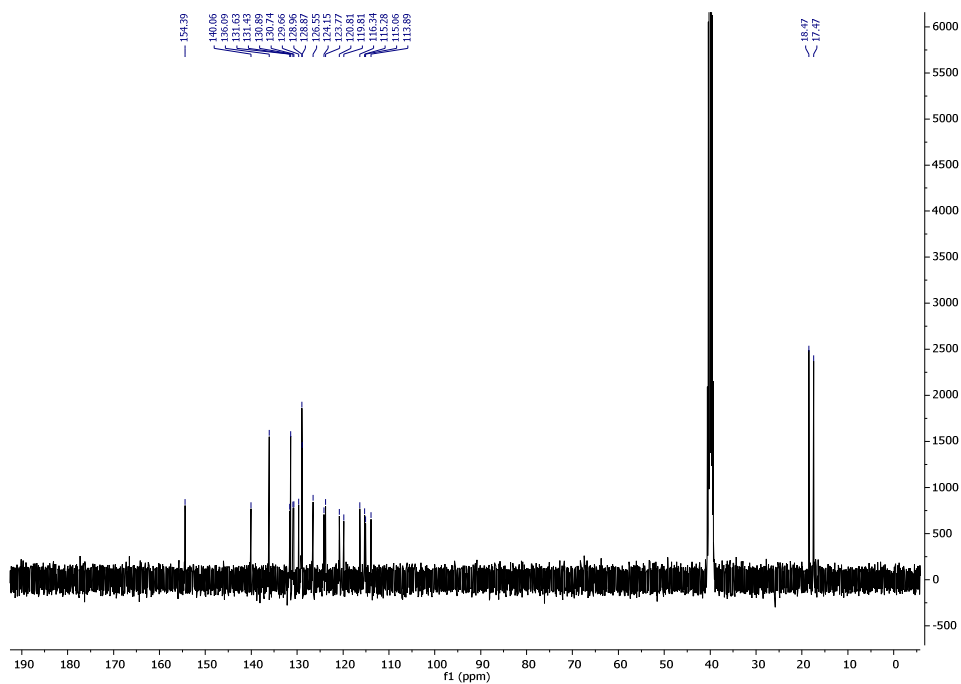
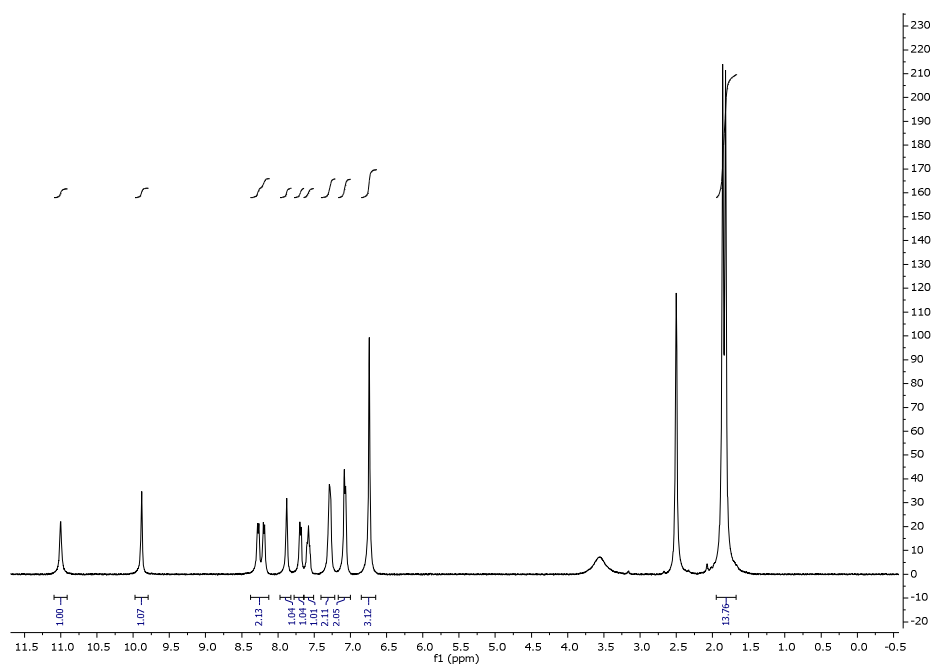
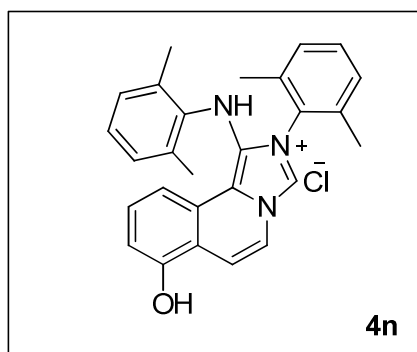
2-cyclohexyl-1-(cyclohexylamino)-7-(methoxycarbonyl)imidazo[5,1-a]isoquinolin-2-ium(4I)



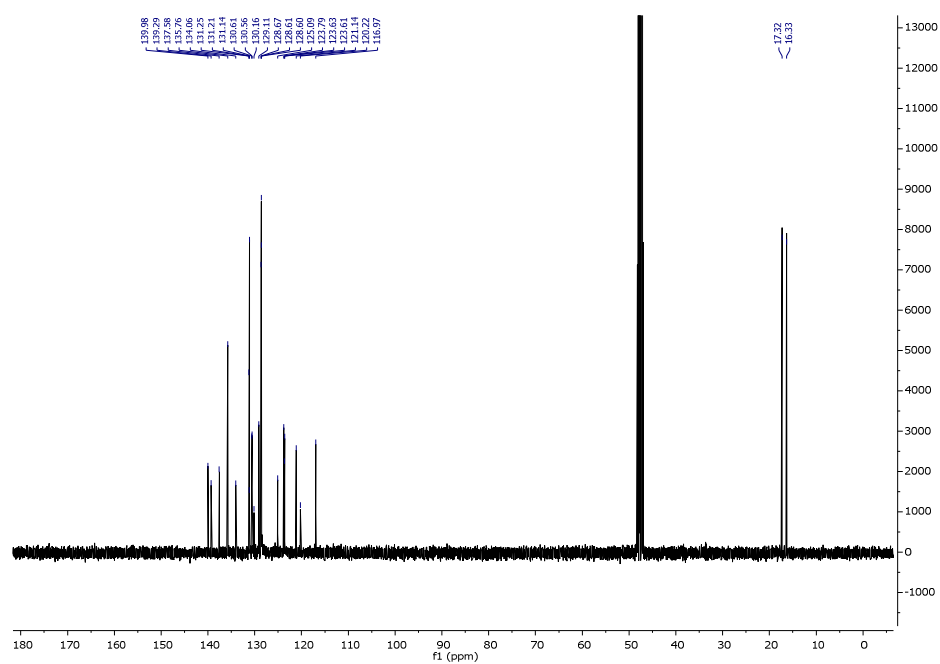
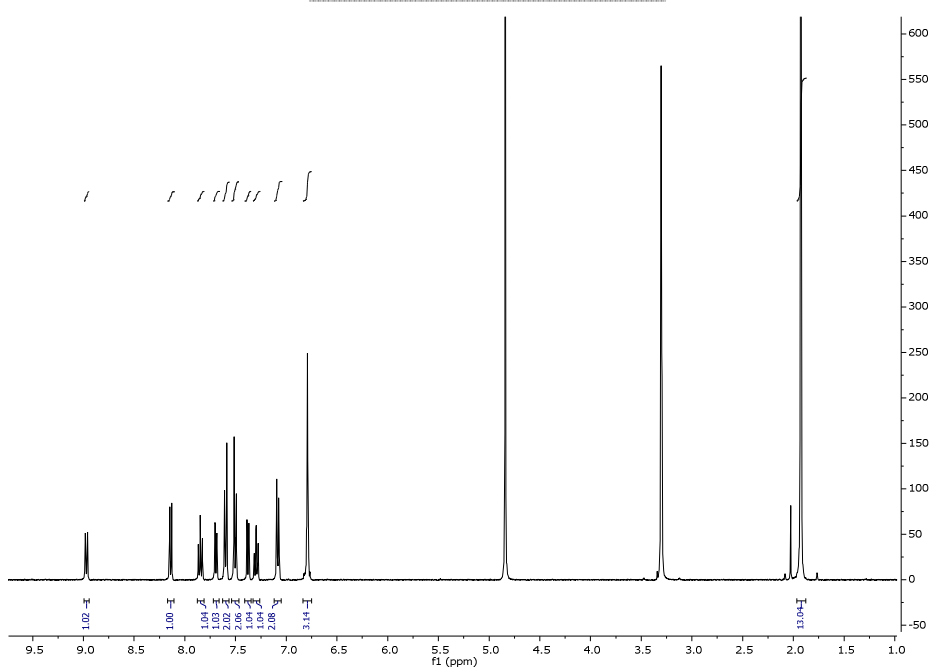
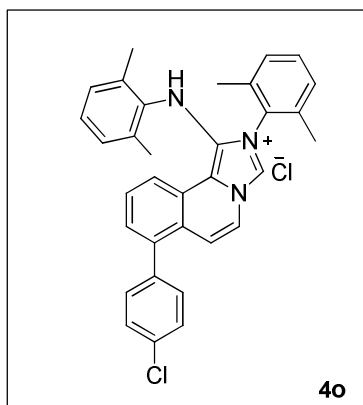
2-cyclohexyl-1-(cyclohexylamino)-7-(morpholine-4-carbonyl)imidazo[5,1-*a*]isoquinolin-2-ium chloride (4m)



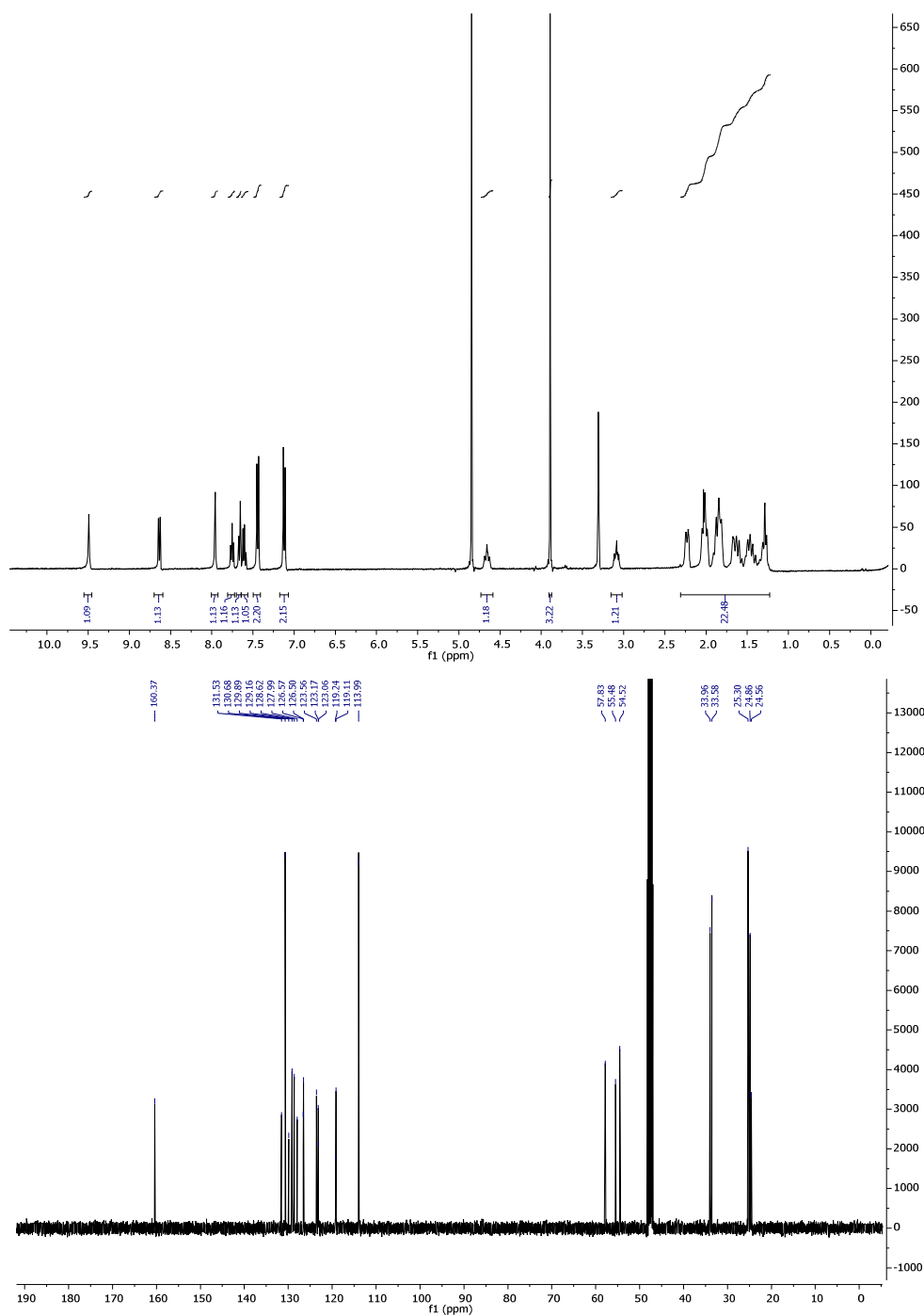
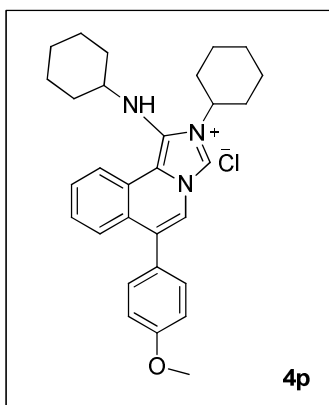
2-(2,6-dimethylphenyl)-1-((2,6-dimethylphenyl)amino)-7-hydroxyimidazo[5,1-*a*]isoquinolin-2-ium chloride (4n)



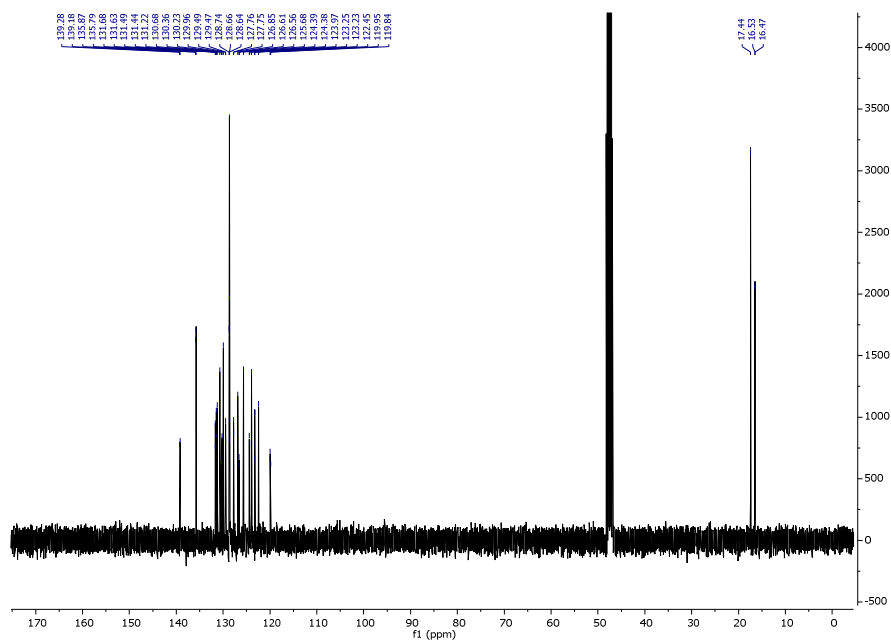
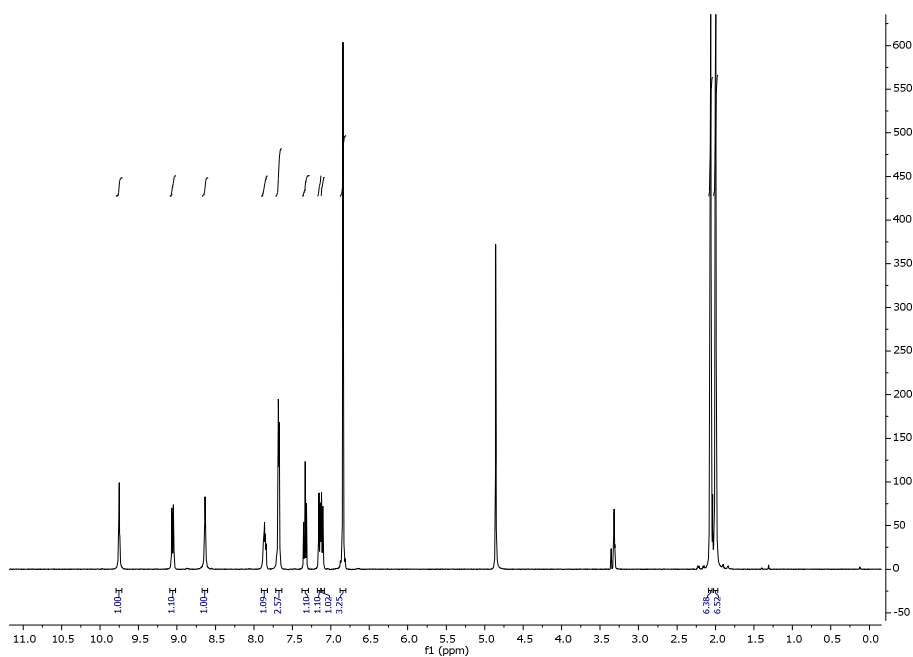
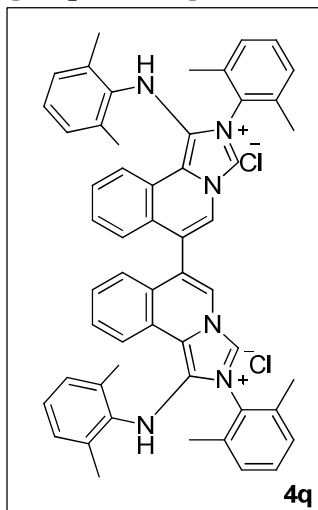
7-(4-chlorophenyl)-2-(2,6-dimethylphenyl)-1-((2,6-dimethylphenyl)amino)imidazo[5,1-a]isoquinolin-2-ium chloride (4o)



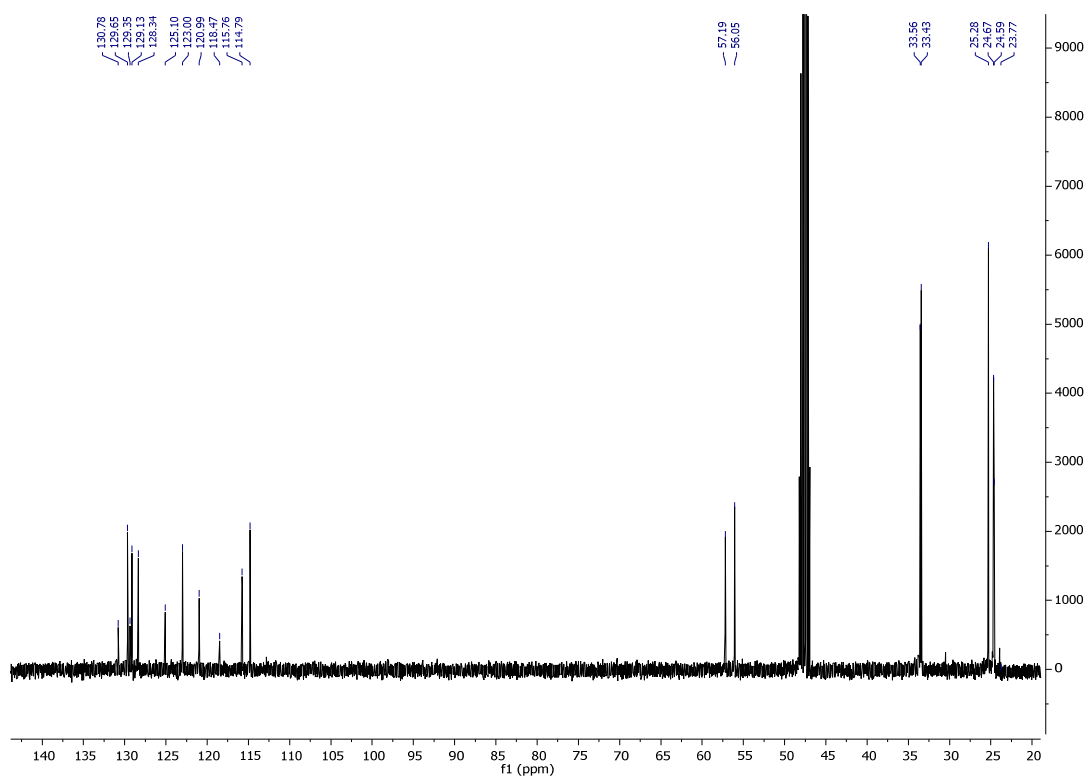
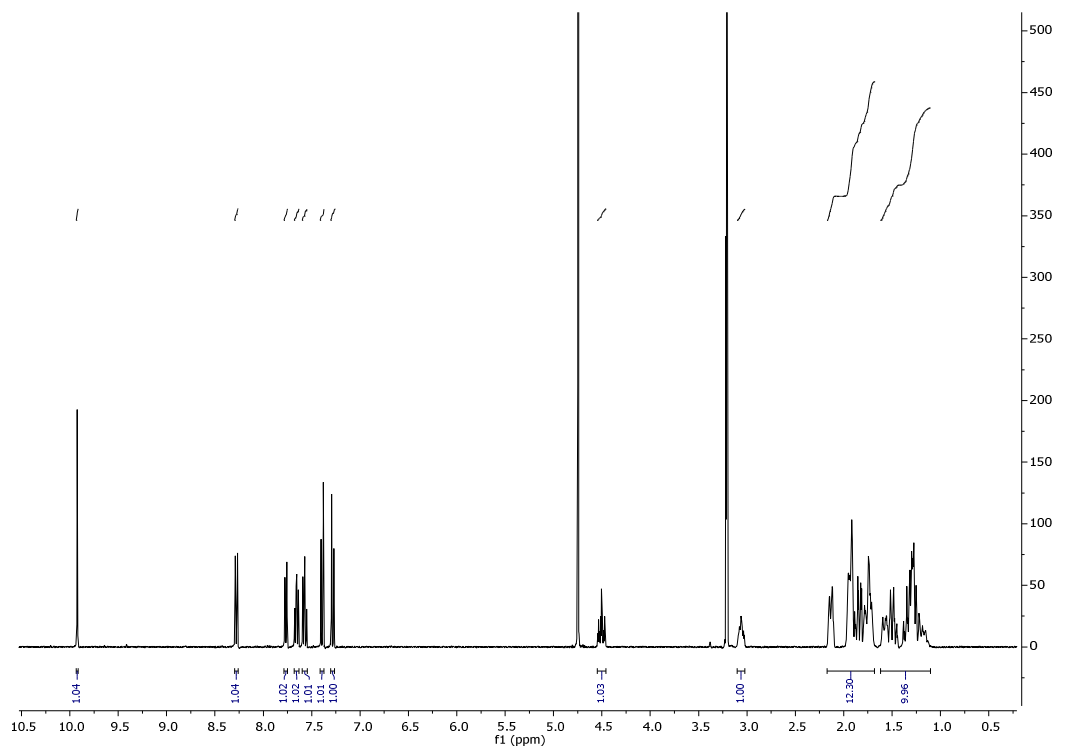
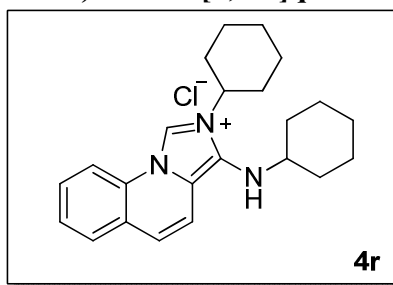
2-cyclohexyl-1-(cyclohexylamino)-6-(4-methoxyphenyl)imidazo[5,1-a]isoquinolin-2-ium chloride (4p)



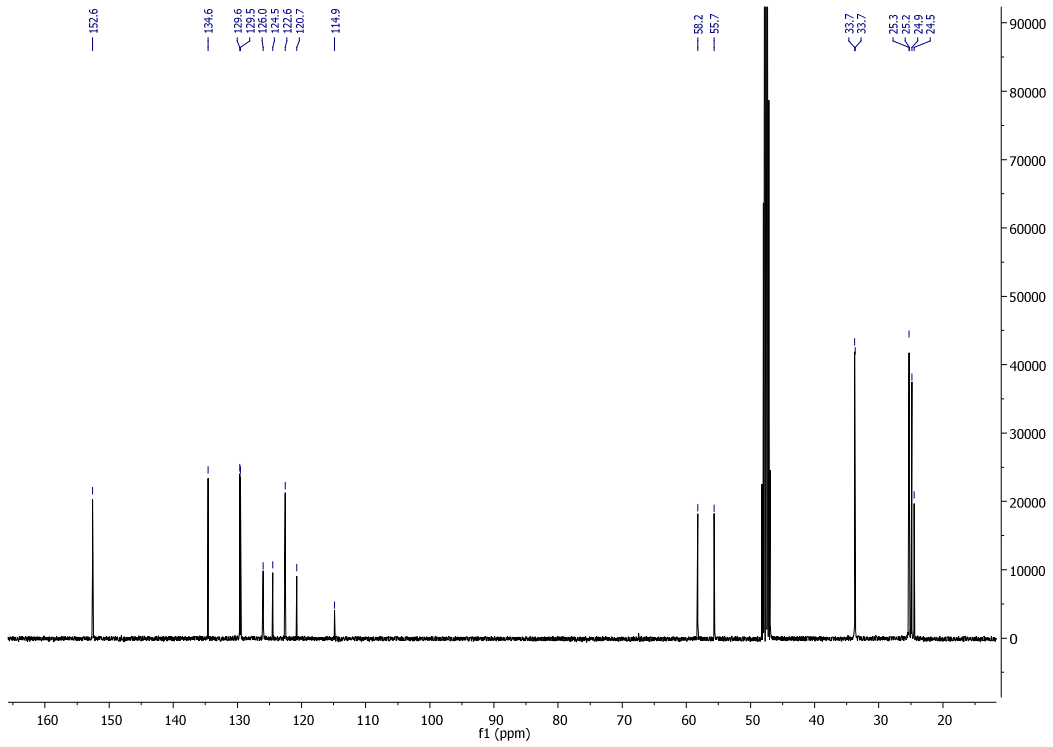
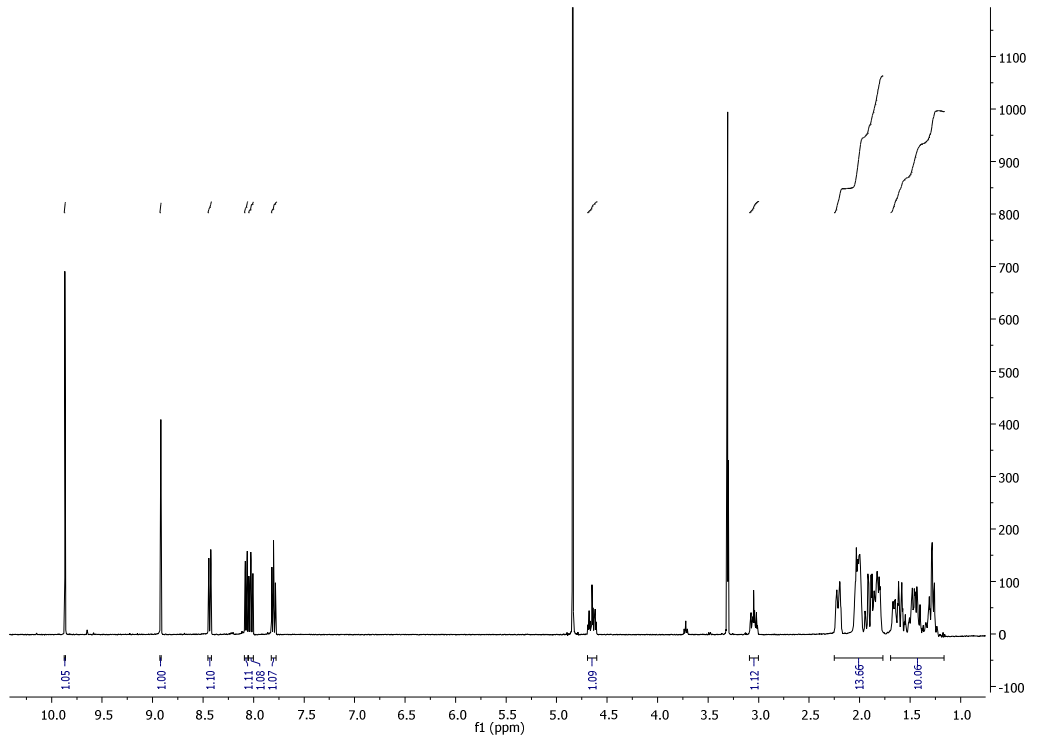
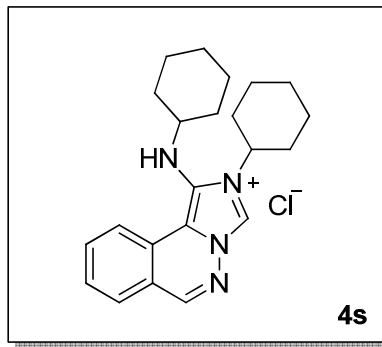
2,2'-bis(2,6-dimethylphenyl)-1,1'-bis((2,6-dimethylphenyl)amino)-[6,6'-biimidazo[5,1-*a*]-isoquinoline]-2,2'-dium chloride (4q)



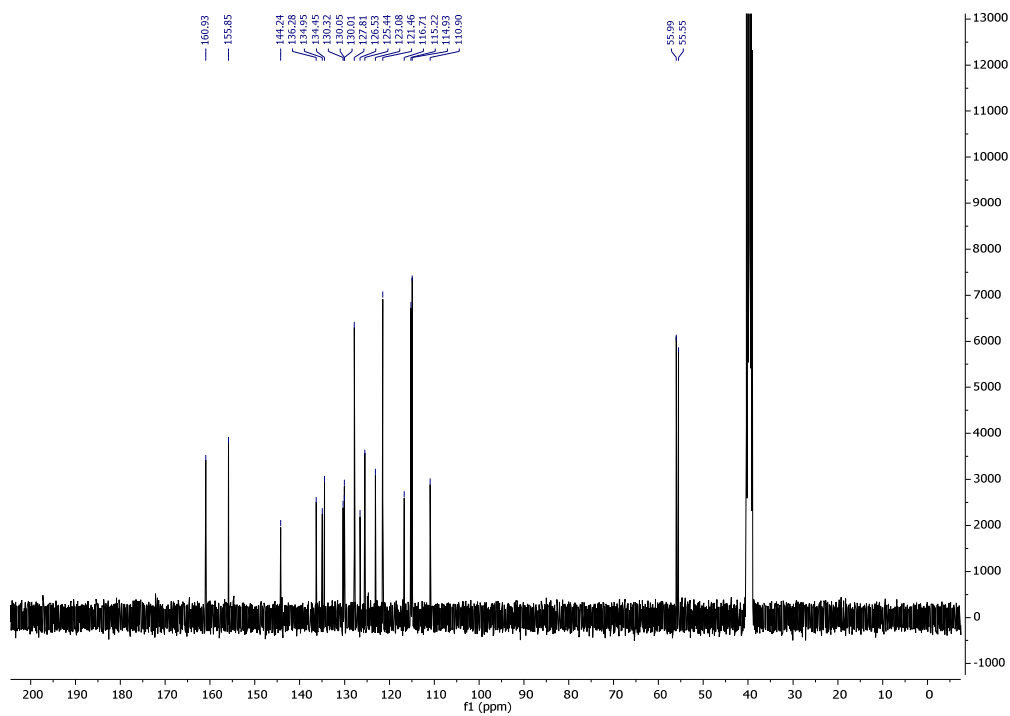
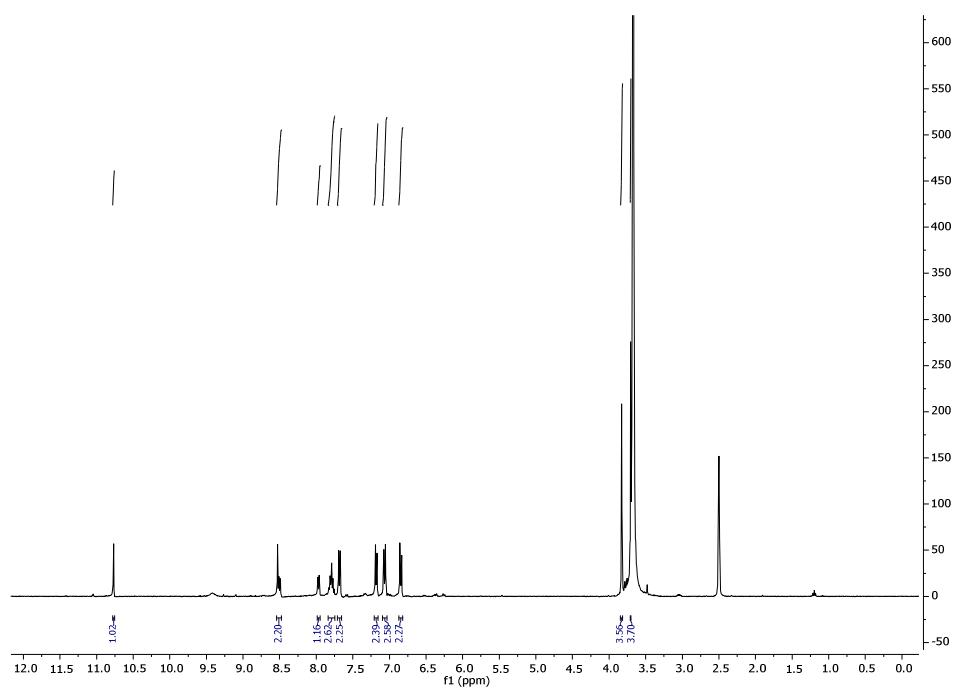
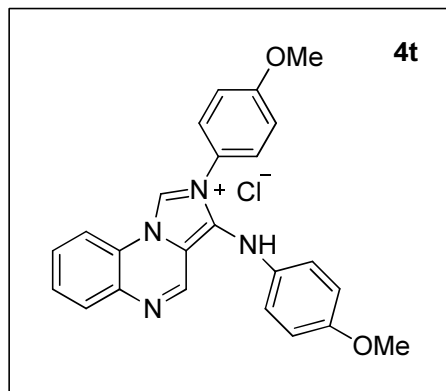
2-cyclohexyl-3-(cyclohexylamino)imidazo[1,5-a]quinolin-2-ium chloride (4r)



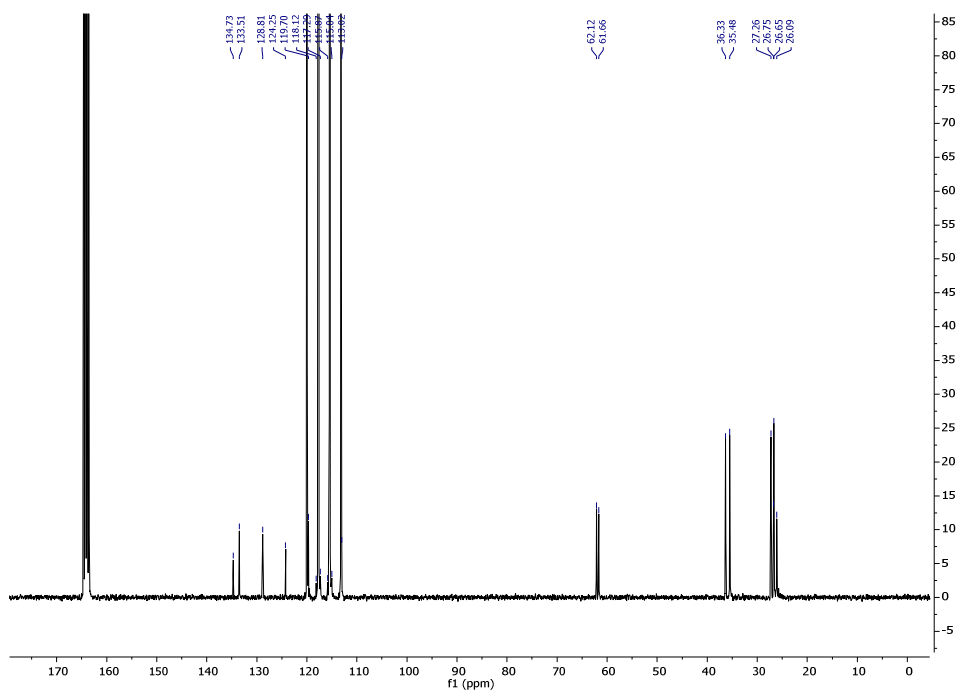
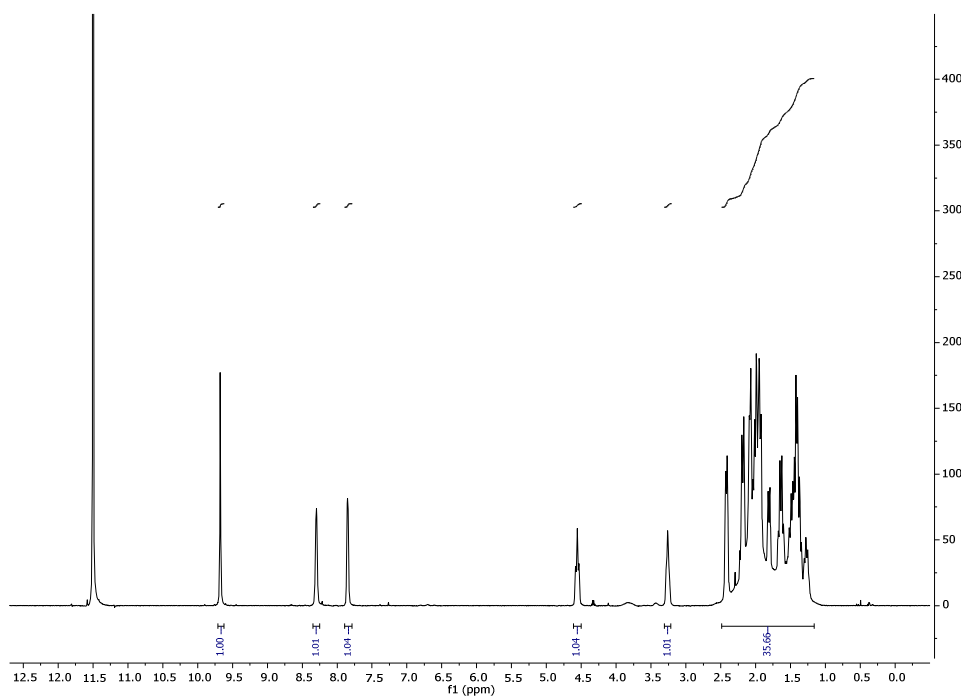
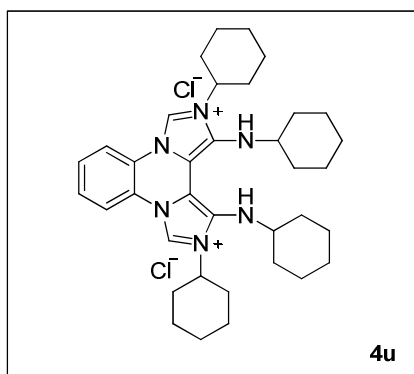
2-cyclohexyl-1-(cyclohexylamino)imidazo[5,1-a]phthalazin-2-ium chloride (4s)



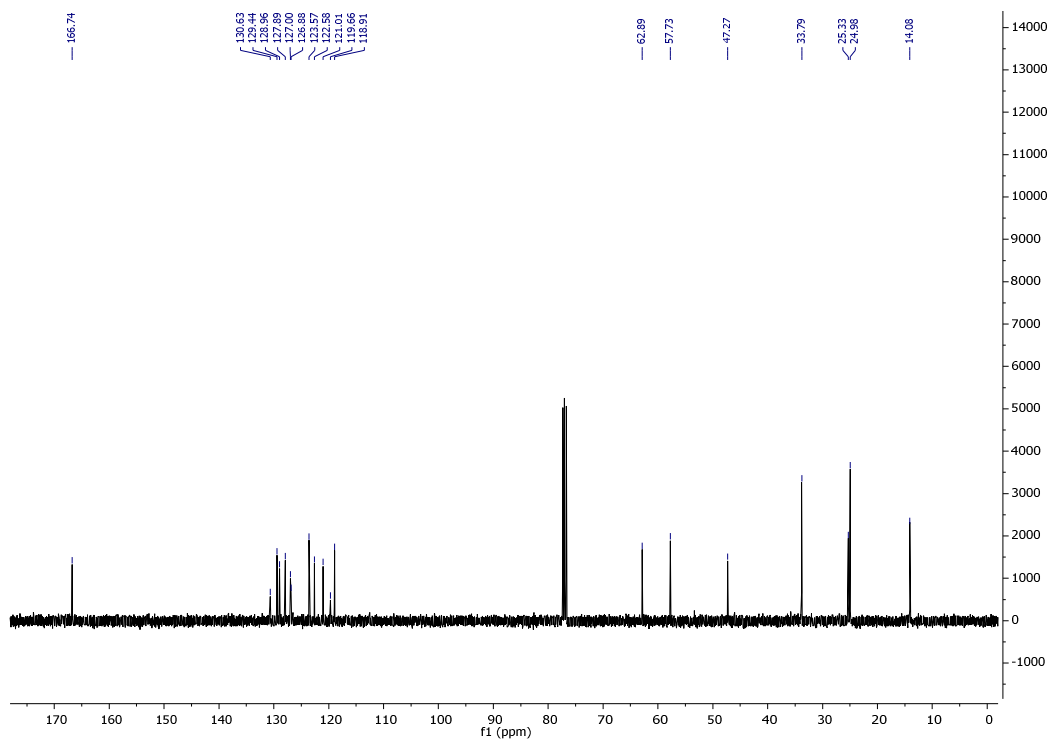
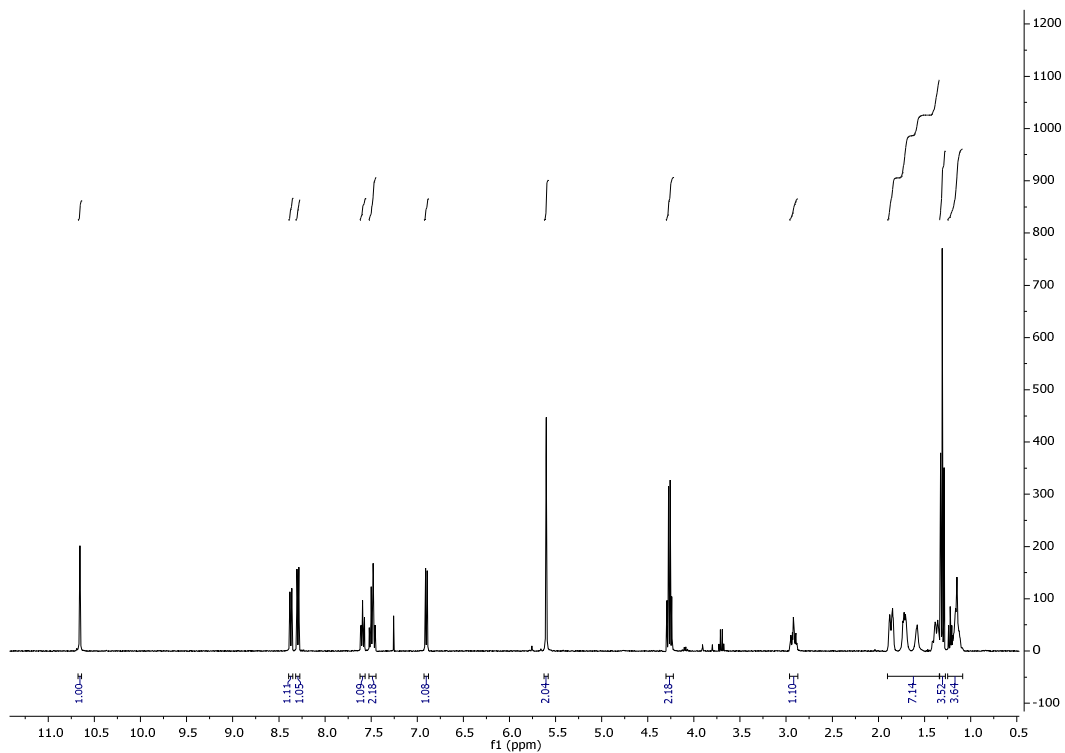
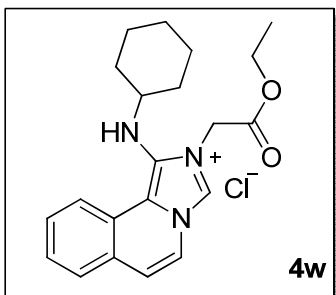
2-(4-methoxyphenyl)-3-((4-methoxyphenyl)amino)imidazo[1,5-a]quinoxalin-2-ium chloride (4t)



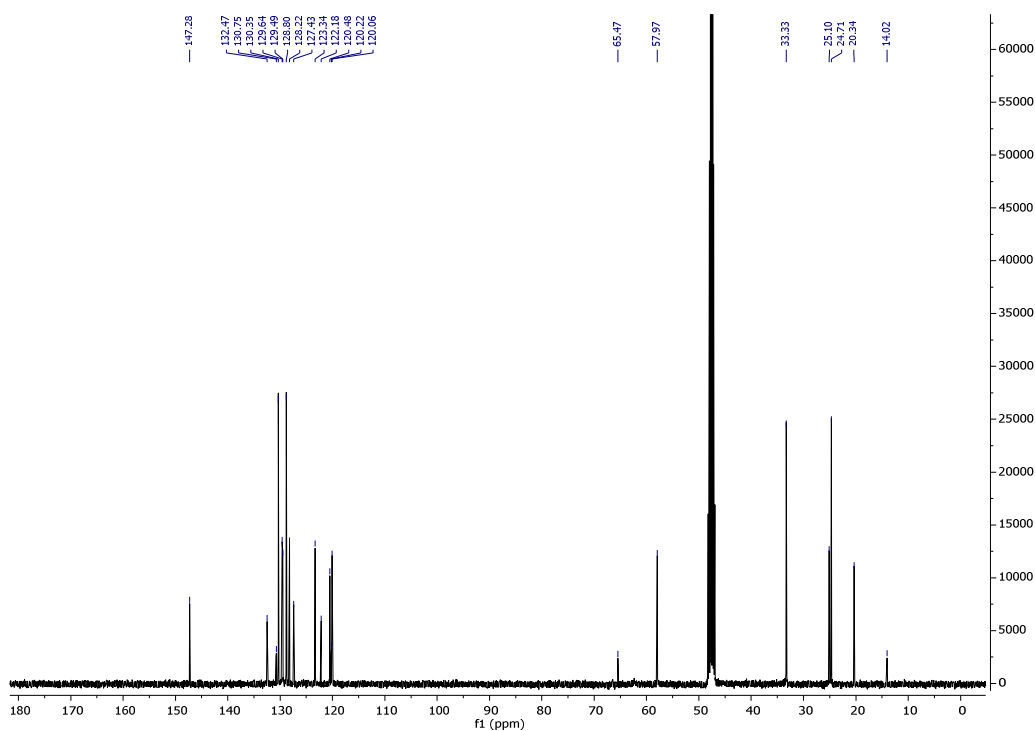
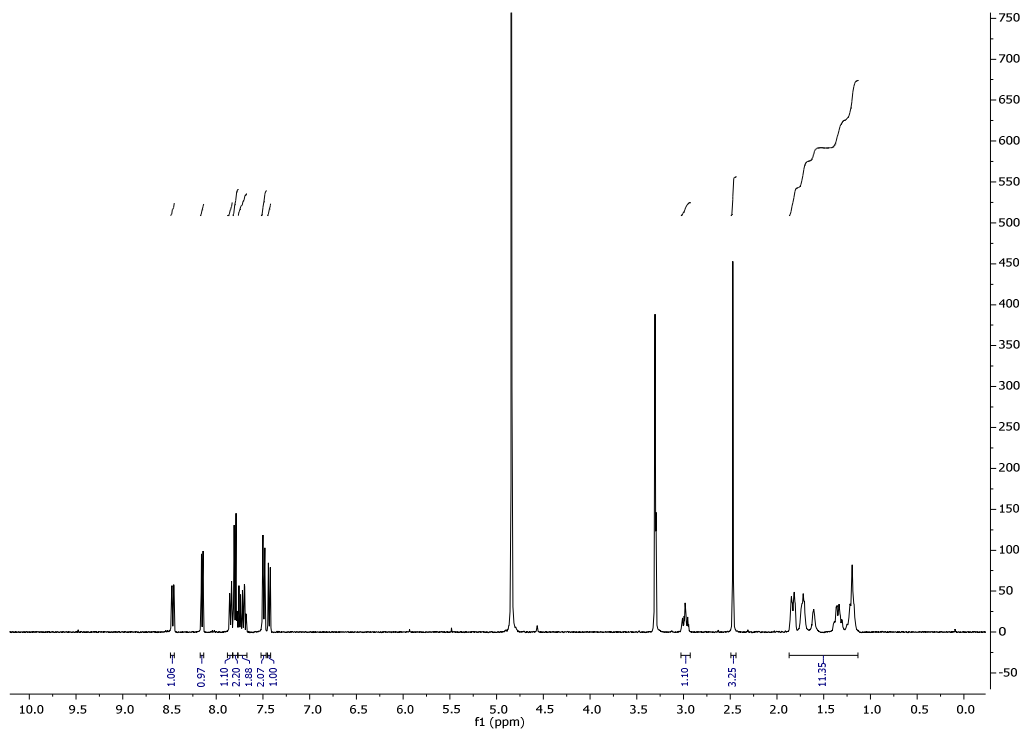
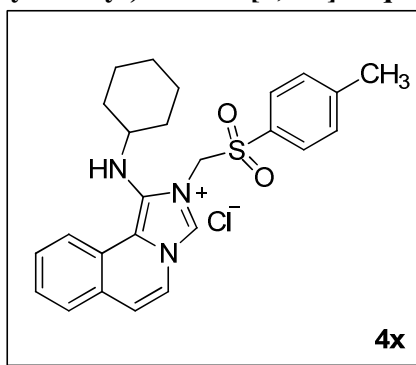
2,11-dicyclohexyl-1,12-bis(cyclohexylamino)diimidazo[1,5-a:5',1'-c]quinoxaline-2,11-dium chloride (4u)



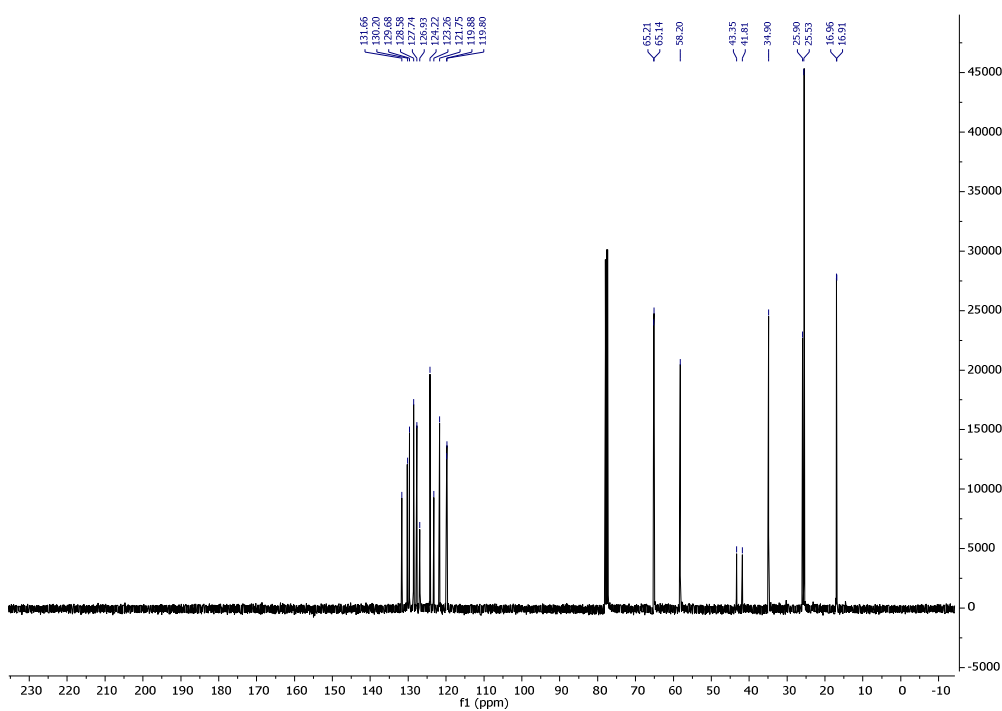
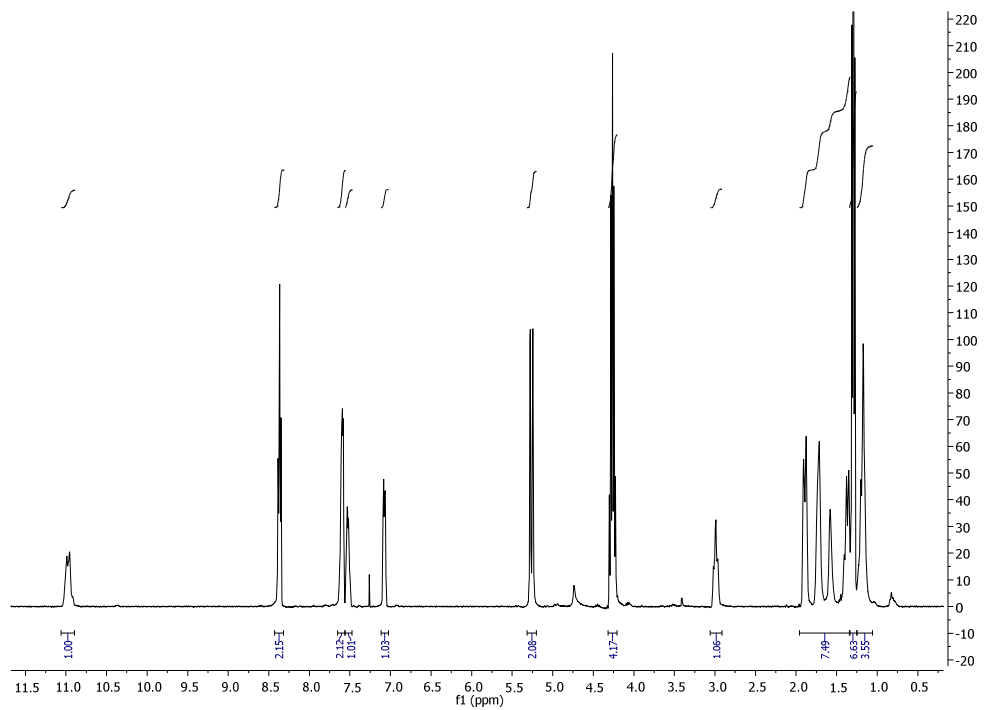
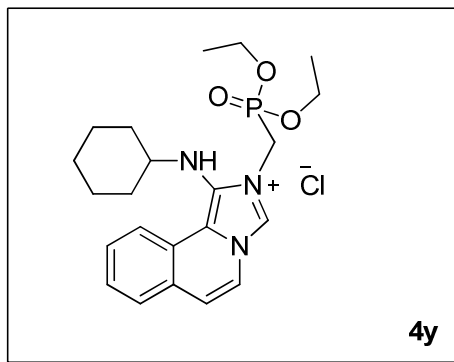
1-(cyclohexylamino)-2-(2-ethoxy-2-oxoethyl)imidazo[5,1-a]isoquinolin-2-ium chloride (4w)



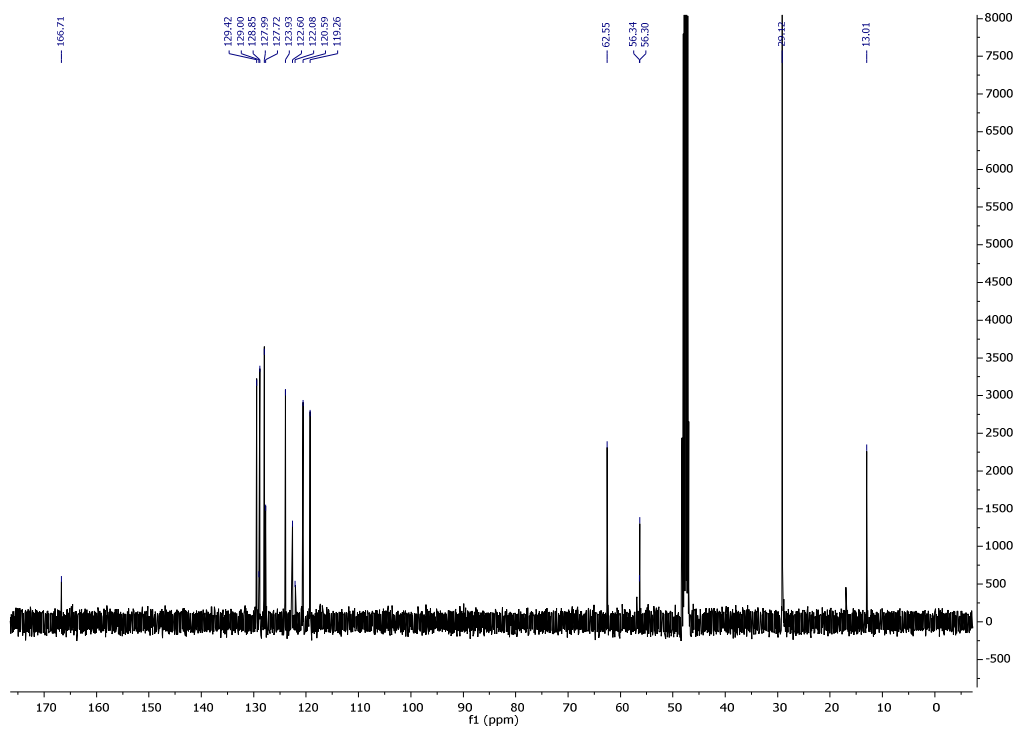
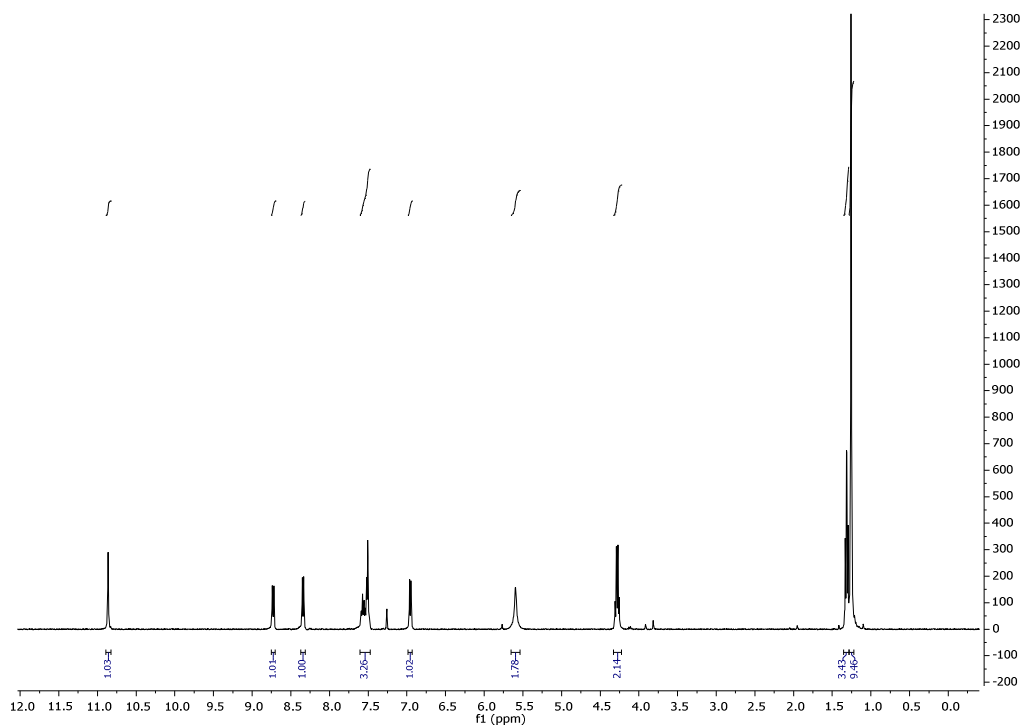
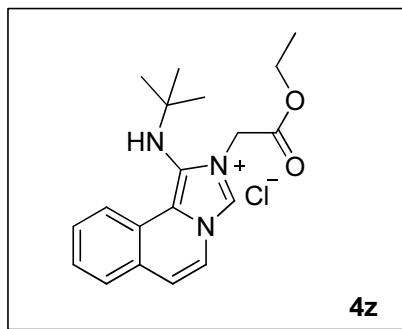
1-(cyclohexylamino)-2-(tosylmethyl)imidazo[5,1-a]isoquinolin-2-ium chloride (4x)



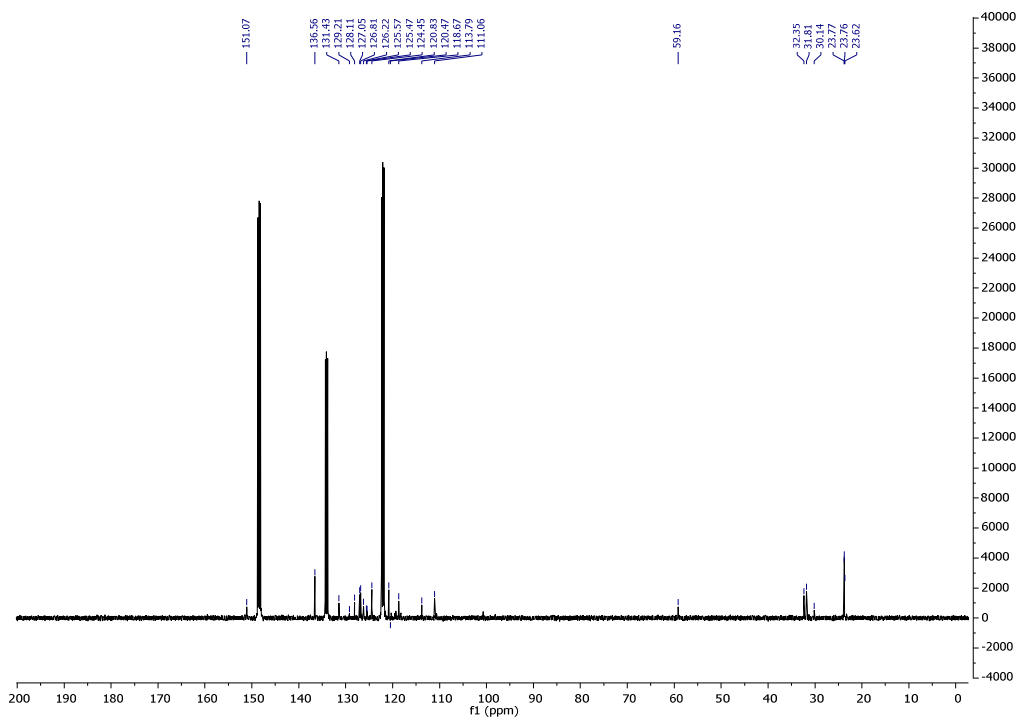
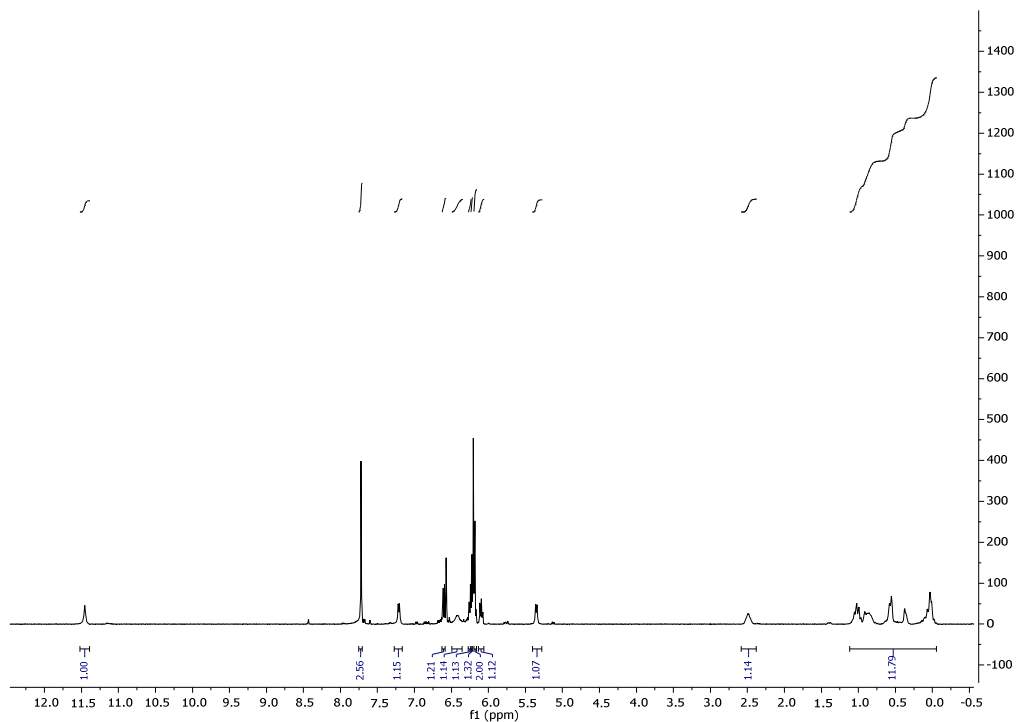
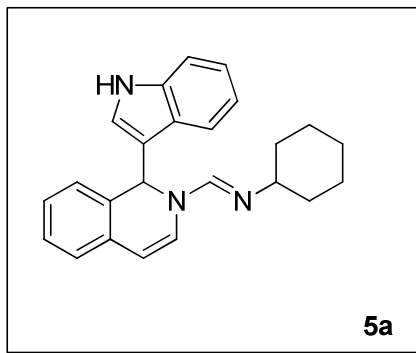
1-(cyclohexylamino)-2-(diethoxyphosphoryl)imidazo[5,1-*a*]isoquinolin-2-ium chloride (4y)



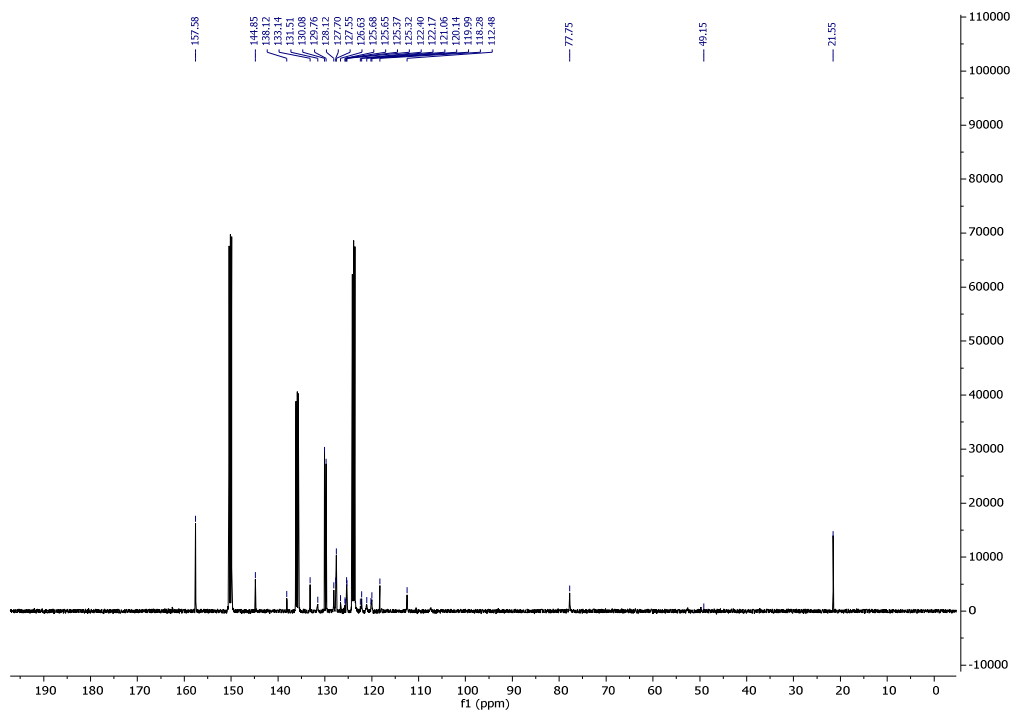
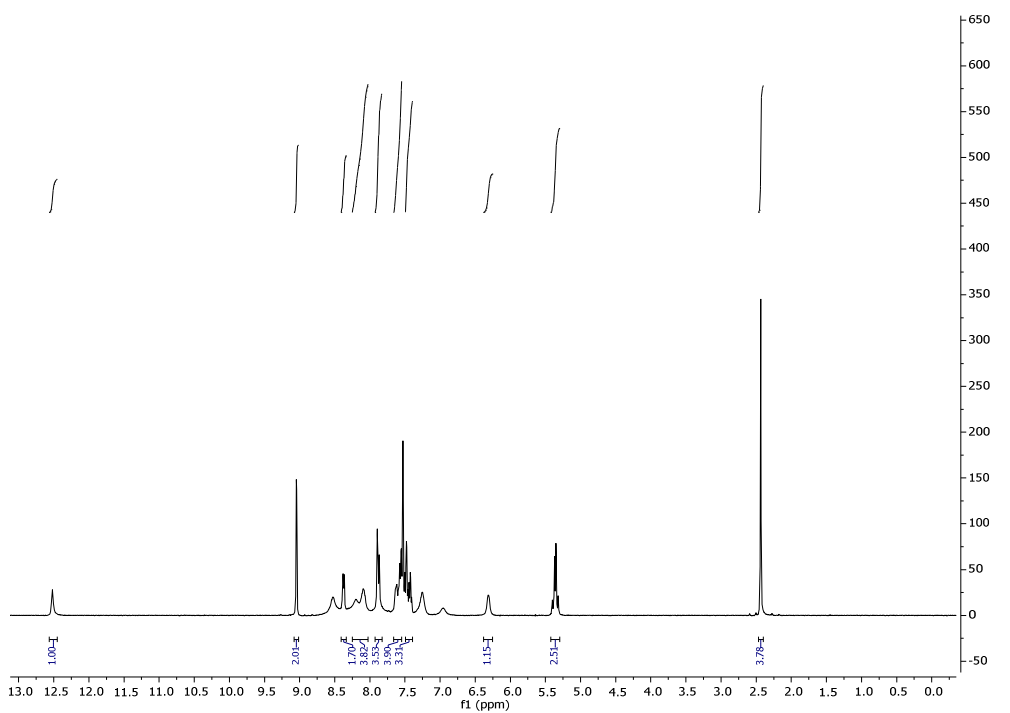
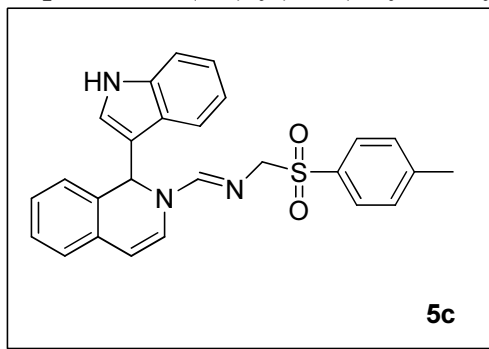
1-(*tert*-butylamino)-2-(2-ethoxy-2-oxoethyl)imidazo[5,1-*a*]isoquinolin-2-ium chloride (4z)



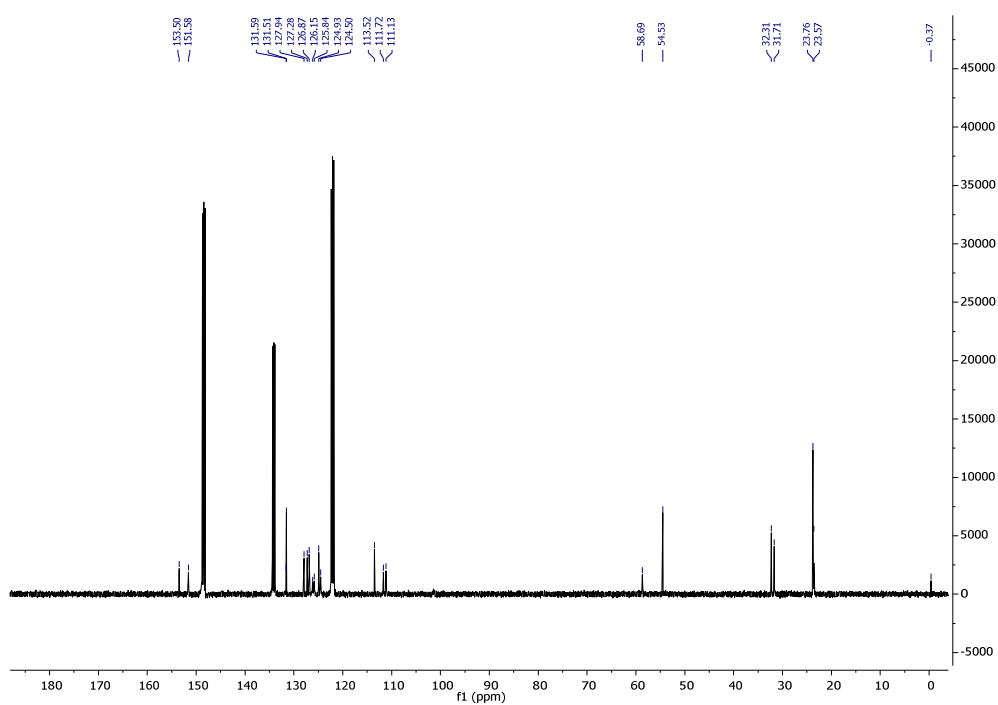
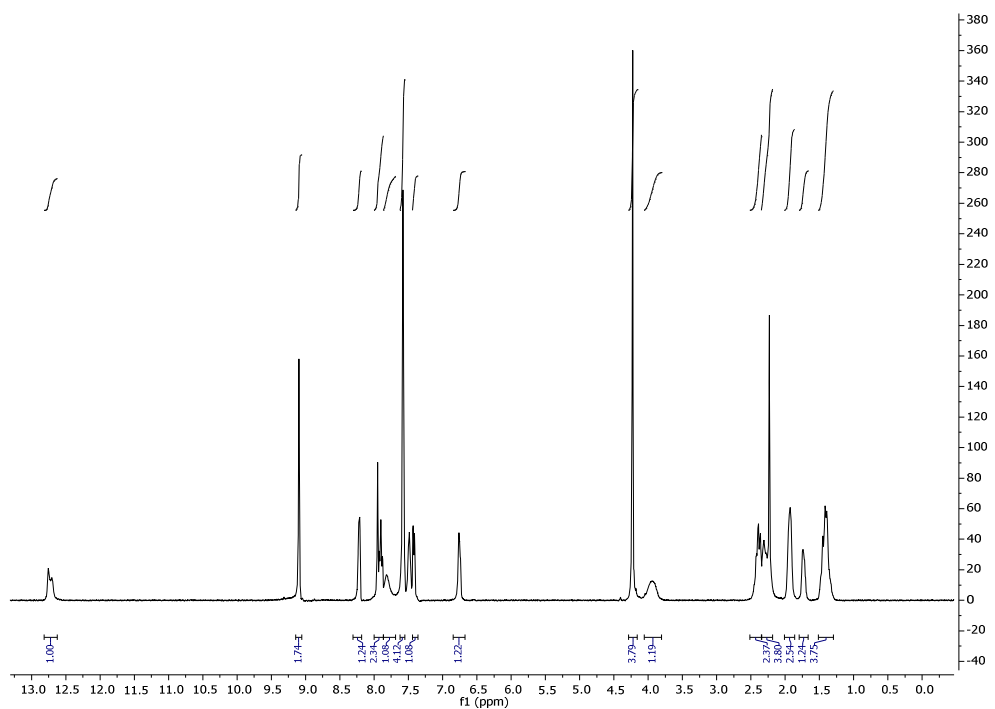
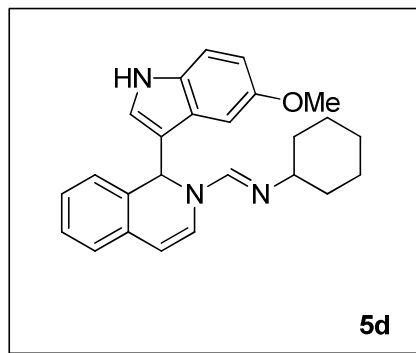
(E)-1-(1-(1H-indol-3yl)isoquinolin-2-(1H)-yl)-N-cyclohexylmethanimine 5a



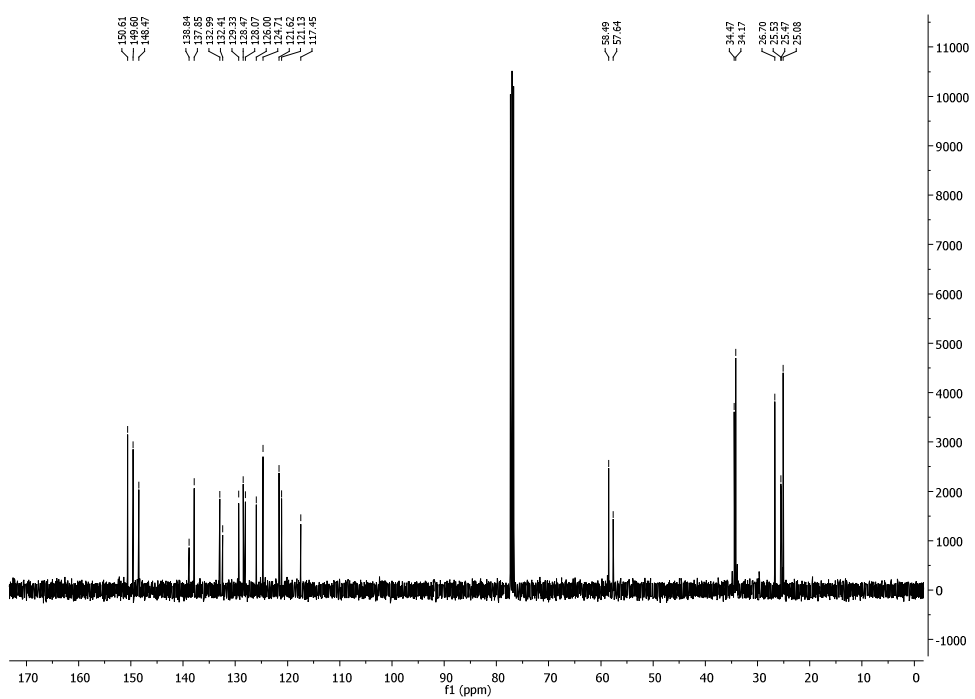
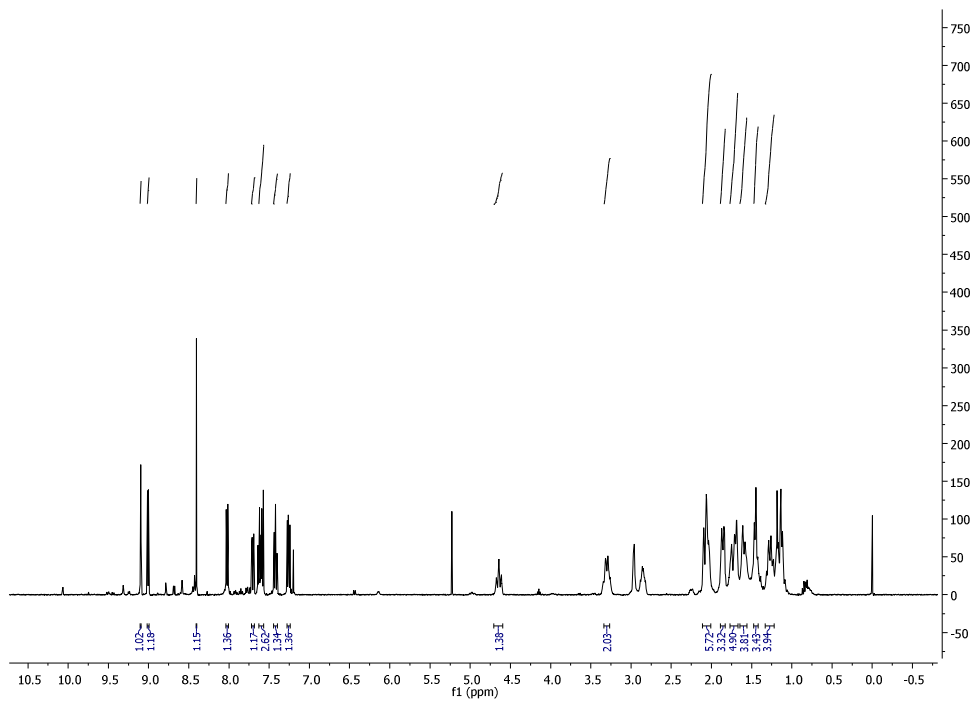
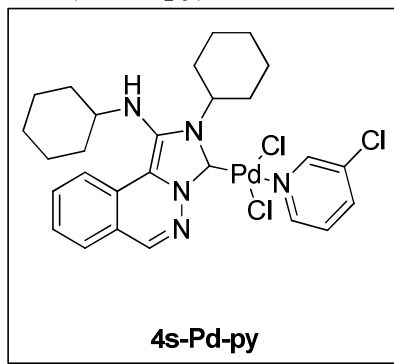
(E)-1-(1-(1H-indol-3yl)isoquinolin-2-(1H)-yl)-N-(tosylmethyl)methanimine 5c



(E)-N-cyclohexyl-1-(1-(5-methoxy-1H-indol-3yl)isoquinolin-2-(1H)-yl)methanimine
5d

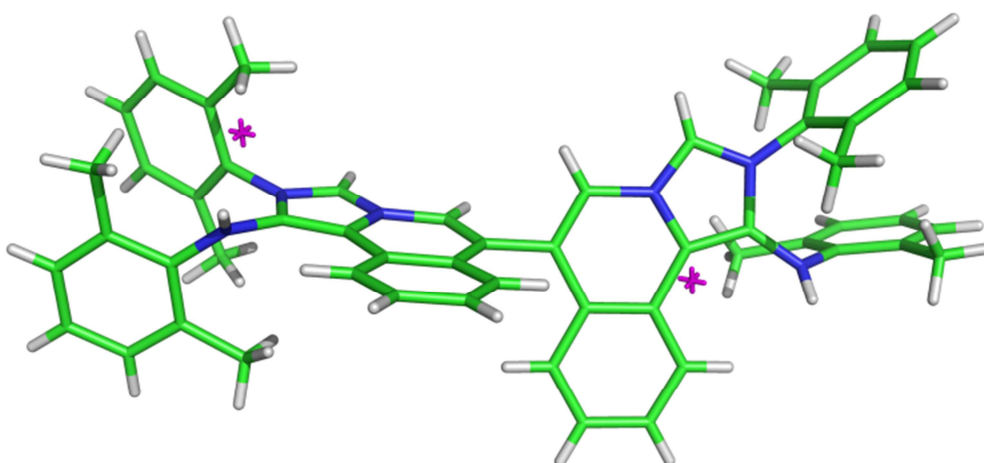
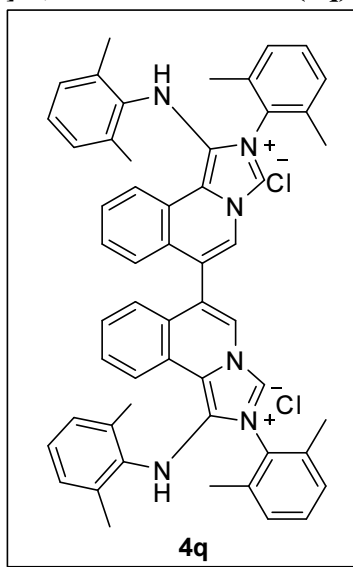


2-cyclohexyl-1-(cyclohexylamino)imidazo[5,1-a]phthalazin-2-ium chloride-PdCl₂ complex with 3-chloropyridine (4s-Pd-py)

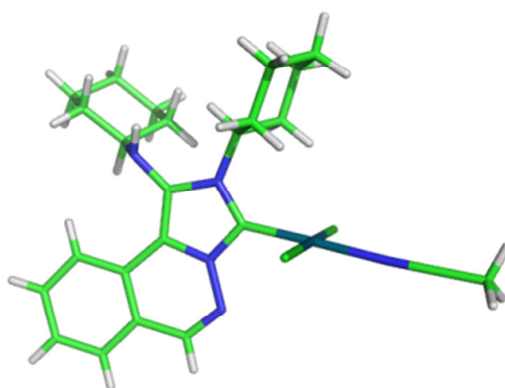
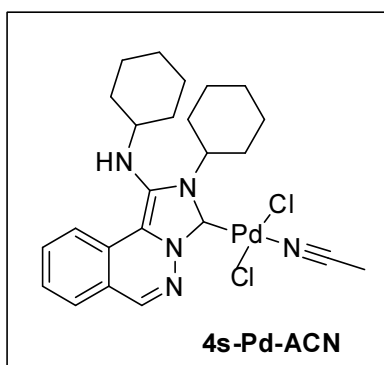


X-ray structures:

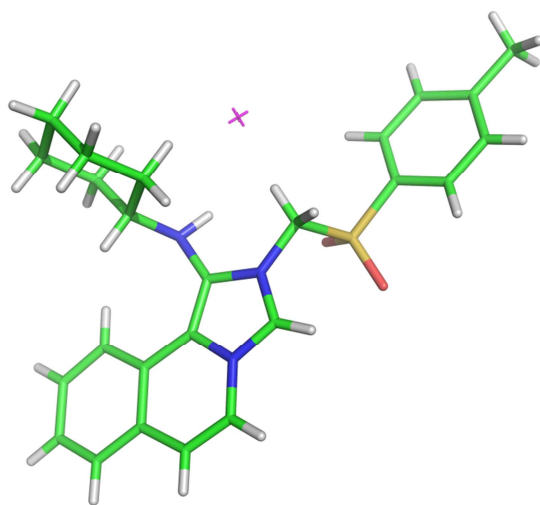
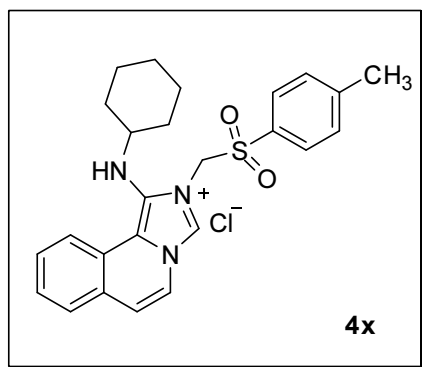
2,2'-bis(2,6-dimethylphenyl)-1,1'-bis((2,6-dimethylphenyl)amino)-[6,6'-biimidazo[5,1-*a*]isoquinoline]-2,2'-dium chloride (4q) (CCDC 1457880)



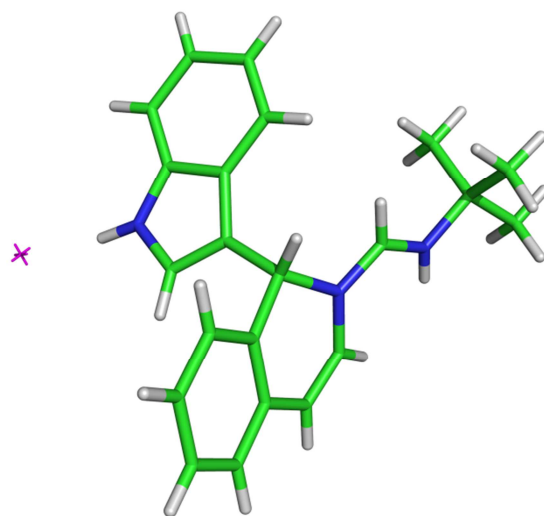
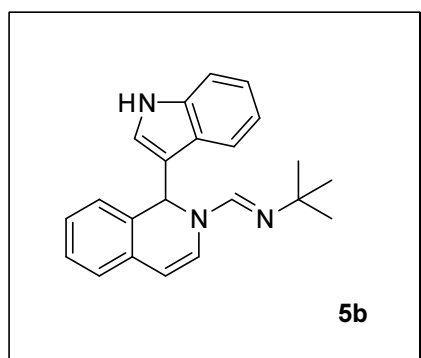
2-cyclohexyl-1-(cyclohexylamino)imidazo[5,1-a]phthalazin-2-ium chloride-PdCl₂ complex with CH₃CN (CCDC 1457879)



1-(cyclohexylamino)-2-(tosylmethyl)imidazo[5,1-a]isoquinolin-2-ium chloride (4x)
CCDC 1457877



**(E)-1-(1-(1*H*-indol-3yl)isoquinolin-2-(1*H*)-yl)-*N*-(*tert*-butyl)methanimine (5b)
(Hydrochloride) CCDC 1457878**



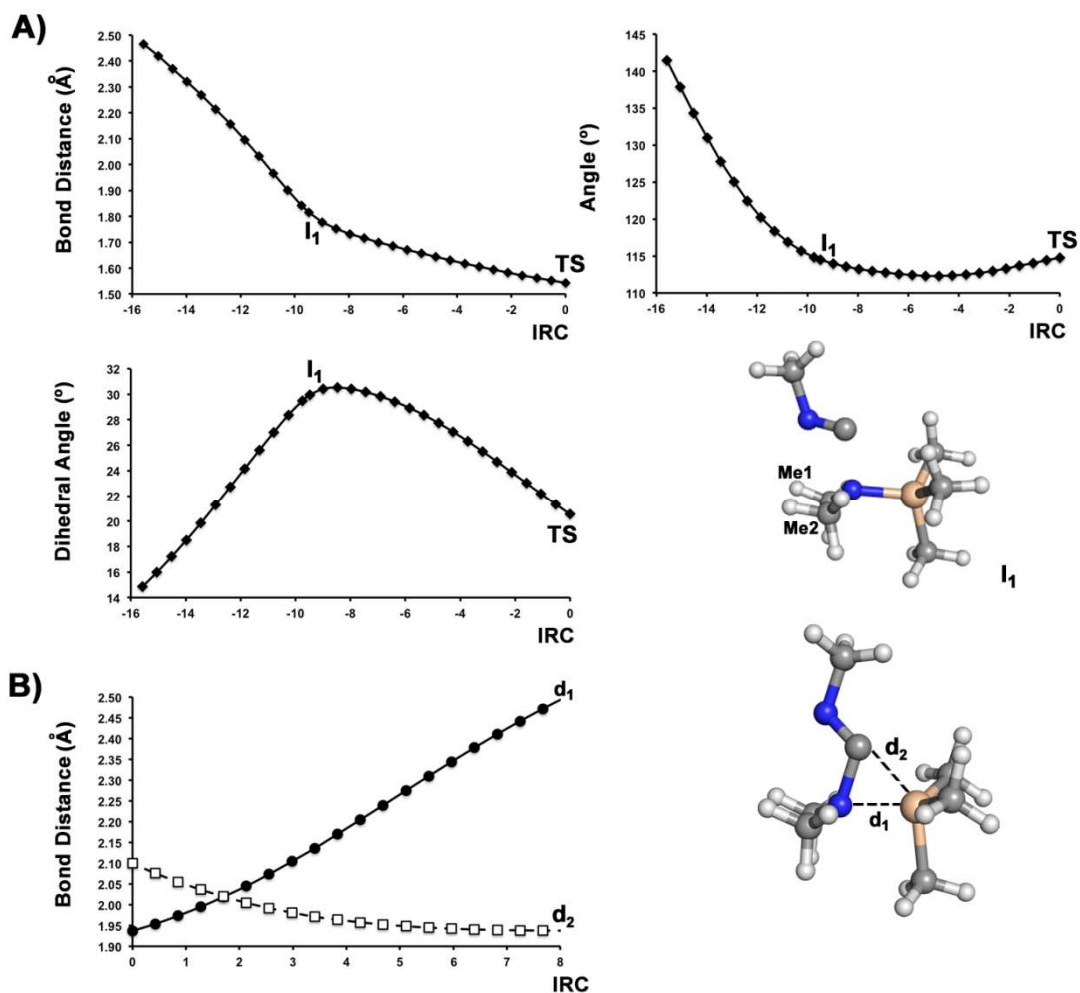
Theoretical methods

The reaction channels leading to the insertion of isocyanide into the N-Si bond were examined by combining MP2^[5,6] calculations and the 6-311+G(d,p)^[7-10] basis set. The geometries were fully optimized and the nature of the stationary points was verified from inspection of the vibrational frequencies using the harmonic oscillator-rigid rotor model. The intrinsic reaction coordinate (IRC) was calculated at the same level of theory to search for the reactants and products related to a given transition state. To further confirm the relative stability of the stationary points along the reaction channels, single-point calculations were also performed at the B2PLYPD3/6-311+G(d,p)^[11] level. This DFT functional, which includes the spin-component scaled MP2 (SCS-MP2)^[12] contribution and Grimme's D3 dispersion term,^[13] has proved to be valuable for the study of reactive processes.^[14] The relative stabilities of the stationary points were obtained by adding the thermal and entropic corrections (determined at 1 atm and 298 K) to the energy differences determined at the MP2 and B2PLYPD3 levels. To this end, the free energy corrections were calculated using Truhlar's quasiharmonic approximation,^[15,16] where real harmonic vibrational frequencies lower than 100 cm⁻¹ were raised to 100 cm⁻¹, as has been utilized in other chemical reactivity studies.^[17,18] Finally, since the reaction leading to compound **6b** was completed in toluene, the effect of solvation was taken into account using the SMD version^[19] of the IEF-PCM^[20] continuum solvation method. SMD calculations were performed at the B3LYP/6-311+G(d,p)^[21] level, which was one of the six electronic structure methods used in the optimization of the SMD method. Accordingly, the free energy in solution was estimated by adding the solvation free energy to the relative stabilities in the gas phase. Finally, Natural Bond Orbital analysis was conducted to examine the changes. All DFT computations were carried out using the keyword Integral(Grid=Ultrafine) as implemented in Gaussian09,^[22] which was used to carry out these calculations.

Mechanism of isocyanide insertion

The reactive channel can be divided into two major events: i) the attack of the DMA-TMS amine nitrogen to the methyl isocyanide, and ii) the formation of the (isocyanide) C-Si (DMA-TMS) bond, and the concomitant breaking of the Si-N bond in DMA-TMS (Figure 3 in the manuscript; see also Figure S7).

Figure S7. Reactive pathway along the intrinsic reaction coordinate (IRC) for the insertion of methyl isocyanide into DMA-TMS. (A) Conversion of the pre-reactant complex (Pre-R) to the transition state (TS) occurs through a metastable intermediate (I1) that orients the isocyanide carbon towards Si, allowing the insertion between the amine N and Si atoms. Change in the distance between isocyanide C and amine N atoms, the CNC angle of methyl isocyanide, and the pyramidalization of the amine N (measured relative to the plane formed by Si, and C atoms from methyl groups, Me1 and Me2). (B) Change in distances from the Si atom to the amine N and the isocyanide C.



The transition from the pre-reactant (**Pre-R**) complex to the intermediate **I1** involves the increased pyramidalization of the amine nitrogen and the progressive loss of the *sp* hybridization of the isocyanide, leading to the attack of the amine nitrogen to the isocyanide and the formation of intermediate **I1** (Figure S2). This process is associated to the loss of linearity of methyl isocyanide, as the CNC angle is 114 degrees, and the lengthening of the N–C bond (from 1.18 Å in Pre-R to 1.26 Å in I1). It is also worth noting the lengthening of the N–Si bond (from 1.76 Å in Pre-R to 1.83 Å in I1). These structural changes are the major contribution to the reaction barrier, as they involve an

energy destabilization close to 25 kcal/mol (Table S1). The presence of a large barrier is not unexpected, as the chemical reaction between *c*-hexyl isocyanide and N-trimethylsilyl pyrrolidine to afford adduct **6b** (Scheme 2 in the manuscript) was performed in toluene at 110 °C.

Table S1. Relative energies and free energies in gas phase and solution (toluene) of the stationary points along the reaction channel leading to the insertion of isocyanide into DMA-TMS (Figure 3 in the manuscript). All values (kcal mol⁻¹) are given relative to the pre-reactant complex (Pre-R in Figure 3).

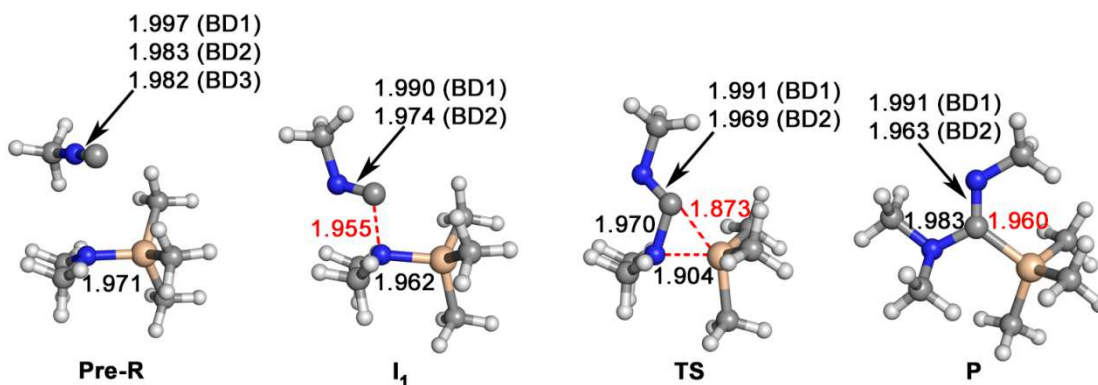
Method	Property	I1	TS	P
MP2				
Gas	E _{rel}	25.5	30.0	-3.5
	G _{rel}	28.0	32.9	0.9
Solution	G _{rel}	25.3	31.6	0.2
B2PLYPD3				
Gas	E _{rel}	25.8	31.4	-3.8
	G _{rel}	28.4	34.3	0.6
Solution	G _{rel}	25.6	33.0	-0.1

Formation of the intermediate **I1** is coupled to a net transfer of 0.33 e from DMA-TMS to methyl isocyanide. This is reflected in the loss of negative charge in the amine nitrogen (by 0.13 e) and Si (by 0.05 e) atoms of DMA-TMS, and the increase in negative charge by the isocyanide C (-0.13 e) and N (-0.11 e) atoms (Table S2). This reflects a large change in the electron density distribution, which encompasses the formation of a lone pair in the isocyanide nitrogen (occupancy of 1.889 e), and a bond between the amine nitrogen and the isocyanide carbon (occupancy of 1.955 e; distance of 1.78 Å; Figure S8). This bond is highly polarized toward the nitrogen atom, as it originates from the overlap between an *sp* hybrid on the nitrogen atom (80.8%) and an *sp* hybrid on the carbon atom (19.2%).

Table S2. Natural atomic charge found over the Si and N atoms in DMA-TMS, and over C and N atoms of isocyanide for the systems represented in Figure 3 of the manuscript.

Species	DMA-TMS		isocyanide	
	Si	N	C	N
Pre-RC	1.85	-0.98	0.28	-0.56
I1	1.90	-0.85	0.15	-0.67
TS	1.78	-0.74	0.09	-0.56
P	1.60	-0.57	0.11	-0.55

Figure S8. Representation of the four states shown in Figure 3 (in the manuscript) together with the occupancy of Natural Bond Orbitals (NBO) for selected bonds along the insertion mechanism (BD denotes the occupancy of the bond orbital).



The changes in both the geometrical parameters and the electron density distribution of methyl isocyanide are needed for the formation of the transition state (**TS**), which is destabilized by only 5 kcal/mol (Table S1).

In the **TS** the isocyanide C is located at 1.54 Å from the amine N, thus revealing the stabilization of this bond, as also noted in the enlarged occupancy (1.970 e; Figure S3) and the reduced polarization of the bond (the contributions of N and C atoms amount to 70.9% and 29.1%, respectively). Remarkably, the lone pair of the isocyanide C has the appropriate arrangement for the attack to the Si atom (distance of 2.10 Å), as noted in the existence of a natural bond (occupancy of 1.873 e; Figure S3) between these atoms, but highly polarized toward the isocyanide C (contributions of 11.5% and 88.5% from the Si and C atoms, respectively). It is also worth noting the weakening of the amine N–Si bond (distance of 1.94 Å), which is enlarged by 0.11 Å relative to the intermediate **I1**, and the occupancy of the natural bond is reduced to 1.904 (Figure S3), while it is also polarized toward the N atom (contributions of 9.9% and 90.1% from the Si and N atoms, respectively).

Overall, the results suggest that the insertion of the isocyanide in DMA-TMS and the subsequent formation of adduct **6b** is primarily conditioned by the nucleophilic attack of the amine N to the isocyanide, which affords the proper configuration for the attack of the isocyanide C to the Si atom.

Biological assays

***T. brucei* culturing and evaluation of trypanocidal activity**

Bloodstream form *T. brucei* (strain 221) were cultured at 37 °C in modified Iscove's medium [23]. Trypanocidal activity was assessed by growing parasites in the presence of various concentrations of the novel compounds and determining the levels which inhibited growth by 50% (IC50) and 90% (IC90). *T. brucei* in the logarithmic phase of growth were diluted back to $2.5 \times 10^4 \text{ mL}^{-1}$ and aliquoted into 96-well plates. The compounds were then added at a range of concentrations and the plates incubated at 37 °C. Each drug concentration was tested in triplicate. Resazurin was added after 48 h and the plates incubated for a further 16 h and the plates then read in a Spectramax plate reader. Results were analysed using GraphPad Prism.

***T. cruzi* culturing and evaluation of trypanocidal activity**

T. cruzi epimastigotes (CL Brener stain) were cultured at 28 °C as described previously [24]. Activity was determined by growing parasites in 96-well plates. Briefly, cultures were diluted to $2.5 \times 10^5 \text{ mL}^{-1}$, aliquoted into wells in triplicate at a range of drug concentrations, and allowed to grow for 4 days. Resazurin was added and the plates incubated for a further 3 days, then read in a Spectramax plate reader as outlined above.

Cytotoxic activity against rat skeletal myoblast L6 cells

Cytotoxicity against mammalian cells was assessed using microtitre plates following a described procedure [25]. Briefly, rat skeletal muscle L6 cells were seeded at $1 \times 10^4 \text{ mL}^{-1}$ in 200 μL of growth medium containing different compound concentrations. The plates were incubated for 6 days at 37 °C and 20 μL resazurin was then added to each well. After a further 8 h incubation, the fluorescence was determined using a Spectramax plate reader.

Table S3: Compounds **4** vs bloodstream form *Trypanosoma brucei*

Compd	EC₅₀ <i>T. brucei</i> (μM)	EC₉₀ <i>T. brucei</i> (μM)	EC₅₀ L cells (μM)	S.I.
4a	0.55 \pm 0.16	0.81 \pm 0.22	10.2 \pm 0.3	18
4b	0.50 \pm 0.02	0.73 \pm 0.02	66.2 \pm 5.8	132
4c	0.93 \pm 0.01	1.19 \pm 0.01	12.5 \pm 0.6	13
4d	>25	>25	nd	-
4f	0.20 \pm 0.01	0.23 \pm 0.01	15.5 \pm 2.2	78
4g	3.43 \pm 0.61	5.83 \pm 1.76	12.2 \pm 0.6	3.6
4h	2.15 \pm 0.06	3.11 \pm 0.05	99.1 \pm 5.8	46
4i	12.1 \pm 2.1	16.4 \pm 0.6	13.6 \pm 1.9	1.1
4j	2.60 \pm 0.07	3.11 \pm 0.03	17.7 \pm 1.9	6.8
4k	5.79 \pm 0.58	8.32 \pm 0.26	6.87 \pm 0.80	1.2
4l	4.07 \pm 0.20	6.33 \pm 1.60	31.2 \pm 1.6	7.7
4m	>20	>20	nd	-
4n	1.78 \pm 0.15	2.30 \pm 0.15	10.7 \pm 0.2	6.0
4o	0.52 \pm 0.04	0.74 \pm 0.07	36.5 \pm 4.1	70
4p	0.083 \pm 0.002	0.104 \pm 0.002	<2.0	-
4r	0.97 \pm 0.01	1.23 \pm 0.01	6.97 \pm 0.62	7.2
4s	0.71 \pm 0.10	1.19 \pm 0.03	39.8 \pm 0.5	56
4t	17.3 \pm 0.7	22.1 \pm 0.3	83.5 \pm 3.9	4.8
4u	0.59 \pm 0.01	0.74 \pm 0.01	9.42 \pm 0.55	16
4x	1.20 \pm 0.06	1.52 \pm 0.02	10.1 \pm 0.4	8.4
4y	9.95 \pm 0.08	12.6 \pm 0.1	>110	>11

S.I.: Selectivity Index

Table S4: Compounds **4** vs *Trypanosoma cruzi* epimastigotes

Compd	EC₅₀ <i>T. cruzi</i> (μM)	EC₉₀ <i>T. cruzi</i> (μM)	EC₅₀ L cells (μM)	S.I.
4a	1.02 \pm 0.03	1.43 \pm 0.18	10.2 \pm 0.3	10
4b	1.53 \pm 0.11	2.66 \pm 0.18	66.2 \pm 5.8	43
4c	1.20 \pm 0.03	2.80 \pm 0.06	12.5 \pm 0.6	10
4d	>25	>25	nd	-
4f	4.02 \pm 0.23	11.2 \pm 0.5	15.5 \pm 2.2	3.9
4g	>20	>20	12.2 \pm 0.6	-
4h	19.7 \pm 0.7	34.9 \pm 3.9	99.1 \pm 5.8	5.0
4i	20.1 \pm 0.6	45.4 \pm 3.3	13.6 \pm 1.9	<1.0
4j	4.04 \pm 0.71	7.99 \pm 0.11	17.7 \pm 1.9	4.4
4k	12.7 \pm 1.2	24.0 \pm 2.6	6.87 \pm 0.80	<1.0
4l	25.1 \pm 2.5	44.1 \pm 4.1	31.2 \pm 1.6	1.2
4m	>20	>20	nd	-
4n	>25	>25	10.7 \pm 0.2	<1.0
4o	17.1 \pm 0.7	37.4 \pm 1.1	36.5 \pm 4.1	2.1
4p	1.90 \pm 0.37	3.26 \pm 0.71	<2.0	<1.0
4q	>12	>12	nd	-
4r	4.86 \pm 0.16	9.96 \pm 0.99	6.97 \pm 0.62	1.4
4s	1.14 \pm 0.13	2.03 \pm 0.16	39.8 \pm 0.5	35
4t	>20	>20	83.5 \pm 3.9	-
4u	>15	>15	9.42 \pm 0.55	-
4x	8.16 \pm 0.81	17.0 \pm 4.8	10.1 \pm 0.4	1.2
4y	>20	>20	>110	-

S.I.: Selectivity Index

Determination of brain permeability: PAMPA-BBB assay

The in vitro permeability (P_e) of the novel compounds and fourteen commercial drugs through lipid extract of porcine brain membrane was determined by using a parallel artificial membrane permeation assay [26]. Commercial drugs and the target compounds were tested using a mixture of PBS:EtOH 70:30. Assay validation was made by comparing the experimental permeability with the reported values of the commercial drugs by bibliography and lineal correlation between experimental and reported permeability of the fourteen commercial drugs using the parallel artificial membrane permeation assay was evaluated ($y=1,6374x-1,3839$; $R^2=0,9203$). From this equation and the limits established by Di et al. for BBB permeation, three ranges of permeability were established: compounds of high BBB permeation (CNS+): $P_e (10^{-6} \text{ cm s}^{-1}) > 5.16$; compounds of low BBB permeation (CNS-): $P_e (10^{-6} \text{ cm s}^{-1}) < 1.89$; and compounds of uncertain BBB permeation (CNS±): $5.16 > P_e (10^{-6} \text{ cm s}^{-1}) > 1.89$.

Table **S5** shows permeability results from the different commercial and assayed compounds (three different experiments in triplicate) and predictive penetration in the CNS. The tested compounds show different permeability to cross the barrier and to reach the central nervous system.

Table S5. Permeability (Pe 10^{-6} cm s^{-1}) in the PAMPA-BBB assay of 14 commercial drugs and tested compounds and predictive penetration in the CNS

Compound	Bibliography value^(a)	Experimental value (n=3) \pm S.D.	CNS Prediction
Verapamil	16,0	25,9 \pm 0,4	
Testosterone	17,0	23,9 \pm 0,3	
Costicosterone	5,1	6,7 \pm 0,1	
Clonidine	5,3	6,5 \pm 0,05	
Ofloxacin	0,8	0,97 \pm 0,06	
Lomefloxacin	0,0	0,8 \pm 0,06	
Progesterone	9,3	16,8 \pm 0,0,3	
Promazine	8,8	13,8 \pm 0,3	
Imipramine	13,0	12,3 \pm 0,1	
Hidrocortisone	1,9	1,4 \pm 0,05	
Piroxicam	2,5	1,7 \pm 0,03	
Desipramine	12,0	17,8 \pm 0,1	
Cimetidine	0,0	0,7 \pm 0,03	
Norfloxacin	0,1	0,9 \pm 0,02	
4a		2,7 \pm 0,1	CNS+/-
4b		5,25 \pm 0,4	CNS+/-
4c		5,4 \pm 0,5	CNS+/-
4d		3,5 \pm 0,2	CNS+/-
4e		3,9 \pm 0,04	CNS-
4f		18,4 \pm 1,4	CNS+
4g		4,2 \pm 0,45	CNS+/-
4i		11,4 \pm 1,5	CNS+
4j		11,5 \pm 1,3	CNS+
4k		4,6 \pm 0,3	CNS+/-
4l		4,4 \pm 0,5	CNS+/-
4m		12,5 \pm 0,9	CNS+
4n		2,7 \pm 0,2	CNS+/-
4q		3,2 \pm 0,2	CNS+/-
4r		7,6 \pm 0,9	CNS+
4s		10,8 \pm 1,0	CNS+
4t		9,6 \pm 0,7	CNS+
4u		16,2 \pm 1,2	CNS+
4v		7,6 \pm 0,5	CNS+
4w		10,5 \pm 0,5	CNS+
4x		>30 \pm 1.0	CNS+
4y		3,5 \pm 0,4	CNS-

a) Taken from Di et al. ^[26].

Calculated molecular properties and CNS MPO desirability scores of the novel isoquinolinium salts and related compounds

Table S6 Molecular properties (Log P, topological polar surface area (TPSA), molecular weight (MW), number of hydrogen bond acceptors (nON), number of hydrogen bond donors (nOHNH), number of rotatable bonds (nrotb), molecular volume (of the cation) , and number of violations of Lipinski's rules (n violations)) calculated using Molinspiration (<http://molinspiration.com>).

compd	miLogP	TPSA	nON	nOHNH	nrotb	nviolations	vol	MW
4a	2.56	20.33	3	3	3	0	348.86	348.51
4b	1.12	20.33	3	1	3	0	301.25	296.44
4c	1.63	20.33	3	1	5	0	345.29	364.47
4d	-0.78	72.94	7	1	9	0	325.14	356.40
4e	-1.19	91.41	9	1	13	0	428.56	484.45
4f	4.18	20.33	3	1	3	0	377.93	392.53
4g	4.90	20.33	3	1	3	0	399.67	436.54
4h	2.69	38.80	5	1	5	0	362.78	396.47
4i	2.08	57.63	5	2	4	0	375.86	392.52
4j	3.29	20.33	3	1	3	0	366.71	427.41
4k	3.32	20.33	3	1	3	0	366.75	427.41
4l	2.34	46.63	5	1	5	0	393.39	406.55
4m	1.32	49.87	6	1	4	0	445.98	461.63
4n	3.91	40.55	4	2	3	0	385.95	408.52
4o	6.61	20.33	3	1	4	2	462.88	503.07
4p	4.34	29.56	4	1	5	0	445.82	454.64
4q	8.07	40.65	6	2	7	2	743.23	783.04
4r	2.45	20.33	3	1	3	0	348.86	348.51
4s	2.02	33.22	4	1	3	0	344.71	349.50
4t	2.16	51.69	6	1	5	0	358.62	397.46
4u	2.31	40.65	6	2	6	1	569.69	568.85
4x	1.58	54.47	5	1	5	0	395.07	434.58
4y	0.67	55.87	6	1	0	7	371.91	402.45

Table S7. CNS MPO scores calculated using the algorithm reported in ref. [27]. TPSA values, MW, and the number of hydrogen bond donors (nOHNH), used in the algorithm, are shown also in Table S6.

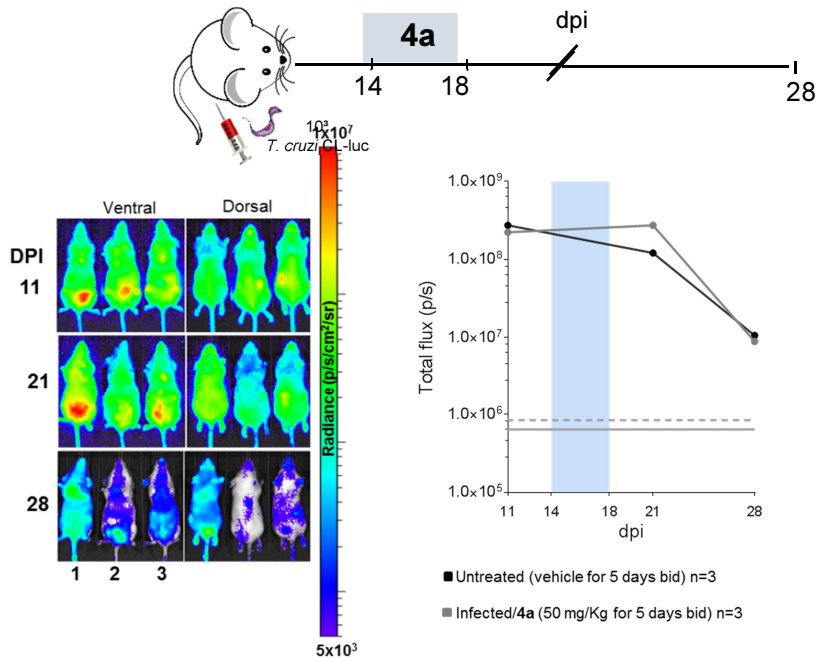
compd	ClogP	clogD	TPSA	MW	HBD	pKa	CNS MPO
4a	2.56	1.01	20.33	348.51	1	-3.16	4.8
4b	1.12	-0.48	20.33	296.44	1	-3.37	4.8
4c	1.63	0.89	20.33	364.47	1	2.60	4.8
4d	-0.78	-2.62	72.94	356.40	1	-5.46	5.8
4e	-1.19	-1.16	91.41	484.45	1	-6.81	4.9
4f	4.18	4.89	20.33	392.53	1	-5.11	3.0
4g	4.9	5.57	20.33	436.54	1	-5.79	2.4
4h	2.69	2.54	38.80	396.47	1	-3.77	5.2
4i	2.08	0.44	57.63	392.52	2	-3.54	5.3
4j	3.29	1.78	20.33	427.41	1	-3.22	4.2
4k	3.32	1.78	20.33	427.41	1	-3.18	4.2
4l	2.34	1.02	46.63	406.55	1	-3.55	5.5
4m	1.32	0.09	49.87	461.63	1	-3.42	5.1
4n	3.91	4.82	40.55	408.52	2	-4.95	3.7
4o	6.61	7.14	20.33	503.07	1	-5.11	1.8
4p	4.34	2.5	29.56	454.64	1	-3.09	3.7
4q	8.07	9.46	40.65	783.04	2	-5.14	2.5
4r	2.45	1.04	20.33	348.51	1	-1.75	4.8
4s	2.02	0.91	33.22	349.50	1	-4.25	5.5
4t	2.16	1.95	51.69	397.46	1	-3.81	5.6
4u	2.31	-0.88	40.65	568.85	2	-5.96	4.5
4x	1.58	0.48	54.47	434.58	1	-3.39	5.3
4y	0.67	-0.15	55.87	402.45	1	-3.33	5.5

In vivo Assays

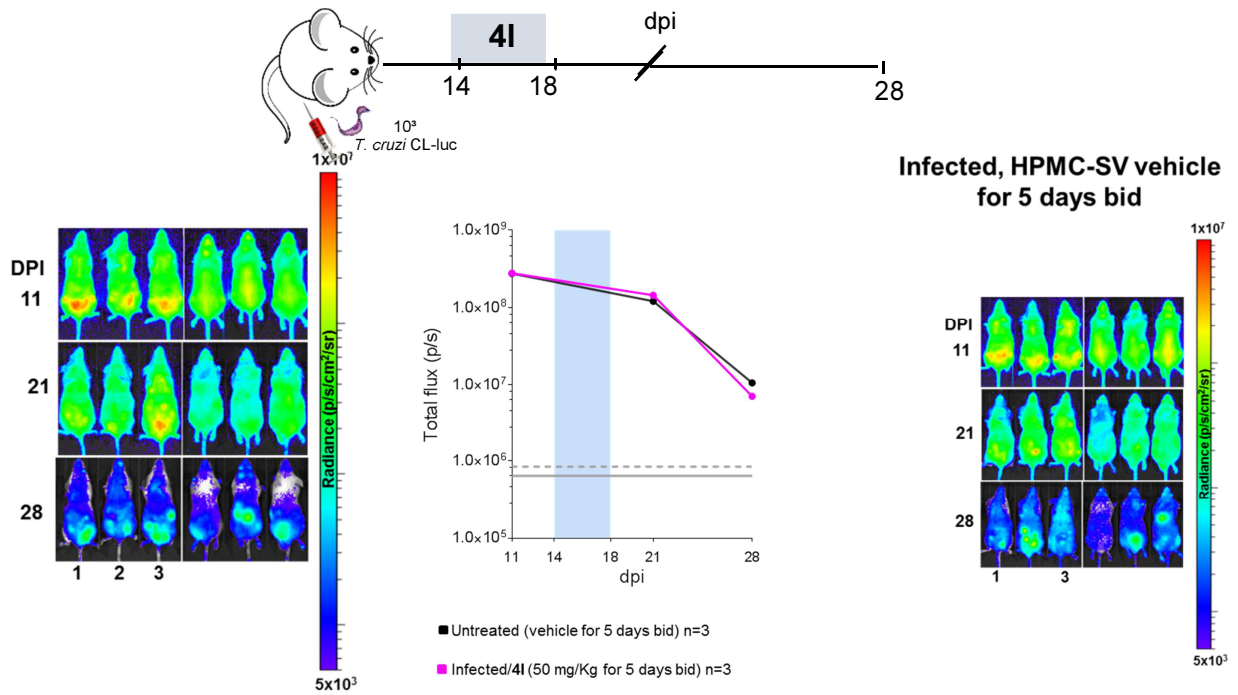
All animal experiments were carried out under UK Home Office licence PPL70/8207. Female BALB/c mice were obtained from Charles River (UK). They were maintained under specific pathogen-free conditions in individually ventilated cages, with a 12 hour light/dark cycle and access to food and water *ad libitum*. Mice aged 8–12 weeks were infected by i.p. injection with 1×10^3 bloodstream trypomastigotes of bioluminescent *T. cruzi* strain CL Brener^[28].

Mice were treated twice daily with test compounds at 50 mg/kg for 5 days, by the oral route, at the peak of the acute stage (days 14-18). Vehicle only (HPMC-SV - aqueous vehicle containing 0.5% (w/v) hydroxypropyl methylcellulose 0.5% (v/v) benzyl alcohol and 0.4% (v/v) Tween 80) was administered to non-treated control mice. For imaging, mice were injected i.p. with 150 mg kg⁻¹ d-luciferin in Dulbecco's Ca²⁺/Mg²⁺ free PBS, then anaesthetized using 2.5% (v/v) gaseous isoflurane in oxygen. Both dorsal and ventral images were obtained by placing mice in an IVIS Lumina II system (Caliper Life Science) 10–20 minutes after d-luciferin administration, using LivingImage 4.3 software. Exposure times varied from 30 seconds to 5 minutes, depending on signal intensity, with anaesthesia maintained throughout via individual nose-cones. Following the peak of the acute stage (day 14), bioluminescence falls with time as the immune system begins to control the infection. By day 60 it will reach a dynamic equilibrium as the disease transits to the chronic stage.

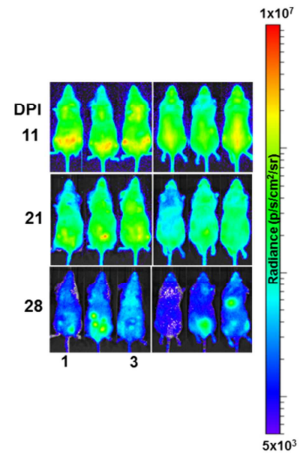
Compound 4a at 50 mg/kg for 5 days bid



Compound 4l at 50 mg/kg for 5 days bid



Infected, HPMC-SV vehicle for 5 days bid



References

- [1] O'Brien, C. J., Kantchev, E. A. B., Valente, C., Hadei, N., Chass, G. A., Lough, A., Hopkinson, A. C. and Organ, M. G. *Chem. Eur. J.*, **2006**, *12*, 4743–4748.
- [2] Xu, L., Chen, W., & Xiao, J. *Organometallics*, **2000**, *19*, 1123-1127.
- [3] A. M. R. Smith, H. S. Rzepa, A. J. P. White, D. Billen, K. K. Hii. *J. Org. Chem.*, **2010**, *75*, 3085–3096.
- [4] F. Chen, Z. Ding, J. Qin, T. Wang, Y. He, Q-H. Fan, *Org. Lett.* **2011**, *13*, 4348-4351.
- [5] C. Møller, M. S. Plesset, *Phys. Rev.* **1934**, *46*, 618-622.
- [6] M. Head-Gordon, J. A. Pople, M. J. Frisch, *Chem. Phys. Lett.* **1988**, *153*, 503-506.
- [7] K. Raghavachari, J. S. Binkley, R. Seeger, J. A. Pople, *J. Chem. Phys.* **1980**, *72*, 650-654.
- [8] A. D. McLean, G. S. Chandler, *J. Chem. Phys.* **1980**, *72*, 5639-5648.
- [9] T. Clark, J. Chandrasekhar, G. W. Spitznagel, P. v. R. Schleyer, *J. Comp. Chem.* **1983**, *4*, 294-301.
- [10] K. Fukui, *Acc. Chem. Res.* **1981**, *14*, 363-368.
- [11] (a) S. Grimme, *J. Chem. Phys.* **2006**, *124*, 034108. (b) S. Grimme, S. Ehrlich, L. Goerigk, *J. Comp. Chem.* **2011**, *32*, 1456-1465.
- [12] S. Grimme, *J. Chem. Phys.* **2003**, *118*, 9095–9102.
- [13] L. Goerigk, S. Grimme, *J. Chem. Theory Comput.* **2011**, *7*, 291-309.
- [14] S. Grimme, L. Goerigk, R. F. Fink. *WIREs Comput. Mol. Sci.* **2012**, *2*, 886-906.
- [15] Y. Zhao, D. G. Truhlar. *Phys. Chem. Chem. Phys.* **2008**, *10*, 2813-2818.
- [16] R. F. Ribeiro, A. V. Marenich, C. J. Cramer, D. G. Truhlar. *J. Phys. Chem. B* **2011**, *115*, 14556-14562.
- [17] A. H. Asari, Y.-H. Lam, M. A. Tius, K. N. Houk. *J. Am. Chem. Soc.* **2015**, *137*, 13191-13199.
- [18] N. Gulzar, K. M. Jones, H. Konnerth, M. Breugst, M. Klussmann. *Chem. Eur J.* **2015**, *21*, 3367-3376.
- [19] A. V. Marenich, C. J. Cramer, D. G. Truhlar, *J. Phys. Chem. B* **2009**, *113*, 6378-6396.
- [20] E. Cancès, B. Mennucci, J. Tomasi, *J. Chem. Phys.* **1997**, *107*, 3032-3041.
- [21] (a) A. D. Becke, *Phys. Rev. A* **1988**, *38*, 3098-3100. (b) C. Lee, W. Yang, R. G. Parr, *Phys. Rev. B* **1988**, *37*, 785-789. (c) P. J. Stephens, F. J. Devlin, C. F. Chabalowski, M. J. Frisch, *J. Phys. Chem.* **1994**, *98*, 11623-11627.

- [22] Gaussian 09, Revision **D.01**, M. J. Frisch, G. W. Trucks, H. B. Schlegel, G. E. Scuseria, M. A. Robb, J. R. Cheeseman, G. Scalmani, V. Barone, B. Mennucci, G. A. Petersson, H. Nakatsuji, M. Caricato, X. Li, H. P. Hratchian, A. F. Izmaylov, J. Bloino, G. Zheng, J. L. Sonnenberg, M. Hada, M. Ehara, K. Toyota, R. Fukuda, J. Hasegawa, M. Ishida, T. Nakajima, Y. Honda, O. Kitao, H. Nakai, T. Vreven, J. A. Montgomery, Jr., J. E. Peralta, F. Ogliaro, M. Bearpark, J. J. Heyd, E. Brothers, K. N. Kudin, V. N. Staroverov, R. Kobayashi, J. Normand, K. Raghavachari, A. Rendell, J. C. Burant, S. S. Iyengar, J. Tomasi, M. Cossi, N. Rega, J. M. Millam, M. Klene, J. E. Knox, J. B. Cross, V. Bakken, C. Adamo, J. Jaramillo, R. Gomperts, R. E. Stratmann, O. Yazyev, A. J. Austin, R. Cammi, C. Pomelli, J. W. Ochterski, R. L. Martin, K. Morokuma, V. G. Zakrzewski, G. A. Voth, P. Salvador, J. J. Dannenberg, S. Dapprich, A. D. Daniels, Ö. Farkas, J. B. Foresman, J. V. Ortiz, J. Cioslowski, and D. J. Fox, Gaussian, Inc., Wallingford CT, 2009.
- [23] S.R. Wilkinson, S.R. Prathalingam, M.C. Taylor, A. Ahmed, D. Horn, J.M. Kelly, *Free Radical Biol. Med.* 2006, *40*, 98–209.
- [24] G. Kendall, A.F. Wilderspin, F. Ashall, F., M.A. Miles, J. M. Kelly, *EMBO J.* **1990**, *9*, 2751-2758.
- [25] C. Bot, B.S. Hall, N. Bashir, M.C. Taylor, N.A. Helsby, S.R. Wilkinson, *Antimicrob. Agents Chemother.* **2010**, *54*, 4246–4252.
- [26] L. Di, E.H. Kerns, K. Fan, O.J. McConnell, G.T. Carter, *Eur. J. Med. Chem.* **2003**, *38*, 223–232.
- [27] T.T. Wager, X. Hou, P.R. Verhoest, A. Villalobos, *ACS Chem. Neurosci.* **2010**, *1* 435-449.
- [28] M.D. Lewis, A. Fortes Francisco, M.C. Taylor, J.M. Kelly. *J. Biomolecular Screening* **2015**, *20*, 36-43.

Chapter IV

Publication IV: Multiple Multicomponent
Reaction Platform for the Selective Access
to N-PolyHeterocyclic Chemotypes with
Relevant Applications in Biology,
Medicine and Materials Science

Multiple Multicomponent Reaction Platform for the Selective Synthesis of a Family of N-PolyHeterocyclic Chemotypes with Relevant Applications in Biology, Medicine and Materials.

Ouldouz Ghashghaei,¹ Samantha Caputo,² Miquel Sintès,¹ Marc, Revés,¹ Nicola Kielland,¹ Rodolfo Lavilla,^{1,3} Carolina Estarellas,⁴ F. Javier Luque,⁴ Anna Aviñó,⁵ Ramón Eritja,^{3,5} Marc Vendrell,⁶ Ryan Treadwell,⁶ Fabio de Moliner,⁶ Javier Sánchez-Céspedes^{7,8}, Ana Serna-Gallego⁷, José Antonio Marrugal-Lorenzo⁷, Jerónimo Pachón^{7,8}, Joan Mendoza⁹

1 Laboratory of Organic Chemistry, Faculty of Pharmacy, University of Barcelona, Barcelona Science Park, Baldiri Reixac 10-12, Barcelona 08028, Spain.

2 Department of Chemistry and Industrial Chemistry, University of Genova, via Dodecaneso 31, 16146 Genova, Italy

3 CIBER-BBN, Networking Centre for Bioengineering, Biomaterials and Nanomedicine, Baldiri Reixac 10-12, Barcelona 08028, Spain.

Correspondence should be addressed to R.L. (email: rlavilla@ub.edu)

4 Departament de Nutrició, Ciència dels Aliments i Gastronomia. Facultat de Farmàcia, and IBUB, Universitat de Barcelona. Prat de la Riba 171, 08921, Santa Coloma de Gramenet (Spain)

5 Dpt. Chemical & Biomolecular Nanotechnology, Institute for Advanced Chemistry of Catalonia (IQAC), CSIC, Jordi Girona 18-26, 08034-Barcelona, Spain.

6 MRC/UoE Centre for Inflammation Research, The University of Edinburgh, 47 Little France Crescent, Edinburgh EH16 4TJ (UK)

7 Clinical Unit of Infectious Diseases, Microbiology and Preventive Medicine, Institute of Biomedicine of Seville (IBiS), University Hospital Virgen del Rocío/CSIC/University of Seville.

8 Department of Medicine, University of Seville, Seville, Spain.

9. Scientific and Technological Centres, Universitat de Barcelona, C/ Lluís Solé i Sabaris, 1-3, 08028 Barcelona (Spain)

Abstract

A range of commercially available alpha di(tri)amino di(tri)azines has been subjected to acid-catalyzed interaction with a wide scope of aldehydes and isocyanides to yield the corresponding 5-7 multicomponent adducts. These multiple Groebke-Bieanymé-Blackburn processes are amenable to direct polycondensation protocols or sequential processes with two different aldehyde/isocyanide pairs to selectively afford non-symmetrical adducts. The obtained products can be engaged with post-synthetic transformations (Ugi, Suzuki, Buchwald, amidation etc.) to yield a variety of compact scaffolds in a straightforward manner. The mechanism explaining the selectivity has been unravelled using computational methods. The resulted adducts have been subject to different assays to prove their wide potential as bioactive molecules. Notably, some of the adducts showed tuneable fluorescence emission covering a broad range of the visible spectrum. Also, some adducts were transformed into novel BODIPY-type derivatives with excellent photophysical properties and bioimaging capabilities as fluorophores for live cell imaging. Also, a variety of multicomponent adducts demonstrate structure-dependent affinity for a variety of DNA structural types and show potent antiviral activity against adenoviruses, at low micromolar concentration and with low cytotoxicity. Finally, conveniently substituted, or modified melamine derivatives have been developed to nanometric dimensions.

Introduction

“Production of properties” is the most fundamental objective of organic synthesis. ^[1] Efficient synthetic pathways have been developed to feed society’s growing need for functional chemotypes in various sectors i.e. health, industry, energy, etc. However, they habitually consist of complex multi-step procedures. ^[2] Discovery of new reactions and advances in catalysis, often lead to shorter synthetic routes. ^[3] The so-called Function Oriented Synthesis (FOS), focuses on the simpler yet better analogues of the useful structurally complex compounds. ^[4]

In this respect, multicomponent reactions (MCRs), processes in which three or more reactants interact to yield an adduct, have been fundamental in the development of modern synthetic methods. ^[5] MCRs offer diversity through rapid access to a library of compounds with a common core structure (Figure 1A). Therefore, they are among the strategies of choice in Diversity Oriented Synthesis (DOS) ^[6] as well as combinatorial chemistry. ^[7]

A step beyond in this direction is the concept of Multiple MCRs, which further increases the synthetic efficiency and diversity of the MCR concept (Figure 1A). In these processes, bi(poly)functional components undergo a productive sequence of MCRs to assemble highly complex scaffolds in a straightforward manner. ^[8] This approach has been successfully used in the synthesis of a variety of complex functional compounds including peptides, hydrogels, supramolecular structures, and natural products derivatives. ^[9] In a recent example, Wessjohan et al. used the strategy for one-pot assembly of hybrid macromulticyclic cages ^[10] (Figure 1B).

Furthermore, heterocycles constitute the most frequent motif found in drugs and bioactive compounds, hence a primary target for synthesis and modification. Consequently, they are privileged reactants to be included in MCRs and the field is receiving considerable attention.

^[11]

Isocyanides are one of the key functional groups in MCRs, and the most fruitful MCR processes are based on their reactivity; the Ugi and Passerini reactions being paradigmatic examples. Isocyanides have extensive applications in synthetic, medicinal, and biological chemistry, as well as material science. ^[12]

Among the many variations of the Ugi 4CR, the Groebcke-Bienaymé-Blackburn reaction (GBB) is a well-stated multicomponent reaction, involving the acid-catalyzed interaction of α -

aminoazines, aldehydes and isocyanides, yielding imidazopyridine cores (Figure 1C) [13]. As it delivers compact heterocyclic adducts amenable to rapid diversification due to its MCR nature, this modern transformation is already having a deep impact in modern medicinal chemistry. [14] Although detailed studies have tackled the substrate scope, solvent, and catalysts range, [15] to our knowledge there are no reports on multiple MCRs involving these processes. In this work, we disclose the exploration of multiple GBB reactions taking place upon a variety of polyaminopolyazines, investigating the chemistry and functions of the novel chemotypes obtained thereof (Figure 1D).

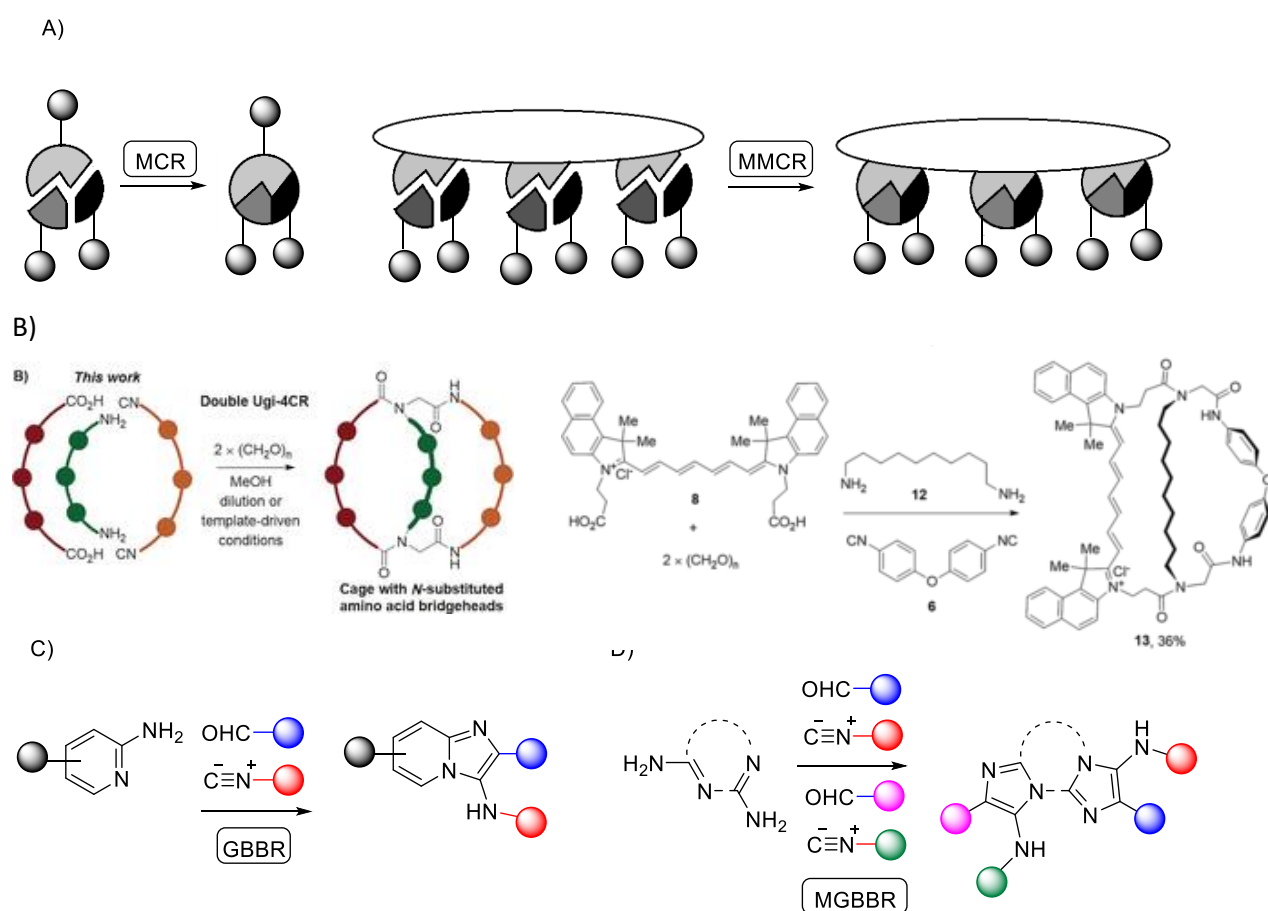


Figure 1. A) Schematic representation of multicomponent reactions (MCRs) and multiple multicomponent reactions. B) A recent example on the applications of multiple MCRs in the synthesis of macromulticyclic cages. C) Groebcke-Bienaymé-Blackburn reaction (GBBR). D) The present work: Multiple GBBRs for the synthesis of polyheterocyclic compounds.

References

1. Editorial. (Chief Editor: Peter Kirkpatrick), *Nature Reviews Drug Discovery* 3, 375 (2004)
2. Wender, P. A., & Miller, B. L. (2009). Synthesis at the molecular frontier. *Nature*, 460(7252), 197-201.
3. Bergbreiter, Dave E., and Shu Kobayashi. "Introduction to facilitated synthesis." (2009): 257-258.
4. Wender, P. A., Verma, V. A., Paxton, T. J., & Pillow, T. H. (2007). Function-oriented synthesis, step economy, and drug design. *Accounts of chemical research*, 41(1), 40-49.
5. a) Zhu, J., & Bienaymé, H. (Eds.). (2006). *Multicomponent reactions*. John Wiley & Sons., b) Ugi, Ivar, Alexander Dömling, and Werner Hörl. "Multicomponent reactions in organic chemistry." *Endeavour* 18.3 (1994): 115-122.
6. a) Burke, M. D., & Schreiber, S. L. (2004). A planning strategy for diversity-oriented synthesis. *Angewandte Chemie International Edition*, 43(1), 46-58. b) Ruijter, E., Scheffelaar, R., & Orru, R. V. (2011). Multicomponent reaction design in the quest for molecular complexity and diversity. *Angewandte Chemie International Edition*, 50(28), 6234-6246.
7. a) Weber, Lutz. "The application of multi-component reactions in drug discovery." *Current medicinal chemistry* 9.23 (2002): 2085-2093. b) Weber, Lutz. "Multi-component reactions and evolutionary chemistry." *Drug Discovery Today* 7.2 (2002): 143-147. c) Bienaymé, Hugues, et al. "Maximizing synthetic efficiency: Multi-component transformations lead the way." *Chemistry—A European Journal* 6.18 (2000): 3321-3329.
8. Eckert, Heiner. "From multi-component-reactions (MCRs) towards multi-function-component-reactions (MFCRs)." *Heterocycles* 73.1 (2008): 149.
9. Wessjohann, Ludger A., Ricardo AW Neves Filho, and Daniel G. Rivera. "Multiple multicomponent reactions with isocyanides." *Isocyanide Chemistry: Applications in Synthesis and Material Science* (2012): 233-262.
10. Wessjohann, Ludger A., Oliver Kreye, and Daniel G. Rivera. "One-Pot Assembly of Amino Acid Bridged Hybrid Macromulticyclic Cages through Multiple Multicomponent Macrocyclizations." *Angewandte Chemie International Edition* 56.13 (2017): 3501-3505.
11. a) Isambert, Nicolas, and Rodolfo Lavilla. "Heterocycles as key substrates in multicomponent reactions: the fast lane towards molecular complexity." *Chemistry—A European Journal* 14.28 (2008): 8444-8454. b) Zhu, Jieping. "Recent Developments in the Isonitrile-Based Multicomponent Synthesis of Heterocycles." *European Journal of Organic Chemistry* 2003.7 (2003): 1133-1144.

12. a) Nenajdenko, Valentine, ed. *Isocyanide Chemistry: Applications in Synthesis and Material Science*. John Wiley & Sons, 2012. b) Ugi, I., B. Werner, and A. Dömling. "The chemistry of isocyanides, their multicomponent reactions and their libraries." *Molecules* 8.1 (2003): 53-66. c) Dömling, Alexander, and Ivar Ugi. "Multicomponent reactions with isocyanides." *Angewandte Chemie International Edition* 39.18 (2000): 3168-3210.
13. a) Groebke, Katrin, Lutz Weber, and Fridolin Mehlh. "Synthesis of imidazo [1, 2-a] annulated pyridines, pyrazines and pyrimidines by a novel three-component condensation." *Synlett* 1998.06 (1998): 661-663. b) Bienayme, Hugues, and Kamel Bouzid. "A new heterocyclic multicomponent reaction for the combinatorial synthesis of fused 3-aminoimidazoles." *Angewandte Chemie International Edition* 37.16 (1998): 2234-2237.
14. Shaaban, Saad, and Bakr F. Abdel-Wahab. "Groebke–Blackburn–Bienaymé multicomponent reaction: emerging chemistry for drug discovery." *Molecular diversity* 20.1 (2016): 233-254.
15. a) Devi, Nisha, Ravindra K. Rawal, and Virender Singh. "Diversity-oriented synthesis of fused-imidazole derivatives via Groebke–Blackburn–Bienayme reaction: a review." *Tetrahedron* 71.2 (2015): 183-232. b) Pericherla, Kasiviswanadharaju, et al. "Recent Developments in the Synthesis of Imidazo [1, 2-a] pyridines." *Synthesis* 47.07 (2015): 887-912.

Results and Discussion

Reactivity and Scope

To examine the possibility of applying multiple GBB condensations on a single substrate, we first examined the interaction of 4-chlorobenzaldehyde and cyclohexyl isocyanide (two equivalents each) with 2,4-diaminopyrimidine (**1a**). Initial screening of common reaction conditions showed that the expected adduct **5a** is formed under PTSA catalysis in DMF (Figure 2A). Also, the reaction can be promoted by microwave irradiation and using catalytic amounts of Yb(OTf)₃ in acetonitrile. In this way, using a variety of common aldehydes and isocyanides, we prepared the double GBB adducts **5a-5f** in good yields (Figure 2B).

Having in mind the access to complex non-symmetric double GBB adducts with four diversity points through this methodology, we studied the innate selectivity of the process. This implies using a reactive mixture of two aldehydes of different electrophilicity^[1] plus two isocyanides of distinct nucleophilicity.^[2] Although in some experiments we detected (HPLC/MS) the

formation of mixed compounds in slight over-statistical ratios, according to the predicted activation levels, the complexity of the mixtures precluded practical use of this approach.

Then we turned our attention towards a sequential approach; forming the mono GBB adduct first, then reacting this intermediate with a different pair of aldehyde-isocyanide to yield the desired non-symmetrical double GBB product. Thus, when equimolar amounts of 2,4-diamino pyrimidine **1a** were reacted with aldehyde **2a** and isocyanide **3a** using Sc(OTf)₃ in acetonitrile, we observed the selective formation of mono GBB adduct **4a**, which was isolated, characterized and its structure secured by X-Ray crystallography (Figure 2, See SI). Then, this compound underwent a second GBB reaction under previously optimized conditions, yielding the expected product **5g**, whose structure was confirmed by X-Ray crystallography (Figure 2A, See SI). Importantly, this means that under the conditions tested, the first GBB step towards mono adduct is faster than the second one, resulting the full control on all four diversity points of scaffold **5**.

In this way, a variety of mono GBB adducts **4a-h** could be formed in high yields using Yb(OTf)₃ in acetonitrile under microwave irradiation. In order to obtain non-symmetrical double GBB adducts, the mono adducts **4** were subjected to a second MCR condensation. These transformations satisfactorily yielded the expected products **5g-m**, offering four diversity points on the new N-fused tricyclic scaffold **5**. As a proof of concept, we prepared the complementary compounds **5h** and **5j**, merely changing the order in which the sequential MCRs are performed. These reactions tolerated a variety of isocyanides including aliphatic (cyclohexyl and tert-Butyl) and substituted aromatics (4-methoxyphenyl, 2-bromophenyl). Moreover, the deactivated isocyanides like ethyl isocyanoacetate and phosmic were successfully incorporated, whereas tosmic resulted unreactive in the standard conditions used. The prepared compounds also feature a variety of aldehydes including aromatics featuring functional groups with different connectivities (2-bromophenyl, 2,6-dichlorophenyl, 2-methylcarboxyphenyl, 2-allyloxyphenyl) as well as aliphatic aldehydes (isopropyl, isopropenyl). Also, heterocyclic aldehydes (2- and 4-pyridyl, 3-indolyl) yielded expected products in good yields. (Figure 2B)

Next, we intended to further explore the reactivity space of this process by changing the diaminodiazine component of the reaction. In our first attempt under the optimized conditions, 2,4-diaminoquinazoline **1b** underwent the mono GBB reaction. Interestingly, the

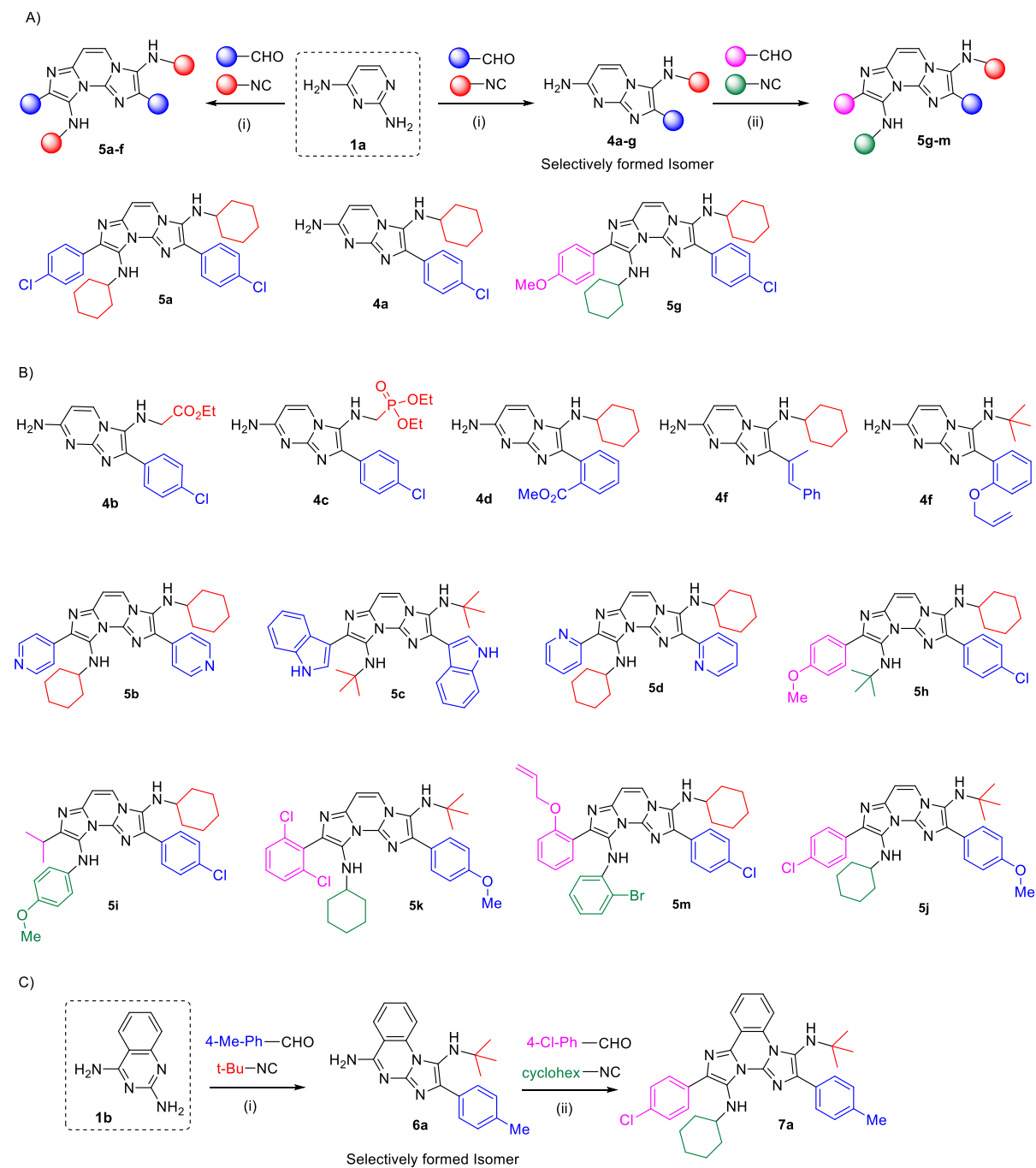
previously observed regioselectivity was maintained as the mono GBB adduct **6a** was isolated as the single product and its structure was confirmed by NMR experiments (See SI). Moreover, a second GBB reaction was performed on **6a** to yield the non-symmetrical double GBB adduct **7a** (Figure 2C).

Later, we studied the reactivity of 3,6-diaminopyridazine **1c** and mono GBB adducts **8a-d** were prepared in moderate yields. The expected double GBB adduct **9a** as well as the non-symmetrical double GBB adduct **9b** were also prepared using the previously optimized conditions (Figure 3A). It is worth mentioning that in case of 3,6-diaminopyridazine **1c**, the double GBB adducts were only formed using aromatic isocyanides, due to their planar geometry, whereas other bulky isocyanides (i.e. tert-butyl and cyclohexyl) failed to yield double GBB adducts, likely because of the steric hindrance of the proximal amino moieties in the final structure.

Interestingly, mono GBB adducts **8**, arising from of 3,6-diaminopyridazine **1c**, underwent Ugi multicomponent reactions to yield another new scaffold **10**, featuring a peptidomimetic residue on treatment with an isocyanide, an aldehyde, and a carboxylic acid. Compound **10a** was generated in a one-pot reaction involving a sequential GBB-Ugi MCRs in the presence of acetic acid (which also catalysed the GBB reaction). Furthermore, adducts **10b** and **10c**, featuring 5 diversity points in the heterocyclic core, were prepared (Figure 3B). Incidentally, applying similar conditions to the mono GBB adducts **4a** (from diaminopyrimidine **1a**) did not afford the GBB-Ugi adduct, but a trace amount of double GBB adduct, the majority of the starting material remaining intact.

Finally, we tackled melamine **1d** as the prototypical triaminotriazine and we could isolate the triple GBB adducts **11a-d**, using a variety of common isocyanides and aldehydes. (Figure 3C). The structure of **11a** was confirmed by X-Ray crystallography, featuring a dimeric secondary structure (See SI). These compounds are of high importance as melamine holds a privileged position as a reactive core in the synthesis of functionalized materials with widespread use in several fields. However, its use in organic synthesis due to its polar nature and low solubility in most organic solvents. Also, there are no reports on the participation of melamine in MCRs. The final scaffold **11** is a novel, tripodal, highly compact N-fused tetracyclic structure that is conveniently synthesized in a single step using readily available starting material. Moreover,

it is highly atom economical, and this formal 7CR features the formation of nine bonds in a single reaction.



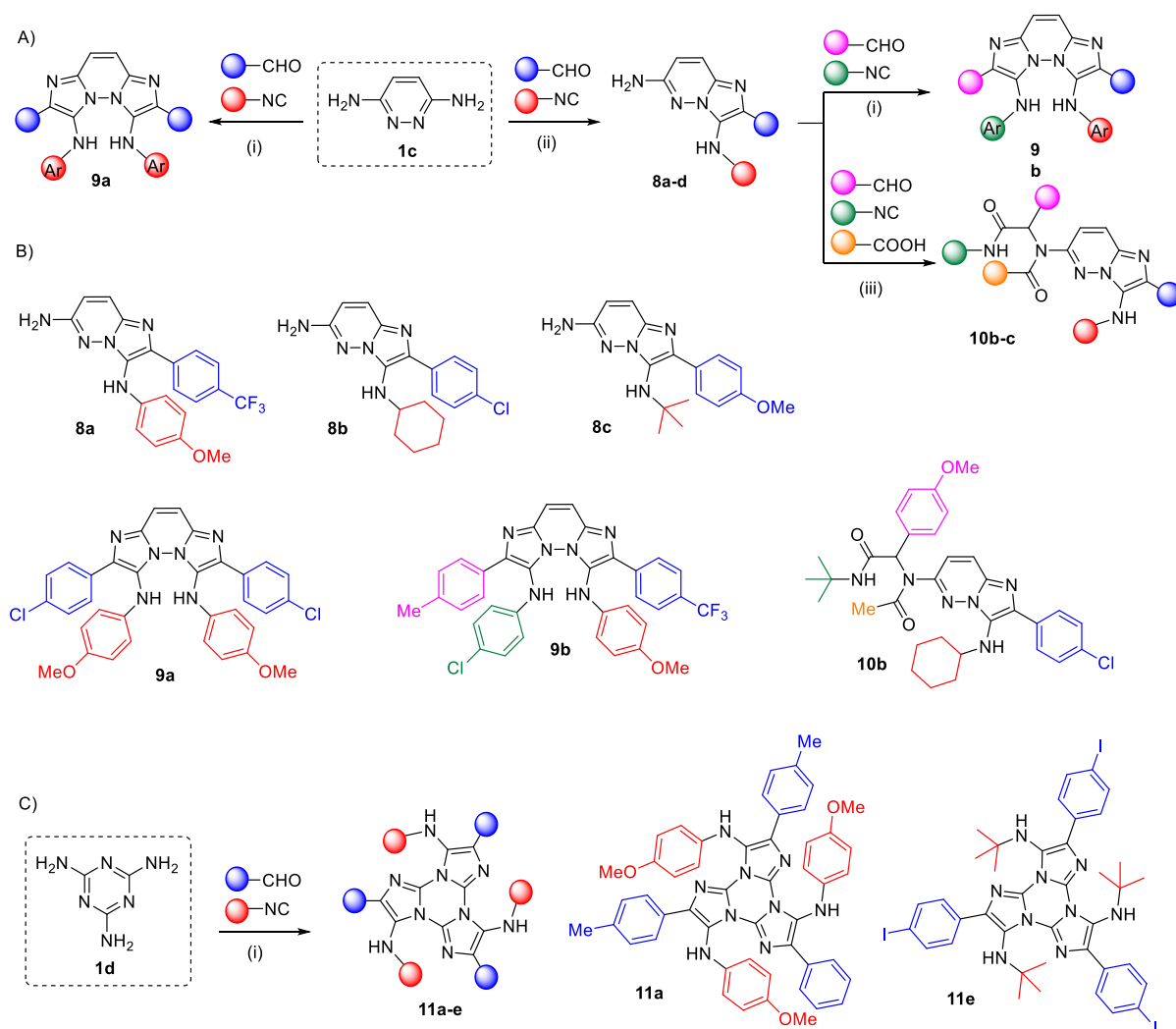


Figure 3. New reactants in GBBs: A) GBB, Double GBBs and GBB-UgiR upon diaminopyridazine (multiple and sequential access). B) Library of GBB adducts formed in the process 3,6-diaminopyridazine. C) Melamine triple GBB processes

References

1. Appel, Roland, and Herbert Mayr. "Quantification of the electrophilic reactivities of aldehydes, imines, and enones." *Journal of the American Chemical Society* 133.21 (2011): 8240-8251.
2. Tumanov, Vasily V., Alexander A. Tishkov, and Herbert Mayr. "Nucleophilicity parameters for alkyl and aryl isocyanides." *Angewandte Chemie International Edition* 46.19 (2007): 3563-3566.

Post-transformation Reactions

Post-transformations of MCR adducts are routinely used to diversify the generated scaffolds, giving access to more complex and valuable chemotypes. In this way, we modified our imidazopyrimidines with a number of representative reactions (Figure 5). In the first experiment, mono adduct **4d** underwent a second GBB reaction using 4-anisaldehyde and *tert*-butylisocyanide. When applying a basic workup, the resulting adduct suffered an intramolecular amide formation, affording pentacyclic lactam **12** (7%, unoptimized) in just one step (Figure 5A). Also, the nucleophilicity of the pyridine moiety present in adduct **5b** was exploited and on interaction with methyl iodide, afforded almost quantitatively, the double *N*-methylpyridinium salt **13**. Interestingly, the NMR studies suggest that the methylation selectively takes place on the pyridine moieties and not on the nitrogen atoms of the main scaffold (Figure 5B). Also, the chloroacetyl moiety of the GBB-Ugi adduct **10c** was cyclized to generate the 2,5-diketopiperazine ring moiety through the standard intermolecular amide *N*-alkylation process ^[1], affording compound **15** in moderate yields. (Figure 5C)

N-fused, conjugated polycyclic scaffolds, normally prepared through complex multistep sequences, are highly appreciated chemotypes in material science, due to versatile applications they display. In this context, we prepared modified expanded chemotypes through metal-catalyzed couplings. First, we applied an intramolecular Buchwald-Hartwig cross-coupling on double GBB adduct **5f** to yield the novel heptacyclic compound **14** (Figure 5D). A similar transformation on the triple melamine GBB adduct **11b** yielded the decacyclic radial derivative **16** in a single step (Figure 5E)^[2].

We also extended the novel tetracyclic scaffold **11**, fitted with aryl iodide residues, via multiple Suzuki couplings to access star-shaped compounds **17a-c**. Noteworthy, the triple reactions take place successfully to yield the corresponding adducts with *meta* and *para* connectivities. It is worth highlighting that compounds **17b** and **17c** have nanometric dimensions, the latter reaching almost 30 Å of lateral length (Figure 5F-G). These examples clearly demonstrate the power and versatility of the methodology to construct functionalized nanosized entities through a short bottom up approach.

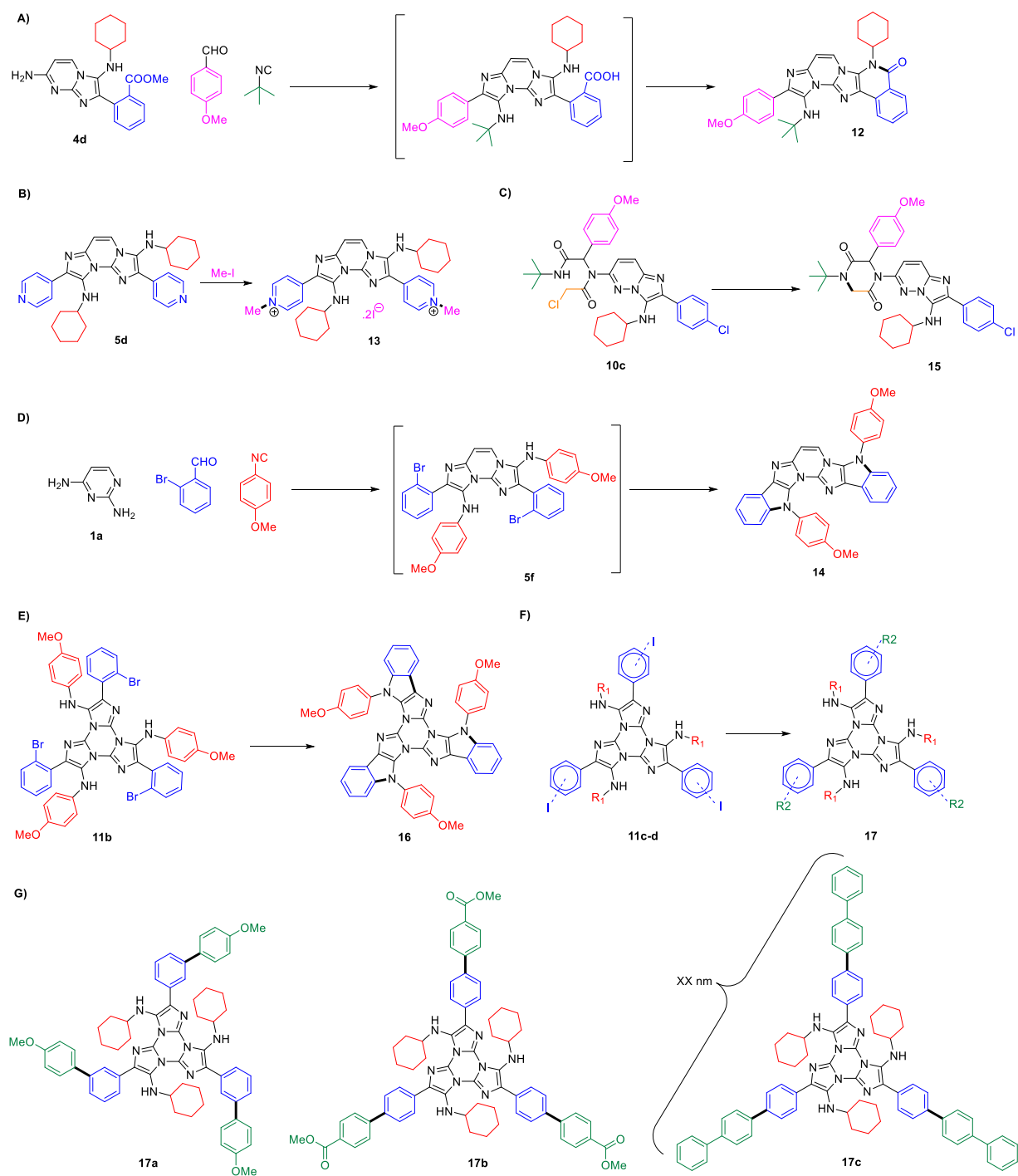


Figure 5. Post-transformations of GBB adducts. A) Lactam formation from compound **4d**. B) Pyridinium salt formation out of pyridine adduct **5d**. C) DKP generation from GBB Ugi adduct **10c**. D and E) Indole formation using Ullman coupling out of pyridazine and melamine adducts. G) Suzuki coupling from bromoaryl melamine GBB adducts.

References

1. Tyagi, V., Khan, S., Bajpai, V., Gauniyal, H. M., Kumar, B., & Chauhan, P. M. (2012). Skeletal diverse synthesis of N-fused polycyclic heterocycles via the sequence of Ugi-type MCR and cui-catalyzed coupling/tandem Pictet–Spengler reaction, *J. Org. Chem.* 77(3), 1414-1421.
2. Wang, B., Lv, X. L., Feng, D., Xie, L. H., Zhang, J., Li, M., & Zhou, H. C. (2016). Highly stable Zr (IV)-based metal-organic frameworks for the detection and removal of antibiotics and organic explosives in water. *J. Am. Chem. Soc.*, 138(19), 6204-6216.
3. Banfi, Luca, Andrea Basso, and Renata Riva. "Synthesis of Heterocycles Through Classical Ugi and Passerini Reactions Followed by Secondary Transformations Involving One or Two Additional Functional Groups." *Synthesis of Heterocycles via Multicomponent Reactions I*. Springer Berlin Heidelberg, 2010. 1-39.

Bioimaging Studies of Selected MGBB Adducts

The need for novel functional fluorescent derivatives has prompted the development of new synthetic strategies to prepare fluorophores that are not easily accessible with classic chemical approaches.^[1] In this context, isocyanide-based MCRs have proven as a valuable chemical platform to afford new fluorescent scaffolds with optimal properties thanks to their intrinsic divergent and combinatorial nature.^[2] In a pioneering work, Balakirev et al. described the combinatorial preparation of fluorescent GBB adducts droplet arrays.^[3] The development of multiple GBB processes allowed us to modulate π -conjugation systems and introduce new functionalities to modify the spectral properties of GBB adducts. Notably, the versatility of GBB reactions allowed us to fine-tune the fluorescent properties and red-shift the emission wavelengths of the adducts by extending their electronic conjugation with C-C connected aryl groups (**13** vs **5b** and **9**, Figure 6A). Our synthetic strategy also enabled the introduction of EWG and EDG at specific sites of the heterocyclic core to generate push-pull fluorophores with bright fluorescence emission in the red region of the visible spectra (**10a**, Figure 6A). The excellent photophysical features of the BODIPY scaffold in bioimaging^[4] encouraged us to explore the generation of novel BODIPY fluorophores derived from our α -pyridylGBB adducts, taking into account the different coordination possibilities between conjugated N atoms to form diazaborane 5/6-member rings. A model GBB compound **18** was reacted with BF_3 in the presence of sodium carbonate^[5] to render selectively the difluoroboron complex **19a**. We confirmed its structure by X-ray diffraction (Figure 6B), which displays a BF_2 unit linking the imino group of the aminopyridine component and the pyridine nitrogen, suggesting that the formation of the 5-member ring is faster than the more conventional 6-membered BODIPY cycle (Figure 6C).^[6] Interestingly, compound **19a** shows cationic nature, featuring a BF_4^- as the counterion, which accounts for the fluoride anion released during its formation. Similarly, the BODIPY-like compound **19b** was obtained from its precursor **5d**. We assigned its structure by NMR, observing high analogy between the structures of the two BODIPY analogues. Remarkably, attempts to obtain a double BF_2 complex from **5d** were unsuccessful. Next, we analyzed the photophysical features of the novel 5-member ring BODIPY fluorophore **19a**, and compared them to its precursor. The coordination of the two N atoms through the BF_2 moiety led to a significant enhancement of their properties as fluorophores. In addition to presenting remarkably longer emission wavelengths (453 nm to 514 nm, Figure 6D), compound **19a**

presented a 40-fold higher fluorescence quantum yield due to the increased rigidification of the BODIPY core (Figure 6E). Unlike its precursor, the fluorescence emission of compound **19a** did not show any pH dependence, asserting its value as a bright green fluorophore for bioimaging assays covering the whole pH physiological range (Figure 6F). We also confirmed the compatibility of compound **19a** for live-cell imaging by incubating human lung A549 epithelial cells and acquiring images under a confocal fluorescence microscope. Compound **19a** showed excellent cell permeability and staining of the cytosolic compartment, as demonstrated by co-incubation with the commercially available LysoTracker and MitoTracker dyes (Figure 6G). Altogether, these results indicate the suitability of multiple GBB reactions to generate novel fluorescent scaffolds with excellent features for bioimaging assays, including novel 5 and 6-member BODIPY-based fluorophores.

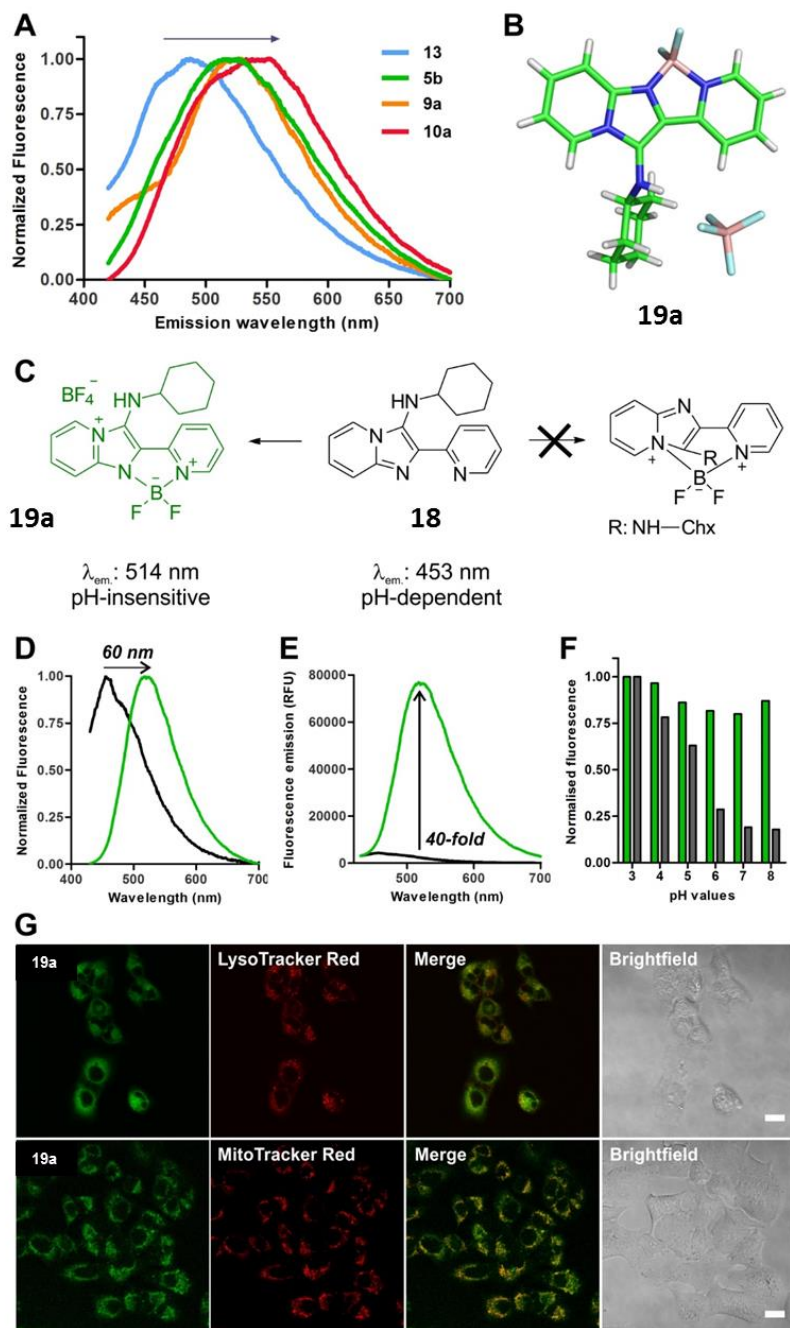


Figure 6. GBB adducts as fluorophores for bioimaging applications. A) Chemical tunability of the fluorescence emission of different GBB adducts with red-shifted emission spectra. B) X-ray diffraction of the fluorescent adduct **19a**. C) Selective incorporation of the BF₂ unit to **18** form the 5-member BODIPY-like fluorophore **19a**. D, E, F) Comparative photophysical analysis of the adduct **19a** and its precursor (**18**) as fluorophores for live cell imaging. G) Brightfield and fluorescence confocal microscope images of human A549 epithelial cells upon incubation with compound **19a** (2 μ M) and the commercially available trackers LysoTracker Red and MitoTracker Red. Scale bar: 10 μ m.

References

- [1] a) F. de Moliner, N. Kielland, R. Lavilla, M. Vendrell, *Angew. Chem. Int. Ed.* **2017**, *56*, 3758–3769; b) L. Levi, T. J. J. Müller, *Chem. Soc. Rev.* **2016**, *45*, 2825–2846.
- [2] a) Kielland, N. et al. *Chem Commun* 2012; b) Vazquez-Romero, A. et al. *JACS* 2013.
- [3] O. N. Burchak, L. Mugherli, M. Ostuni, J. Jacques Lacapère, M. Y. Balakirev, *J. Am. Chem. Soc.* **2011**, *133*, 10058–10061.
- [4] a) N. Boens, V. Leen, W. Dehaen, *Chem. Soc. Rev.*, **2012**, *41*, 1130–1172; b) A. Loudet, K. Burgess, *Chem. Rev.*, **2007**, *107*, 4891-4932; c) Kikuchi et al. *Chem Soc. Rev.* 2015
- [5] For a related process see: Z. Zhang, W-Y. Cha, N. J. Williams, E. L. Rush, M. Ishida, V. M. Lynch, D. Kim, J. L. Sessler, *J. Am. Chem. Soc.* **2014**, *136*, 7591–7594.
- [6] a) C. Yu, E. Hao, T. Li, J. Wang, W. Sheng, Y. Wei, X. Mu, L. Jiao, *Dalton Trans.*, **2015**, *44*, 13897–13905; b) X. Liu, M. Chen, Z. Liu, M. Yu, L. Wei, Z. Li, *Tetrahedron*, **2014** *70*, 658-663; c) W. Li, W. Lin, J. Wang, X. Guan, *Org. Lett.*, **2013**, *15*, 1768–1771.

Antiviral Activity of MGBB Adducts

The relevance of GBB adducts in medicinal chemistry and their presence in a number of drugs suggests that the imidazoazine core is a highly bioactive scaffold ^[1]. To corroborate this potential in our library of molecules we addressed the exploration of their bioactivity in an unmet medical need. Human adenoviruses (HAdV) are non-enveloped viruses responsible for a wide range of diseases that had been rarely associated with severe clinical symptoms in healthy individuals. However, nowadays it is well known that HAdV infections are associated with high morbidity and mortality in immunosuppressed patients, like those receiving solid organ or hematopoietic stem cells transplantation, and in immunocompetent individuals with community-acquired pneumonia ^[2,3]. The lack of approved specific antiviral drugs with probed efficacy and safety against HAdV further complicates the treatment of these patients ^[4,5]. In this context, a series of representative compounds (Figure 7A) were tested to determine their antiviral activity against HAdV using different susceptibility assays.

Fifty percent of the compounds constituent of this small library showed significant anti-HAdV activity in the plaque assay when evaluated at a concentration of 10 μ M (Figure 7B). Our dose-response assays showed that only compounds **5h** and **12** presented a dose-dependent activity (Figure 7C), with IC_{50} values of 1.19 and 3.42 μ M, respectively (Table 1). Compounds **5b** and **10a** showed significant CC_{50} with values of 22.9 and 62.8 μ M, respectively (Table 1), so the observed anti-HAdV activity of these compounds may be explained because of their cytotoxicity. Compound **10b** showed a safe value of CC_{50} (132.2 μ M) and a significant anti-HAdV activity at concentration of 10 μ M (Table 1; Figure 7B) but it did not present a dose-dependent activity, at concentrations under 10 μ M it did not show anti-HAdV activity (data not showed). The more cytotoxic molecules, **5b** and **10a** presented the lowest selectivity index (SI), because of their high cytotoxicity, whilst molecules **5h** and **12** showed the highest (Table 1). Interestingly, when comparing molecules **5h**, **10b** and **12** HAdV yield reductions, the one with the lower activity at a concentration of 10 μ M and exerting a dose-independent activity, showed a significantly higher reduction (Table 1). These results are encouraging given the low number of screened hits and the observed Structure-Activity relationship (SAR) dependence, as slight differences in connectivity lead to major changes in antiviral potency (for instance, GBB adducts **5h** and **5g**, sharing the same diaminopyrimidine scaffold display very different

activity levels, the former being more potent; see Figure 7). Similarly, the Ugi-GBB diaminopyridazine adduct **10b** is considerably more active than its double GBB analogue **9a**. This trend suggests further improvement on programmed exploration of the substituent and scaffold range around the new GBB scaffold. The results obtained in this work support the generation of a new library of compounds based on the SAR of the compounds evaluated here in order to optimize their anti-HAdV and identify a hit candidate for the clinical development of a specific anti-HAdV drug to address this emergent unmet medical need in the treatment of HAdV life-threatening infections.

Table 1. Summary of the activities; CC₅₀, IC₅₀ and HAdV yield reduction

Compound	IC₅₀ (μM)	CC₅₀ (μM)	Selectivity index (SI)	Virus yield reduction (Fold-reduction)
5h	1,19±0,08	112,5±2,94	94,38	11,54±5,98
10b	---	132,2±1,41	17,67	157,72±0,00
5b	2,46±0,00	22,9±2,24	9,31	115,42±59,76
12	3,42±1,33	215,22±8,53	62,93	24,88±12,87
10a	7,86±2,01	62,8±12,53	7,98	11,54±5,98

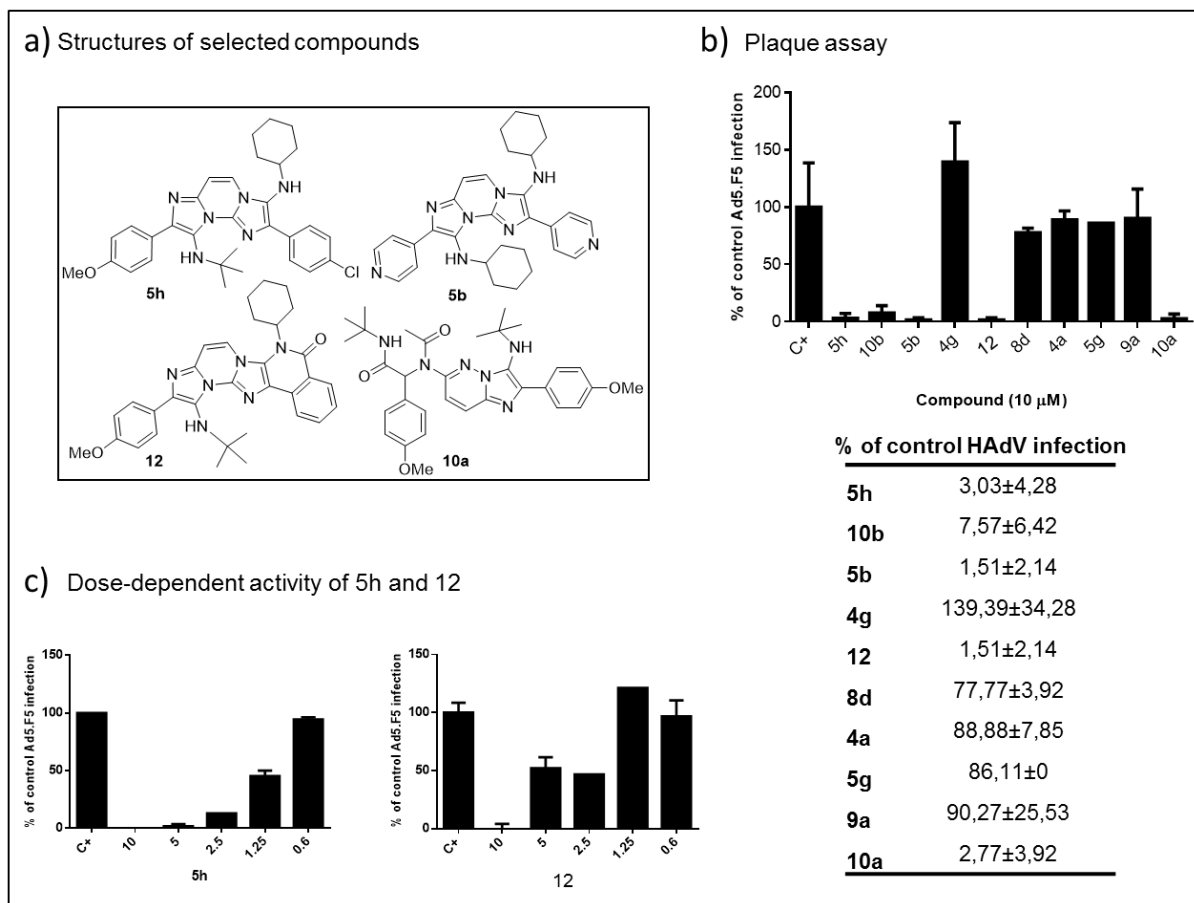


Figure 7. Inhibitory activity of the MCR adducts: A) Structures of selected compounds; B) Plaque assay at 10 μM concentration; and C) Dose-dependent activity of the MCR adducts. The results represent means ± SD of triplicate samples from three independent experiments.

References

- [1] N. Devi, R. K. Rawal, V. Singh; *Tetrahedron* **2015**, *71*, 183-232.
- [2] P. Martínez-Aguado, Ana Serna-Gallego, J. A. Marrugal-Lorenzo, I. Gómez-Marín, J. Sánchez-Céspedes; *Drug Discov. Today*. **2015**, *20*,1235-42.
- [3] D. Tan, Y. Fu, J. Xu, Z. Wang, J. Cao, J. Walline, H. Zhu, X. Yu; *J. Thorac. Dis.* **2016**, *8(5)*,848-54.
- [4] M. M. Y. Wayne, C. W. Sing; *Pharmaceuticals* **2010**, *3*, 3343-3354.
- [5] J- Sánchez-Céspedes, P. Martínez-Aguado, M. Vega-Holm, A. Serna-Gallego, J. I. Candela, J. A. Marrugal-Lorenzo, J.Pachón, F. Iglesias-Guerra, J. M. Vega-Pérez; *J. Med. Chem.* **2016**, *59*, 5432–5448.

Affinity of MGBB compounds to DNA

The topological plasticity of DNA, leading to a variety of stable structures, has deep consequences in biology. In this respect, it is crucial to have selective binders to study their features and roles in a suitable manner. There is an intense effort going on to find such compounds as preliminary step to develop medicines ^[1]. We are concerned with topology-dependent selectivity and especially relevant here are G-quadruplexes, because of their wide presence in the genome, mainly involved in the maintenance of chromosomes and in the transcriptional regulation of genes ^[2]. Therefore, selective ligands binding these topologies may display a prominent role in biological and medicinal chemistry ^[3,4].

Flat N-heteroaromatic compounds having polar or cationic groups are among the chemotypes frequently found in active binders, stabilizing the G-tetrads by π -stacking and electrostatic interactions, although often non-selective for a defined substructure. In this context, we explored the selectivity of a selected set of our synthesized MGBB-type compounds adducts **5b**, **11b**, **13** and **19b** in the interaction with model DNA oligonucleotides. To this means, we performed competitive dialysis experiment was carried out with 10 oligonucleotides representing prototypical nucleic acid structures: including single and double strands, and especially quadruplexes including the human telomere sequence (TEL22 ^[5]), the aptamer DL-40 ^[6], the conserved DNA quadruplex element found in the transcriptional activation site of the promoter of the protooncogene c-kit (GG1 ^[7]) and the promoter sequence of the antiapoptotic gene bcl-2 (24bcl ^[8]) (see Figure 8 and SI). These sequences represent different G-quadruplex topologies (parallel, antiparallel and hybrid ^[5-8]) and some of them have been demonstrated to be sensitive to G-quadruplex binders causing down regulation of oncogene expression in cancer cells ^[9]. The more adduct being accumulated in the dialysis bag indicates a higher binding affinity, the analysis performed by fluorescence ^[10]. Further digestion (DSS) allowed the accurate determination of the binding affinities.

Initial results showed that the melamine adduct **11b** interacts with all the sequences. However, its interaction with single strand T20 was significantly higher. This could be explained by the Nitrogen-rich and planar structure of the melamine core. Compound **5b** showed undefined and week affinity to a number of sequences. However, its dimethylated salt **13** displayed potent and selective affinity to the hybrid quadruplex 24bcl. Less significant affinities were also observed with quadruplexes Tel22 and GG1. The distinct improvement in

the interactions of compounds **5b** and **13** may be partially explained through the charged nature of the salt **13**. Furthermore, the charged BODIPY adduct **19b** showed affinity to the same hybrid quadruplex 24bcl. (Figure 8B)

To further study the selective affinity of compound **13** with quadruplexes, we carried out fluorescence titrations quadruplex GG1 and hybrid quadruplex 24bcl with double strand DS26 as the negative control. The titration curves show that the increase in the relative oligonucleotide-drug concentration from 0 to 18 folds, results in the significant increase in the fluorescence in quadruplex 24bcl-**13** combination. A similar, yet less potent, trend is observed with quadruplex GG1-**13** combination. However, in case of double strand DS26, no change is observed. Considering the fact that oligonucleotides are not fluorescent and the concentration of the drug is kept constant, the observed increase in the fluorescence levels arise from the formation of oligomer-drug complexes. Thus, these results provide further evidence that compound **13** has selective affinity to the quadruplex structures especially 24bcl (Figure 8C) and may serve as a lead to develop a new class of selective binders for this type of DNA structures.

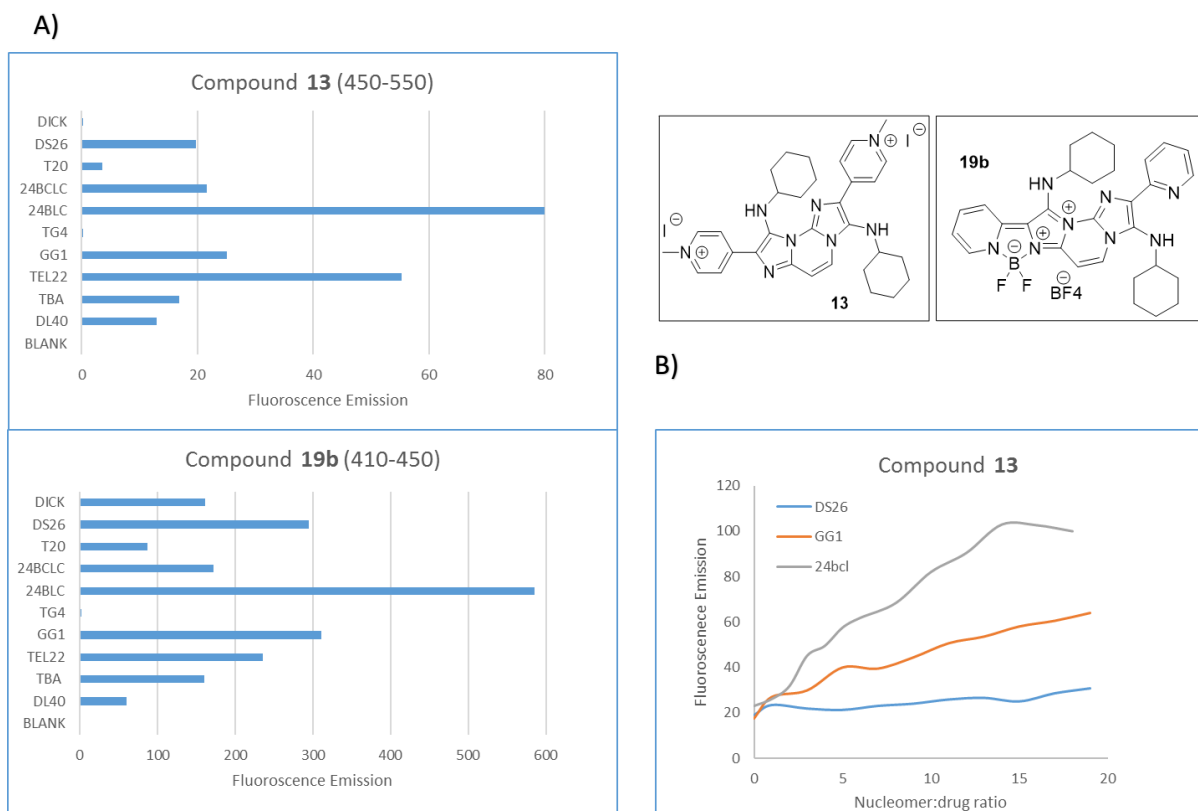


Figure 8. A) Results obtained by the competitive dialysis assays of 10 oligonucleotide and compounds **13** and **19b**. B) Fluorescence spectra of a 0.2 μM solution of the GBB adduct **13** after the addition of increasing amounts of oligonucleotides DS26, GG1 and 24bcl (from 0 to 10 μM) in potassium phosphate buffer.

References

- [1] A. Ali; S. Bhattacharya; *Bioorg. Med. Chem.* **2014**, *22*, 4506–4521.
- [2] D. Rhodes, H. J. Lipps; *Nucleic Acids Res.* **2015**, *43*, 8627–8637.
- [3] S. Alcaro, C. Musetti, S. Distinto, M. Casatti, G. Zagotto, A. Artese, L. Parrotta, F. Moraca, G. Costa, F. Ortuso, E. Maccioni, C. Sissi; *J. Med. Chem.* **2013**, *56*, 843–855.
- [4] G. W. Collie, G. N. Parkinson; *Chem. Soc. Rev.* **2011**, *40*, 5867–5892.
- [5] Y. Wang, D. J. Patel; *Structure*, **1993**, *1*, 263–282.
- [6] V. Kuryavyi, A. Majumdar, A. Shallop, N. Chernichenko, E. Skripkin, R. Jones, D. J. Patel; *J. Mol. Biol.* **2001**, *310* 181-194.
- [7] H. Fernando, A. P. Reszka, J. Huppert, S. Ladame, S. Rankin, A. R. Venkitaraman, S. Neidle, S. Balasubramanian; *Biochemistry* **2006**, *45*, 7854-7860.
- [8] J. Dai, T. S. Dexheimer, D. Chen, M. Carver, A. Ambrus, R.A. Jones, D.Z. Yang; *J. Am. Chem. Soc.* **2006**, *128*, 1096–1098.
- [9] K. McLuckie, Z. Waller, D. A. Sanders, D. Alves, R. Rodriguez, J. Dash, G. J. McKenzie, A. R. Venkitaraman, S. Balasubramanian; *J. Am. Chem. Soc.* **2011**, *133*, 2658-2663.
- [10] R. Ferreira, A. Aviñó, R. Perez-Tomás, R. Gargallo, R. Eritja; *J. Nucleic Acids* **2010**, Article ID 489060 (doi:10.4061/2010/489060.)

Initial applications of MGBB compounds in Material science

In the context of the search of novel scaffolds in materials science ^[1] and considering the key role of triazines and specially melamine in this field ^[2-4], we started the exploration of some properties arising from the representative structures prepared through our methodology. Remarkably the combinatorial synthesis of these GBB adducts features a wide reactant scope, and a convenient *bottom up* approach to nanometric size star-shaped molecules, resembling N-doped nanographene ribbons ^[5,6], privileged chemotypes in material science.

First, we analyzed the structural features of the triphenyl-melamine GBB compound **17c**, suitably obtained through a multiple MCR followed by a Suzuki coupling. The X-ray diffraction shows a triangular molecule of considerable size (around 28 Å length each side) with a planar core and some conformational freedom detected in the cyclohexyl residues. The aromatic arms linearly extend in a regular atropisomeric pattern (Figure 9a). The crystal packing features an interesting docking arrangement of the central π system, and an efficient intertwining of the triaryl groups (Figure 9A- 9C). The needle-type crystals were also analysed by electron-diffraction, which allowed the description of additional structural motifs, by scanning distinct sections of the crystalline material. The structural variety of the crystalline packing modes attained by the different molecules analysed is remarkable. Further work in this section is ongoing and will be reported in due course.

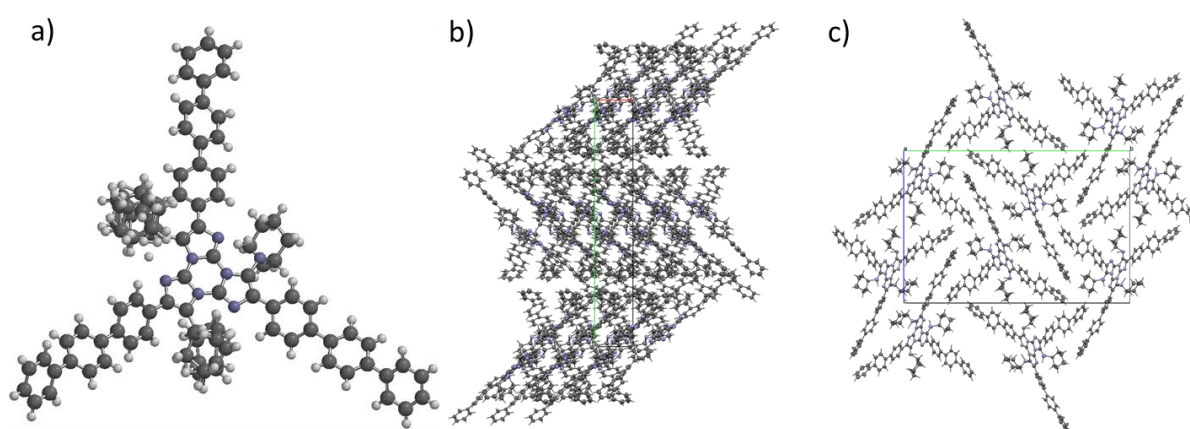


Figure 9. Structural features of nanometric star shaped compounds: A) X-ray structures of compound **17c**. B and C) Molecular packing arrangement of **17c**.

References

- [1] K. Müllen; Chemistry in a Materials World; *Angew. Chem. Int. Ed.* **2015**, *54*, 10040 – 10042.
- [2] P. Puthiaraj, Y.-R. Lee, S. Zhang, W.-S. Ahn; *J. Mater. Chem. A*, **2016**, *4*, 16288–16311.
- [3] B. Roy, P. Bairia, A. K. Nandi; *RSC Adv.*, **2014**, *4*, 1708–1734.
- [4] J. Lim, E. E. Simanek; *Adv. Drug Deliv. Rev.* **2012**, *64*, 826–835.
- [5] For instance, see: H. Wang, T. Maiyalagan, X. Wang; *ACS Catal.* **2012**, *2*, 781–794.
- [6] M. Daigle, A. Picard-Lafond, E. Soligo, J.-F. Morin; *Angew. Chem. Int. Ed.* **2016**, *55*, 2042 –2047.
- [7] C. Delaney, G. M. Ó. Máille, B. Twamley, S. M. Draper; *Org. Lett.* **2016**, *18*, 88–91.
- [8] A. L. Pinaridi, G. Otero-Irurueta, I. Palacio, J. I. Martinez, C. Sanchez-Sanchez, M. Tello, C. Rogero, A. Cossaro, A. Preobrajenski, B. Gómez-Lor, A. Jancarik, I. G. Stará, I. Starý, M. F. Lopez, J. Méndez, J. A. Martin-Gago; *ACS Nano* **2013**, *7*, 3676-3684.
- [9] W. Liu, X. Luo, Y. Bao, Y. P. Liu, G.-H. Ning, I. A., L. Li, C. T. Nai, Z. G. Hu, D. Zhao, B. Liu, S. Y. Quek; K. P. Loh; *Nature Chem.*, **2017**, doi:10.1038/nchem.2696

Conclusions

In summary, the Multiple GBB reaction approach upon polyaminopolyazines, involving heterocyclic cores of pyrimidine, pyridazine and melamine, is a very robust and fruitful source of highly functional materials. Although the innate selectivity is quite limited, a sequential mode allows the performance of consecutive reactions leading to the programmed incorporation of up to 6-diversity points, in formally 5- and 7-multicomponent reactions. The generated adducts are compact, small molecules suitably diversifiable, amenable of straightforward post-transformation processes and constitute novel scaffolds with remarkable properties as antiviral compounds, fluorescent probes, selective DNA binders and also as nanometric blocks in materials science. Having demonstrated these properties and the extremely fast and reliable synthetic approach for these compounds, their molecular tuning, either by design or combinatorially, should be direct and lead to improved hits in all these fields.

Acknowledgement

We thank the funding of DGICYT-Spain (CTQ2015-67870-P) and Generalitat de Catalunya (2014 SGR 137).

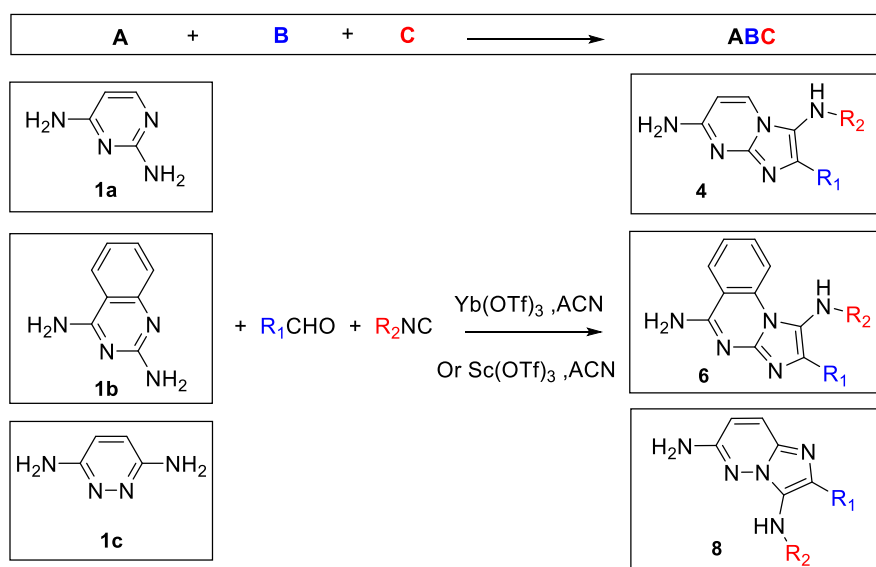
Publication IV: Selected Supporting Information

General Information

Unless stated otherwise, most of reactions were carried out in a Microwave Reactor (CEM Focused TM Synthesis, Discoverer SP System). Commercially available reactants were used without further purification. Thin-layer chromatography was performed on pre-coated Merck silica gel 60 F254 plates and visualized under a UV lamp. ^1H , and ^{13}C NMR spectra were recorded on a Varian Mercury 400 (at 400 MHz, and 100 MHz respectively). Unless otherwise stated, NMR spectra were recorded using residual solvent as the internal standard ^1H NMR: $\text{CDCl}_3 = 7.26$, $\text{CD}_3\text{OD} = 4.87$; $(\text{CD}_3)_2\text{SO} = 2.50$; $\text{D}_2\text{O} = 4.79$ and ^{13}C NMR: $\text{CDCl}_3 = 77.0$; $\text{CD}_3\text{OD} = 49.0$; $(\text{CD}_3)_2\text{SO} = 39.52$; $\text{CF}_3\text{COOD} = 164.2, 116.6$. Data for ^1H NMR spectra are reported as follows: chemical shift (δ ppm), multiplicity, coupling constants (Hz) and integration. Data for ^{13}C NMR spectra are reported in terms of chemical shift (δ ppm). IR spectra were recorded using a Thermo Nicolet Nexus spectrometer and are reported in frequency of absorption (cm^{-1}). High resolution mass spectrometry was performed by the University of Barcelona Mass Spectrometry Service.

Experimental Procedures

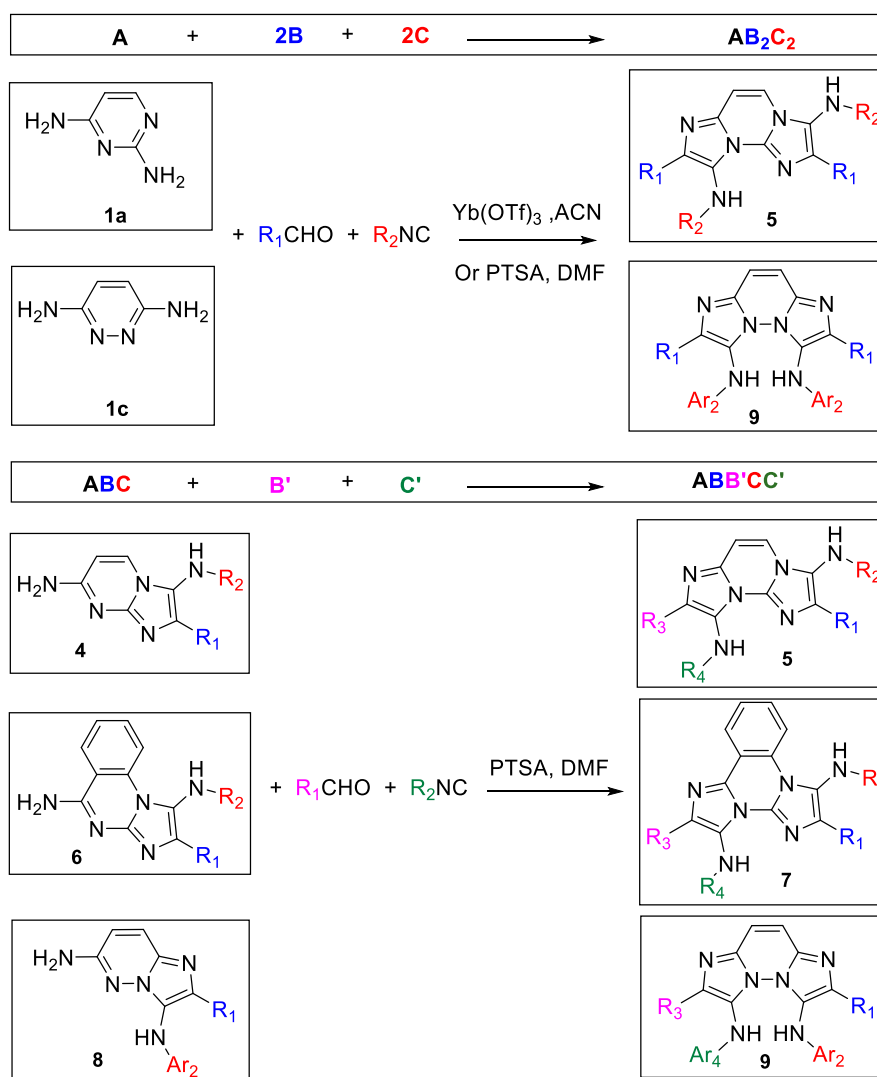
General Procedure for the Synthesis of Mono GBB Adducts (4a-h, 6, 8a-d)



General Procedure A: A solution of polyaminopolyazaine **1** (1 mmol, 1 eq) and aldehyde (1 mmol, 1 eq) in ACN (2 mL) was transferred to a microwave reactor tube followed by the addition of $\text{Sc}(\text{OTf})_3$ or $\text{Yb}(\text{OTf})_3$ (0.2 mmol, 0.2 eq) at room temperature. After 10 min, the suitable isocyanide (1 mmol, 1 eq) was added to the stirring reaction mixture; the vessel was sealed and heated by microwave irradiation

to 80° C for 30-60 min. After reaction completion was confirmed by TLC or HPLC, in some cases solid precipitate of the product appeared, which was filtered off, washed and triturated from appropriate solvent (DCM/Et₂O or Hexane/Et₂O). In other cases, ACN was evaporated, and DCM was added until everything was dissolved. The mixture was treated with saturated NaHCO₃ aqueous solution to pH 8. The organic layer was separated, dried over MgSO₄ and evaporated under reduced pressure. The pure product was obtained by flash chromatography (DCM/MeOH or EtOAc/Hexane as eluent).

General Procedure for the Synthesis of Double GBB Adducts (5a-m, 7, 9a-b)



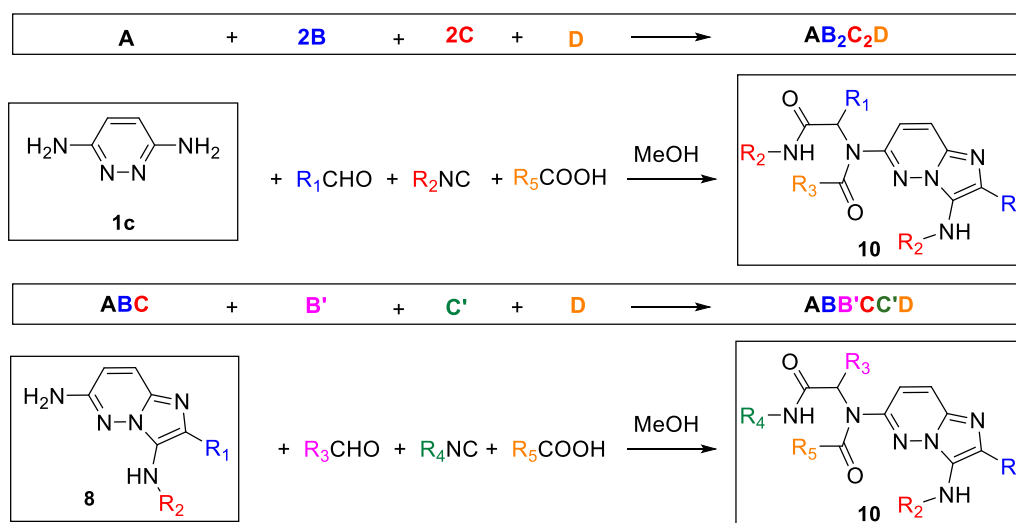
General Procedure B: A solution of 2,4-Diaminopyrimidine (1 mmol, 1 eq) and aldehyde (2 mmol, 2 eq) in ACN (2 mL) was transferred to a microwave reactor tube followed by the addition of Yb(OTf)₃ (0.2 mmol, 0.2 eq) at room temperature. After 10 min, the suitable isocyanide (2 mmol, 2 eq) was added to the stirring reaction mixture, the vessel sealed and heated by microwave irradiation to 100°C for 60-90 min. After reaction completion was confirmed by TLC or HPLC, the solvent was evaporated and

DCM was added until everything was dissolved. The mixture was treated with saturated NaHCO_3 aqueous solution to pH 8. The organic layer was separated, dried over MgSO_4 and evaporated under reduced pressure. The pure product was obtained by flash chromatography (DCM/MeOH or EtOAc/Hexane as eluent).

General Procedure C: A solution of 2,4-diaminopyrimidine (1 mmol, 1 eq) and aldehyde (2 mmol, 2 eq) in DMF (2 mL) was transferred to a microwave reactor tube followed by the addition of PTSA (0.2 mmol, 0.2 eq) at room temperature. After 10 min, the suitable isocyanide (2 mmol, 2 eq) was added to the stirring reaction mixture, the vessel sealed and heated by microwave irradiation to 150°C for 90 min. After reaction completion was confirmed by TLC or HPLC, the mixture was treated with saturated NaHCO_3 aqueous solution to pH 8 and extracted with DCM (3 x 5 mL). The combined organic layer was washed with 5% aqueous LiCl (4 x 5 mL) and then with brine (3 x 5 mL), dried over MgSO_4 and evaporated under reduced pressure. The pure product was obtained by flash chromatography (DCM/MeOH or EtOAc/Hexane as eluent).

General Procedure D: A solution of compound **1** (1 mmol, 1 eq) and aldehyde (1 mmol, 1 eq) in DMF (2 mL) was transferred to a microwave reactor tube followed by the addition of PTSA (0.2 mmol, 0.2 eq) at room temperature. After 10 min, the suitable isocyanide (1 mmol, 1 eq) was added to the stirring reaction mixture, the vessel sealed and heated by microwave irradiation to 150°C for 90 min. After reaction completion was confirmed by TLC or HPLC, the mixture was treated with saturated NaHCO_3 solution to pH 8 and extracted with DCM (3 x 5 mL). The combined organic layer was washed with 5% aqueous LiCl (4 x 5 mL) and then with brine (3 x 5 mL), dried over MgSO_4 and evaporated under reduced pressure. The pure product was obtained by flash chromatography (DCM/MeOH or EtOAc/Hexane as eluent).

Procedure for the Synthesis of GBB-Ugi adducts (**10**)



Synthesis of N-(tert-butyl)-2-(N-(3-(tert-butylamino)-2-(4-methoxyphenyl)imidazo[1,2-b]pyridazin-6-yl)acetamido)-2-(4-methoxyphenyl)acetamide (10a)

The *p*-anisaldehyde (1 mmol, 2 eq), 3,6-diaminopyridazine **1c** (0.5 mmol, 1 eq) and *tert*-butyl isocyanide (1 mmol, 2 eq) were dissolved in MeOH (3mL). Glacial acetic acid (4eq) was added. The reaction mixture was stirred at 80°C overnight. The reaction mixture was concentrated under vacuum. The residue was taken up in KHCO₃, extracted with EtOAc (x3), dried with MgSO₄, filtered and concentrated under vacuum. The resultant residue was purified by flash column chromatography (DCM/MeOH) to afford the pure product.

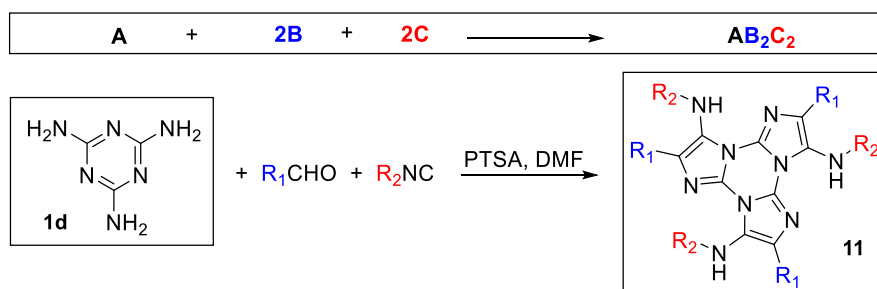
Synthesis of N-(tert-butyl)-2-(N-(2-(4-chlorophenyl)-3-(cyclohexylamino)imidazo[1,2-b]pyridazin-6-yl)acetamido)-2-(4-methoxyphenyl)acetamide (10b)

A solution of **8b** (0.29 mmol, 1 eq, 100 mg) in dry MeOH (1 mL) was treated, in the following order, with *p*-anisaldehyde (0.35 mmol, 1.2 eq, 43 µL), acetic acid (1.45 mmol, 5 eq, 83 µL) and *tert*-butyl isocyanide (0.35 mmol, 1.2 eq, 39 µL). The reaction mixture was stirred for 48 h at 80°C. After reaction completion was confirmed by TLC or HPLC, the solvent was evaporated, the crude was treated with saturated NaHCO₃ aqueous solution to pH 8 and extracted with DCM (3 x 5 mL). The combined organic layer was washed with brine, dried over MgSO₄ and evaporated. The pure product was obtained by flash chromatography (EtOAc/Hexane 60:40 as eluent).

Synthesis of N-(tert-butyl)-2-(2-chloro-N-(2-(4-chlorophenyl)-3-(cyclohexylamino)imidazo[1,2-b]pyridazin-6-yl)acetamido)-2-(4-methoxyphenyl)acetamide (11c)

A solution of **8b** (0.29 mmol, 1 eq, 100 mg) in dry MeOH (1 mL) was treated, in the following order, with *p*-anisaldehyde (0.35 mmol, 1.2 eq, 43 µL), PTSA (0.029 mmol, 0.1 eq, 6 mg), chloroacetic acid (0.44 mmol, 1.5 eq, 42 mg) and *tert*-butyl isocyanide (0.35 mmol, 1.2 eq, 39 µL). The reaction mixture was stirred for 48 h at 80°C. After reaction completion was confirmed by TLC or HPLC, the solvent was evaporated, the crude was treated with saturated NaHCO₃ solution to pH 8 and extracted with DCM (3 x 5 mL). The combined organic layer was washed with brine, dried over MgSO₄ and evaporated to dryness. The pure product was obtained by flash chromatography (EtOAc/Hexane 40:60 as eluent).

General Procedure for the Synthesis of Triple GBB Adducts (11)



General Procedure E: Melamine **1d** (0.5 mmol, 1 eq) was suspended in 1 ml of DMF in a Schlenk tube. The appropriate aldehyde (2 mmol, 4 eq), PTSA (0.1 mmol, 0.2 eq) and finally the suitable isocyanide (2.5 mmol, 5 eq) was added to the stirring reaction mixture at room temperature; The tube was sealed and heated to 130 °C overnight. After reaction completion was confirmed by TLC or HPLC, the reaction mixture was concentrated to a syrup consistency. The pure product was obtained by precipitation using ether and in some cases methanol.

Synthesis of 1-(tert-butylamino)-7-cyclohexyl-2-(4-methoxyphenyl)imidazo[1'',2'':3',4']pyrimido[2',1':2,3]imidazo[4,5-c]isoquinolin-8(7H)-one (12)

A solution of compound **4d** (0.33 mmol, 1 eq, 120 mg) and *p*-anisaldehyde (0.33 mmol, 1 eq, 40 μL) in DMF (0.5 mL) was transferred to a microwave reactor tube followed by the addition of PTSA (0.066 mmol, 0.2 eq, 13 mg) at room temperature. After 10 min, the tert-butyl isocyanide (0.33 mmol, 1 eq, 37 μL) was added to the stirring reaction mixture, the vessel sealed and heated by microwave irradiation to 150 °C for 2 h. After reaction completion was confirmed by TLC or HPLC, the mixture was treated with saturated NaHCO₃ solution to pH 8 and extracted with DCM (3 x 5 mL). The combined organic layer was washed with 5% aqueous LiCl (4 x 5 mL) and then with brine (3 x 5 mL), dried over MgSO₄ and evaporated under reduced pressure. The pure product was obtained by using column chromatography (EtOAc/ Hexane 50:50 + 1% MeOH as eluent).

Synthesis of 4,4'-(3,9-bis(cyclohexylamino)diimidazo[1,2-a:1',2'-c]pyrimidine-2,8-diyl)bis(1-methylpyridin-1-ium) iodide (13)

A solution of compound **5b** (0.05 mmol, 1eq, 25 mg) in MeOH (0.5 mL) was treated with iodomethane (0.2 mmol, 4 eq, 13 μL). The reaction mixture was stirred for 3 h at room temperature. The solvent was evaporated and the crude was triturated by Et₂O/DCM to afford the pure compound **13**.

Synthesis of double GBB-Buchwald adduct (14)

Compound **5f** was synthesized through *General Procedure C*. The resultant residue from the work up was analyzed by HPLC MS and NMR. As the crude mixture was directly subject to the Buchwald–Hartwig amination process without further purification. The procedure reported by Chauhan et al.⁸ was applied as follows: Compound **5f** (0.2 mmol, 1 eq), the CuI (20 mol %), 1,10-phenanthroline (20 mol %), were placed in a dry Schlenk tube which was purged with argon. DMF (1 mL) was added and the tube was sealed. The solution was stirred and heated at 120 °C overnight. After completion of the reaction as indicated by HPLC, the mixture was cooled to room temperature and filtered through a pad of Celite. The Celite was rinsed with DCM. The solvent was evaporated under reduced pressure using toluene, and the residue was purified by flash column chromatography on silica gel (eluent: DCM) to afford the pure product.

Synthesis of 1-(tert-butyl)-4-(2-(4-chlorophenyl)-3-(cyclohexylamino)imidazo[1,2-b]pyridazin-6-yl)-3-(4-methoxyphenyl)piperazine-2,5-dione (15)

A solution of the Ugi adduct **10c** (0.09 mmol, 1 eq, 60 mg) and Cs₂CO₃ (0.18 mmol, 2 eq, 60 mg) in DMF (2 mL) was stirred for 3 h at room temperature. The reaction was quenched with 5 mL of saturated NH₄Cl aqueous solution and extracted with DCM (3 x 5 mL). The combined organic layer was washed with 5% aqueous LiCl (4 x 5 mL) and then with brine (3 x 5 mL), dried over MgSO₄ and evaporated under reduced pressure. The crude was crystallized from diethyl ether to afford pure 2,5-diketopiperazine **14**.

Synthesis of triple GBB-Buchwald adduct (16)

The procedure reported by Chauhan et al.⁹ was applied as follows: Compound **11b** (0.5 mmol, 1 eq), the CuI (30 mol %), 1,10-phenanthroline (30 mol %), were placed in a dry Schlenk tube which was purged with argon. DMF (2 mL) was added and the tube was sealed. The solution was stirred and heated at 120 °C overnight. After completion of the reaction as indicated by HPLC, the mixture was cooled to room temperature and filtered through a pad of Celite. The Celite was rinsed with DCM. The solvent was evaporated under reduced pressure using toluene, and the residue was purified by flash column chromatography on silica gel (eluent: DCM) to afford the pure product.

⁸ Tyagi, V., Khan, S., Bajpai, V., Gauniyal, H. M., Kumar, B., & Chauhan, P. M. (2012). Skeletal diverse synthesis of N-fused polycyclic heterocycles via the sequence of Ugi-type MCR and cui-catalyzed coupling/tandem Pictet–Spengler reaction. *The Journal of organic chemistry*, 77(3), 1414-1421.

⁹ Tyagi, V., Khan, S., Bajpai, V., Gauniyal, H. M., Kumar, B., & Chauhan, P. M. (2012). Skeletal diverse synthesis of N-fused polycyclic heterocycles via the sequence of Ugi-type MCR and cui-catalyzed coupling/tandem Pictet–Spengler reaction. *The Journal of organic chemistry*, 77(3), 1414-1421.

Procedure for the Synthesis of TripleGBB-Suzuki adducts (17)

The procedure reported by Lavilla et al.¹⁰ was applied as follows: A Schlenk vessel was charged with appropriate melamine adduct (**11c**, **11d**) (0.1 mmol, 1eq). After three argon/vacuum cycles, toluene (3 mL) was added. The appropriate boronic acid (0.6 mmol, 6 eq) was dissolved in ethanol (1 mL) and was added to the tube. A 2M water solution of Na₂CO₃ (1 mL, 2.0 mmol) was also added. The mixture was degassed and was stirred for 10 min. Pd(PPh₃)₄ (30%, 0.03 mmol) was added quickly under a flow of argon. Three more argon/vacuum cycles were made, and the mixture was stirred at 100 °C overnight. The mixture was cooled to room temperature and filtered through a celite pad, washing with DCM. The resulting solution was extracted with DCM (3x10 mL). The combined organic extracts were dried (Na₂SO₄) and filtered. The solvent was removed under reduced pressure and the residue was purified by column chromatography on silica (Hexanes/DCM) to yield the desired products.

Synthesis of N-cyclohexyl-2-(pyridin-2-yl)imidazo[1,2-a]pyridin-3-amine (18)

2-aminopyrimidine (1,06 mmol, 1 eq), picolinaldehyde (1,06 mmol, 1 eq) and cyclohexyl isocyanide (1,06 mmol, 1 eq) dissolved in acetonitrile (2 mL) in presence of ytterbium (III) trifluoromethanesulfonate (134 mg, 0,213 mmol) at 100°C in a microwave reactor for one hour. The reaction mixture was then washed with saturated NaHCO₃ (10 mL) and extracted three times with dichloromethane (3 x 15 mL). The organic layers were dried over MgSO₄ and were evaporated. The crude was purified via column chromatography in silica (CH₂Cl₂/MeOH) to afford the pure product.

Synthesis of MonoGBB-BODIPY adduct (19a)

Compound **17** (0.34 mmol, 1 eq) was dissolved in acetonitrile (5 mL). Na₂CO₃ (1.37 mmol, 4 eq) and BF₃·OEt₂ (574.05 mmol, 12 eq) were added. The mixture was set to reflux at 90°C for 48h. The reaction mixture was washed with saturated NaHCO₃ (15 mL) and extracted three times with dichloromethane (3 x 20 mL). The organic layers were dried over MgSO₄ and evaporated. The crude was purified via column chromatography in silica (DCM/MeOH) to afford the desired product.

Synthesis of DoubleGBB-BODIPY adduct (19b)

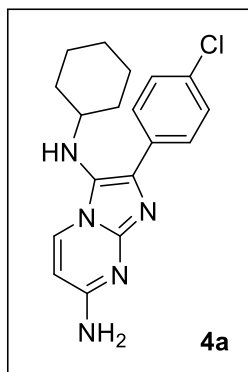
Compound **5d** (0.2 mmol, 1 eq) was dissolved in acetonitrile (5 mL), sodium carbonate anhydrous (1.58 mmol, 8 eq) and boron trifluoride diethyl etherate (4.47 mmol, 22 eq) were added to the solution. The reaction mixture was heated to reflux at 100°C for 48 hours. The solvent was evaporated and the

¹⁰ Kielland, N., Vicente-García, E., Revés, M., Isambert, N., Arévalo, M. J., & Lavilla, R. (2013). Scope and Post-Transformations for the Borane-Isocyanide Multicomponent Reactions: Concise Access to Structurally Diverse Heterocyclic Compounds. *Advanced Synthesis & Catalysis*, 355(16), 3273-3284.

residue washed with NaHCO_3 (sat) and extracted with DCM (3x20 mL). The resulting organic phase was dried over MgSO_4 and evaporated under reduced pressure. The crude was then purified via column chromatography on silica (Hexanes/DCM) to afford the desired product.

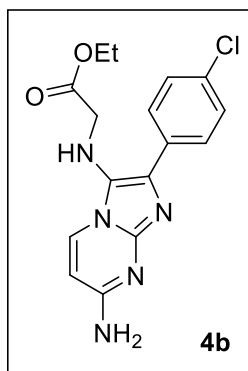
Characterization data

2-(4-chlorophenyl)- N^3 -cyclohexylimidazo[1,2-a]pyrimidine-3,7-diamine (4a)



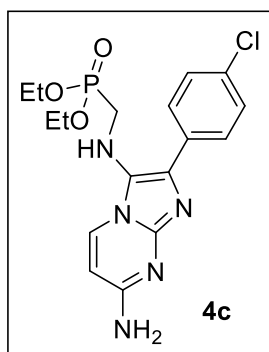
Compound **4a** was obtained as an ivory powder (80%). $^1\text{H NMR}$ (400 MHz, DMSO) δ = 8.20 (d, $J=7.3$, 1H), 8.11 (d, $J=8.7$, 2H), 7.43 (d, $J=8.6$, 2H), 6.86 (s, 2H), 6.30 (d, $J=7.3$, 1H), 4.59 (d, $J=5.4$, 1H), 2.80 – 2.64 (m, 1H), 1.79 – 1.44 (m, 5H), 1.28 – 1.01 (m, 5H). $^{13}\text{C NMR}$ (100 MHz, DMSO) δ = 158.20, 145.00, 133.48, 131.61, 130.51, 129.79, 128.07, 127.67, 123.08, 99.81, 56.64, 33.41, 25.42, 24.46. **HRMS (ESI)**: m/z calculated for $\text{C}_{18}\text{H}_{21}\text{ClN}_5^+$ [$\text{M} + \text{H}$] $^+$: 342.1480, found 342.1484.

Ethyl 2-((7-amino-2-(4-chlorophenyl)imidazo[1,2-a]pyrimidin-3-yl)amino)acetate (4b)



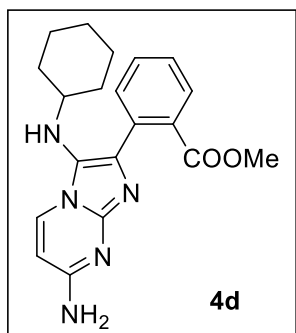
Compound **4b** was obtained as a yellow powder (23%). $^1\text{H NMR}$ (400 MHz, DMSO) δ = 8.34 (d, $J=7.3$, 1H), 8.06 – 8.01 (m, 2H), 7.47 – 7.39 (m, 2H), 6.80 (s, 2H), 6.29 (d, $J=7.3$, 1H), 5.16 (t, $J=6.1$, 1H), 4.00 (q, $J=7.1$, 2H), 3.71 (d, $J=6.1$, 2H), 1.09 (t, $J=7.1$, 3H). $^{13}\text{C NMR}$ (100 MHz, DMSO) δ = 171.73, 158.07, 144.98, 133.49, 132.13, 130.53, 128.91, 128.21, 127.52, 123.60, 99.24, 60.29, 49.03, 13.94. **IR (KBr)** $\ddot{\nu}$ (cm^{-1}): 3433, 2250, 2124, 1646, 1468, 1379, 1205, 1056, 1028, 1008, 823, 760. **HRMS (ESI)**: m/z calculated for $\text{C}_{16}\text{H}_{17}\text{ClN}_5\text{O}_2^+$ [$\text{M} + \text{H}$] $^+$: 346.1066, found 346.1074.

Diethyl (((7-amino-2-(4-chlorophenyl)imidazo[1,2-a]pyrimidin-3-yl)amino)methyl)phosphonate (4c)



Compound **4c** was obtained as a yellow powder (30%). $^1\text{H NMR}$ (400 MHz, CD_3OD) δ = 8.30 (d, $J=7.4$, 1H), 7.98 (d, $J=8.6$, 2H), 7.43 (d, $J=8.6$, 2H), 6.39 (d, $J=7.4$, 1H), 4.01 (p, $J=7.1$, 4H), 3.41 (d, $J=9.9$, 2H), 1.21 (t, $J=7.1$, 6H). $^{13}\text{C NMR}$ (100 MHz, CD_3OD) δ = 160.57, 147.44, 133.81, 133.22, 129.81, 129.60, 129.41, 129.31, 129.28, 100.84, 63.70, 63.64, 44.48, 16.58, 16.52. **IR (KBr)** $\ddot{\nu}$ (cm^{-1}): 3327, 3207, 2958, 2925, 2854, 1728, 1650, 1519, 1467, 1403, 1259, 1092, 1025, 803. **HRMS (ESI)**: m/z calculated for $\text{C}_{17}\text{H}_{22}\text{ClN}_5\text{O}_3\text{P}^+$ [$\text{M} + \text{H}$] $^+$: 410.1144, found 410.1151.

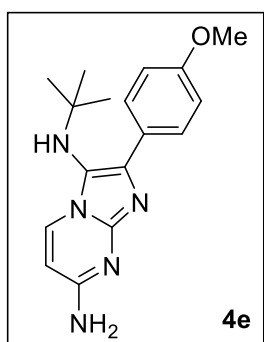
Methyl 2-(7-amino-3-(cyclohexylamino)imidazo[1,2-a]pyrimidin-2-yl)benzoate (4d)



Compound **4d** was obtained as a pale brown powder (37%). $^1\text{H NMR}$ (400 MHz, DMSO) δ = 8.19 (d, $J=7.3$, 1H), 7.85 (d, $J=7.7$, 1H), 7.57 – 7.51 (m, 2H), 7.34 (m, 1H), 6.79 (s, 2H), 6.30 (d, $J=7.3$, 1H), 4.29 (d, $J=4.5$, 1H), 3.65 (s, 3H), 2.64 (s, 1H), 1.63 – 1.36 (m, 5H), 1.05 – 0.99 (m, 5H). $^{13}\text{C NMR}$ (100 MHz, DMSO) δ = 206.49, 169.47, 157.68, 144.73, 131.96, 131.54, 130.07, 129.41, 129.37, 128.22, 126.33, 122.65, 99.47, 56.10, 51.83, 32.91, 25.45, 24.11. **IR (KBr)** $\ddot{\nu}$ (cm^{-1}): 3336, 3209, 2926, 2853, 1719, 1654, 1648, 1597,

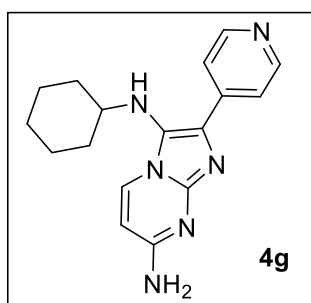
1560, 1542, 1522, 1508, 1466, 1378, 1287.

N^3 -(tert-butyl)-2-(4-methoxyphenyl)imidazo[1,2-a]pyrimidine-3,7-diamine (4e)



Compound **4e** was obtained as a yellow powder (93%). $^1\text{H NMR}$ (400 MHz, DMSO) δ = 8.21 (d, $J=7.4$, 1H), 8.01 (d, $J=8.8$, 2H), 6.91 (d, $J=8.8$, 2H), 6.65 (s, 2H), 6.22 (d, $J=7.3$, 1H), 4.32 (s, 1H), 3.77 (s, 3H), 0.98 (s, 8H). **IR (KBr)** $\ddot{\nu}$ (cm^{-1}): 3342, 3148, 2966, 2836, 1651, 1508, 1466, 1296, 1273, 1247, 1221, 1177. **HRMS (ESI)**: m/z calculated for $\text{C}_{17}\text{H}_{22}\text{N}_5\text{O}^+$ [$\text{M} + \text{H}$] $^+$: 312.1819, found 312.1816.

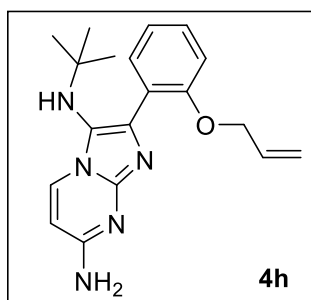
N^3 -cyclohexyl-2-(pyridin-4-yl)imidazo[1,2-a]pyrimidine-3,7-diamine (4g)



Compound **4g** was obtained as a yellow powder (93%). $^1\text{H NMR}$ (400 MHz, $\text{D}_2\text{O}/\text{CF}_3\text{COOD}$) δ = 9.03 – 8.96 (m, 2H), 8.78 (d, $J=7.1$, 1H), 8.56 – 8.50 (m, 2H), 8.45 – 8.38 (m, 2H), 6.81 (d, $J=7.7$, 1H), 3.05 (m, 1H), 1.90 (m, 2H), 1.69 (m, 2H), 1.57 (m, 1H), 1.18 (m, 5H). N-H overlapped with solvent signal (D_2O). $^{13}\text{C NMR}$ (100 MHz, $\text{D}_2\text{O}/\text{CF}_3\text{COOD}$) δ = 163.89, 146.64, 144.12, 142.77, 134.12, 133.37, 128.71, 123.84, 106.28, 59.34,

35.07, 26.55, 26.16.

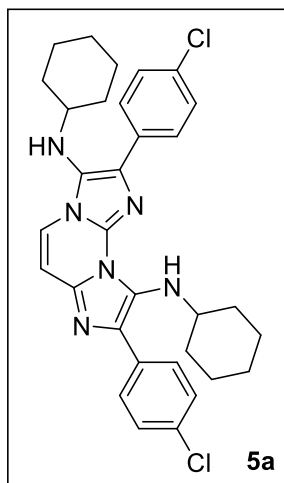
2-(2-(allyloxy)phenyl)- N^3 -(tert-butyl)imidazo[1,2-a]pyrimidine-3,7-diamine (4h)



Compound **4h** was obtained as a yellow foam (54%). $^1\text{H NMR}$ (400 MHz, CDCl_3) δ = 8.13 (d, $J=7.3$, 1H), 7.81 (dd, $J=7.6$, 1.8, 1H), 7.29 – 7.22 (m, 1H), 7.04 (m, 1H), 6.95 (dd, $J=4.6$, 3.9, 1H), 6.37 (d, $J=7.4$, 1H), 6.22 (s, 2H), 6.10 – 5.97 (m, 1H), 5.41 – 5.27 (m, 2H), 4.55 (d, $J=5.6$, 2H), 3.69 (s; 1H), 0.89 (s, 9H). $^{13}\text{C NMR}$ (100 MHz, CDCl_3) δ = 158.55, 154.84, 145.69, 132.94, 131.82, 131.75, 130.91, 128.87, 123.93, 123.34, 121.77, 118.96,

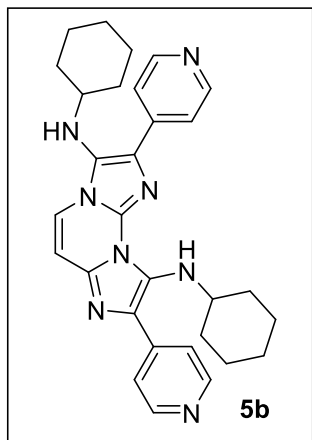
112.80, 100.42, 70.15, 55.68, 29.83. IR (KBr) \ddot{u} (cm^{-1}): 3341, 3183, 2967, 1667, 1644, 1538, 1471, 1362, 1225, 1031, 995.

2,8-bis(4-chlorophenyl)- N^3, N^9 -dicyclohexyldiimidazo[1,2-a:1',2'-c]pyrimidine-3,9-diamine (5a)



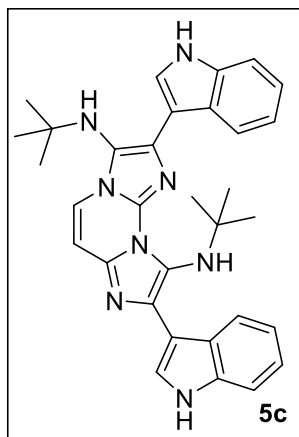
According to procedure B, compound **5a** was obtained as a pink powder (70%). $^1\text{H NMR}$ (400 MHz, CDCl_3) δ = 7.98 (dd, J = 11.6, J = 8.6, 4H), 7.59 (d, J = 7.7, 1H), 7.43 (dd, J = 14, 8.6, 4H), 6.91 (d, J = 7.7, 1H), 5.64 (d, J = 9.4, 1H), 3.23 – 3.11 (m, 1H), 2.98 (m, 2H), 1.88 (m, 4H), 1.75 (m, 4H), 1.65 (m, 1H), 1.54 (m, 1H), 1.41 – 1.15 (m, 10H). $^{13}\text{C NMR}$ (100 MHz, CDCl_3) δ = 135.43, 134.70, 132.78, 132.71, 132.19, 132.16, 131.02, 129.87, 128.76, 128.44, 127.81, 127.34, 124.70, 119.24, 103.04, 57.34, 55.90, 34.17, 33.77, 25.72, 25.60, 24.77, 24.60. IR (KBr) \ddot{u} (cm^{-1}): 3316, 3055, 2297, 2852, 1627, 1594, 1488, 1448, 1403, 1091, 833. HRMS(ESI): m/z calculated for $\text{C}_{32}\text{H}_{35}\text{Cl}_2\text{N}_6^+$ [$\text{M} + \text{H}$] $^+$: 573.2295, found 573.2312.

N^3, N^9 -dicyclohexyl-2,8-di(pyridin-4-yl)diimidazo[1,2-a:1',2'-c]pyrimidine-3,9-diamine (5b)



According to procedure A, compound **5b** was obtained as a yellow powder (62%). $^1\text{H NMR}$ (400 MHz, CDCl_3) δ = 8.66 (ddd, J = 16.7, 4.7, 1.5, 4H), 7.90 – 7.84 (m, 4H), 7.58 (d, J = 7.8, 1H), 6.89 (d, J = 7.7, 1H), 5.76 (d, J = 9.9, 1H), 3.27 – 3.15 (m, 1H), 3.07 (d, J = 5.2, 1H), 3.03 – 2.97 (m, 1H), 1.75 (m, 10H), 1.46 – 1.14 (m, 10H). $^{13}\text{C NMR}$ (100 MHz, CDCl_3) δ = 150.21, 149.82, 141.94, 140.97, 135.84, 135.02, 133.53, 127.99, 127.33, 126.18, 120.61, 120.11, 119.49, 103.94, 57.70, 56.33, 34.34, 33.98, 25.70, 25.60, 24.89, 24.69. IR (KBr) \ddot{u} (cm^{-1}): 3302, 3029, 2927, 2852, 1629, 1599, 1448, 1322, 1144, 1091, 990, 833. HRMS (ESI): m/z calculated for $\text{C}_{30}\text{H}_{35}\text{N}_8^+$ [$\text{M} + \text{H}$] $^+$: 507.2980, found 507.2979.

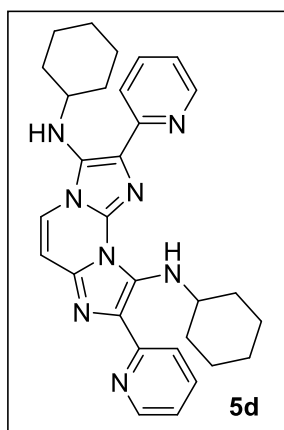
N³,N⁹-di-tert-butyl-2,8-di(1H-indol-3-yl)diimidazo[1,2-a:1',2'-c]pyrimidine-3,9-diamine (5c)



According to procedure A, compound **5c** was obtained as a pale brown powder (86%). ¹H NMR (400 MHz, DMSO) δ = 11.24 (s, 1H), 11.19 (s, 1H), 8.44 (d, J=7.7, 1H), 8.35 (d, J=7.4, 1H), 8.07 (d, J=2.5, 1H), 7.99 (d, J=7.7, 1H), 7.87 (d, J=2.4, 1H), 7.42 (dd, J= 11.3, 8.0, 2H), 7.17 – 7.05 (m, 4H), 6.99 (d, J=7.7, 1H), 5.06 (s, 1H), 4.67 (s, 1H), 1.07 (s, 18H). ¹³C NMR (100 MHz, DMSO) δ = 136.80, 136.01, 135.96, 134.62, 132.78, 129.76, 126.17, 125.89, 125.73, 124.38, 124.32, 122.09, 121.77, 121.39, 121.19, 121.06, 120.99, 118.74, 118.67, 111.44, 111.30, 110.10, 108.88, 101.47, 56.89, 55.26, 30.02, 29.37. IR (KBr) $\ddot{\nu}$ (cm⁻¹): 3407, 2964, 1693, 1621, 1567, 1453,

1388, 1334, 1239, 1194, 742. HRMS (ESI): m/z calculated for C₃₂H₃₅N₈⁺ [M + H]⁺: 531.2980, found 531.2981.

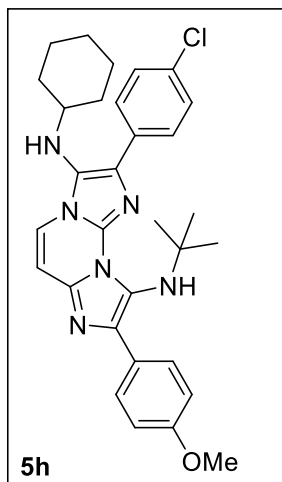
N³,N⁹-dicyclohexyl-2,8-di(pyridin-2-yl)diimidazo[1,2-a:1',2'-c]pyrimidine-3,9-diamine (5d)



According to procedure B, compound **5d** was obtained as a pale brown powder (97%). ¹H NMR (400 MHz, CDCl₃) δ = 8.60 – 8.56 (m, 1H), 8.52 – 8.49 (m, 1H), 8.06 (d, J=8.0, 1H), 7.99 (d, J=8.0, 1H), 7.75- 7.69 (m, 3H), 7.5 (d, J=7.7, 1H), 7.11-7.06 (m, 2H), 6.83 (d, J= 7.7, 1H), 6.15 (d, J=9.9, 1H), 4.10 (m, 1H), 3.06 (m, 1H), 2.13 (m, 2H), 1.95 (m, 2H), 1.81 – 1.71 (m, 5H), 1.25 (m, 11H). ¹³C NMR (100 MHz, CDCl₃) δ = 155.05, 154.79, 148.36, 136.48, 136.37, 135.99, 135.34, 133.37, 131.88, 126.71, 124.35, 120.45, 120.41, 120.04, 120.02, 119.47, 103.43, 57.21, 56.95, 34.11, 34.07, 26.12, 25.88, 25.22, 25.09. IR (KBr) $\ddot{\nu}$ (cm⁻¹): 3265, 3050, 2927, 2852, 1632, 1607, 1590,

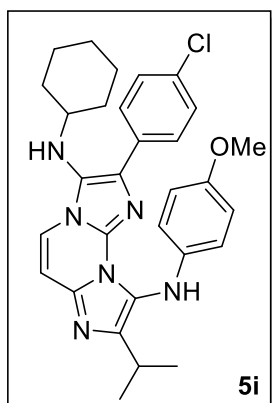
1481, 1448, 1411, 1290, 1263, 1180, 1087, 891, 789, 740. HRMS (ESI): m/z calculated for C₃₀H₃₅N₈⁺ [M + H]⁺: 507.2980, found 507.3001.

N⁹-(tert-butyl)-2-(4-chlorophenyl)-N³-cyclohexyl-8-(4-methoxyphenyl) diimidazo[1,2-a:1',2'-c]pyrimidine-3,9-diamine (5h)



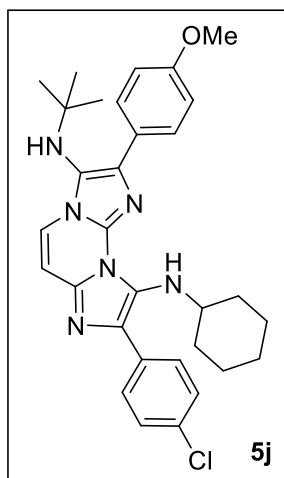
According to procedure C, compound **5h** was obtained as a yellow powder (50%). ¹H NMR (400 MHz, CD₃OD) δ = 8.10 (d, J= 8.8, 2H), 7.98 (d, J= 8.6, 2H), 7.60 (d, J=7.6, 1H), 6.94 (d, J= 8.9, 2H), 6.90 (d, J=7.6, 1H), 4.87 (s, 1H), 3.85 (s, 3H), 2.95 (m, 2H), 1.86 (m, 2H), 1.77 – 1.69 (m, 2H), 1.62 (m, 1H), 1.29 – 1.17 (m, 5H), 1.14 (s, 9H). ¹³C NMR (100 MHz, CD₃OD) δ = 153.98, 144.41, 140.23, 137.74, 134.54, 132.73, 132.48, 130.58, 128.77, 127.64, 124.66, 122.52, 119.81, 116.59, 114.79, 103.27, 57.52, 55.82, 34.29, 26.17, 25.77, 24.91, 22.32. IR (KBr) $\ddot{\nu}$ (cm⁻¹): 3320, 3091, 2929, 2854, 1627, 1612, 1507, 1491, 1441, 1390, 1246, 1173, 1091, 1012, 835. HRMS (ESI): m/z calculated for C₃₁H₃₆ClN₆O⁺ [M + H]⁺: 543.2634, found 543.2638.

2-(4-chlorophenyl)-N³-cyclohexyl-8-isopropyl-N⁹-(4-methoxyphenyl) diimidazo[1,2-a:1',2'-c]pyrimidine-3,9-diamine (5i)



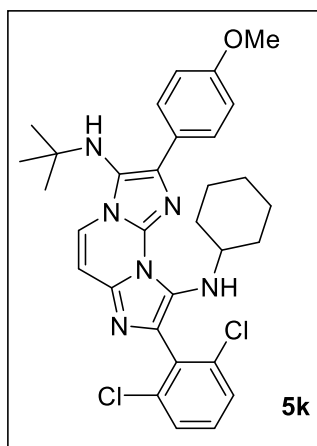
According to procedure C, compound **5i** was obtained as a white powder (57%). ¹H NMR (400 MHz, CDCl₃) δ = 7.86 – 7.78 (m, 2H), 7.61 (d, J=7.7, 1H), 7.39 – 7.34 (m, 2H), 6.92 (d, J=7.6, 1H), 6.85-6.76 (m, 4H), 6.32 (s, 1H), 3.75 (s, 3H), 3.17 – 3.05 (m, 1H), 2.91 (m, 2H), 1.81 (m, 2H), 1.68 (m, 3H), 1.36 (s, 3H), 1.34 (s, 3H), 1.28 – 1.12 (m, 5H). ¹³C NMR (100 MHz, CDCl₃) δ = 153.98, 144.41, 140.22, 137.74, 134.54, 132.73, 132.47, 130.57, 128.77, 127.64, 124.66, 122.52, 119.80, 116.59, 114.78, 103.26, 57.52, 55.81, 34.28, 26.16, 25.76, 24.90, 22.32. IR (KBr) $\ddot{\nu}$ (cm⁻¹): 3355, 3240, 2961, 2929, 2854, 1630, 1607, 1508, 1449, 1390, 1235, 1091, 821. HRMS (ESI): m/z calculated for C₃₀H₃₄ClN₆O⁺ [M + H]⁺: 529.2478, found 529.2480.

N³-(tert-butyl)-8-(4-chlorophenyl)-N⁹-cyclohexyl-2-(4-methoxyphenyl) diimidazo[1,2-a:1',2'-c]pyrimidine-3,9-diamine (5j)



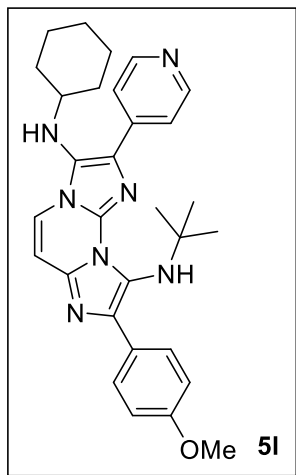
According to procedure C, compound **5j** was obtained as an almond powder (40%). ¹H NMR (400 MHz, CDCl₃) δ = 7.98 (d, J=8.6, 2H), 7.85 (d, J=8.8, 2H), 7.65 (d, J=7.7, 1H), 7.39 (d, J=8.6, 2H), 6.99 (d, J=8.8, 2H), 6.82 (d, J=7.7, 1H), 5.70 (d, J=9.1, 1H), 3.16 (m, 1H), 2.99 (s, 1H), 1.87 (m, 2H), 1.72 (m, 2H), 1.52 (m, 1H), 1.35 (m, 2H), 1.20 (m, 4H), 1.10 (s, 9H). ¹³C NMR (100 MHz, CDCl₃) δ = 159.00, 135.82, 135.20, 133.44, 133.34, 132.07, 131.16, 128.74, 128.53, 127.96, 127.87, 127.08, 122.53, 120.11, 113.91, 102.56, 56.12, 55.43, 33.90, 30.55, 25.91, 24.82. IR (KBr) $\tilde{\nu}$ (cm⁻¹): 3306, 3068, 2929, 2854, 1627, 1597, 1512, 1488, 1450, 1394, 1248, 1173, 1090, 836, 738.

N³-(tert-butyl)-N⁹-cyclohexyl-8-(2,6-dichlorophenyl)-2-(4-methoxyphenyl) diimidazo[1,2-a:1',2'-c]pyrimidine-3,9-diamine (5k)



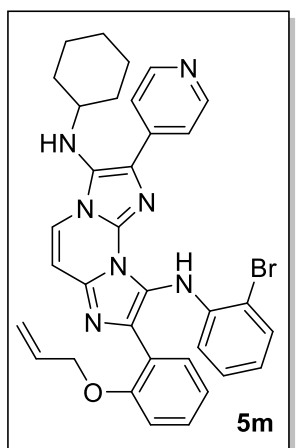
According to procedure C, compound **5k** was obtained as a pale brown powder (32%). ¹H NMR (400 MHz, CDCl₃) δ = 7.83 (d, J=8.9, 2H), 7.57 (d, J=7.7, 1H), 7.42 – 7.39 (m, 2H), 7.27 (m, 1H), 6.97 (d, J=8.8, 1H), 6.79 (d, J=7.8, 1H), 3.86 (s, 3H), 2.87 – 2.72 (m, 1H), 1.83 (m, 1H), 1.64 (m, 10H – water signal overlapped), 1.45 – 1.38 (m, 1H), 1.25 (s, 3H), 1.10 (s, 9H). ¹³C NMR (100 MHz, CDCl₃) δ = 158.90, 137.77, 135.76, 133.94, 133.68, 132.93, 129.80, 128.73, 127.84, 127.19, 123.42, 122.53, 118.90, 113.87, 110.16, 103.18, 56.14, 55.43, 53.28, 33.84, 30.52, 25.83, 24.52.

N⁹-(tert-butyl)-N³-cyclohexyl-8-(4-methoxyphenyl)-2-(pyridin-4-yl)diimidazo[1,2-a:1',2'-c]pyrimidine-3,9-diamine (5l)



According to procedure C, compound **5l** was obtained as a yellow powder (50%). ¹H NMR (400 MHz, CDCl₃) δ = 8.67 (m, 2H), 8.09 (d, J=8.4, 2H), 7.93 (m, 2H), 7.59 (d, J=7.6, 1H), 6.98 – 6.89 (m, 3H), 4.82 (m, 1H), 3.03 (m, 2H), 1.81 (m, 6H), 1.35 – 1.24 (m, 6H- Et₂O signals overlapped), 1.15 (s, 9H), 0.87 (m, 2H). ¹³C NMR (100 MHz, CDCl₃) δ = 158.99, 150.10, 141.57, 136.98, 135.97, 135.48, 129.17, 128.21, 128.06, 127.60, 127.09, 120.30, 119.33, 113.63, 104.04, 57.87, 57.73, 55.36, 34.44, 30.25, 25.73, 24.99. IR (KBr) $\ddot{\nu}$ (cm⁻¹): 3320, 3040, 2929, 2854, 1628, 1603, 1506, 1443, 1391, 1246, 1117, 1033, 836.

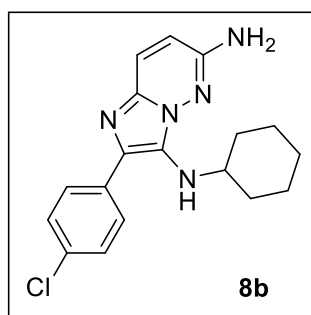
8-(2-(allyloxy)phenyl)-N⁹-(2-bromophenyl)-N³-cyclohexyl-2-(pyridin-4-yl)diimidazo[1,2-a:1',2'-c]pyrimidine-3,9-diamine (5m)



According to procedure C, compound **5m** was obtained as a yellow powder (13%). ¹H NMR (400 MHz, CDCl₃) δ = 8.59 (d, J=5.5, 2H), 7.97 (s, 1H), 7.86 – 7.81 (m, 2H), 7.75 (dd, J=7.6, 1.8, 1H), 7.66 (d, J=7.7, 1H), 7.52 (dd, J=7.9, 1.5, 1H), 7.05 (td, J=7.5, 1.0, 1H), 7.00 (d, J=7.7, 1H), 6.84 – 6.76 (m, 2H), 6.60 (ddd, J=7.9, 7.3, 1.5, 1H), 6.36 (dd, J=8.2, 1.5, 1H), 5.96 (ddt, J=17.3, 10.5, 5.3, 1H), 5.31 – 5.16 (m, 2H), 4.41 (d, J=5.3, 2H), 3.05 (d, J=5.0, 1H), 3.00 (m, 1H), 1.93 – 1.87 (m, 2H), 1.79 – 1.58 (m, 8H), 1.36 – 1.18 (m, 8H), 0.93 – 0.82 (m, 2H). ¹³C NMR (100 MHz, CDCl₃) δ = 155.78, 149.96, 141.32, 137.34, 133.51, 132.34, 131.09, 130.87, 129.43, 128.72, 127.60, 127.28,

123.97, 123.40, 121.07, 120.49, 120.36, 119.83, 117.75, 115.05, 112.36, 110.93, 103.95, 69.46, 57.84, 34.39, 25.73, 24.97.

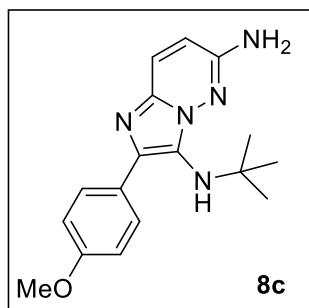
2-(4-chlorophenyl)-N³-cyclohexylimidazo[1,2-b]pyridazine-3,6-diamine (8b)



Compound **8b** was obtained as a yellow powder (50%). ¹H NMR (400 MHz, CDCl₃) δ = 8.05 – 8.01 (m, 2H), 7.60 (d, J=9.4, 1H), 7.41 – 7.38 (m, 2H), 6.38 (d, J=9.4, 1H), 4.38 (s, 2H), 3.68 (m, 1H), 3.09 (m, 1H), 1.85 – 1.51 (m, 5H), 1.25 – 1.13 (m, 5H). ¹³C NMR (100 MHz, CDCl₃) δ = 153.30, 133.94, 133.02, 132.67, 130.86, 130.70, 128.96, 128.05, 126.58, 109.49, 56.31, 34.62, 26.19, 25.35. IR (KBr) $\ddot{\nu}$ (cm⁻¹): 3312, 3176, 2927, 2853,

1625, 1548, 1489, 1090,802. **HRMS (ESI):** m/z calculated for C₁₈H₂₁ClN₅⁺ [M + H]⁺: 342.1480, found 342.1482.

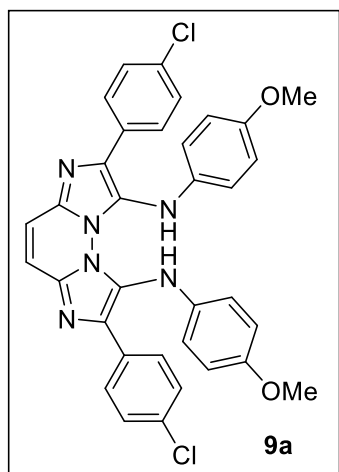
N³-(tert-butyl)-2-(4-methoxyphenyl)imidazo[1,2-b]pyridazine-3,6-diamine (8c)



Compound **8c** was obtained as a yellow powder (60%). **¹H NMR** (400 MHz, CDCl₃) δ = 8.11 – 8.06 (m, 2H), 7.62 (d, J=9.4, 1H), 6.94 (d, J= 8.9 2H), 6.40 (d, J=9.4, 1H), 4.35 (s, 2H), 3.84 (s, 3H), 1.10 (s, 9H). **¹³C NMR** (100 MHz, CDCl₃) δ = 159.06, 152.78, 137.04, 133.59, 128.99, 128.33, 127.97, 126.29, 113.77, 109.41, 57.29, 55.50, 30.65. **IR (KBr)** \ddot{u} (cm⁻¹): 3301, 3199, 2967, 2835, 1624, 1610, 1551, 1507, 1386, 1246, 1181.

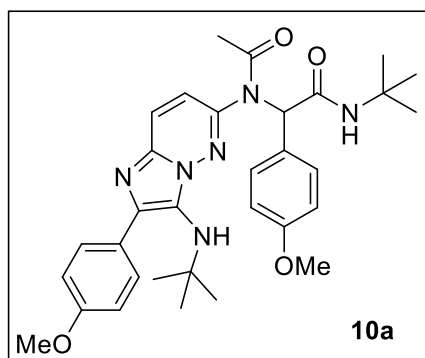
HRMS (ESI): **HRMS (ESI):** m/z calculated for C₁₇H₂₂N₅O⁺ [M + H]⁺: 312.1819, found 12.1822.

2,7-bis(4-chlorophenyl)-N¹,N⁸-bis(4-methoxyphenyl)diimidazo[1,2-b:2',1'-f]pyridazine-1,8-diamine (9a)



Compound **9a** was obtained as a dark green powder (38%). **¹H NMR** (400 MHz, CDCl₃) δ = 7.74 (d, J = 8.7 Hz, 4H), 7.46 (s, 2H), 7.25 (d, J = 8.7 Hz, 4H), 6.76 (d, J = 8.9 Hz, 4H), 6.47 (d, J = 8.9 Hz, 4H), 5.78 (s, 2H), 3.72 (s, 6H). **¹³C NMR** (101 MHz, CDCl₃) δ= 154.16, 137.94, 137.12, 135.80, 133.80, 131.00, 128.65, 128.12, 122.16, 117.32, 115.50, 114.73, 55.56. **HRMS (ESI):** m/z calculated for C₃₄H₂₇Cl₂N₆O₂⁺ [M + H]⁺: 621.1494, found 621.1510.

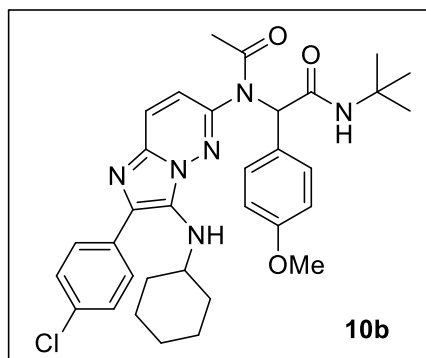
N-(tert-butyl)-2-(N-(3-(tert-butylamino)-2-(4-methoxyphenyl)imidazo[1,2-b]pyridazin-6-yl)acetamido)-2-(4-methoxyphenyl)acetamide (10a)



Compound **10a** was obtained as an orange powder (14%). **¹H NMR** (400 MHz, CDCl₃) δ = 8.11 – 8.03 (m, 2H), 7.61 (d, J = 9.3 Hz, 1H), 7.25 – 7.18 (m, 1H), 7.10 – 7.00 (m, 2H), 6.89 – 6.82 (m, 2H), 6.63 – 6.51 (m, 2H), 5.93 (s, 1H), 5.76 (s, 1H), 3.83 – 3.74 (m, 3H), 3.61 (s, 3H), 1.90 (s, 3H), 1.32 (s, 9H), 0.95 (d, J = 12.8 Hz, 9H). **¹³C NMR** (100 MHz, CDCl₃) δ = 170.40 (s), 168.83 (s), 159.59 (s), 159.37 (s), 148.97 (s), 139.69 (s), 134.57 (s), 131.40

(s), 128.99 (s), 127.83 (s), 127.11 (s), 125.61 (s), 125.11 (s), 118.30 (s), 114.00 (s), 113.56 (s), 64.36 (s), 56.94 (s), 55.19 (s), 55.10 (s), 51.79 (s), 30.34 (s), 28.69 (s), 23.25 (s).

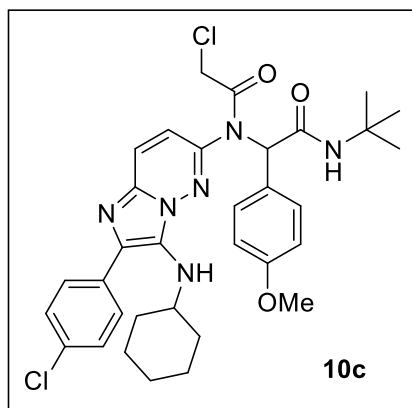
N-(tert-butyl)-2-(N-(2-(4-chlorophenyl)-3-(cyclohexylamino)imidazo[1,2-b]pyridazin-6-yl)acetamido)-2-(4-methoxyphenyl)acetamide (10b)



Compound **10b** was obtained as a yellow powder (77%). ¹H NMR (400 MHz, CDCl₃) δ = 8.05 (d, J=8.6, 2H), 7.66 (d, J=9.3, 1H), 7.40 (d, J=8.6, 2H), 7.27 (d, J=9.0, 1H), 7.13 (d, J=8.7, 2H), 6.66 (d, J=8.7, 2H), 5.98 (s, 1H), 5.80 (s, 1H), 3.67 (s, 3H), 3.57 (m, 1H), 2.97 (m, 1H), 1.99 (s, 3H), 1.68 (m, 8H), 1.39 (s, 9H), 1.16 (m, 2H). ¹³C NMR (100 MHz, CDCl₃) δ = 170.50, 168.95, 159.76, 149.61, 133.72, 133.46, 133.06, 132.68, 131.49,

130.81, 128.88, 128.03, 125.63, 125.54, 118.03, 114.06, 64.56, 56.22, 55.23, 52.00, 34.40, 28.84, 25.76, 25.09, 23.41. IR (KBr) $\ddot{\nu}$ (cm⁻¹): 3321, 3055, 2963, 2929, 2854, 1674, 1534, 1366, 1259, 1199, 1091, 1033, 836, 803. HRMS (ESI): m/z calculated for C₃₃H₄₀ClN₆O₃⁺ [M + H]⁺: 603.2845, found 603.2848.

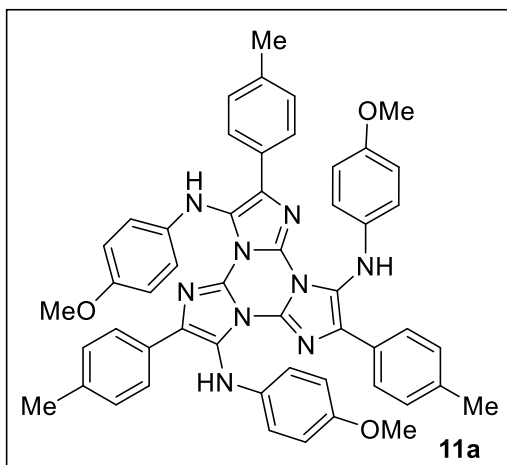
N-(tert-butyl)-2-(2-chloro-N-(2-(4-chlorophenyl)-3-(cyclohexylamino)imidazo[1,2-b]pyridazin-6-yl)acetamido)-2-(4-methoxyphenyl)acetamide (10c)



Compound **10c** was obtained as a yellow powder (61%). ¹H NMR (400 MHz, CDCl₃) δ = 8.05 (d, J=8.7, 2H), 7.67 (d, J=9.4, 1H), 7.41 (d, J=8.6, 2H), 7.33 (d, J=9.4, 1H), 7.14 (d, J=8.7, 2H), 6.66 (d, J=8.8, 2H), 5.99 (s, 1H), 5.73 (s, 1H), 4.14 – 3.88 (m, 2H), 3.67 (s, 3H), 2.99 (m, 1H), 1.80 (m, 1H), 1.72 – 1.53 (m, 5H), 1.40 (s, 9H), 1.28 – 1.07 (m, 4H).. ¹³C NMR (100 MHz, CDCl₃) δ = 168.21, 166.51, 159.92, 148.16, 133.64, 133.58, 133.46, 132.53, 131.53, 130.85, 128.89, 128.06, 125.66, 124.77, 117.39, 114.13, 65.11,

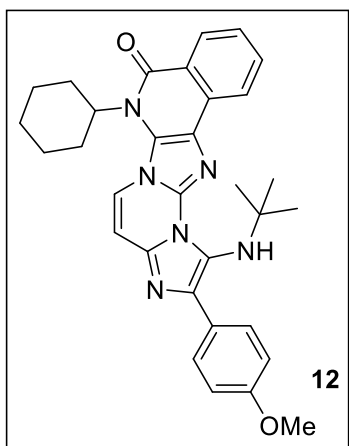
56.17, 55.23, 52.15, 42.53, 34.40, 28.79, 25.72, 25.06. IR (KBr) $\ddot{\nu}$ (cm⁻¹): 3331, 3055, 2930, 2854, 1683, 1532, 1406, 1365, 1252, 1199, 1089, 1033, 836, 803, 737. HRMS (ESI): m/z calculated for C₃₃H₃₉Cl₂N₆O₃⁺ [M + H]⁺: 637.2456, found 637.2451.

N³,N⁷,N¹¹-tris(4-methoxyphenyl)-2,6,10-tri-p-tolyltriimidazo[1,2-a:1',2'-c:1'',2''-e][1,3,5]triazine-3,7,11-triamine (11a)



Compound **11a** was obtained as a pink powder (42%). ¹H NMR (400 MHz, CDCl₃) δ = 7.89 (d, *J* = 8.2 Hz, 6H), 7.24 (d, *J* = 8.0 Hz, 6H), 6.65 (d, *J* = 9.0 Hz, 6H), 6.46 (d, *J* = 8.9 Hz, 6H), 6.00 (s, 3H), 3.67 (s, 9H), 2.41 (s, 9H). ¹³C NMR (100 MHz, CDCl₃) δ = 153.50, 137.44, 137.24, 131.89, 130.79, 129.04, 128.92, 126.13, 121.50, 115.91, 114.30, 77.16, 55.30, 21.18.

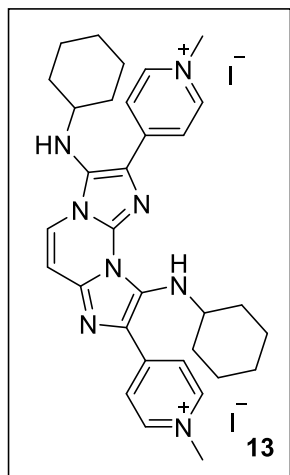
1-(tert-butylamino)-7-cyclohexyl-2-(4-methoxyphenyl)imidazo[1'',2'':3',4']pyrimido[2',1':2,3]imidazo[4,5-c]isoquinolin-8(7H)-one (12)



Compound **12** was obtained as a pink powder (7%). ¹H NMR (400 MHz, CDCl₃) δ = 8.40 (d, *J*=7.8, 1H), 8.17 – 8.10 (m, 3H), 7.77 (ddd, *J*=8.2, 7.2, 1.3, 1H), 7.70 (d, *J*=7.9, 1H), 7.49 (ddd, *J*=8.3, 7.2, 1.2, 1H), 7.01 (d, *J*=7.9, 1H), 6.96 (d, *J*=8.8, 1H), 5.03 (s, 1H), 4.32 – 4.23 (m, 1H), 3.86 (s, 3H), 2.95 (m, 2H), 2.06 – 1.93 (m, 4H), 1.77 (m, 2H), 1.48 – 1.42 (m, 2H), 1.17 (s, 9H). ¹³C NMR (100 MHz, CDCl₃) δ = 162.74, 159.11, 136.37, 136.27, 135.62, 133.11, 131.71, 129.16, 129.00, 128.99, 127.31, 126.60, 125.53, 125.29, 121.09, 120.51, 119.85, 113.67, 104.73, 61.32, 58.05, 55.38, 30.24, 29.83, 26.54, 25.14. IR (KBr) $\tilde{\nu}$ (cm⁻¹):

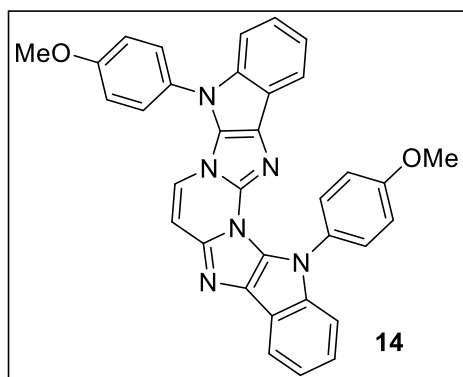
¹): 3324, 3062, 2931, 2856, 1651, 1633, 1515, 1410, 1247, 1117, 1033.

4,4'-(3,9-bis(cyclohexylamino)diimidazo[1,2-a:1',2'-c]pyrimidine-2,8-diyl)bis(1-methylpyridin-1-ium) iodide (13)



Compound **13** was obtained as an orange powder (78%). ¹H NMR (400 MHz, CD₃OD) δ = 8.74 – 8.64 (m, 4H), 8.54- 8.47 (m, 4H), 8.34-8.28 (m, 2H), 8.07 (d, J=6.2, 1H), 8.01 – 7.91 (m, 2H), 7.03 – 6.87 (m, 1H), 4.30 – 4.21 (m, 6H), 3.05-2.89 (m, 2H), 2.05 – 1.85 (m, 6H), 1.80-1.65 (m, 6H), 1.62 – 1.34 (m, 10H), 1.28-1.16 (m, 10H) overlap with solvents signal in the aliphatic part (2.05-1.16). IR (KBr) $\ddot{\nu}$ (cm⁻¹): 3448, 3210, 2928, 2853, 1635, 1604, 1560, 1512, 1466, 1389. HRMS (ESI): m/z calculated for C₃₃H₄₀ClN₆O₃⁺ [M + H]⁺: 603.2845, found 603.2848.

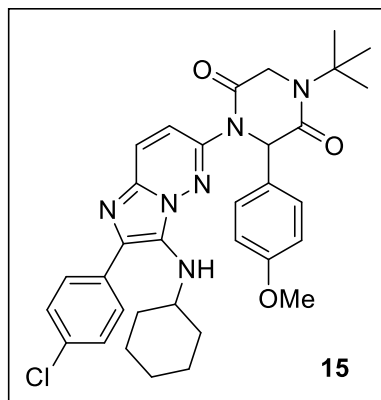
Aminopyrimidine GBB adduct- Indole compound (14)



Compound **14** was obtained as a gray powder (67%). ¹H NMR (400 MHz, CDCl₃) δ = 8.05 – 7.99 (m, 1H), 7.51 (dt, J = 3.1, 1.8 Hz, 1H), 7.48 (d, J = 8.9 Hz, 2H), 7.33 (d, J = 8.9 Hz, 2H), 7.30 – 7.11 (m, 7H), 7.09 (d, J = 8.9 Hz, 2H), 7.04 (d, J = 8.9 Hz, 2H), 6.88 (d, J = 7.8 Hz, 1H), 3.97 (s, 3H), 3.85 (s, 3H). ¹³C NMR (100 MHz, CDCl₃) δ = 159.84, 159.46, 143.14, 140.30, 139.48, 134.93, 131.97, 130.67, 130.48, 129.83, 129.26, 128.73, 127.93, 124.41, 123.37, 122.25, 120.95,

120.91, 119.01, 118.82, 118.68, 117.82, 117.59, 115.28, 113.93, 111.81, 110.74, 102.98, 55.77, 55.66.

1-(tert-butyl)-4-(2-(4-chlorophenyl)-3-(cyclohexylamino)imidazo[1,2-b]pyridazin-6-yl)-3-(4-methoxyphenyl)piperazine-2,5-dione (15)

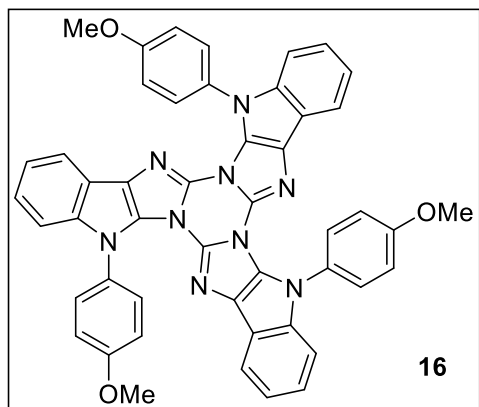


Compound **15** was obtained as a yellow powder (43%). ¹H NMR (400 MHz, CDCl₃) δ = 8.13 – 8.08 (m, 2H), 7.80 (d, J=9.8, 1H), 7.72 (d, J=9.8, 1H), 7.38 (dd, J=9.9, 7.9, 4H), 6.92 (d, J=8.8, 2H), 5.99 (s, 1H), 4.26 (d, J=17.5, 1H), 3.91 (d, J=17.5, 1H), 3.78 (s, 3H), 3.31 (m, 1H), 2.86 (m, 1H), 1.59 (m, 12H- overlap with solvent signals), 1.43 (s, 9H), 0.91 (m, 6H). ¹³C NMR (100 MHz, CDCl₃) δ = 167.28, 166.24, 159.66, 147.59, 133.22, 132.60, 128.76, 127.94, 126.62, 126.15, 125.48, 114.49, 112.99, 97.30, 65.24, 58.22, 55.86, 55.33, 48.01,

34.07, 33.97, 29.76, 25.51, 24.62. IR (KBr) $\ddot{\nu}$ (cm⁻¹): 3299, 2927, 2853, 1681, 1668, 1511, 1409, 1312,

1288, 1199, 836, 804. **HRMS (ESI):** m/z calculated for $C_{33}H_{37}ClN_6O_3^+$ $[M + H]^+$: 600.2616, found 600.2690.

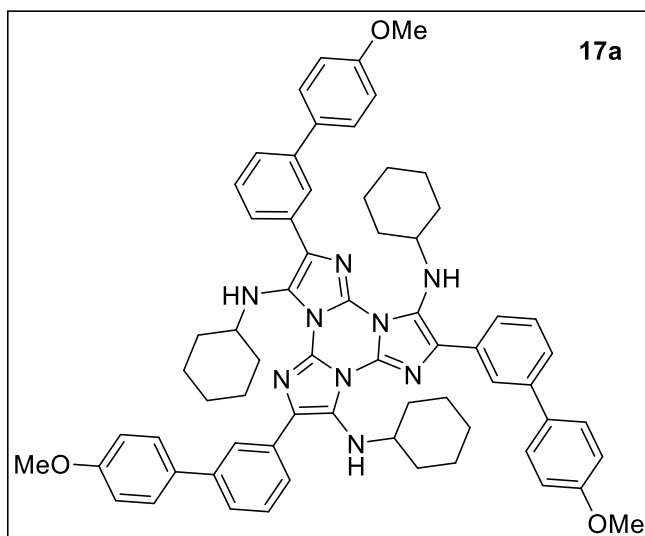
Melamine GBB Adduct- Indole Compound (16)



Compound **16** was obtained as a very pale blue powder (47%). **1H NMR** (400 MHz, d^7 -toluene) δ = 7.91 (d, J = 7.7 Hz, 1H), 7.43 (d, J = 8.5 Hz, 2H), 7.37 (d, J = 8.2 Hz, 1H), 7.28 (t, J = 7.2 Hz, 1H), 7.21 (t, J = 7.0 Hz, 1H), 7.07 – 7.00 (m, 2H, Overlapped by the toluene signals), 3.59 (s, 3H). **^{13}C NMR** (100 MHz, DMSO) δ = 159.82, 141.11, 133.25, 130.52, 130.41, 130.35, 123.70, 122.75, 121.43, 118.11, 116.97, 114.36, 112.16, 56.11. **HRMS (ESI):** m/z calculated for

$C_{48}H_{34}N_9O_3^+$ $[M + H]^+$: 784.2706, found 784.2748.

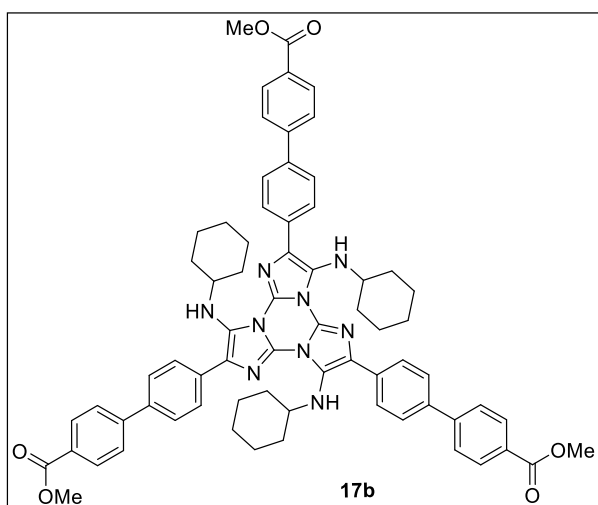
N^3,N^7,N^{11} -tricyclohexyl-2,6,10-tris(4'-methoxy-[1,1'-biphenyl]-3-yl)triimidazo[1,2-a:1',2'-c:1'',2''-e][1,3,5]triazine-3,7,11-triamine (17a)



Compound **17a** was obtained as a pale orange powder (37%). The isolated compound contained impurities of PPh₃O. **1H NMR** (400 MHz, $CDCl_3$) δ = 8.31 (s, 3H), 8.01 (dt, J = 7.1, 1.5 Hz, 3H), 7.63 (d, J = 8.7 Hz, 6H), 7.46 – 7.39 (m, 6H), 6.99 (d, J = 8.7 Hz, 6H), 4.71 (s, 1H), 3.87 (s, 9H), 3.26 (s, 3H), 1.97 – 1.16 (m, 22H, Overlapped by Trace impurities). **^{13}C NMR** (100 MHz, $CDCl_3$) δ = 159.09, 140.33, 135.20, 134.22, 133.82, 130.19, 128.59, 128.40, 127.97, 127.63,

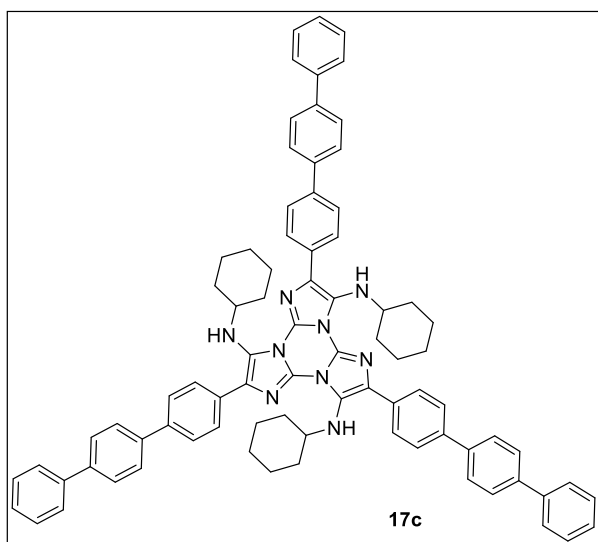
125.96, 124.46, 124.36, 114.12, 56.50, 55.33, 33.61, 25.87, 24.69. **HRMS (ESI):** m/z calculated for $C_{66}H_{70}N_9O_3^+$ $[M + H]^+$: 1036.5523, found 1036.5617.

trimethyl 4',4''',4''''-(3,7,11-tris(cyclohexylamino)triimidazo[1,2-a:1',2'-c:1'',2''-e][1,3,5]triazine-2,6,10-triyl)tris([1,1'-biphenyl]-4-carboxylate) (17b)



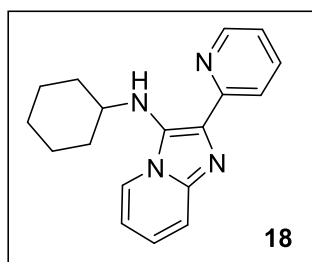
Compound **17b** was obtained as a light brown powder (31%). $^1\text{H NMR}$ (400 MHz, CDCl_3) δ = 8.15 (d, J = 6.7 Hz, 6H), 8.13 (d, J = 6.6 Hz, 6H), 7.76 (d, J = 6.5 Hz, 6H), 7.74 (d, J = 6.5 Hz, 6H), 5.05 (d, J = 8.4 Hz, 3H), 3.96 (s, 9H), 3.26 (s, 3H), 2.00 (d, J = 11.2 Hz, 6H), 1.85 – 1.69 (m, 6H), 1.48 – 1.38 (m, 3H), 1.32 – 1.18 (m, 3H).

2,6,10-tri([1,1':4',1''-terphenyl]-4-yl)- $\text{N}^3, \text{N}^7, \text{N}^{11}$ -tricyclohexyltriimidazo[1,2-a:1',2'-c:1'',2''-e][1,3,5]triazine-3,7,11-triamine (17c)



Compound **17c** was obtained as a cream powder (49%). $^1\text{H NMR}$ (400 MHz, CDCl_3) δ = 8.09 (d, J = 8.5 Hz, 6H), 7.71 (d, J = 6.9 Hz, 6H), 7.69 (d, J = 7.0 Hz, 6H), 7.64 (d, J = 8.5 Hz, 6H), 7.61 (dd, J = 8.3, 1.2 Hz, 6H), 7.41 (t, J = 7.6 Hz, 6H), 7.30 (t, J = 7.4 Hz, 3H), 4.97 (s, 3H), 3.23 (s, 3H), 1.96 (d, J = 12.8 Hz, 6H), 1.77 – 1.66 (m, 6H), 1.57 – 1.33 (m, 9H, Overlapped by signal of H_2O), 1.27 – 1.17 (m, 9H).

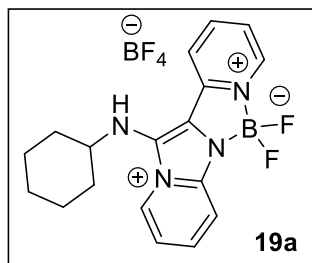
N -cyclohexyl-2-(pyridin-2-yl)imidazo[1,2-a]pyridin-3-amine (18)



Compound **18** was obtained as a yellowish powder (84%). $^1\text{H NMR}$ (400 MHz, CD_3OD) δ = 8.59 (ddd, J = 4.9, 1.8, 0.9 Hz, 1H), 8.16 (dt, J = 6.9, 1.1 Hz, 1H), 8.05 (dt, J = 8.0, 1.1 Hz, 1H), 7.85 (ddd, J = 8.0, 7.6, 1.8 Hz, 1H), 7.49 (dt, J = 9.1, 1.1 Hz, 1H), 7.28 – 7.22 (m, 2H), 6.93 (td, J = 6.8, 1.1 Hz, 1H), 3.21 – 3.12 (m, 1H), 1.86 (d, J = 10.2 Hz, 2H), 1.71 (dd, J = 9.2, 4.0 Hz, 2H), 1.55 (d, J = 13.3 Hz, 1H), 1.32 – 1.21 (m, 5H). $^{13}\text{C NMR}$ (100 MHz, CD_3OD) δ = 154.19, 148.27,

140.83, 136.63, 130.58, 129.47, 124.47, 123.18, 121.33, 119.89, 116.33, 112.12, 54.95, 33.40, 25.44, 24.43.

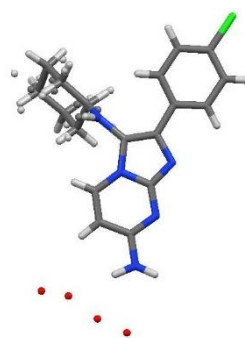
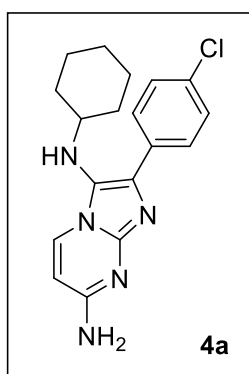
Aminopyridine GBB-BODIPY Adduct (**19a**)



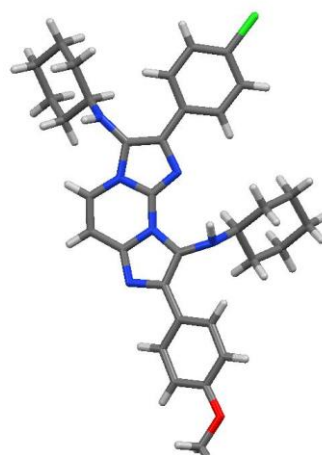
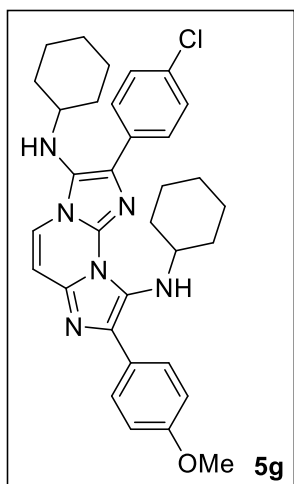
Compound **19a** was obtained as a yellow powder (58%). $^1\text{H NMR}$ (400 MHz, CD_3CN) δ = 8.75 (d, J = 5.7 Hz, 1H), 8.53 (d, J = 6.8 Hz, 1H), 8.49 (d, J = 7.0 Hz, 1H), 8.25 (d, J = 8.0 Hz, 1H), 7.99 – 7.92 (m, 1H), 7.92 – 7.85 (m, 1H), 7.81 (d, J = 9.0 Hz, 1H), 7.44 (t, J = 7.3 Hz, 1H), 4.82 (d, J = 8.4 Hz, 1H), 3.28 – 3.15 (m, 1H), 2.07 (d, J = 13.5 Hz, 3H), 1.78 (d, J = 9.6 Hz, 2H), 1.64 (d, J = 9.1 Hz, 1H), 1.46 (dd, J = 21.6, 12.9 Hz, 3H), 1.37 – 1.22 (m, 5H). $^{13}\text{C NMR}$ (101 MHz, CD_3CN) δ = 147.37, 143.73, 136.38, 127.72, 127.16, 122.53, 117.93, 113.55, 58.23, 34.86, 26.12, 25.71.

X-Ray Crystallography

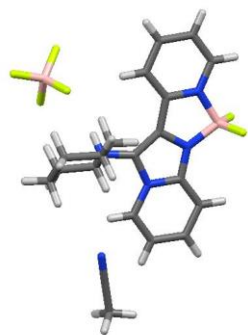
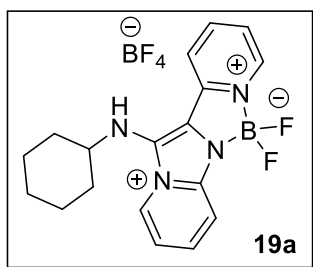
2-(4-chlorophenyl)- N^3 -cyclohexylimidazo[1,2-a]pyrimidine-3,7-diamine (**4a**)



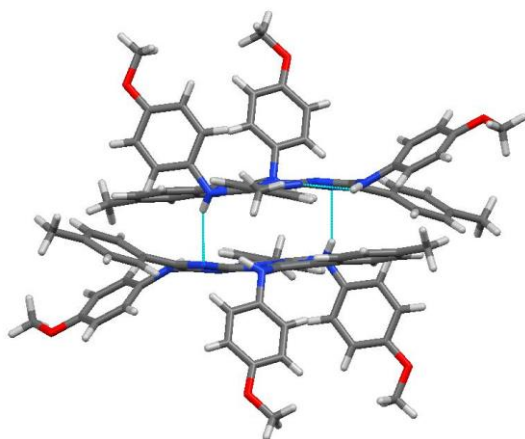
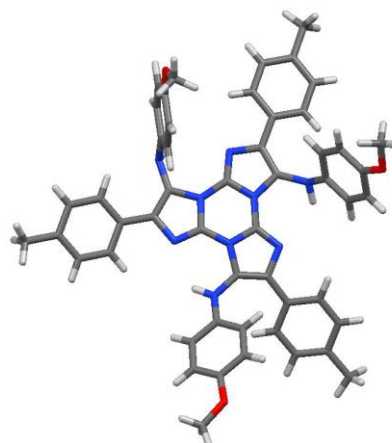
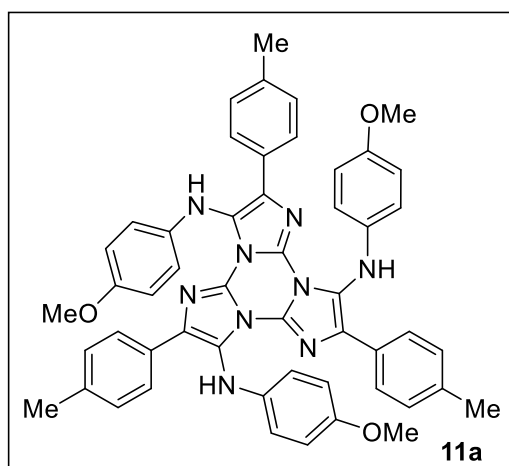
2-(4-chlorophenyl)- N^3, N^9 -dicyclohexyl-8-(4-methoxyphenyl)diimidazo[1,2-a:1',2'-c]pyrimidine-3,9-diamine (**5g**)



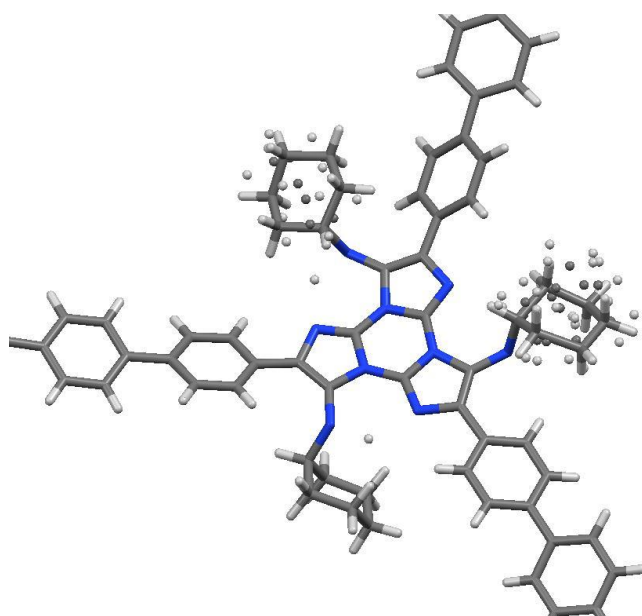
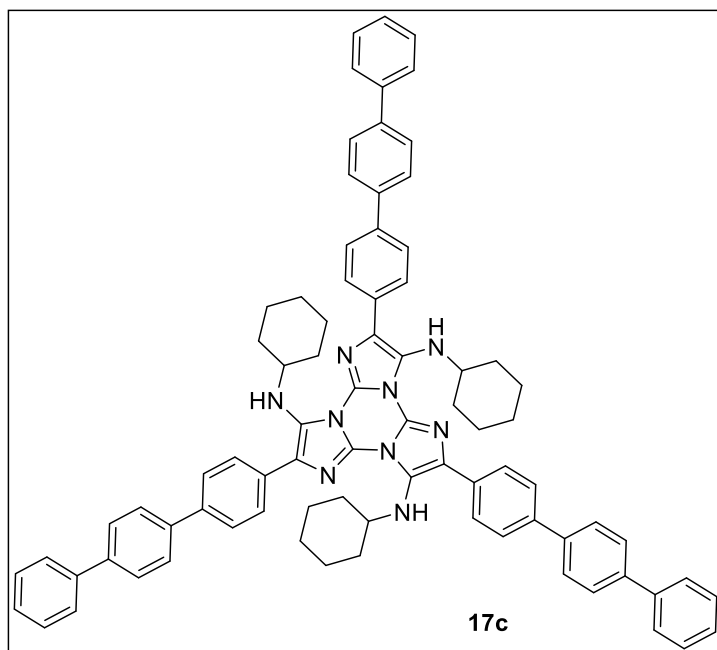
Aminopyridine GBB-BODIPY Adduct (19a)



N³,N⁷,N¹¹-tris(4-methoxyphenyl)-2,6,10-tri-p-tolyltriimidazo[1,2-a:1',2'-c:1'',2''-e][1,3,5]triazine-3,7,11-triamine (11a)

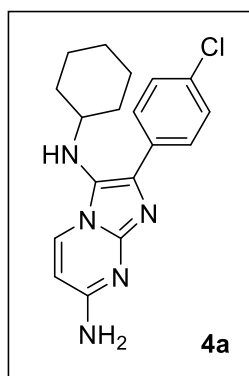
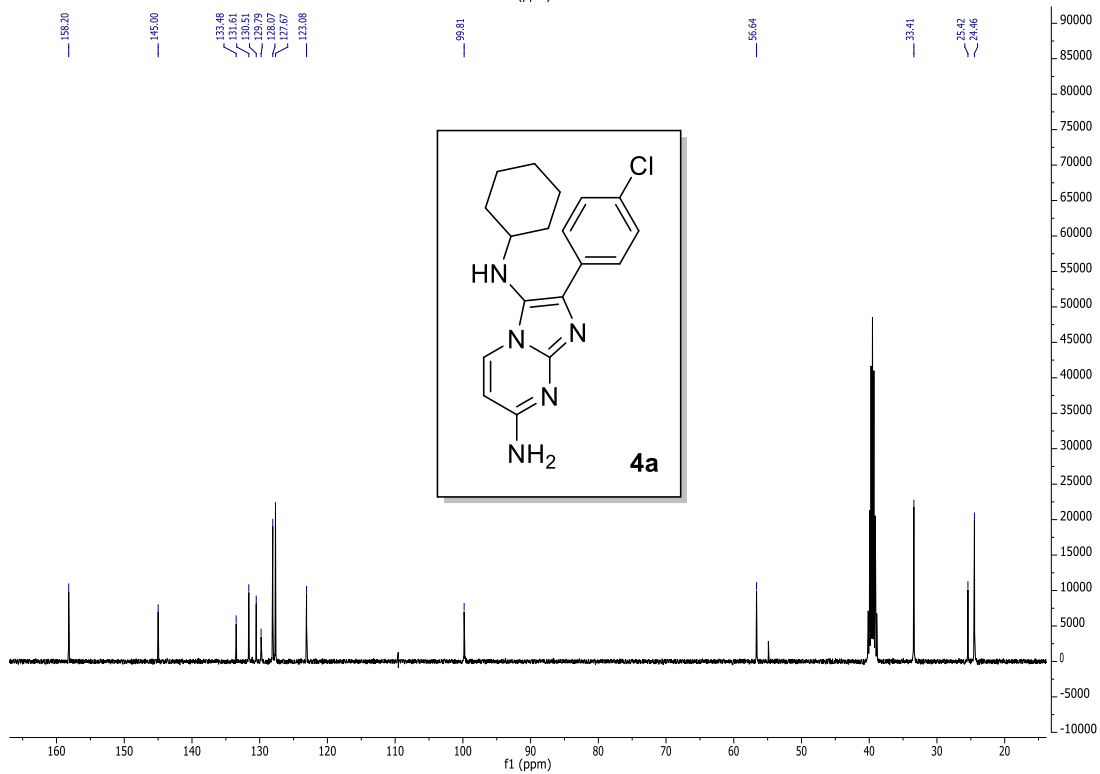
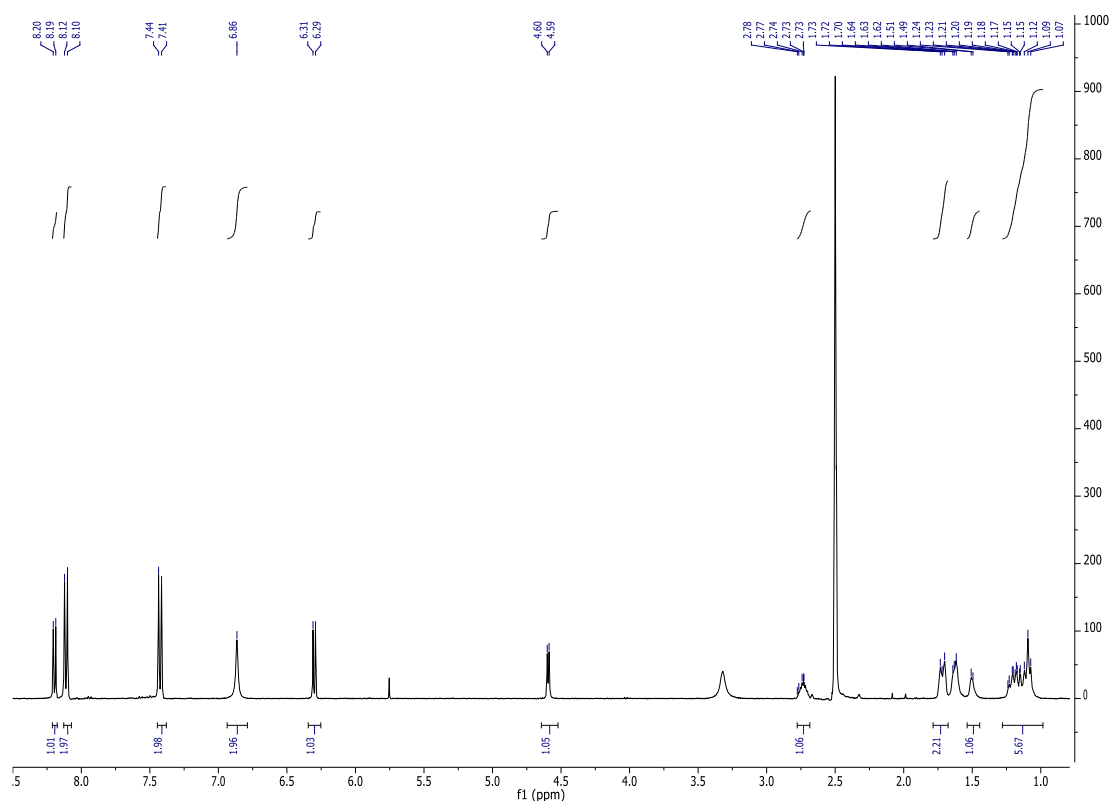


2,6,10-tri([1,1':4',1''-terphenyl]-4-yl)-N³,N⁷,N¹¹-tricyclohexyltriimidazo[1,2-a:1',2'-c:1'',2''-e][1,3,5]triazine-3,7,11-triamine (17c)

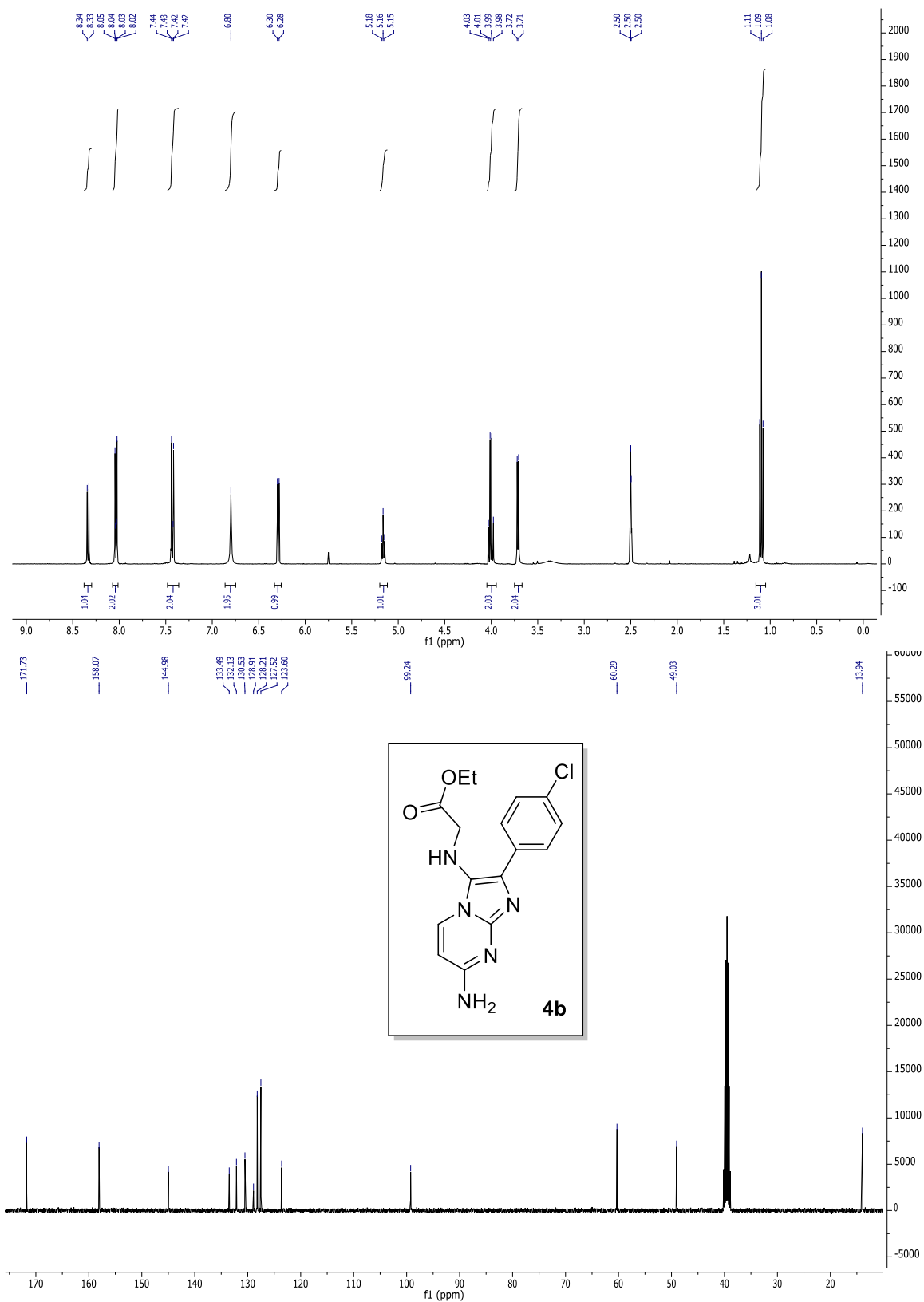


Copies of NMR Spectra

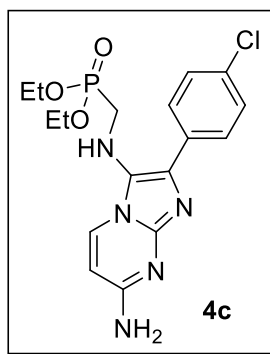
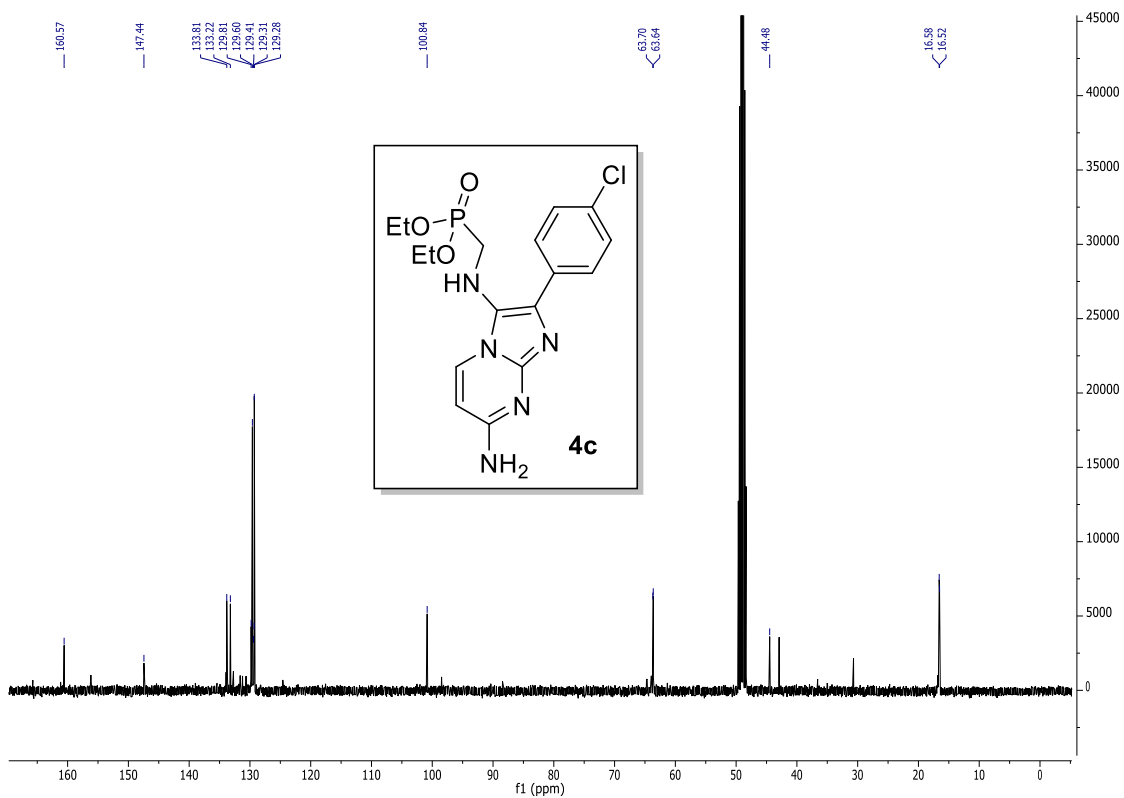
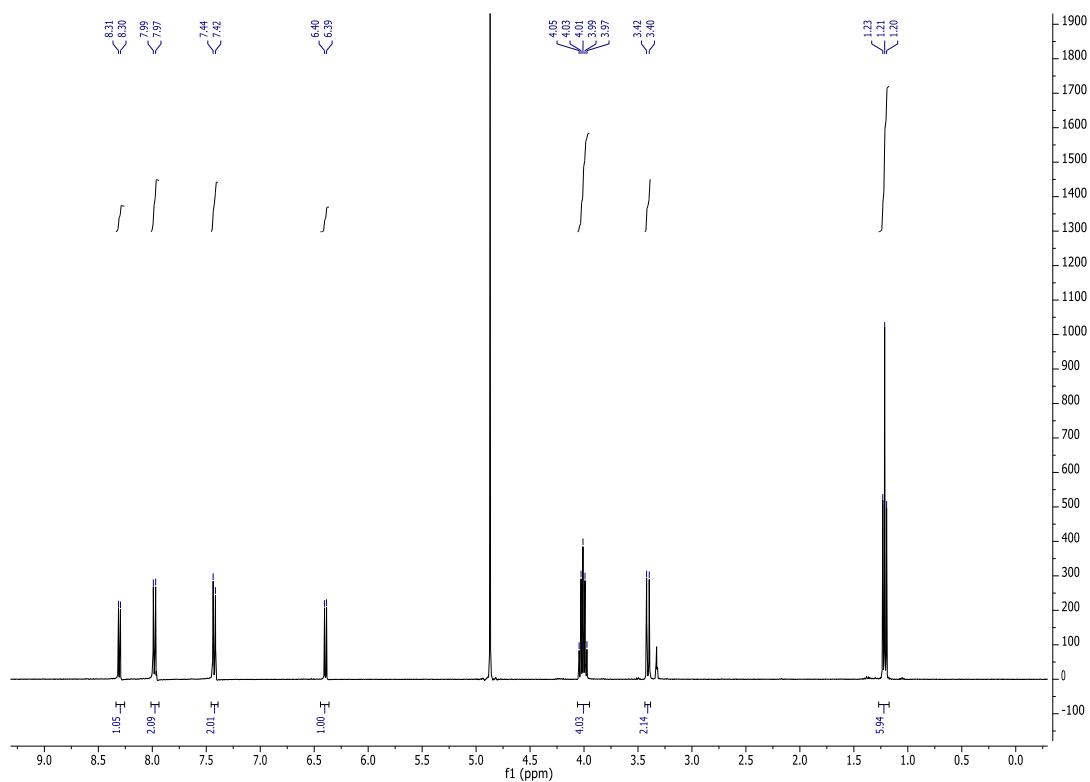
2-(4-chlorophenyl)-N³-cyclohexylimidazo[1,2-a]pyrimidine-3,7-diamine (4a)



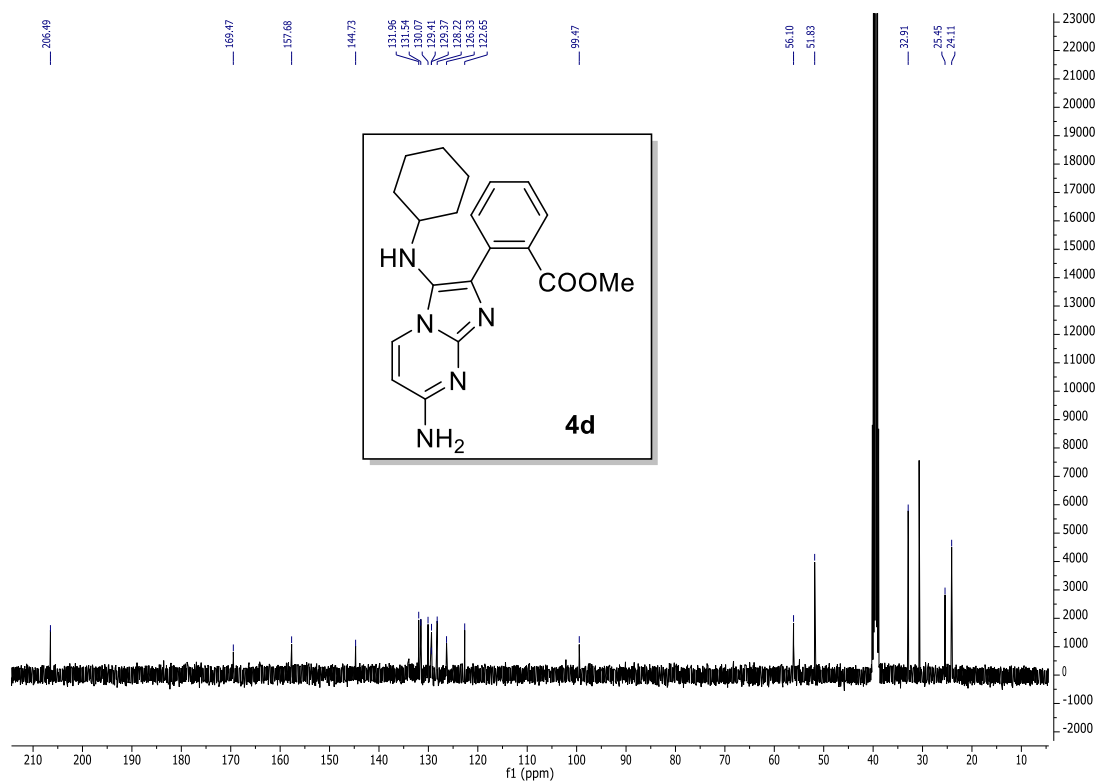
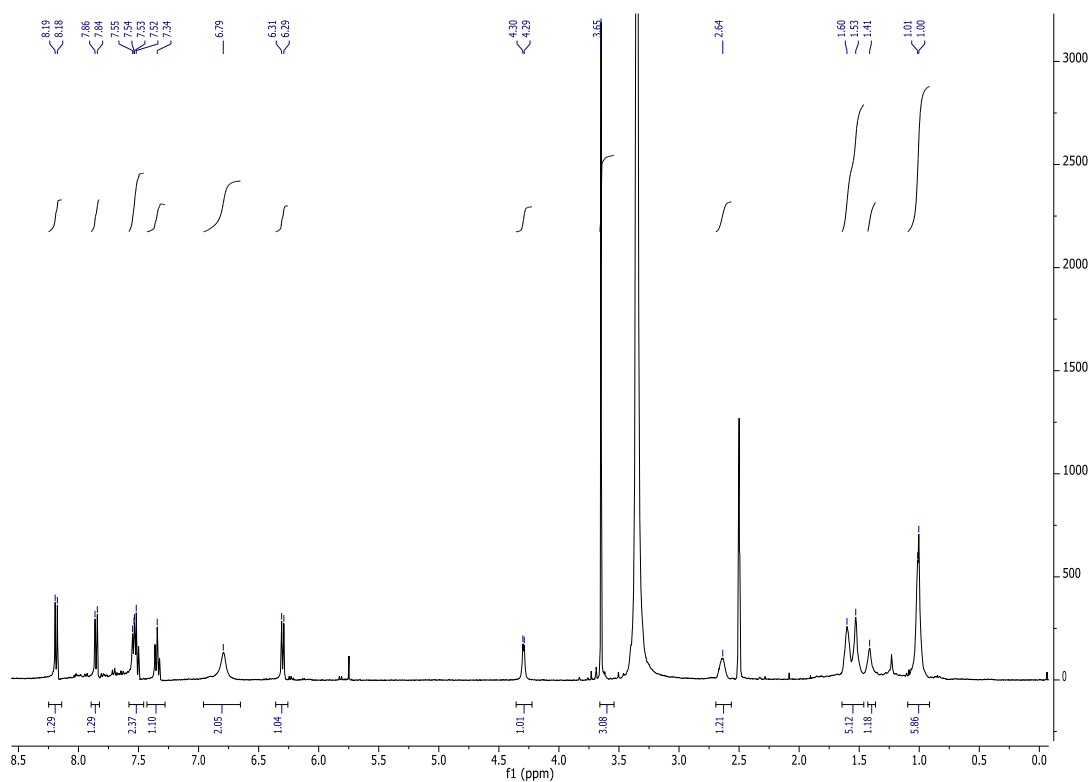
Ethyl 2-((7-amino-2-(4-chlorophenyl)imidazo[1,2-a]pyrimidin-3-yl)amino)acetate (4b)



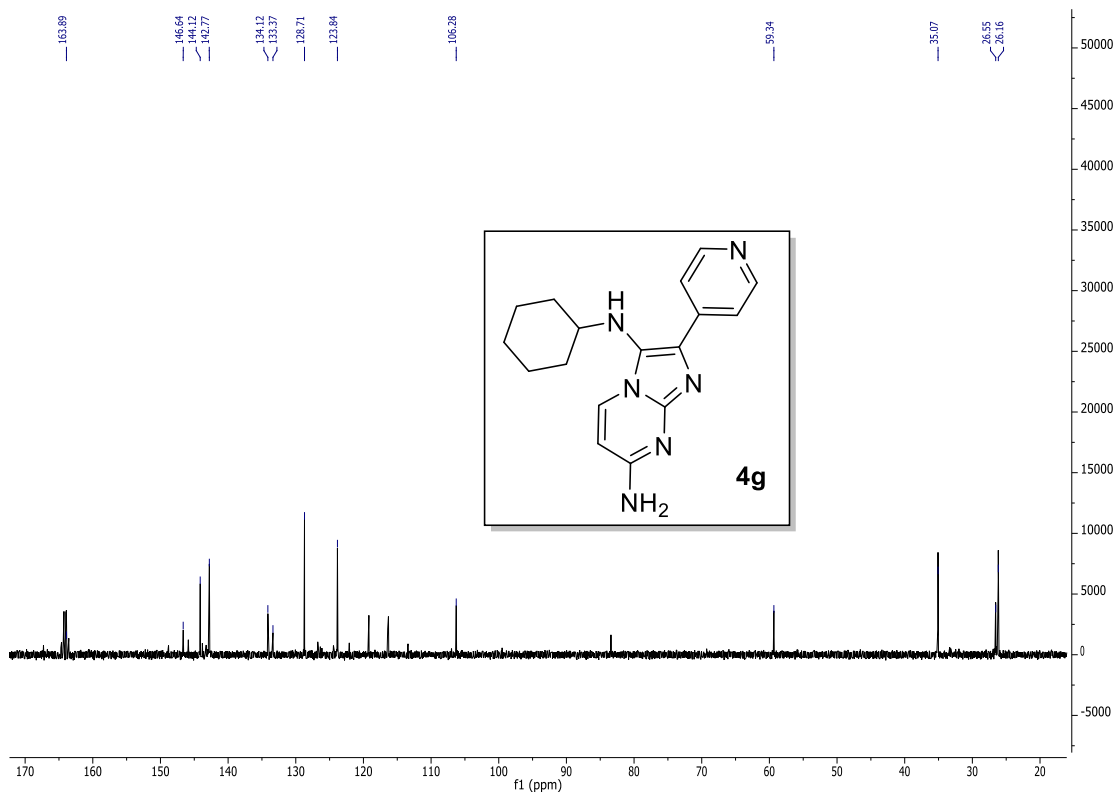
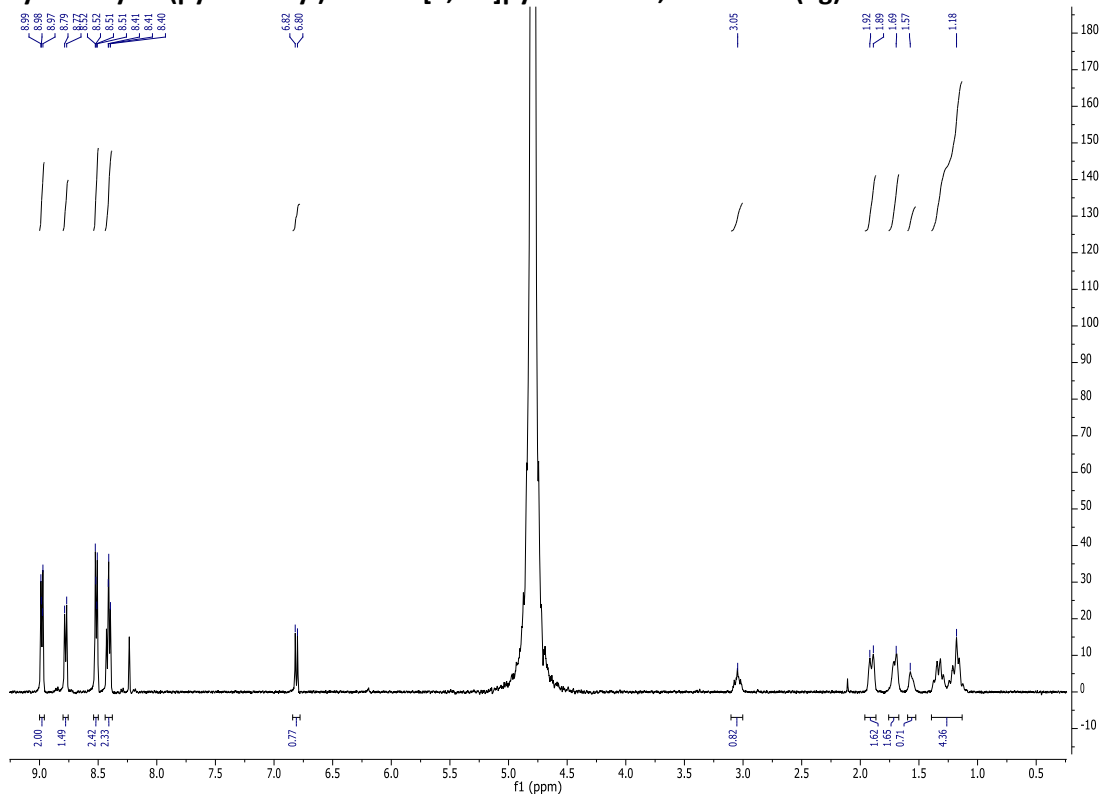
Diethyl (((7-amino-2-(4-chlorophenyl)imidazo[1,2-a]pyrimidin-3-yl)amino)methyl)phosphonate (4c)



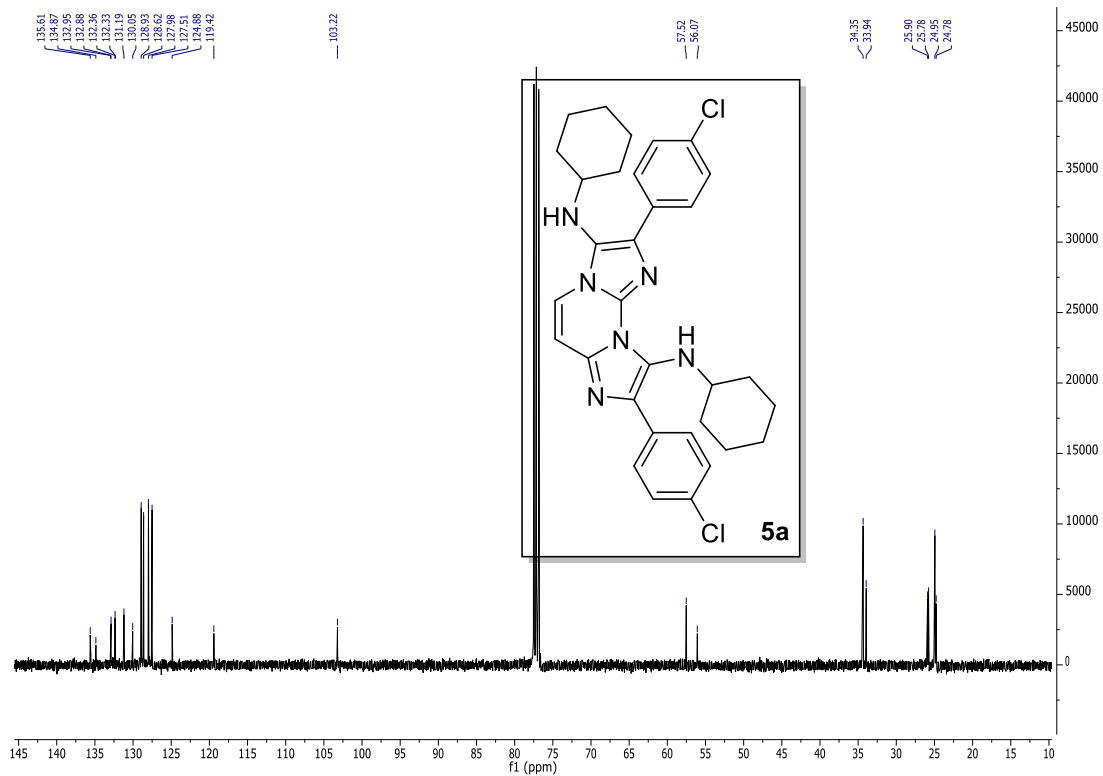
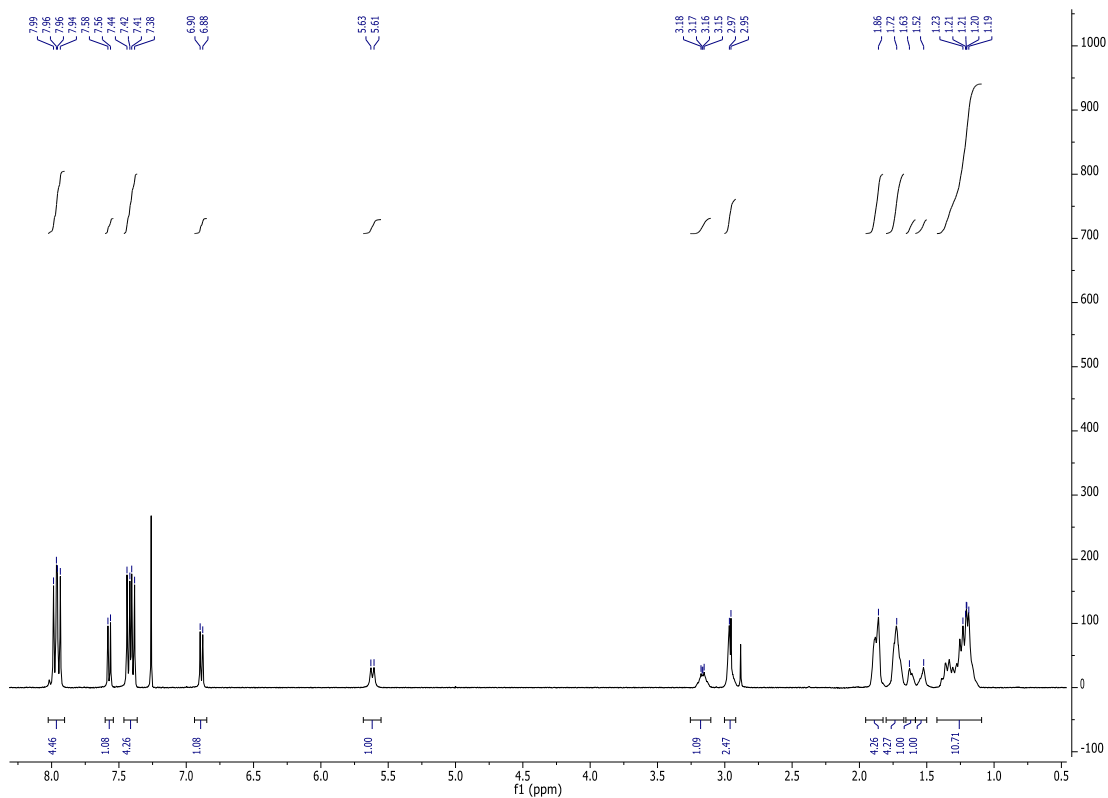
Methyl 2-(7-amino-3-(cyclohexylamino)imidazo[1,2-a]pyrimidin-2-yl)benzoate (4d)



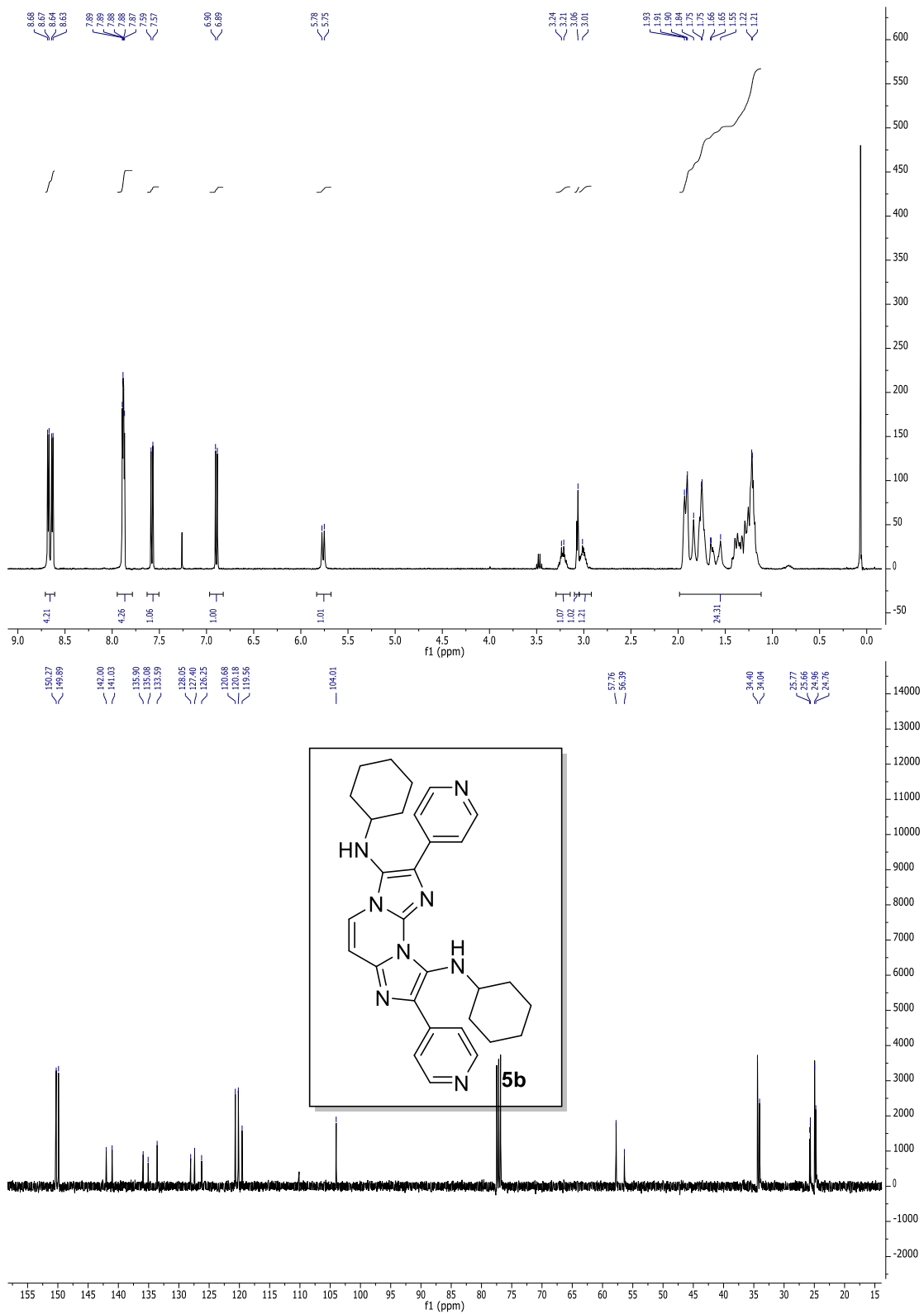
N³-cyclohexyl-2-(pyridin-4-yl)imidazo[1,2-a]pyrimidine-3,7-diamine (4g)



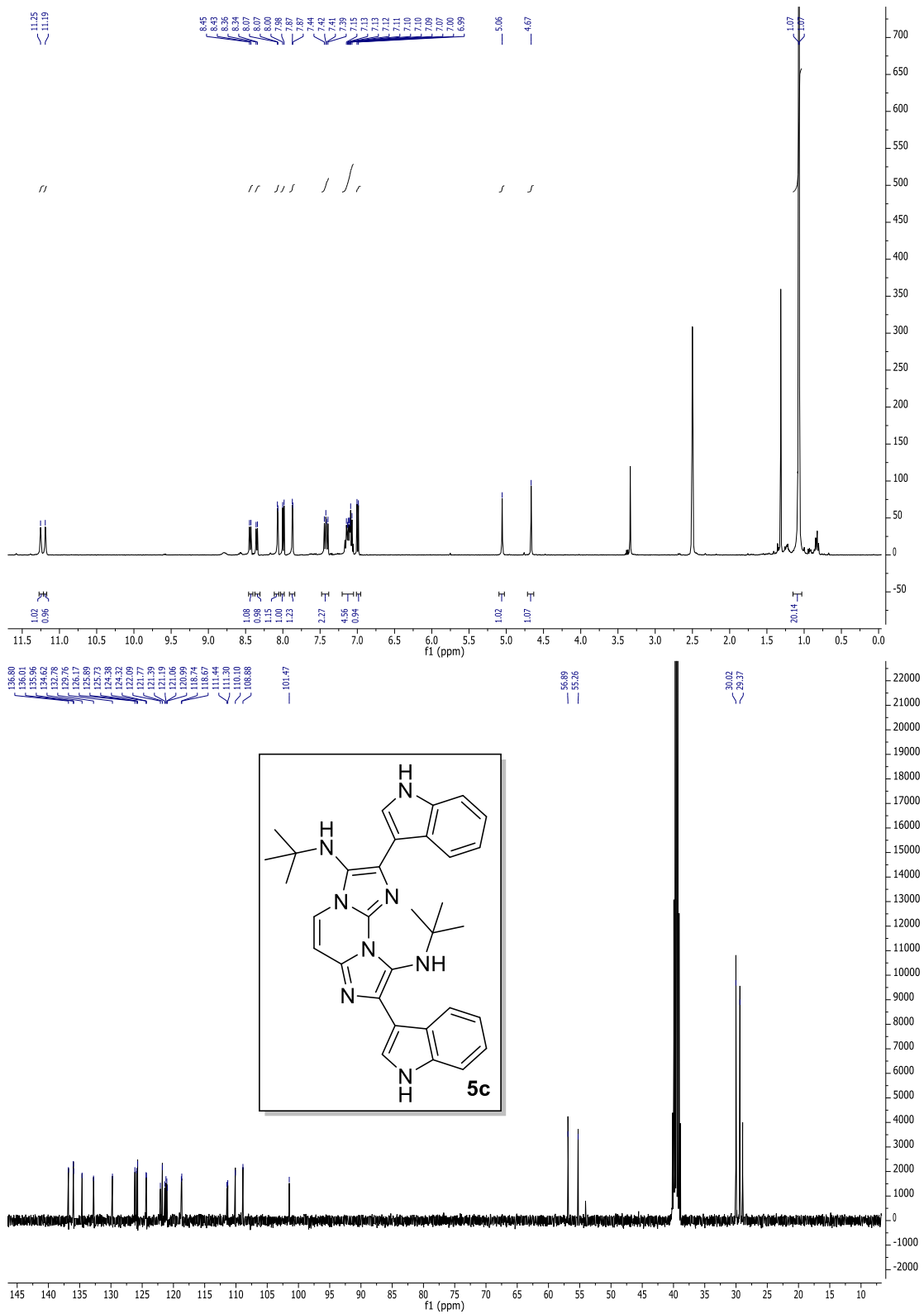
2,8-bis(4-chlorophenyl)-N³,N⁹-dicyclohexyldiimidazo[1,2-a:1',2'-c]pyrimidine-3,9-diamine (5a)



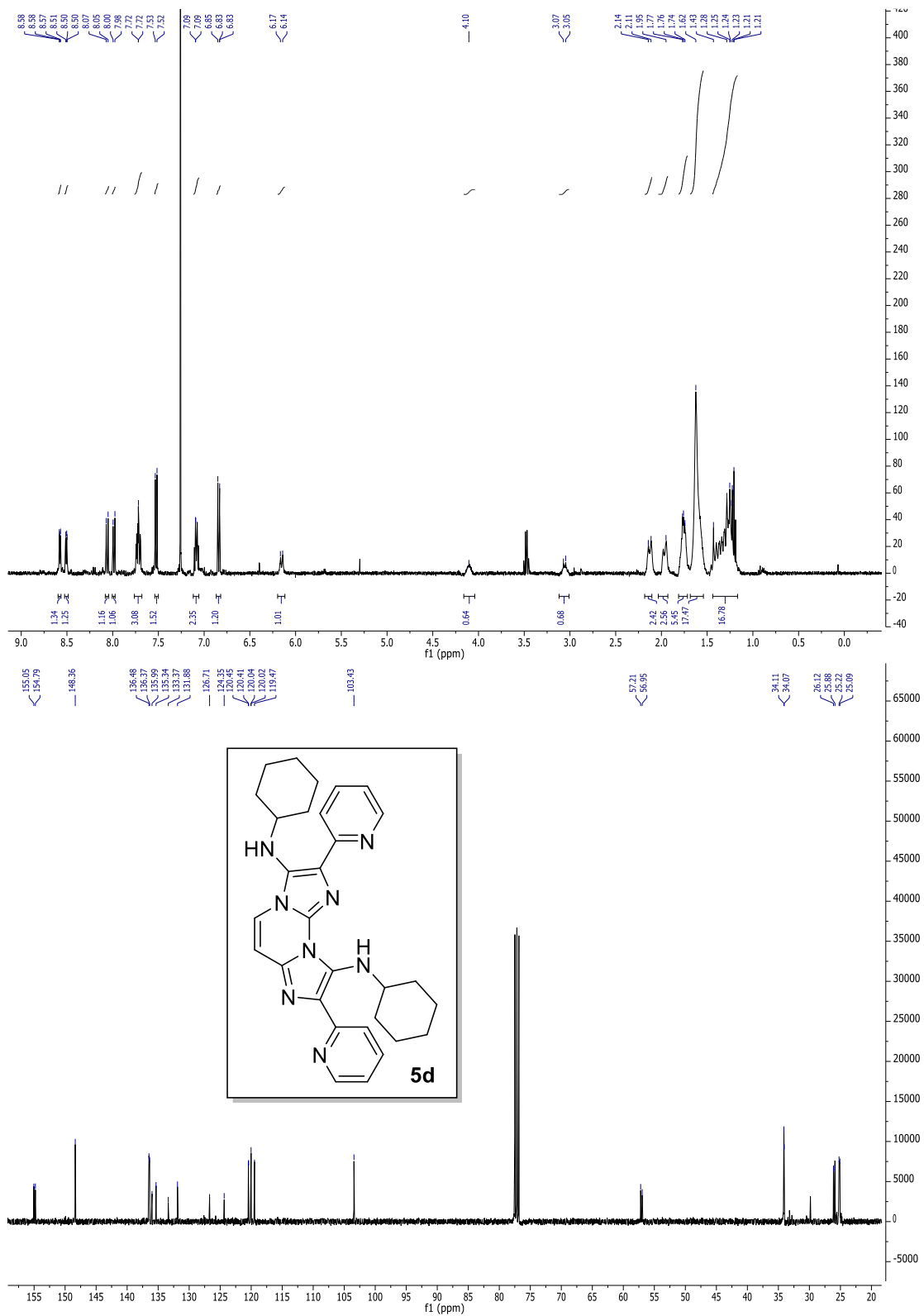
N³,N⁹-dicyclohexyl-2,8-di(pyridin-4-yl)diimidazo[1,2-a:1',2'-c]pyrimidine-3,9-diamine (5b)



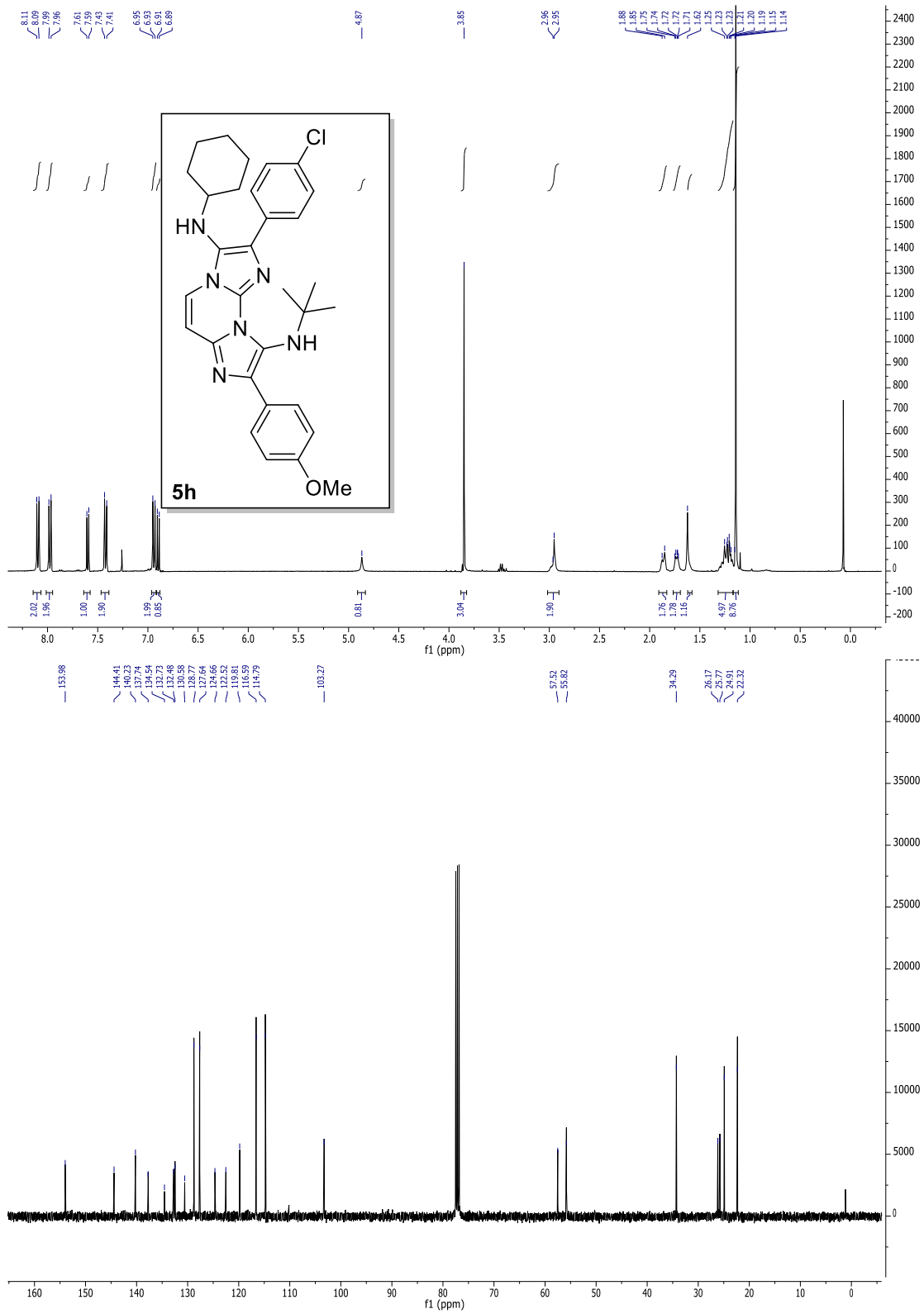
N³,N⁹-di-tert-butyl-2,8-di(1H-indol-3-yl)diimidazo[1,2-a:1',2'-c]pyrimidine-3,9-diamine (5c)



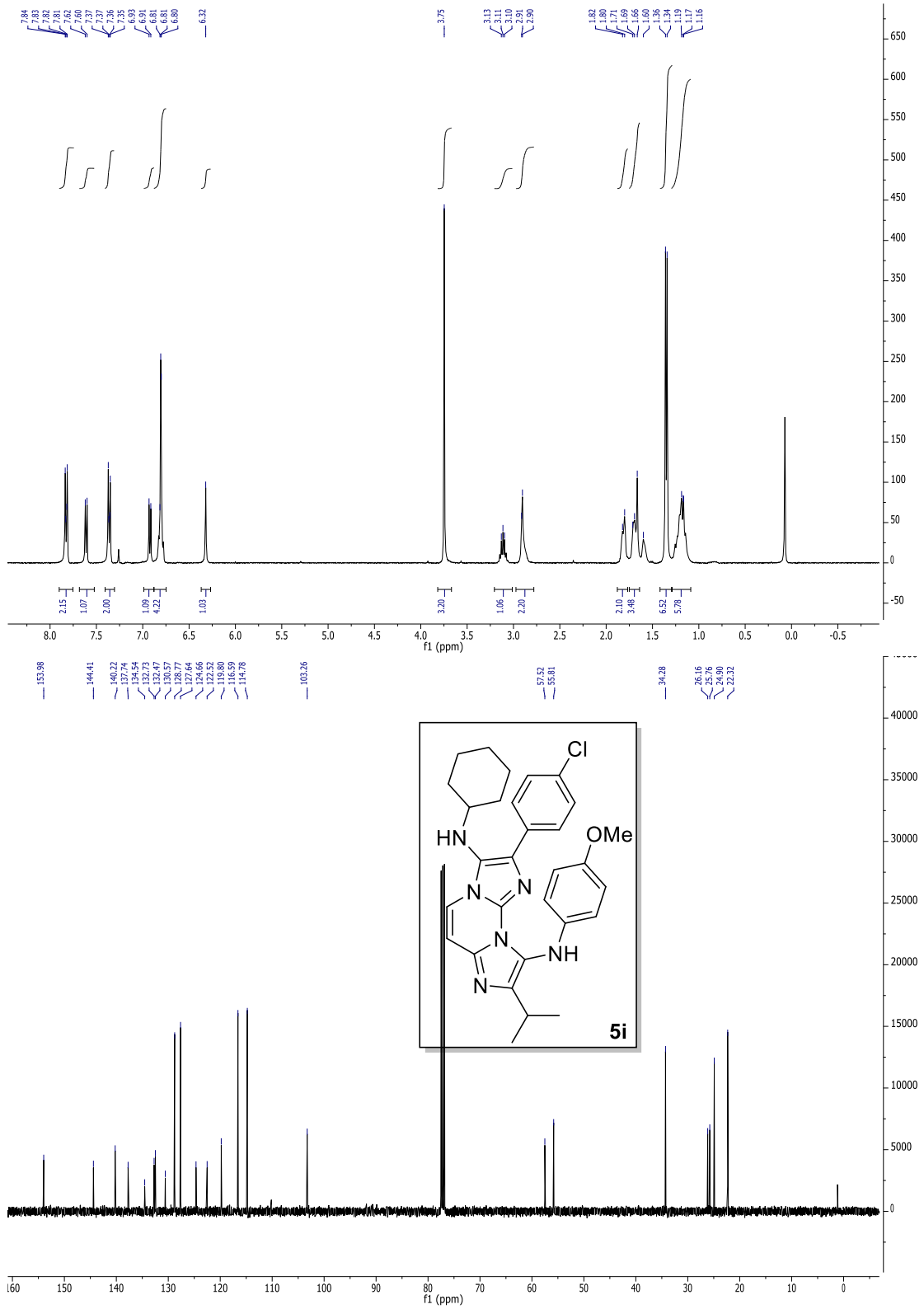
N³,N⁹-dicyclohexyl-2,8-di(pyridin-2-yl)diimidazo[1,2-a:1',2'-c]pyrimidine-3,9-diamine (5d)



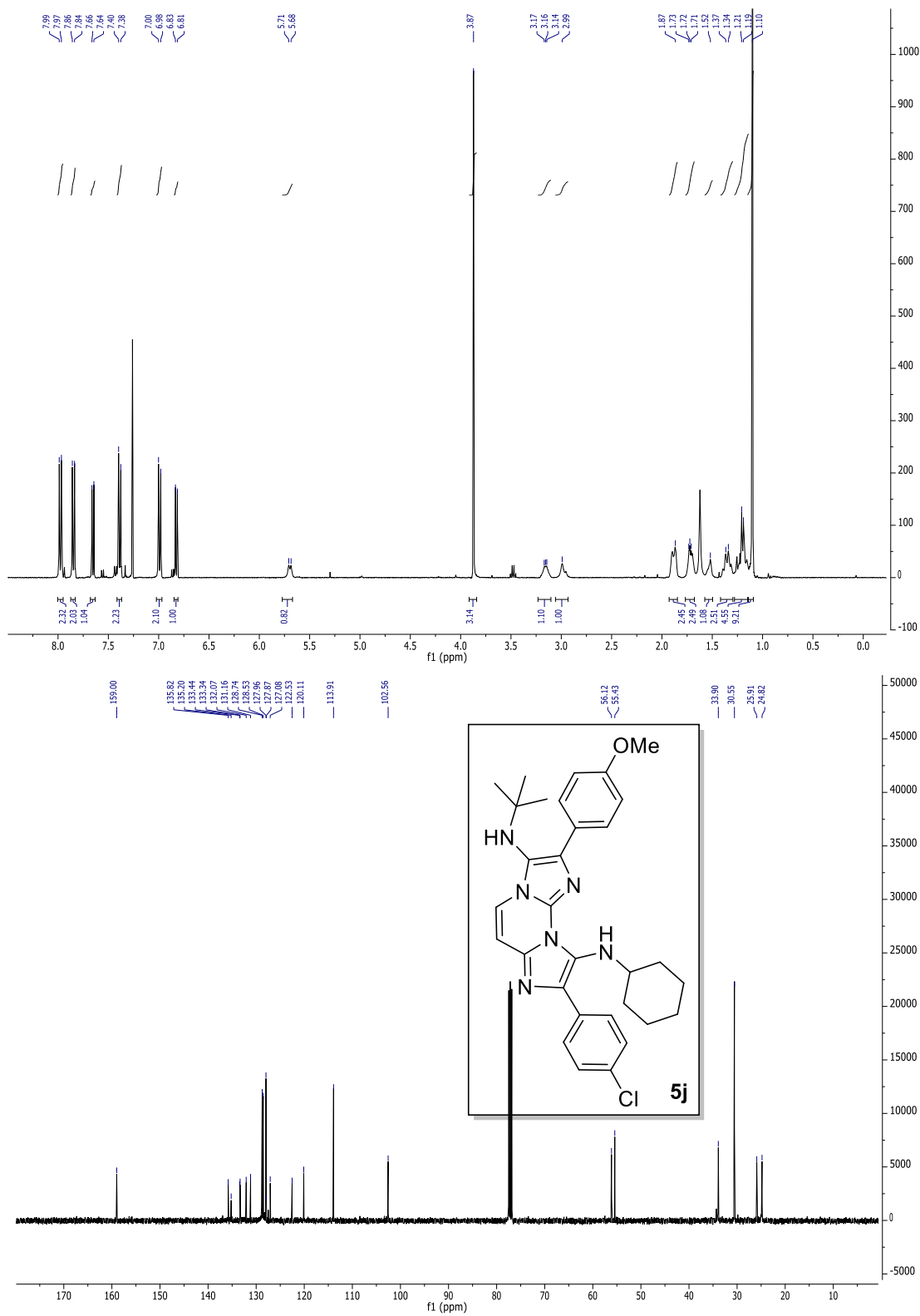
N⁹-(tert-butyl)-2-(4-chlorophenyl)-N³-cyclohexyl-8-(4-methoxyphenyl) diimidazo[1,2-a:1',2'-c]pyrimidine-3,9-diamine (5h)



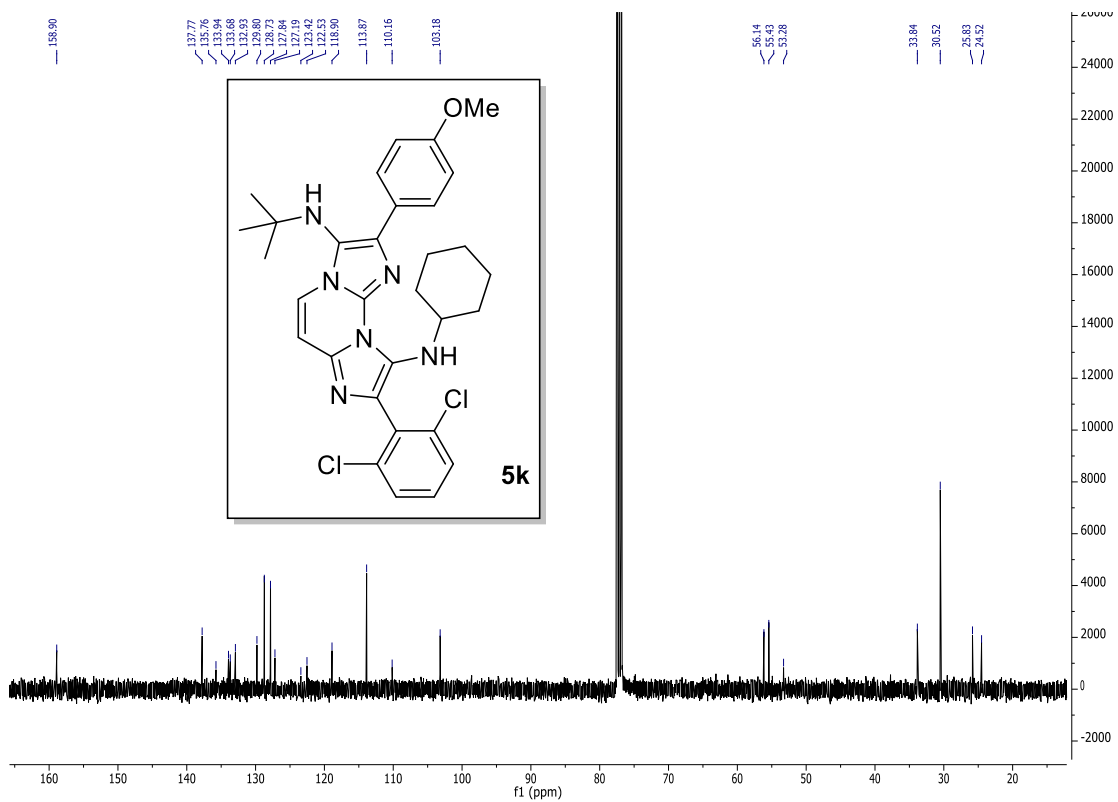
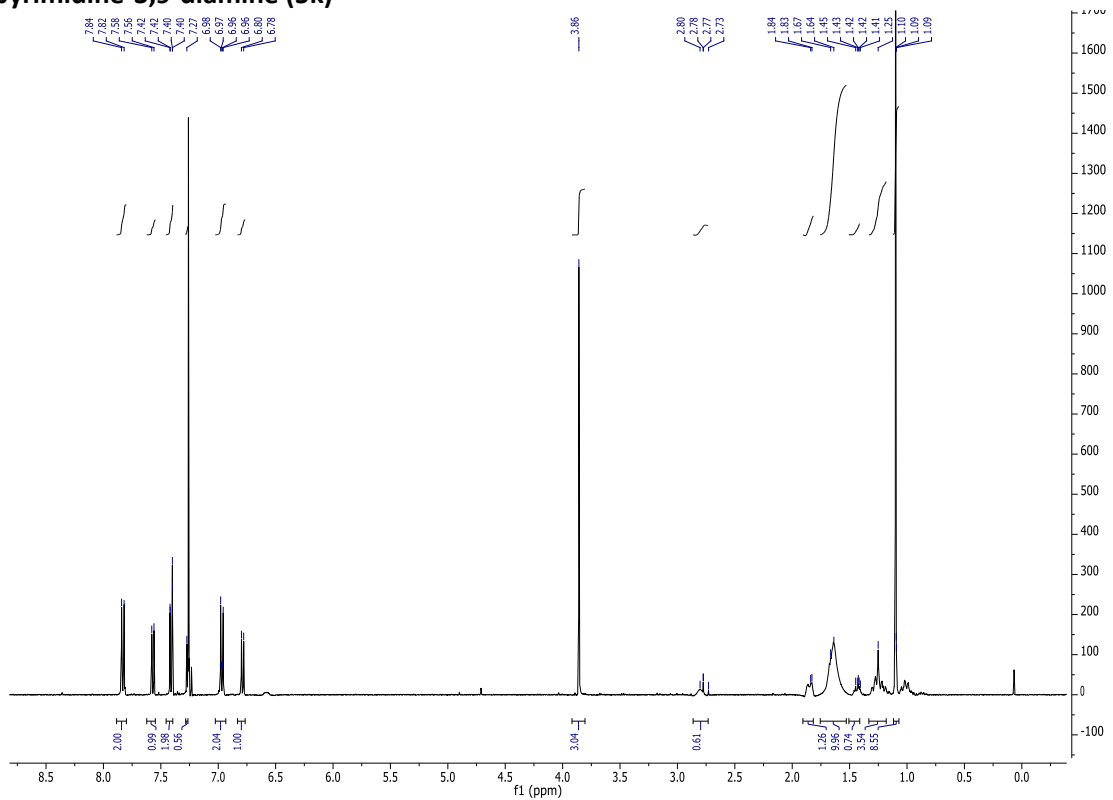
2-(4-chlorophenyl)-N³-cyclohexyl-8-isopropyl-N⁹-(4-methoxyphenyl) diimidazo[1,2-a:1',2'-c]pyrimidine-3,9-diamine (5i)



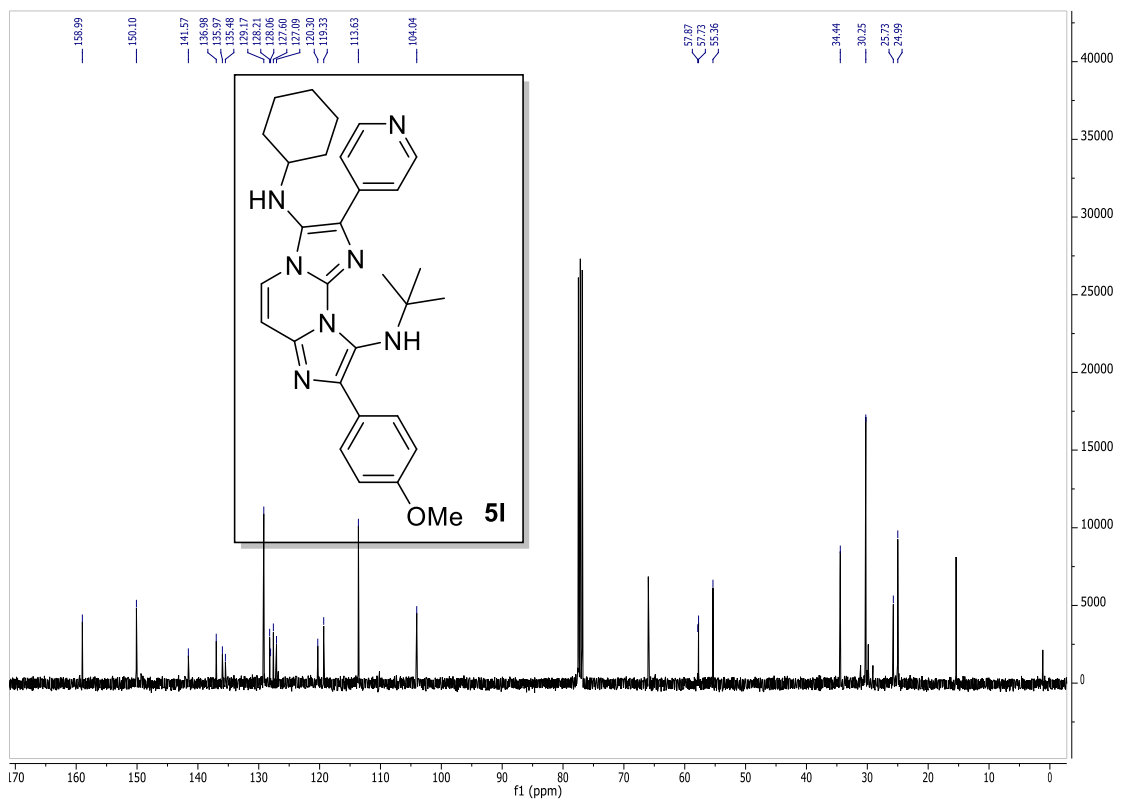
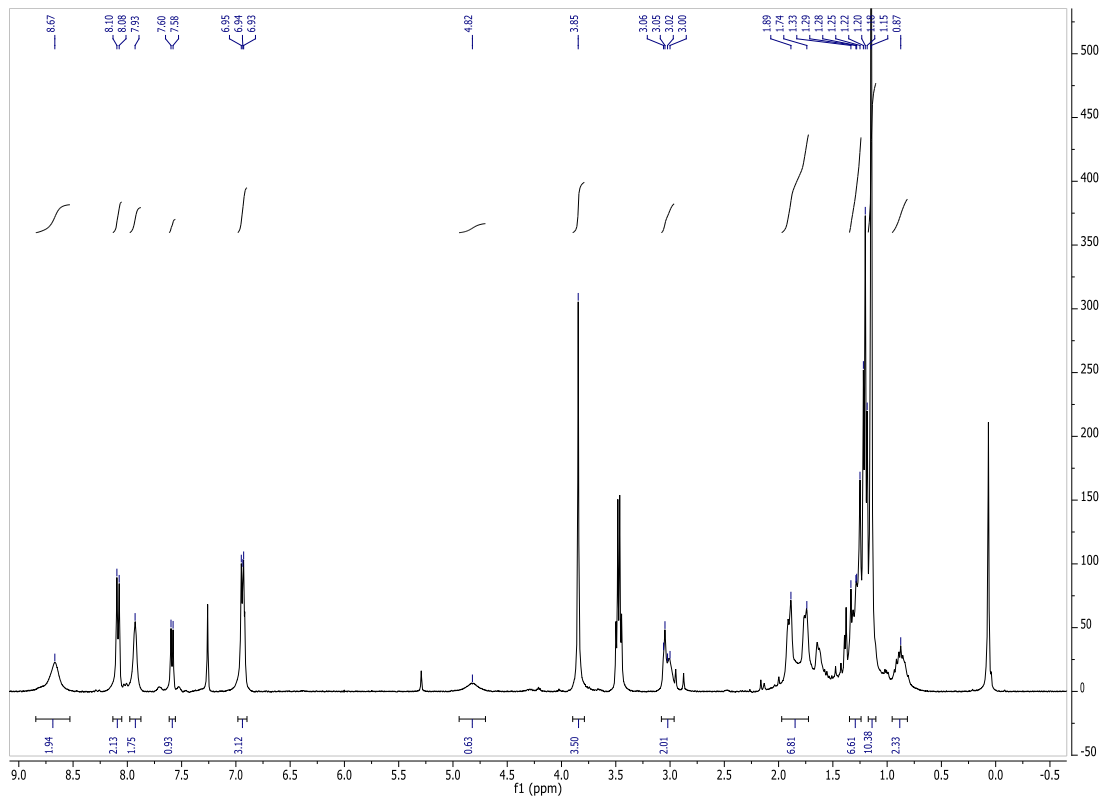
N³-(tert-butyl)-8-(4-chlorophenyl)-N⁹-cyclohexyl-2-(4-methoxyphenyl) diimidazo[1,2-a:1',2'-c]pyrimidine-3,9-diamine (5j)



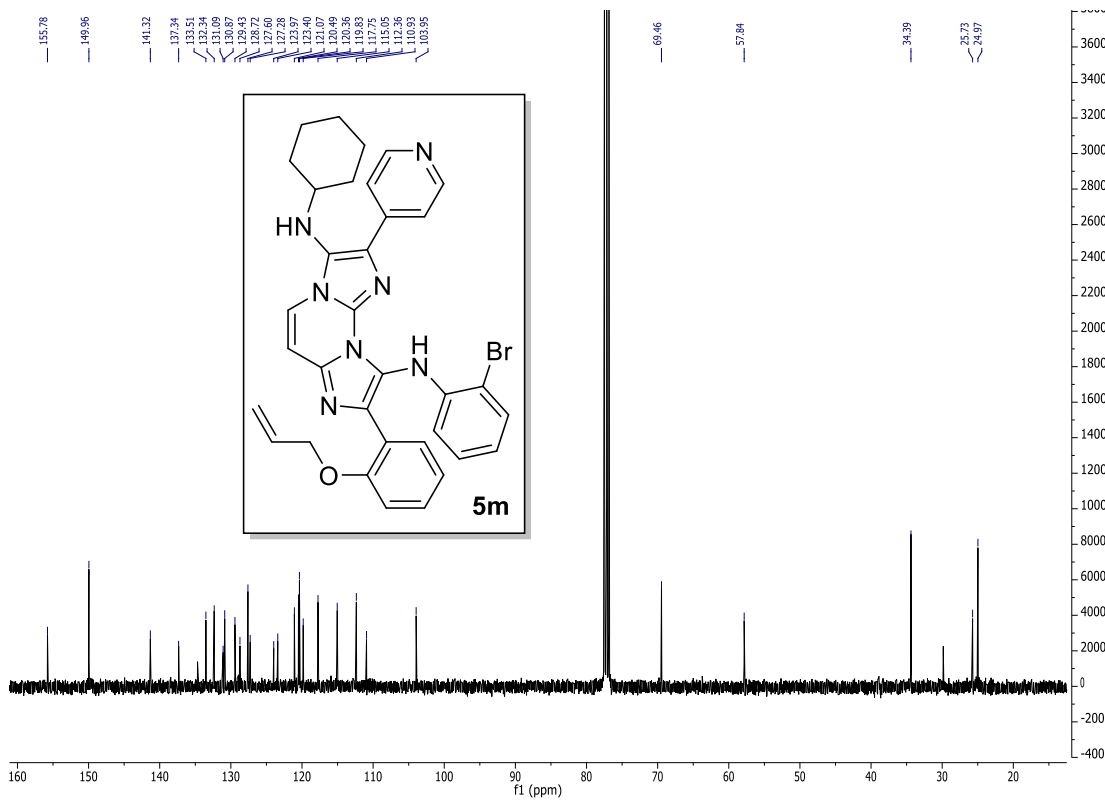
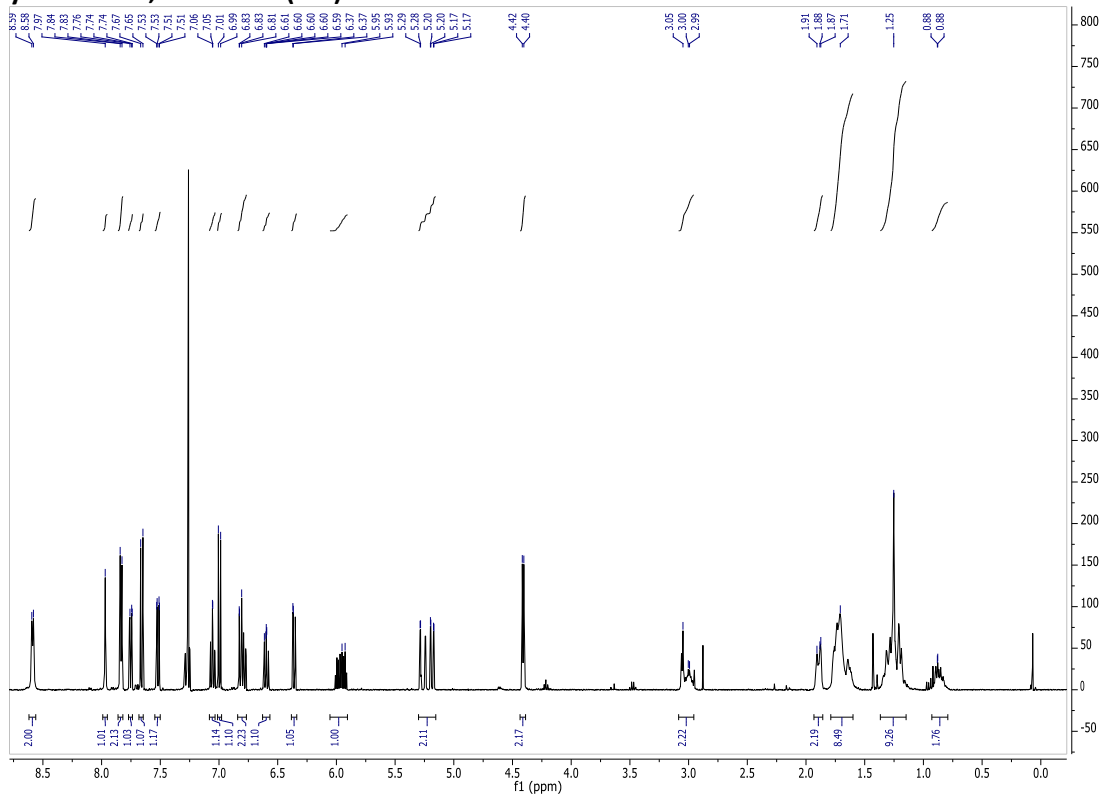
N³-(tert-butyl)-N⁹-cyclohexyl-8-(2,6-dichlorophenyl)-2-(4-methoxyphenyl) diimidazo[1,2-a:1',2'-c]pyrimidine-3,9-diamine (5k)



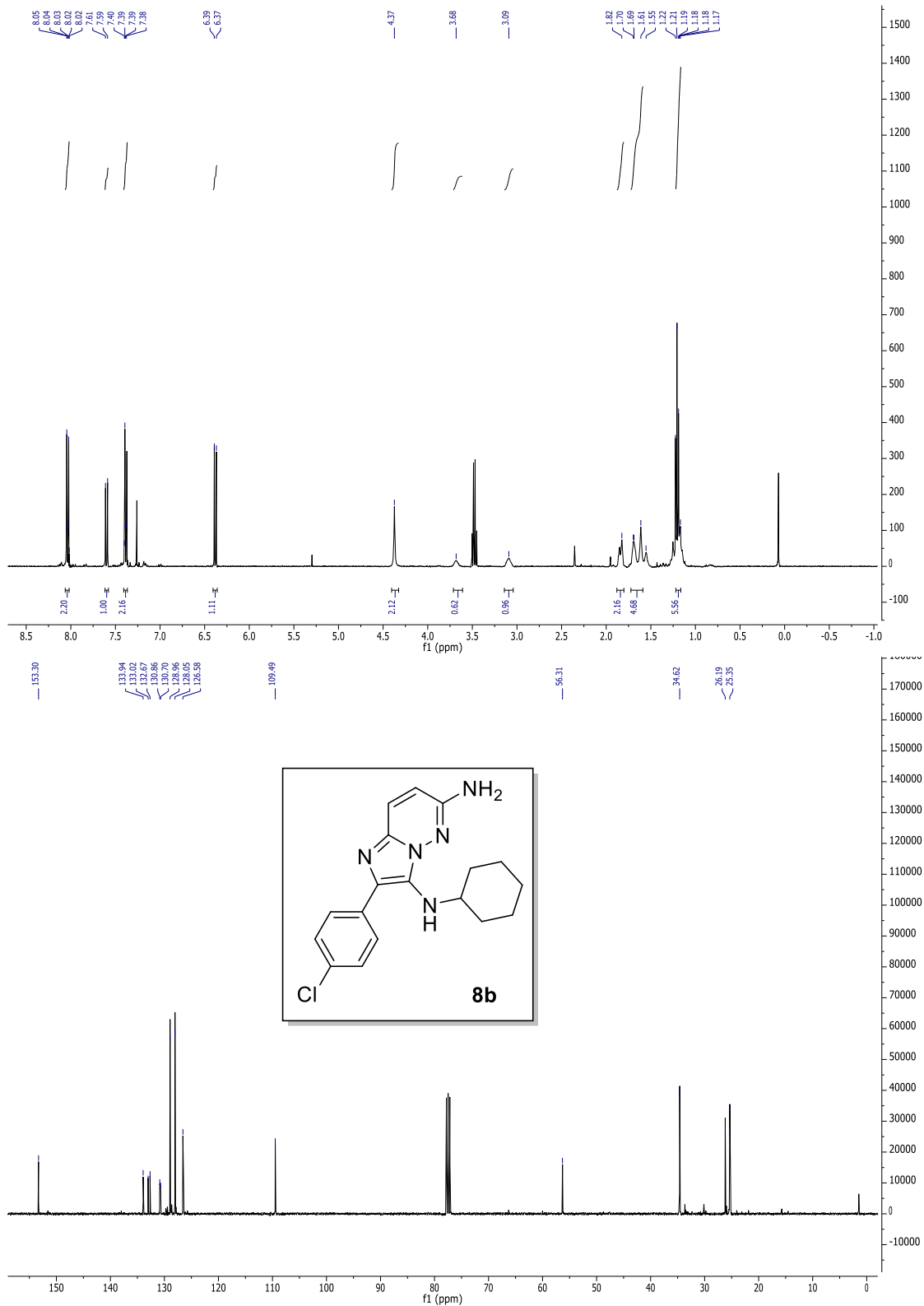
N⁹-(tert-butyl)-N³-cyclohexyl-8-(4-methoxyphenyl)-2-(pyridin-4-yl)diimidazo[1,2-a:1',2'-c]pyrimidine-3,9-diamine (5I)



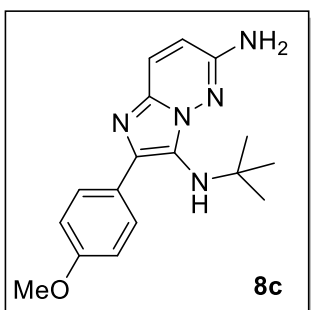
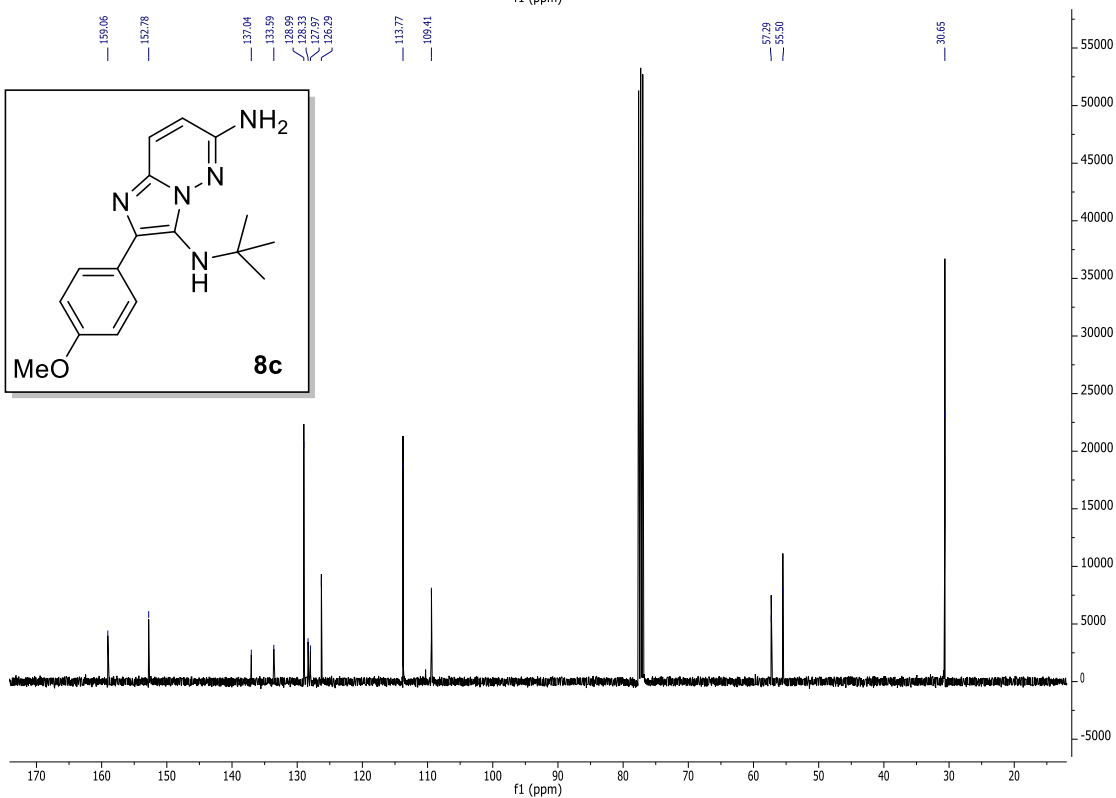
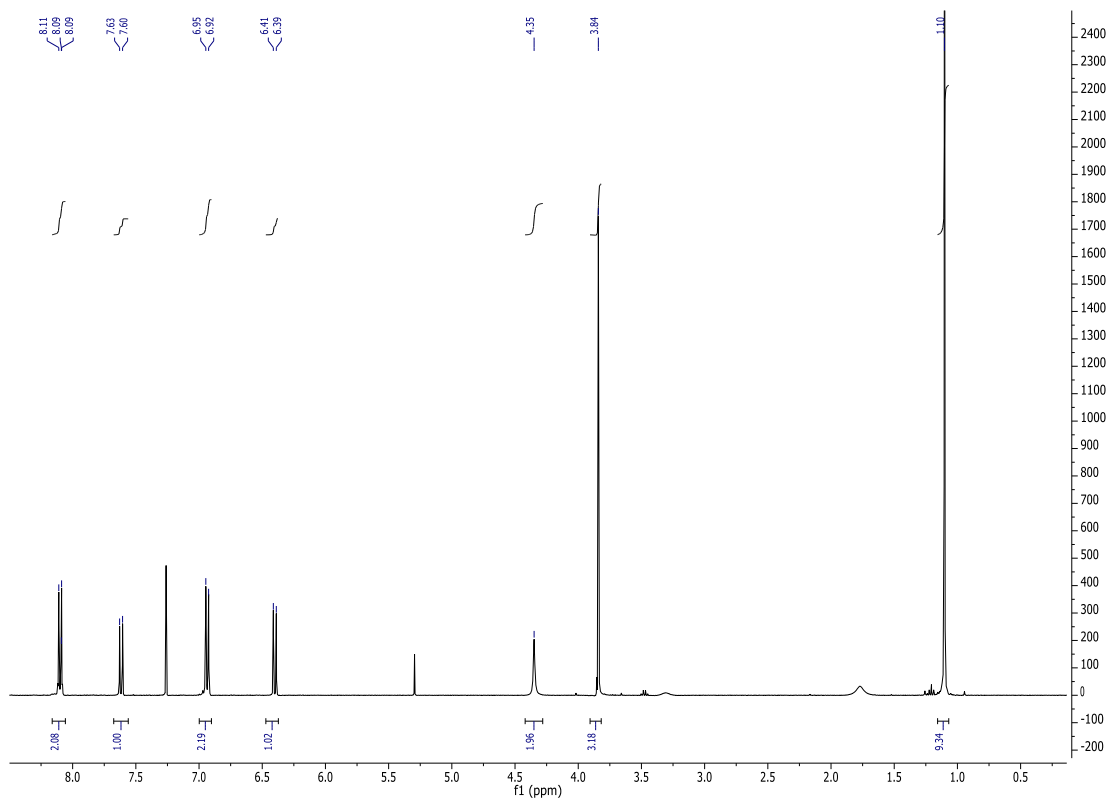
8-(2-(allyloxy)phenyl)-N⁹-(2-bromophenyl)-N³-cyclohexyl-2-(pyridin-4-yl)diimidazo[1,2-a:1',2'-c]pyrimidine-3,9-diamine (5m)



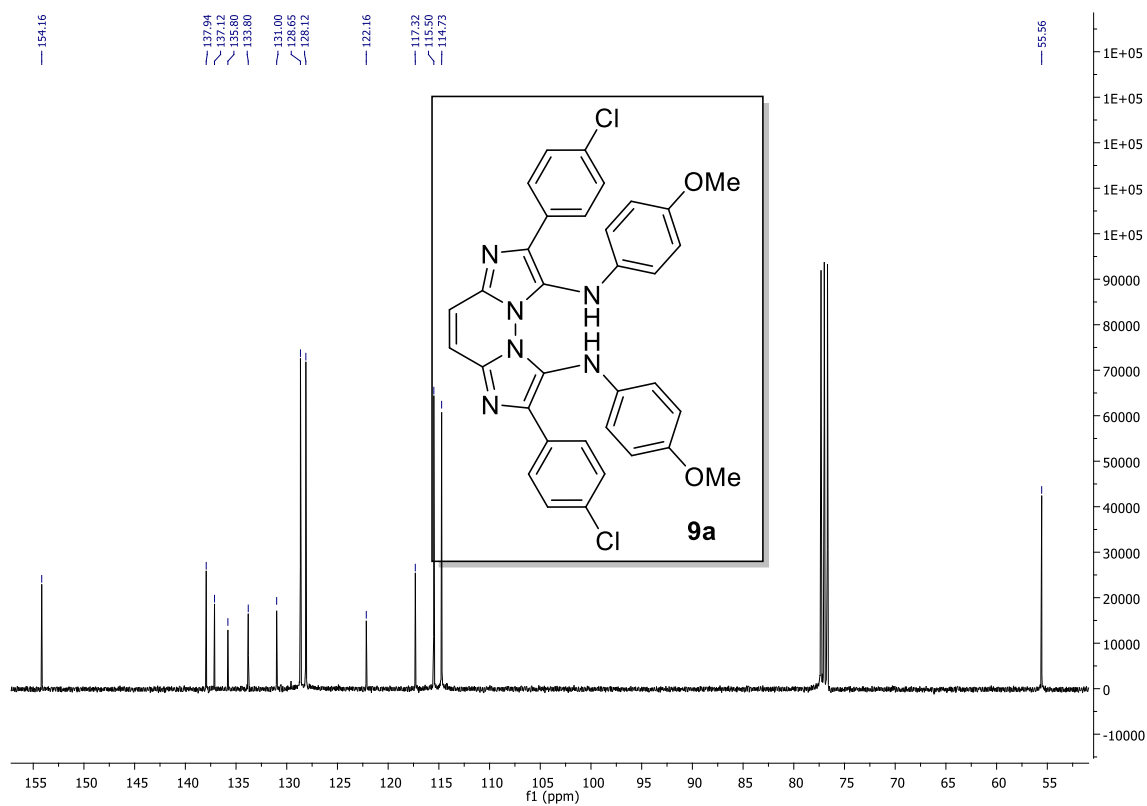
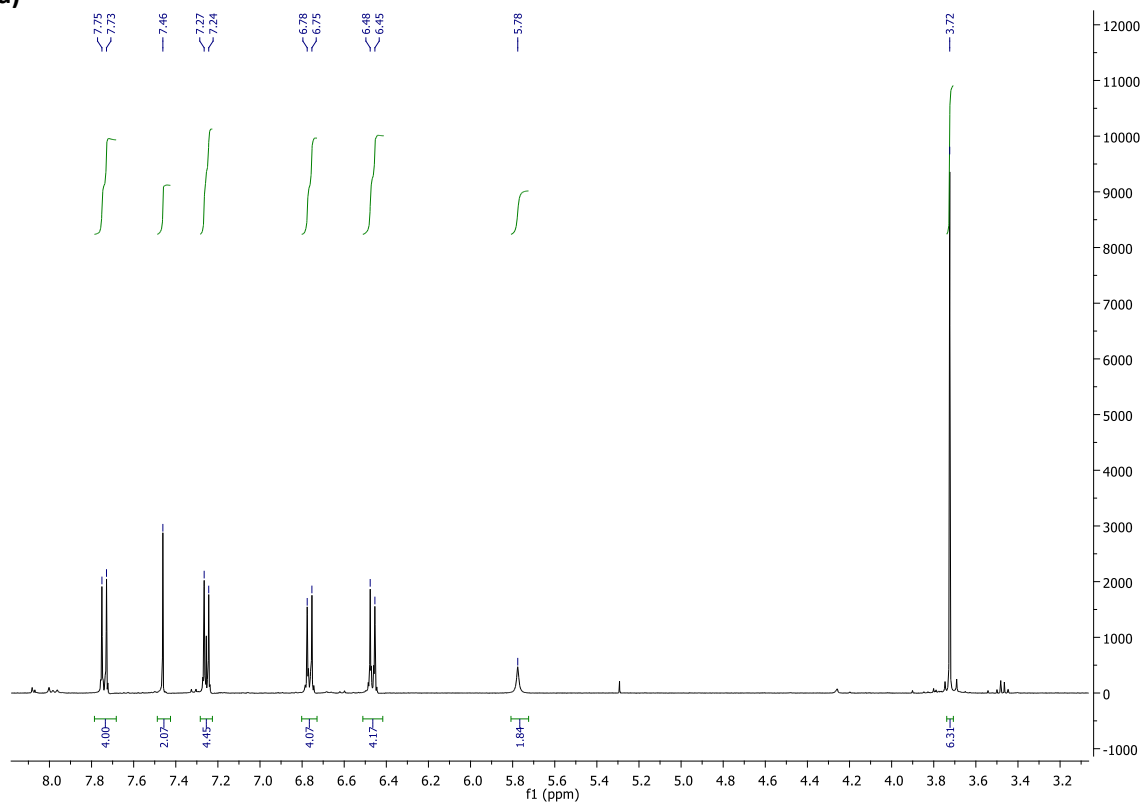
2-(4-chlorophenyl)-N³-cyclohexylimidazo[1,2-b]pyridazine-3,6-diamine (8b)



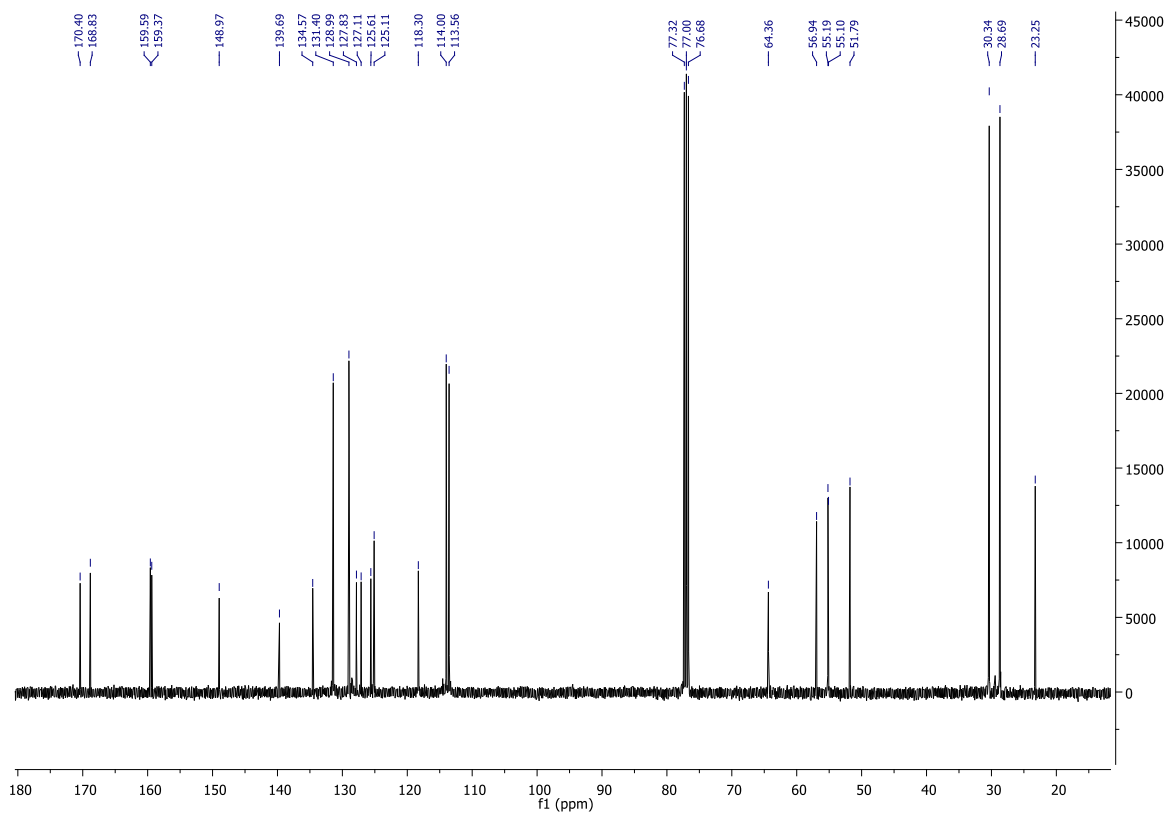
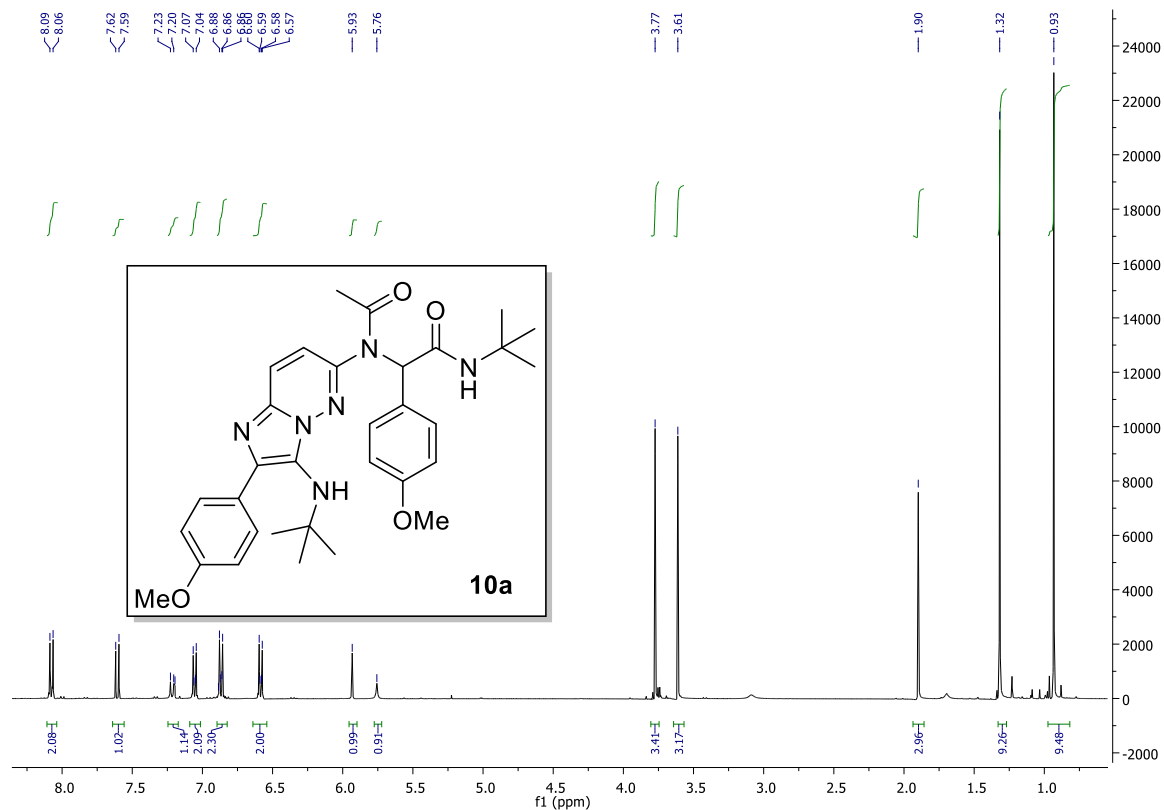
N³-(tert-butyl)-2-(4-methoxyphenyl)imidazo[1,2-b]pyridazine-3,6-diamine (8c)



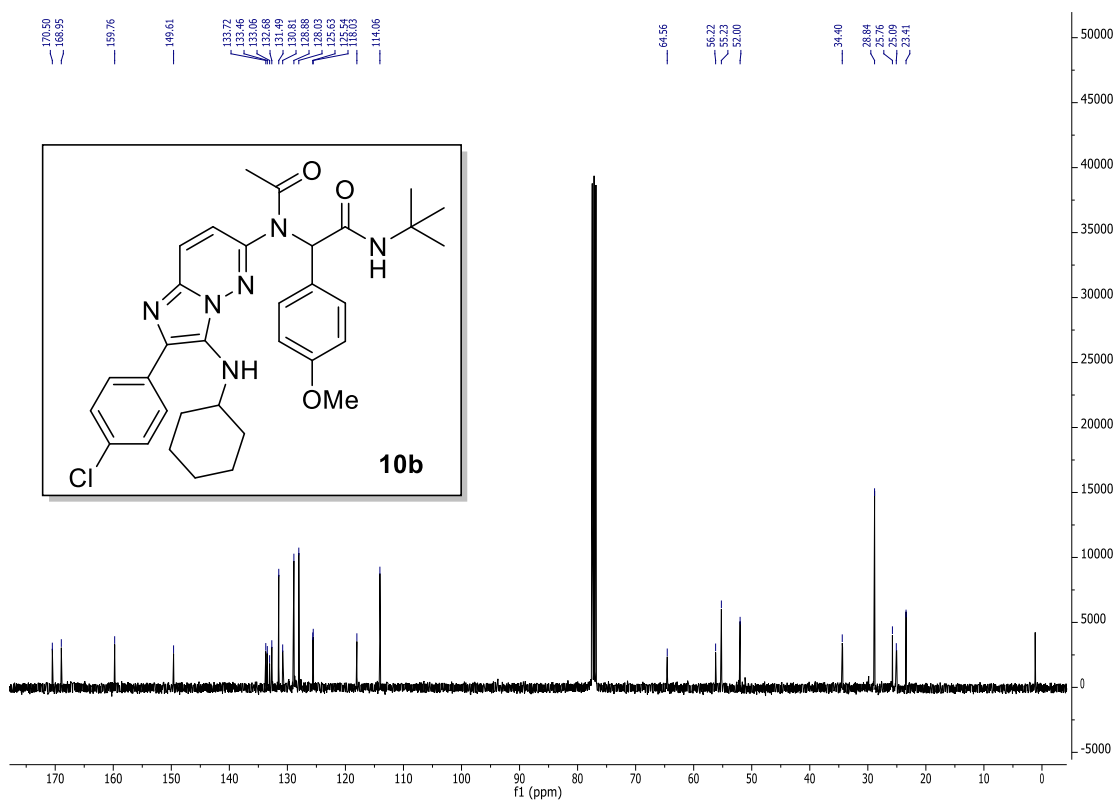
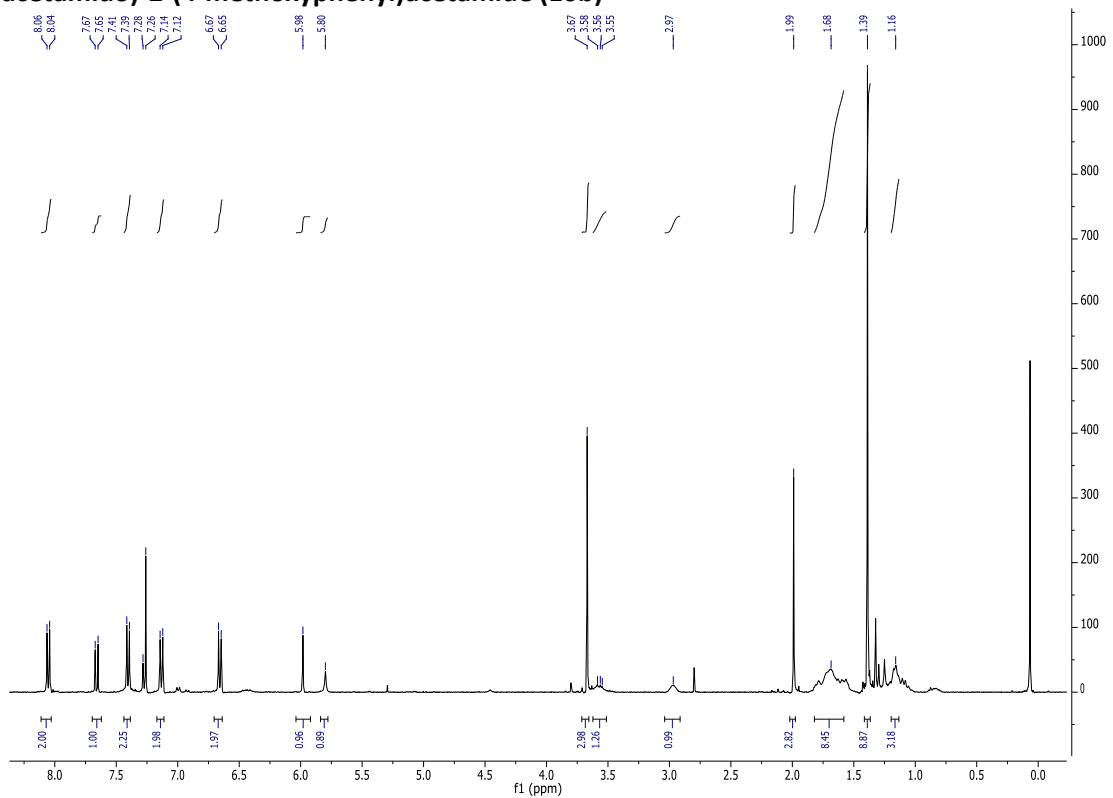
2,7-bis(4-chlorophenyl)-N¹,N⁸-bis(4-methoxyphenyl)diimidazo[1,2-b:2',1'-f]pyridazine-1,8-diamine (9a)



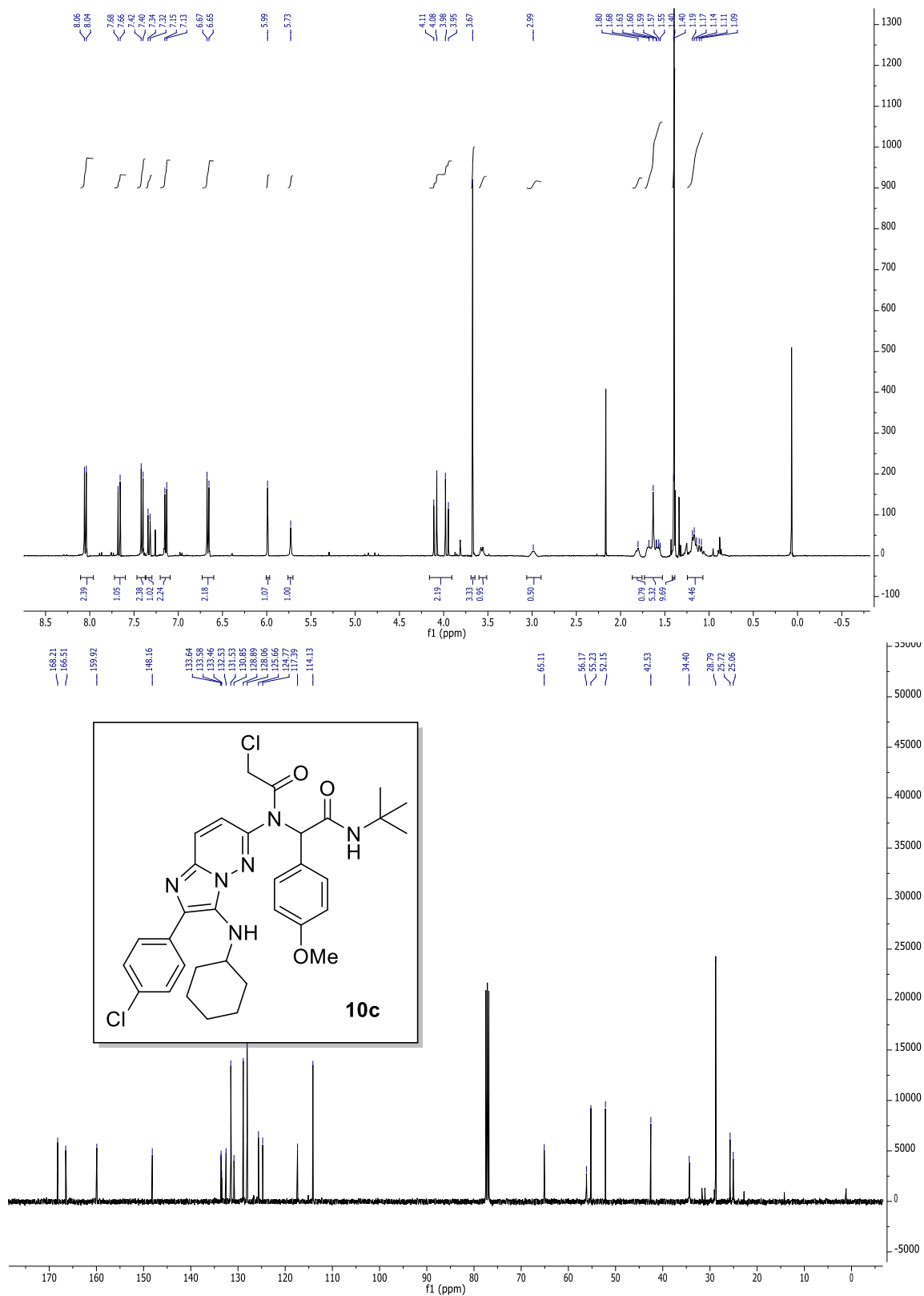
N-(tert-butyl)-2-(N-(3-(tert-butylamino)-2-(4-methoxyphenyl)imidazo[1,2-b]pyridazin-6-yl)acetamido)-2-(4-methoxyphenyl)acetamide (10a)



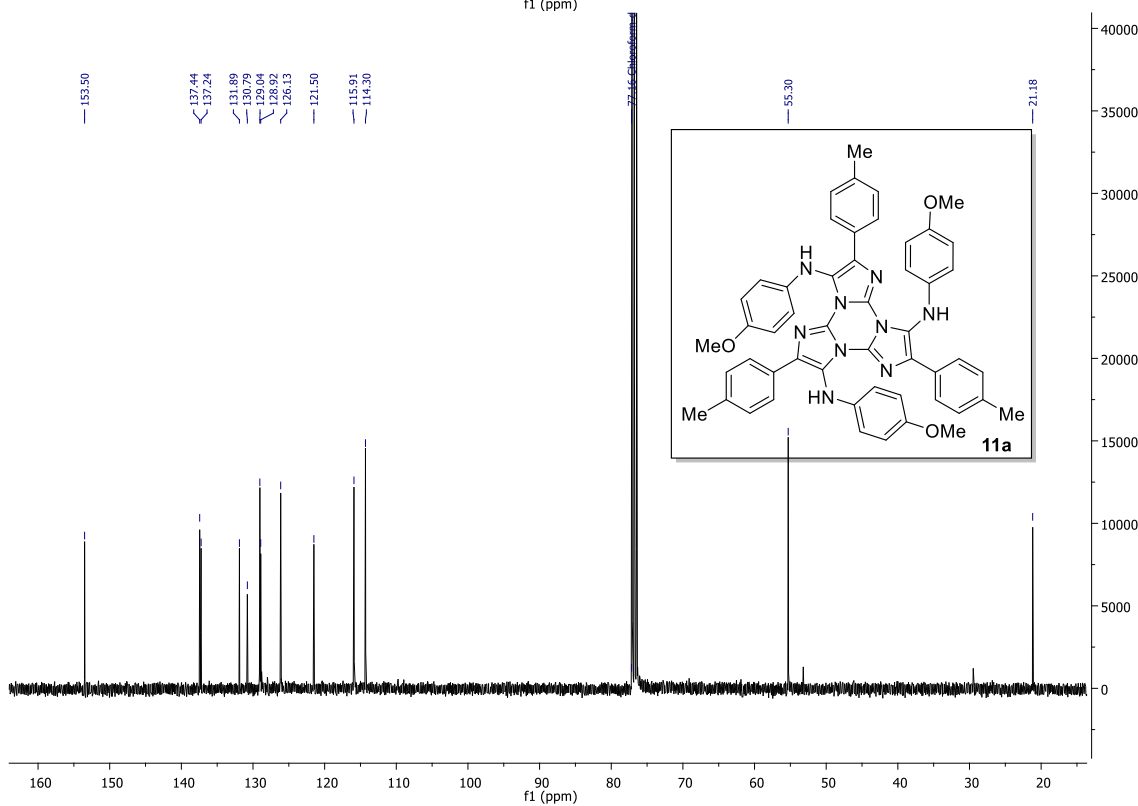
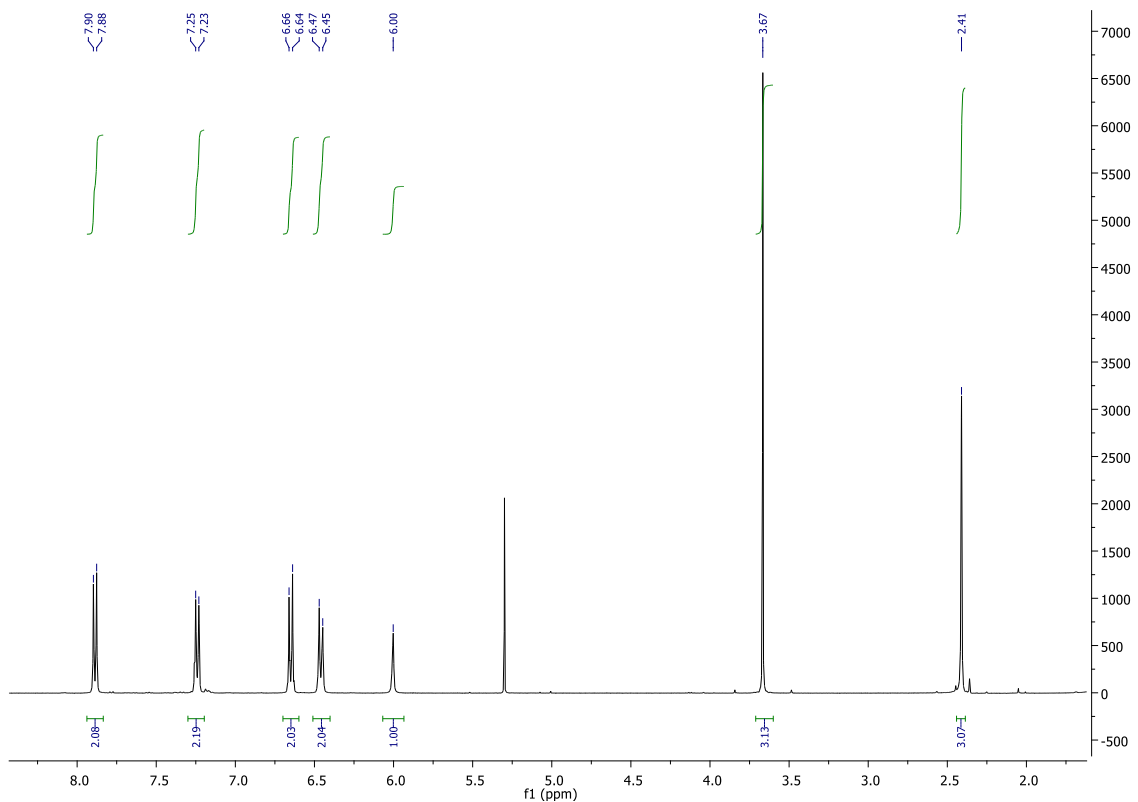
N-(tert-butyl)-2-(N-(2-(4-chlorophenyl)-3-(cyclohexylamino)imidazo[1,2-b]pyridazin-6-yl)acetamido)-2-(4-methoxyphenyl)acetamide (10b)



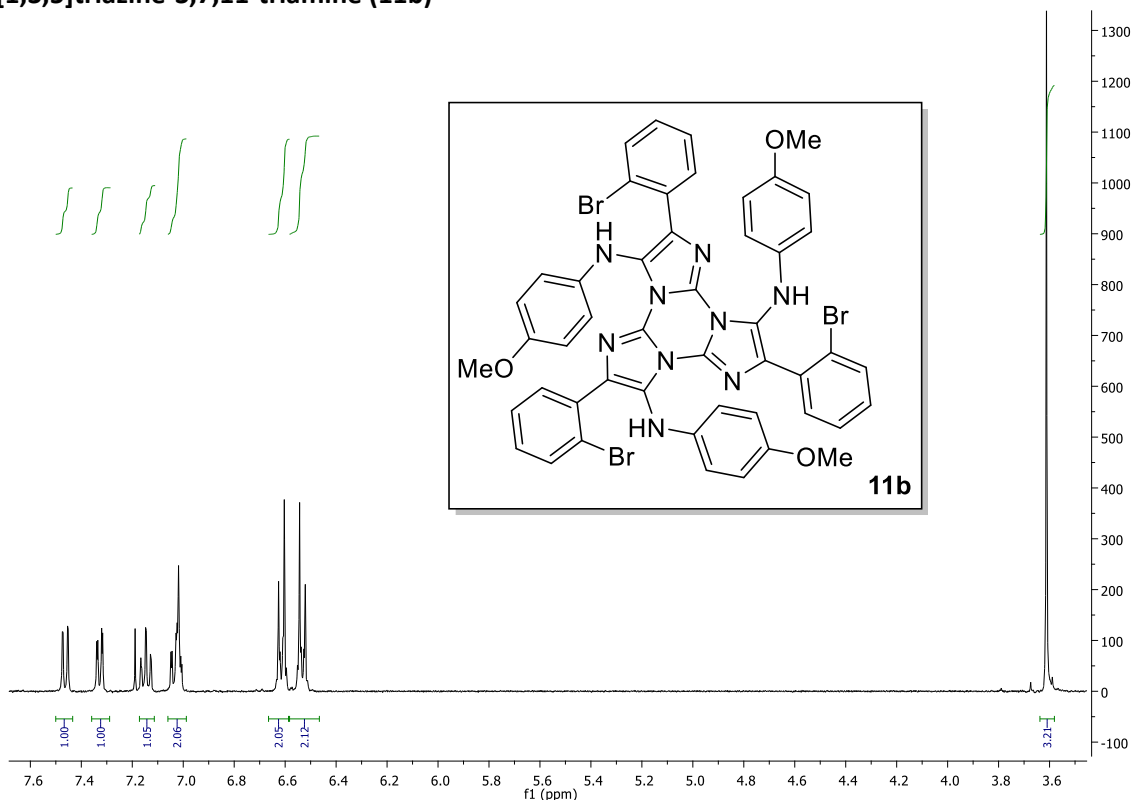
N-(tert-butyl)-2-(2-chloro-N-(2-(4-chlorophenyl)-3-(cyclohexylamino)imidazo[1,2-b]pyridazin-6-yl)acetamido)-2-(4-methoxyphenyl)acetamide (10c)



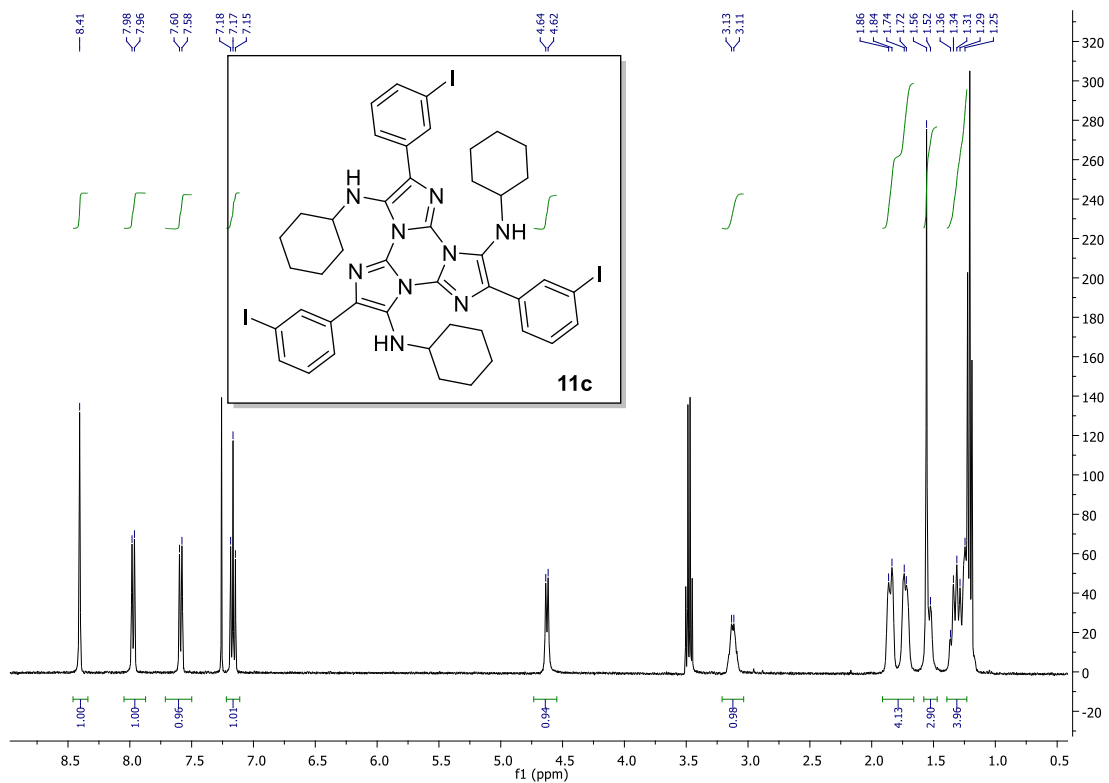
N³,N⁷,N¹¹-tris(4-methoxyphenyl)-2,6,10-tri-p-tolyltriimidazo[1,2-a:1',2'-c:1'',2''-e][1,3,5]triazine-3,7,11-triamine (11a)



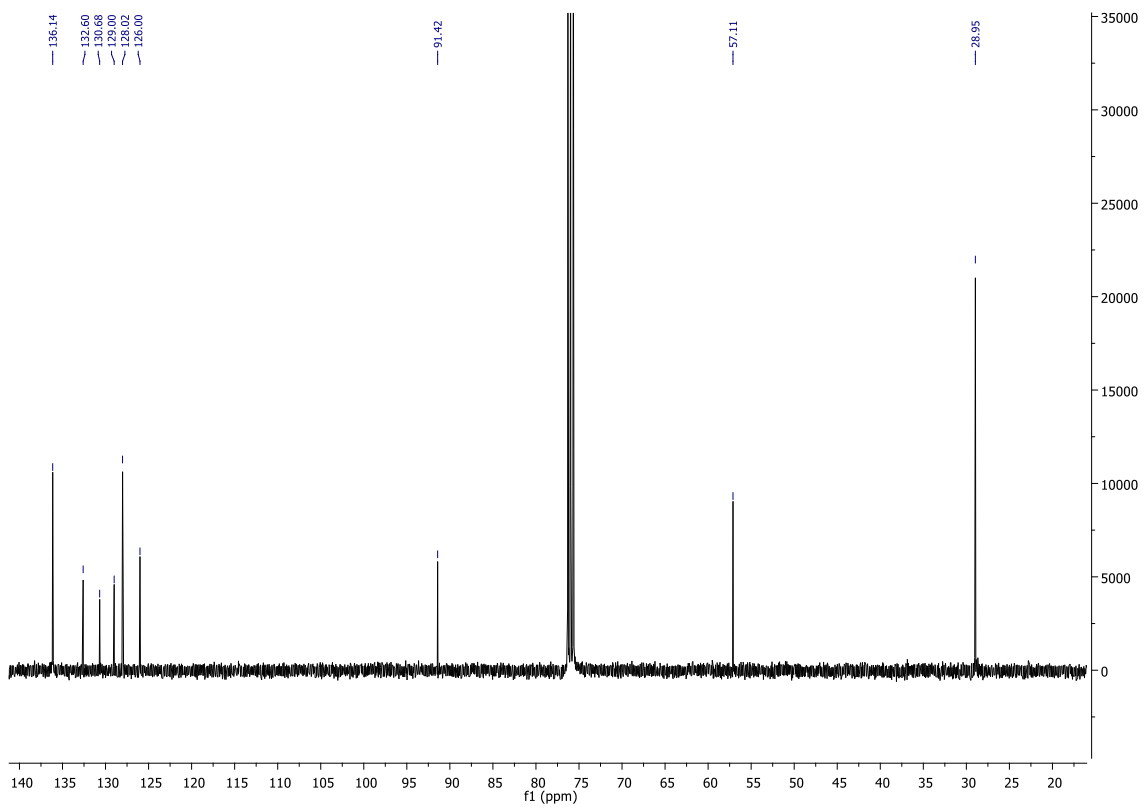
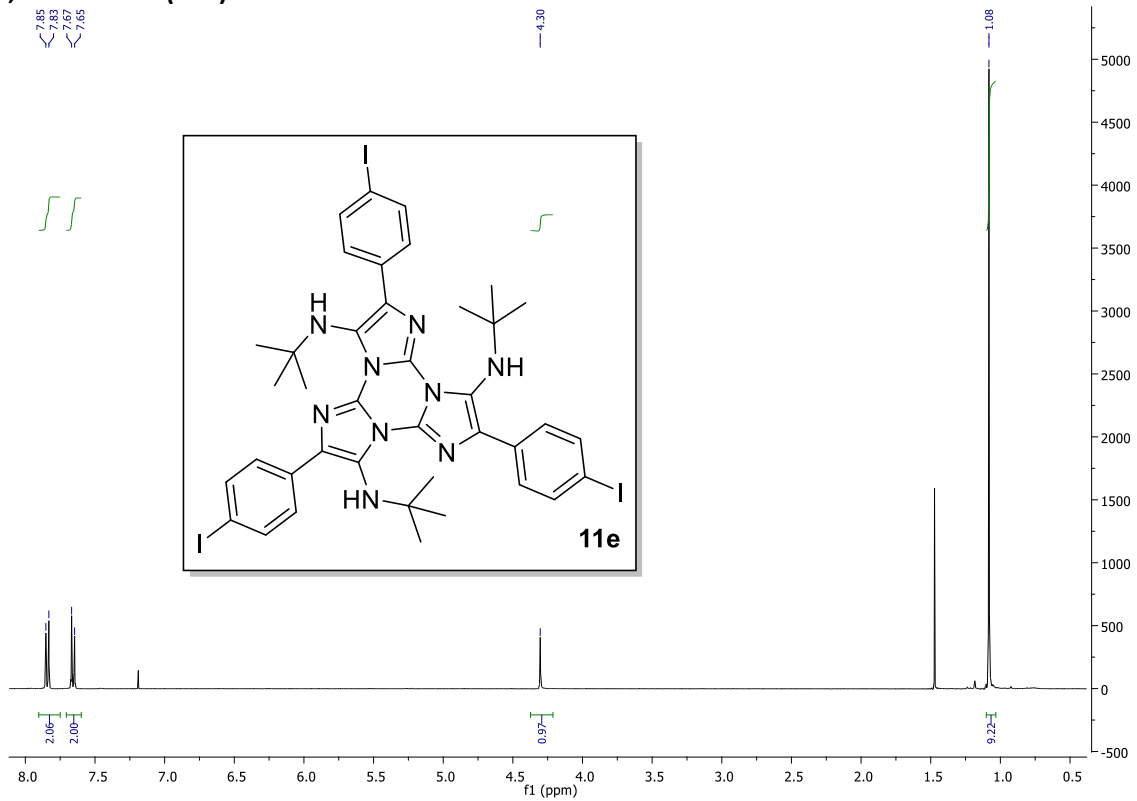
2,6,10-tris(2-bromophenyl)-N³,N⁷,N¹¹-tris(4-methoxyphenyl)triimidazo[1,2-a:1',2'-c:1'',2''-e][1,3,5]triazine-3,7,11-triamine (11b)



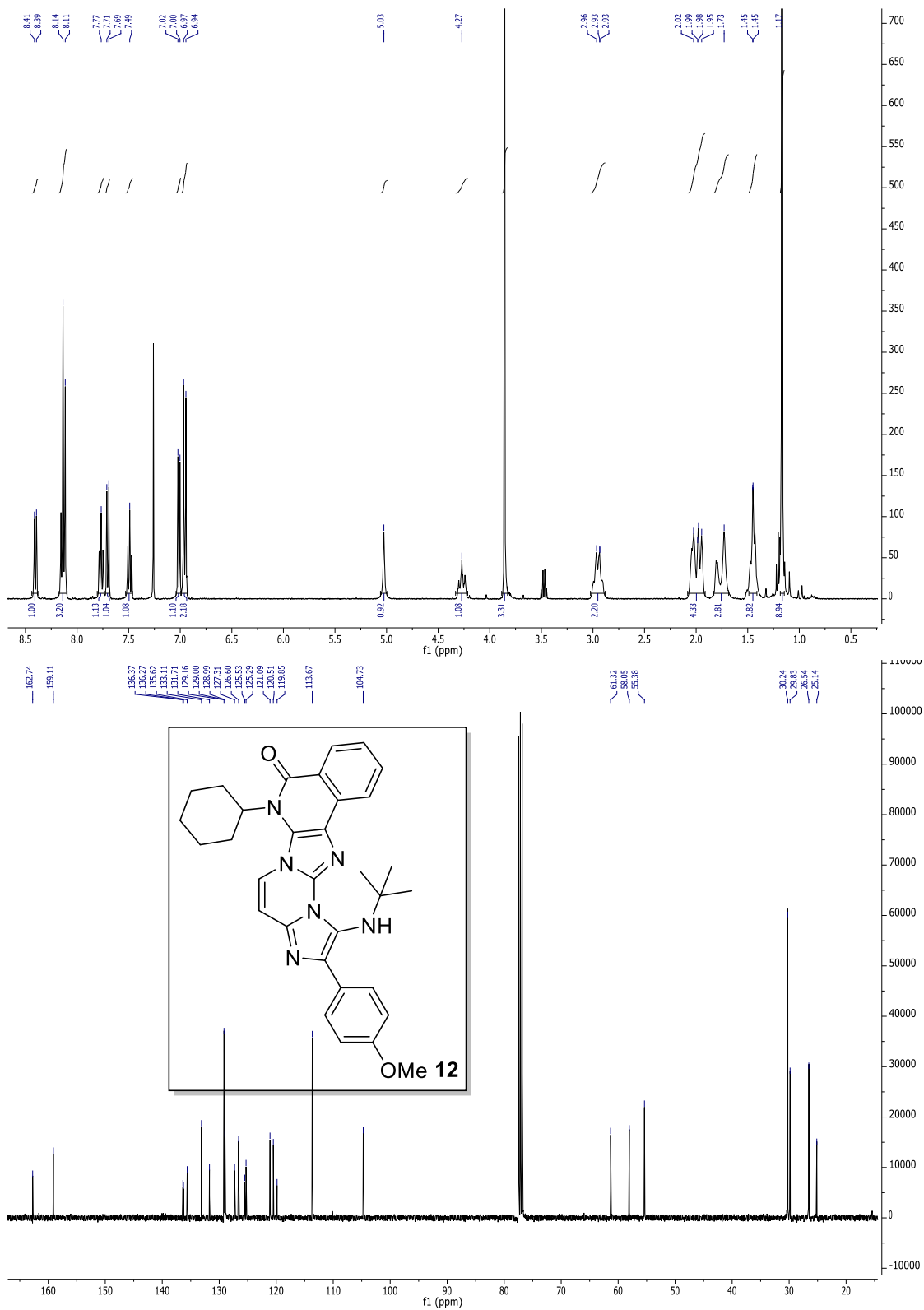
N³,N⁷,N¹¹-tricyclohexyl-2,6,10-tris(3-iodophenyl)triimidazo[1,2-a:1',2'-c:1'',2''-e][1,3,5]triazine-3,7,11-triamine (11c)



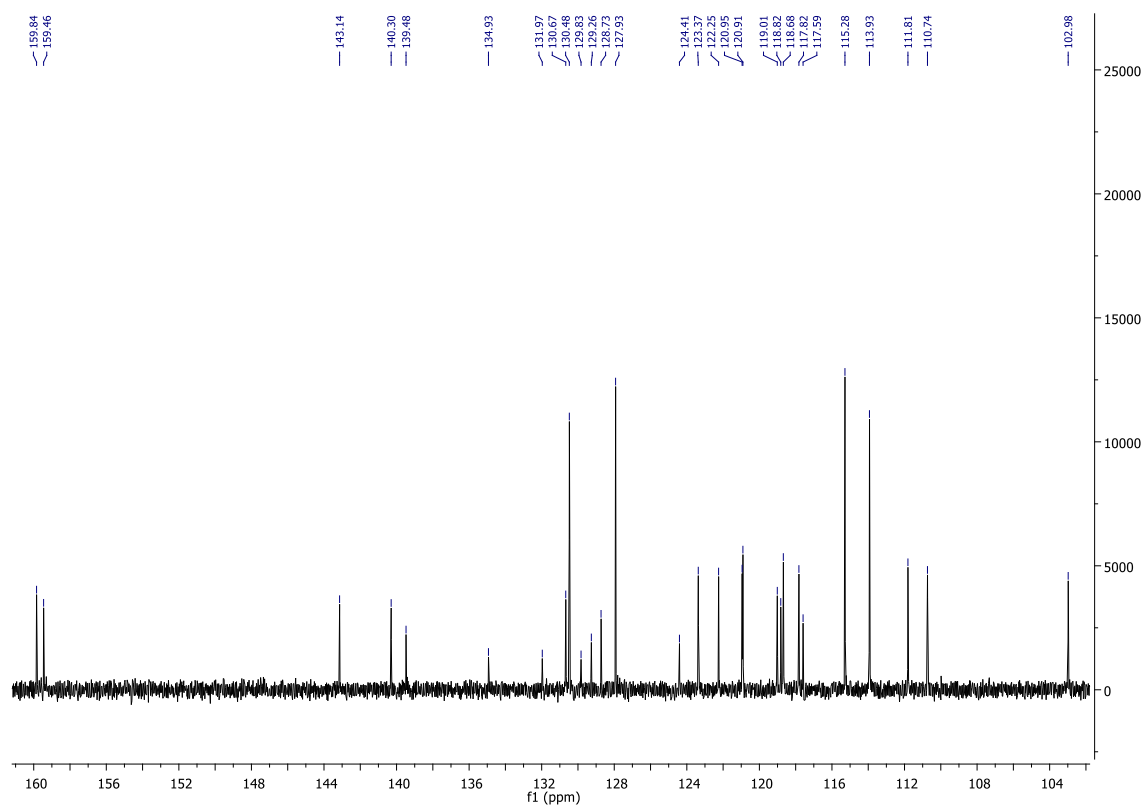
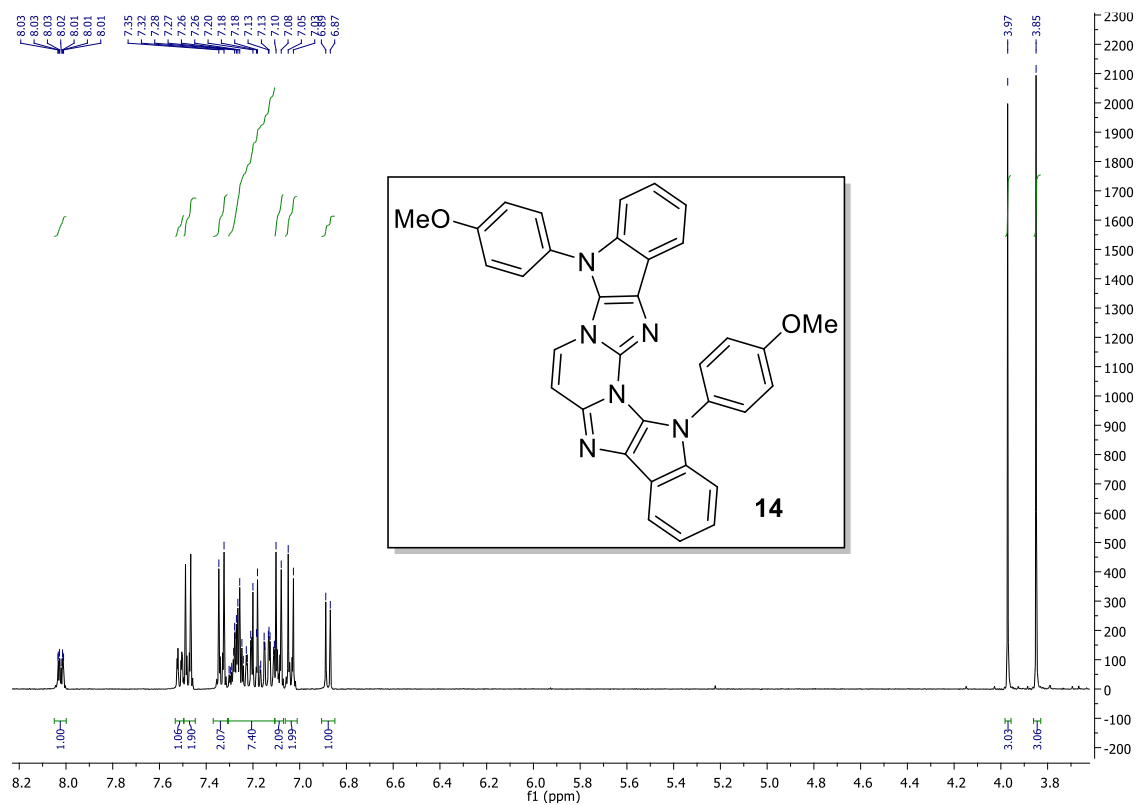
N³,N⁷,N¹¹-tri-tert-butyl-2,6,10-tris(4-iodophenyl)triimidazo[1,2-a:1',2'-c:1'',2''-e][1,3,5]triazine-3,7,11-triamine (11e)



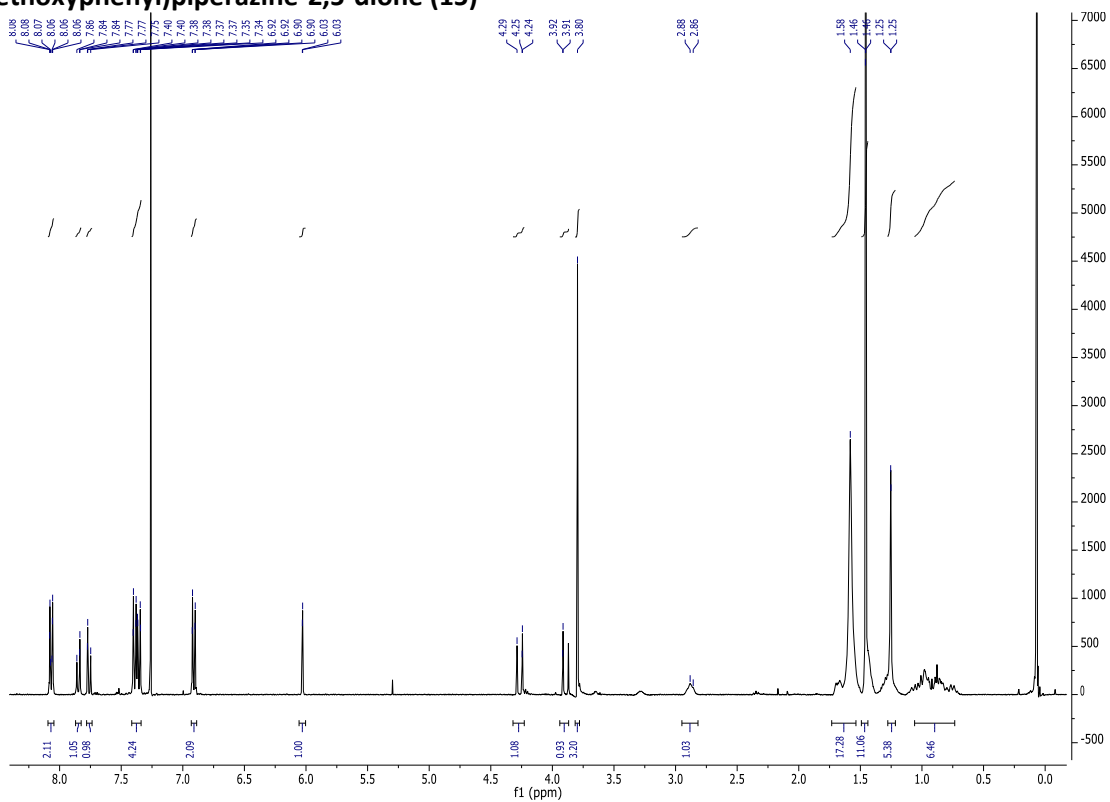
**1-(tert-butylamino)-7-cyclohexyl-2-(4-methoxyphenyl)imidazo[1'',2'':3',4']
pyrimido[2',1':2,3]imidazo[4,5-c]isoquinolin-8(7H)-one (12)**



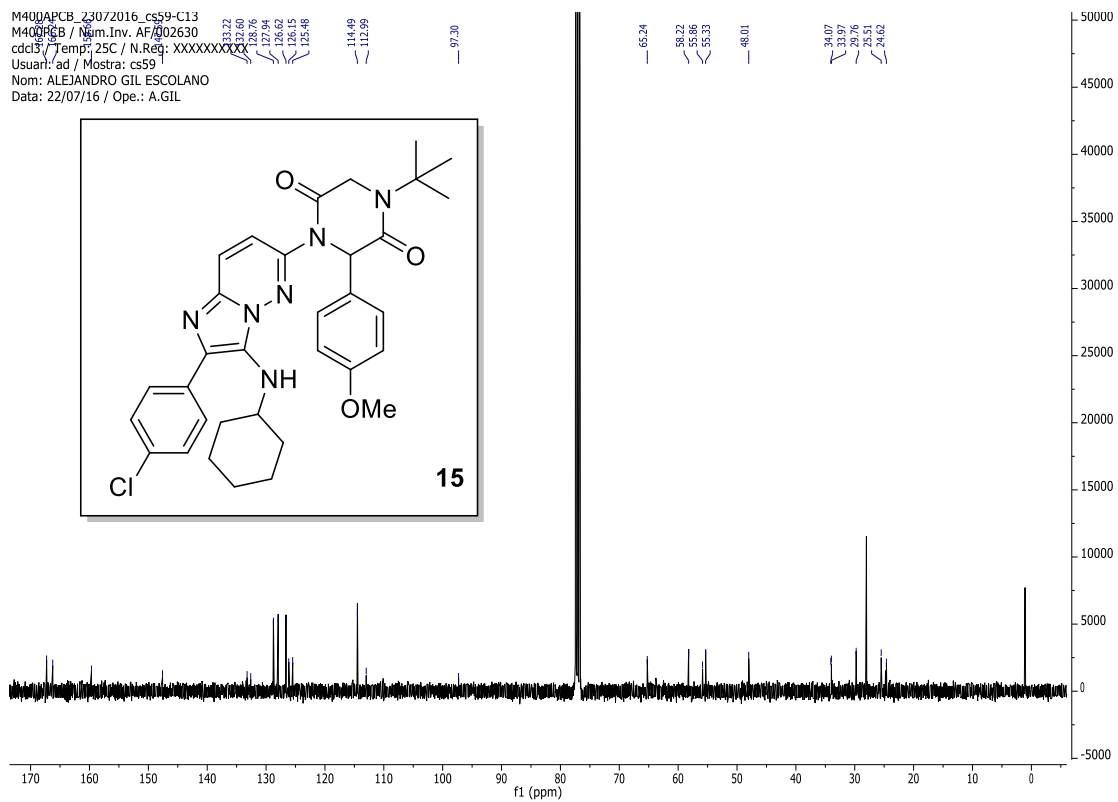
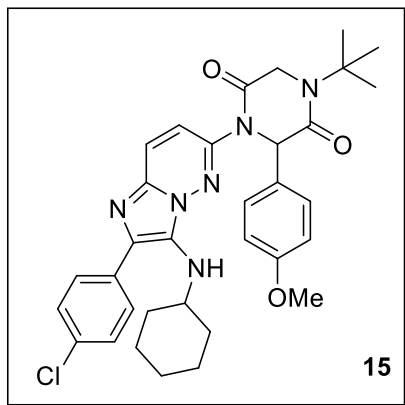
Diaminopyrimidine GBB adduct- Indole compound (14)



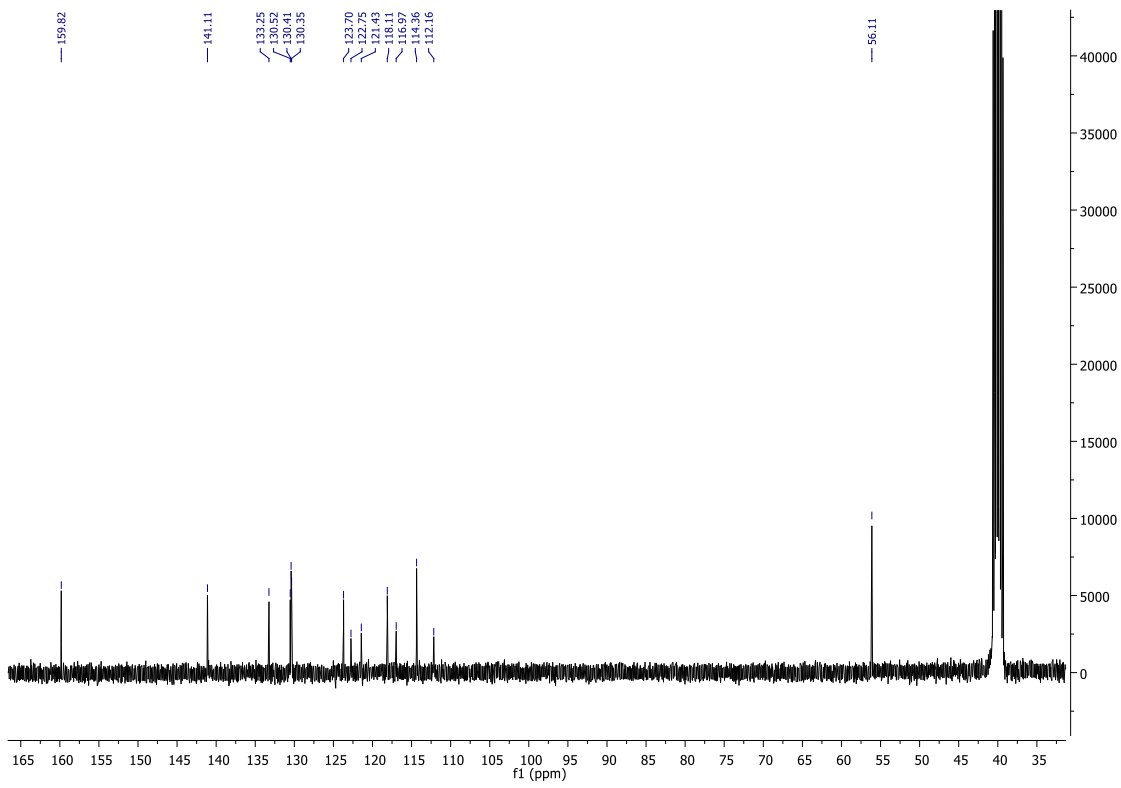
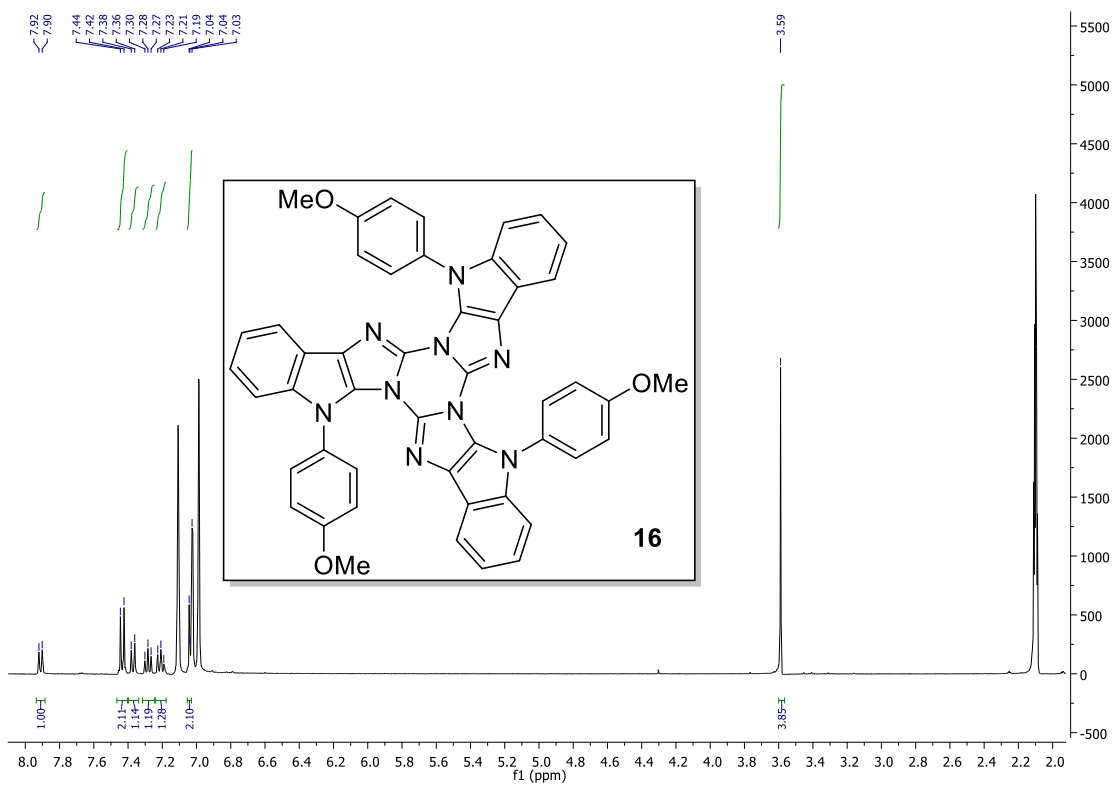
1-(tert-butyl)-4-(2-(4-chlorophenyl)-3-(cyclohexylamino)imidazo[1,2-b]pyridazin-6-yl)-3-(4-methoxyphenyl)piperazine-2,5-dione (15)



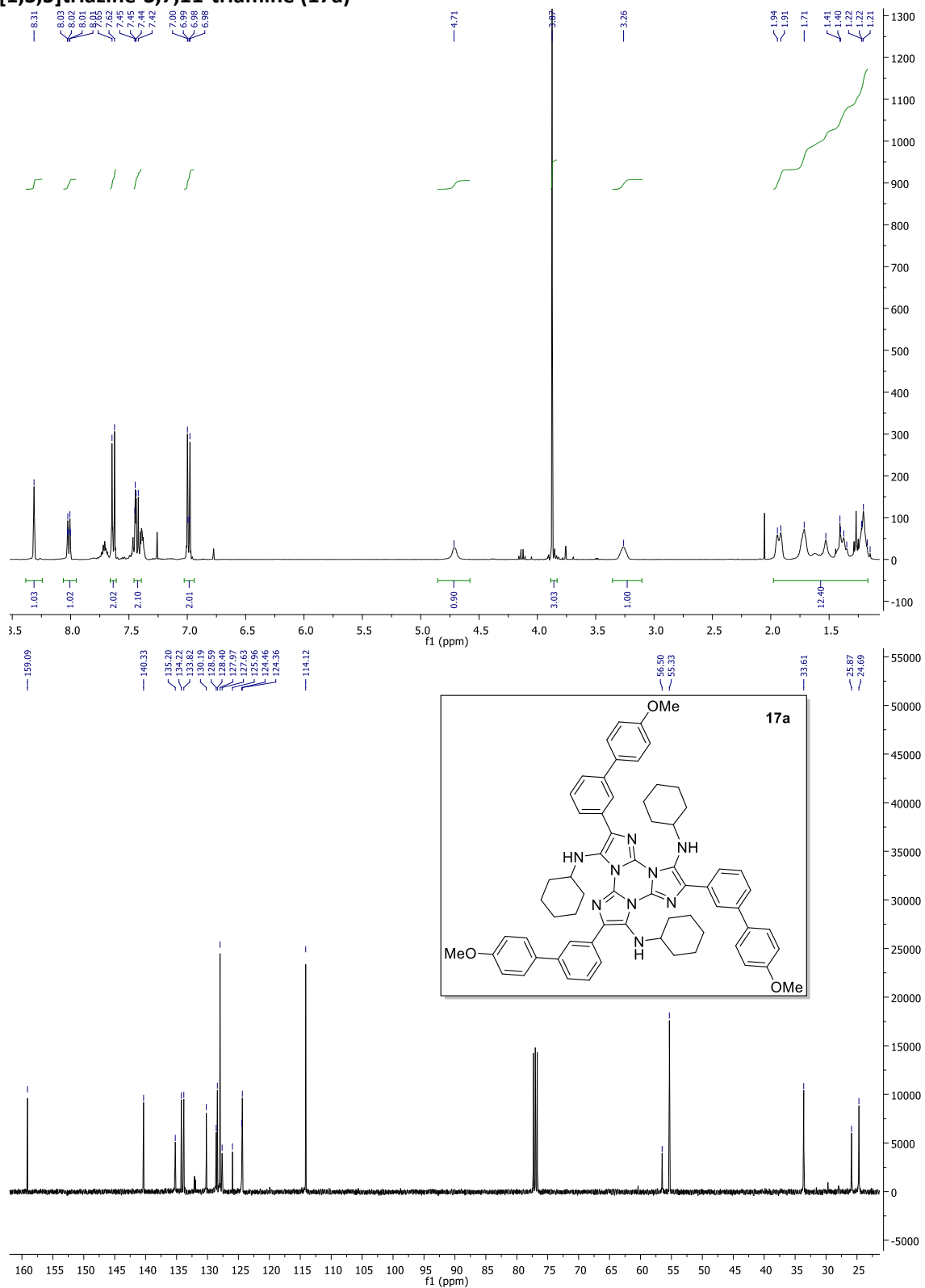
M400APCB_23072016_cs59-C13
 M400REB / Num.Inv. AF/002630
 cdcl3 / Temp: 25C / N.Reg: XXXXXXXXXX
 Usuar: ad / Mostra: cs59
 Nom: ALEJANDRO GIL ESCOLANO
 Data: 22/07/16 / Ope.: A.GIL



Melamine GBB adduct- Indole compound. (16)



N³,N⁷,N¹¹-tricyclohexyl-2,6,10-tris(4'-methoxy-[1,1'-biphenyl]-3-yl)triimidazo[1,2-a:1',2'-c:1'',2''-e][1,3,5]triazine-3,7,11-triamine (17a)



Material and Methods for Medicinal Studies

Cells and virus

Human A549 and 293 cell lines were from the American Type Culture Collection (ATCC, Manassas, VA). The 293 β 5 stable cell line overexpressing the human β 5 integrin subunit was kindly provided by Dr. Glen Nemerow (Nguyen et al., 2010). These cell lines were propagated in Dulbecco's modified Eagle medium (DMEM, Life Technologies/Thermo Fisher) supplemented with 10% fetal bovine serum (FBS) (Omega Scientific, Tarzana, CA), 10 mM HEPES, 4 mM L-glutamine, 100 units/ml penicillin, 100 μ g/ml streptomycin, and 0.1 mM non-essential amino acids (complete DMEM).

Wild-type HAdV5 was obtained from ATCC. The HAdV5-GFP used in this work is a replication-defective virus containing a CMV promoter-driven enhanced green fluorescent protein (eGFP) reporter gene cassette in place of the E1/E3 region (Nepomuceno et al., 2007). HAdV were propagated in 293 β 5 cells and isolated from cellular lysate by cesium chloride (CsCl) density gradient combined with ultracentrifugation.

Cytotoxicity assay

The cytotoxicity of the compounds was evaluated using the Alamar Blue Cell Viability Assay (Invitrogen) according to the manufacturer's instructions. Actively dividing A549 cells were incubated with the salicylanilide anthelmintic drugs for 48 h. After this incubation the Alamar Blue Reagent was added to the cells (1/10th Alamar Blue Reagent in culture medium) for an extra 4 h. The 50% cytotoxic concentration (CC₅₀) of the molecules was calculated according to Cheng *et al.* (Cheng et al., 2002). The selectivity index (SI) was evaluated as the ratio of CC₅₀ to IC₅₀, where the IC₅₀ is defined as the concentration of compound that inhibits HAdV infection by 50%.

Plaque assay

To test the antiviral activity of these molecules 293 β 5 cells were seeded in 6-well plates at a density of 4×10^5 cells per well. When cells reached 80–90% confluency, they were infected with HAdV5-GFP (0.06 vp/cell) and rocked for 2 h at 37°C. The inoculum was then removed, and the cells were washed once with PBS. The cells were then carefully overlaid with 2 mL/well of equal parts of 1.6% (water/vol) Difco Agar Noble (Becton, Dickinson & Co., Sparks, MD) and 2 \times EMEM (Minimum Essential Medium Eagle, BioWhittaker) supplemented with 2 \times penicillin/streptomycin, 2 \times Lglutamine, and 10% FBS. Following incubation for 7 days at 37°C,

plates were scanned with a Typhoon 9410 imager (GE Healthcare Life Sciences) and plaques were quantified with ImageJ. Molecules that showed an inhibition of HAdV plaque formation higher $\geq 90\%$ were further tested in a dose–response assay using 0.06 vp/cell and molecule concentrations ranging from 10 to 0.6 μM .

Virus yield reduction

The effect of the active molecules on virus production was evaluated in a burst assay. A549 cells were infected with wild-type HAdV5 (MOI 100) in the presence or absence of 50 μM of each molecule. After 48 h, cells were harvested and subjected to three rounds of freeze/thaw. Serial dilutions of clarified lysates were titrated on A549 cells, and TCID₅₀ values were calculated using a previously reported end-point dilution method (Reed and Muench, 1938).

Statistical Analyses

Statistical analyses were performed with the GraphPad Prism 5 suite. Data are presented as the mean of triplicate samples \pm standard deviation (SD).

DNA binding studies

The DNA binding studies were carried out following the procedure reported by Eritja et al.¹¹

Competitive Dialysis Assays.

100µL of a 50µM oligonucleotide (Table 1) in potassium phosphate buffer (185mM NaCl, 185mM KCl, 2mM NaH₂PO₄, 1mM Na₂EDTA, 6mM Na₂HPO₄ at pH 7) was introduced into a separated dialysis unit. A blank sample containing only buffer without oligonucleotide was also prepared. All 11 dialysis units were then placed in the beaker containing the 1µM solution of the synthesized GBB adducts. The samples were allowed to equilibrate with continuous stirring at room temperature overnight. After the equilibration period, DNA samples were removed to an Eppendorf tube. In order to measure the compound retained in the dialysis unit, samples were treated with snake-venom phosphodiesterase to degrade the DNA and release the GBB from oligomer. 350µL of potassium phosphate buffer (without EDTA), buffer at pH 8.5, 50µL of 100mM MgCl₂, and 1 µm of snakevenom phosphodiesterase solution were added for an additional overnight incubation at 37°C. Finally, the fluorescence of each sample was measured (λ_{ex} and λ_{em} were set based on the results from photophysical studies)

Fluorescence Assays.

The study of the interaction equilibrium of acridine derivatives and oligonucleotides consists of recording the fluorescence spectra of a 0.2µM solution of the GBB derivative after the addition of increasing amounts of oligonucleotide (from 0 to 10µM) in potassium phosphate buffer (185mM NaCl, 185mM KCl, sodium phosphate, 1mM EDTA, pH 7). These experiments were carried out by adding small volumes of an oligonucleotide stock solution to the 0.2µM solution of the GBB derivative. After each addition, the emission spectra of the resulting solutions were recorded.

¹¹ R. Ferreira, A. Aviñó, R. Perez-Tomás, R. Gargallo, R. Eritja; J. Nucleic Acids **2010**, Article ID 489060 (doi:10.4061/2010/489060.)

Table 2: The oligonucleotides used for the screening experiments against GBB adducts

	Name	Sequence	Type
1	DL40	5' GGTTTTGGCAGGGTTTTGGT3'	Antiparallel QUADRUPLEX
2	TBA	5' GGTTGGTGTGGTTGG 3'	Antiparallel QUADRUPLEX
3	TEL22	5' AGGGTTAGGGTTAGGGTTAGGG 3'	Antiparallel/parallel QUADRUPLEX
4	GG1	5' GGGCGGGCGCGAGGGAGGGT 3'	Parallel QUADRUPLEX
5	TG4	5' TGGGGT 3'	Parallel QUADRUPLEX
6	24BCLC	5' CCCGCCCTTCTCCCGCCTCCG 3'	I MOTIF
7	T20	5' TTTTTTTTTTTTTTTTTT 3'	SINGLE STRAND
8	DS26	5' CAATCGGATCGAATTCGATCCGATTG 3'	DUPLEX
9	DICK	5' CGCGAATTCGCG 3'	DUPLEX
10	24BCL	5' CGGGCGCGGGAGGAAGGGGGCGG 3'	HYBRID QUADRUPLEX

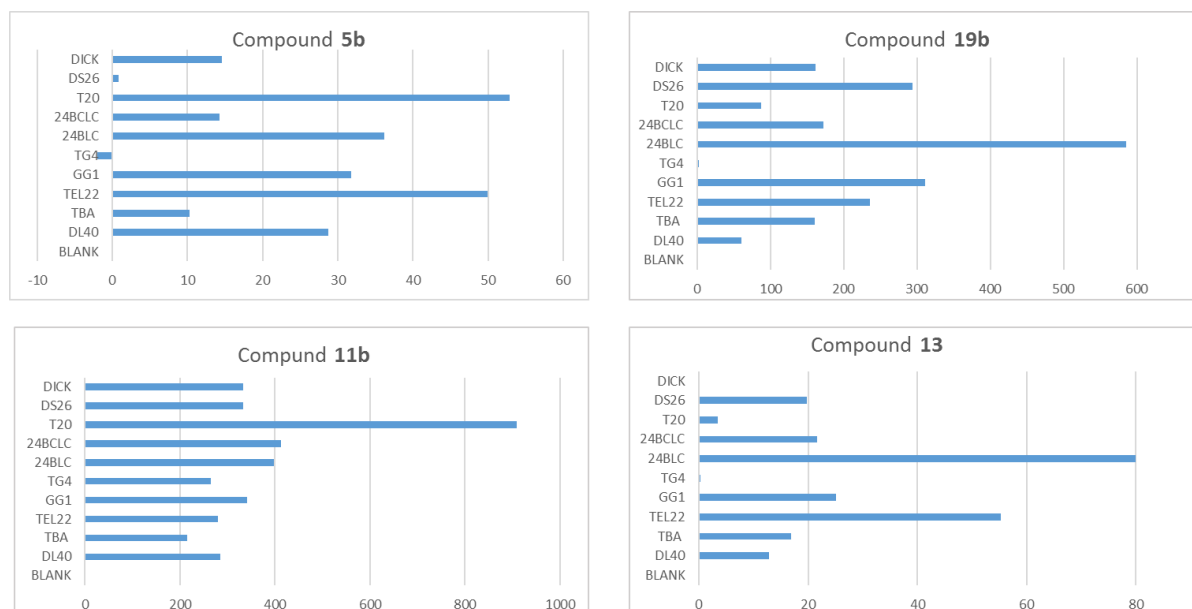


Figure 1. Results obtained by the competitive dialysis assay. The amount of ligand bound to each DNA structure is shown as a bar.

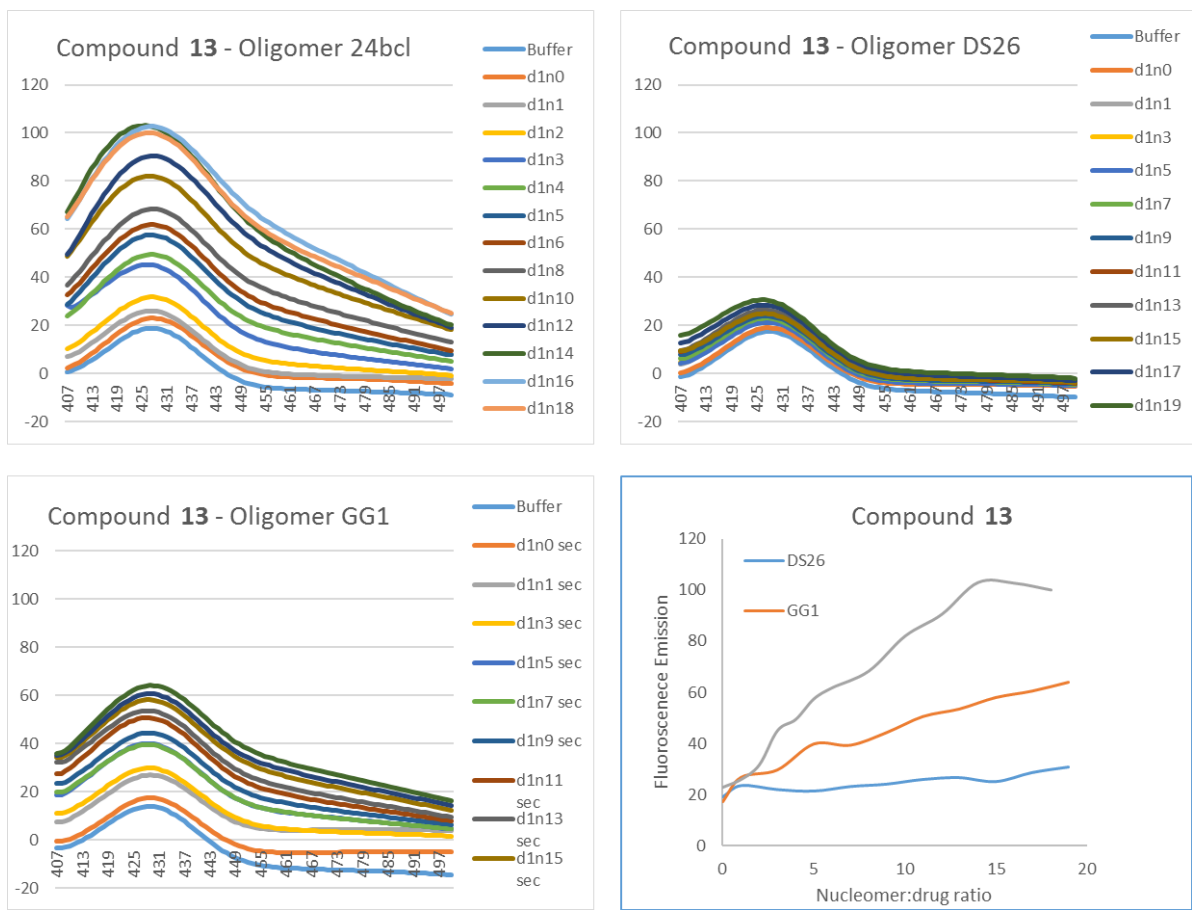
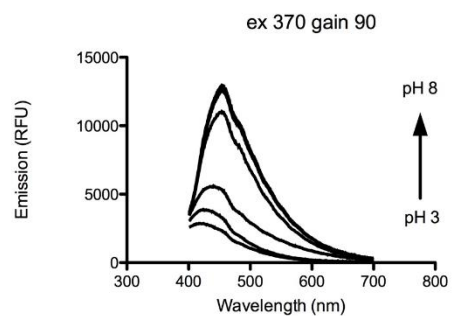
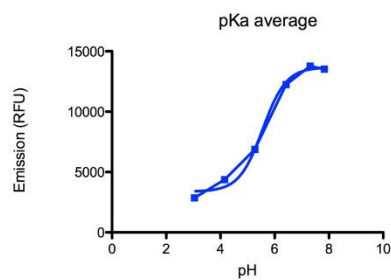
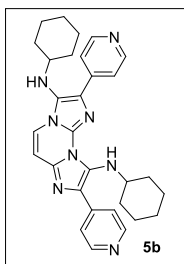
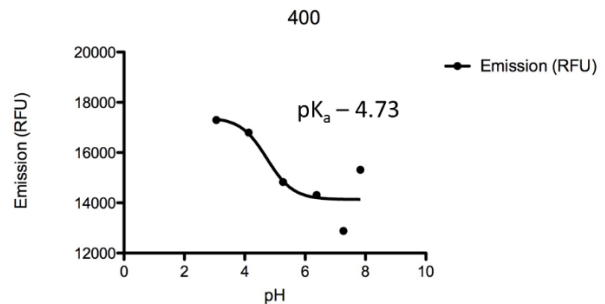
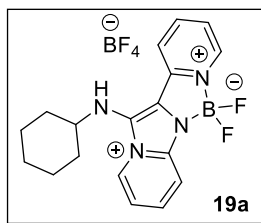
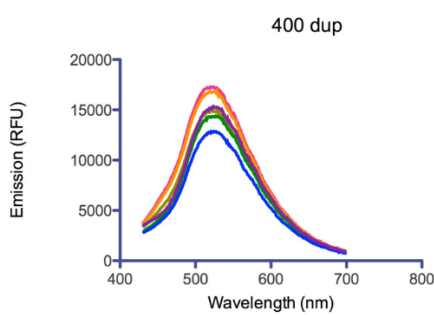
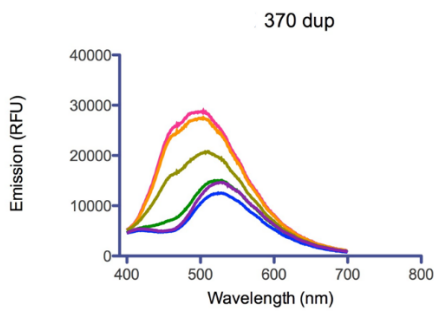
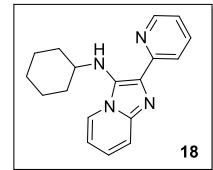
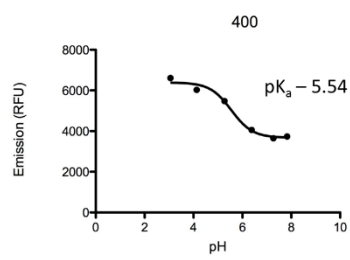
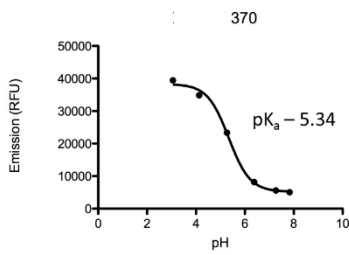
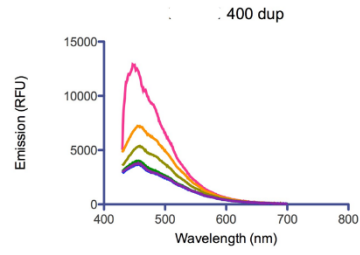
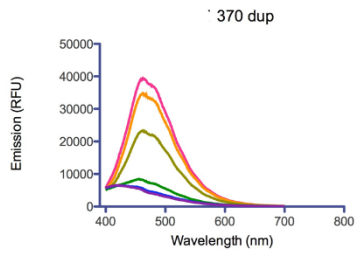
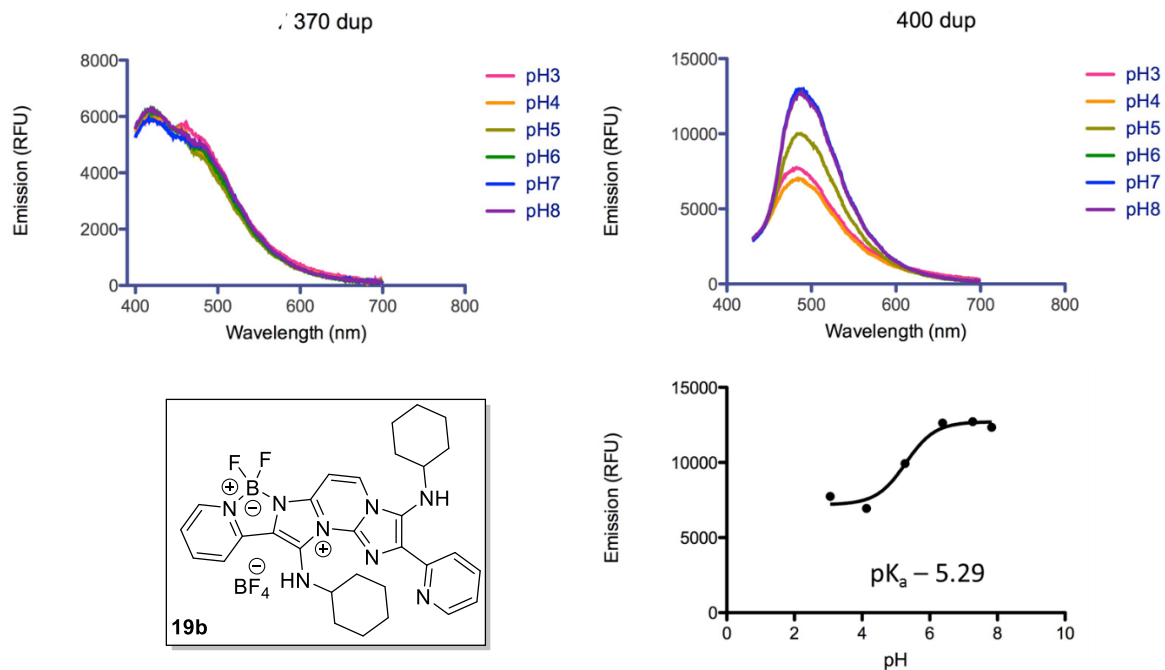


Figure 2. Fluorescence titration spectra. Fluorescence spectra of a 0.2 μ M solution of the Compound **13** after the addition of increasing amounts of quadruplex oligonucleotides 24bcl and GG1, and duplex DS26 as negative control (from 0 to 10 μ M) in potassium phosphate buffer.

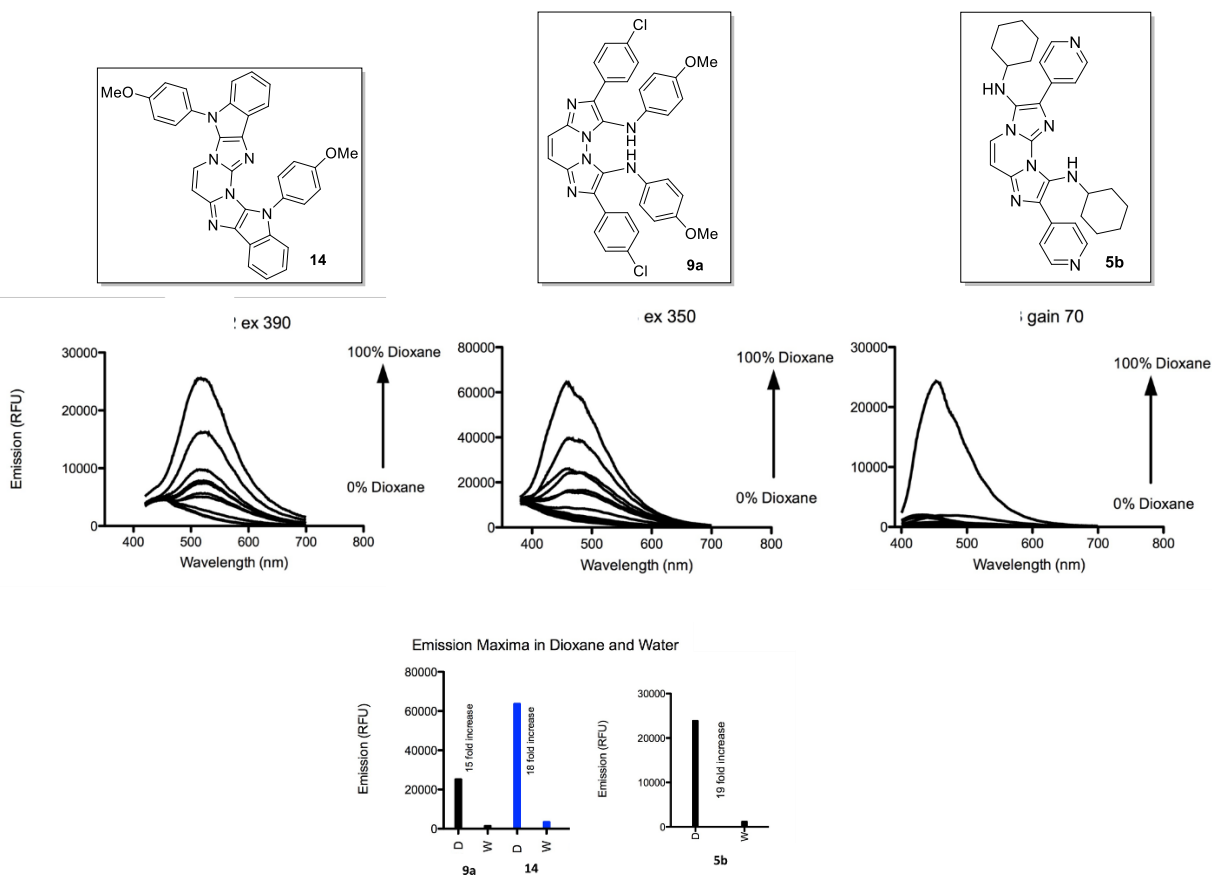
Photophysical properties of GBB adducts

pH dependent Absorbance of GBB adducts





Lipophilicity-dependent Absorbance of GBB adducts



Conclusions

Conclusions:

1. It was observed that the interaction of imines and isocyanides in the presence of a Lewis acid can lead to a variety of scaffolds including α -aminoamides, α -aminoamidines, indoles and diiminoazetidines. The reaction conditions were optimized to yield the later as the main product. Screening the scope of amines, aldehydes and isocyanides led to a small library of azetidine adducts. Also, a few spiro-azetidine adducts were prepared using isatine ketimines. A unified mechanism was proposed to explain the structural diversity that the process offers. In case of the main azetidine adduct, the process goes through consecutive insertion of two isocyanides followed by a 4-exo-dig cyclization. The structural elucidation of the azetidine compounds confirms the unexpected *syn* nature of the formed imine bonds.
2. It was shown that N-insertion of isocyanides to N-substituted propargylamines in the presence of HCl yields 1,3,4,5-tetrasubstituted imidazolium salts. As the propargylamines arise from A³ reactions, the scope of the process in terms of aldehydes, amines, alkynes, and isocyanides was studied. The described conditions do not apply for aliphatic amines as opposed to the Zhu reaction ^[1] who used a different activation method (dual metallic catalysis). However, mild reaction conditions allow the incorporation of tert-Bu isocyanide, avoiding undesired elimination, as in Zhu conditions. Furthermore, the A³ reaction was successfully combined with the new reaction to obtain the imidazolium salts in a one pot process. We also explored the properties of the MCR adducts: As a proof of concept, an adduct was used as an NHC ligand to catalyze a standard Suzuki coupling. Interestingly, some of the obtained compounds displayed potent antiparasitic activity against *Trypanosoma brucei* and *T. cruzi* at nanomolar level.
3. A TMSCl- catalyzed Reissert type MCR was studied. The process features the insertion of isocyanide to N-Si bond as the mechanistical key step. Computational and experimental methods were applied to study this novel interaction of isocyanides and N-Si bonds. The reaction yields aminoimidazolium salts from the incorporation of two isocyanide units into azines. The new activation mode offers significantly wider scope. Regioselective incorporation of two distinct isocyanides was successfully performed. Furthermore, some obtained adducts demonstrated potent antiparasitic properties against *Trypanosoma Brucei* and *Cruzi*.

[1] S. Tong, Q. Wang, M.-X. Wang, J. Zhu, *Angew. Chem. Int. Ed.* **2015**, 54, 1293–1297.

The paper of Zhu group was published when the project was in the course of manuscript writing.

4. The application of multiple Groebcke-Bienaymé-Blackburn reactions on di- and triaminoazines leads to the formation of a variety of new N-fused heterocyclic scaffolds (aminoimidazopyridines) with several diversity points. The selective reactivity mode of diaminopyrimidine provides controlled synthesis of non-symmetrical adducts. The scope of reaction was studied (analyzing the range of the aldehyde, isocyanide and aminoazine components) and post- modifications were applied to further diversify the rich structural outcome of the process. Adducts arising from melamine were structurally enlarged, exploiting cross-coupling reactions to achieve nanosized tripodal structures. The synthesized adducts displayed interesting pH and environment sensitive fluorescent properties. Interestingly, a novel borylated BODYPY-type adduct was successfully synthesized and used for staining lysosomes in mammal cells. Moreover, some adducts demonstrated potent antiviral activity against Adenovirus. Furthermore, selected compounds showed selective affinity to G-quadruplex DNA sequences, suggesting potential applications in medicinal and biological chemistry.

Summaries

Chapter I.

Publication I. Studies on the interaction of isocyanides with imines: reaction scope and mechanistic variations.

Ouldouz Ghashghaei, Consiglia A. Manna, Esther Vicente-García, Marc Revés, Rodolfo Lavilla.

Beilstein Journal of Organic Chemistry, **2014**, *10*, 12–17

Imine surrogates have a significant presence as intermediates in isocyanide-based multicomponent reactions. In many IMCRs, a repeating reaction pattern is the formation of an imine followed by the nucleophilic attack of an isocyanide, yielding a nitrilium ion. Imine based IMCRs normally differ in the manner the nitrilium ion evolves into the final product. For instance, in the named Ugi reaction, the nitrilium ion is trapped by a carboxylic acid and a Mumm rearrangement yields the final adduct.

Although Ugi-type MCRs have been thoroughly studied, the interactions of imines and isocyanides in the absence of other trapping agents have been overlooked. An interesting variation in the reaction happens when the formed nitrilium ion is attacked by a second isocyanide and is cyclized to give diiminoazetidines scaffolds. The present work focuses on the structural diversity arising from the interaction of imines and isocyanides, highlighting the synthesis of diiminoazetidines.

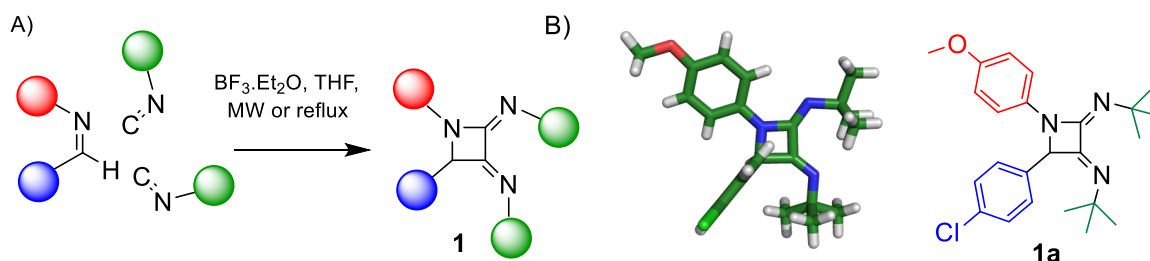


Figure 1. A) Synthesis of diiminoazetidines from the reaction of imines and two units of isocyanides B) structural elucidation of compound **1a** using X-Ray crystallography

Application of the Lewis acid $\text{BF}_3 \cdot \text{Et}_2\text{O}$ as catalyst and microwave irradiation leads to the formation of a small library of azetidine adducts **1**. The reaction scope was studied and a range common of aromatic and aliphatic amines, aldehydes, and isocyanides with different connectivities were productive. Moreover, some spiroazetidine adducts were prepared using isatine ketimines.

The proposed unified reaction mechanism justifies the formation of the expected azetidine structures as well as other observed scaffolds like indoles, aminoamidines, and triiminopyrroles. giving a more general picture of the isocyanide/imine interaction, where the first intermediate nitrilium ion is either

trapped by a second (third) unit of an isocyanide, then by the nucleophilic N atom of the starting imine, or by another nucleophilic moiety, giving rise to a family of structures.

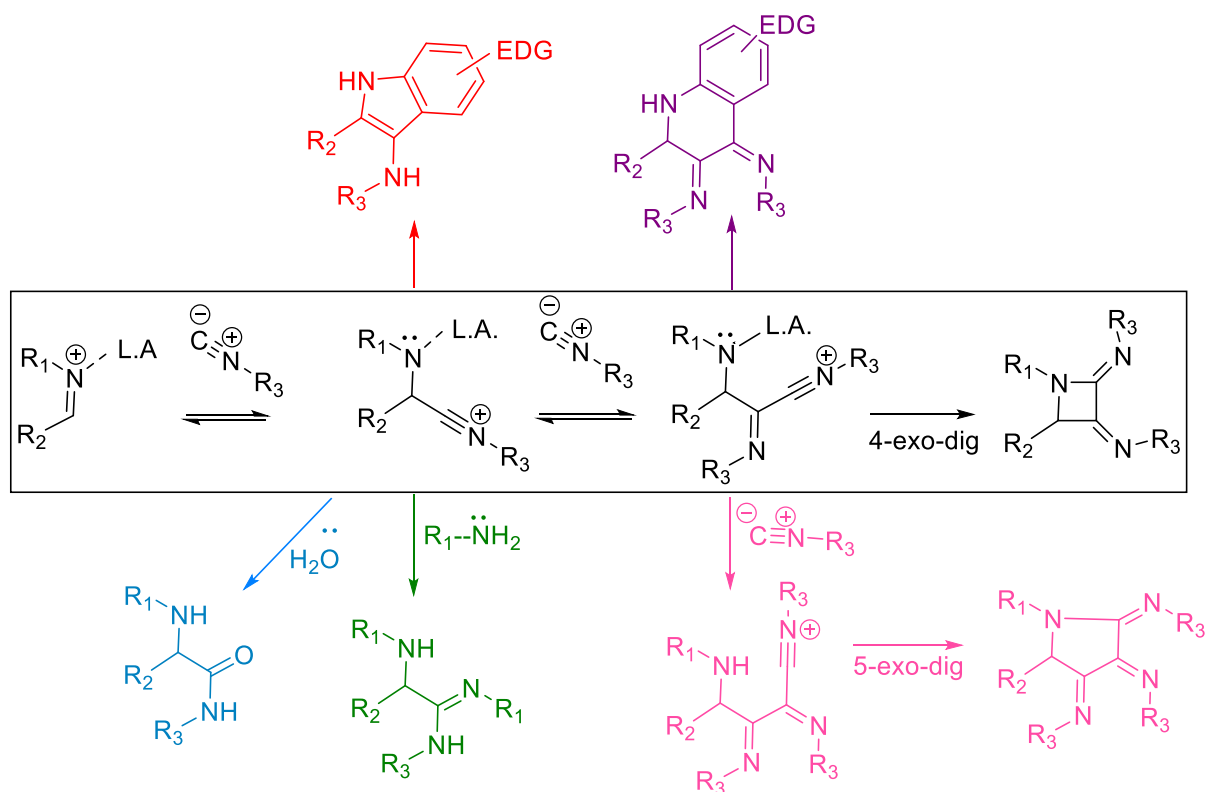


Figure 2. Unified reaction mechanism for interaction of amines and isocyanides

Chapter II.

Publication II. Modular Access to Tetrasubstituted Imidazolium Salts through Acid-Catalyzed Addition of Isocyanides to Propargylamines.

Ouldouz Ghashghaei, Marc Revés, Nicola Kielland, Rodolfo Lavilla.

European Journal of Organic Chemistry, **2015**, 4383–4388.

Following our interest to study new MCR processes involving isocyanides, we decided to study the unprecedented interaction of isocyanides and propargylamines. Propargylamines are attractive substrates as they could be prepared from the incorporation of amines, aldehydes, and terminal alkynes in an MCR process called A³ condensation.

The reaction was expected to proceed through nucleophilic addition of isocyanide to the triple bond or the alternative N-insertion process instead. The isocyanide N-insertion into amines has long been known. The process is reported to be mainly catalysed by acids or metal catalysts. The formed amidine structure has been used as the key step in the synthesis of a variety of heterocyclic compounds.

In this case, the interaction starts from the N-insertion of isocyanides to propargylamines. The amidine intermediates undergo cyclization upon the alkyne unit and isomerization, to form imidazolium salts in a tandem process.

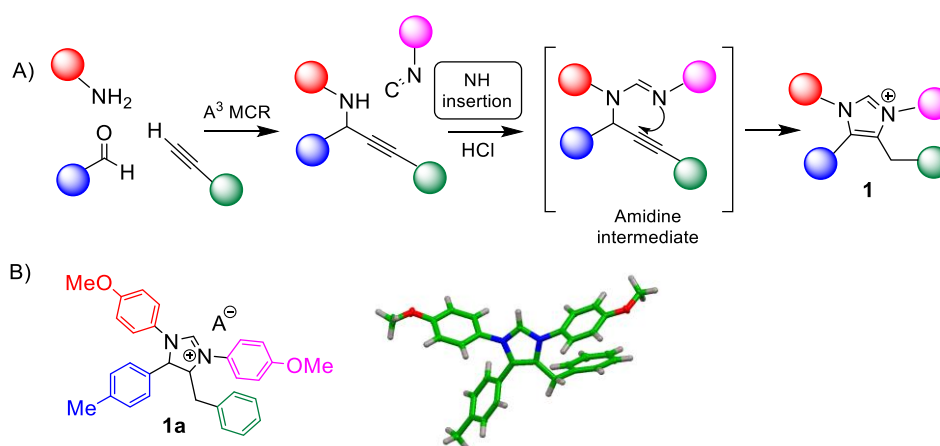


Figure 1. A) Synthesis of tetrasubstituted imidazolium salts from the reaction of propargylamines and isocyanides B) structural elucidation of compound **1a** using X-Ray crystallography

The shown procedure was repeated for a combination of common aromatic and aliphatic aldehydes and alkynes, aromatic amines to preform propargyl amines, which yielded a small library of imidazolium salts. Moreover, a tandem procedure was also designed, where the *in situ* formed propargylamine reacted with isocyanide to form the expected adduct in a one pot manner. However,

Isocyanides were inert in reaction with tertiary propargylamines, propargylalcohols and alkynes, suggesting that nucleophilic addition of isocyanides to the triple bond is not productive under the described reaction conditions.

Imidazolium salts are of great interest in transition metal- and organo-catalysis as the natural precursors of NHC ligands. As a proof of concept, the Pd-complex of imidazolium salt **1b** catalysed a Suzuki coupling reaction involving an aryl chloride and phenylboronic acid.

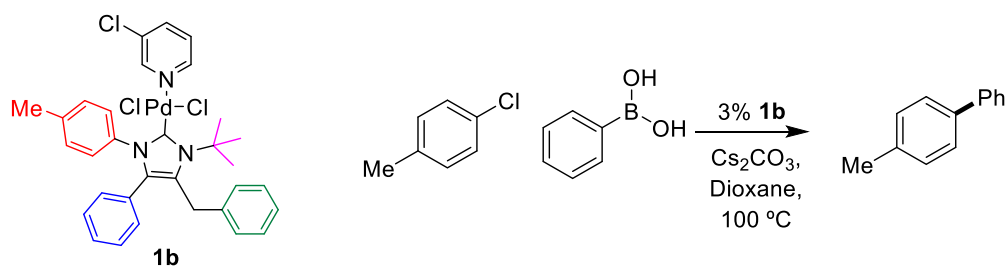


Figure 1. Pd complex of imidazolium salt **1b** used as a PEPSY type catalyst in an unconventional Suzuki coupling.

Experiments showed that the synthesized imidazolium adducts could have possible applications in biomedicine as they feature potent antiparasitic activity against *T.Brucei* and *T.Cruzi* which cause Chagas and sleeping diseases.

Chapter III.

Publication III. Insertion of Isocyanides into N–Si Bonds: Multicomponent Reactions with Azines Leading to Potent Antiparasitic Compounds.

Kranti G. Kishore[#], Ouldouz Ghashghaei[#], Carolina Estarellas[#], M. Mar Mestre, Cristina Monturiol, Nicola Kielland, John M. Kelly, Amanda Fortes Francisco, Shiromani Jayawardhana, Diego Muñoz-Torrero, Belén Pérez, F. Javier Luque, Rocío Gámez-Montaño, Rodolfo Lavilla

[#]These authors contributed equally to this work

Angewandte Chemie International Edition, 2016, 55, 8994-8998.

Following the previous studies on unprecedented reactivity patterns of isocyanides, we intended to investigate the interaction of isocyanides with silylated species. In this way, a Reissert-type MCR process involving an azine and two units of isocyanides was chosen. The reaction was catalyzed by trimethylsilyl chloride (TMSCl) instead of previously reported Brønsted acids, featuring milder conditions. The new activation mode was successfully used on a wide variety of azines and isocyanides resulting in a significant expansion in the scope of reaction, highlighting the diversity of azines and isocyanides. Some complex double-Reissert adducts were also prepared using diazine substrates. Moreover, regioselective formation of a single adduct was achieved from a mixture of two distinct isocyanides with different nucleophilicities. Furthermore, amidine adducts were isolated replacing one isocyanide with different nucleophiles such as indoles or dicarbonyl species.

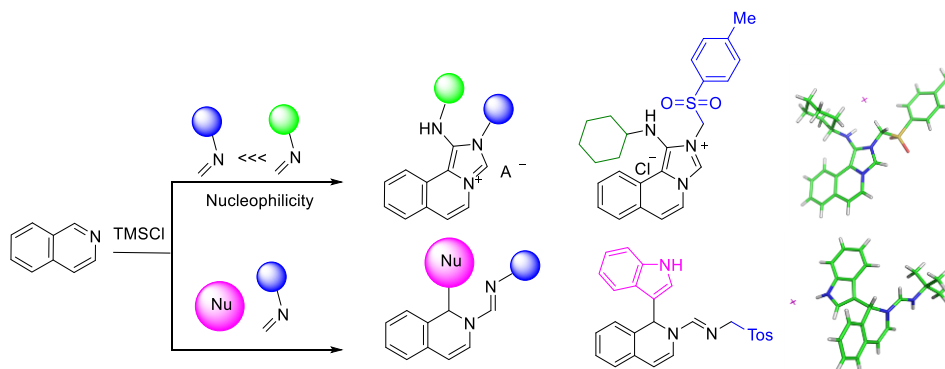


Figure 1. Regioselective synthesis of aminoimidazolium salts via a TMSCl-catalysed Reissert-type MCR.

Computational studies on the reaction mechanism revealed that the process goes through a rare insertion of isocyanide into the N-Si bond, justifying the observed improvement in the reactivity.

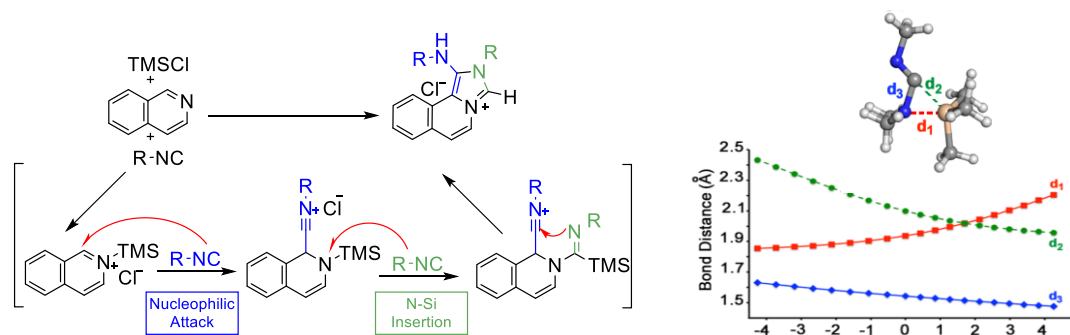


Figure 2. Proposed reaction mechanism featuring a rare N-Si isocyanide insertion.

The final adducts also feature interesting biomedical properties, being an extremely potent antiparasite chemotype against *T. Brucei* and *T. Cruzi*. Although the physicochemical properties and the *in vitro* experiments were extremely promising, the initial *in vivo* tests on mice fail, likely due to metabolic inactivation or poor biodistribution. However, structurally modified analogues could be easily accessed through the designed synthetic methodology.

Chapter IV.

Publication IV. Multiple Multicomponent Reaction Platform for the Selective Synthesis of a family of N-PolyHeterocyclic Chemotypes with Relevant Applications in Biology and Material Science.

Ouldouz Ghashghaei, Samantha Caputo, Miquel Sintes, Marc, Revés, Nicola Kielland, Carolina Estarellas, F. Javier Luque, Anna Aviñó, Ramón Eritja, Marc Vendrell, Ryan Treadwell, Fabio de Moliner, Javier Sánchez-Céspedes, Ana Serna-Gallego, José Antonio Marrugal-Lorenzo, Jerónimo Pachón, Joan Mendoza, Rodolfo Lavilla.

Manuscript in preparation, 2017.

Multiple multicomponent reactions are powerful tools for the rapid assembly of large scaffolds. They have been widely used for the synthesis of large structures like macrocycles and molecular cages. However, their potentials in the assembly of complex polyheterocyclic compounds have not been exploited. The Groebke–Blackburn–Bienaymé reaction (GBBR) is an MCR in which an aldehyde, an isocyanide and an amidine (α -aminoazine) yield substituted aminoimidazoloazines. Although the GBBR scope and applications have been widely studied, it almost exclusively uses aminopyridines as the amidine component in isolated processes.

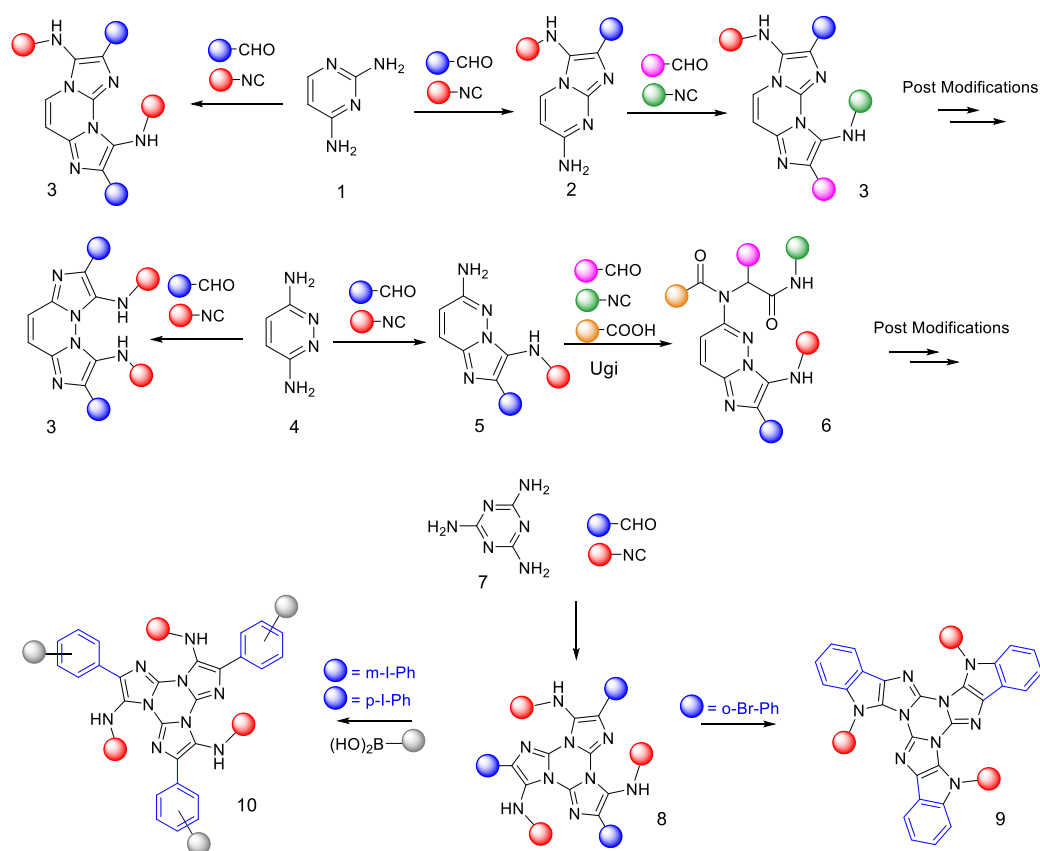


Figure 1 Diversity oriented synthesis of N-fused polyheterocycles using multiple GBB MCRs.

These scaffolds served as substrates for post modifications to access more complex chemotypes: diaminodiazine **4** was involved in a union process of GBB-Ugi MCR, introducing five diversity points into the final adduct **6**. Cross coupling reactions were used to transform adducts **8** into polycyclic heterocycle **9** and tripodal structures **10**.

Also, some adducts **3** are fluorescent probes that show pH- and environment-sensitive behavior. They also have relevant applications in medicinal chemistry as they demonstrate antiviral activity against adenoviruses. Moreover, they have selective interaction with quadruplex DNA sequences. Finally, the BODIPY-type derivative **11** is a fluorescent dye that selectively stains lysosomes in living cells. Compounds **11** and **12** are the first BODIPY derivatives of GBB adducts, which feature non-conventional 5-membered borono-cyclic moieties.

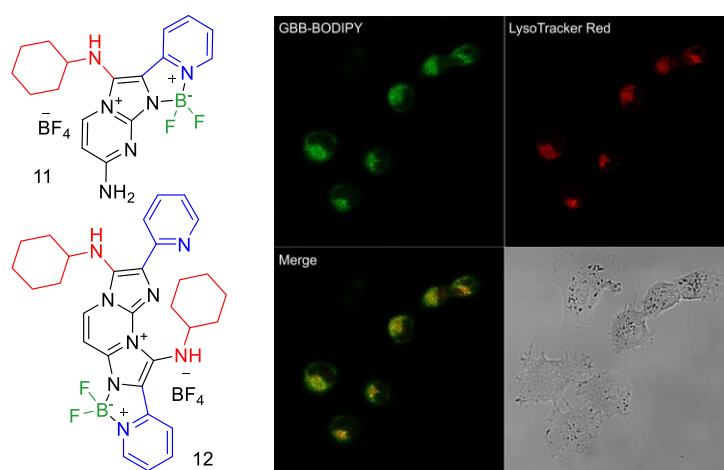


Figure 2. BODIPY-type fluorescent derivatives of GBB adducts, used as dyes to stain lysosomes in living cells.

Personal Contributions

Personal Contribution to the Presented Publications.

Publication I. Studies on the interaction of isocyanides with imines: reaction scope and mechanistic variations.

Ouldouz Ghashghaei, Consiglia A. Manna, Esther Vicente-García, Marc Revés, Rodolfo Lavilla.

Beilstein Journal of Organic Chemistry, **2014**, *10*, 12–17

In this paper, I participated in optimizing the reaction conditions. I also performed the major number of experimentation related to the synthesis and characterization of azetidines. Finally, I contributed in the preparation of the final manuscript (writing, revision, etc.).

Publication II. Modular Access to Tetrasubstituted Imidazolium Salts through Acid-Catalyzed Addition of Isocyanides to Propargylamines.

Ouldouz Ghashghaei, Marc Revés, Nicola Kielland, Rodolfo Lavilla.

European Journal of Organic Chemistry, **2015**, 4383–4388.

In this work, I carried out the majority of experimental tasks including the synthesis of propargylamine substrates, optimization of reaction conditions, as well as the synthesis and characterization of the final imidazolium adducts and in the exploration of their catalytic properties as well. Finally, I also took part in the preparation of the final manuscript (writing, revision, etc.).

Publication III. Insertion of Isocyanides into N–Si Bonds: Multicomponent Reactions with Azines Leading to Potent Antiparasitic Compounds.

Kranti G. Kishore[#], Ouldouz Ghashghaei[#], Carolina Estarellas[#], M. Mar Mestre, Cristina Monturiol, Nicola Kielland, John M. Kelly, Amanda Fortes Francisco, Shiromani Jayawardhana, Diego Muñoz-Torrero, Belén Pérez, F. Javier Luque, Rocío Gámez-Montaño, Rodolfo Lavilla

[#]*These authors contributed equally to this work*

Angewandte Chemie International Edition, **2016**, *55*, 8994–8998.

In the present work, I was involved in the experiments to investigate the reaction mechanism and the trapping of the silylated intermediates. I also collaborated in the characterization of the final adducts and contributed in the manuscript preparation. Although not primarily, I also took part in designing the computational section and the pharmacological part, working in the analysis of the results and the consequences.

Publication IV. Multiple Multicomponent Reaction Platform for the Selective Synthesis of a family of N-PolyHeterocyclic Chemotypes with Relevant Applications in Biology and Material Science.

Ouldouz Ghashghaei, Samantha Caputo, Miquel Sintès, Marc Revés, Nicola Kielland, Carolina Estarellas, F. Javier Luque, Anna Aviñó, Ramón Eritja, Marc Vendrell, Ryan Treadwell, Fabio de Moliner, Javier Sánchez-Céspedes, Ana Serna-Gallego, José Antonio Marrugal-Lorenzo, Jerónimo Pachón, Joan Mendoza, Rodolfo Lavilla.

Manuscript in preparation, 2017.

In the most recent work, I have been involved in the synthesis of double GBB adducts from pyrimidine and pyridazine. I also carried out the synthesis and characterization of compounds arising from melamine and other aminoazines. I assisted the structural elucidation of the novel scaffolds and in the post-transformation reactions. Moreover, I collaborated in the studies on the interaction of the GBB adducts and DNA sequences. Furthermore, I contributed to the preparation of the final manuscript. I also participated in designing the experimentation and analysis of the bioimaging, materials science and medicinal chemistry sections.

